Studies in Systems, Decision and Control 350

Alla G. Kravets
Alexander A. Bolshakov
Maxim V. Shcherbakov *Editors*

Cyber-Physical Systems

Digital Technologies and Applications

Springer

Studies in Systems, Decision and Control

Volume 350

The series "Studies in Systems, Decision and Control" (SSDC) covers both new developments and advances, as well as the state of the art, in the various areas of broadly perceived systems, decision making and control–quickly, up to date and with a high quality. The intent is to cover the theory, applications, and perspectives on the state of the art and future developments relevant to systems, decision making, control, complex processes and related areas, as embedded in the fields of engineering, computer science, physics, economics, social and life sciences, as well as the paradigms and methodologies behind them. The series contains monographs, textbooks, lecture notes and edited volumes in systems, decision making and control spanning the areas of Cyber-Physical Systems, Autonomous Systems, Sensor Networks, Control Systems, Energy Systems, Automotive Systems, Biological Systems, Vehicular Networking and Connected Vehicles, Aerospace Systems, Automation, Manufacturing, Smart Grids, Nonlinear Systems, Power Systems, Robotics, Social Systems, Economic Systems and other. Of particular value to both the contributors and the readership are the short publication timeframe and the world-wide distribution and exposure which enable both a wide and rapid dissemination of research output.

Indexed by SCOPUS, DBLP, WTI Frankfurt eG, zbMATH, SCImago.

All books published in the series are submitted for consideration in Web of Science.

More information about this series at http://www.springer.com/series/13304

Alla G. Kravets · Alexander A. Bolshakov ·
Maxim V. Shcherbakov
Editors

Cyber-Physical Systems

Digital Technologies and Applications

Springer

Editors
Alla G. Kravets
Volgograd State Technical University
Volgograd, Russia

Maxim V. Shcherbakov
Volgograd State Technical University
Volgograd, Russia

Alexander A. Bolshakov
Peter the Great St. Petersburg
Polytechnic University
St. Petersburg, Russia

ISSN 2198-4182 ISSN 2198-4190 (electronic)
Studies in Systems, Decision and Control
ISBN 978-3-030-67891-3 ISBN 978-3-030-67892-0 (eBook)
https://doi.org/10.1007/978-3-030-67892-0

This Springer imprint is published by the registered company Springer Nature Switzerland AG
The registered company address is: Gewerbestrasse 11, 6330 Cham, Switzerland

Preface

This book dwells with cyber-physical systems' progress and proposes ideas and finding around digital tools and technologies and their application. In this book, the authors confirm the scientific, practical, and methodological approaches to the digital technologies application in cyber-physical systems, including digital twins, computer linguistics and computer vision paradigms, implementations of IoT, and solutions for cybersecurity. The authors both analyzed and improved existing approaches to solving problems and demonstrated new ways by showing their perspective view on the subject matter. Implemented breakthrough systems, models, programs, and methods that could be used in real processes to predict and lead cyber-physical systems functions, states, and evolution.

There are five original chapters in the book grouped into five parts. Part "Cyber-Physical Systems and Digital Twins" presents brand new ideas of digitization of processes and manufactures via digital twins' ideas. The next part "IoT for Cyber-Physical Systems" includes results for enhancing approaches of communication and information transferring between cyber-physical systems connected with the Internet of things platforms. A chapter "Computer Linguistic for Cyber-Physical Systems" presents findings in the handling of semi-formalized information via artificial intelligence and machine learning approaches. A part "Intelligent Cybersecurity" contains chapters covering the very important issue of secure data collecting and transferring inside and outside of a system of systems. The last part "Computer Vision for Cyber-Physical Systems" shows how computer vision approaches and systems help to improve digital technologies and increase their efficiency during implementation and application.

The additional benefits of the book that authors determine key foreseen challenges and the main features of complex processes. The implementations of the developed prototypes, including testing in real industries, which have collected and analyzed big data and proved their effectiveness, are presented.

The book is for researchers and practitioners who are interested in digital technologies development and their applications for increasing efficiency.

Edition of the book is dedicated to the 130th Anniversary of Kazan National Research Technological University and 35th Anniversary of Computer-Aided Department at Volgograd State Technical University. Also, it is technically supported by the Project Laboratory of Cyber-Physical Systems of Volgograd State Technical University.

Volgograd, Russia — Alla G. Kravets
St. Petersburg, Russia — Alexander A. Bolshakov
Volgograd, Russia — Maxim V. Shcherbakov
January 2021

The book was prepared with the financial support of the Russian Foundation for Basic Research, project No. 20-08-20032.

Contents

Cyber-Physical Systems and Digital Twins

A Generalized Stacking for Implementing Ensembles of Gradient Boosting Machines

Andrei V. Konstantinov and Lev V. Utkin

Abstract The gradient boosting machine is one of the powerful tools for solving regression problems. In order to cope with its shortcomings, an approach for constructing ensembles of gradient boosting models is proposed. The main idea behind the approach is to use the stacking algorithm in order to learn a second-level meta-model which can be regarded as a model for implementing various ensembles of gradient boosting models. First, the linear regression of the gradient boosting models is considered as the simplest realization of the meta-model under the condition that the linear model is differentiable with respect to its coefficients (weights). Then it is shown that the proposed approach can be simply extended on arbitrary differentiable combination models, for example, on neural networks that are differentiable and can implement arbitrary functions of gradient boosting models. Various numerical examples illustrate the proposed approach.

Keywords Regression · Gradient boosting · Stacking · Ensemble · Neural network · Machine learning

1 Introduction

One of the ways to enhance the machine learning models and to produce improved results is to apply ensemble-based techniques which are based on combining a set of the so-called base or weak models (classifiers, regressors) [18, 21, 24, 25, 34]. All approaches to combining models can be conditionally divided into three main groups: bagging, stacking, and boosting. The first group consists of bagging methods [5], which are based on using bootstrapped samples. One of the most well-known bagging models is the random forest [7] using a large number of randomly built classification or regression decision trees whose predictions are combined to get the overall random forest prediction. Random forests often use the combination of the bagging and the random subspace method [16] for building trees. In contrast to bagging methods, the boosting assigns weights to elements of a training set in accordance with special

A. V. Konstantinov (✉) · L. V. Utkin
Peter the Great St.Petersburg Polytechnic University, Saint-Petersburg, Russia

A. G. Kravets et al. (eds.), *Cyber-Physical Systems*, Studies in Systems, Decision and Control 350, https://doi.org/10.1007/978-3-030-67892-0_1

rules. One of the first efficient boosting algorithms is AdaBoost [13]. Among boosting methods, we have to highlight the gradient boosting machines (GBMs) [14, 15]. In accordance with these methods, the training of each base model depends on models that have already been trained. The interpretation of GBMs in terms of regression is the following. By using the first guess as a prediction, the residuals are computed as differences between guessed predictions and target variables. These residuals are used instead of target variables to build the next base model, for example, a regression tree which is used in turn to predict new residuals. The boosting regression model is constructed by means of iterative computing the sum of all previous regression trees and updating residuals to reflect changes in the boosting regression model. In other words, a set of regression trees is computed in the GBM such that each successive tree predicts the residuals of the preceding trees given an arbitrary differentiable loss function [25]. The gradient boosting has a lot of modifications. One of the most popular modifications is the XGBoost [8] which is much faster than other models. An efficient gradient boosting method is CatBoost [9].

Another interesting ensemble-based technique is stacking [6, 31]. This technique is used to combine different base models by means of a meta-learner that takes into account which base model are reliable and which are not. One of the combination stacking models is when outputs of the base models are used as training data for the meta-learner to approximate the same target function. A detailed review of stacking algorithms can be found in [26].

It should be noted that the above division of the ensemble-based approaches is rather rough because there are models that do not belong to these groups. Moreover, there are a lot of models that can be viewed as a combination of the above approaches, for example, the deep forest or gcForest which was proposed by Zhou and Feng [35]. Due to many outperforming properties of the deep forest and due to its architecture which is similar to the multi-layer architecture of neural networks (NNs), several modifications of the deep forest have been developed, for example [28, 29]. We have to point out also a very interesting combination of ideas of the gradient boosting and the deep forest, which is called the multi-layered gradient boosting decision tree forest [11]. It learns hierarchical distributed representations by stacking several layers of regression gradient boosting decision trees as its building blocks.

A lot of surveys have been published due to the remarkable properties of ensemble-based models [10, 12, 17, 18, 21–23, 32, 33]. Most ensemble-based models are thoroughly studied in Zhou's book [34].

By returning to the GBMs, it should be pointed out that there are some shortcomings of the technique, which are explicitly described by Natekin and Knoll [19]. One of the important shortcomings is that there is currently no a fast and efficient model and the corresponding implementation of the smooth continuous base learner that captures interactions between variables which may play a crucial role in the particular predictive model design. Moreover, the GBM can be regarded as a linear combination of base models with some weights, and errors of the base models are correlated for some examples of the training set such that the GBM overfits. In order to overcome this shortcoming, we propose to extend the standard GBM towards constructing ensembles of the models, i.e., ensembles of ensembles, to reduce the impact of errors caused by overfitting. The ensemble is organized by using the generalized stacking algorithm where inputs of the meta-model are predictions of the ensemble of GBMs, and the meta-model can be implemented as any differentiable machine learning model, i.e., the ensemble of ensembles of GBMs is constructed by using arbitrary differentiable models, for example, NNs. Moreover, the proposed approach allows us to reduce the number of tuning parameters, that is many parameters become to be trainable. It is important to note that the idea of a combination of NNs and GBMs has been considered in the literature. In particular, Bilal [4] proposed the so-called deep gradient boosting where the GBM was incorporated into the NN backpropagation algorithm at every layer of the NN for updating the NN weights. Another combination of the GBM and the NN was proposed by Badirli et al. [1] where the authors use shallow NNs as base learners in the GBM. The same combination of the NN and XGBoost was proposed by Weldegebriel et al. [30]. Ideas of the NN and GBM combination have been also studied by other authors, for example [2, 20]. However, our approach differs from the available ones. We apply the NN as a possible tool for implementing the stacking algorithm and the second-level ensemble of GBMs.

The peculiarities of the proposed approach open a door to develop a large class of efficient ensembles of regression gradient boosting models. Various numerical examples illustrate the efficiency of the proposed ensembles of GBMs.

The chapter is organized as follows. Sections 2 and 3 provide descriptions of the standard regression problem statement and the GBM. An idea of using the stacking algorithm for implementing the linear combination of GBMs is considered in Sect. 4. An extension of the linear combination of GBMs towards the generalization of the proposed approach is given in Sect. 5. Numerical examples with real data are provided in Sect. 6. Concluding remarks can be found in Sect. 7.

2 Regression Problem Statement

Let us formally state the standard regression problem. Given N training data (examples, instances, patterns) $D = \{(x_1, y_1), \dots, (x_N, y_N)\}$, in which x_i may belong to an arbitrary set $\mathcal{X} \subset \mathbb{R}^m$ and represents a feature vector involving m features, and $y_i \in \mathbb{R}$ represents the observed output or target value such that $y_i = f(x_i) + \varepsilon$. Here ε is the random noise with expectation 0 and unknown finite variance. Machine learning aims to construct a regression model or an approximation g of the function f that minimizes the expected risk or the expected loss function

$$L(f) = \mathbb{E}_{(x,y)\sim P}\, l(y, g(x)) = \int_{\mathcal{X}\times\mathbb{R}} l(y, g(x))\mathrm{d}P(x, y),$$

with respect to the function parameters. Here $P(x, y)$ is a joint probability distribution of x and y. The loss function $l(\cdot, \cdot)$ may be represented, for example, as follows:

$$l(y, g(x)) = (y - g(x))^2.$$

There are many powerful machine learning methods for solving the regression problem, including regression random forests [3, 7], the support vector regression [27], etc. One of the powerful methods is gradient boosting [15], which will be considered below.

3 The Gradient Boosting Algorithm

Let us consider the gradient boosting decision tree algorithm [15]. The algorithm is an iterative construction of a model as an ensemble of base (weak) prediction models built in a stage-wise fashion where each base model is constructed, based on data obtained using an ensemble of models already built on previous iterations, as an approximation of the loss function derivative. A model of the size M is a linear combination of M base models:

$$g_M(x) = \sum_{t=1}^{M} \gamma_t h_t(x),$$

where h_i is the i-th base model; γ_i is the i-th coefficient or the i-th base model weight.

The gradient boosting algorithm can be represented as the following steps:

1. Initialize the zero-base model $h_0(x)$, for example, with the constant value.
2. Calculate the residual $r_i^{(t)}$ as a partial derivative of the expected loss function $L(x_i, y_i)$ at every point of the training set, $i = 1, \dots, N$.
3. Build the base model $h_t(x)$ as regression on residuals $\left\{ \left(x_i, r_i^{(t)} \right) \right\}$;
4. Find the optimal coefficient γ_t at $h_t(x)$;
5. Update the whole model $g_t(x) = g_{t-1}(x) + \gamma_t h_t(x)$;
6. If the stop condition is not fulfilled, go to step 2.

Here the loss function depends on the machine learning problem solved (classification or regression). Let us consider all the above in detail. Suppose that $(M - 1)$ steps produce the model $g_{M-1}(x)$. For constructing the model $g_M(x)$, the model $h_M(x)$ has to be constructed, i.e., there holds

$$g_M(x) = \sum_{t=1}^{M} \gamma_t h_t(x) = g_{M-1}(x) + \gamma_M h_M(x).$$

The dataset for constructing the model $h_M(x)$ is chosen in such a way as to approximate the expected loss function partial derivatives with respect to the function of the already constructed model $g_{M-1}(x)$. Let us denote residuals $r_i^{(M)}$ defined as the values of the loss function partial derivative at the point $g_{M-1}(x_i)$ in the current iteration M,

$$r_i^{(M)} = -\left.\frac{\partial L(z, y_i)}{\partial z}\right|_{z=g_{M-1}(x_i)}.$$

By using the residuals, a new training set D_M can be formed as follows:

$$D_M = \left\{\left(x_i, r_i^{(M)}\right)\right\}_{i=1}^N,$$

and the model h_M can be constructed on D_M by solving the following optimization problem

$$l = \min \sum_{i=1}^N \left\| h_M(x_i - r_i^{(M)}) \right\|^2.$$

Hence, an optimal coefficient γ_M of the gradient descent can be obtained as:

$$\gamma_M = \arg\min_{\gamma} \sum_{i=1}^N L\big[g_{M-1}(x) + \gamma h_M(x_i), y_i\big].$$

Then we get the following model at every point x_i of the training set

$$g_M(x) = g_{M-1}(x) + \gamma_M h_M(x) \approx g_{M-1}(x) - \gamma_M \left.\frac{\partial L(z, y_i)}{\partial z}\right|_{z=g_{M-1}(x_i)}.$$

If the loss function is the squared difference, then minimizing l corresponds to minimizing the loss function. This implies that the choice of the optimal step γ_M is not required, and its value is 1. In order to reduce overfitting, the step γ_M is reduced by its multiplying by a constant called the learning rate. By introducing the learning rate, it is possible to reduce the impact of model h_M errors on the ensemble error.

The above algorithm allows us to minimize the expected loss function by using decision trees as base models. However, it requires to select of the decision tree parameters, for example, depths of trees, as well as the learning rate, in order to simultaneously provide a high generalization and accuracy depending on a specific task.

The gradient boosting algorithm is a powerful and efficient tool for solving regression problems, which can cope with complex non-linear function dependencies [19]. However, it has a number of shortcomings. One of them is caused by the "greedy" concept used in the model implementation. The GBM $g_M(x)$ constructed using the above algorithm is an ensemble of base models itself, i.e., a linear combination of base models with given weights γ_i. However, each model is regarded as the "greedy" one, which means that errors of base models are correlated in the worst case when the base models are poorly approximating residuals for a set of points. As a result, the loss function can be minimized in the vicinity of such points only by overfitting. Therefore, it makes sense to construct ensembles of GBMs in order to reduce the variance of the error caused by overfitting.

4 An Ensemble of GBMs

The main idea behind the construction of a more accurate ensemble of GBMs is to apply the stacking algorithm [31], which trains the first-level learners using the original training dataset. The stacking algorithm generates a new dataset for training the second-level learner (meta-model) such that the outputs of the first-level learners are regarded as input features for the second-level learner while the original labels are still regarded as labels of new training data.

Let us compose an ensemble $E_M^K(x)$ of K GBMs of the size M. It can be represented as follows:

$$E_M^K(x) = \left(g_M^{(j)}(x)\right)_{j=1}^{K}.$$

First, we consider a linear regression model for implementing the meta-model of the stacking algorithm, which is of the form:

$$S_w(t) = t \cdot w + b = \sum_{j=1}^{K} t_j w_j + b,$$

where $w = (w_1, \dots, w_K) \in \mathbb{R}^K$ is a vector of weights; $t = (t_1, \dots, t_K) \in \mathbb{R}^K$ is a vector of the ensemble model predictions; b is the bias.

We will assume for simplicity purposes that the bias b is zero. Weights of the linear regression model can be computed by means of the standard well-known approaches depending on the regularization method used (the L_1 or L_2 norms). Suppose that a differentiable expected loss function $L(\hat{y}, y)$ is given, where y is a true class label, $\hat{y}$ is the model prediction. Let us set the initial approximation of the weights $w^{(0)}$. We are searching for the optimal vector of weights using gradient descent:

$$w^{(q)} = w^{(q-1)} - \alpha \frac{1}{N} \sum_{i=1}^{N} \nabla_w L\left(S_w\left(E_M^K(x_i)\right), y_i\right)\Big|_{w=w^{(q-1)}}.$$

Here $S_w\left(E_M^K(x_i)\right)$ is the prediction of the ensemble for the input feature vector x_i.

Note that the model $S_w(t)$ is differentiable both by the vector of weights and by the vector t of the ensemble predictions. It has been shown that the use of the gradient boosting algorithm allows us to minimize the differentiable loss functions by constructing new models approximating values proportional to their derivatives.

We will use this peculiarity to optimize not only linear regression weights but also the ensemble of GBMs.

Let us define a new differentiable loss function as follows:

$$\mathcal{L}(t, y) = L(S_w(t), y).$$

Intuitively, such a loss functional "hides" the linear regression block S_w. Since the gradient boosting algorithm allows iteratively minimizing an arbitrary differentiable loss function, we apply it to minimize $\mathcal{L}$. Each GBM in the ensemble minimizes the corresponding loss function:

$$\mathcal{L}_i(t_i, y) = L(S_w(t), y).$$

By using gradient boosting for each fixed set of weights of the linear model, we can construct such an ensemble of GBMs, which minimizes the loss function

$\mathcal{L}(t, y)$. Similarly, optimal weights of the linear model can be determined for a fixed ensemble of GBMs. We combine these two steps into one step, i.e., we simultaneously optimize weights of the linear model and construct the ensemble of GBMs.

Suppose that an ensemble of K GBMs is composed such that every its GBM is initialized by a constant value, for example, by the mean value of the corresponding target variable. Initial weights of the linear model are set as:

$$w^{(0)} = \frac{1}{K}.$$

Denote the residual of the j-th GBM for point x_i at step q as $r^q_{i,j}$, and differentiate the loss function $\mathcal{L}$ as:

$$r^q_{i,j} = -\left.\frac{\partial \mathcal{L}(t, y_i)}{\partial t_j}\right|_{t=E^K_{q-1}(x_i)} = -\left.\frac{\partial L(z, y_i)}{\partial z}\right|_{z=S_w(t)} \cdot \left.\frac{\partial S_w(t)}{\partial t_j}\right|_{t=E^K_{q-1}(x_i)}.$$

The partial derivative with respect to the j-th component of the linear regression model is nothing else but the weight w_j in the expression for $S_w(t)$ corresponding to this component. Hence, there holds:

$$r^q_{i,j} = -\left.\frac{\partial L(z, y_i)}{\partial z}\right|_{z=S_w(t)} \cdot w_j^{(q-1)}.$$

Let us construct a function which approximates residuals as:

$$h^j_q(x) = \underset{h\in\mathcal{F}}{\operatorname{argmin}} \sum_{i=1}^{N} \left\| h\left(x_i - r^q_{i,j}\right) \right\|.$$

where $\mathcal{F}$ is a set of admissible functions.

We simultaneously optimize the weights of the linear model and each GBM in the ensemble as follows:

$$\begin{cases} w^{(q)} = w^{(q-1)} - \alpha \frac{1}{N} \sum_{i=0}^{N} \nabla_w L\big(S_w\big(E_M^K(x_i)\big), y_i\big)\big|_{w=w^{(q-1)}}, \\ g_q^{(j)} = g_{q-1}^{(j)} + \gamma_q^{(j)} h_q^j(x). \end{cases}$$

For simplicity, $\gamma_q^{(j)}$ will be taken identical for all models and iterations. In sum, the learning algorithm consists of the following steps:

1. Initialize an ensemble of K GBMs.
2. Initialize model weights S_w.
3. Until the stop condition is fulfilled, at step q:

   a. calculate the partial derivative of the loss function by weights of the linear model;
   b. calculate the residuals $r_{i,j}^q$;
   c. construct base models $h_q^j(x)$ approximating the corresponding residues $r_{i,j}^q$.

The resulting model will be called an adaptive ensemble of GBMs because each member of the GBM ensemble adapts to a new loss function corresponding to each iteration.

It should be noted that the results of the traditional gradient boosting algorithm are strongly influenced by the choice of parameters of base models (decision trees). For every specific problem, the most appropriate parameters exist. However, it is necessary to construct the GBM many times to find the parameters and to apply one of the evaluation methods, for example, the cross-validation method. In the adaptive ensemble of GBMs, many different parameters of the base models can be immediately included as follows. In each GBM of the ensemble, we use a unique set of parameters corresponding to the GBM throughout the entire training of the ensemble. As a result of training, the largest weights are assigned to models with the most appropriate parameters.

As a rule, decision trees in traditional gradient boosting algorithms are used as base models. In order to construct a model $h_q^j(x)$ approximating the residuals $r_{i,j}^q$, a tree is built that minimizes the quadratic norm of the difference between the model predictions and the residual $h_q^j(x)$. The decision tree model approximating residuals implements a piecewise constant function with a small number of unique values. That is, at each iteration of the ensemble training, the accuracy of a prediction of the partial derivative of the loss function $r_{i,j}^q$ is not high. Moreover, it is difficult to control the accuracy of the approximation under the condition of a fixed tree depth for each specific GBM. Hence, ensembles of GBMs with a larger depth of trees will learn “faster” than GBM with a smaller depth, although trees of a smaller depth may be more preferable for a specific task. The basic idea behind the problem solution is to use more complex base models, namely, GBMs. Such models allow us to approximate the residuals with higher accuracy by using trees of a fixed depth. It is important to note that the ensemble of GBMs, which uses GBMs as base models, is also a linear combination of decision trees, however, the algorithm at each step more accurately approximates the partial derivative of the loss function $\mathcal{L}_i(t_i, y)$.

Let us consider various ways of initializing an ensemble of deep GBMs:

1. An exact initialization using the training set: each GBM is constructed by optimizing the loss function L directly over a certain number of iterations M_{init}. The larger the number of iterations, the greater the correlation between the model predictions.
2. A random initialization: each GBM includes only a single base model built on the basis of the training set where values of free variables repeat those of D, and reference values of the target variable are selected as observations of a random variable from the normal distribution whose parameters, the mean and the variance, coincide with the sample mean and the sample variance of the reference target variable.
3. An exact initialization using subsets of the training set: in order to get the most diverse GBMs in the ensemble (the diversity reduces the correlation of the model prediction errors), the GBMs can be constructed on pairwise disjoint subsets of the training set.
4. An initialization with the average value of the target variable.

Weights of the linear model can be initialized with optimal values under the condition that the ensemble of GBMs is fixed.

5 Generalization of the GBM Ensemble

Note that only a few conditions have to be fulfilled for training the aggregate model by means of the proposed algorithm:

- the loss function L has to be differentiable;
- the model $S_w(t)$ has to be differentiable with respect to the parameter w and the argument t.

This implies that the obtained approach can be generalized by replacing the linear regression model with an arbitrary differentiable model $\mathcal{S}_\theta^K(t)$, whose input is a vector of size K. The learning procedure for the model $\mathcal{S}_\theta^K(t)$ can be carried out not only by gradient descent but also by another algorithm, for example, by means of the support vector method. However, the model, in this case, has to be rebuilt after each update of the ensemble of GBMs. Therefore, we will consider only differentiable models $\mathcal{S}_\theta^K(t)$ from the class of NNs of forwarding propagation $\mathcal{F}$:

$$\mathcal{F} = \left\{ f : \mathbb{R}^I \times \Theta \to \mathbb{R}^T \right\},$$

where I is the dimensionality of the NN input space; Θ is the set of admissible parameters of the NN; T is the dimensionality of the target variable.

Any method of initializing the GBM ensemble among the considered above can be used for the case $T = 1$, and the dimension of the input space is equal to the number of models: $I = K$. If $T > 1$, then it is possible to exactly initialize every GBM in the ensemble using the training set only by constructing models with several outputs such that every GBM is a function whose values are in a space of dimension T. In this case, there holds $I = T \cdot K$, and the prediction of the GBM ensemble is the concatenation of predictions of every GBM. In the case of large values of T, the construction of the GBM ensemble with several outputs may be computationally expensive. For example, if the target variable corresponds to images of sizes 100×100, and the ensemble contains 100 GBMs, then the dimension of the input space of the NN will be 10^6. When the size of the training set is equal to 1000 in this case, the number of values that should be fed to the NN input is one billion. Therefore, it makes sense in such cases to use the random initialization which allows us to directly control the value of I by setting the number of models K.

We can construct a model on the basis of the proposed algorithm using both the advantages of learning algorithms for base models, for example, for decision trees, and the advantages of differentiable models, including the NN. The GBM ensemble is actually a mapping from the original feature space into a new intermediate space of dimension I, which is more informative in the context of a specific problem. Moreover, such the GBM ensemble has the following advantages of traditional ensembles based on decision trees:

- possibility of training the ensemble of trees on a sample of small dimension;
- interpretability of models, in particular, an assessment of the effects of specific features of input data on predictions;
- availability of deterministic algorithms for constructing decision trees;
- lack of assumptions about the existence of a linear relationship between features.

Note that the aggregate model inherits a part of the above properties, namely the interpretability and the lack of assumptions about the existence of a linear relationship between features, while the useful properties of the NN are potentially preserved, including generating high-dimensional outputs (for example, images), simultaneous solving several types of tasks (multi-task learning), parameterizing the loss function of a neural network, and so on. But it is very important that the number of NN parameters can be reduced, and, as a result, the NN can be trained on small samples because the processing of the initial features is carried out to the NN.

6 Numerical Experiments

In order to illustrate the proposed approach, we investigate the model for real data sets from the R Package "data microarray" which contains DNA microarrays. Table 1 is a brief introduction to the investigated datasets, while more detailed information

Table 1 A brief introduction about the DNA microarray data sets

Data set	Type	m	n	C
Alon	Colon Cancer	2000	62	2
Borovecki	Huntington's Disease	22,283	31	2
Chin	Breast Cancer	22,215	118	2
Chowdary	Breast Cancer	22,283	104	2
Golub	Leukemia	7129	72	3
Gravier	Breast Cancer	2905	168	2
Pomeroy	CNS Disorders	7128	60	2
Nakayama	Sarcoma	22,283	105	10
Sorile	Breast Cancer	456	85	5
Singh	Prostate Cancer	12,600	102	2

can be found from, respectively, the data resources. Table 1 shows the number of features m for the corresponding data set, the number of examples n, and the number of classes C. All these datasets are for solving the classification task. It can be seen from Table 1 that the number of features of every dataset is much more than the number of training examples. Accuracy measure A used in numerical experiments is the proportion of correctly classified cases on a sample of data. To evaluate the average accuracy, we perform cross-validation with 100 repetitions, where in each run, we randomly select $n_{\text{tr}} = 3n/4$ training data and $n_{\text{test}} = n/4$ testing data.

The numerical results of the DNA microarray classification are shown in Table 2. Four models are compared: the linear ensemble of GBMs (Linear GBM) in accordance with $S_w(t)$; a combination of the NN and ensemble of GBMs (NN + GBM), the standard GBM, and the random forest with the numbers of decision trees equal to 100 or 1000. The learning rates 0.1 or 0.01 are taken for training GBMs. Ensembles of GBMs consist of 20 machines with depths of trees from 2 to 21. The epoch number

Table 2 Comparison of four models on the DNA microarray datasets

Data set	Linear GBM	NN + GBM	GBM	Random Forest
Alon	0.708	0.833	0.771	0.762
Borovecki	0.979	1.000	0.958	0.925
Chin	0.987	0.894	0.900	0.933
Chowdary	0.987	1.000	0.962	0.992
Golub	0.861	0.991	0.889	0.911
Gravier	0.730	0.766	0.778	0.748
Pomeroy	0.511	0.422	0.556	0.453
Nakayama	0.577	0.590	0.526	0.585
Sorile	0.627	0.714	0.683	0.857
Singh	0.929	0.897	0.897	0.862

Table 3 A brief introduction to the regression data sets

Data set	Abbreviation	*m*	*n*
House Prices: Advanced Regression	HouseART	79	1460
ML housing	Boston	13	506
Diabetes	Diabetes	10	442
Longley's Economic Regression	Longley	7	16
Friedman 1	Friedman 1	10	100
Friedman 2	Friedman 2	4	100
Scikit-Learn Regression	Regression	100	100

is 10, and the learning rate of every ensemble is 0.05. The fully connected NN having 3 layers of size 10 with tanh as an activation function. The best performance for each dataset is shown in bold. It can be seen from Table 2 that the combinations of the NN and ensemble of GBMs provide better results for most datasets. Moreover, 7 datasets from 10 ones show outperforming results by using the proposed approach (2 datasets by using Linear GBM and 5 datasets by using NN + GBM).

In order to study the proposed approach for solving regression problems, we apply the datasets described in Table 3. The datasets are taken from open sources, in particular, Boston Diabetes, Longley can be found in the corresponding R Packages; HouseART can be found in the Kaggle platform; Friedman 1 and 2 are described at the site: https://www.stat.berkeley.edu/breiman/bagging.pdf; Regression is available in package "Scikit-Learn".

Numerical results in the form of the mean squared errors for the regression datasets are shown in Table 4. We again use the four models described above. Ensembles of GBMs consist of 100 machines now. The NN having 3 layers of size 20 is used. Other parameters of numerical experiments are the same as in the previous experiments. It can be seen from Table 4 that the combinations of the NN and ensemble of GBMs provide better results for 4 datasets from 7 ones.

We can conclude after analyzing the numerical results that the proposed approach provides outperforming results for cases of small datasets (see, for example, most DNA microarray datasets and the Longley dataset). This implies that ensembles of

Table 4 Comparison of four models on the regression datasets

Data set	Linear GBM	NN + GBM	GBM	Random Forest
HouseART	6.43×10^8	2.02×10^8	8.02×10^8	9.26×10^8
Boston	1.42×10^1	1.16×10^1	1.47×10^1	1.64×10^1
Diabetes	4.06×10^3	3.73×10^3	3.48×10^3	3.74×10^3
Longley	1.01×10^0	6.04×10^0	1.91×10^0	1.65×10^0
Friedman 1	8.07×10^0	1.13×10^1	6.82×10^0	9.41×10^0
Friedman 2	2.06×10^3	6.35×10^3	2.40×10^3	3.85×10^3
Regression	1.15×10^4	1.84×10^4	1.06×10^4	1.34×10^4

GBMs partially solve the problem of overfitting, which takes place for datasets with a small number of training examples.

7 Conclusion

A new approach for combining GBMs by using the stacking algorithm has been proposed in the chapter. It has many advantages in comparison with the GBM as well as with deep differentiable models such as NNs:

- the “greedy” stacking algorithm of GBMs does not guarantee the achievement of the loss function optimum because the optimization procedure is carried out in turn. The simultaneous optimization solves this problem;
- NNs consider linear combinations of input features, which lead to a serious problem of overfitting when working with tabular data consisting of features of different nature, for example, mass and length, as well as by a large number of features and small sizes of training samples. The proposed approach allows us to process features using decision trees and to construct arbitrarily deep models taking advantage of NNs.

It should be noted that many important questions and studies remain outside the scope of our study in this chapter. In particular, it is interesting to consider various types of regularization which could improve the models. Moreover, it is interesting to consider a procedure that removes a training example from the gradient descent procedure when a current residual corresponding to the example is smaller than some threshold. This improvement may reduce learning time and increase model accuracy. The above questions can be regarded as directions for further research.

References

1. Badirli, S., Liu, X., Xing, Z., Bhowmik, A., Keerthi, S.: Gradient boosting neural networks: Grownet (Feb 2020), arXiv:2002.07971
2. Bengio, Y., Roux, N., Vincent, P., Delalleau, O., Marcotte, P.: Convex neural networks. In: Advances in neural information processing systems, pp. 123–130 (2006)
3. Biau, G., Scornet, E.: A random forest guided tour. Test **25**(2), 197–227 (2016)
4. Bilal, E.: Deep gradient boosting—layer-wise input normalization of neural networks (Oct 2019), arXiv:1907.12608
5. Breiman, L.: Bagging predictors. Mach. Learn. **24**(2), 123–140 (1996)
6. Breiman, L.: Stacked regressions. Mach. Learn. **24**(1), 49–64 (1996)
7. Breiman, L.: Random forests. Mach. Learn. **45**(1), 5–32 (2001)
8. Chen, T., Guestrin, C.: Xgboost: A scalable tree boosting system. In: Proceedings of the 22nd ACM SIGKDD International Conference on Knowledge Discovery and Data Mining, pp. 785–794. ACM, New York, NY (2016)
9. Dorogush, A., Ershov, V., Gulin, A.: Catboost: gradient boosting with categorical features support (Oct 2018), arXiv:1810.11363

10. Fawagreh, K., Gaber, M., Elyan, E.: Random forests: from early developments to recent advancements. Syst. Sci. & Control. Eng. **2**(1), 602–609 (2014)
11. Feng, J., Yu, Y., Zhou, Z.H.: Multi-layered gradient boosting decision trees. In: Advances in neural information processing systems, pp. 3551–3561. Curran Associates, Inc. (2018)
12. Ferreira, A., Figueiredo, M.: Boosting algorithms: A review of methods, theory, and applications. In: Zhang, C., Ma, Y. (eds.) Ensemble Machine Learning: Methods and Applications, pp. 35–85. Springer, New York (2012)
13. Freund, Y., Schapire, R.: A decision theoretic generalization of on-line learning and an application to boosting. J. Comput. Syst. Sci. **55**(1), 119–139 (1997)
14. Friedman, J.: Greedy function approximation: a gradient boosting machine. Ann. Stat. **29**, 1189–1232 (2001)
15. Friedman, J.: Stochastic gradient boosting. Comput. Stat. & Data Anal. **38**(4), 367–378 (2002)
16. Ho, T.: The random subspace method for constructing decision forests. IEEE Trans. Pattern Anal. Mach. Intell. **20**(8), 832–844 (1998)
17. Jurek, A., Bi, Y., Wu, S., Nugent, C.: A survey of commonly used ensemble-based classification techniques. Knowl. Eng. Rev. **29**(5), 551–581 (2014)
18. Kuncheva, L.: Combining Pattern Classifiers: Methods and Algorithms. Wiley-Interscience, New Jersey (2004)
19. Natekin, A., Knoll, A.: Gradient boosting machines, a tutorial. Front. Neurorobotics **7**(Article 21), 1–21 (2013)
20. Nitanda, A., Suzuki, T.: Functional gradient boosting based on residual network perception (Feb 2018), arXiv:1802.09031
21. Polikar, R.: Ensemble learning. In: Zhang, C., Ma, Y. (eds.) Ensemble Machine Learning: Methods and Applications, pp. 1–34. Springer, New York (2012)
22. Ren, Y., Zhang, L., Suganthan, P.N.: Ensemble classification and regression-recent developments, applications and future directions [review article]. IEEE Comput. Intell. Mag. **11**(1), 41–53 (2016)
23. Rokach, L.: Ensemble-based classifiers. Artif. Intell. Rev. **33**(1–2), 1–39 (2010)
24. Rokach, L.: Ensemble Learning: Pattern Classification Using Ensemble Methods. World Scientific **85** (2019)
25. Sagi, O., Rokach, L.: Ensemble learning: A survey. WIREs Data Min. Knowl. Discov. **8**(e1249), 1–18 (2018)
26. Sesmero, M., Ledezma, A., Sanchis, A.: Generating ensembles of heterogeneous classifiers using stacked generalization. WIREs Data Min. Knowl. Discov. **5**, 21–34 (2015)
27. Smola, A., Scholkopf, B.: A tutorial on support vector regression. Stat. Comput. **14**, 199–222 (2004)
28. Utkin, L.: An imprecise extension of SVM-based machine learning models. Neurocomputing **331**, 18–32 (2019)
29. Utkin, L., Konstantinov, A., Meldo, A., Ryabinin, M., Chukanov, V.: A deep forest improvement by using weighted schemes. In: Proceedings of the 24th Conference of Open Innovations Association FRUCT. pp. 451–456. IEEE, Moscow, Russia (2019)
30. Weldegebriel, H., Liu, H., Haq, A., Bugingo, E., Zhang, D.: A new hybrid convolutional neural network and extreme gradient boosting classifier for recognizing handwritten ethiopian characters. IEEE Access **8**, 17804–17818 (2019)
31. Wolpert, D.: Stacked generalization. Neural Netw. **5**(2), 241–259 (1992)
32. Wozniak, M., Grana, M., Corchado, E.: A survey of multiple classifier systems as hybrid systems. Inf. Fusion **16**, 3–17 (2014)
33. Yang, P., Yang, E., Zhou, B., Zomaya, A.: A review of ensemble methods in bioinformatics. Curr. Bioinform. **5**(4), 296–308 (2010)
34. Zhou, Z.H.: Ensemble Methods: Foundations and Algorithms. CRC Press, Boca Raton (2012)
35. Zhou, Z.H., Feng, J.: Deep forest: Towards an alternative to deep neural networks. In: Proceedings of the 26th International Joint Conference on Artificial Intelligence (IJCAI'17), pp. 3553–3559. AAAI Press, Melbourne, Australia (2017)

Role of Simulation in the Development of a Digital Twin of a Food Item

Marina Nikitina

Abstract Simulation is closely related to such categories as abstraction, analogy, hypothesis, etc. The chapter suggests that a mathematical model of a food item, which includes the whole variety of factors (physical and chemical, functional and technological, structural, and mechanical) is a "digital model" of such item. The example of creating a functional product in the form of a sausage product shows the stages of forming the model. At the first stage, the nutritional, biological, and energy value of the product is designed. By varying structural ratios of recipe components, taking into account input constraints, it is possible to see how nutritional and biological values of the product, as well as the protein-to-fat ratio, etc. change. The second stage is associated with the development of structural forms of the product. In our particular example, the Fourier equation of heat conduction in cylindrical coordinates is used for this purpose. Initial conditions—temperature distribution over the thickness of the product at the initial time. Third-type boundary conditions characterize the law of convective heat transfer between the body surface and the environment. To implement the stages, it is necessary to have a large scope of data not only on physical and chemical parameters: moisture, fat, protein, etc. but also on functional and technological properties of raw materials; kinetics of biochemical and colloidal-chemical processes in food systems, analytical and empirical dependencies characterizing main patterns of behavior of heterogeneous dispersed systems with varying physical and chemical factors. A digital model of a food item will allow a research scientist to expand the possibilities of conducting a scientific experiment, forecasting, and making a decision.

Keywords Simulation modeling · Mathematical model · Digital twin · Food items · Database · Bank of models · Knowledge bbase

M. Nikitina (✉)
V.M. Gorbatov Federal Research Center for Food Systems of RAS, Moscow 26, Str. Talalikhina, 109316, Russia
e-mail: nikitinama@yandex.ru

A. G. Kravets et al. (eds.), *Cyber-Physical Systems*, Studies in Systems, Decision and Control 350, https://doi.org/10.1007/978-3-030-67892-0_2

1 Introduction

One of the scientific tools of modern biotechnology that allows studying the behavior of an object (food product) using its mathematical description is modeling.

Among the existing types of modeling [1, 2], it can be assumed that simulation of a specific food product is its virtual model, i.e. a digital twin or digital prototype.

A simulation model of the process and object allows (1) reducing the number of laboratory experiments; (2) making changes to the physical and chemical composition of raw materials (since raw materials are heterogeneous in composition) at the input and getting feedback at the output; (3) observing interaction effects of main factors and cross-factor interactions; (4) altering and varying variables (ingredients, recipe); (5) avoiding or reducing the number of gross and systematic errors, which are an integral part of traditional research methods.

This hypothesis is based on one of the definitions of a digital twin [3–10], namely "a digital twin is the use of a digital copy of a physical system for real-time optimization" [6].

Solving the problem of obtaining a "digital twin" of a food product at different stages is associated with finding optimal structural ratios, technological modes, and processes, and determining material balance according to the selected criteria between the input and output flows.

A food product is a complex food system. When designing a food system, a symbiosis of knowledge in the field of food chemistry, food biotechnology, engineering, and computer modeling is required.

The process of creating a "digital twin" of a food product (virtual model) is not only a reasonable choice of ingredients and structural relations between them, taking into account various restrictions, i.e. solving the problem of food combinatorics. But also "giving" the product necessary physical, chemical, structural, mechanical, functional, and technological properties. A reasoned choice of optimal technological modes.

The chapter considers the issue of creating a virtual model of a food product, which includes the following stages: (1) preparation of initial data for design; (2) structural optimization taking into account specified requirements and restrictions; (3) formation of structural forms; (4) overall quality assessment.

2 Methodology Description and Results' Discussion

2.1 Preparing Initial Data for Design. Analysis of Raw Materials of Animal and Vegetable Origin

When developing a food product model with specified properties, one of the main tasks is to fill in the missing nutrients in the diet, the optimal ratio of nutrients that meet the medical and biological requirements of FAO/WHO.

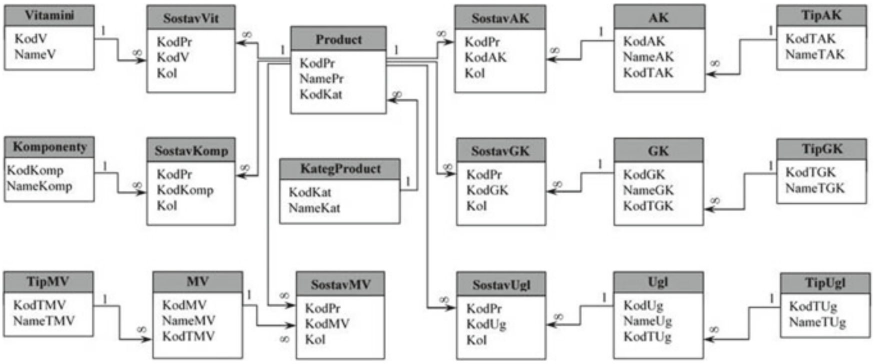

Fig. 1 Logical structure of the database

Thus, *the first stage* is associated with the selection of components of the future recipe. Analysis of raw materials for various properties, such as physical and chemical composition, functional properties, presence of bioactive peptides, etc. allows to further provide the future product with certain functional properties and orientation. Structural optimization allows setting necessary ratios of protein: fat: carbohydrates, food, biological and energy values of the food product.

To implement the first stage, one needs to know main indicators of raw materials of animal and vegetable origin, and auxiliary ingredients—moisture, protein, fat, carbohydrates, energy value, amino acid, fatty acid, vitamin, and mineral compositions, as well as information about functional, technological, structural and mechanical properties, and the index of atherogenicity. In addition, the database should contain information about rheological properties of raw materials, the rate of kinetic reactions of biochemical and colloidal chemical processes; physical laws, equations of mathematical physics, mathematical dependencies characterizing the behavior of complex food systems.

A relational approach was used when developing the database structure (Fig. 1). Data is structured as tables with the rows presented as records (tuples) [11].

2.2 *Food Combinatorics. Recipe Optimization Issue*

The second stage is associated with mathematical modeling of a combined food product and solving the problem of structural and recipe optimization.

The recipe composition is calculated according to the physical and chemical parameters of the nutrient composition of ingredients of animal and vegetable origin selected from the database. The modeled recipe must meet established FAO/WHO biomedical requirements and balance limits as much as possible.

Table 1 Indicators of food and energy value, and the balance of amino acids in the control and experimental recipe of emulsified meat product

Indicator name	Control Sample	Development Type
Moisture, %	60.15	44.36
Fat, %	23.31	18.24
Protein, %	13.02	13.65
Energy value, kcal	264	220
Minimum score, %	79.57	85.30
Utility coefficient, decimal quantity	0.82	0.84
Coefficient of difference of amino acid score, %	18.09	16.89
Biological value, %	81.91	83.11

As a criterion for optimizing a multicomponent food product, the criterion for minimizing the sum of squared deviations of a group of indicators, for example, food or biological value, from the reference (or desired) structures, can be used.

The principles for assessing the quality of protein and the balance of amino acid composition in products are based on formulas and criteria proposed by Mitchell-Block in the middle of the last century [12–14]. They are still relevant. They include coefficients of utility and rationality of amino acid composition, comparable redundancy, as well as the index of essential amino acids, the minimum score characterizing the limiting amino acid, and the indicator of biological value.

Using the example of an emulsified meat product, we will show an assessment of nutritional and energy value, as well as the balance of amino acids in the product designed and control sample. The recipe composition of which, respectively, includes: 2nd grade trimmed beef—48% (35%); semi-fat pork—30% (23%); trimmed fat pork—20% (20%); potato starch—2% (2%); soy protein—0% (4%); water for the hydration of soy protein—0% (16%) [15] (Table 1).

Along with the listed coefficients and indicators, the authors [16] proposed another criterion of the amino acid compliance of protein for the quantitative assessment of the protein composition of the designed gerodietetic product.

The criterion evaluates the ratio of essential amino acids such as methionine and cystine, tryptophan, and lysine, taking into account the role of isoleucine, leucine, phenylalanine, and tyrosine as gerontological competitors of tryptophan in the design of a gerodietetic product. Ideally, the criterion should be equal to one.

$$K = \frac{a_{(Met+Cys)}}{a_{Lys} \cdot C_{Trp}} \cdot \frac{\sum_{J=1}^{4} a_{jn}}{\sum_{J=1}^{4} a_{jэ}} \to 1$$

where K is the coefficient of amino acid compliance, decimal quantity;

$a_{(Met+Cys)}, a_{Lys}$—mass fractions of methionine + cystine, lysine amino acids, g/100 g of protein;

C_{Trp}—the score of tryptophan amino acid in the protein of a gerodietetic product in relation to the FAO/WHO standard, decimal quantity;

$a_{jn}, a_{j э}$—mass fractions of j-th amino acid in the protein and the FAO/WHO standard, respectively, g/100 g of protein;

the j is the index identifies respectively 1—isoleucine amino acid; 2—leucine amino acid; 3—phenylalanine amino acid; 4—tyrosine amino acid.

Metadata of articles published over the past decades shows that the issue of the computer-aided design of food products is well studied and mastered. A detailed review of publications on food combinatorics is presented in the work [17].

2.3 Building Structural Forms of Designed Food Product

The third stage is associated with the design of structural forms of a food product. As it is known, the optimal model system of the product without taking into account rheological properties obtained at the second stage does not guarantee the production of a product with required structural and mechanical properties. For example, instead of "persistent" pudding, we may get a spreading liquid.

The appearance, consistency, smell, texture, connectivity, etc. of a food product depend on the course of colloidal chemical reactions during the entire technological process.

In meat food systems, the main structure-forming agent is protein. Reactions like "protein-protein", "protein-water", "protein-fat"," water-protein-fat" depend primarily on the native properties of the protein, i.e. on its natural properties: vegetable, dairy, meat (muscle, connective), etc. properties, and many other factors, such as pH, temperature, ionic interaction force, the degree of minced meat grinding, the depth of autolytic changes having occurred with meat raw materials, etc. [18–20].

In the production of emulsified meat products, the most important stage is heat treatment. Equations of mathematical physics are used to calculate thermal conductivity [21]. As an example, we may consider the Fourier thermal conductivity equation in cylindrical coordinates (implicit scheme). The advantage of using an implicit scheme is that the time step change does not depend on the spatial coordinate step change. This reduces the time to solve the issue. The partial differential equation of thermal conductivity has the following form:

$$\frac{dU}{dt} = a\left(\frac{d^2U}{dr^2} + \frac{1}{r}.\frac{dU}{dr}\right)$$

where $0 \le r \le R$ for a given initial temperature distribution over the radius of the rod of $U(r, 0) = f(r)$ and conditions of convective heat exchange with the environment on the rod's side (third-type boundary conditions)

$$\frac{dU(R,t)}{dr} = \frac{\lambda}{\alpha}[\varphi(t) - U(R,t)]$$

where λ, α, a, $\varphi(t)$ are coefficients of heat transfer, thermal conductivity, thermal diffusivity, and the law of heating medium variation, respectively.

The Fourier thermal conductivity equation has innumerable solutions. To determine the uniqueness of their solution, it is necessary to specify the system's state at the beginning of the process (initial condition) and the nature of the interaction of the system under consideration with the environment (boundary condition).

The following initial data were taken as an example of a solution: thermal diffusivity coefficient of a = 0.0015; heat transfer coefficient of $\alpha = 0.004$; thermal conductivity coefficient of $\lambda = 0.004$; the initial temperature of $U_0 = 15$; duration of Tm = 14,400 s. (or 240 min, or 4 hours); time division step of l = 30 s.; loaf radius of r = 3; the number of division points by the radius of n = 6 [21].

As a result of solving the thermal conductivity equation (implicit method) in the R programming language in the Jupiter Notebook environment, we have obtained the temperature distribution during the technological process and managed to construct the temperature field of internal points (Fig. 2a, b)

The temperature field shows the temperature distribution over time (t), both on the surface of the sausage product and inside. As a rule, the most interesting thing for technologists is the temperature on the surface of the sausage product, since the heating and cooling process is evaluated based on it.

All food products belong to complex food systems with a design that must take into account rheological properties.

For example, in the baking industry, rheological properties acquired by the product during proofing and baking are important. The results of modeling [22–24] allow correlating the recipe with the final cell structure and understanding better the main mechanisms.

In the dairy industry, fermentation processes play a great role in the production of fermented milk products. The works [25–27] have predicted the use of ultrasonic processing as a technological tool for creating an environment that would stimulate the accumulation of functional components in fermented dairy products.

2.4 Quality Assessment

Each of the stages of developing a "digital twin" includes a number of criteria. This set of criteria is open and can be supplemented with other criteria that are significant for the development of different types of food products.

The set of solutions corresponds to the achievement of the global extremum for each criterion separately. To generalize and structure the results obtained, convolution in the form of an integral quality indicator is required.

To solve this issue, the author suggests using a "weighted" quality functional that varies from 1 to 0 [16]

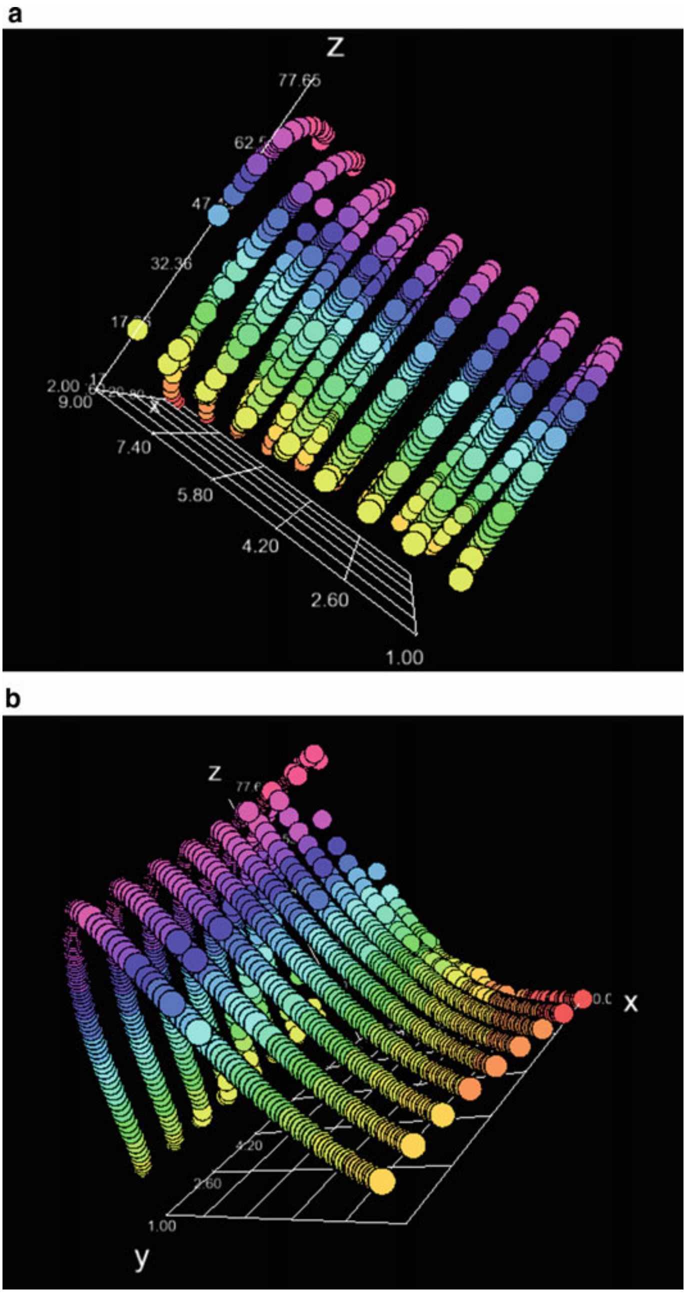

Fig. 2 **a**. Visual result of solving the thermal conductivity equation under the given initial and boundary conditions—the “Temperature field”. **b**. Visual result of solving the thermal conductivity equation under the given initial and boundary conditions—the “Temperature field” (*from a different angle*)

$$\Phi(z) = 1 - \sqrt{\sum_{k=1}^{n} b_k z_k^2}$$

where b_i, z_i are the weight coefficient of the *i-th* criterion and the relative dimensionless estimate.

The optimal solution of the issue is related to the achievement of the functional value equal to 1. This indicates the maximum likelihood of the "digital twin" to meet established requirements.

Along with the functionality proposed by the author, other convolutions can be used [28], such as the Saati scale [29], or the Harington desirability function [30].

3 Conclusion

The use of simulation as a tool in creating "digital twins" allows expanding researcher's boundaries in conducting a scientific experiment with any combination of factors and interaction effects.

Using the "digital twin" of a food product before launching it into production, process engineers can analyze the nutritional, biological, and energy value and other properties of the product. By changing and adjusting the spread of parameters and properties of biological raw materials in real-time operating conditions, it can be compensated by choosing optimal strategies for redistributing components and rearranging technological schemes depending on the actual resource and component composition of biological raw materials. Thus, each possible state of the input flow of biological raw materials will be opposed to a certain structural and mode-setting option ensuring maximum processing of products from a unit of raw materials at the maximum approximation to standard indicators.

Acknowledgements This chapter is published as part of a scientific research theme No. 0585-2019-0008 under the state assignment of the federal state budgetary scientific institution V.M. Gorbatov's Federal Research Centre for Food Systems of RAS.

References

1. Glinskij, B.A., Gryaznov, B.S., Dynin, B.S., Nikitin, E.P: Modeling as a method of scientific research: gnoseological analysis. MGU Publishing House, Moscow (1965)
2. Sovetov, B.Ya., Yakovlev, S.A.: Modeling of Systems. 7nd end. Yurajt, Moscow (2019)
3. Claessgen, E., Stargel, D.: The digital twin paradigm for future NASA and US Air Force vehicles. In: 53rd AI-AA/ASME/ASCE/AHS/ASC Structures, Structural Dynamics and Materials Conference 20th AIAA/ASME/AHS Adaptive Structures Conference 14th AIAA, vol. 8. pp. 7247–7260 (2012)

4. Lee, J., Bagheri, B., Kao, H.A.: A cyber-physical systems architecture for industry 4.0-based manufacturing system. Manufacturing letters **3**, 18–23 (2015)
5. El, S.A.: Digital twins: the convergence of multimedia technologies. IEEE Multimedia **25**(2), 87–92 (2018)
6. Söderberg, R., Wärmefjord, K., Carlson, J.S., Lindkvist, L.: Toward a Digital Twin for real-time geometry assurance in individualized production. CIRP Ann. **66**(1), 137–140 (2017)
7. Bolton, R.N., McColl-Kennedy, J.R., Cheung, L., Gallan, A., Orsingher, C., Witell, L., Zaki, M.: Customer experience challenges: bringing together digital, physical and social realms. J. Serv. Manag. **29**(5), 766–808 (2018)
8. Tao, F., Sui, F., Liu, A., Qi, Q, Zhang, M., Song, B., Guo, Z., Lu, S.C.-Y., Nee, A.Y.C.: Digital twin-driven product design framework. Int. J. Prod. Res. **57**(12), 3935–3953 (2019)
9. Tarassov, V.B.: Enterprise total agentification as a way to industry 4.0: forming artificial societies via goal-resource networks. In: Abraham, A., Kovalev, S., Tarassov, V., Snasel, V., Sukhanov, A. (eds). Proceedings of the Third International Scientific Conference "Intelligent Information Technologies for Industry" (IITI'18). IITI'18 2018. Advances in Intelligent Systems and Computing, vol. 874. Springer, Cham (2019)
10. Suyatinov, S.I.: Conceptual approach to building a digital twin of the production system. In: Alla G. Kravets, A.G., Bolshakov, A.A., Shcherbakov M.V. (eds). Cyber-Physical Systems: Advances in Design & Modelling, vol. 259, pp. 279–290. Springer, Cham (2020)
11. Nikitina, M.A., Lisitsyn, A.B., Zakharov, A.N., Sus', E.B., Pilyugina, S.A., Dydykin, A.S., Ustinova, A.V: Food products. Certificate of database registration. Rospatent RU 2015620557 (2015)
12. Mitchell, H.H., Block, R.I.: Some relationships between amino acid contents of proteins and their nutritional value for the rat. J. Biol. Chem. **163**, 599–617 (1946)
13. Oser, B.L.J.: Method for integrating essential amino acid content in nutritional evaluation of proteins. J. Am. Diet. Assoc. **27**, 396–402 (1951)
14. Mitchell, H.H.: Comparative nutrition of man and domestic animals. New York **2**, 596–604 (1964)
15. Rogov, I.A., Zharinov, A.I., Ivashkin, YuA, Dunchenko, N.I., Nikitina, M.A., Popova, MYu., Kuptsova, S.V.: Designing Combined Foods. Mosk. Gos. Univ. Prikl. Biotekhnol, Moscow (2005)
16. Ivashkin, YuA, Yudina, S.B., Nikitina, M.A., Azarova, N.G.: Information technologies for food design. Meat Ind. **5**, 40–41 (2000)
17. Lisitsyn, A.B., Chernukha, I.M., Nikitina, M.A.: Russian methodology for designing multicomponent foods in retrospect. Foods Raw Mater. **8**(1), 2–11 (2020)
18. Zharinov, A. I.: Fundamentals of modern meat processing technologies. Part 1. Emulsified and coarsely ground meat products. In: Voyakin, M.P. ITAR-TASS, Moscow (1994)
19. Texture in food. Semi-solid foods. In: McKenna, B.M. (eds.). Woodhead Publishing (2003)
20. Moelwyn-Hughes, E.A.: The Kinetics of Reactions in Solution. The Oxford Press, New York (1933)
21. Lisitsyn, A.B., Chernukha, A.M., Borodin, A.V: Application of mathematical modeling for automated calculation of thermograms for heat treatment of meat products. Bulletin of the Don State Technical University **1**(40), 110–120 (2009)
22. Bikard, J., Coupez, T., Valle, G.D., Vergnes, B.: Simulation of bread making process using a direct 3D numerical method at microscale: Analysis of foaming phase during proofing. J. Food Eng. **85**, 259–267 (2008)
23. Stanke, M., Zettel, V., Schutze, S., Hitzmann, B.: Measurement and mathematical modeling of the relative volume of wheat dough during proofing. J. Food Eng. **131**, 58–64 (2014)
24. Babin, P., Della Valle, G., Chiron, H., Cloetens, P., Hoszowska, J., Pernot, P., Réguerre, A.L., Salvo, L., Dendievel, R.: Fast X-ray tomography analysis of bubble growth and foam setting during breadmaking. J. CeR. Sci. **43**, 393–397 (2006)
25. Potoroko, I., Kalinina, I., Botvinnikova, V., Krasulya, O., Fatkullin, R., Bagale, U.: Ultrasound effects based on simulation of milk processing properties. Ultra-Sonochemistry **48**, 463–472 (2018)

26. Ojha, K.S., Mason, T.J., O'Donnell, C.P., Kerry, J.P., Tiwari, B.K.: Ultrasound technology for food fermentation applications. Ultra-Sonochemistry **34**, 410–417 (2017)
27. Lee, H., Zhou, B., Liang, W., Feng, H., Martin, S.E.: Inactivation of Escherichia coli cells with sonication, manosonication, thermosonication, and manothermosonication: microbial responses and kinetics modeling. J. Food Eng. **93**, 354–364 (2009)
28. Verhoef, A., Huijberts, G., Vaessen, W.: Introduction of a quality index, based on generalizability theory, as a measure of reliability for univariate- and multivariate sensory descriptive data. Food Qual. Prefer. **40**, 296–303 (2015)
29. Saaty, T.L.: The Analytic Hierarchy Process: Planning, Priority Setting, Resource Allocation (Decision Making Series). McGraw-Hill, New York (1980)
30. Harrington Jr., E.C.: The desirability Function. Ind. Qual. Control. **21**(10), 494–498 (1965)

The Application of Statistical Methods for the Analysis of Multi-Parameter Data of Complex Composite Objects in the Field of Cyber-Physical Systems

Sergey Demin, Oleg Panischev, Valentin Yunusov, and Sergey Timashev

Abstract We design a scheme of an automated intelligent system for monitoring the evolution of complex composite objects. We develop new methods for the analysis of multi-parameter data for further possible applications in the industry of cyber-physical systems. We describe the possibilities of the Memory Function Formalism and Flicker-Noise Spectroscopy in the analysis of collective phenomena realized in complex systems of a living and astrophysical nature. We determine diagnostic criteria for photosensitive epilepsy by the analysis of the power spectra of magnetoencephalogram signals of healthy subjects and patients. We establish different mechanisms of disk accretion by the study of cross-correlations in radio emission signals of quasars at different frequencies. The effects of frequency phase synchronization are studied based on the construction of 3D cross-correlators. We performed calculations of the dynamic and spectral characteristics of simultaneously recorded signals in the MatLab environment. We note prospects of using methods of statistical physics in the development of integrated data analysis systems in the field of the Internet of Things.

Keywords Cyber-physical systems · Internet of things · Automated intelligent system · Monitoring of complex systems evolution · Statistical data analysis · Collective phenomena · Cross-correlations · Effects of synchronization

1 Introduction

The complex systems play a special role in the diversity of objects around the world. The time series of dynamic variables and spatial maps of the structural characteristics of complex systems carry meaningful information about their evolution, which can

S. Demin (✉) · O. Panischev · V. Yunusov
Kazan Federal University, Kremlevskaya Str., 18, Kazan 420008, Russian Federation
e-mail: serge_demin@mail.ru

S. Timashev
Karpov Institute of Physical Chemistry, Vorontsovo Pole Str., 10, Moscow 105064, Russian Federation
e-mail: serget@mail.ru

A. G. Kravets et al. (eds.), *Cyber-Physical Systems*, Studies in Systems, Decision and Control 350, https://doi.org/10.1007/978-3-030-67892-0_3

be extracted using mathematical methods of statistical physics. For example, significant information on the functioning of the human brain is collected by medical devices—electroencephalographs (EEG, electroencephalogram) and magnetoencephalographs (MEG, magnetoencephalogram). Methods of intellectual analysis and machine learning, software tools using neural networks, etc. are effectively used for processing large arrays of collected experimental data (Big Data). In regard to this, the development of cyber-physical systems to integrate modern computing resources with real objects of animate and inanimate nature seems to be very relevant. The development of cyber-physical systems in healthcare is of particular importance under the conditions of a gradual transition to "personalized" medicine of the future. In this case, the Internet of Things (IoT), as one of the areas of development of cyber-physical systems, will allow developing the methods for the prevention of human pathologies, facilitating their diagnosis and treatment, based on the individual characteristics of the patient. The collection of biomedical data is carried out by standard medical equipment; the assessment can be performed by software-analytical complexes using methods of statistical physics.

Complex systems have unique properties, primarily, non-equilibrium dynamics, nonstationarity, and nonlinearity, fundamentally distinguishing them from other objects. The first property means that a complex system is far from equilibrium with the environment. The second one means that the system is evolving, i.e. continuously changing the nature of its dynamics. The third property establishes that the processes within the system and the response to external influences are nonlinear. The specified properties, on the one hand, give complex systems their extraordinary "flexibility", and on the other hand, make the task of describing them quite difficult.

In addition, the description of the evolution of composite objects is complicated due to the presence of a large number of interacting components. On the one hand, the components generate their own dynamics, and on the other, they are in close interaction with the environment and act as a whole. Then the key factor in the stability of a complex system is the collective processes that arise as a result of interaction or redistribution of relationships.

There are a considerable number of approaches for describing the coordination processes implemented in complex systems. First of all, it is necessary to single out the concepts of phase and frequency synchronizations [1–4], which are based on the detection of characteristic frequencies and analysis of the phase difference of the signals produced by parts of a complex system. In practice, frequencies and phases of oscillations other than harmonic can be established within the framework of the "analytical signal" model using Fourier, Hilbert [1–3] or Wavelet transform [4]. Besides the phase model, stochastic synchronization models are being used, the essence of which is a comparative analysis of the topological structure of attractors describing the dynamics of nonlinear interacting oscillators; "generalized" synchronization [5]; and also synchronization of time scales.

The description of the mutual dynamics of parameters of complex systems based on the study of cross-correlations, i.e. probabilistic relationships between two sequences of random variables—time series recording of dynamic variables. The Random-matrix method is widely used in the study of financial systems [6];

detrended cross-correlation analysis is used to study power dependencies in cross-correlations between non-stationary time series [6–8]. Besides that, there is a group of methods that directly use cross-correlation functions [9–13].

The logic of the chapter is a preliminary description of the authors' statistical methods for monitoring and analyzing the dynamic states of complex composite systems, with further application of the obtained results in the design of an automated cyber-physical system and analytical services, e.g. for the healthcare sector.

2 Theoretical Approaches to the Analysis of Multi-Parameter Data

2.1 Memory Function Formalism

In this chapter, we present the possibilities of describing cross-correlations and synchronization effects in complex systems based on statistical analysis methods: the Memory Function Formalism (MFF) and Flicker-Noise Spectroscopy (FNS). Memory Function Formalism [11, 14, 15] is a theoretical approach to the study of auto- and cross-correlations generated by complex systems with discrete-time. The effects of statistical memory in a more general sense describe the complex and hidden nature of the birth, distribution, and attenuation of correlations. From a physical point of view, the time scales of processes associated with correlations and memory effects cannot be arbitrary. For a quantitative comparison of these processes, as well as for a description of the relationships between them, functions and measures of statistical memory are introduced that characterize the rate of change of random variables at different levels of the statistical description.

The studied signals are presented as a sequence of values $\{x_j\}$, $\{y_j\}$ of two random variables X, Y:

$$X = \{x(T), x(T + \tau), x(T + 2\tau), \ldots, x(T + (N - 1)\tau\},$$

$$Y = \{y(T), y(T + \tau), y(T + 2\tau), \ldots, y(T + (N - 1)\tau\},$$

where T is the initial time, $(N–1)\tau$ is the signal recording time, τ is the sampling time step.

For the specified sequences mean values X,Y, fluctuations δx_j, δy_j and variances σ_x, σ_y are calculated:

$$\langle X\rangle = \frac{1}{N}\sum_{j=0}^{N-1} x(T + j\tau), x_j = x(T + j\tau), \delta x_j = x_j - \langle X\rangle, \sigma_x^2 = \frac{1}{N}\sum_{j=0}^{N-1} \delta x_j^2;$$

$$\langle Y\rangle = \frac{1}{N}\sum_{j=0}^{N-1} y(T+j\tau),\ y_j = y(T+j\tau),\ \delta y_j = y_j - \langle Y\rangle,\ \sigma_y^2 = \frac{1}{N}\sum_{j=0}^{N-1}\delta y_j^2.$$

We write the expression for the time cross-correlation function (CCF) as:

$$c(t) = \frac{1}{(N-m)\sigma_x\sigma_y}\sum_{j=0}^{N-m-1}\delta x(T+j\tau)\delta y(T+(j+m)\tau),$$

$$t = m\tau,\ 1 \le m \le N-1.$$

Based on MFF [11], higher-order memory functions $M_{n-1}^{XY}(t)$ are calculated, as well as expressions for the kinetic λ_n^{XY} and relaxation Λ_n^{XY} parameters:

$$M_{n-1}^{XY}(t) = \frac{\left\langle \mathrm{W}_{n-1}^{X}\left\{1+i\tau\hat{L}_{22}\right\}^{m}\mathrm{W}_{n-1}^{Y}\right\rangle}{\left\langle \mathrm{W}_n^X\mathrm{W}_n^Y\right\rangle},$$

$$\lambda_n^{XY} = \frac{\left\langle \mathrm{W}_{n-1}^{X}\hat{L}\mathrm{W}_{n-1}^{Y}\right\rangle}{\left\langle \mathrm{W}_{n-1}^{X}\mathrm{W}_{n-1}^{Y}\right\rangle},\ \Lambda_n^{XY} = i\frac{\left\langle \mathrm{W}_n^X\mathrm{W}_n^Y\right\rangle}{\left\langle \mathrm{W}_{n-1}^{X}\mathrm{W}_{n-1}^{Y}\right\rangle}.$$

Where W_i^X,W_i^Y are dynamic orthogonal vectors derived from state vectors $\mathrm{A}_k^0(0)$, $\mathrm{B}_k^0(0)$ using recurrence relations:

$$\mathrm{A}_k^0 = \mathrm{A}_k^0(0) = \{\delta x_0, \delta x_1, \ldots, \delta x_{k-1}\},$$

$$\mathrm{B}_k^0 = \mathrm{B}_k^0(0) = \{\delta y_o, \delta y_1, \ldots, \delta y_{k-1}\}.$$

$$\mathrm{W}_0^X = \mathrm{A}_k^0,\ \mathrm{W}_1^X = \left(i\hat{L} - \lambda_1^{XY}\right)\mathrm{W}_0^X,\ \mathrm{W}_2^X = \left(i\hat{L} - \lambda_2^{XY}\right)\mathrm{W}_1^X - \Lambda_1^{XY}\mathrm{W}_0^X, \ldots,$$

$$\mathrm{W}_0^Y = \mathrm{B}_k^0,\ \mathrm{W}_1^Y = \left(i\hat{L} - \lambda_1^{XY}\right)\mathrm{W}_0^Y,\ \mathrm{W}_2^Y = \left(i\hat{L} - \lambda_2^{XY}\right)\mathrm{W}_1^Y - \Lambda_1^{XY}\mathrm{W}_0^Y, \ldots.$$

$\hat{L}$ is the Liouville's quasi operator.

For analyzing the frequency phase synchronization, the power spectra of the memory functions are used:

$$\mu_0^{XY}(\nu) = \left|\Delta t\sum_{j=0}^{N-1} c\left(t_j\right)\cos 2\pi\nu t_j\right|^2, \ldots, \mu_i^{XY}(\nu) = \left|\Delta t\sum_{j=0}^{N-1} M_i^{XY}\left(t_j\right)\cos 2\pi\nu t_j\right|^2.$$

2.2 Flicker-Noise Spectroscopy

The prospects for using Flicker-Noise Spectroscopy to study signals generated by complex systems [13, 16] are due to the introduction of information parameters characterizing the components of the analyzed signals in different frequency ranges. The extracted information includes low-frequency “resonances” that are specific for each signal, as well as parameters of chaotic components.

The parameters introduced in FNS are determined on the basis of the “image” of the autocorrelation function, which is basic for statistical physics:

$$\psi(\tau) = \langle V(t)V(t+\tau)\rangle_{T-\tau}, \langle(\ldots)\rangle_{T-\tau} = \frac{1}{T-\tau}\int\limits_0^{T-\tau}(\ldots)\mathrm{d}t,$$

where τ is the “lag” time parameter, $0 \le \tau \le T_M$ ($T_M \le T/2$). To extract the information contained in $\psi(\tau)$ (we set $\langle V(t)\rangle = 0$), it is more convenient to analyze some transformations of this function, namely, the cosine transform $S(f)$ (f is the frequency):

$$S(f) = 2\int\limits_0^{T_M}\langle V(t)V(t+t_1)\rangle_{T-\tau}\cos 2\pi f t_1 \mathrm{d}t_1$$

and its difference moments (Kolmogorov transient “structure” functions) $\Phi^{(2)}(\tau)$ of the second-order:

$$\Phi^{(2)}(\tau) = \langle[V(t) - V(t+\tau)]^2\rangle_{T-\tau}.$$

Two-parameter cross-correlators introduced in the framework of the FNS allow obtaining direct information on the dynamics of correlation relationships between simultaneously measured signals—dynamic variables—$V_i(t)$ and $V_j(t)$, measured at spatially separated points i and j of the studied system or signals of different nature. The corresponding expression for “two-point” correlators or cross-correlators is represented as [16]:

$$q_{ij}(\tau,\theta_{ij}) = \left\langle\left[\frac{V_i(t) - V_i(t+\tau)}{\sqrt{\Phi_i^{(2)}(\tau)}}\right]\left[\frac{V_j(t+\theta_{ij}) - V_j(t+\theta_{ij}+\tau)}{\sqrt{\Phi_j^{(2)}(\tau)}}\right]\right\rangle_{T-\tau-|\theta_{ij}|},$$

where τ is the “lag” time (we set $\tau > 0$), θ_{ij} is the “time shift” parameter.

3 The Study of Collective Phenomena in Complex Systems Based on Intelligent Data Analysis

Further, as an example, the results of studying the frequency phase synchronization in the activity of individual regions of the human cerebral cortex at photosensitive epilepsy (PSE) and healthy subjects will be presented. Signals [17, 18] are magneto-electric responses caused by flickering light stimuli. The disease is a type of epilepsy in which seizures are triggered by the flickering light of high intensity. MEG signals were recorded by a Neuromag-122 installation (Neuromag Ltd., Finland) using 61 SQUID (Superconducting QUntum Interference Device) sensors with a sampling frequency of 500 Hz. The group of subjects included 9 healthy people (age 22–27 years) and a patient with PSE. The red-blue stimulus was projected onto a special screen 80 times in two seconds with an interval of three seconds. The results of all repetitions were averaged.

Consider the signals recorded by sensors from the left- (№ 37) and right-temporal (№ 60) areas of the cerebral cortex. In Fig. 1 the power spectra $\mu_0^X(\nu)$, $\mu_0^Y(\nu)$ of the autocorrelation functions and the cross-correlation function $\mu_0^{XY}(\nu)$ for the signals of one of the healthy subjects are shown. A comparative analysis of the amplitude bursts of the spectra (for example, peaks 1 and 2) allows us to establish the frequencies at which the synchronization of the signals of the cerebral cortex is realized.

The power spectra of the initial CCF calculated for the signals of a healthy test subject (Fig. 2a) and a patient (Fig. 3a) have a clear fractal structure. Significant differences can be detected using the following relaxation levels (Fig. 2b–d, Fig. 3b–d) on

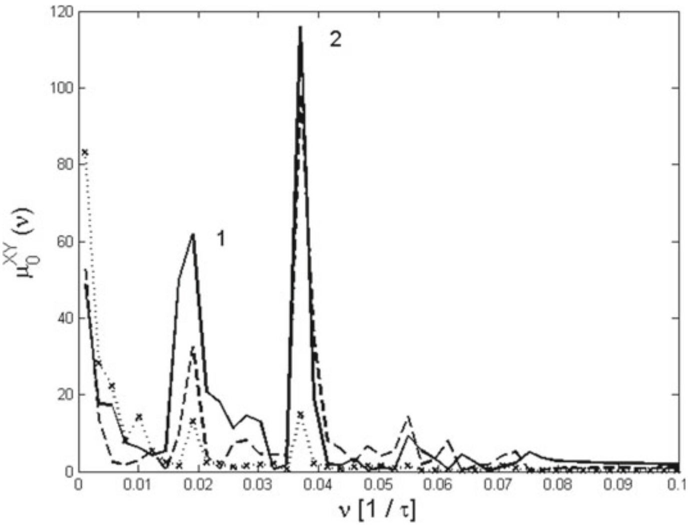

Fig. 1 Power spectra of autocorrelation functions calculated for two MEG signals (dashed lines), in comparison with the power spectrum of the cross-correlation function (solid line)

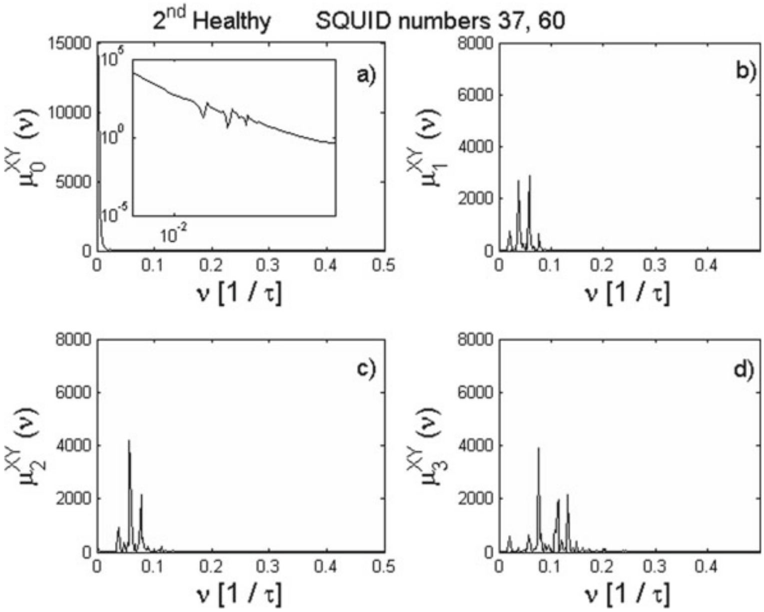

Fig. 2 Power spectra of the cross-correlation function (**a**) and memory functions (**b**–**d**) for the mutual dynamics of the neuromagnetic responses of a healthy subject

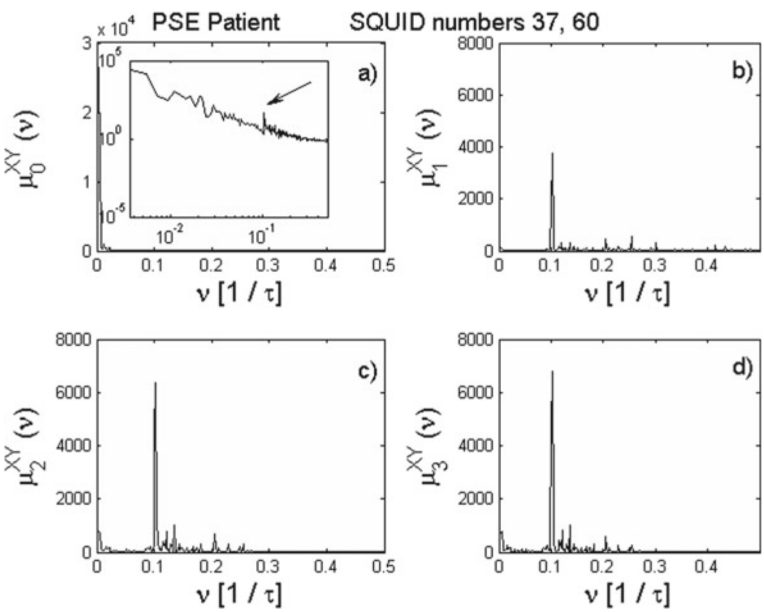

Fig. 3 Power spectra of the cross-correlation function (**a**) and memory functions (**b**–**d**) for the mutual dynamics of neuromagnetic responses of a patient with photosensitive epilepsy

the spectra of memory functions. The spectra of CCF power and memory functions for signals of a healthy subject are characterized by a pronounced low-frequency dynamics with the presence of significant bursts in the range up to 50 Hz, which correspond to physiological rhythms. Rhythms reflect the complex psychophysiological processes of brain activity. The picture is different for the spectra of CCF and memory functions for signals of a patient with PSE (Fig. 3). The process with a frequency of about 50 Hz is dominant. At the same time, additional quasiperiodic processes appear in the region of higher frequencies.

The results suggest that there are processes that compensate for the development of the abnormally high collective activity of neurons in spatially separated areas of the cerebral cortex of healthy subjects in response to light exposure.

In the framework of Flicker-Noise Spectroscopy, we study the effects of synchronization in the dynamics of the spectral density of the radio emission flux of the quasars 0420m014 and 2251p158 at frequencies of 2.7 GHz and 8.1 GHz [19]. According to the most common concepts, quasars are active nuclei of distant galaxies that are at the formation stage, in which a supermassive black hole absorbs matter from a gas-dust disk. When the layers of the incident substance move, collective effects, and resonance phenomena arise, which ultimately affect the dynamics of the radiation of the quasar.

In Fig. 4 3D cross-correlators for the radio emission of the quasars under consideration at frequencies of 2.7 and 8.1 GHz are presented. Cross-correlation dependencies for 0420m014 quasar signals show a clear oscillating structure, reflecting the dominance in the dynamics of a certain frequency. The sequential maximum values of $q_{ij}(\tau,\theta_{ij})$, represented in Fig. 4a when $\theta_{ij} > 0$, mean that the signal at a frequency of 2.7 GHz follows with a certain frequency the signal at a frequency of 8.1 GHz. At the same time, sequential maximum values of $q_{ij}(\tau,\theta_{ij})$, calculated when $\theta_{ij} < 0$, mean that the signal at a frequency of 8.1 GHz with the same periodicity precedes the signal at a frequency of 2.7 GHz.

In the dependence of $q_{ij}(\tau,\theta_{ij})$ for the radiation of 2251p158 quasar (Fig. 4b), a low-frequency diffuse large-scale structure can be observed. The absence of the generated set of natural frequencies in the dynamics of quasar 2251p158 signals

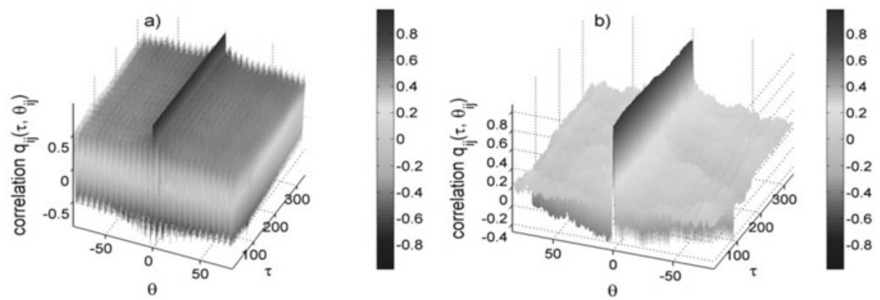

Fig. 4 3D dependencies of cross-correlators $q_{ij}(\tau,\theta_{ij})$ for radio emission of the quasars 0420m014 (**a**) and 2251p158 (**b**) at frequencies of 2.7 GHz and 8.1 GHz

leads to a lower level of synchronization than it's observed for quasar 0420m014. At the same time, the significant influence of dynamic intermittency effects leads to asymmetry of the 3D structure of the cross-correlator.

4 The Design of a Cyber-Physical System for Monitoring the Evolution of Complex Systems

Based on the proposed methods, we develop a software-analytical complex for monitoring the evolution of complex systems as an example of the integration of computing and physical resources optimized in an automated cyber-physical system.

The software-analytical complex includes the following modules:

1. Experimental data collection module: can be represented by a remote or built-in standard or specialized recording and control-measuring equipment (e.g. electroencephalography);
2. Database: includes input experimental data, intermediate data, quantitative and qualitative characteristics, and parameters obtained after calculations;
3. Calculation module: performs numerical calculations based on the author's theoretical approaches; carries out the construction of analytical diagrams and the calculation of the numerical values of qualitative indicators (Fig. 5). Designed for processing and parameterization of digitized recordings of signals in order to identify their dynamic and spectral features, correlation features, synchronization effects, as well as the degree of manifestation of statistical memory effects for various dynamic states of a complex system;
4. Analytical module: an autonomous diagnostic system that allows making the decision about the state of the system, including the abnormal one;
5. Knowledge base: contains decision-making algorithms based on the data obtained; contains information about the decisions taken and their subsequent adjustment;
6. Interface module (user information input/output module): visualizes the decision; allows making adjustments to the software-analytical complex; interacts with the user.

5 Conclusion

In this chapter, we consider the results of applying the author's methods: the Memory Functions Formalism and Flicker-Noise Spectroscopy to the study of synchronization effects between parts of a complex system. The first method is based on the use of power spectra of memory functions to identify sets of frequencies at which synchronization occurs. Using the presented method, the characteristic frequencies were established at which the neuromagnetic signals are synchronized for various areas of the cerebral cortex of healthy subjects. Disturbance or suppression of these

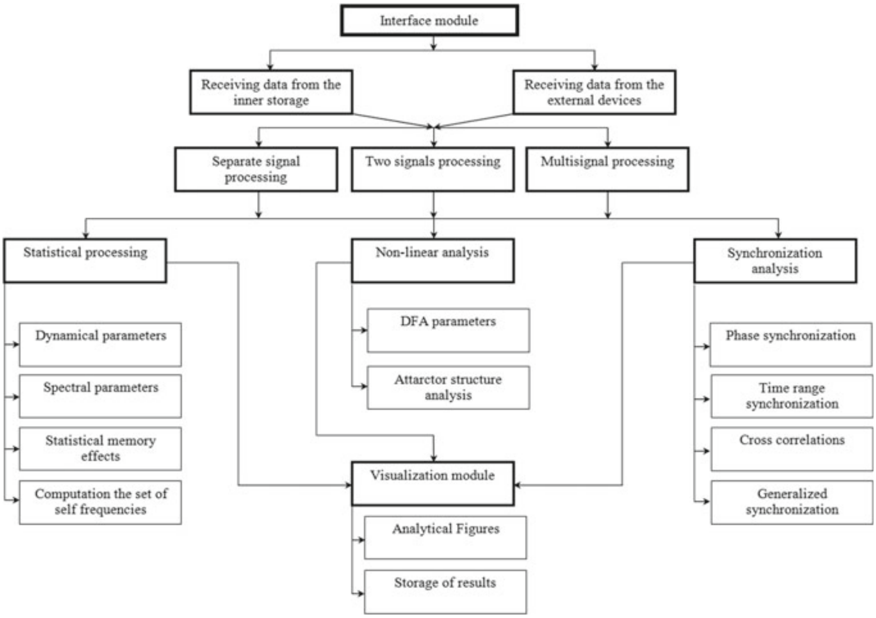

Fig. 5 The structure of the calculation module of the proposed cyber-physical system (software-analytical complex)

periodic processes served as the basis for the discovery of diagnostic criteria for pathological brain activity for photosensitive epilepsy. The second method is based on the use of two-parameter cross-correlators, the structure of which reflects collective phenomena manifested in the system. The effects of frequency phase synchronization discovered in the radioactivity signals of quasars at different frequencies contributed to the establishment of different mechanisms of their disk accretion.

The presented methods for analyzing multi-parameter data of complex systems: the Memory Functions Formalism and Flicker-Noise Spectroscopy, as separate areas of "Data Science" or "Complexity Science", show a possible way of developing an intelligent analysis of biomedical and observational space data in order to search for diagnostic and prognostic criteria for human neurological diseases, identification of astrophysical objects. The combined use of MFF and FNS with other machine learning methods for studying cross-correlations and synchronization effects (see, for example, [20–24]) will allow advancing in understanding the collective phenomena realized in complex composite objects of animate and inanimate nature, as well as economic and financial systems [25, 26]. The results obtained during the research can be applied in the economy when developing cyber-physical and robotic systems for actions in emergency situations and conditions; the creation of automated diagnostic and treatment centers [27]; personified medicine.

The use of theoretical approaches and numerical algorithms for the analysis of time signals will become the basis for a software-analytical complex that is adaptable, e.g. to monitoring physiological conditions, identifying and predicting human pathological states. The purpose of the software package will be to identify individual parameters of a person, accumulate a knowledge base, intellectual decision-making support when making a diagnosis (Internet of Things).

Acknowledgements This paper has been supported by the Kazan Federal University Strategic Academic Leadership Program. This work has been supported by the Russian Science Foundation (project no. 20-12-00105).

References

1. Rosenblum, M., Pikovsky, A., Kurths, J.: Phase synchronization of chaotic oscillators. Phys. Rev. Lett. **76**(11), 1804–1807 (1996)
2. Mormann, F., Lehnertz, K., David, P., Elger, C.E.: Mean phase coherence as a measure for phase synchronization and its application to the EEG of epilepsy patients. Physica D **144**(1), 358–369 (2000)
3. Rossberg, A.G., Bartholome, K., Voss, H.U., Timmer, J.: Phase synchronization from noisy univariate signals. Phys. Rev. Lett. **93**(1), 154103–1–4 (2004)
4. Lachaux, J.-P., Rodriguez, E., Martinerie, J., Varela, F.J.: Measuring phase synchrony in brain signals. Hum. Brain Mapp. **8**(1), 194–208 (1999)
5. Rulkov, N.F., Sushchik, M.M., Tsimring, L.S., Abarbanel, H.D.I.: Generalized synchronization of chaos in directionally coupled chaotic systems. Phys. Rev. E **51**(1), 980–994 (1995)
6. Plerou, V., Gopikrishnan, P., Rosenow, B., Amaral, L.A.N., Stanley, H.E.: Universal and nonuniversal properties of cross correlations in financial time series. Phys. Rev. Lett. **83**(7), 1471–1474 (1999)
7. Podobnik, B., Stanley H.E.: Detrended cross-correlation analysis: a new method for analyzing two nonstationary time series. Phys. Rev. Lett. **100**(8), 084102–1–4 (2008)
8. Zhou,W.-X.: Multifractaldetrended cross-correlation analysis for two nonstationary signals. Phys. Rev. E. **77**(6), 066211–1–4 (2008)
9. Ginzburg, I., Sompolinsky. H.: Theory of correlations in stochastic neural networks. Phys. Rev. E. **50**(4), 3171–3191 (1994)
10. Arianos, S., Carbone, A.: Cross-correlation of long-range correlated series. J. Stat. Mech.: Theory and Experiment 03037 (2009)
11. Panischev, O.Y., Demin, S.A., Bhattacharya, J.: Cross-correlation markers in stochastic dynamics of complex systems. Phys. A **389**(21), 4958–4969 (2010)
12. Panischev, O.Y., Demin, S.A., Kaplan, A.Y., Varaksina, N.Y.: Use of cross-correlation analysis of EEG signals for detecting risk level for development of Schizophrenia. Biomed. Eng. **47**(3), 153–156 (2013)
13. Timashev, S.F., Polyakov, Y.S., Yulmetyev, R.M., Demin, S.A., Panischev, O.Y., Shimojo, S., Bhattacharya, J.: Frequency and phase synchronization in neuromagnetic cortical responses to flickering-color stimuli. Laser Phys. **20**(3), 604–617 (2010)
14. Yulmetyev, R., Hanggi, P., Gafarov, F.: Stochastic dynamics of time correlation in complex systems with discrete time. Phys. Rev. E **62**, 6178–6194 (2000)
15. Yulmetyev, R., Demin, S., Emelyanova, N., Gafarov, F., Hänggi, P.: Stratification of the phase clouds and statistical effects of the non-Markovity in chaotic time series of human gait for healthy people and Parkinson patients. Phys. A **319**, 432–446 (2003)

16. Timashev, S.F.: Flicke-noise spectroscopy: information in chaotic signals. Fizmatlit, Moscow (2007)
17. Watanabe, K., Imada, T., Nihei, K., Shimojo, S.: Neuromagnetic responses to chromatic Flicker: implications for photosensitivity. Neurorep. **13**(16), 2161–2165 (2002)
18. Bhattacharya, J., Watanabe, K., Shimojo, S.: Nonlinear dynamics of evoked neuromagnetic responses signies potential defensive mechanisms against. Int. J. Bifur. Chaos. **14**(8), 2701–2719 (2004)
19. Tanizuka, N., Khan, M.R.: Dynamical structure of quasar radio wave intensity fluctuations from daily to yearly period. In: Sikula, J. (ed.) Noise and Fluctuations, ICNF-2003, pp. 813–816. Brno University of Technology, Brno (2003)
20. Pikovsky, A., Rosenblum, M., Kurths, J.: Synchronization. Cambridge University Press, Cambridge (2001)
21. Goelman, G., Dan, R., Růžička, F., Bezdicek, O., Růžička, E., Roth, J., Vymazal, J., Jech, R.: Frequency-phase analysis of resting-state functional MRI. Sci. Rep. **7**, 43743 (2017)
22. Blythe, D., Nikulin, V., Müller, K.: Robust Statistical Detection of Power-Law Cross-Correlation. Sci. Rep. **6**, 27089 (2016)
23. Ma, Z., Zhou, W., Zhang, Y., Geng, S.: Epileptogenic zone localization and seizure control in coupled neural mass models. Biol. Cybern. **109**, 671–683 (2015)
24. Maharaj, E.A., Teles, P., Brito, P.: Clustering of interval time series. Stat. Comput. **29**, 1011–1034 (2019)
25. Cipra, T.: Time series in economics and finance. Springer International Publishing, Basel (2020)
26. Proletarsky, A., Berezkin, D., Popov, A., Terekhov, V., Skvortsova, M.: Decision support system to prevent crisis situations in the socio-political sphere. In: A.G. Kravets et al. (eds.), Cyber-Physical Systems: Industry 4.0 Challenges, Studies in Systems, Decision and Control, SSDC 260, pp. 301–314 (2020)
27. Buldakova, T., Krivosheeva, D.: Data Protection During Remote Monitoring of Person's State. In: O. Dolinina et al. (eds.), Recent Research in Control Engineering and Decision Makin, Studies in Systems, Decision and Control, SSDC 199, pp. 3–14 (2019)

The Methodology of Hybrid Modelling for Gas Turbine Subsystems Prescriptive Analytics

Sergei Nikolaev, Sergei Belov, Tatiana Greenkina, Tikhon Uglov, and Vadim Leshchev

Abstract This chapter proposes a methodology for building hybrid models of gas turbine power plants for solving the task of prescriptive and predictive plant health analytics. The hybrid models are built based on the physics model of the power plant subsystem and machine learning methods. The combination of physics-based models and machine learning models allows predicting the occurrence of malfunctions and predicting internal parameters of subsystems influencing the gas turbine plant's technical health. The proposed methodology was implemented as a special software system, and it was tested on the field data from mobile gas turbine plants.

Keywords Prescriptive analytics · Physics-based modelling · Gas turbine condition monitoring

1 Introduction

A frequent problem appearing during predictive analytics of machinery such as gas turbines is the lack of field data. Machine health prognostics is complicated due to the small amount of available data that characterize malfunctions and malfunctions' development. Health monitoring could be realized at the initial stage of machine operation, but it only provides the monitoring of faults' development when the machine's operating regime becomes abnormal [1]. Usually, operators do not have a lot of labeled data to make a prescriptive model, which would determine the exact reason for the malfunction and provide operators with information on how they should act [2].

Another approach to monitoring the system during its lifecycle is model-based systems engineering [3]. Software tools like Simulink, Simcenter Amesim, Dymola, or OpenModelica allow engineers to develop, change, and manage the system from design to operation. Physics-based modeling allows simulating the system's behavior by solving equations of mechanics, thermal, and fluid dynamics. Physics-based

S. Nikolaev (✉) · S. Belov · T. Greenkina · T. Uglov · V. Leshchev
Skolkovo Institute of Science and Technology, Moscow, Russia
e-mail: s.nikolaev@skoltech.ru

A. G. Kravets et al. (eds.), *Cyber-Physical Systems*, Studies in Systems, Decision and Control 350, https://doi.org/10.1007/978-3-030-67892-0_4

models play an essential role in some cases where the system's structural complexity or operating conditions (for example, high temperature) make it impossible to place sensors and acquire the data.

For most gas turbines on the market, the primary maintenance strategy is designed by the manufacturer. It suggests some scheduled actions which are needed to be performed. These actions are based on equipment tests, historical operation data, and expert knowledge. These scheduled actions are not connected with the operation condition of the gas turbine. Thus, plant operators desire to perform maintenance actions when they are needed.

That is why predictive and prescriptive maintenance is so desirable. Predictive models connected with real operation equipment determine the possible malfunctions in the future and recommend the actions. A prediction of the maintenance model should be accurate. False-negative results can lead to equipment damage, whereas false-positive results cause unnecessary maintenance and high expenditures.

The advantages of pure data-driven and physics-based approaches could be combined using a hybrid modeling technique (Fig. 1). The hybrid approach should include a two-phase methodology for prognostics, where the first phase develops a physics-based model for both healthy and malfunctioning conditions, and the second phase computes the residuals when comparing the measurements with the simulation results.

In this chapter, we propose a methodology for developing a prescriptive model, which is based both on machine learning models and physics-based models. The methodology is implemented in special in-house software, which is tested on real field data.

Fig. 1 Hybrid modelling approach

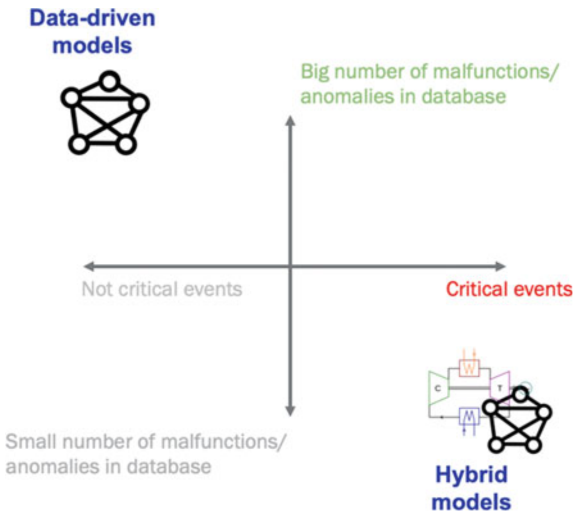

2 Prediction of Malfunctions in the Gas Turbine Power Plant Subsystems Using Data-Driven Approach

The term “malfunction” means an event indicating the gas power plant’s technical condition is inoperable, and it requires to repair and/or restoration works to make the system operational. For choosing malfunctions for machine learning modeling, it is important to take into account two criteria. The first criterion is the rate of occurrence. The event must occur often enough so that the training set has enough instances of this or other events occurring. The second criterion is the severity (significance) of the event.

The task of malfunction detection is to predict the time of occurrence of the event to prevent an emergency shutdown. Solving this task means predicting the time of event occurrence for each predicted shutdown. As events follow one after another, the closest event is predicted for each moment of time. Then, based on the event occurrence rate, the optimal prediction time is determined.

The prediction horizon is the maximum time where the machine learning model can predict the event’s occurrence. The model does not predict beyond the prediction horizon. For choosing optimal prediction time, the maximum time to the event is taken into account, and it is checked that no more than one event takes place. This concept is implemented by transforming the event occurrence data by limiting the prediction time (for each moment of time to the nearest event, if the time is greater than the prediction horizon, the time values are set to the prediction time). The obtained values are then normalized (Fig. 2) from one (the event cannot be detected) to zero (the event is detected).

As the occurrence of the emergency shutdown occurrence is often characterized by complex change of all parameters of the system, data from different subsystems having the least correlation are used for analyzing events. The data is formed as a set

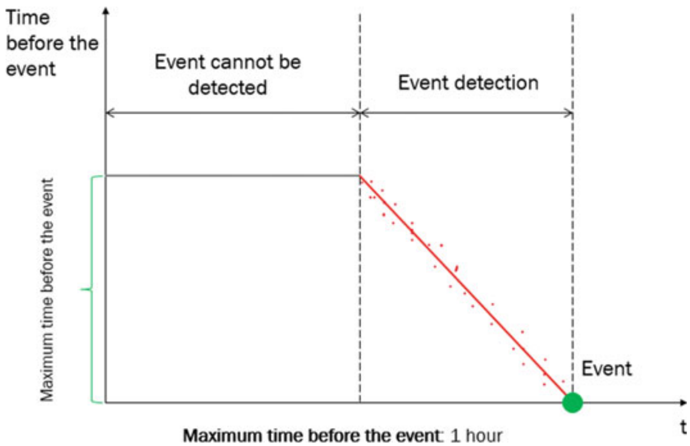

Fig. 2 Transformation of data for prediction

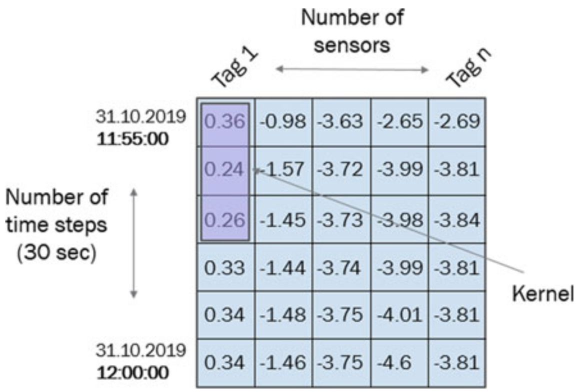

Fig. 3 Input data convolution

of examples having a selection of all selected tags for a certain time interval (number of time steps). A Convolutional Neural Network [4] is used to solve this type of problem; the idea is to form a set of features for different data channels. Thus, the power plant technical condition is represented as a generalized vector by sequentially processing sensor time series by convolution layers (Fig. 3).

The prediction is conducted using a fully connected layer with the Exponential Linear Unit (ELU) activation function. The dimension of the output layer is equal to the number of processed events. Thus, the machine learning model is capable of predicting time for each of the selected events.

For the malfunction identification problem, predicting the malfunction is more important than predicting the absence of it. Thus, for calculating the error function, the difference between the response and the reference value is multiplied by the penalty coefficient 0.9 if the reference value is less than 1 (time to malfunction is less than one hour) and 0.1 if the reference value is 1 (time to malfunction is more than one hour).

Aside from applying the penalty function mentioned above, the balancing of the training set is conducted. The training set is comprised of the instances of the gas turbine power plant state and the set of times to events. Compared to normal operation, malfunctions are rare, so the number of malfunction instances in the training set is very small. Such an imbalance of the training set can cause model overfitting on data without malfunctions, causing reduced prediction accuracy of the model on data with malfunctions. The number of instances of current power plant operation is reduced to the number of instances of malfunctions, thus balancing the training set.

The proposed approach was tested for the case of the Mobile Gas Turbine Unit. The training history is shown in Fig. 4.

Figure 5 shows the model prediction for the test set.

Aside from the accurate prediction of time to malfunction, the obtained model should also accurately detect the malfunction itself.

Similar to the classification models, the malfunction detection model must determine where an event will occur in the system at the nearest time or not at any moment of time. To that end, models must be evaluated by the precision and recall metrics.

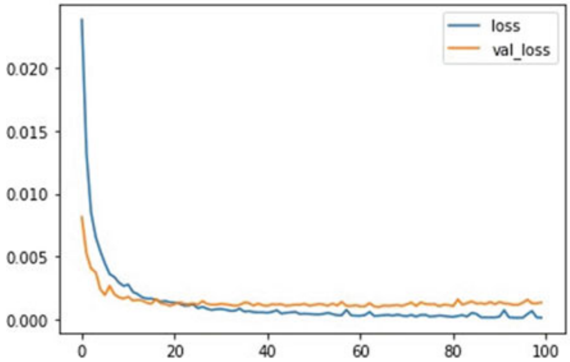

Fig. 4 Training error history for the training and the validation sets

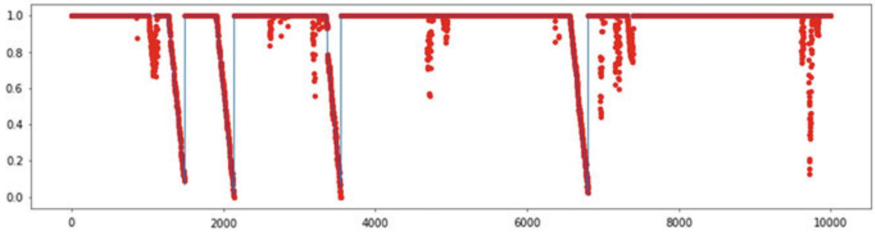

Fig. 5 Training error history for the training and the validation sets

As the model does not respond as a classifier (malfunction is present or not), the following algorithm was developed to transform the model responses:

The model responses and the reference responses whose values are equal to 1 are classified as "no malfunction";

The intervals of reference data with the value less than 1 are classified as "malfunction are present";

The model responses can be classified as "malfunction is present" if the intervals where the model responses are less than zero and form a straight line with the slope equal to that of the reference like on the interval with data classified as "malfunction is present."

Based on the assumption that the model responses replicate the straight line of reference values, a model straight line is fitted using the least-squares method, and its slope is evaluated.

Based on the developed algorithm, the model can be classified using the precision and recall metrics. Table 1 shows the evaluation results.

Table 1 Model quality metrics

Metric	Training dataset	Test dataset
Precision	0.86	0.66
Recall	0.88	0.70
F1-score	0.82	0.68

3 Physic-Based Model of Subsystems for the Case of Hydraulic Subsystem

To build hybrid predictive models, physics-based models of each subsystem of a gas turbine power plant should be developed. The main purpose of the physics-based model is to identify dependencies between observed variables (measured by sensors) and internal parameters of the subsystem, which could not be measured. The principle of such a physics-based model is presented on the example of a hydraulic subsystem.

3.1 Description of the Hydraulic Subsystem

The hydraulic system's designation is to ensure the operation of the Inlet Guide Vanes (IGV) and Variable Stator Vanes (VSV). The oil for the hydraulic pump is taken from the gas generator lube system after inlet filters. The pump is installed on the main gearbox and is driven from the pinions/vertical shaft connected to the High-Pressure Compressor (HPC). The oil passes through the filter with an internal bypass. The pressure regulator maintains the required pressure by bypassing excess oil in the gas generator lube system. The filter pressure differential is determined using pressure sensors at the filter inlet and outlet. If the differential pressure is high, an alarm signal is issued, and a controlled shutdown is conducted upon reaching the upper limit of the pressure differential.

3.2 Assumptions of the Model

The following empirical assumptions are made during model development. The elements whose state is constant for the steady-state operation were either extremely simplified or neglected. For valves, the model considered their section as fully opened during steady-state operation. The study considered the system's variant where verification can be done based on the current values of displacements of rods of hydraulic cylinders of the VSV and IGV.

3.3 Model Architecture

Figure 6 shows the architecture of the physics-based model of the hydraulic system

The gear pump supplies hydraulic pressure for the VSV/IGV control system through the filter. The pressure coming to the system from the oil supply system is recorded by pressure gauges, by which the modeled system pressure is compared to real sensor readings. The filter is modeled as a block similar to the real filter having through holes with corresponding diameters. After the filter, the oil passes to the servo valve; if a threshold (750 psi) is breached, a pressure regulator opens and sends the excess oil into the oil tank. The servo valve control signal is formed based on the difference between the hydraulic cylinder rod's target and current positions. Both hydraulic cylinders VSV and IGV are identical and have the same working mechanism: rod pro-tracts and retracts depending on what inlet the pressure is supplied to. The leaks from cylinders can be set as a parameter in the corresponding component. In the model, the oil tank is simplified as a component with a certain pressure and temperature where fluids can be drained.

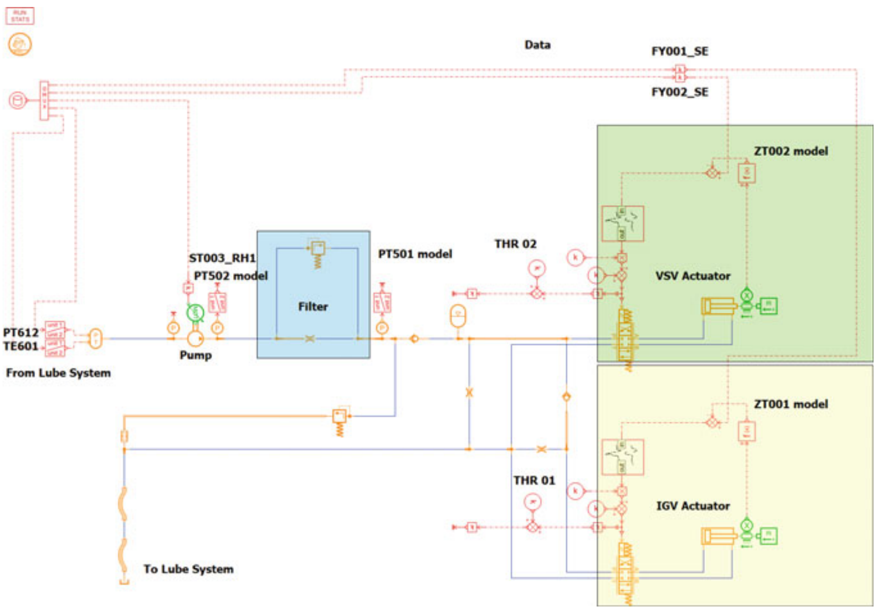

Fig. 6 Physics-based model of the hydraulic subsystem

3.4 Model Verification

The verification of the subsystem was done as follows. For each variable at the subsystem output mean absolute error is calculated on 10 random time intervals of the plant operation when the high-performance compressor rotor speed is greater than 10,000 rpm. The error is determined as follows:

$$MAPE_{TAG} = \frac{1}{n}\sum\left|\frac{TAG_{real} - TAG_{sim}}{TAG_{real}}\right| \quad (1)$$

where TAG_{real} is real data from the plant, and TAG_{sim} is the value of an output variable of the model. The model is considered verified if the error for each output variable is less than 10%. In this case, the errors were less than 1%.

3.5 Modeling of Malfunctions

Using the developed model of the hydraulic system, it is possible to conduct modeling of the system with occurring faults. For example, let us consider the fault related to the system filter clogging. In this model, the filter is modeled as a component with the following parameters: the number of bores and the diameter of each bore. The filter works correctly if the number of holes is 10,000, and the hole diameter is 0.2. If the filter is clogged, the number of holes decreases, which can be set as the component parameter value. The filter clogging results can be seen from the differential pressure, as shown in Fig. 7. The greater the clogging, the less the number of holes is, and the greater the pressure difference is.

4 Health Prediction of Gas Turbine Power Plant Using Hybrid Modeling

For predicting the gas power plant's health, an approach based on hybrid modeling is used. The model's essence is in representing the technical health of a subsystem of the plant as the difference between the "ideal" functional physics-based model of a subsystem and its real indicators.

The "ideal model" is understood as the model determining the healthy subsystem behavior under current operating conditions. It is assumed that the system's critical events are pre-defined by the degradation of parameters of its subsystems, allowing early warning about possible disorders at the early stages of degradation. It makes sense to track not the parameters itself but rather the difference between its measured values and the "ideal" model indicators. This approach determines the deviation of the current state of the subsystem from the normal state and predicts a deviation

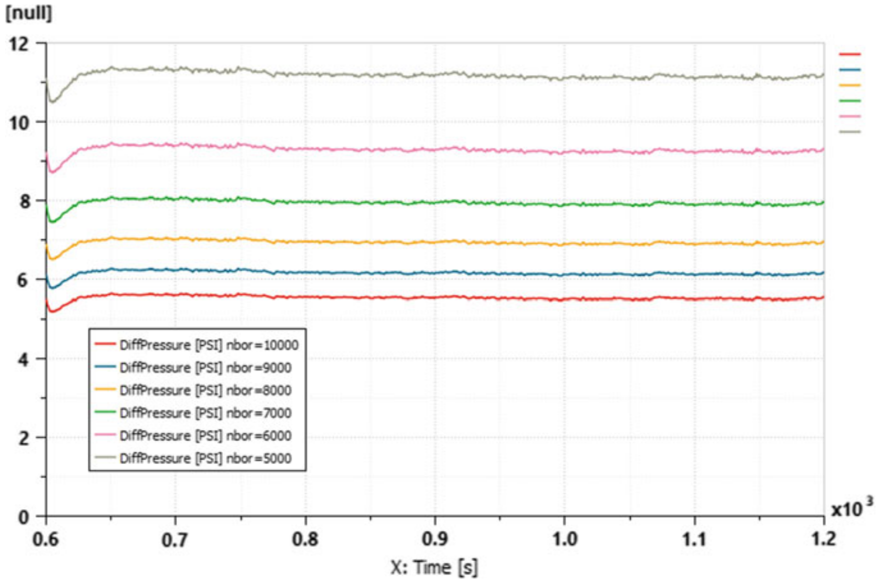

Fig. 7 Time histories of differential pressure with a reduced number of bores

Fig. 8 Trend prediction

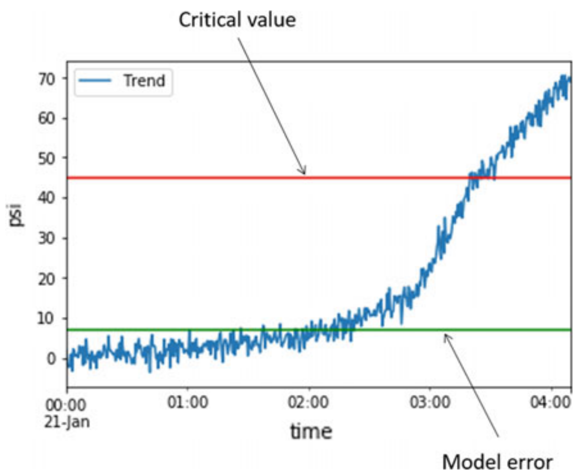

trend. As soon as the trend exceeds the model error, the difference starts to grow until it reaches its critical value (malfunction), as shown in Fig. 8.

The physics model error is calculated as a mean absolute percentage error (MAPE).

$$MAPE = \frac{1}{n}\sum_{t=1}^{n}\left|\frac{y_{true} - y_{model}}{y_{true}}\right| \tag{2}$$

So, the health index (HI) is calculated as the difference between the modeled parameters and the real sensor data biased by the value of mathematical model error and scaled from zero to one.

$$HI = \begin{cases} 1, trend \leq error \\ 1 - \frac{trend - error}{y_{crit} - error}, trend > error \end{cases} \quad (3)$$

where the parameters *trend* and *error* are calculated as follows:

$$trend = y_{true} - y_{model} \quad (4)$$

$$error = MAPE * y_{true} \quad (5)$$

As the deviation trend is time series, prediction can be made using standard machine learning methods. Long Short-Term Memory [5, 6] recurrent neural network is an example of these methods. This network can predict the system state by analyzing its current status.

The prediction task is to determine the future values of the difference between the modeled values of the system's parameters and real sensor data [6]. For the current time interval with a set time window, the data come to the prediction model's input, and the model predicts future values, Fig. 9.

For the hydraulic system, the data characterizing a progressing malfunction (oil filter clogging) were modeled. The data served as the training set for the LSTM model. The model predicted future values with a 20-minute prediction horizon for 30 min. The model was comprised of a recurrent layer (LSTM) with 100 neurons, followed by a fully connected layer (MLP) with the ELU activation function. The model error function was MSE, and the training algorithm was ADAM [7].

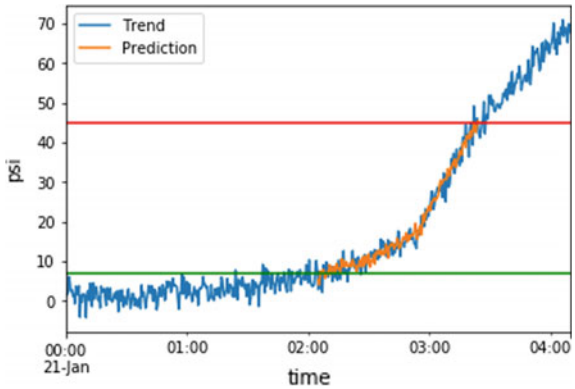

Fig. 9 Trend of deviation of the model parameters from the "ideal" model

5 Software for Technical Health Monitoring and Prediction

The software for Technical Health Monitoring and Prediction (THMP) was developed for automating the tasks of monitoring and predicting the technical health of gas turbine power generating plants based on mathematical models of mobile gas turbine plants. The software implements a combination of a data-driven approach for predicting often events and a hybrid modeling approach to analyze and predict health index.

The software conducts the analysis of the technical health of gas turbine subsystems:

- High- and low-pressure compressors;
- High- and low-pressure turbines;
- Combustion chamber with flame tubes and fuel spray nozzles;
- Fuel system;
- Oil system;
- Air intake system;
- Thrust balance system;
- Hydraulic VSV control system;
- Hydraulic launch system;
- Power turbine.

The software has a monolithic server architecture with three logical layers.

- Business logic layer;
- Resource layer;
- Communications layer.

Software architecture is shown in Fig. 10.

The business logic layer is comprised of:

- The complex of functional physics-based models of the gas turbine power plant subsystems having a detailed mathematical formulation of the interconnections and physical processes taking place in the subsystems of the physical object in the form of algebraic and differential equations.
- Modules implementing the algorithms for analysis and prediction of the gas turbine power plants' technical health based on machine learning methods.

The business logic layer inputs data sets of physical values from real sensors in the generator subsystems and runs mathematical models to obtain readings from the virtual sensors used to calculate deviations in measurements to detect malfunctions in the generator subsystems.

The resource layer is implemented using the NoSQL database having a system cache for storing modeling parameters, modeling results, and previous sensor readings to provide the fastest access to them. Also, file storage is located at this level.

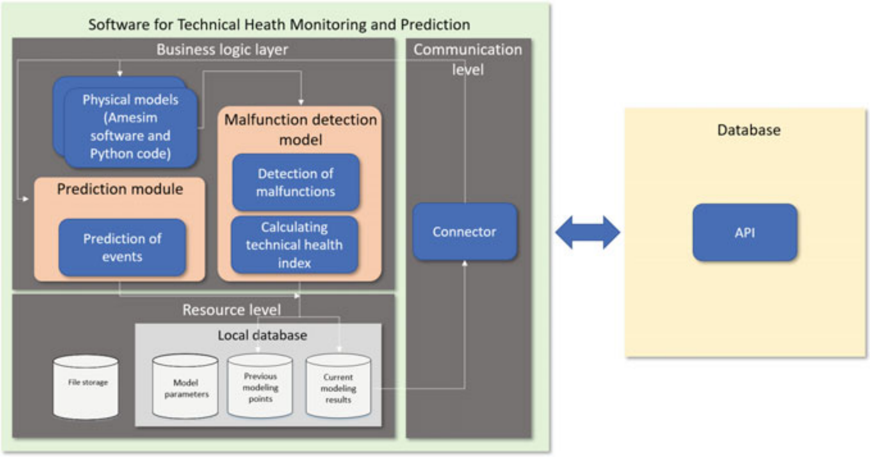

Fig. 10 Software structure

The communication level is developed as methods implementing API queries to the database. The communication to the external database service is implemented via an HTTP protocol using REST API.

Given architecture allows us to analyze and predict the technical conditions of the gas turbines in real-time. The developed software is used for predictive analytics of mobile gas turbines and is under test exploitation at an energy production company.

6 Conclusion

The methodology, based on a combination of data-driven and physics-based modelling is presented in this chapter. This methodology is implemented for gas turbine power plant predictive analytics and implemented in special in-house software.

The presented hybrid modeling approach enables malfunction detection with a small amount or even no labeled malfunction data. The following advantages of the combined approach present the research interest in this field:

- Very little operation data is required to tune the model for a real turbine;
- Compared to the pure data-driven approach, the combined model allows operators not only to determine abnormal behavior of gas turbines but also reveal the causes thereof;
- Many malfunctions can be simulated as soon as the model is validated. In this part of the work, tight cooperation with field engineers and operators is required.

Acknowledgements The authors would like to express their gratitude to colleagues Vladimir Kalnikov and Oleg Babarin and Maxim Shcherbakov from the company JSC "Mobile Gas Turbine Electrical Systems" for their support and engineering insights.

Grant Information

This work was supported by the federal program "Research and development in priority areas for the development of the scientific and technological complex of Russia for 2014–2020" via grant RFMEFI60619X0008.

References

1. Jacobs, J., Brotherton, T., Jahns, G., Wroblewski, D.: Prognosis of faults in gas turbine engines. IEEE Aerospace (2000)
2. Allen, Cody W., Holcomb, Chad M., de Oliveira, Mauricio: Gas turbine machinery diagnostics: a brief review and a sample application. Proceedings of the ASME Turbo Expo (2017)
3. Madni, A.M.; Madni, C.C.; Lucero, S.D.: Leveraging dgital twin technology in model-based systems engineering. Systems (2019)
4. LeCun, Y., Bengio, Y., et al.: Convolutional networks for images, speech, and time series. Handb. Brain Theory Neural Netw. **3361**, 1995 (1995)
5. Gers, F.A., Schmidhuber, J., Cummins, F.: Learning to forget: continual prediction with LSTM. In: 1999 Ninth International Conference on Artificial Neural Networks ICANN 99. (Conf. Publ. No. 470). pp. 850–855 vol. 2 (1999)
6. Siami-Namini, S., Tavakoli, N., Siami Namin, A.: A Comparison of ARIMA and LSTM in Forecasting Time Series. In: 2018 17th IEEE International Conference on Machine Learning and Applications (ICMLA). pp. 1394–1401 (2018)
7. Kingma, D.P., Ba, J.: Adam: A method for stochastic optimization. arXiv Prepr. arXiv1412.6980 (2014)

Automation of Assembly Batches Installation in Hot Rolling Mills

Alexander Galkin and Vladimir Istomin

Abstract The study presents the process of forming assembly batches installation in a hot rolling mill. There has been developed an algorithm for the optimal formation of assembly batches at a hot rolling mill based on the genetic algorithm considering technological restrictions imposed on the production process. The optimization of the set of assembly batches consists of the construction of a set with maximum productivity, which is achieved by reducing the time for the reconstruction of the equipment when switching to different width and thickness of rolling stock. A program for automatic formation of assembly batches at a hot-rolled steel mill has been implemented. It is now possible to save each batch included in the generated set to a separate file, as well as write general information about the entire set to a file. The algorithm was tested when forming assembly batches from a set of slabs available at the warehouse. Calculations on the formation of optimal assembly batches have been carried out. The presented results of the study show the increase of the formed assembly batches' productivity and their compliance with all technological restrictions.

Keywords Production planning · Hot rolled products · Formation of installation batches · Rational picking · Optimization · Genetic algorithms

1 Introduction

Hot rolled steel [1–3] is in great demand in many industries. The sorting of hot rolled steel is not corrosive, is very advantageous in terms of price and quality, is produced in plastics with high strength, hardly requires treatment, is resistant to high temperatures, and mechanical damage [4].

Metal rolling on a continuous broadband mill is carried out in mounting batches [5], for the required quality of which a number of technological restrictions on

A. Galkin (✉) · V. Istomin
Lipetsk State Technical University, 30 Moscovskaya, Lipetsk 398055, Russia
e-mail: avgalkin82@mail.ru

V. Istomin
e-mail: istomin96@mail.ru

A. G. Kravets et al. (eds.), *Cyber-Physical Systems*, Studies in Systems, Decision and Control 350, https://doi.org/10.1007/978-3-030-67892-0_5

temperatures and mechanical damage are imposed [6–9]. In addition to quality characteristics, productivity is the most important indicator of production, including hot rolled steel [10]. In this case, production optimization consists of planning installation batches that minimizes the total time of their rolling, i.e. increases productivity, while observing all the specified restrictions that affect the quality of rolled products. Thus, the development of optimization methods, as well as the introduction of new methods for forming assembly batches at hot rolled mills, is one of the current research topics in the direction of metal production.

2 Initial Mathematical Formulation and Research Methodology

In the process of studying the topic under consideration, an algorithm for forming assembly batches based on the specified restrictions was developed. The information about the availability and characteristics of slabs in the warehouse is used as input data. The programming block of the Mathcad [11] package is used to implement the algorithm. Optimization is implemented through the use of genetic algorithms [12–19]. Let us perform the task formalization.

There is a set of vectors $X = \{X_1, \ldots, X_n\}$ consisting of slabs X_i. It is necessary to create such a sequence of execution of orders $Y_u(X)$ for rolling at the mill to achieve the maximum rolling performance V of the formed assembly batches. Productivity refers to the ratio of the length of the rolled tape to the duration of the process.

Enter the following notation to describe slabs and assembly batches:

$$X_i = \begin{bmatrix} x_1 \\ \vdots \\ x_{13} \end{bmatrix},\ Y_u = \begin{bmatrix} X_r \\ \vdots \\ X_m \end{bmatrix},$$

where $i = 1 \ldots n$; n—the number of slabs, u—the number of the installation batch, r and m—respectively, the first and last elements of the installation batch; x_l—a parameter that contains information about the slab, $l = 1 \ldots 13$.

The necessary parameters are selected from the array of data about available slabs received from the warehouse, and rows with missing data, as well as those that are obviously incorrect, are removed. The final selection includes the following columns:

x_1—slab rolling time (s);
x_2—steel grade;
x_3—surface finishing group;
x_4—route;
x_5—slab thickness (mm);
x_6—slab width (mm);
x_7—length of the slab (mm);
x_8—slab weight (t);

x_9—target roll thickness (mm);
x_{10}—target roll width (mm);
x_{11}—strip length (m);
x_{12}—destination shop;
x_{13}—note.
Objective function:

$$V(Y_1, \ldots, Y_z) = \frac{1}{z}\sum_{u=1}^{z} v(Y_u) = \frac{1}{z}\sum_{u=1}^{z} \frac{d(Y_u)}{t(Y_u)} \to \max, \quad (1)$$

where z—number of batches, v—performance u-nd installation batch, d—the total length of the u-nd installation batch, t—the total time for rolling all slabs of the u-th installation batch.

The time for rolling is calculated using the formula:

$$t = x_1 + tp,$$

$$tp = \begin{cases} 120, \ \text{if } (x_{10,w} \neq x_{10,w+1}), \\ 60, \ \text{if } (x_{9,w} \neq x_{9,w+1}) \wedge (x_{10,w} = x_{10,w+1}), \\ 0, \end{cases}$$

where tp—time to reconfigure the mill, w—the serial number of the slab in the u-th installation batch.

Taking into account the restrictions described in [6], the following conditions must be met for installation batches $G(Y(X))$:

$$G(Y(X)) = \begin{cases} \sum_{w=1}^{q} x_{8,w} \leq 4000, \\ x_{10,w+1} - x_{10,w} \leq 250, \\ x_{9,w+1} - x_{9,w} \leq 1.5, \\ \sum_{w=1}^{q} x_{11,w} \leq 40000, \ (x_{10,w} = x_{10,w+1}) \forall w = 1, \ldots, q, \end{cases}$$

where q—the number of slabs in the u-th installation batch.

The entire array of reading data is divided into the following subsamples, which have conditions set for them:

1. *Rabv*—the included metal after handling the work rolls.
2. *km7_60*—the length of the installation from 7 to 60 km.
3. *km97*—the installation length is up to 97 km.
4. *km120*—the installation length is up to 120 km.
5. *km121_*—the length of the installation after 120 km.

Production batches are compiled from the sub-samples received in accordance with technological restrictions for these groups. Also, each installation batch takes into account a number of restrictions imposed on the entire installation.

The scheme of the developed algorithm is shown in Fig. 1.

The optimization algorithm is implemented as follows. An Excel file with the prepared selection is read. The received data is sorted by bandwidth—from wide to narrow. It also reads steel grades that belong to certain groups: $uglPDS$—carbon steel rolling for PDS; $xolkS$—cold rolled steel grades; $tovarS$—commercial steel grades; $electrS$—electro-technical steel grades [20]. These groups of brands are required when forming installations to meet the imposed technological restrictions.

At the first step of the genetic algorithm, initial populations are compiled in order to complete slabs from the warehouse into assembly batches. The formation of batches stops if there are no slabs in any of the subsamples. So they are made up sequentially one after the other and have the following form:

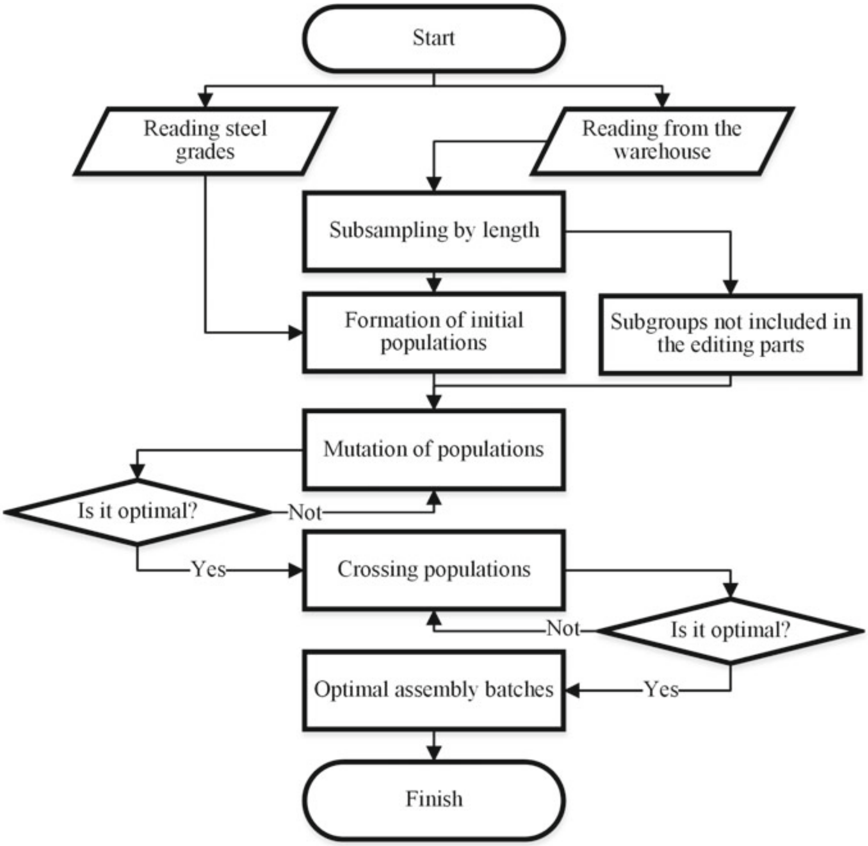

Fig. 1 The block diagram of the program

$$mont_u = \begin{pmatrix} J_1 & \cdots & J_g \\ D_1 & \cdots & D_g \\ M_1 & \cdots & M_g \\ T_1 & \cdots & T_g \\ k_1 & \cdots & k_g \\ y_1 & \cdots & y_g \\ ogshDL_1 & \cdots & ogshDL_g \end{pmatrix}, \quad J = \begin{pmatrix} j_1 \\ \vdots \\ j_k \end{pmatrix},$$

where $mont_u$—generated installation number of subsamples, $g = 1, \ldots, 5$—the number of subsamples; J_g – vector column with sequence numbers selected in the installation of slabs from the warehouse, k—the number of slabs in the sub-sample g installation u; D_g—the total length of the installation in the sub-sample g subject to the preceding sub-groups (mm); M_g—total weight of installation in a subsample of g subject to the pre-pacing subgroups (t); T_g—the total rolling time of all mounting slabs in the sub-sample g taking into account the preceding subgroups (s); y_g—rows of selected slabs in the g sub-sample; $ogshDL_g$—the total length of consecutive slabs of the same width.

Assembly batches that are made in accordance with technological restrictions are combined into a set of installations.

The slabs that were not included in the assembly batches are distributed in subsamples of the same structure that were used for forming the initial populations of the genetic algorithm. They will be called free subsamples.

The scheme of formation of initial populations is shown in Fig. 2.

A fragment of the obtained initial populations (montages) is shown in Fig. 3.

The next step is to mutate the resulting set of montages.

The mutation operator changes an arbitrary number of elements in an individual to other arbitrary ones. In fact, it is a kind of dissipative element, on the one hand pulling from local extremes, on the other—bringing new information to the population.

The population mutation scheme is shown in Fig. 4.

Under the conditions of the problem being solved, the mutation operator will change an arbitrary number of subsamples from montages with random free subsamples. Mutated mounts are combined into a set and so several individuals are obtained. Among the available individuals of descendants, the most adapted one is selected, i.e. the set of mounts with the highest productivity (1), which will become the parent for the next generation of mutants. The cycle repeats until the productivity of new generations is less than or equal to that of their ancestor. At the same time, the installations inside the set are checked for compliance with the entered restrictions.

The best set of montages obtained by mutations passes through crossing among the montages included in this set. Free sub-selections are discarded.

This genetic algorithm uses uniform cross-breeding, otherwise called monolithic or single-stage, performed in accordance with a pre-selected standard that specifies which genes should be inherited from the first parent (the remaining genes are taken from the second parent).

The population crossing diagram is in Fig. 5.

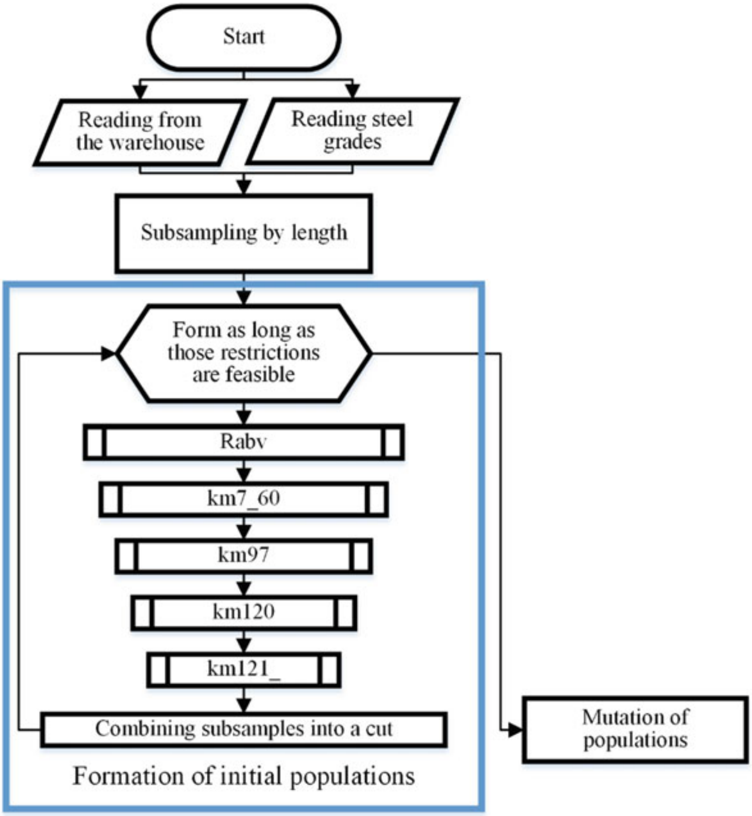

Fig. 2 Scheme of initial populations formation

$$mont_{10} = \begin{pmatrix} \{9,1\} & \{50,1\} & \{33,1\} & \{35,1\} & \{28,1\} \\ 6.403 \times 10^3 & 5.996 \times 10^4 & 9.658 \times 10^4 & 1.195 \times 10^5 & 1.36 \times 10^5 \\ 276.73 & 1.61 \times 10^3 & 2.49 \times 10^3 & 3.316 \times 10^3 & 3.951 \times 10^3 \\ 1.01 \times 10^3 & 5.561 \times 10^3 & 8.743 \times 10^3 & 1.091 \times 10^4 & 1.305 \times 10^4 \\ 9 & 50 & 33 & 35 & 28 \\ \{9,1\} & \{50,1\} & \{33,1\} & \{35,1\} & \{28,1\} \\ 6.403 \times 10^3 & 1.276 \times 10^4 & 8.953 \times 10^3 & 3.185 \times 10^4 & 8.209 \times 10^3 \end{pmatrix}$$

Fig. 3 Fragment of the obtained initial populations

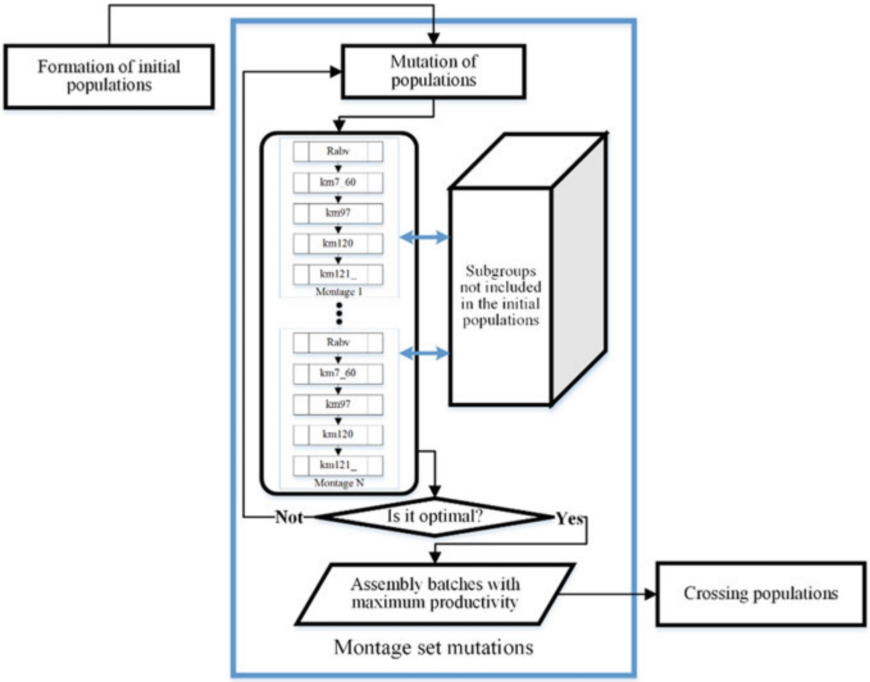

Fig. 4 Diagram of mutations in populations

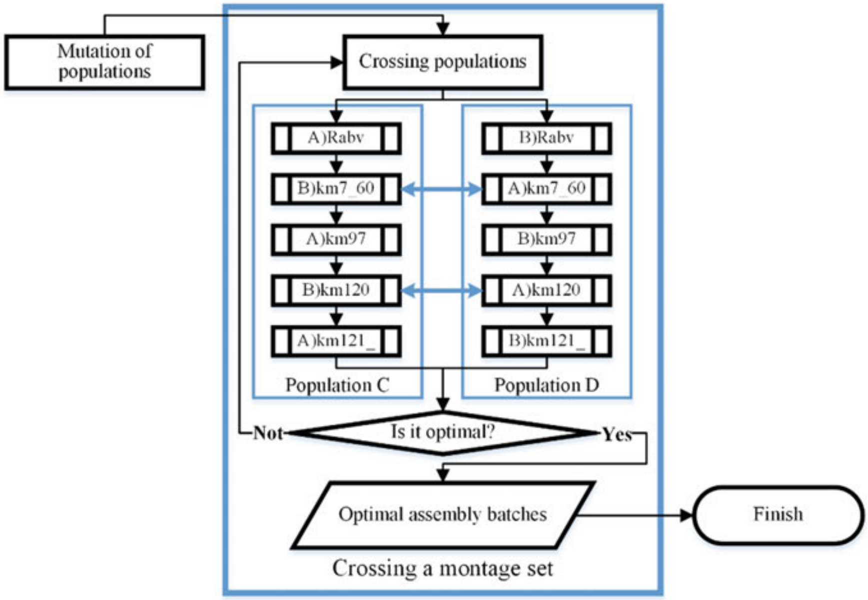

Fig. 5 Scheme of interbreeding populations

Randomly selected individuals from a set of mutated montages are selected in pairs to perform the crossing operator:

$$mont_a = \left([Rabv]_a \; [km7\_60]_a \; [km97]_a \; [km120]_a \; [km121\_]_a \right)$$
$$mont_b = \left([Rabv]_b \; [km7\_60]_b \; [km97]_b \; [km120]_b \; [km121\_]_b \right)$$

in which the following replacement occurs:

$$mont_c = \left([Rabv]_a \; [km7\_60]_b \; [km97]_a \; [km120]_b \; [km121\_]_a \right)$$
$$mont_d = \left([Rabv]_b \; [km7\_60]_a \; [km97]_b \; [km120]_a \; [km121\_]_b \right)$$

the resulting montages are a new generation of individuals. They have combined again into a set. In this way, several randomly crossed sets are formed. The crossing stop criterion is the same as the mutation stop criterion (1). At the end of the crossing operator's work, the optimal set of mounting batches will be found, which is the result of the genetic algorithm.

3 Interpretation and Discussion of Research Results

A study on the operation of the implemented algorithm has been conducted. The information provided by the metallurgical plant about slabs from the warehouse is used. The information necessary for the algorithm is selected from the received data.

With the help of the program for forming assembly batches of hot rolled steel products, 276,000 rows of data from the warehouse were processed, resulting in 14 unique sets of assembly batches. Each set is formed on non-overlapping input data ranges of 20 thousand samples in the first 13 sets and 16 thousand in the last one. General information on the sets is provided in Table 1.

In Table 1 №—dial number, Km—number of installations in the set (PCs), Kp—number of rolled products in a set (PCs), Ln—total length of the rental set (km), Mn—total weight of rolled products in a set (t), Tp—required rolling time (h), Vn—the performance of the kit after the application of genetic algorithms (km/h), ΔVn—increase the performance of the hire after the application of genetic algorithms (km/h).

The average productivity increase was 0.56 (km/h), which indicates the relevance of the method used for forming and optimizing the composition of assembly batches at hot rolled mills. The mutation operator had a greater effect on performance changes.

A comparison of the performance of mounting sets before and after applying the genetic algorithm is shown in Fig. 6.

In total, the algorithm obtained 507 installations with an average productivity of 30.34 (km/h), which corresponds to an increase in rolling efficiency by 1.9%.

Table 1 Information about installation kits

№	*Km*	*Kp*	*Ln*	*Mn*	*Tp*	*Vn*	*ΔVн*
1	40	5952	5626.81	143772.51	183.50	30.66	0.68
2	42	6360	5830.02	155523.89	198.06	29.44	0.34
3	41	6118	5726.41	147124.89	186.37	30.73	0.31
4	35	5367	5014.91	129461.26	166.36	30.14	1.21
5	32	4702	4446.35	113782.32	147.38	30.17	0.36
6	37	6012	5678.48	146602.34	187.64	30.26	0.00
7	40	6547	6141.22	158462.54	201.55	30.47	0.00
8	37	5640	5358.69	135655.05	171.73	31.20	0.39
9	43	6399	6016.90	158217.29	199.88	30.10	0.62
10	38	5677	5348.68	140675.45	174.30	30.69	0.74
11	34	5040	4742.33	124922.34	155.59	30.48	0.60
12	28	4092	3929.63	102252.99	130.77	30.05	1.18
13	35	5260	4910.13	127793.26	165.73	29.63	0.53
14	25	3701	3558.23	91074.60	114.88	30.97	0.89

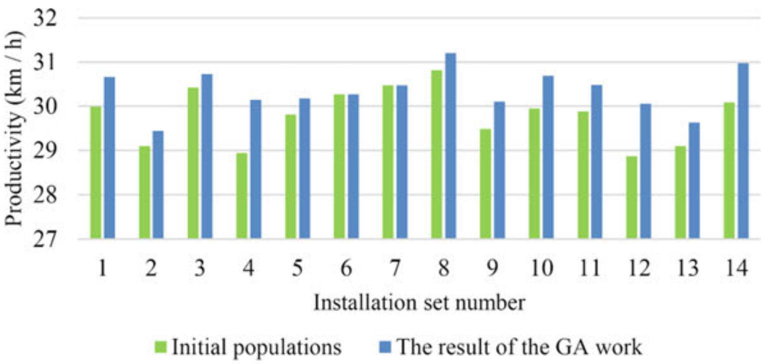

Fig. 6 Comparison of performance after GA operation

4 Conclusion

Thus, there is presented the algorithm for optimal assembly batches installation at a hot rolling mill based on genetic approaches. The crossing and mutation operators were applied. The algorithm considers the technological restrictions imposed on the production process. The optimality criterion is obtaining the maximum performance during installation, which is achieved by reducing the time for re-building equipment when switching to different widths and thicknesses of rolled products. Based on the obtained results, the developed model of optimal assembly batches installation at the hot rolling mill of metallurgical production allows us to increase the productivity of the mill and reduce energy consumption.

References

1. Linchevsky, B.V., Sobolevsky, A.L., Kalmenev, A.A.: Metallurgy of Ferrous Metals. Metallurgy, Moscow (1986)
2. Metal heater. Training manual for the training of workers in the production of hot rolled products. 1st edn. Printing house of PJSC “NLMK”, Lipetsk (2011)
3. Jung, C., Zaefferer, M., Bartz-Beielstein, T., et al.: Metamodel-based optimization of hot rolling processes in the metal industry. Int. J. Adv. Manuf. Technol. **90**, 421–435 (2017)
4. Tse, F.S., Morse, I.E., Hinkle, R.T.: Mechanical Vibrations. Allyn and Bacon, Boston (1963)
5. Mazur, I.P., Cherkashina, T.I.: Mathematical and physical modeling of soft cobbing process of hot rolling steels. Mater. Sci. Forum **704–705**, 160–164 (2012)
6. Production of rolled products at the mill 2000 in the HRP. 2nd edn. Printing house of PJSC “NLMK”, Lipetsk (2016)
7. Operating instructions for heating furnaces with walking beams of the hot rolled shop. 2nd edn. Printing house of PJSC “NLMK”, Lipetsk (2017)
8. Operating instructions for push-type heating furnaces of the hot rolled shop. 2nd edn, Printing house of PJSC “NLMK”, Lipetsk (2017)
9. Mittal, P., Malik, A., Mohanty, I., Mitra, K.: Comparative Study of Multi/Many-Objective Evolutionary Algorithms on Hot Rolling Application. In: Datta, S., Davim, J. (eds.) Optimization in Industry: Management and Industrial Engineering. Springer, Cham (2019)
10. Lugovskoy, V.M.: Algorithms of Automation Systems for Sheet Mills. Metallurgy, Moscow (1974)
11. Makarov, E.G.: Engineering Calculations in Mathcad 15. Peter, St. Petersburg (2011)
12. Gladkov, L.A., Kureichik, V.V., Kureichik, V.M.: Genetic algorithms. FIZMATLIT, Moscow (2006)
13. Sytnik, K.I.: Development and research of optimization algorithms for evolutionary computations based on the unification of hybridization methods. Dis. … Cand. tech. Sciences: 05.13.18. Voronezh State Technical University, Voronezh (2015)
14. Mitra, K.: Genetic algorithms in polymeric material production, design, processing and other applications: A review. Int. Mater. Rev. **53**, 275–297 (2008)
15. Man, K.F., Tang, K.S., Kwong, S.: Genetic Algorithms in Production Planning and Scheduling Problems. In: Genetic Algorithms. Advanced Textbooks in Control and Signal Processing. Springer, London (1999)
16. Costa, C.B.B., Wolf Maciel, M.R., Maciel Filho, R.: Factorial design technique applied to genetic algorithm parameters in a batch cooling crystallization optimization. Comput. Chem. Eng. **29**(10), 2229–2241 (2005)
17. Yu-guang, Zhong, Bo, Ai.: A modified ant colony optimization algorithm for multi-objective assembly line balancing. Soft Computing, vol. 21, Issue 22, pp. 6881–6894. Springer (2017)
18. Kucukkoc, I.: Integrating ant colony and genetic algorithms in the balancing and scheduling of complex assembly lines. Int. J. Adv. Manuf. Technol. **82**, 265–285. Springer (2016)
19. Samigulina, G.A.: Immune network modeling technology for complex objects intellectual control and forecasting system: Monograph. Science Book Publishing House, Yelm, WA, USA (2015)
20. Istomin, V.A., Galkin, A.V.: Formation of initial populations of assembly batches at hot rolling mills. In: XVI All-Russian School-Conference of Young Scientists “Management of Large Systems”, vol.1, pp. 52–57. Tambov State Technical University, Tambov (2019)

Software Application for Modeling the Fractionation Process Based on the Principle of Maximum Entropy

Alexander I. Balunov, Maksim A. Smirnov, and Sergey Yu. Boykov

Abstract The chapter considers software designed for modeling and optimization of the process of multicomponent fractionation based on the entropy-informational approach. The process is described mathematically based on the informational principle of maximum entropy, and the informational criterion of a relative estimate of system organization bears the role of the target function in the optimization. The application allows a user to calculate the most probable values of the main parameters of the process and can be used for decision support both at designing new fractionation devices and at the optimization of existing devices.

Keywords Fractionation · Mathematical modeling · Maximum entropy principle · Optimization · Windows application

1 Introduction

The last decade saw the informational principle of maximum entropy as a way to solve problems of uncertainty (Jaynes' formalism [1, 2], entropy modeling method [3]). This principle provides an opportunity to obtain the most probable result based on an accurate but incomplete information source [4]. The maximum entropy principle is known to be used in physics [5, 6], ecology [7–9], biology [10], social studies [11], and other fields.

Since the mid-seventies of the last century, the school of V. P. Maykov develops a system-informational approach to modeling and optimization of chemical engineering processes through their works [12–14]. This approach intends the maximum entropy principle to be used to describe technological processes mathematically.

A. I. Balunov (✉) · M. A. Smirnov · S. Yu. Boykov
Yaroslavl State Technical University, 88 Moskovskiy Avenue, Yaroslavl 150023, Russia
e-mail: balunovai@ystu.ru

M. A. Smirnov
e-mail: maks11041998@rambler.ru

S. Yu. Boykov
e-mail: boykovsy@ystu.ru

A. G. Kravets et al. (eds.), *Cyber-Physical Systems*, Studies in Systems, Decision and Control 350, https://doi.org/10.1007/978-3-030-67892-0_6

Among those, the most fully developed is the fractionation theory, in which the law of distribution of components in the column streams, when described, is assumed to be the most probable, corresponding to the maximum of information entropy when the balance constraints are taken into account. The constraints also include the equation specific to the entropy method of modeling, which introduces the properties of components and specifies the degree of stream separation.

The mathematical description of multicomponent fractionation of close-to-perfect mixtures determines Shannon's entropy as the criterion of maximum likelihood. It measures the uncertainty of the presence of microparticles (molecules) of each component in a mixture. Since the probability of detecting particles of a specific type in such mixtures is equal to their molar fraction, Shannon's entropy can be calculated based on the molar composition of the mixture [12, 13, 15]. Generally, this probability is related to the size of microparticles. It means that to describe the processes of mixture separation, the non-ideality of which is caused by the difference in the size of component molecules (athermic mixtures), we propose an extended version of the maximum entropy principle [14, 16]. In this version, the criterion of likelihood is the information entropy of a complex experiment. This entropy includes conditional entropy and conditional probabilities [17].

The criterion of likelihood within the description of processes of separation of (oil) mixtures is the information entropy of a continuum [18, 19].

Thus, the entropy method provides a way to describe the fractionation process of both ideal [15] and non-ideal (athermic) mixtures [14, 16], both multi-component [14–16] and continuous systems [18, 19], as well as a tray and packed columns on a unified methodological basis.

The optimization of processes based on the system-informational approach sees the criterion of a relative estimation of the degree of system organization as the main target function [20]:

$$\eta = \frac{H_{\text{in}} - H_{\text{out}}}{H_{\text{in}}}$$

H_{in} and H_{out} here are information entropies used to evaluate the disorder of streams at the input and the output of the system.

It proves to be helpful when evaluating the separation power of the fractional column—the higher the η, the higher the separation power of the column, and the better the quality of separation. The maximum possible separation of power is $\eta = 1$. This corresponds to the hypothetical case of separation of a binary mixture into pure products or a multicomponent mixture into two pure fractions. On the contrary, when the process is reduced to a simple separation of a mixture into two parts of an equal initial composition, then $\eta = 0$.

In the thermodynamic interpretation, the criterion η represents the relation of the thermodynamic work of fractioning the initial, close to the ideal mixture into given products to the similar work of fractioning into pure products. It is known that such a criterion does not contradict the criteria based on technical and economic evaluation [15].

2 Mathematical Model of the Process

The application of the entropy method to the description of the fractionation process has made it possible to reproduce previously known theoretical results as well as new ones. In determining the law of the most probable distribution of components in the product streams of the column, we obtain the proportions that meet the Fenske-Anderwood equation known in the theory of equilibrium fractionation. The analog of the number of theoretical trays in the column is one of the Lagrange multipliers in the conditional extreme task of calculating the most probable distillate and distillation residue compositions. The obtained dependencies can be used both in the project and verification settings of the column calculation problem [15]. In the first case, we set the separation quality of the mixture, while product stream compositions and the conditional height of the column (Lagrange multiplier) are to be determined. In the second case, we set the conditional height of the column (model identification parameter), and the product stream compositions are to be determined. Verification calculation to analyze the work and optimization of the existing fractional apparatus.

Similar dependencies have been obtained for calculation of the most probable compositions of streams leaving the column volume limited by two arbitrary sections with known compositions of input streams [15]. Here, one of the Lagrange multipliers acquires the physical meaning of the parameter that determines the degree of separation of output streams.

As a result of the combination of these dependencies with the equations of material balance of the top (reinforcing) and bottom (exhaustive) sections of the column, we have obtained the recurrence ratios for calculation of the most probable distributions of components in adjacent sections at the step-counterflow scheme of streams in the column [15]. Generally, the calculation is possible for both equilibrium (the degree of separation of streams is one) and non-equilibrium (the degree of separation is less than one) contact steps. While calculating per equilibrium (theoretical) steps, the received ratios completely coincide with generally accepted dependencies of per-tray calculation. However, it should be noted that the degree of stream separation here is not introduced from the outside as, for example, tray efficiency in traditional methods, but follows from the solution of the problem itself—it is a Lagrange multiplier in a conditional extreme problem.

The separation of the mixture in the column reduces the disordered nature of the source stream evaluated by entropy. It is natural to require the work of each part of the column to be subordinated to that goal. However, in the feed node, due to mixing streams, the disorder does not only decrease but even increases somewhat. Therefore, the optimal location of the feed input to the column should provide the minimum possible increase of disorder. As a result of the optimization problem solution, we have obtained dependencies for the calculation of such compositions in the feed node sections, which minimize entropy production in it [15].

3 Calculation Algorithms

Progressively solving the problems above makes it possible to use two algorithms for calculating the column depending on the volume of initial information. The first algorithm, which is called the “main” algorithm, is more focused on the project calculation of the column, and the second algorithm—“decompositional”—can be used both at project and calibration calculation.

Calculation using the main algorithm is performed in the following sequence.

The first step, calculate compositions of product streams of the column, as well as the value of the Lagrange multiplier at the project calculation (the minimum number of theoretical contact steps in a non-selective one). The initial information for the calculation is molar composition and relative volatility of the components of the shared mixture, product selection, as well as the concentration of one of the components in the product streams (project calculation) or the parameter that reflects the conventional height of the column (verification calculation).

The second step, determine the compositions of streams in the cross-sections of the optimal feed node. To do this, the evaporation fraction and the phase composition of the feed, as well as the phlegm number, are additionally specified (or calculated).

In the third step, calculate the compositions in sections of the column and determine the number of equilibrium or non-equilibrium contact steps in each of them at a given degree of separation of output streams of the step. It is calculated with the recurrence ratios in mind from one section to another in the direction from the product streams to the feed node. Particularly, when the vapor stream at the top of the column condenses in a full condenser, and the distillation residue evaporates in a full evaporator, the streams compositions at the end sections of the column are considered to be equal compositions of product streams. Generally, at the partial condenser and boiler, the compositions at the end sections of the column are calculated using known dependencies of single condensation and evaporation.

The condition of joining sections with the feed node is the equality of the average energy parameter for the sections of the column and feed node [15]. To comply with this condition, it is necessary to vary the degree of separation of streams at the contact steps adjacent to the feed node, which is equivalent to crushing them.

The main algorithm assumes that the compositions of distillate and distillation residue do not depend on phlegm mode and feed input location. This information is omitted, i.e. it is assumed that the given separated can be related to a variety of constructive and mode parameters defined at the next steps of calculation. If this information (or a part of it) is known, it is possible to clarify the solution of the problem somewhat using the decompositional calculation algorithm, which contains only two steps [19, 21].

The first step, find the most probable component distributions in the end cross-sections of the column sections and, thus, decompose the column into two subsystems—the exhaustive and reinforcing sections. The initial information for the column calculation is evaporation ratio and phase composition of the feed, the relative volatility of the mixture components, product selection, phlegm number, as well as, in the case of the project calculation, the concentration of the target component in the product streams and the value of the parameter defining the conditional height of one of the sections, and in the case of verification—the value of these parameters for each section.

When determining the compositions of output streams of column sections, the dependencies are usually used to calculate the compositions of product streams of the entire column. Thus, an input stream of the reinforcing section is a total vapor stream arriving in it from a feed node and the liquid arriving from a dephlegmator, while in the exhaustive section, it is a total stream of the liquid arriving from a feed node and vapor from a boiler. The relationship between the material streams of the sections is determined by the equations of the material balance of the feed node. Since compositions of output streams of sections depend on compositions of input streams, which are not known initially, the calculation is iterative and consists of multiple alternating calculations of each section before the stabilization of compositions in boundary sections. The practice of calculations has shown that the compositions of streams are stabilized to the fourth decimal in 5–7 iterations.

In the second step, the column sections are calculated similarly to the main algorithm, using the components obtained at the first step of component distribution in the boundary cross-sections of the column sections.

It should be emphasized that although the decomposition algorithm leads to the need to introduce iterative procedures, the latter are much simpler and more reliable compared to traditional calculation methods. At the same time, the algorithm preserves the main advantages of the entropy method—a smaller volume of source information and a significant reduction in calculation time.

4 Software Functionality

To model and optimize the process of fractionation of multicomponent mixtures based on the system-informational approach, we have developed a special software—MS Windows application, in which both calculation algorithms are implemented (Fig. 1). To make the algorithm more convenient, it starts with determining compositions of product streams of a column in a non-selective mode (the first step of the basic algorithm) for the chosen calculation option, and then depending on the chosen algorithm, compositions are calculated either in optimal feed node or in boundary cross-sections of column sections. The compositions are then found in the cross-sections of the top and bottom sections of the column, and the optimality criterion is calculated.

The user interface language can be selected in the application. The main interface window with the active tab "Concentration Profiles" is shown in Fig. 2.

In the left part of the window, the user can enter new source data or load previously entered data from saved files, as well as select an algorithm (main or decompositional) and option (project or verification) of column calculation. If there are no source data required for the next calculation step, the user can either enter them and

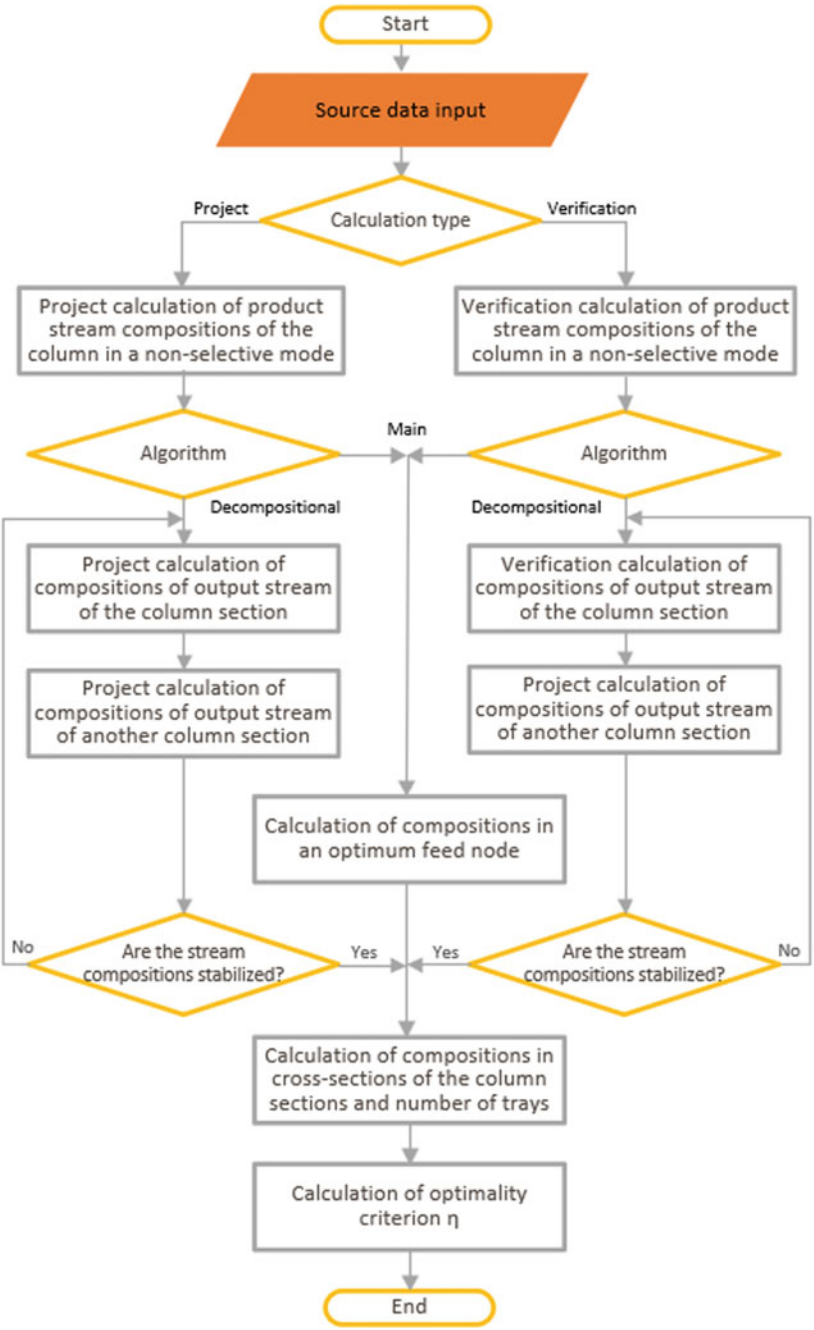

Fig. 1 Flowchart of the fractional column calculation algorithm

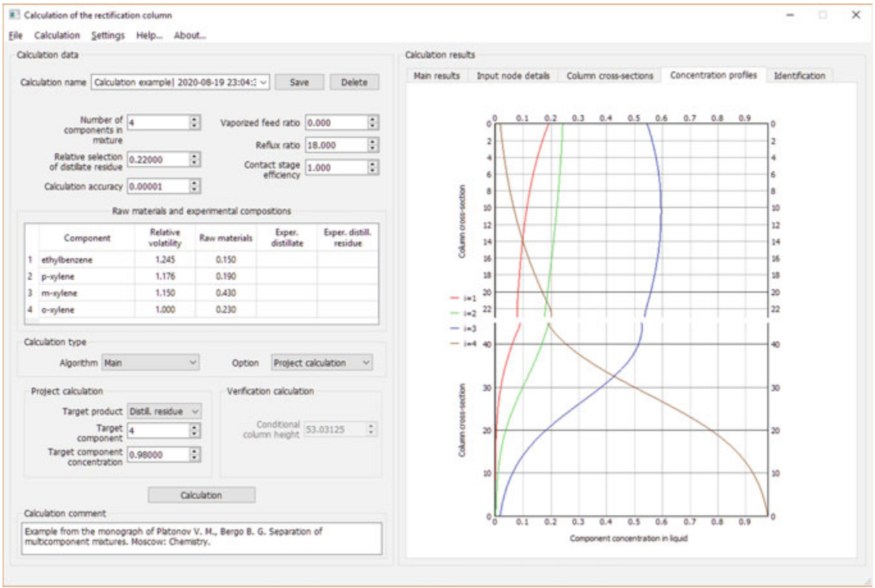

Fig. 2 Application interface: "Concentration Profiles" tab

continue with the calculation or finish the calculation. Here the user can also enter the experimental compositions of product streams of the column and identify the verification mathematical model. The identification parameter, as mentioned above, is the Lagrange multiplier, which defines the separation power of the column.

There are five tabs on the right side of the window: "Basic Results", "Detailed Input Node", "Column Cross-Sections", "Concentration Profiles", "Identification", the results of calculations are presented as a spreadsheet and a chart, which can also be printed.

The application is developed in Python using third-party libraries:

- «Pyside2»—user interface design;
- «NumPy»—multi-dimensional arrays operation;
- «PyQtGraph»—plotting graphs of component concentration distribution along with the height of column sections;
- «Skipy»—an approximation of component concentration distribution along with the height of column sections using the Interp1d class;
- «PyFPDF»—*.pdf results output.

5 Conclusion

This software can be used for decision-making support both at designing new fractionation devices and at the optimization of existing devices. It can also be included as one of the hierarchical levels in the system strategy for calculating multicolumn fractionation units. As a result, the fractionation system will be calculated in the following sequence: choice of the optimal scheme of separation (system structure), optimal decomposition of the system into subsystems (columns), and calculation of each column separately.

References

1. Tribus, M.: Thermostatics and Thermodynamics. D. Van Nostrand Co Inc, Princeton (1961)
2. Maron, A.I.: Assessment of service quality for complex technical devices based on the Jaynes' information principle. Bus. Inform. **4**(38), 47–51 (2016)
3. Wilson, A.G.: Entropy in Urban and Regional Modeling. Pion Limited, London (1970)
4. Jaynes E.T.: Probability Theory: The Logic of Science, p 727. Cambridge University Press, Cambridge (2003)
5. Pressé S., Ghosh K., Julian L., et. al.: Principles of maximum entropy and maximum caliber in statistical physics. Rev. Mod. Phys. **85**(3), 1115–1241 (2013)
6. Banavar J.R., Maritan A., Volkov I.: Applications of the principle of maximum entropy: from physics to ecology. J. Phys.: Condens. Matter. **22**(6), 063101 (2010)
7. Merow C., Smith M.J., Silander Jr J.A. Ecography: A practical guide to MaxEnt for modeling species' distributions: what it does, and why inputs and settings matter. Ecography **36**(10):1058–1069 (2013)
8. Phillips, S.J., Anderson, R.P., Schapire, R.E.: Maximum entropy modeling of species geographic distributions. Ecolog. Model. **190**, 231–259 (2006)
9. Elith J., Phillips S.J., Hastie T., et. al.: A statistical explanation of MaxEnt for ecologists. Divers. Distrib. **17**(1), 43–57 (2011)
10. Bowler, M.G.: Species abundance distributions, statistical mechanics and the priors of MaxEnt. Theor. Popul. Biol. **92**, 69–77 (2014)
11. Luzzi, R., Mesquita, M.V., Madureira, J.R.: An information-theoretic-based (MaxEnt) approach to social dynamical systems. J. Math. Sociology. **25**(2), 179–224 (2001)
12. Theory and calculation of separation systems. System-information approach./Chief ed. Maykov V.P. Moscow. MIKhM. 128 p. (1975)
13. Protsessy i apparati khimicheskoy tekhniki. [Processes and apparatus of chemical technology] System-information approach./Chief ed. Maykov V.P. Moscow. MIKhM. 160 p. (1975)
14. Maykov V.P., Balunov A.I.: Rectification of athermal mixtures. System-information approach. Moscow. MIKhM. 160 p. (1979)
15. Balunov, A.I., Maykov, V.P.: Entropy and information in theory of rectification. Izv. Vyssh. Uchebn. Zaved., Khim. Khim. Tekhnol. **46**(9), 54–67 (2003)
16. Balunov, A.I.: Compositions calculation of complex distillation system product flows based on the extended version of the maximum entropy principle. Izv. Vyssh. Uchebn. Zaved., Khim. Khim. Tekhnol. **63**(1), 99–104 (2020)
17. Maykov, V.P., Balunov, A.I.: Conditional entropy in description of athermal properties. Izv. Vyssh. Uchebn. Zaved., Khim. Khim. Tekhnol. **47**(8), 76–81 (2004)
18. Maykov, V.P., Morugin, K.K., Karavaev, N.M.: Calculation of distillate and distillation residue compositions during fractionation of continuous and discrete-continuous mixtures based on probability (information) model. Dokl. Akad. Nauk SSSR **239**(5), 1157–1160 (1978)
19. Balunov, A.I., Dzuba, O.V., Maykov, V.P.: Thermodynamic method of calculation of separation product compositions at fractionation of continuous and discrete-continuous mixtures. Izv. Vyssh. Uchebn. Zaved., Khim. Khim. Tekhnol. **39**(1–2), 86–89 (1996)
20. Ashby, W.: Ross: An Introduction to Cybernetics. Chapman & Hall, London (1956)
21. Balunov A.I.: Decomposition algorithm for calculating multicomponent rectification. Mathematical methods in engineering and technology—MMTT. 2011, Vol. 3, pp. 65–67 (2011)

Identification of a Technological Process with Application of Neural Network Modeling

A. S. Aleksandrova, A. G. Shumikhin, and B. V. Kavalerov

Abstract A conceptual scheme for identifying a controlled process using neural network modeling is proposed. A cyber-physical system including a technological object and a control system is considered. The conceptual scheme is based on the hidden information potential of the cyber-physical system, which consists of the data on its functioning registered during operation. Neural network technology allows us to realize this potential, using the accumulated data to build a process model. Further, the neural network model is used to conduct computational experiments on it in order to identify the model of the object. In accordance with the presented conceptual scheme, the model of the controlled technological process of maintaining the temperature of the gas-raw material mixture at the furnace outlet of the catalytic reforming unit of the oil fraction was identified.

Keywords Cyber-physical system · Control object · Identification · Passive identification · Frequency identification · Neural network modeling · Automation regulation

1 Introduction

In recent years, modern industrial enterprises of the chemical industry have paid increased attention to the issues of production efficiency [1, 2], the situation is similar in the electric power industry, for example, in the production of electricity by gas turbine power plants of small and medium power [3]. Modern production in a broad sense is a cyber-physical system that includes technological processes and objects, as well as an automatic control system. Automation systems for technological processes play an important role in solving issues of increasing efficiency. The competent design of automatic control systems, selection of the correct configuration, and timely

A. S. Aleksandrova (✉) · A. G. Shumikhin · B. V. Kavalerov
Perm National Research Polytechnical University, Komsomolsky Prospect 29, Perm 614990, Russia

B. V. Kavalerov
e-mail: kbv@pstu.ru

A. G. Kravets et al. (eds.), *Cyber-Physical Systems*, Studies in Systems, Decision and Control 350, https://doi.org/10.1007/978-3-030-67892-0_7

adjustment of algorithm parameters can significantly improve the quality indicators of technological processes. For example, to increase the yield of the product, to reduce the costs of technological processes, to reduce the costs associated with the loss of the product, and for energy [4].

There is a demand for the implementation of strategies for advanced control of technological processes (Advanced Process Control) [5], while often the potential of the implemented control systems remains unrealized. This leads to a decrease in the efficiency of systems for advanced control of technological processes, or the functions of the control system are shifted to the upper-level subsystem.

First of all, it is necessary to ensure the optimal operation of the control algorithms, to perform their correct adjustment and timely adaptation with the changing characteristics of the object [6, 7].

Calculation or reconfiguration of automatic control systems requires the construction of an object model [8]. There are three main approaches to building a model of a technological object. This is the construction of an analytical model based on the regularities of the ongoing physical and chemical processes, the identification of a certain model of the object based on the results of an active experiment on the object, and the building of a model of the object based on the results of a passive experiment using statistical methods.

The creation of analytical models is costly and time-consuming. The use of such models for tuning control algorithms for a technological object is impossible without their additional adaptation to the current conditions of its functioning [9].

The most common and reliable method for identifying models is identification based on the methods of active experiment on the object [10, 11]. There are technical limitations to the applicability of these methods. Limitations may be related to the impossibility of physical implementation of the test signal at the input of the object or the inadmissibility of turning off the control system of a technological object for conducting experiments. When identifying by conducting an active experiment, it is necessary to ensure the stabilization of all influencing signals except the test signal, which is practically impossible for real industrial objects exposed to the influence of many different kinds of recorded and unrecorded disturbing influences. However, carrying out an active experiment at an operating industrial facility increases the risk of deterioration in the quality of the functioning of a technological facility, which leads to a deterioration in finished products and an increase in resource consumption, and also increases the threat of reducing the safety of hazardous industrial facilities.

It is especially difficult to obtain a satisfactory model of an object from the data of its normal operation for the case when the object is part of an automatic control system. The disadvantages of this approach to determining the characteristics of control channels based only on data from the normal operation are explained by deviations of the statistical properties of controlled variables from the prerequisites under-lying the known mathematical methods for identifying multidimensional objects. The known methods of modeling and identification based on the results of passive observation do not allow constructing an adequate mathematical model of a technological object in the presence of feedbacks in the control circuit and insufficient dispersion of input actions during normal operation [12].

Therefore, the use of active identification methods is a necessary measure. It is necessary to strive to optimize the active identification procedure itself, minimizing the negative influence of some factors on the process of controlling the identification procedure by reducing the time of the active experiment, reducing the amplitudes of the test signals, and also by mutual compensation of the influence of the test signals.

The development of methods for modeling and identification of multiparametric, controlled technological objects, allowing to minimize the intervention of the researcher in the operation of the control system, is an urgent task [13–15].

It should be noted that at present the vast majority of continuous technological processes are cyber-physical systems and are equipped with modern control systems that include a real-time database. In such systems, the registration and storage of the values of technological parameters are realized with a rather small discreteness in comparison with the inertia of the processes and for a long period of time, as a rule, several years. Considering a system that includes a technological object and a control system as a single cyber-physical system, it is possible to discover the information potential hidden in the arrays of accumulated data on the technological process during its operation. Such data may contain information necessary for building a model of an object [13].

The technology of neural networks allows realizing this potential [16–20]. Recurrent neural networks with delay are able to simulate the behavior of dynamic objects [21, 22]. Neural networks make it possible to use the operating data of a technological object [23] to build a model, while the requirements for the characteristics of the processes are softer than when conducting an active or passive experiment. In particular, signal trends can be used during the period of emergency situations, significant disturbing influences, changes in the operating mode of the object, etc.

Even when it is necessary to conduct an active experiment on-site, no specific test signal waveforms are required. The impact on the object can be of a random nature and, when acting on the modeled object, at the same time partially compensate for the influence of the test signals. There are also no special requirements for the characteristics of random test signals.

2 Conceptual Scheme of Technological Process Identification Using Neural Network Modeling

Figure 1 shows a conceptual scheme for identifying a technological process using neural network modeling.

The conceptual identification scheme includes two stages - the stage “Building a neural network model” and the stage of “Identification by a neural network model”.

The stage “Building a neural network model” includes three steps. The first step “Data collection” includes collecting information about the object under study. The main data source is the control system database. The most unstable states of the technological process, periods of the greatest influence of disturbing influences, etc.

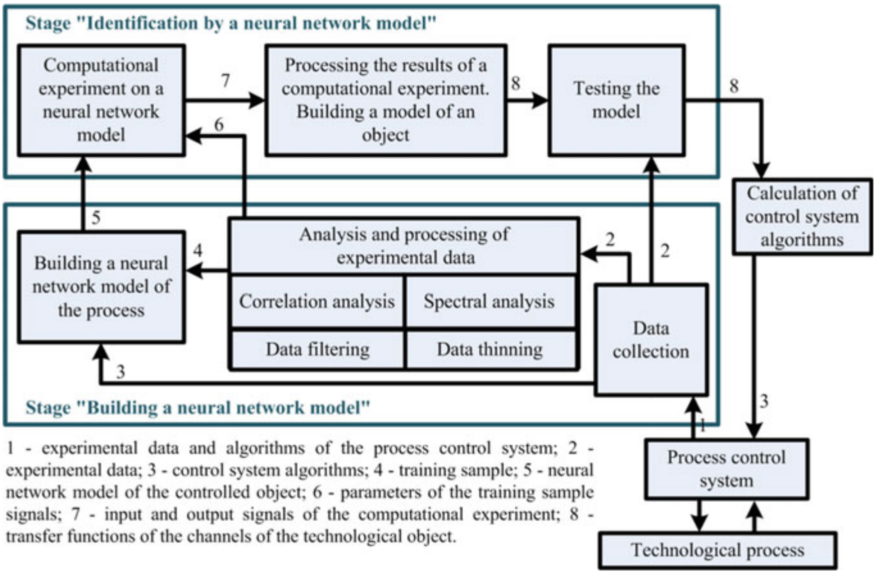

Fig. 1 A conceptual scheme for identifying a controlled technological object according to its neural network model

should be chosen. If necessary, tests can be carried out in the form of effects on the investigated technological process within the required operating mode. The data (2) is transferred to the step "Analysis and processing of experimental data" in the form of technological parameter trends. Also, information about automatic control algorithms (3) in the case of modeling a controlled object is transmitted to the step "Building a neural network model of the process".

The step "Analysis and processing of experimental data" includes a correlation analysis, during which technological parameters that affect the output parameter of the model are determined. Research on the neural network model should be carried out for those channels, the correlation function of which indicates the presence of a linear relationship, and exclude interdependent signals, leaving one of them, the least noisy or earlier influencing the output value. Depending on the time of the first peaks of the correlation functions, the maximum required delay for the neural network model is calculated. For controlled objects, it is necessary to calculate the values of the correlation functions from the investigated parameters and the control action.

In the case of noise, the signals are passed through a smoothing filter. For inertial processes, it is advisable to thin out the data. For the technological parameters selected for building a neural network model, a spectral analysis is carried out, during which the harmonic composition of the signal is determined. The results of the spectral analysis (6) are transferred to the stage "Identification by neural network model". At the step "Analysis and processing of experimental data" training and test samples are formed (4), which are transferred to the step "Building a neural network model of the process".

The step "Building a neural network model of the process" includes the process of training a neural network based on the date of the training sample. At this step, a neural network model is formed. For a controlled object, the neural network model includes a regulator model. In the case of successful testing, the model (5) is transferred to the stage "Identification by the neural network model".

At the stage "Identification by a neural network model" methods of the active experiment is used, a distinctive feature of which is the use of a neural network model of an object instead of a full-scale object for carrying out a computational experiment on it. So by the method of a computational experiment on a neural network model, a series of experiments is carried out with the supply of periodic test signals with the parameters of characteristics (amplitude, frequency). For tests on a neural network model, it is necessary to use signals with the same characteristics as the signals of the training sample. Signal parameters are determined based on the results of spectral analysis of the training sample at the stage "Building a neural network model" at the step "Analysis and processing of experimental data".

Further, the results of the computational experiment are transferred to the next stage, where the results of the computational experiment are processed and the object model is constructed. As a result of processing the results of the computational experiment, the complex frequency response is formed, which is approximated by a certain transfer function. The resulting model of the technological process in the form of transfer functions is further tested on experimental data, which ensures the adequacy of the resulting model.

3 Identification of the Model of a Controlled Technological Process in Accordance with the Presented Conceptual Scheme Is Performed

In accordance with the presented conceptual scheme, the model of the controlled technological process of maintaining the temperature (TIRCSA1_09) of the gas-feed mixture at the outlet of the furnace of the catalytic reforming unit of the oil fraction was identified (Fig. 2).

After heating in Furnace E-1 (Fig. 2), the raw material is sent for purification from sulfur, nitrogen, and oxygen and further to the reforming reactor. With an increase in the temperature of the gas-raw mixture, the intensity of the reactions of hydrodesulfurization and hydrogenation of unsaturated hydrocarbons increases. At the same time, the intensity of hydrocracking reactions increases to a greater extent. As a result of these reactions, there is a loss of raw materials that turn into gases. Insufficient heating of raw materials leads to insufficient purification from sulfur, nitrogen, and oxygen. The presence of these impurities in the gas-feed mixture

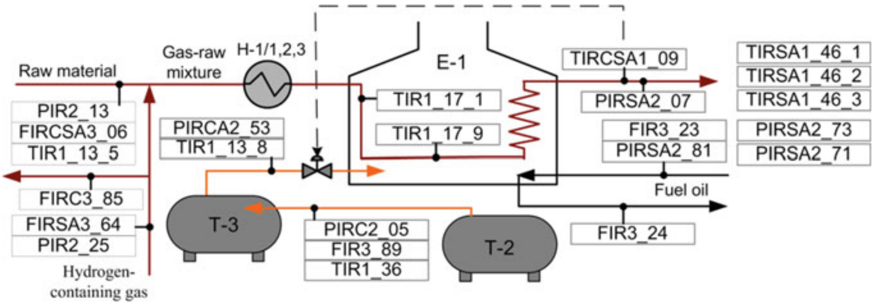

Fig. 2 Furnace of a catalytic reforming unit with preliminary hydrotreating of the feedstock

poisons the reforming catalyst. The strategy for controlling the temperature of the gas-raw mixture consists of maintaining the temperature at the minimum value required for hydrotreating reactions, while the regime is always carried out with a certain quality margin. Those the temperature must be kept several degrees higher than necessary. The better the temperature is stabilized, the smaller the quality margin is needed, and the less the likelihood of rejects and the less loss of raw materials for hydrocracking.

The consumption of raw materials in the tee of mixing with a circulating hydrogen-containing gas is regulated by the device pos. FIRCSA3_06. The pressure and temperature of the raw material supplied to the mixing tee are recorded by the devices pos. PIR2_13 and TIR1_13_5. The flow rate and pressure of the hydrogen-containing gas supplied to the mixing tee are recorded by the devices pos. FIRA3_64 and PIR2_25. For unloading the E-1 furnace, a part of the hydrogen-containing gas is discharged in addition to the hydrotreating unit. The flow rate of excess hydrogen-containing gas, in addition to the hydro-cleaning unit, is regulated by the device pos. FIRC3_85. After the mixing tee, the gas-raw mixture passes through the annular space of the heat exchangers H-1/1,2,3, then the convection part of the E-1 furnace passes in two parallel flows, where it is heated by the exhaust flue gases and the combined flow of the gas-raw mixture enters the radiant chamber of the E-1 furnace. The temperature of the total flow at the entrance to the convection chamber and the exit from the chamber is recorded by devices pos. TIR1_17_1 and pos. TIR1_17_9. The temperature of the gas-raw mixture at the outlet of the E-1 furnace into the reactor is controlled by the device pos. TIRCSA1_09, the control valve is installed on the fuel gas supply line to the E-1 furnace. The temperature of the flue gases over the E-1 passes is controlled by devices pos. TIRSA1_46_1 – TIRSA1_46_3. The pressure at the entrance to E-1 is recorded by the device pos. PIRSA2_07. The E-1 hydrotreating furnace operates on combined fuel - liquid and gaseous. Liquid fuel consumption (direct and reverse) is recorded by devices pos. FIR3_23 and FIR3_24. The pressure of the liquid fuel to the furnaces is recorded by the device pos. PIRSA2_81. Gaseous fuel - the fuel gas flows from the manifold to the T-3 fuel gas separator, where the blow-off gases from the T-2 tank and the gas after separation into the irrigation tanks are sent. The pressure in the tank T-2 is regulated by the device pos. PIRC2_05. The temperature of the fuel gas on the furnace is recorded by the device pos. TIR1_13_8. The fuel gas pressure in front of T-3 is regulated by the device pos. PIRCA2_53. Flare gas consumption from T-2 to T-3 is recorded by the device pos. FIR3_89. The temperature of the flare gas from E-2 to B-3 is recorded by the device pos. TIR 1-36. The fuel gas pressure to the main burner is recorded by the device pos. PIRSA2_73. The fuel gas pressure to the pilot burner is recorded by the device pos. PIRSA2_73.

Collected experimental data on 23 technological parameters within 5 h with a recording period of 1 s by downloading their values from the database of the control system. Correlation analysis for technological parameters and control action of the temperature regulator of the gas-fired mixture at the furnace outlet is carried out. Correlation functions from 5 parameters (PIR2_13, PIR2_25, PIRSA2_07, FIRA3_64, and FIRC3_85) and control activities are almost the same, and the correlation coefficients between these parameters are close to 1.0. So of these 5 parameters, it is advisable to choose one with the maximum value of the extremum of the correlation function (this is the parameter PIRSA2_07). The value of the correlation function at the extremum point for the parameter FIR3_23 and the control action can be considered insignificant, i.e. the parameter has no significant effect on the controlled value. Similar results were obtained for the parameter PIRC2_05. Correlation functions for a number of parameters (TIR1_13_8, TIR1_36, FIR3_89 have a maximum at time 0 s, which indicates the presence of a connection between these parameters, but not through an adjustable value because it is known that the transmission channel “control action - controlled variable” has a delay.

Based on the results of the analysis of the experimental data, training and test samples were formed to build a neural network model, which include, as input parameters for the neural network model, the disturbing parameters - the pressure of the gas-raw mixture at the entrance to the furnace (PIRSA2_07) and the control action of the temperature controller (TIRCSA1_09). At the output, the trained neural network model outputs the temperature value of the gas-raw mixture after the furnace. So an imitation neural network model of a controlled object is built, shown in Fig. 3, including a regulator, which ensures adequate operation of the neural network model.

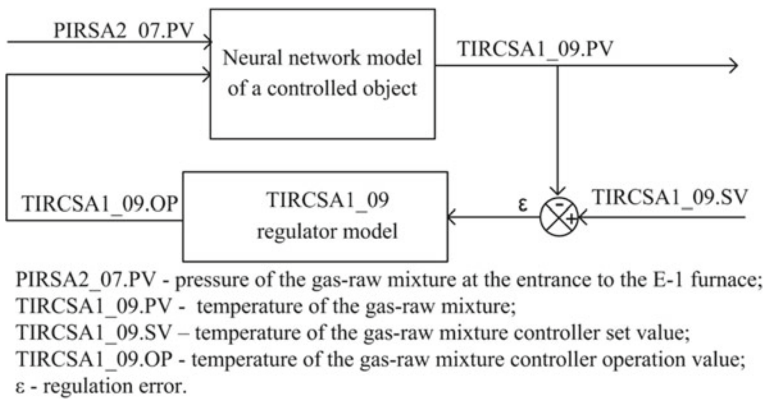

Fig. 3 Neural network model of a controlled object

Figure 4 shows the results of testing a simulation neural network model of a controlled object.

The trained neural network model is transferred to the stage "Identification by a neural network model" for performing computational experiments on it. A series of computational experiments are carried out with the input of the model of periodic test signals with different frequencies. The frequencies are selected in accordance with the results of the spectral analysis of the training sample of the neural network model. In the course of the computational experiment, a Nyquist diagram was obtained, shown in Fig. 5.

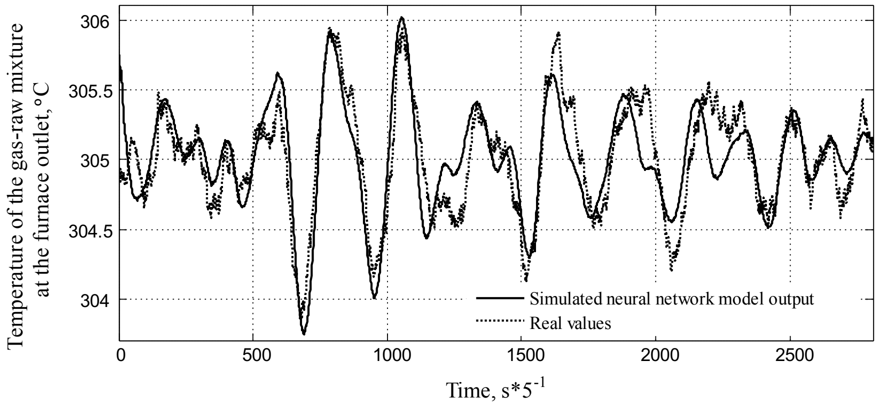

Fig. 4 Results of testing the simulation neural network model of the controlled object

Fig. 5 Nyquist diagram of the controlled object along the channel "pressure of the gas-raw mixture at the entrance to the furnace - temperatures of the gas-raw mixture after the furnace"

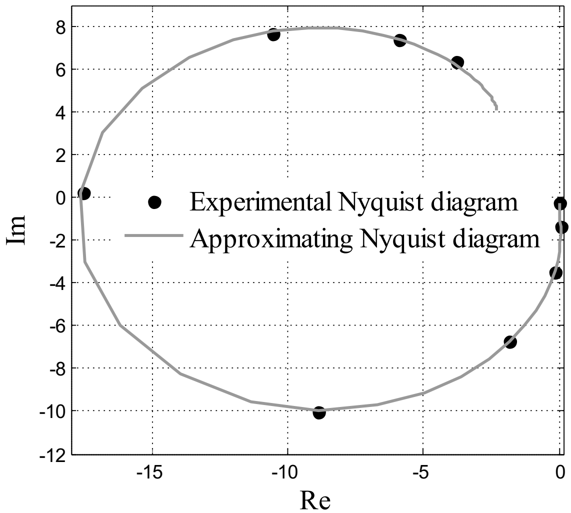

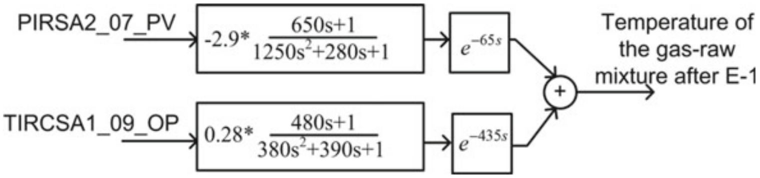

Fig. 6 Simulation model of the technological process in the form of transfer functions

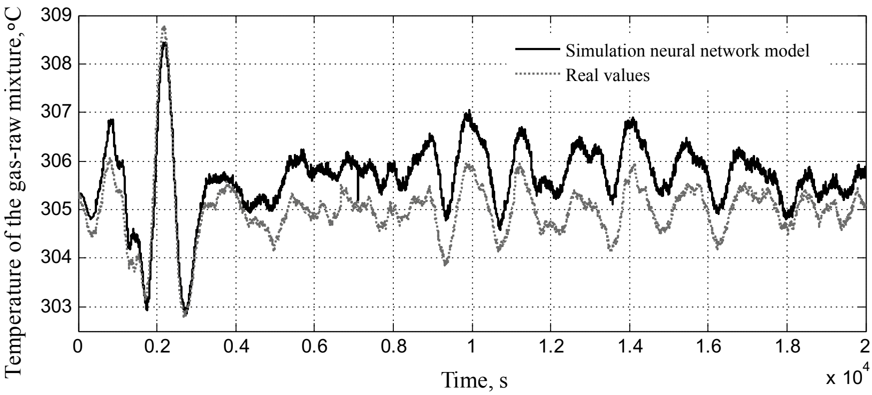

Fig. 7 Testing the model of the technological process of maintaining the temperature of the gas-raw mixture at the outlet of the furnace, identified following the conceptual scheme

The Nyquist diagram is approximated by transfer functions. The simulation model of the technological process in the form of transfer functions is shown in Fig. 6.

The results of testing the technological process model in the form of transfer functions, identified following the conceptual scheme, are presented in Fig. 7.

The mean square error of the model output from the real values does not exceed 0.57 °C. The maximum absolute error does not exceed 1.6 °C.

4 Conclusion

The conceptual scheme for identifying a process model is based on the representation of a controlled process as a cyber-physical system containing performance data used to identify the process model. The presented approach to the identification of technological processes using neural network modeling makes it possible to combine the methods of passive and active experiments, minimizing the disadvantages of these methods and optimizing the procedure of collecting information about the technological process necessary for building its model.

The conceptual identification scheme includes validation procedures by testing a neural network model and a simulation model in the form of transfer functions on a test sample, which ensures the adequacy of the results obtained. A feature of the proposed concept is the use of test signals for conducting computational experiments on a neural network model with characteristics similar to those of signals in the training sample formed from data on the functioning of the technological process.

Acknowledgements The study was carried out with the financial support of the Russian Federal Property Fund and the Perm region as part of the scientific project № 19-48-590012.

References

1. Alanqar, Anas, Durand, Helen, Christofides, Panagiotis: Fault-Tolerant Economic Model Predictive Control Using Empirical Models. IFAC-PapersOnLine. **50**, 3517–3523 (2017). https://doi.org/10.1016/j.ifacol.2017.08.940
2. Moshev E., Meshalkin V., Romashkin M.: Development of Models and Algorithms for Intellectual Support of Life Cycle of Chemical Production Equipment. In: Kravets A., Bolshakov A., Shcherbakov M. (eds.) Cyber-Physical Systems: Advances in Design & Modelling. Studies in Systems, Decision and Control, vol 259. Springer, Cham (2020)
3. Kavalerov, B.V., Bakhirev, I.V., Kilin, G.A.: Using neural networks in controlling low- and medium-capacity gas-turbine plants//Russian. Electr. Eng. **90**, 737–740 (2020)
4. Onori, S.: Model-based optimal energy management strategies for hybrid electric vehicles. In: Waschl, H., Kolmanovsky, I., Steinbuch, M., del Re, L. (eds.) Optimization and Optimal Control in Automotive Systems—Lect. Notes in Control Science, pp. 199–218. Springer, New York (2014)
5. Hu, H., Xu, Y., Liang, W., Forrest, J., Liu, M., Liu, L., Hu, P., Peng, X., Peng, Y.: Advanced process control applied to distributed control systems. Kybernetes. **39**, 946–953 (2010). https://doi.org/10.1108/03684921011046717
6. Zhenhai, Dou, Lianyun, Sun: Design of temperature controller for heating furnace in oil field. Physics Procedia. **24**, 2083–2088 (2012). https://doi.org/10.1016/j.phpro.2012.02.305
7. Zajic, I., Larkowski, T., Burnham, K., Hill, D.: Control analysis and tuning of an industrial temperature control system. In: IFAC Proceedings Volumes (IFAC-PapersOnline), 2 (2012)
8. Alberer, D., Hjalmarsson, H., Re, L.: Identification for automotive systems. Lect. Notes Control. Inf. Sci. **418**, 1–10 (2012)
9. Kutlu, C., Erdinc, M. T., Li, J., Su, Y., Pei, G., Gao, G., & Riffat, S. (2020). Evaluate the validity of the empirical correlations of clearance and friction coefficients to improve a scroll expander semi-empirical model. Energy, 202,
10. Karimshoushtari, Milad, Novara, Carlo: Design of experiments for nonlinear system identification: A set membership approach. Automatica. **119**, 109036 (2020). https://doi.org/10.1016/j.automatica.2020.109036
11. Hofreiter, Milan: Alternative identification method using biased relay feedback. IFAC-PapersOnLine **51**, 891–896 (2018). https://doi.org/10.1016/j.ifacol.2018.08.491
12. Myshlyaev, L., Rykov, A., & Lvova, E. The principles, methods and algorithms of industrial objects identification in control systems. In: IFAC Proceedings Volumes (IFAC-PapersOnline), vol. 42, pp. 1895–1900 (2009). IFAC Secretariat. https://doi.org/10.3182/20090603-3-RU-2001.0394
13. Bakhtadze N.N., Lototsky V.A. (2016) Knowledge-Based Models of Nonlinear Systems Based on Inductive Learning. In: Różewski P., Novikov D., Bakhtadze N., Zaikin O. (eds) New Frontiers in Information and Production Systems Modelling and Analysis. Intelligent Systems Reference Library, vol 98. Springer, Cham

14. Yadykin, Igor, Lototsky, V., Bakhtadze, Natalia, Maximov, E., Nikulina, I.: Soft Sensors of Power Systems Stability Based on Predictive Models of Dynamic Discrete Bilinear Systems. IFAC-PapersOnLine **51**, 897–902 (2018). https://doi.org/10.1016/j.ifacol.2018.08.456
15. Jafarov, S.M., Mustafayeva, A.M.: Identification of dynamic objects under uncertainty and non-stationarity using etalon transformers. In: Procedia Computer Science, vol. 120, pp. 561–567 (2017). Elsevier B.V. https://doi.org/10.1016/j.procs.2017.11.279
16. Muravyova, E.A., Mustaev, R.R.: Development of an artificial neural network for controlling motor speeds of belt weighers and separator in cement production. Opt. Mem. Neural Networks **26**, 289–297 (2017). https://doi.org/10.3103/S1060992X17040087
17. Shumikhin, A.G., Boyarshinova, A.S.: Identification of a complex control object with frequency characteristics obtained experimentally with its dynamic neural network model. Avtomat. i Telemekh. **4**, 125–134; Autom. Remote Control **76**:4 (2015), 650–657
18. Shumikhin, A.G., Aleksandrova, A.S.: Identification of a controlled object using frequency responses obtained from a dynamic neural network model of a control system. Comput. Res. Model. **9**(5), 729–740 (2017)
19. Korobiichuk I. et al. (2020) Identification of Technological Objects on the Basis of Intellectual Data Analysis. In: Szewczyk R., Krejsa J., Nowicki M., Ostaszewska-Liżewska A. (eds) Mechatronics 2019: Recent Advances Towards Industry 4.0. MECHATRONICS 2019. Advances in Intelligent Systems and Computing, vol 1044. Springer, Cham
20. Ghorbani, H., Wood, D., Choubineh, A., Tatar, A., Ghazaeipour, P., Madani, M., Mohamadian, N.: Prediction of oil flow rate through an orifice flow meter: Artificial intelligence alternatives compared. Petroleum (2018). https://doi.org/10.1016/j.petlm.2018.09.003
21. Li T., Gong Q. (2013) A Novel Artificial Neural Network Learning Algorithm. In: Du Z. (eds) Proceedings of the 2012 International Conference of Modern Computer Science and Applications. Advances in Intelligent Systems and Computing, vol 191. Springer, Berlin, Heidelberg
22. Schürholz, Klemens, Brückner, Daniel, Gresser, Melissa, Abel, Dirk: Modeling of the Three-way Catalytic Converter by Recurrent Neural Networks. IFAC-PapersOnLine. **51**, 742–747 (2018). https://doi.org/10.1016/j.ifacol.2018.09.166
23. Ghorbani, H., Wood, D.A., Choubineh, A., et al.: Performance comparison of bubble point pressure from oil PVT data: Several neurocomputing techniques compared. Exp. Comput. Multiph. Flow **2**, 225–246 (2020). https://doi.org/10.1007/s42757-019-0047-5

Development of Digital Twin of Plant for Adaptive Calculation of Development Stage Duration and Forecasting Crop Yield in a Cyber-Physical System for Managing Precision Farming

Petr Skobelev, Igor Mayorov, Elena Simonova, Oleg Goryanin, Alexey Zhilyaev, Aleksey Tabachinskiy, and Vladimir Yalovenko

Abstract The chapter proposes a formalized model of a digital twin of the plant on the basis of a graph of transitions of states corresponding to stages of plant development, a description of which is contained in the knowledge base. The graph of states is based on a mathematical model of the "tube" of ranges in values of parameters at each stage during the normal development of the plant, as well as in case of dangerous weather events and going beyond critical boundaries, which leads to partial or complete loss of yield. The software implementation of the digital twin of the plant uses a conceptual (ontological) model for representing domain knowledge (ontology of crop production). The created ontological models of the development of plant varieties are loaded into a multi-agent system for planning stages of plant development and generating yield forecast for each stage, presented by its own software agent. A prototype of an intelligent system of the digital twin of the plant has been developed, in which, among others, the functions of modeling duration of plant development stages and forecasting crop yield are implemented depending on weather and climatic conditions and external events. The digital twin can help systematize, formalize and accumulate knowledge for decision-making in each farm and automate management processes when introducing precision farming technologies.

P. Skobelev (✉) · I. Mayorov · A. Zhilyaev · A. Tabachinskiy
Samara State Technical University, 443100 Samara Molodogvardeyskaya Str., 244,, Russia

E. Simonova
Samara National Research University, 443086 Samara Moskovskoe Shosse, 34,, Russia
e-mail: simonova@smartsolutions-123.ru

O. Goryanin
Samara Federal Research Scientific Center RAS, Samara Scientific Research Agriculture Institute Named After N.M. Tulaykow, 446250 Karl Marx Str., 41, Samara Region, Bezenchuk, Russia

V. Yalovenko
Peschanokopskaya Agrarian Laboratory, 347561 Rostov Region, Peschanokopskiy District, Razvilnoe Village Usadba SKhT Str., Building 3, Office 12,, Russia

A. G. Kravets et al. (eds.), *Cyber-Physical Systems*, Studies in Systems, Decision and Control 350, https://doi.org/10.1007/978-3-030-67892-0_8

Keywords Cyber-physical system · Digital twin · Multi-agent system · Ontology · Knowledge base · Decision making · Precision farming

1 Introduction

A report of the international research agency MarketsandMarkets determines the following leading segments in precision farming: Farm Labor Management and Crop Scouting (monitoring and forecasting the harvest) [1]. Global climate changes create risks for crop production, associated primarily with changes in average annual temperatures (in most cases—their increase) and precipitation (an increase in some regions and a decrease in others). Therefore, patterns of plant development, well known for the preceding decades, cease to be fulfilled. In addition, there is a growing impact of soil degradation and a number of other factors that disrupt the existing seasonal “recipes” for agrotechnical operations. Therefore, an increasingly urgent and significant problem for modern farms of precision farming is end-to-end enterprise management, in which the role of knowledge of qualified agronomists is significantly increasing as it is essential for managerial decisions on the choice of crops and technologies, planning crop rotation for the season and further daily planning agrotechnical measures taking into account the available human, material and technical resources.

The chapter proposes the creation of a digital twin (DT) of plant, intended for automated decision-making processes by agronomists when implementing precision farming technologies. The introduction of this chapter substantiates the relevance of developing a plant DT for management of a precision farming enterprise, which must be accurate not only “place-wise”, but also “time-wise”. The second chapter formulates the problem statement for developing a DT as part of an intelligent cyber-physical system for managing precision farming (ICPS) to support managerial decisions at all stages of crop development. The third chapter provides an overview of the existing developments of CPS and DT in precision farming. The fourth chapter defines an approach to the development of an intelligent digital twin (IDT) of plant-based on multi-agent technology and semantic representation of knowledge about stages of plant growth and development in the form of a plant production ontology. The fifth chapter proposes a new model and method for calculating the duration of stages and assessing the yield, which is based on the concepts and relations of ontology as an “explanatory dictionary” for agents. The sixth chapter describes the software package for DT implementation. In the seventh chapter, experiments are described to estimate the duration of plant development stages and changes in the yield of the selected crop—winter wheat—with the help of created plant DT. The eighth chapter discusses prospects for further development of plant DT and directions of its use as part of ICPS for precision farming.

2 Problem Statement

Let us define the "digital twin" of the plant as a software program that models stages of plant development depending on parameters of the external environment, which is synchronized with the growth of a real plant, for example, through regular inspections of crops by agronomists. Intelligent "digital twin" (IDT) is an intelligent system built on the basis of a specialized knowledge base about stages of plant development and methods of reasoning or decision-making. The plant IDT should accumulate, formalize and represent knowledge that is currently acquired by agronomists throughout their life, and should also allow for modeling the plant development under different conditions, at least at a qualitative level, acting as the basis for construction and functioning of the intelligent cyber-physical precision farming management system.

The knowledge of how each subsequent microstage of plant development should look like at any moment in time [2, 3] will help the agronomist to more accurately model and predict plant growth, plan and carry out special agrotechnical measures in time if there is a deviation of the actual development of the real plant from the "ideal" (norms). Moreover, this is possible from the earliest stages of such a deviation. The presence of plant DT in the CPS of precision farming management changes the approach to the management of machinery. ICPS should combine analysis of data on the state and progress of plant growth and development, obtained from agronomists, as well as data received from sensors in fields or unmanned aerial vehicles, with the weather forecast, creating and adaptively changing machinery routes. The digital twin of the plant as part of ICPS will provide agronomists with decision support based on formalized knowledge about the rate of plant development and real data on growth in microstages, setting the temporal pace and rhythm of the enterprise.

Thus, at present, the management of precision farming enterprises requires a model of control object—the "digital twin" of plant, which will be the basis for an intelligent cyber-physical system that determines the production plan of the enterprise.

3 Review of Existing Cyber-Physical Systems and Digital Twins in Precision Farming

An analysis of available Russian and foreign software developments of intelligent cyber-physical systems in agriculture and precision farming has shown that there are no ready-made solutions in this area. However, various cyber-physical systems are being actively developed to solve the problems of increasing the efficiency of managing an agricultural enterprise.

[4] describes the structure of a typical CPS for precision farming, which should consist of four parts: sensors and receiving units, computing units of the control center

for issuing commands to specialists and resources of a farm, as well as communication means.

The A-FARM solution represents a universal cyber-physical platform consisting of a set of microservices, implemented on the ATLAS framework, designed to deploy precision farming systems and manage data of complex agricultural production systems. However, the versatility of the platform and lack of knowledge base and decision support module is its significant drawback [5].

[6] describes the following projects: Sensing Change and Smart Water Management Platform (SWAMP), which combine software developments in agriculture and the Internet of Things (IoT) platform for irrigation management. Within the project, a CPS has been created, which can collect data on plants from sensors and display them on the dashboard, i.e. create a digital shadow that reflects the state of the object. However, this is not a digital twin of the plant. It also allows users to regulate watering. This is a research project and it has not been brought to industrial use.

Nowadays, in plant growing, industrial ICPS is almost absent, with the exception of one accelerating direction of their development for research laboratories and greenhouses, where such systems are already used to control and optimize the application of nano fertilizers, for example, a project of the Taiwanese company Landgreen Technology & Co [7].

[8] describes a project which made an attempt to develop a DT in the field of aquaponics based on a simulation model with feedback from sensors. The main challenge was the combination of a large number of interacting nonlinearly connected elements (hydroponics, aquaculture, and IoT systems). As a result, only two of a large number of parameters (pH and total dissolved solids) were successfully modeled using DT.

The Taiwan Agricultural Research Institute of the Council of Agriculture is developing the technology Digital Twin Solutions for Smart Farming in order to build up farmers' knowledge of production and provide intelligent, adaptive, and dynamic facility management tools, as well as proposals for decision-making in real-time [9]. It is fulfilled within the Smart Agriculture R&D program with the goal of combining human intelligence (HI) with artificial intelligence (AI). However, this development uses neural networks, and there is no plant model as such.

The development of a DT for a complex physical object and the processes occurring in it can be divided into two main stages. Initially, a mathematical model of a physical object and/or processes is built in the form of systems of algebraic or differential equations, the solution of which at a given moment in time gives the state of the object. In their absence, it can also be built based on the expert knowledge of agronomists. At the second stage, the created model is converted into digital form by creating a software program, for example, for the numerical solution of the above-mentioned system of equations, or for modeling the processes of the object's functioning, as well as forming the corresponding arrays of time series or databases for managing the object [10]. Further, to process this data, machine learning algorithms can be used, available as cloud services [11]. By processing data for each season, it is possible to estimate the harvest of the next year at the beginning of the next season more and more accurately—however, only if climatic conditions, characteristics of plant varieties, their cultivation technology, fertilizers, or plant protection products, do not change, which is, of course, almost impossible.

These models and methods can be used to accumulate certain statistics, but for the first step, a conceptual model is needed that will help formalize the expert knowledge of agronomists and make it applicable to obtain estimates of stage duration and forecast the yield depending on parameters of the external environment. Thus, the analysis showed that the creation of a data center and CPS for precision farming is an urgent and significant task, and its solutions are still being designed in order to ensure greater adaptability, scalability, fault tolerance, safety, and usability, surpassing the capabilities of embedded systems.

4 Approach to Developing Intelligent Digital Twin of Plant-Based on Multi-agent Technology

The model of stages of plant growth and development has been taken as the basis for developing the DT; wheat has been chosen as the object of research. It goes through about 100 microstages of plant development, organized into 10 main macrostages [2, 3]. These can be formalized for the purpose of more accurate and frequent control of plant development by continuous real-time comparison of the expected (average) and actual (observed) states at each step of cultivation. If one of the phases of plant development is delayed or values of controlled parameters are reduced at the exit of the phase, then the forecast of plant development for the next stages should also be recalculated, which, in fact, will determine the possible plan for future agrotechnical measures, for example, for application of fertilizers.

To implement such "wave" recalculations by stages, which can be started from any stage, if parameters of external environment change, multi-agent technology is proposed [12–14]. Currently, multi-agent technology is considered as a universal new approach to solving a variety of complex problems, such as planning and optimization of resources, pattern recognition, or design of complex products. However, applications for modeling living systems are not yet known.

Each stage of plant development should be represented by its own agent, which reads the weather forecast, performs calculations, rebuilds its forecast for values of output parameters, and then transmits the obtained data to agents of the next stages along the chain—until the final yield forecast from the last stage is obtained. After adjustment and approval by the agronomist, this forecast will lead to an adaptive change in composition, timing, and volume of fertilization and other agrotechnical operations performed by teams of workers, as well as unmanned vehicles and field robots in the future.

For the operation of plant stage DT agents, a knowledge base is required that deter-mines the graph of transitions by micro-stages of plant development, including parameters of each micro-stage, possible relations between them, signs of the average rate of plant development and possible deviations, temporal characteristics, etc. It is advisable to build the knowledge base operating with the ontology toolkit that has been actively developing recently within the Semantic Internet approach [15]. This requires the definition of classes of concepts and relations, specific to the description of plant development micro-stages, and their linking with existing ontologies in agronomy, plant physiology, etc. [16–18].

The general structure of the intelligent DT system for planning stages and forecasting plant yield is shown in Fig. 1. The system includes the following main modules:

1. Ontology editor—allows users to create an ontology for the development of plant stages;
2. The knowledge base—a repository of ontological models of plant varieties development, built on the basis of the ontology of plant stages development;
3. Knowledge base editor—allows users to create and edit ontological models of plant varieties development;
4. Multi-agent system (MAS) for plant growth and development planning—allows users to build a plant development plan and simulate the impact of different factors, as well as synchronize (adjust) the resulting plan according to the survey data from agronomists;

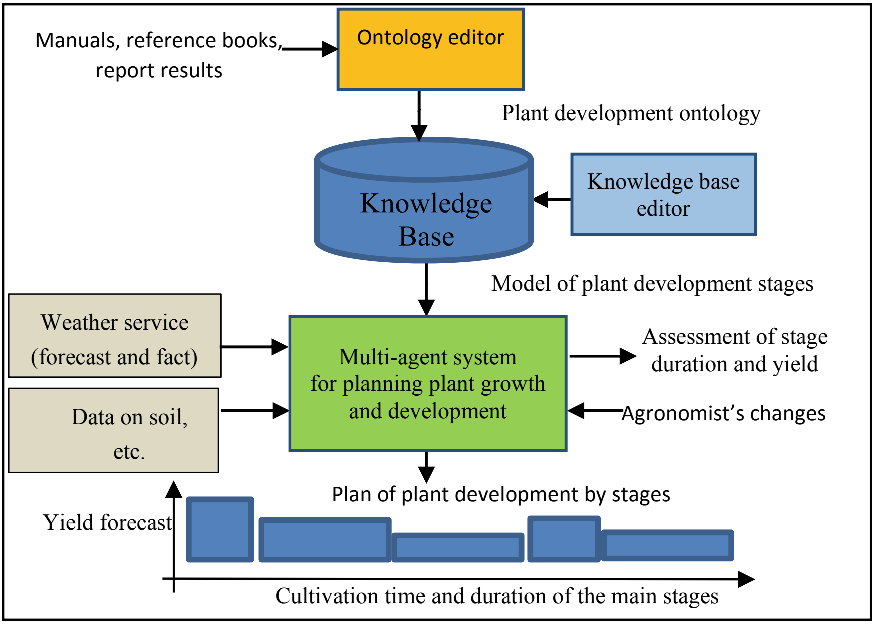

Fig. 1 The general structure of the intelligent DT system for planning stages and forecasting plant yield

5. Plant development plan by stages—shows the expected timing for the onset of each stage and the yield forecast.

Based on the constructed and always up-to-date plant development plan in a specific field, it is possible to plan measures for influencing the plant, for example, choosing the time points for fertilizing and the number of applied substances, as well as planning the work of precision farming machinery exactly on time [19]. A more detailed description of plant IDT within ICPS is described in [20].

5 Method for Assessing Duration of Development Stages and Forecasting Plant Yield Based on the "Tube" Parameters

In the developed intelligent DT system, a method is proposed for assessing the yield and duration of plant development stages based on the concept of a working "tube" of changing the most important parameters. The "tube" of parameters is understood as the ideal (nominal) range for each parameter (Fig. 2) that affects plant development. As the first step in describing plant growth and development at different stages, it is proposed to use linear relations of different types. This means that the deviation of the input parameter of the external environment from the ideal will cause a linear (proportional) change in the yield and timing of stages in one direction or another. If the parameter values go beyond the permissible limit values, then the plant, as a rule, dies, and the yield is lost. In some cases, for such a parameter, it is proposed to indicate the resulting effect through an expert "if-then" rule, which connects the input and output variables of the plant.

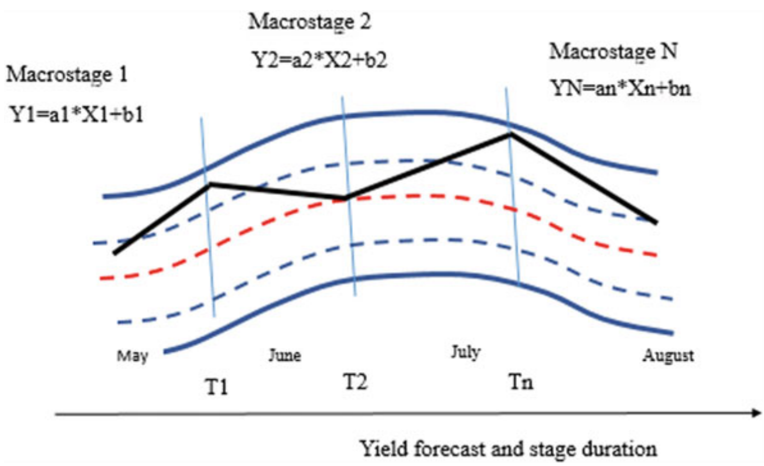

Fig. 2 Model of the range of changes in plant parameters ("tube")

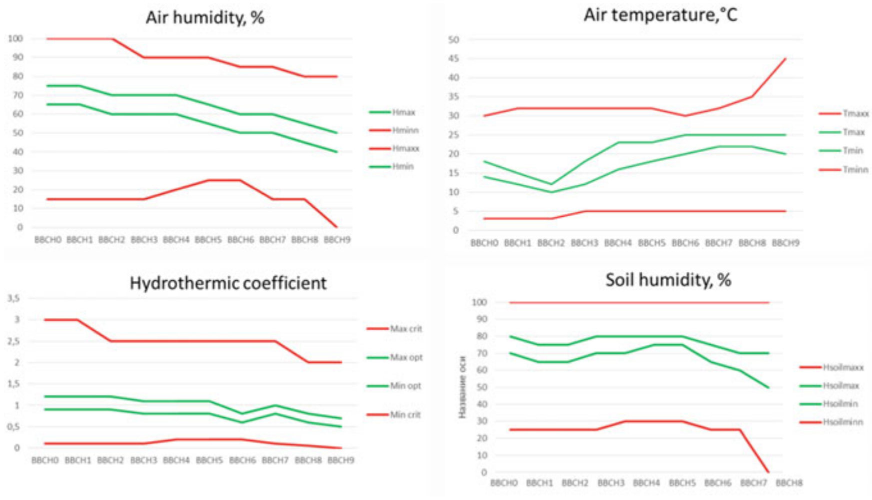

Fig. 3 Models of the "tube" for the main parameters of plant DT

As a result of a survey of agronomists and analysis of results, the following most important weather parameters for assessing the yield and duration of plant development stages have been identified: air temperature and humidity, soil moisture, hydrothermal coefficient. The ranges of these parameters have been collected and studied for winter wheat in the Samara region on the basis of available monographs and reference books and formalized for DT in the form of "tube" models (Fig. 3). The drop in crop yield due to unfavorable external conditions is proposed to be modeled using the "bonuses and penalties" function, where the initial estimate is taken as 100%.

The model for assessing the yield and duration of plant development stages is based on the concepts and relations of ontology as an "explanatory dictionary" for agents. At the top level, the digital twin ontology is defined, which consists of the most general and reusable classes of concepts and relations. In a specialized ontology of plant growing, domain-specific details are described, and instances of these concepts for specific plant varieties are formed in the knowledge base.

Figure 4 shows a fragment of the ontology of the digital twin of the plant. The key concept here is "Order" (for sowing) to obtain "Product" (yield), for which the plant needs to complete a sequence of certain "Tasks" (stages). For tasks, the rules for calculating the duration and values of parameters of the product (for example, assessing the yield) are determined. Compliance with these rules depends on parameters of the external environment (temperature, humidity, etc.), data on which are provided by third-party services. Environment parameters are tied to certain "locations" (fields) on which "orders" are placed, thus, each field and sowing forms its own external environment.

One of the concepts in ontology is the "Parameter calculation rule" (Fig. 5). Parameters are divided into two groups: environmental parameters and parameters

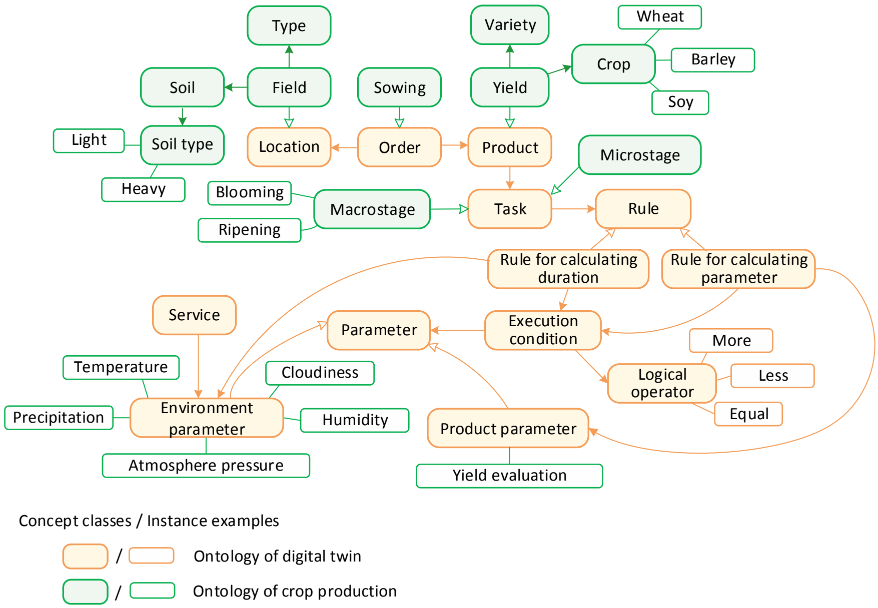

Fig. 4 Fragment of plant DT ontology

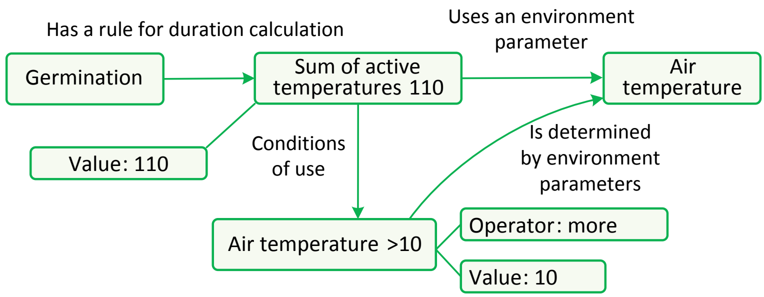

Fig. 5 The rule for calculating duration in ontology

of plant development (the “Product”). “Yield Assessment” is a “Product” parameter. “Stage duration”—a “Tasks” parameter. The rules for calculating the duration of a stage are set through the sum of a certain parameter, for example, temperature. Several “Condition” objects are associated with the “Parameter calculation rule” object. Each condition has a link to the parameter for which this condition is defined, an operator (>, <, =), and a value for comparison. Such a system is universal and can be used to calculate not only stage duration but also other parameters, for example, yield.

The specified data will be read by the stage agent for each stage to ensure appropriate calculations and transfer of results to subsequent agents in the chain.

6 Description of the Prototype Plant DT

To implement the proposed approach to creating plant DTs, an intelligent system has been developed. To work with the DT, an agronomist's workstation and mobile application for data synchronization with DT of real plants have been implemented. These tools allow for receiving data from weather services, entering DT data, entering events and viewing plans, receiving and adjusting data on stages of plant development and yield forecast, as well as modeling behavior of the plant in response to unforeseen events. Figure 6 shows the knowledge base and representation of a class in crop production ontology in the table and semantic format.

To obtain data about the external environment, a service registration mechanism is used. Each service implements an API interface that provides access to values of a certain parameter for the selected field at a specified time interval. To do this, it implements methods for receiving and setting parameter values (for entering external events). For example, the "weather service", included in the software package, unloads historical and forecast data from files of a structured format and associates them with parameters described in ontology, such as temperature, air humidity, cloudiness, etc. Data and results for all environment parameters defined in the model are plotted on a timeline.

The multi-agent system for planning stages of plant development performs formation and adaptive restructuring of the plant development plan, taking into account prevailing environmental conditions. The system creates and configures instances of agents, provides a multithreaded environment for their execution, determines

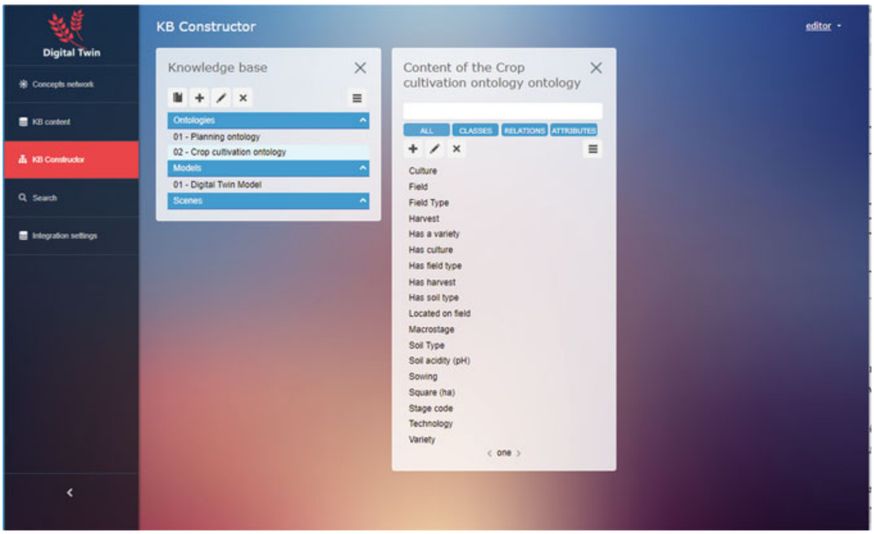

Fig. 6 Representation of a class in the knowledge base

the order and algorithm of their work, and interaction protocols. As a result of the module's work, the following plant development plans are formed:

1. Nominal—a plan for the development of plants in ideal conditions;
2. Preliminary—a plan for the development of plants in a specific field, built at the beginning of the season, at the time of sowing according to a long-term weather forecast;
3. Current (actual)—a plan that takes into account the actual fact of real weather for the current date and the nearest short-term forecast;
4. Modeled—a plan for assessing the possible consequences of weather changes or implementation of agricultural activities.

The constructed plans for each field can be exported to Excel for further processing.

7 Experiments with Plant DT

We will conduct experiments to assess the duration of plant development stages and changes in the yield of winter wheat. Let us create two fields—in the north of the Samara region (Klyavlino) and the south (Bezenchuk). On the tab displaying fields with DT attributes, we will set data on the average daily temperature, air humidity, and amount of precipitation for the entire time interval from sowing to harvesting. A fragment of data showing the differences in temperatures in the selected fields is given in Table 1.

Based on the temperature data, the MAS of plant stage planning determines the duration of crop development stages. Due to the difference in climatic conditions, there is a difference in crop development: in the southern part of the region, crops ripen in 323 days, and the northern part—in 342 days. It is possible to compare the duration of plant development by stages (based on the rule of temperature accumulation): in the southern field, faster development of wheat is observed already at the first stage.

The system also provides the ability to add events to simulate various situations, in response to which the planning system rearranges the plant development schedule. Let us add an event of temperature rise in September in the southern field (Fig. 7).

On the "Plan" tab, you can see that the seed ripening occurred two days earlier due to the reduction of the "Seedling growth" stage, in accordance with the rule described in the ontology.

The "Indicators" tab shows the change in yield estimate according to calculation rules using the "bonuses and penalties" functions (Fig. 8). The graph shows a gradual

Table 1 Average daily temperature in the selected fields

Date	05.09	05.11	05.01	05.03	05.05	05.07
Klyavlino (north)	11.5	2.5	−1.4	−0.6	18.7	22.2
Bezenchuk (south)	12.2	4.5	0.1	0.8	19.8	26.1

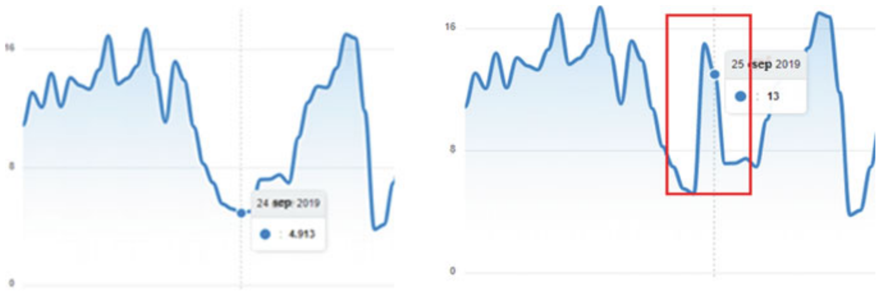

Fig. 7 Graph of air temperature changes before and after the temperature increase

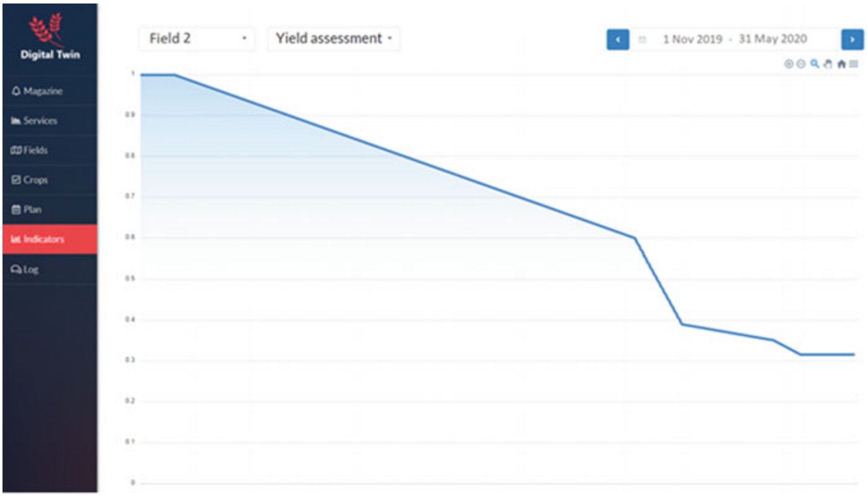

Fig. 8 Changes in duration of plant development stages

decrease in the yield estimate due to imposed fines, and for crops in various fields, different dynamics of yield changes can be observed.

8 Conclusions

The chapter discusses the development of plant DT, which is the main part of an intelligent cyber-physical system. It proposes a method for calculating stages of plant development and forecasting yield, based on the concept of the "tube" of plant parameters, an ontological model of a plant variety, and a multi-agent technology for associated calculation of stage parameters. The first DT prototype has been created, which makes it possible to carry out model experiments to determine the duration of plant development stages and yield forecast, setting various environmental conditions.

Further development of plant DTs will include the following additions: introduction of various regionalized wheat varieties into the knowledge base, development of a "tube" model of parameter values for them; development of a soil model, taking into account its granulometric composition, acidity, moisture, availability of nitrogen, phosphorus, exchangeable potassium; development of typical combinations of the DT model parameters; checking the performance of the DT system on data from 5–10 seasons; development of a plant model in terms of constructing agents of the root, stem, leaves, and fruits of a plant with the possibility of integration based on the developed method of knowledge about physical, chemical and biological dependencies.

Development of an ICPS for managing a precision farming enterprise on the basis of plant DT will allow for solving the urgent and significant problem of optimizing plant cultivation, taking into account variability of the plant habitat for the most efficient organization of the crop production process.

Acknowledgements This work has been supported by the Ministry of Education and Science of the Russian Federation within contract #075-15-2019-1691—unique project identifier RFMEFI60419X0224.

References

1. Precision farming software market. https://www.marketsandmarkets.com/Market-Reports/precision-farming-software-market-88781005.html. Accessed 15 July 2020
2. Zadoks growth scale (agriculture and food). https://www.agric.wa.gov.au/grains/zadoks-growth-scale. Accessed 10 Aug 2020
3. Uwe Meier (ed.): BBCH Monograph. Federal Biological Research Centre for Agriculture and Forestry. Berlin and Braunschweig, 2nd ed. (2001)
4. An, W., et al.: Agriculture cyber-physical systems. In: Cyber-Physical Systems, pp 399–417. Academic Press (2017)
5. Antonopoulos, K., Panagiotou, C., Antonopoulos, C.: A-FARM precision farming CPS platform. In: Proceedings of 10th IISA Conference, pp. 1–3. PATRAS, Greece (2019)
6. Gomes Alves, R., Souza, G., Filev, R., et al.: A digital twin for smart farming. In: 2019 IEEE GHTC Conference, pp. 1–4. IEEE, Seattle, WA, USA, 17–20 Oct. (2019)
7. Landgreen Technology&Co, Ltd. https://www.lgt.tw/. Accessed 12 Aug 2020
8. Ahmed, A., Zulfiqar, S., Ghandar, A, et al.: Digital twin technology for aquaponics: towards optimizing food production with dynamic data driven application systems. In: Tan, G., Lehmann, A., Teo, Y., Cai, W. (eds.) Methods and Applications for Modeling and Simulation of Complex Systems. AsiaSim (2019)
9. Digital Twin Solutions for Smart Farming. R&D World. https://www.rdworldonline.com/rd100/. Accessed 15 July 2020
10. Tao, F., Cheng, J., Qi, Q., et al.: Digital twin-driven product design, manufacturing and service with big data. Int. J. Adv. Manuf. Technol. **94**, 3563–3576 (2018)
11. Vasisht, D., Kapetanovic, Z., Won, J., et al.: FarmBeats: An IoT platform for data-driven agriculture. In: 14th USENIX NSDI 17 Symposium, pp. 515–529 (2017)

12. Müller, J., Fischer, K.: Application impact of multi-agent systems and technologies: a survey. In: Agent-Oriented Software Engineering, pp. 27–53. Springer, Berlin (2014)
13. Rzevski, G., Skobelev, P.: Managing Complexity. WIT Press, London and Boston (2014)
14. Skobelev, P.: Multi-agent systems for real time adaptive resource management. In: Leitão, P., Karnouskos, S. (ed.) Industrial Agents: Emerging Applications of Software Agents in Industry, pp. 207–230. Elsevier (2015)
15. Sicilia, M.-A. (ed.): Semantic Web. Handbook of Metadata, Semantics and Ontologies. World Scientific (2013)
16. Bei, Z., Zhao, G.: Application Study of Precision Agriculture Based on Ontology in the Internet of Things Environment, pp. 374–380. Springer (2011)
17. Rajbhandari, S., Keizer, J.: The AGROVOC concept scheme—a walkthrough. J. Integr. Agric. **11**(5), 694–699 (2012)
18. The Planteome database: an integrated resource for reference ontologies, plant genomics and phenomics. Nucleic Acids Research. D1168–D1180, vol. 46. Database issue, 23 November 2017. https://doi.org/10.1093/nar/gkx1152
19. Leung, J.: Handbook of Scheduling: Algorithms. Models and Performance Analysis. Chapman & Hall, CRC Computer and Information Science Series (2004)
20. Laryukhin, V., Skobelev, P., Lakhin, O., et al.: The multi-agent approach for developing a cyber-physical system for managing precise farms with digital twins of plants. Cybern. Phys. **8**(4), 257–261 (2019)

Forecasting the Future State of a Dynamic System by a Neural Network as a Task for a Cyber-Physical System

Sergey Masaev and Yuri Bezborodov

Abstract The issues of utility and the complexity of the use (opposition) of neural networks in management, the use of their prognostic abilities using the example of a nonlinear dynamic system with unknown environmental parameters as one of the tasks of the cyber-physical system are considered. The experiment uses a layered network structure with a teacher, an "anti-rotation" learning optimization algorithm, neurons with sigmoid nonlinearity, a fully connected network for predicting the state of a dynamic system. The activity of a special economic zone under the influence of environmental parameters was taken as a cyber-physical system. The parameters of the neural network were revealed: for which the weighting coefficients of the neurons closed the calculation at the saturation point and thereby led to its paralysis. Also, the modes of stalling the calculation into a local minimum or maximum of any local function of the system were revealed, depending on the period and the importance of this parameter in this period. As a result of the experiment, the cyber-physical system obtained a prediction of a set of output values from a set of input values based on the experience obtained by the neural network while minimizing the forecast discrepancy. A set of competencies is proposed to improve the accuracy of the neural network forecast and control the cyber-physical system (special economic zone).

Keywords Control theory · Dynamic system · Neural network · Special economic zone · Forecast · Cyber-physical systems

1 Introduction

The development of neural networks is associated with the formalization in 1943 of a mathematical model of a biological neuron by the names of W. McCallock and

S. Masaev (✉) · Y. Bezborodov
Siberian Federal University, 79 Svobodny, Krasnoyarsk 660041, Russia
e-mail: faberi@list.ru

Y. Bezborodov
e-mail: ybezborodov@sfu-kras.ru

A. G. Kravets et al. (eds.), *Cyber-Physical Systems*, Studies in Systems, Decision and Control 350, https://doi.org/10.1007/978-3-030-67892-0_9

W. Pitts, and in 1949 D. Habb outlined the law of learning. In 1962, F. Rosenblatt published his monograph with a detailed description of the perceptron, which had a significant impact on the development of the theory of neural networks. The use of neural networks is quite extensive due to the fact that a person experiences a natural craving to simplify the adoption of complex decisions in his activities. Human activity generates a large amount of data and repeated operations in management [1–25], and the use of a neural network allows you to perform these operations much orders of magnitude faster than the personnel of the organization.

The task of predicting the behavior of an economic object as a cyber-physical system remains relevant, taking into account the desire of participants to find a method that forms, and confirms the accuracy of their control. Classically, works in this area include A.G. Granberg, L.V. Kontorovich, V.V. Leontyev, V.F. Krotov [1–3], and foreign authors [4–10]. Often, the developed economic forecasts contradict each other and confuse managers. The recurring financial crises show the imperfection of the management methods used. The indicated activity gives rise to some repeating field of factual data, decisions, external environment, and controls [1–10]. Then we assume that the neural network is able to notice and predict such a field much faster than human analytical abilities, other analytical methods, and expect the benefits of such a forecast in the speed of decision-making, regardless of the complexity of the control object. The original approaches to the application of neural network planning are the works of the authors: Alex Krizhevsky, Ilya Sutskever, Geoffrey E. Hinton, and M.V. Pokrovskaya [11, 12].

The chaotic behavior of a complex economic object is described by the behavior of a deterministic system. In nonlinear dynamics methods, there are effective approaches to the analysis of phenomena (physics, chemistry, biology, sociology, economics) of time series even in experimental data [1–15].

However, in the analysis of complex economic objects, traditional mathematical methods of modeling are unacceptable. It is impossible to determine the parameters of nonlinear dynamics (the dimension of the attractor, entropy, Lyapunov parameters), due to the large dimension of the data of a large number of participants in this process and their display. We suggest that a neural network can help find the function of the dependence of the function $Y = F(x_1, x_2, \ldots, x_n)$ on the selected input parameters.

Objective: to investigate the prognostic ability of a neural network to predict the state of a nonlinear dynamic system (an economic object is a special economic zone) as a task of a cyber-physical system.

2 Initial Mathematical Formulation of System and Research Methodologies

The study uses a fully connected multilayer neural network where each neuron is connected to all the axons of the neurons of the previous layer and the first layer is connected to all inputs, respectively. The training of a single-layer network (single-layer perceptron) does not usually cause difficulties. It is not difficult to adjust synaptic connections, minimize error, for a known output of correct values.

It is impossible to train a multilayer perceptron in this way, since the required exact values of the output parameters of all layers are unknown and, therefore, the magnitude of the error is not indicative. In this case, it is necessary to select the output signals corresponding to the input for each layer of the neural network. Another way is to adjust the weight coefficients of the synapses, which allows you to find slightly variable parameters that affect the accuracy of training in the output parameters. The first two methods are very cumbersome to perform, so the third method will be used. The third method is the reverse direct feed of the signal from the output of the neural network to its inputs during normal operation (backpropagation).

Consider the third method in more detail.

By the least-squares method, the objective error function is minimized:

$$E(w) = \frac{1}{2}\sum_{j,p}(y_{j,p}^{(N)} - d_{j,p})^2, \tag{1}$$

where $y_{j,p}^{(N)}$—the actual state of the neuron j at the output of the neural N network layer with a signal at the input p of the image; $d_{j,p}$—parameters of the reference state of the same neuron.

All the outputs of the neurons in all images are added up. The gradient descent method is being implemented. The weighting coefficients are adjusted according to the formula:

$$\Delta w_{ij}^{(n)} = -\eta \cdot \frac{\partial E}{\partial w_{ij}}, \tag{2}$$

where $\Delta w_{ij}^{(n)}$—the weight coefficient of the synaptic connection connecting i the layer neuron $n-1$ to the layer j neuron n, η—learning rate factor, $0 < \eta < 1$.

Next, we count

$$\frac{\partial E}{\partial w_{ij}} = \frac{\partial E}{\partial y_j} \cdot \frac{dy_j}{ds_j} \cdot \frac{\partial s_j}{\partial w_{ij}}, \tag{3}$$

where y_j neuron output signal j, s_j—a weighted sum of neuron input signals j (activation function argument). We calculate the hyperbolic tangent (classical sigmoid)

$$\frac{dy}{ds} = 1 - s^2. \tag{4}$$

Then $\partial s_j/\partial w_{ij}$ is equal to the output of the neuron of the previous layer $y_i^{(n-1)}$.

Multiplier $\partial E/\partial y_j$ (3) can be imagined:

$$\frac{\partial E}{\partial y_j} = \sum_k \frac{\partial E}{\partial y_k} \cdot \frac{dy_k}{ds_k} \cdot \frac{\partial s_k}{\partial y_j} = \sum_k \frac{\partial E}{\partial y_k} \cdot \frac{dy_k}{ds_k} \cdot w_{jk}^{(n+1)}, \tag{5}$$

where the sum k of layer neurons $n + 1$.

From

$$\delta_j^{(n)} = \frac{\partial E}{\partial y_j} \cdot \frac{dy_j}{ds_j} \tag{6}$$

we have a recursive calculation of the layer $\delta_j^{(n)}$ value n from the value $\delta_k^{(n+1)}$ of the next layer $n + 1$

$$\delta_j^{(n)} = \left[\sum_k \delta_k^{(n+1)} \cdot w_{jk}^{(n+1)} \right] \cdot \frac{dy_j}{ds_j}. \tag{7}$$

Values for the course layer

$$\delta_l^{(N)} = (y_l^{(N)} - d_l) \cdot \frac{dy_l}{ds_l}. \tag{8}$$

Formula (2) is converted:

$$\Delta w_{ij}^{(n)} = -\eta \cdot \delta_j^{(n)} \cdot y_i^{(n-1)}. \tag{9}$$

By adjusting the weights, you can adjust the "dynamics" of the process, quenching sharp and unit jumps on the surface of the objective function, then in (9) the weight in the previous operation changes

$$\Delta w_{ij}^{(n)}(t) = -\eta \cdot (\mu \cdot \Delta w_{ij}^{(n)}(t-1) + (1-\mu) \cdot \delta_j^{(n)} \cdot y_i^{(n-1)}) \tag{10}$$

where μ—inertia coefficient, t—current iteration number.

Having considered the theoretical aspects of the calculation, we can identify an algorithm for calculating experimental data.

Step 1. The input of the neural network is set in the mode of its normal operation. Calculate output parameter values

$$s_j^{(n)} = \sum_{i=0}^{M} y_i^{(n-1)} \cdot w_{ij}^{(n)} \tag{11}$$

where M—the number of neurons in the $n - 1$ layer, taking into account a neuron with a constant output state of +1, which sets the displacement; $y_i^{(n-1)} = x_{ij}^{(n)}$—$i$ input of neuron j layer n.

$$y_i^{(n)} = f(s_j^{(n)}), \tag{12}$$

where f—sigmoid (13).

$$y_q^{(0)} = I_q, \quad (13)$$

where I_q—q input image vector component.

Step 2. Using the formula (8), determine $\delta^{(N)}$ for the output layer. According to the formulas (9) or (10), the weight of $\Delta w^{(N)}$ the layer N.

Step 3. Using formulas (7) and (9) (or (7) and (10)), calculate $\delta^{(n)}$, and $\Delta w^{(n)}$, respectively, for the remaining layers, $n = N - 1, \ldots, 1$.

Step 4. Perform weight adjustment

$$w_{ij}^{(n)}(t) = w_{ij}^{(n)}(t-1) + \Delta w_{ij}^{(n)}(t). \quad (14)$$

Step 5. Check the accuracy of the forecast. If the error is not within the requirements of the process control, then start step 1. Otherwise, the end of the algorithm.

Now it is necessary to move on to the dynamic characteristics of the observation object, for which the algorithm will be used in predicting its future state.

The dynamic object in the research is a special economic zone (hereinafter referred to as the SEZ). SEZ is a geographic unified territory on which various economic objects with preferential tax regimes perform economic activity [16–21].

The activity of the SEZ is given as a dynamic system through the equation

$$y(t) = A(t)x(t) + B(t)(x(t)u(t)) + v(t) \quad (15)$$

where $C = \{c_1, \ldots, c_i\}$—list of enterprises, I—their total number. $T = \{t : t = 1, \ldots, T\max\}$—many points in time (months).

$x(t) = \left[x_1^1(t), x_2^1(t), \ldots, x_N^i(t)\right]^T$—$N$—a vector of the economic parameter i of the enterprise, where $x_N^i(t)$ the value of the element n of costs/incomes (order of the Ministry of Finance of the Russian Federation of October 31, 2000 No. 94n and PBU No. 10/99) i enterprise at the time of t subspace X^i space Ω.

There is some g regulation for planning the allocation of available resources to functions x_i for an enterprise based on the values of past periods x^*, then $x = g(x^*)$ with criterion $X_i(t) = \sum_{t=1}^{T} \sum_{i=1}^{n} TX^i \to \max$.

The planning function $x^*(t)$ is performed according to past economic indicators with a lag of l periods $x(t) = g(x(t-l), \varepsilon(t))$, if $\varepsilon(t)$—the error is 0, then the plan is equal to the fact $x^*(t) = x(t)$ [18, 20].

$u(t) = \left[u_1(t), u_2(t), \ldots, u_M(t)\right]^T$—$M$—control vector, where u_i is the above control action by the state in the form of changes in tax interest rates (tax code of the Russian Federation), subsidies to the industry, and benefits aimed at increasing the gross national product (GRP) at the time of t u_1—income tax rate to the budget of the subject of the Russian Federation, u_2—income tax rate in the consolidated budget of the Russian Federation, u_3—transport tax, u_4—electricity cost, u_5—tariffs for transportation of products, u_6—the average value of contributions to the pension fund of the Russian Federation (PF RF), the territorial compulsory medical insurance fund (FOMS) of the Krasnoyarsk Territory, the Federal compulsory medical insurance fund (FFOMS), the social insurance fund of the Russian Federation (FSS RF), u_7—the rental price of land (land rent), u_8—the rental price of a forest plot (forest rent).

Control for the goals of the SEZ in general: $J = J(W) \to \inf_{W \in \mho^*}$, where q neural network prediction of the states of a dynamic system at different points in time t, $W = [w_{ij}]$—$Q \times N$—control structure matrix, where J is the target parameter of the system states for various q, defining a set of control matrices $\mho^*$, taking into account the restrictions and requirements for the dynamics of the process of control a neural network $u = W(q)y$.

$y(t) = \left[y_1(t), y_2(t), \ldots, y_K(t)\right]^T$—$K$—observation vector, where $y_i(t)$ observed values of GRP (gross regional product) at an instant t.

$v(t) = \left[v_1(t), v_2(t), \ldots, v_K(t)\right]^T$—interference acting on $x(t)$ or other known factors that we cannot influence: v_1—resource prices, v_2—outrunning salary growth (in the model +4% annually), v_3—investment from the owner, v_4—technological innovations, v_5—a movement of material flows, v_6—project logistics improvement measures, v_7—labor resources, v_8—technology prices, v_9—inflation (in the 4% model annually), v_{10}—dollar exchange rate (in the model it is assumed 70 rubles per dollar).

$A(t) - N \times N$—a matrix that determines the speed of development of the SEZ, through the use of financial resources and the impact of other activities. a_{ij}—the degree of influence of economic parameters on each other x_i on x_j.

$B(t) - N \times M$—matrix determining the development of the SEZ, when changing control rules. b_{ij}—the degree of influence of the control action $u_j(t)$ on the development of j the economic parameter of the enterprise $x_j(t)$.

$H(t) - K \times N$—matrix $H(t)$ of observations of the actual state, allowing to obtain an assessment of measures $y_j(t)$ by the actual level $x_j(t)$.

3 Interpretation and Discussion of Research Results

The task was solved by a neural network with a teacher. It is expected that a prediction of a set of output values over a set of input will be obtained based on the experience gained by the neural network while minimizing the prediction discrepancy. For training, we used the "anti-rotation" optimization algorithm BFGS (Gorban-Rossiev), neurons with sigmoid nonlinearity, and a fully connected network. The neural network solved the problem in the form of a vector predictor that provides the output of a vector of predicted numerical values from a set of input numerical values of actual data and values of control parameters.

An economic object—a special economic zone (SEZ) of eight enterprises (an example of the structure and operating modes of such enterprises is disclosed in separate works [21–25]) 9.6 million values were modeled at each time step. The

SEZ control dimension was reduced through the matrix of the control structure W. The SEZ as a nonlinear dynamic system is characterized by a sample $(\bar{Y}_k, \overline{U}_{k+1})$ of 45 values over a 3-year time interval. The calculation is presented see tab. 1 and see Fig. 1.

It was found that the neural network, for a given sample of values, from one and four layers of neurons, in principle, is not able to solve the forecast task posed in the experiment. With the network, parameters indicated see tab. 1, lines 1, 2, 3, and 5, calculations were paralyzed. Based on (7) and (8), neural network learning stops. An exception is training a network with a parameter of 0.5 sigmoid neurons and a council of 5 neural networks with 4 layers of 100 neurons per layer and there are two reasons for this.

Table 1 Predictive ability of a neural network

No.	Number of hidden layers	Number of neurons in one layer	Sigmoid neuron parameter	The ability to calculate a neural network (well no)
1	2	100	norm	The network is paralyzed
2	3	100	norm	The network is paralyzed
3	3	100	0.7	The network is paralyzed
4	4	100	0.5	Possibly
5	4	100	0.7	The network is paralyzed
6	Council of neural networks			Possibly

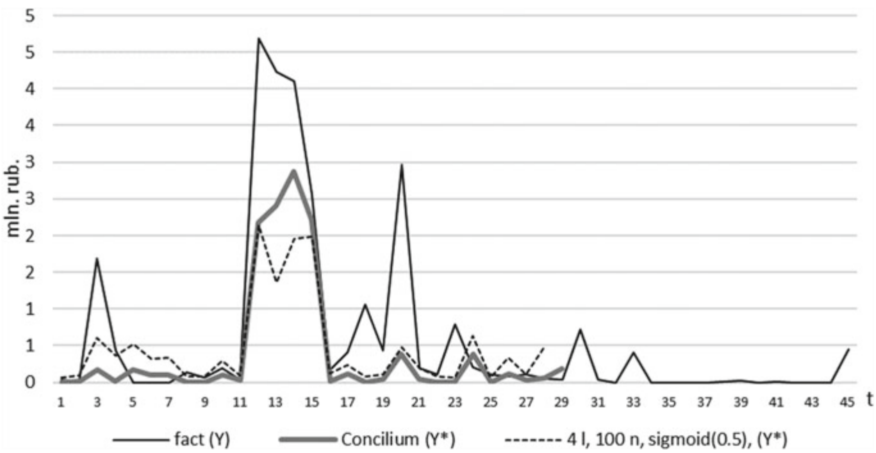

Fig. 1 Predicted trajectories found by the non-network

The first reason—the values of the weight coefficients shifted the resulting values to the saturation point. Based on (7) and (8), neural network learning stops.

The second reason is that the system falls into local minima in the economic object of any function. This is understandable because in the economic object there are incomes and expenses, and the economic object achieves its effectiveness by engaging in certain important functions in any period.

To obtain global optimization, the sigmoid with the exponent was transformed to

$$f(x) = -0.5 + 1/(1 + e^{-\alpha \cdot x}).$$

The hit in the local minimum was excluded by fixing the weight coefficients. Then we increased η to start the gradient descent from a new point. When repeating the calculation algorithm, the neural network came, with a slight deviation, to one result. Then we can say that a global minimum or maximum of a dynamic object is found and our forecast is conditionally correct.

Good accuracy of forecasting the parameters of the special economic zone of 15–17% was achieved. Some SEZ parameters were not predictable or were forecasted with an error of 85–95%, which leads to a situation where the costs of controlling and finalizing the forecast by the neural network exceed the reasonable time for generating the forecast by ten times limit their use and cause criticism from the management. It turns out that when finalizing the forecast for individual parameters, it is necessary to conduct a whole scientific study that exceeds the budget and the time of the process of controlling a special economic zone.

Here, it is worth noting separately that the observed parameters that have single bursts (random from the point of view of the experiment) and, accordingly, do not have clear observation intervals of the phenomena, the neural network predicts poorly or does not predict their value at all. Due to the fact that the factor (4) dy_j/ds_j is a derivative of this function with respect to its argument. The values of the output parameters, i.e. their function should be determined on the entire abscissa axis. Therefore, parameters with constant seasonal fluctuations are predicted much more accurately.

In this regard, in order to avoid rejection of the neural network (confrontation) and the use of cyber-physical systems by the management, the most important task is to increase staff competencies at the level of deputy heads of an economic facility due to the following competencies: to be able to process large volumes of information, apply experience from one area to another, understand interdisciplinary the relation-ship of the managed object, synthesize professional knowledge and experience, create new applied knowledge in a specific field and/or at the junction of areas, identify sources (search for information) necessary for the development of activities, which will allow decentralizing the use of neural network planning in the areas of work of a special economic zone and its de-departments. These operations will improve the accuracy of forecasting and managing SEZ as a cyber-physical system.

4 Conclusion

Decentralization of responsibility in the cyber-physical system for the result of neural network forecasting in a dynamic system (economic object) allows and determines their use "tomorrow" and "the day after tomorrow" in large (multidimensional) systems for solving complex control problems.

The obtained accuracy of the forecast, the state of the SEZ, is 80–95%. The forecast accuracy is 15% higher than similar calculations at an economic facility (enterprise) 57–70%, performed in a separate study [12].

The goal of the work, to investigate the prognostic ability of a neural network to predict the state of a nonlinear dynamic system (an economic object is a special economic zone) as a task of the cyber-physical system has been achieved.

References

1. Granberg, A.G.: Vasily Leontiev in world and domestic economic science. Econ. J. VSHE: Zhurnal **3**, 471–491 (2006)
2. Kantorovich, L.V.: Mathematical and Economic Work, pp. 760. Nauka, Novosibirsk (2011)
3. Krotov, V.F.: The Basics of Optimal Management, pp. 430. Graduate School (1990)
4. Chen, H., Li, B.Y., Zhang, B.W., Zhang, L.: Global finite-time partial stabilization for a class of nonholonomic mobile robots subject to input saturation. Int. J. Adv. Rob. Syst. **12**(11), 159 (2015)
5. Haddad, W.M., L'Afflitto, A.: Finite-time partial stability and stabilization, and optimal feedback control. J. Franklin Inst. **352**(6), 2329–2357 (2015)
6. Binazadeh, T., Shafiei, M.H., Bazregarzadeh, E.: New approach in guidance law design based on finite-time partial stability theorem. J. Space Sci. Technol. **8**, 1–7 (2015)
7. Golestani, M., Mohammadzaman, I., Yazdanpanah, M.J.: Robust finite-time stabilization of uncertain nonlinear systems based on partial stability. Nonlinear Dyn. **85**(1), 87–96 (2016)
8. L'Afflitto, A.: Differential games, finite-time partial-state stabilization of nonlinear dynamical systems, and optimal robust control. Int. J. Control **90**(9), 1861–1878 (2017)
9. Rajpurohit, T., Haddad, W.M.: Stochastic finite-time partial stability, partial-state stabilization, and finite-time optimal feedback control. Math. Control Signals Syst. **29**(2), 10 (2017)
10. Jammazi, C., Abichou, A.: Controllability of linearized systems implies local finite-time stabilizability: applications to finite-time attitude control. J. Math. Control. Inf. **35**(1), 249–277 (2018)
11. Krizhevsky, A., Sutskever, I., Hinton, G.: ImageNet classification with deep convolutional neural networks. Neural Inf. Process. Syst. **25** (2012). https://doi.org/10.1145/3065386
12. Pokrovskaya, M.V.: Creation of a subsystem for forecasting production volumes as part of an automated control system of an industrial enterprise using an apparatus of neural networks abstract: Vologda (2006)
13. Ustugova, S., Parygin, D., Sadovnikova, N., Finogeev, A., Kizim, A.: Monitoring of social reactions to support decision making on issues of urban territory management. In: Procedia Computer Science: Proceedings of the 5th International Young Scientist Conference on Computational Science, YSC 2016, vol. 101, pp. 243–252. Krakow, Poland, Elsevier (2016). https://doi.org/10.1016/j.procs.2016.11.029
14. Parygin, D.S., Malikov, V.P., Golubev, A.V., Sadovnikova, N.P., Petrova, T.M., Finogeev, A.G.: Categorical data processing for real estate objects valuation using statistical analysis. In: Journal of Physics: Conference Series: Proceedings of the International Conference on Information

Technologies in Business and Industry 2018, vol. 1015, Art. No. 032102, pp. 1–6. Tomsk, Russia, IOP Publishing (2018). https://doi.org/10.1088/1742-6596/1015/3/032102
15. Donchenko, D., Ovchar, N., Sadovnikova, N., Parygin, D., Shabalina, O., Ather, D.: Analysis of comments of users of social networks to assess the level of social tension. In: Procedia Computer Science: Proceedings of the 6th International Young Scientist Conference on Computational Science (YSC 2017), vol. 119. pp. 359–367. Kotka, Finland, 1–3, Elsevier (2017). https://doi.org/10.1016/j.procs.2017.11.195
16. Rahoof, A.T., Arul, P.G.: An evaluation of special economic zones (SEZs) performance post SEZs Act 2005. Univers. J. Ind. Bus. Manag. **4**(2), 44–52 (2016)
17. Wei, L., Hong-Bo, S., Zhe, Z., Sang-Bing, T., Yuming, Z., Quan, C., Jiangtao, W.: The development evaluation of economic zones in China. Int. J. Environ. Res. Public Health **15**(56), 1–14 (2018)
18. Jenkins, M., et al.: Export Processing Zones in Latin America. Harvard Institute for International Development, Development Discussion Paper No. 646 (1998)
19. Schminke, A., Van Biesebroeck, J.: Using export market performance to evaluate regional preferential policies in China. Rev. World Econ., Kiel Inst. World Econ. (Springer; Institut für Weltwirtschaft) **149**(2), 343–367 (2013)
20. Zohir, S.C.: Gender balance in the EPZ: a socio-economic study of Dhaka export processing zone in Bangladesh. Bangladesh Institute of Development Studies (2001)
21. Masaev S. N.: Problemy upravleniya osoboj ekonomicheskoj zonoj v rezhime sankcij (Problems of management of special economic area in the sanction regime), vol. 5, pp. 57–60. Informatization and Communication. Moscow, Russia (2019)
22. Harlov, Y., Masaev, S.: «Mastier» LLC jointly develops priority investment projects in the Russian Federation in the field of wood further processing. Industrialized wood deep processing organization. Trade Representation of the Russian Federation in the People's Republic of China, Beijing, p. 32. unpublished. http://www.russchinatrade.ru/assets/files/ru-offer/OOO_master.pdf (2019)
23. Masaev, S.N.: Evaluation of the personnel management strategy of a resident of a special economic zone as a task of modeling the state of a multidimensional dynamic system, vol. 4, pp. 71–90. Informatization and Communication. Moscow, Russia (2019)
24. Masaev, S.N.: Program complex for evaluating the effectiveness of special economic zones taking into account infrastructure projects for the construction of railways. International scientific-practical conference "Transport of Russia: problems and prospects—2019". St. Petersburg: IPT RAS and FSBEI HE St. Petersburg University of the State Fire Service of the Ministry of Emergencies of Russia (2019)
25. Masaev, S.N.: Destruction of the Resident Enterprise in the Special Economic Zone with Sanctions, 2019 Twelfth International Conference "Management of large-scale system development" (MLSD), Moscow, IEEE, Russia, pp. 1–5 (2019). https://doi.org/10.1109/mlsd.2019.8910997

Computer Linguistic for Cyber-Physical Systems

Predicting Research Trend Based on Bibliometric Analysis and Paper Ranking Algorithm

Viet T. Nguyen, Alla G. Kravets, and Tu Q. H. Duong

Abstract One of the most essential investigation demands in the computational evaluation of scientific publications is whether the immense collections of scientific papers hold significant indication about the dynamics included in the development of science; signs that may help predict the growth and decline of scientific methods, ideas, and even fields. The research presented in this paper focuses on a general approach to analyze and predict the thematic evolution of a given research field by pointing out uptrend keywords. In particular, we propose a dataflow of method and a paper ranking algorithm. This results in ranking papers, from there we select the best 20 papers and extract from them meaningful keywords (concerned with research field/subfield, algorithms, methods, etc.). After that, we formulate the final score for keywords by summing up scores of papers containing them and then group the obtained results by year. Therefore, we can demonstrate scores of keywords through years in time series and observe which keywords are displaying an upward tendency. As a case study, the proposed approach is applied to analyze the thematic evolution of the Artificial Intelligence research field in the period 2005–2016 from the Web of Science database. Ultimately the method is evaluated by checking occurrences of predicted keywords in true prominent keywords in timeframe 2017–2019 and provides precision 73.33%.

Keywords Trend research prediction · Thematic evolution · Bibliometric analysis · Paper ranking · Artificial Intelligence · Web of Science Database

---

V. T. Nguyen (✉) · A. G. Kravets · T. Q. H. Duong
Volgograd State Technical University, Volgograd, Russia

A. G. Kravets
e-mail: agk@gde.ru

V. T. Nguyen
Training Department, Pham Van Dong University, Quang Ngai, Vietnam

A. G. Kravets
Dubna State University, Dubna, Moscow Region, Russia

A. G. Kravets et al. (eds.), *Cyber-Physical Systems*, Studies in Systems, Decision and Control 350, https://doi.org/10.1007/978-3-030-67892-0_10

1 Introduction

The amount of scientific publications is growing at a fast pace and it becomes increasingly difficult to remain up to date with everything that has been published. Moreover, the importance of experimental contributions has resulted in large and fragmented research directions. This interferes in accumulating intelligence and actively collecting relevant achievements through a collection of previous research documents. Hence, literature reviews are progressively undertaking a principle role in synthesizing previous research results to effectively utilize the state of the art knowledge base, advance a direction of research, and supply evidence-based comprehension of the practice, expert support, and professional judgment [1].

Scholars utilize various quantitative and qualitative literature reviewing methods to digest and systematize previous findings. Among these, bibliometrics is a transparent, systematic, and reproducible inspection process form by the statistical measurement of scientific activities, scientists, or overall science [2]. Unlike other approaches, bibliometrics generates more reliable and objective analyses. The immense quantity of conceptual developments, new research information, and experimental data is the condition where bibliometrics becomes advantageous by rendering a structured analysis to a huge set of data, to forecast researched themes trends over time, detect shifts in the boundaries of disciplines, to identify the most productive institutions and scholars, and to represent the "wide picture" of the present research. Numerous research fields employ bibliometric approaches to discover the impact of a set of scholars, the impact of the field, or the impact of specific papers [3–5]. Furthermore, the ability to predict research trends in advance would likely revolutionize the strategy science is carried out, e.g., by enabling funding agencies to optimize the allocation of resources towards promising research areas [6].

For this reason, the main aim of the paper is to present a general approach to analyze and predict the thematic evolution of a given research field by pointing out uptrend keywords. This approach presents a dataflow of the method, a paper ranking algorithm, and science mapping for detecting and visualizing thematic research trends. As a case study, the proposed approach is applied to analyze the thematic evolution of the Artificial Intelligence (AI) research field. The rest of the paper is organized as follows: Sect. 2 introduces bibliometric analysis, collected dataset, and some derived results from bibliometrics. Section 3 describes a method for paper ranking, adopts the proposed method to collect meaningful keywords, and illustrates thematic research trend results by pointing out uptrend keywords; then the method is evaluated by detecting occurrences of predicted keywords in true prominent keywords set. Finally, Sect. 4 presents the conclusion and future directions of the study.

2 Analyzing Research Trends Based on Bibliometric Analysis

There are two important procedures in bibliometrics: performance analysis and science mapping. Performance analysis focuses on evaluating scientific element groups (researchers, departments, universities, and countries) and their activity impact on bibliographic data. Science mapping is a graphic representation of how academic papers, authors, disciplines, and fields are related to one another [7]. Standard workflow for science mapping comprises four principal steps: Study design, Data collection, Data analysis, and Data visualization [8].

2.1 Study Design

In the study design, scholars specify the research questions and select suitable bibliometric methods that can solve the problems. By utilizing bibliometrics, three general kinds of research questions for science mapping can be: (i) discovering the intelligence base of a topic or research field and its knowledge structure; (ii) studying the research front (or conceptual structure) of a topic or research field; and (iii) constructing a social network structure of a specific scientific community. In this paper, the second (ii) question is considered in detail.

2.2 Data Collection

Data collection consists of three steps. The first step is data retrieval. Numerous online bibliographic databases, where metadata of academic publications are stored, can be sources of bibliographic information, e.g., Scopus (scopus.com), Clarivate Analytics Web of Science (webofknowledge.com), Google Scholar (scholar.google.com). Other analogous databases were generated for specific disciplines (e.g., Data System, Astrophysics, Medline), patent data, and digital libraries (e.g., CiteSeerXPatent, arXiv, DBPL).

The second step is data conversion in which scholars need to convert data into an appropriate format for the adopted bibliometric tools.

The final step is data cleaning. The result value depends on the quality of the data. Various preprocessing methods can be utilized, e.g., detecting duplicates and misspelled words, removing punctuations. Despite most of the bibliometric data are dependable, cited references may include various versions of the same publication and multiple alternative names of an author. Moreover, cited journals can also be presented in slightly varied forms. Books may have several editions, which will be cited as different references.

In this paper for the case study, we select Clarivate Analytics—Web of Science core collection for the bibliometric database. Then a search with keywords "Artificial intelligence" was implemented with timespan from 2005 to the 2016 year and category filter "Computer science Artificial intelligence". At the time of writing this paper, 6696 publication results were scraped for our experiment. Furthermore, 3211 publications of timeframe 2017–2019 were collected for evaluating the proposed method.

2.3 Data Analysis

Data analysis includes descriptive analysis and network extraction. Examples of descriptive analysis are topmost cited references or authors, topmost frequent keywords, authors' dominance ranking, topmost productive author, etc. Figure 1 demonstrates the top 10 most frequent author keywords of the AI field in timeframe 2005–2016, which was obtained by using R-package Biblioshiny [9].

At the same time, several approaches have been advanced to extract networks utilizing different units of analysis. For instance, the co-word analysis adopts the most substantial words of documents to explore the conceptual structure of an examined field. It is the only method that exploits the plain text of documents to establish a

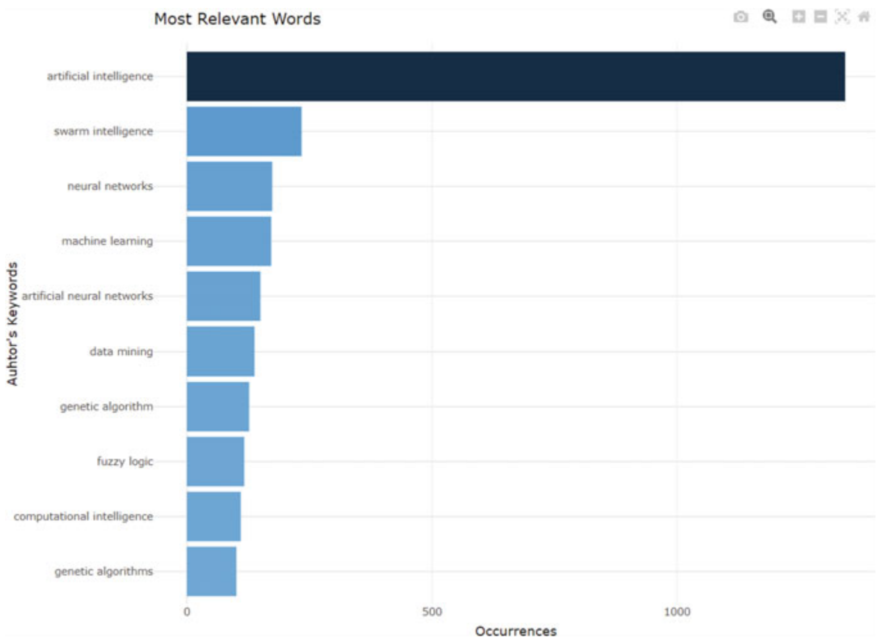

Fig. 1 Top 10 most frequent author keywords of the AI field in 2005–2016

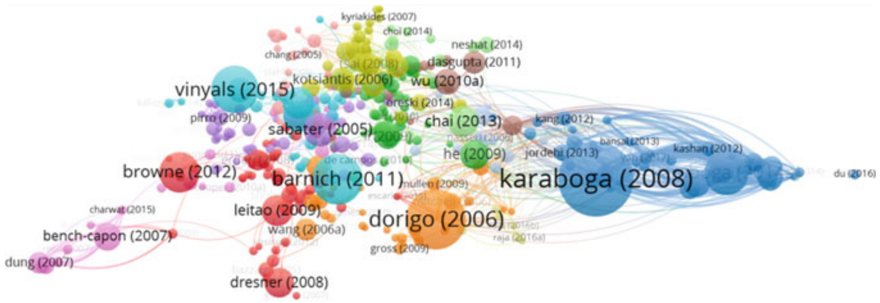

Fig. 2 Bibliographic coupling network of AI field in period 2005–2016

similarity measure, while the others link publications via citations. Co-word analysis generates semantic maps of a field that help understand its cognitive structure. This analysis can be applied for paper keywords, full texts, or abstracts.

On the other hand, citation analysis is the most usual analysis in bibliometrics. It utilizes citation amounts as a similarity measurement between documents, journals, and authors. Citation analysis consists of the direct citation, bibliographic coupling, and co-citation analysis. Examples are author coupling, author co-citation, journal coupling, and journal co-citation, etc.

More specifically, bibliographic coupling analyses the citing documents, whereas co-citation analysis examines the cited ones. Despite the fact that bibliographic coupling is advantageous in exploring the association between research groups [10], co-citation analysis observed over time slices is also useful in discovering a shift in schools of thought and paradigms. The selection of the method to utilize depends on the purposes of the analysis. Typically, co-citation analysis is executed for mapping older papers (prospective analysis—it is dynamic and best exploited in various time slices), whereas bibliographic coupling is utilized to represent an existing research front (retrospective analysis). VOSviewer software [11] is used to demonstrate a bibliographic coupling network of collected papers with a minimum number threshold of citations 30 (Fig. 2).

2.4 Data Visualization

Analysis methods allow us to extract valuable knowledge from data and to demonstrate it according to intuitive visualizations or maps such as social networks, dendrograms, and bi-dimensional maps. Network analysis allows performing a statistical analysis upon the generated maps to present numerous measures of the entire network, measures of the relationship, or the overlap of the various detected clusters.

Visualization techniques are employed to demonstrate the science map and the outcome of diverse analyses. For instance, networks can be presented by thematic areas [12], or by maps in which the distance between elements displays their similarity in VOSviewer software [13]. In particular, by using VOSviewer a co-occurrence analysis map can be constructed and depicted in Fig. 3 to demonstrate keyword prominence detection and their interrelation (minimum number of occurrences is 20).

On the other hand, to illustrate the research evolution in sequential time periods, cluster strings [14] and thematic areas can be utilized. Figure 4 shows thematic areas evolution of author keywords in consecutive time periods over collected data of the AI field, which is derived from R-package Biblioshiny.

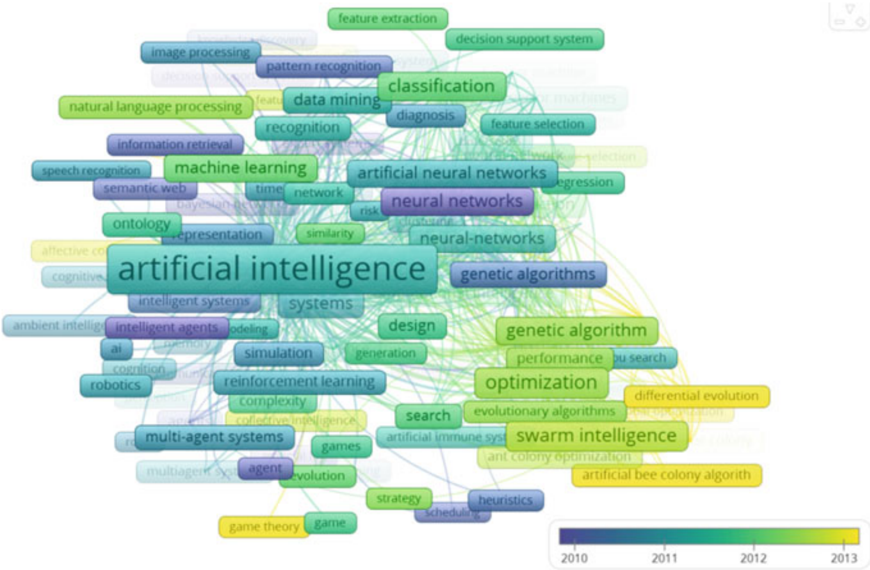

Fig. 3 Co-occurrence map of keywords for detecting prominent themes in years

Fig. 4 Thematic evolution map of author keywords

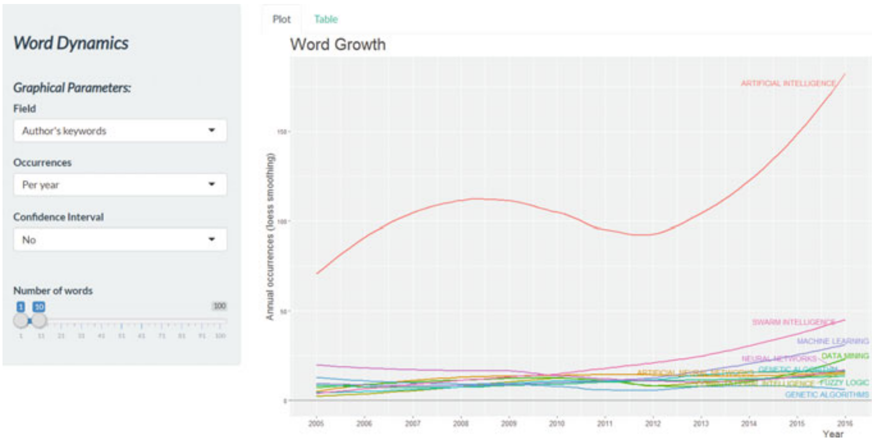

Fig. 5 Author keywords dynamics in the AI papers from 2005 to 2016

Alternatively, temporal analysis performs the conceptual, intellectual, or social evolution of the research field by detecting seasonality, patterns, trends, and outliers. Among them, burst detection is a temporal analysis that discovers feature, which have notable intensity in various time periods [15]. To demonstrating thematic intensity in time periods, Fig. 5 represents author keywords dynamics of the AI field in timeline 2005–2016 derived from R-package Biblioshiny.

3 Predicting Research Trend Based on Paper Ranking Algorithm

To the best of our knowledge, the drawback of mentioned techniques is not aggregating together Titles, Abstracts, Author keywords, and Keywords plus (in Web of Science, Keywords Plus are index terms automatically generated from the titles of cited articles and are ordered from multi-word phrases to single terms). Moreover, the expectation is analyzing and synthesizing all aspects of the most prestigious and influential papers (impact factor). On the other hand, the research trend topics and word dynamics are simply identified by word frequency, not considering the impact factor of papers containing these keywords. Additionally, all mentioned above results do not indicate clearly thematic evolution through timespan.

Subsequently, we propose a new method of tracking scores of keywords in consecutive time periods to help predict research trends. The dataflow of the proposed method is illustrated in Fig. 6.

In the following, we describe in detail some of the most important parts of our method.

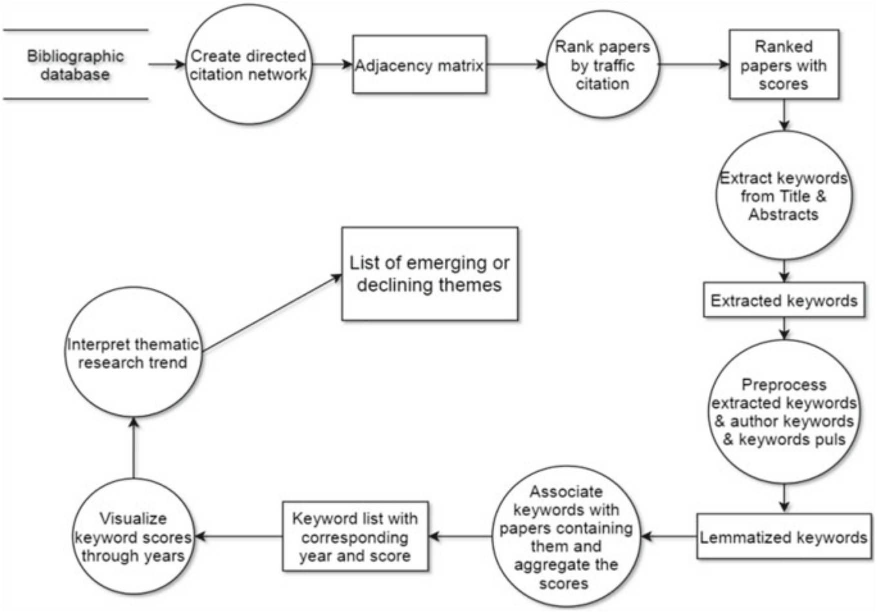

Fig. 6 Dataflow diagram of the proposed method

3.1 Paper Ranking Algorithm

Klavans and Boyack [16] recently recommended that direct citations are more reliable in pointing out a research front than co-citation and bibliographic coupling. Subsequently, this ranking method is based on the graph structure of the direct citation network formed by research papers. The impact of a scientific publication is approved fair by the peer vote, in other words being cited by the others. Research papers cite the others, from which they obtain inspiration, rationales and there is a well-connected graph structure within the network of these academic documents. The importance of a research paper is directly proportional to the importance, quality, and amount of the ones that cite it. We use this assumption in our algorithm to rank the research papers by assigning each of them an authoritative (impact) score.

Let G be the directed citation graph of n papers and m citations. Then $V(G)$ is the set of papers and $E(G)$ *i*s the set of citations. Furthermore, let $p_i, p_j \in V(G)$, then paper $\mathrm{p_i}$ cites paper p_j if $e = \{p_i, p_j\} \in E(G)$. Using this graph notation to describe a paper p, the references in paper p's reference list is the set $C_G^+(p) = \{r \in V(G) | (p, r) \in E(G)\}$, the capacity of which is identified by the out-degree of a vertex $p : O(p)$—number of vertices adjacent from p.

While the number of citations that paper p received is $I(p)$—the number of vertices adjacent to p, which is capacity of the set $C_G^-(p) = \{r \in V(G) | (r, p) \in E(G)\}$. It follows that $|C_G^-(p)| = I(p)$, and $|C_G^+(p)| = O(p)$.

In the following we describe how to compute paper ranking, which is denoted by vector $\vec{\boldsymbol{r}} = [r_1, \ldots, r_i, \ldots, r_n]$, where r_i is authoritative (influential) score of paper i. The normalized constrain is: $\sum_{i=1}^{n} r_i = 1$.

The initial scores at iteration t = 0 are : $r_i^{(t=0)} = \frac{1}{n}, i = \overline{1, n}$

At each iteration (t) the paper score r_i is calculated by formula:

$$r_i^{(t)} = \sum_{j \in C_G^-(i)} \frac{r_j^{(t-1)}}{O(j)}$$

$$r_i^{(t)} = r_i^{(t)} + \frac{1 - \sum_{k=1}^{n} r_k^{(t)}}{n}$$

The loop stops when score vector $\vec{\boldsymbol{r}}$ converges with a predefined precision ε, this is equivalent to:

$$\left\| \vec{\boldsymbol{r}}^{(t)} - \vec{\boldsymbol{r}}^{(t-1)} \right\| < \varepsilon$$

Furthermore, we need to take into account the time characteristic in research papers ranking to diminish the disadvantage against the recent documents which receive less time for being investigated and consequently less cited by the scholars when comparing to the older papers. Based on the idea of m-index [17], which is defined by h/y, where h is h-index, y is the number of years since the first published paper of the scientist, to get the final scores we divide paper scores by their corresponding ages (a factor of 100 was adopted so that the later visualization was more visual):

$$s_i = 100 \frac{r_i}{y_i}, \ i = \overline{1, n}$$

where s_i : final paper score, r_i : paper score after exiting the iteration, y_i: paper age.

3.2 Predicting Research Trend of Artificial Intelligence

Applying the proposed algorithm on collected data of the AI field in the timeline 2005–2016 to rank papers, we get scores of each paper and sort them by scores in descending order, which is represented in Table 1.

Then we create a corpus by combining Title, Abstract, Author keywords, Keyword plus of top 20 papers from above ranking table. Afterward, we use functionality “Create a map based on text data” in VOSviewer software to create a term co-occurrence map based on the derived corpus and then extract all terms (keywords)

Table 1 Top-20 best (influential) papers obtained by proposed algorithm

1	Authors	Title	Source	Year	doi	cit_score	PaperRank	Score	Abstract	Author_keywords	Keyword_plus
2	karaboga, d; ba:	on the performance of artificial	applied soft cor	2008	10.1016/j.aso	117	0.01757	0.19525	Artificial bee colony (ABC) algorithm is a	swarm intelligence;	DIFFERENTIAL EVOLU
3	karaboga, d; gor	a comprehensive survey: artifici	artificial intellig	2014	10.1007/s104	31	0.00163	0.05449	Swarm intelligence (SI) is briefly defined	Swarm intelligence;	QUANTUM EVOLUTI
4	singh, a	an artificial bee colony algorithr	applied soft cor	2009	10.1016/j.aso	35	0.00341	0.04263	Given an undirected, connected, weight	Artificial bee colony	ABC ALGORITHM; OP
5	browne, cb; pov	a survey of monte carlo tree sea	ieee transactior	2012	10.1109/tciai	21	0.00208	0.04162	Monte Carlo tree search (MCTS) is a rec	Artificial intelligence	GAME
6	karaboga, d; aka	a modified artificial bee colony (	applied soft cor	2011	10.1016/j.aso	24	0.00168	0.02806	Artificial Bee Colony (ABC) algorithm wa	Swarm intelligence;	EVOLUTIONARY ALG
7	perez-liebana, d	the 2014 general video game pl	ieee transactior	2016	10.1109/tciai	1	0.00027	0.02651	This paper presents the framework, rule	Competitions; evolutionary algorithms; g	
8	banharnsakun, a	the best-so-far selection in artif	applied soft cor	2011	10.1016/j.aso	28	0.00157	0.02612	The Artificial Bee Colony (ABC) algorithn	Artificial Bee Colony	IMAGE REGISTRATIO
9	napoles, g; grau	a granular intrusion detection s	recent advance	2016	10.1007/978-	1	0.00024	0.0241	Security in computer networks is an acti	Intrusion detection	FUZZY; DECISION; EX
10	hoey, j; schrode	affect control processes: intellig	artificial intellig	2016	10.1016/j.arti	1	0.00024	0.0241	This paper describes a novel method for	Affect; Emotion; So	EMOTION; IDENTITIE
11	garro, ba; rodrig	classification of dna microarray	applied soft cor	2016	10.1016/j.aso	1	0.00024	0.0241	DNA microarray is an efficient new tech	DNA microarrays; A	PARTICLE SWARM OP
12	ueno, m	computational interpretation o	distributed com	2016	10.1007/978-	1	0.00024	0.0241	Understanding intellectual products suc	Computational model of comics; Comic e	
13	treur, j	dynamic modeling based on a te	biologically insp	2016	10.1016/j.bic	1	0.00024	0.0241	This paper presents a dynamic modeling	Modeling; Dynamic;	RECURRENT NEURAL
14	muller, vc; bostr	future progress in artificial intel	fundamental is:	2016	10.1007/978-	1	0.00024	0.0241	There is, in some quarters, concern abo	Artificial intelligence	AI
15	faia, r; pinto, t; v	optimization of electricity mark	trends in practi	2016	10.1007/978-	1	0.00024	0.0241	The electricity markets environment has	Artificial intelligence; Electricity markets;	
16	besold, tr; rober	when thinking never comes to a	fundamental is:	2016	10.1007/978-	1	0.00024	0.0241	The recognition that human minds/brai	Cognitive systems; (	APPROXIMABILITY; C
17	legg, s; hutter, m	universal intelligence: a definitic	minds and mac	2007	10.1007/s110	21	0.00222	0.02224	A fundamental problem in artificial intel	AIXI; complexity the	SCIENCE
18	legg, s; hutter, m	a universal measure of intelliger	19th internatio	2005		2	0.00258	0.02154			
19	alvarado-perez,	artificial and natural intelligenc	distributed com	2015	10.1007/978-	1	0.00042	0.02109	The large amount of data generated by	Data mining; visualization; machine learni	
20	patel, vl; shortlif	the coming of age of artificial in	artificial intellig	2009	10.1016/j.arti	12	0.00154	0.01929	This paper is based on a panel discussior	Artificial intelligence	DECISION-SUPPORT;
21	stilman, b; yakh	the primary language of ancient	international jo	2011	10.1007/s130	8	0.00108	0.01807	Linguistic Geometry (LG) is a type of gar	Linguistic Geometry; Primary Language; A	

from the co-occurrence map [18]. In VOSviewer the term identification stage consists of the following five steps:

- Removal of copyright statements in abstracts.
- Using the sentence detection algorithm given by the Apache OpenNLP library, the text data is split up into sentences.
- Using the part-of-speech tagging algorithm given by the Apache OpenNLP library, each word is assigned a part of speech, e.g., noun, verb, preposition, adjective, etc.
- Noun phrase identification: VOSviewer specifies noun phrase as a chain of one or many successive words from a sentence, in which the last word of the phrase is a noun and each of the remaining words is either an adjective or a noun. To define noun phrases, VOSviewer processes only the longest feasible noun phrases that can be detected in a sentence.
- Noun phrase unification: Eliminating most non-alphanumeric characters, deleting accents from characters, changing plurals to singulars, and changing upper case characters to lower ones.

In the next stage, starting from the collection of identified terms (keywords), the selection is made by excluding terms with occurrence threshold, by excluding terms with a low relevance score, and also by manually excluding certain terms. More specifically, we include only meaningful terms concerned with method, algorithms, field or subfield of research and exclude manually all general or uninformative terms like "direction", "first step", "action", etc.

Using the scores of the research papers calculated by above mentioned algorithm, we formulate final scores for keywords by summing up scores of papers containing them, and then group obtained results by year. Therefore, we can demonstrate scores of keywords through years in time series and observe which keywords are retaining uptrend. For the sake of clarity, we keep only quite frequent and recent keywords (appear at least in the last 4 years in papers) and divide them into 4 groups. The dynamics of keywords scores are illustrated in Fig. 7. From the figure we collect 30 clearly uptrend keywords, these are also predicted research trends after the 2016 year: 'artificial neural network', 'computational intelligence', 'diagnosis', 'disease',

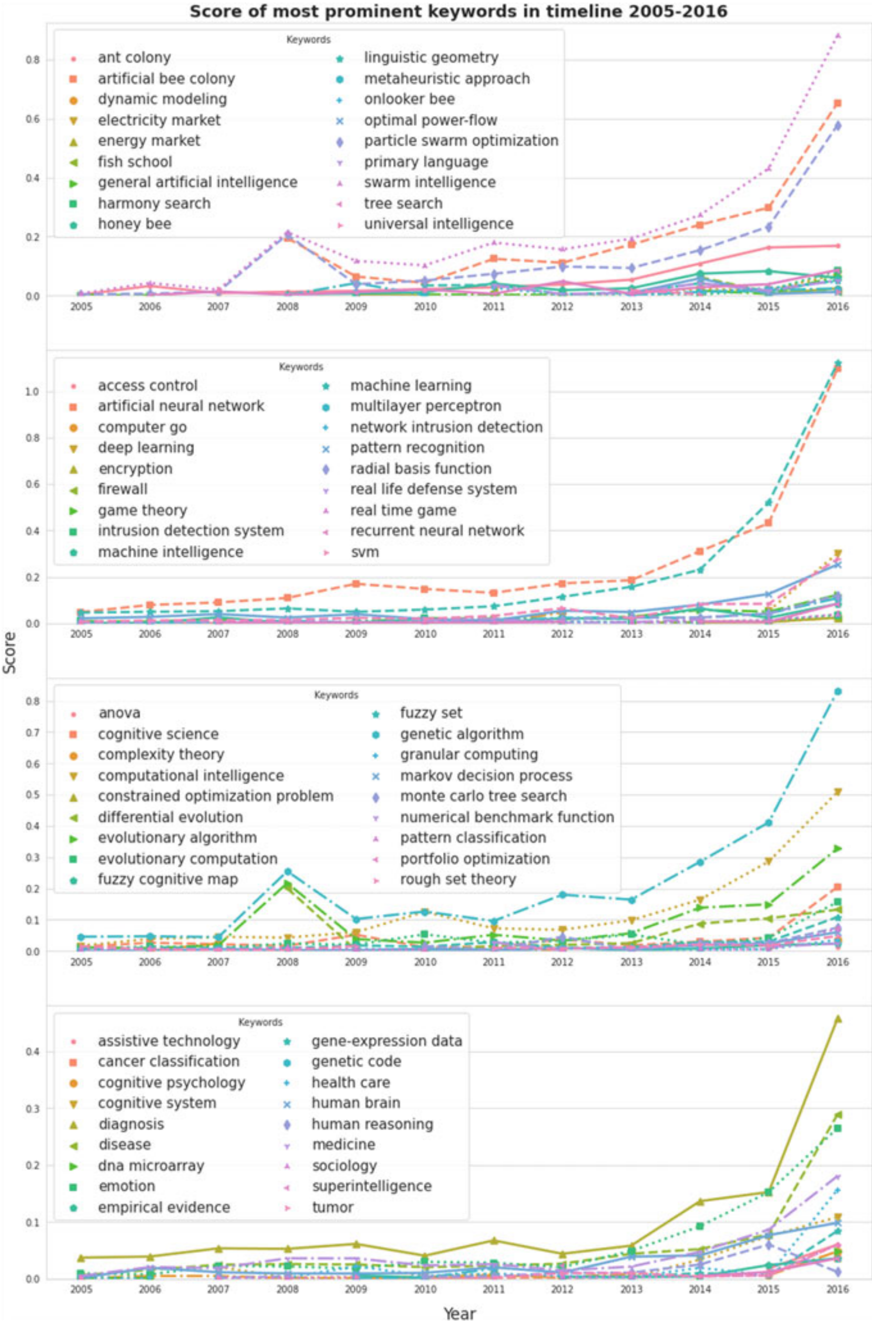

Fig. 7 Dynamics of keywords scores in time series

Fig. 8 Word cloud of 30 keywords research trend after the 2016 year

'emotion', 'genetic algorithm', 'machine learning', 'ant colony', 'cognitive science', 'evolutionary algorithm', 'evolutionary computation', 'fuzzy set', 'game theory', 'granular computing', 'human brain', 'intrusion detection system', 'machine intelligence', 'markov decision process', 'medicine', 'multilayer perceptron', 'particle swarm optimization', 'pattern recognition', 'radial basis function', 'support vector machine', 'swarm intelligence', 'cognitive psychology', 'health care', 'rough set theory', 'tree search', 'fuzzy cognitive map', 'pattern classification', 'recurrent neural network', 'artificial bee colony', 'cognitive system', 'differential evolution', 'empirical evidence', 'honey bee', 'human reasoning', 'network intrusion detection', 'sociology', 'tumor', 'computer go', 'electricity market', 'gene-expression data'.

Alternatively, these keywords are also demonstrated by the word cloud in Fig. 8. Among them, keywords like 'artificial neural network', 'computational intelligence', 'disease', 'emotion', 'genetic algorithm', 'machine learning' show high-speed evolution, and logically we can predict that these thematic researches still appear strongly in later years.

3.3 Method Evaluation

To the extent of its isolation and deepening, each field of knowledge develops its own special language, which makes it inaccessible to specialists in other fields. Therefore, a statistical analysis of the publication keywords allows us to trace the dissemination depth of new ideas and methods, which can be set by the occurrence frequency of words encoding whole concepts. Thus, in order to evaluate the proposed method, the results are evaluated against collected papers from the bibliographic WoS database, category "Computer science Artificial Intelligence" in the timeframe 2017–2019.

Firstly we create corpus by combining Title, Abstract, Author keywords, Keyword plus of all papers from the dataset. Subsequently, we again use functionality "Create a map based on text data" in VOSviewer software to create a term co-occurrence map based on the derived corpus, and then extract all keywords from the co-occurrence map with occurrence threshold 50. Similarly, we include only meaningful terms concerned with method, algorithms, field or subfield of research and exclude manually general and uninformative terms like "argument", "distance", "thing", etc. This results in a set of most 50 frequent keywords in descending order of occurrences with corresponding relevance scores, which are presented in Fig. 9. Terms owning high relevance scores are likely to express particular topics discovered in the text

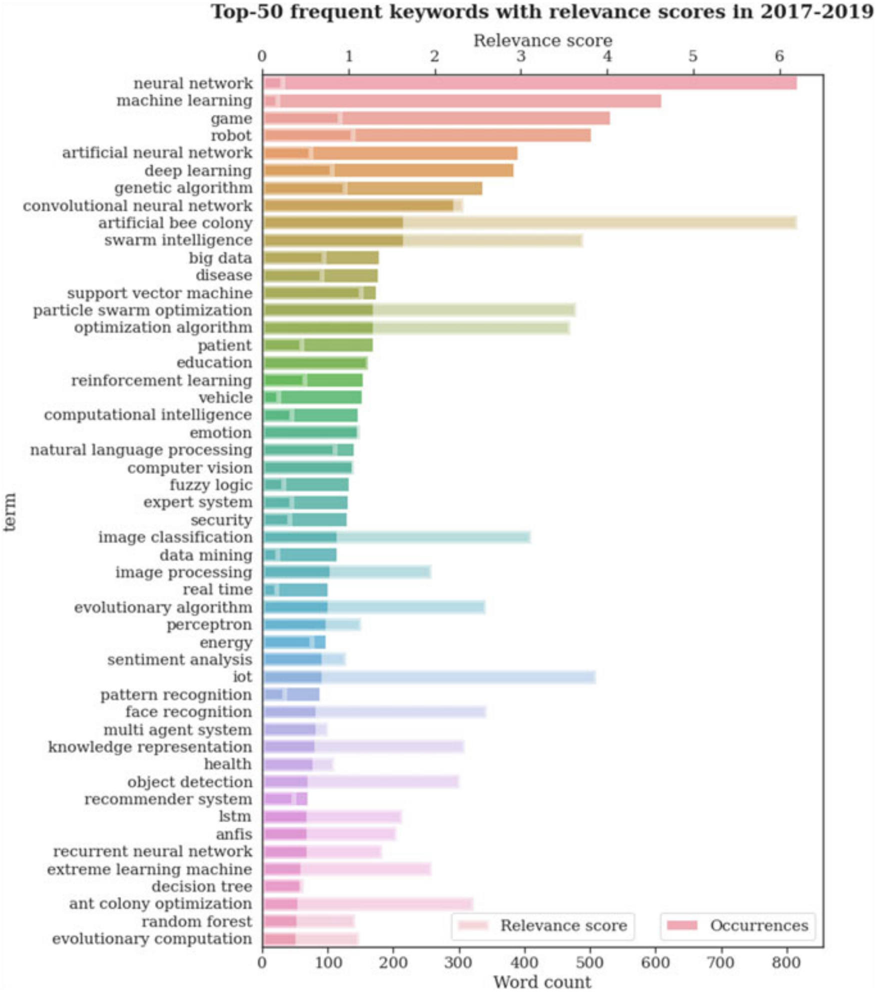

Fig. 9 Most frequent research topics (keywords) in timeline 2017–2019

data, whereas terms with a low relevance score obtain only general meanings, thus these are not representative of any certain topic. By excluding general terms with low relevance scores one obtains particular and informative terms [13].

These terms are considered to be focus research trends in the period 2017–2019, and we will determine how the accuracy of our prediction is by comparing the occurrence of predicted keywords with real prominent keyword set. More specifically, the comparison between keywords is executed not only by explicit match but also by approximate match (e.g., ‘game theory’ and ‘game’, ‘fuzzy cognitive map’ and ‘fuzzy logic’ are considered same keywords). Thus, we detected 22 keywords (of overall 30 predicted uptrend keywords) in the keyword set (50 items) of true focus research trends. Therefore, the prediction precision is about 73.33% (22/30).

4 Conclusion

Because of the fast augmentation in the number of academic publications, it is difficult to remain an overview of the dynamic and structure evolution of a certain science field, as well as all scientific domains. However, understanding of prominent trend topics or shifts of focus in specific research areas is a significant factor of supporting resource allocation decisions in governmental institutions, research laboratories, and corporations. Bibliometrics becomes advantageous by providing a structured analysis to a large body of information, to infer trends over time, themes researches and identify shifts in the boundaries of the disciplines. However, there are some drawbacks of the described bibliometric methods, including not aggregating all metadata and not indicating clearly thematic evolution over a period of time.

This paper introduces some bibliometric analysis tools and presents a general approach to analyze and predict the thematic evolution of a given research field by pointing out uptrend keywords. The proposed method includes a dataflow diagram and a paper ranking algorithm for detecting and visualizing thematic research trends. As a case study, the proposed approach is applied to predict the emerging thematic evolution of the Artificial Intelligence research field in the period 2005–2016 from the WoS database. Finally, the method evaluation is implemented by detecting occurrences of predicted keywords in real prominent keywords in timeframe 2017–2019. The derived prediction precision is 73.33%. In the future, we plan to improve prediction precision by enhancing paper ranking algorithms and accounting more features such as authors and journals impact factors or conference proceedings ranking.

Acknowledgements The reported study was funded by RFBR according to the research project № 19-07-01200 and 20-37-90092.

References

1. Kravets, A.G.: On approach for the development of patents analysis formal metrics. In: Kravets, A.G., Groumpos, P.P., Shcherbakov, M., Kultsova, M. (eds.) 3rd Conference on Creativity in Intelligent Technologies and Data Science, CIT&DS 2019, vol. 1083, pp. 34–45. Springer, Verlag (2019)
2. Iqbal, W., Qadir, J., Tyson, G., Mian, A.N., Saeed-ul, H., Crowcroft, J.: A bibliometric analysis of publications in computer networking research. Scientometrics **119**(2), 1121–1155 (2019)
3. Merigó, J.M., Pedrycz, W., Weber, R., de la Sotta, C.: Fifty years of information sciences: A bibliometric overview. Inf. Sci. **432**, 245–268 (2018)
4. Wang, Q.: A bibliometric model for identifying emerging research topics. J. Assoc. Inf. Sci. Technol. **69**(2), 290–304 (2018)
5. Robinson-Garcia, N., Sugimoto, C.R., Murray, D., Yegros-Yegros, A., Lariyiere, V., Costas, R.: The many faces of mobility: Using bibliometric data to measure the movement of scientists. J. Informetrics **13**(1), 50–63 (2019)
6. Nguyen, T.V., Kravets, A.G.: Analyzing recent research trends of computer science from academic open-access digital library. In: Saxena, A. Kr., Parygin, D., Ather, D., Yadav, V. (eds.) 8th International Conference on System Modeling and Advancement in Research Trends, pp. 31–36. IEEE UP Section, New Delhi (India) (2019)
7. Cobo, M.J., Jurgens, B., Herrero-Solana, V., Martinez, M.A., Herrera-Viedma, E.: Industry 4.0: A perspective based on bibliometric analysis. In: 6th International Conference on Information Technology and Quantitative Management, vol. 139, pp. 364–371 (2018)
8. Zupic, I., Cater, T.: Bibliometric methods in management and organization. Organ. Res. Methods **18**(3), 429–472 (2015)
9. Aria, M., Cuccurullo, C.: Bibliometrix: An R-tool for comprehensive science mapping analysis. Journal of Informetrics **11**(4), 959–975 (2017). https://doi.org/10.1016/j.joi.2017.08.007
10. Yang, S., Han, R., Wolfram, D., Zhao, Y.: Visualizing the intellectual structure of information science (2006–2015): Introducing author keyword coupling analysis. J. Informetrics **10**(1), 132–150 (2016)
11. Van Eck, N.J., Waltman, L.: Citation-based clustering of publications using CitNetExplorer and VOSviewer. Scientometrics **111**(2), 1053–1070 (2017)
12. Moral-Muñoz, J.A., Arroyo-Morales, M., Herrera-Viedma, E., Cobo, M.J.: An overview of thematic evolution of Physical Therapy research area from 1951 to 2013. J. Data Inf. Sci. **3**(2), 1–19 (2018)
13. Van Eck, N.J., Waltman, L.: Visualizing bibliometric networks. In: Y. Ding, R. Rousseau, D. Wolfram (eds.) Measuring Scholarly Impact: Methods and Practice, pp. 285–320 (2014)
14. Upham, S.P., Small, H.: Emerging research fronts in science and technology: Patterns of new knowledge development. Scientometrics **83**(1), 15–38 (2010)
15. Sohrabi, B., Vanani, I.R., Jalali, S.M.J., Abedin, E.: Evaluation of research trends in knowledge management: A hybrid analysis through burst detection and text clustering. J. Inf. Knowl. Manage. **18**(4), 27 (2019)
16. Klavans, R., Boyack, K.W.: Which type of citation analysis generates the most accurate taxonomy of scientific and technical knowledge? J. Assoc. Inf. Sci. Technol. **68**(4), 984–998 (2017)
17. Roldan-Valadez, E., Salazar-Ruiz, S.Y., Ibarra-Contreras, R., Rios, C.: Current concepts on bibliometrics: A brief review about impact factor, Eigenfactor score, CiteScore, SCImago Journal Rank, Source-Normalised Impact per Paper, H-index, and alternative metrics. Ir. J. Med. Sci. **188**(3), 939–951 (2019)
18. Vasiliev, S.S., Korobkin, D.M., Kravets, A.G., Fomenkov, S.A., Kolesnikov, S.G.: Extraction of cyber-physical systems inventions structural elements of Russian-language patents. In: Kravets, A.G., Bolshakov, A.A., Shcherbakov, M.V. (eds.) Cyber-Physical Systems: Advances in Design & Modeling, vol. 259, pp. 55–68. Springer Nature, Switzerland AG (2020)

Development of a Module for Predictive Modeling of Technological Development Trends

Alla G. Kravets, Natalia A. Salnikova, and Elena L. Shestopalova

Abstract In this work, the problem of forecasting technological development trends was solved. A review of the sources of the global patent space, an analysis of technological development trends, a survey of data sources for training the neural network were carried out. Existing data mining techniques were analyzed for more accurate and faster forecasting. A module for predictive modeling of trends in technological development is developed, algorithms for the module for predictive modeling of trends in technological development are described.

Keywords Patent search · Neural network · Decision trees · Gradient boosting · Deep study · Forecasting · Technology trends

1 Introduction

Patent activity indicators are currently used in technological forecasting and in competitive intelligence often. An important role is played by forecasting the development of patent trends in individual countries and around the world, which makes it possible to identify the main priority areas of technology development [1, 2].

In the context of the globalization of the economy and the rapidly changing competitive environment, the problem of choosing a technological development strategy is of particular importance. The relevance and, as a consequence, the effectiveness of this choice is largely determined by how accurately the subject of macro-,

A. G. Kravets (✉)
Volgograd State Technical University, 28 Lenin Av, Volgograd 400005, Russia
e-mail: agk@gde.ru

Dubna State University, Dubna, Moscow Region, Russia

N. A. Salnikova
Volgograd Institute of Management, Russian Presidential Academy of National Economy and Public Administration, 8 Gagarin St, Volgograd 400131, Russia

E. L. Shestopalova
Volgograd State Medical University, 1, Pavshikh Bortsov Sq, Volgograd 400131, Russia

A. G. Kravets et al. (eds.), *Cyber-Physical Systems*, Studies in Systems, Decision and Control 350, https://doi.org/10.1007/978-3-030-67892-0_11

meso- or microeconomics takes into account global and regional and technological trends [3, 4].

The formation of technological trends is influenced, first of all, by the objective processes of development of world markets, as well as the processes of development and change of technological patterns. In addition, the formation of technological trends is affected by measures of state regulation of the economy, taking into account social, environmental, political and other factors. The results of the analysis of global economic processes and trends are formalized in the form of program documents of government bodies, such as forecasts and strategies for socio-economic development; framework programs, studies and forecasts of large consulting companies, as well as international financial institutions. These documents and forecasts are based on deep and comprehensive research and, as a rule, they demonstrate high comparability [5, 6].

Thus, the task of developing methods for predictive modeling of technological development trends is relevant.

It is necessary to solve the following tasks for achievement this goal:

- To analyze the global patent space;
- Conduct a survey of data sources for the analysis of technological trends;
- Conduct an analysis of technological development trends;
- Conduct a survey of data sources for training the neural network;
- Conduct data mining;
- To form structural and functional modeling of technological development trends;
- Describe the methods used for data mining (DM);
- Design a module for predictive modeling of technological development trends;
- Describe the algorithms of the module for predictive modeling of trends in technological development;
- Test the module for predictive modeling of technological development trends.

The aim of the work is to develop software and information tools for predicting trends in technological development.

The object of research is the technological development trends.

The subject of the research is the methods of predictive modeling of trends in technological development of modeling.

Scientific novelty lies in the proposed and software-implemented formal methodology for predictive modeling of technological development trends, in contrast to existing ones, which are based on statistical data from open sources, which allows one to obtain trend forecasts for both technologies introduced into production and for promising technologies in terms of patenting.

2 Analysis of the Global Patent Space

One of the tools for analyzing technological trends is the analysis of patent landscapes. Patent Landscape is an analytical tool in the field of patenting, which allows to outline the technological context of any issue, invention or solution in the field of intellectual property. Introducing the patent analysis tools as a whole, patent landscapes repeatedly enhance the potential of patent search results and patent analysis through visualization methods and multidimensional analytical representations. The analysis of the patent landscape becomes an essential step preceding any research and development in conditions of a significant volume and complex nature of information [7, 8].

Indeed, patent documents are not the only source of information in a detailed analysis of a technological trend. Important sources of information are also data on scientific and technical publications, data on the results of research and development, including in the framework of federal target programs, as well as market information. At the same time, a significant number of publications devoted to the use of patent information in order to determine technological trends indicates the indisputable advantages of using patent documentation in the analysis of technological landscapes, as well as forecasting promising areas of development of various industries [9, 10]. At the same time, however causal relationships between patent indicators have been identified and systematized in literary sources not deeply and fully to solve practical problems, despite a significant number of studies and publications,, on the one hand, and strategic and tactical decisions in the field of technological development, on the other hand [11, 12].

Every year, more and more companies want to patent their inventions. That is why the number of patent applications is increasing from year to year. The increasing flow of applications and more than 70 million issued patents increase the time that patent examiners should spend on considering all incoming applications [13, 14]. Sometimes incoming applications wait for examination up to several years. Sometimes an examiner has to make hundreds of searches and manually process thousands of existing patents during the examination process to decide whether to approve or reject the application. This process can take him more than 20 h. The growing workload of patent offices has necessitated the development of automated decision support systems to assist examiners in the examination process. The system of automatic positioning of application materials for obtaining a patent for an invention in the global patent space is based on the statistical and semantic approaches of the E-patent Examiner—a decision-making system by experts during the examination of a patent application [15, 16].

The task of examining patent applications can be divided into two main sub-tasks: the task of finding the relevant issued patents—a search according to the prior art and the task of automatically deciding on the patentability of an application. The implementation of the system will reduce substantive expertise. The main tasks of the development of the system are:

- providing automatic positioning of application materials for obtaining a patent for an invention in the global patent space based on statistical and semantic approaches;
- optimization of processing of technological processes associated with the examination of the invention, based on the results of the automatic positioning of

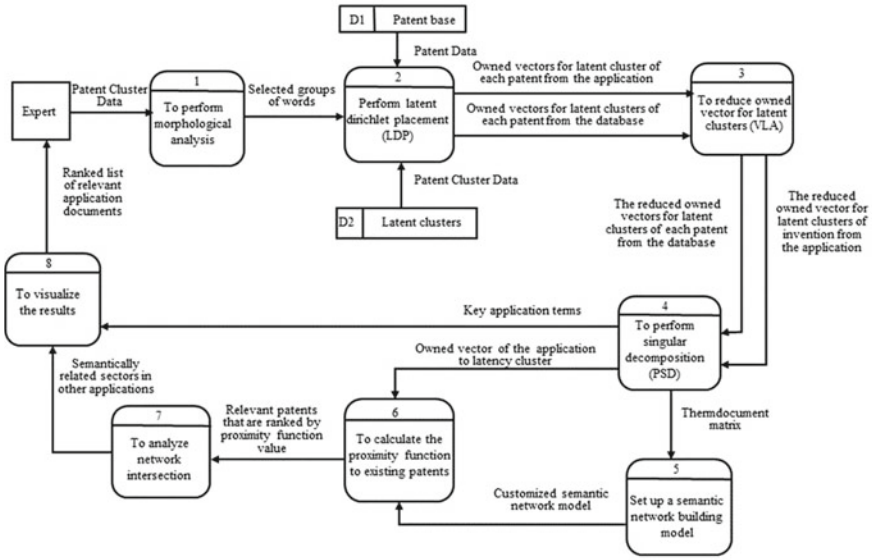

Fig. 1 Data streams of the automatic positioning method

application materials to obtain a patent for an invention in the global patent space based on statistical and semantic approaches.

The proposed algorithm (Fig. 1) for the search for patent analogues is performed using the statistical analysis method, where the procedure of comparing membership vectors for unnamed clusters obtained by the LDA method, semantic analysis of text in natural language, consisting of the following stages: preprocessing, morphological analysis, construction of semantic sentence trees, is applied, assessment of the similarity of semantic trees using a modified Levenstein algorithm.

3 Data Mining

An analysis was made of a number of systems for searching statistical data for training a neural network.

The World Intellectual Property Organization (WIPO) Statistics Data Center for Intelligent Systems is an online service that provides access to WIPO statistics on intellectual property worldwide. Users can select from a wide range of indicators and view or download the latest available as well as historical data according to their needs.

The WIPO Statistics Center covers the following types of indicators: patent, trademark, industrial design, utility model, and PCT, Madrid, and Hague systems. Most indicators related to patents, trademarks, industrial design, and utility models relate to the period starting in 1980.

SJCR (The SCImago Journal & Country Rank) is a publicly accessible portal that includes journals and national scientific indicators based on information contained in the Scopus® database (Elsevier BV). These indicators can be used to evaluate and analyze scientific areas. Logs can be compared or analyzed separately. Country ratings can also be compared or analyzed separately. Magazines can be grouped by subject area (27 main subject areas), subject category (313 specific subject categories) or by country. Citation data is taken from more than 34,100 titles from more than 5,000 international publishers and country performance indicators from 239 countries.

SHAPE OF SCIENCE is an information visualization project whose goal is to uncover the structure of science. Its interface was developed to access the database of bibliometric indicators of the SCImago Journal & Country Rank portal. SHAPE OF SCIENCE shows a very intuitive image of the relationship of various subject areas from the perspective of magazines. Separate log profiles can be accessed from this interface.

The world report—offers detailed information to analyze the world and each of the eight major geographical regions. Numerous indicators are presented here and tables and trend charts are shown (1996–2017) for all or one of the 27 main subject areas and for all or one of the regions corresponding to the selected parameters. The following indicators are presented: H index, reliable documents, citations, self-quoting and citations per document. The report also shows the development during the period 1996–2017.

A comparative analysis of the functionality of these systems was made after analyzing the above systems for the search for statistical data after analyzing the above systems for the search for statistical data. The results are shown in Table 1.

As a result of the comparative characteristics of search engines it was concluded that these sites do not provide an opportunity to predict trends in technological development, but using the data they publish is quite possible.

As a rule, these initial data represent large arrays of structured and unstructured data for the analysis and identification of hidden patterns in which data mining (DM) is widely used. Various DM methods are implemented in software products of Russian and foreign companies, such as IBM (IBM SPSS Modeler computer program) [17], StatSoft (Statistica statistical package), WizSoft (WizWhy analytical system), BaseGroup (Deductor analytical system), IntefralSolutions, Microsoft, etc.

A comparative table is below (Table 2), which reflects the advantages and disadvantages of existing methods for modeling customer churn and their implementation in existing software products.

Table 1 Comparative characteristics of search engines

System	Technology selection	Time interval selection	Country selection	Document type selection
WIPO	+	+	+	–
SJR	+	–	+	+

Table 2 Analysis of IAD methods

Models and methods	Benefits	Disadvantages	Software products
Associative rule search	Finds very simple and intuitive rules	Identifying frequently occurring sets of elements requires large computational and time resources	Deductor studio, SPSS Modeler, STATISTICA, SAS Enterprise Miner
Neural networks	Resistant to noise. Solve problems with unknown patterns. Retrained when the environment changes. Fast acting. Fault tolerant	The reasons for the decision may be unclear. No guarantee of unambiguous repeatable results	Deductor studio, SPSS Modeler, STATISTICA, SAS Enterprise Miner
Maps of Kohonen	Resistant to noisy data. Fast and unmanageable training. The ability to render	Heuristic learning algorithm. The predetermination of the number of clusters. Dependence on initial network settings	Deductor studio, SPSS Modeler, STATISTICA, SAS Enterprise Miner
Random decision forests	Effective with data with a large number of characteristics and classes. Work with continuous and discrete features. Insensitive to monotonous transformations	They are prone to retraining in case of noisy data. Large dimension models	SPSS Modeler, STATISTICA, SAS Enterprise Miner
Decision trees	The speed of training. Extracting rules in a natural language. Intuitive classification model. High accuracy of the forecast. Construction of nonparametric models	The decision only classification issues. Inability to work with a continuous target field	Deductor studio, SPSS Modeler, STATISTICA, SAS Enterprise Miner
Cox regression	Able to work with censored data and categorical variables. The ability to render	Censorship of data reduces the sample, which may result in inconsistent results	SPSS Modeler, STATISTICA, SAS Enterprise Miner
Binary logistic regression	Is simple. Quickly received. Well interpreted. Widely applicable. Accurate enough. It has tools for assessing the quality of models	It has difficulties due to the nonlinearity of the relationship between the outflow and the factors influencing it. The predicted parameter is usually a number from a continuous range	Deductor studio, SPSS Modeler, STATISTICA, SAS Enterprise Miner

Each of the considered IAD methods has its limitations and features as well as the advantages of using it. It is worth noting that the neural network, and in particular, the Kohonen self-organizing map, have a number of advantages, such as self-learning and resistance to noisy data [18].

4 Development of a Formal Methodology for Predictive Modeling of Technological Development Trends

The steps of a formal technique consist of the following steps:

- downloading statistics from WIPO and SJR sites;
- formation of a training sample;
- providing a trained model;
- request for technology analysis (trending or not).

The formation of the training sample is carried out manually by creating a file of the.csv format. In the created file, you need to create two columns: year (year) and the number of patents per year (total). Then transfer the data from the downloaded files to the created document.

After the sampling is completed, this file is loaded into the software module, which in turn reads the data from it and makes a prediction based on these data. Based on the results of the program module, based on the constructed trend, the user makes a request for technology analysis. The development of technology is clearly visible on the chart.

Then, structural and functional modeling of technological development trends is carried out. We use the IDEF0 methodology, which prescribes the construction of a hierarchical system of diagrams for the process of predicting the modeling of trends in technological development.

Figure 2 shows a general view of the process of predictive modeling of technological processes.

A process analysis request is received at the input of the process. The rules of data sampling and rules of parsing control acts.csv. The user, the analyst, the software and the data sources will play the role of the mechanism. The forecast of patented technologies, the forecast of the dynamics of patenting and the forecasting of introduced technologies will be revealed at the output. The data flow diagram is shown in Fig. 3.

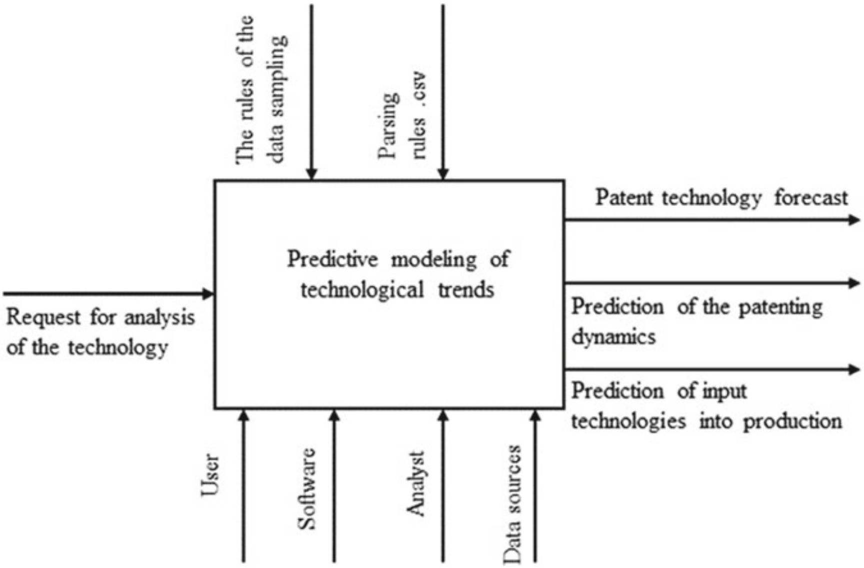

Fig. 2 General functional model of the technique

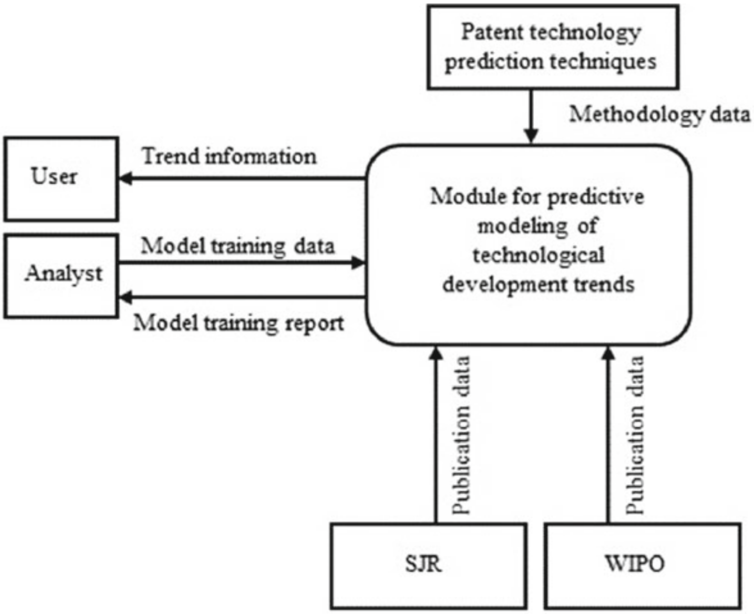

Fig. 3 Data flow diagram

5 A Designing a Module for Predictive Modeling of Technological Development Trends

A preliminary model can be represented in the form of functional diagrams of precedents.

The diagram is a reflection of the actors who interact with the system, and its the reaction of the information system to their actions.

A chart of precedents describing the information system is shown in Fig. 4.

The first step of the program is to read the.csv file format. Next is the training of the model. Since the module cannot predict the data immediately ahead for several years and each subsequent prediction is recorded in the total array and the year is recorded in the year array. The module is retrained after changing the data array. Thus, the total parameter can be predicted for each unlimited number of years in advance. The program builds a graph where the X axis is the year and the Y axis is the number of patents after predicting the required number of years.

Figure 5 shows the algorithm of the software module.

After testing the module for predictive modeling of technological development trends, we can conclude that the trained module makes a fairly accurate forecast for the first 5 years. The forecasting accuracy directly depends on the size of the training sample.

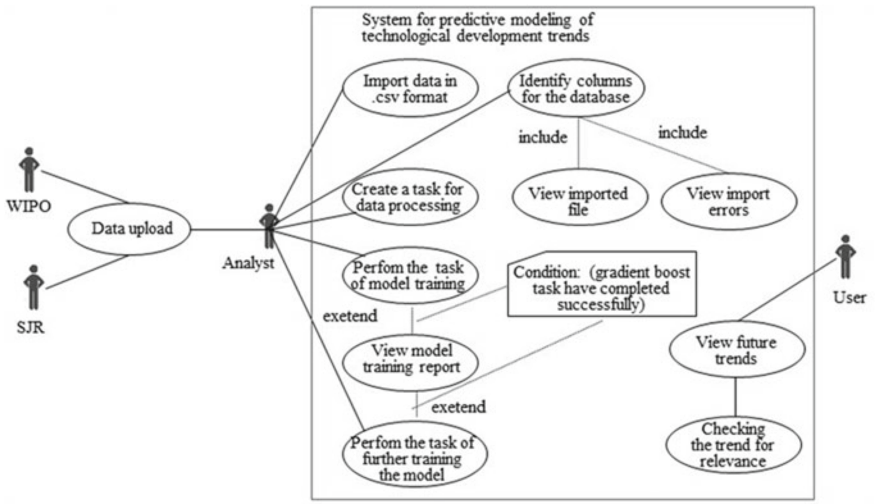

Fig. 4 Functional behavior of the system

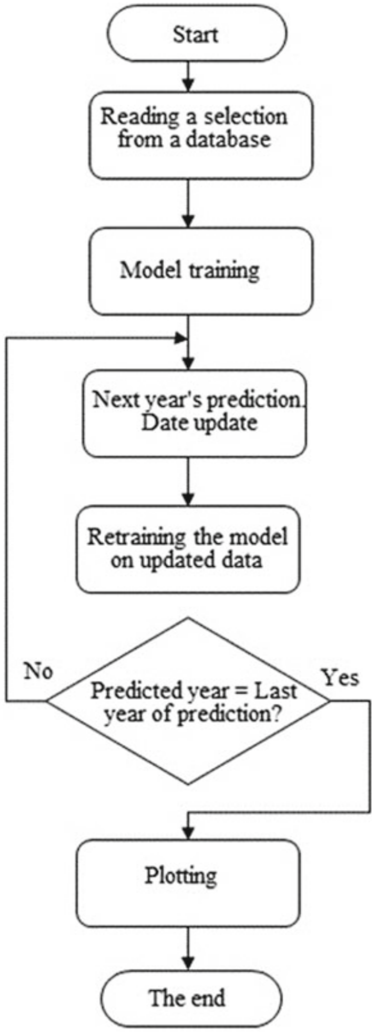

Fig. 5 The algorithm of the module for predictive modeling of trends in technological development

6 Conclusion

In this work, the problem of forecasting technological development trends was solved. Existing data mining techniques were analyzed for more accurate and faster forecasting. One of these methods turned out to be gradient boosting. Gradient boosting is a machine learning technique for classification and regression that builds a prediction model in the form of an ensemble of weak predictive models, usually decision trees.

A module for predicting trends in technological development in Python with the CatBoost library was developed. The process of the system involves 2 main stages:

training and forecasting. The experiment results showed that the trained module makes a fairly accurate forecast for the first 5 years and the accuracy of forecasting directly depends on the size of the training sample. As a result, the developed software module can be used as part of the tasks of predicting trends in technological development.

Acknowledgements The reported study was funded by RFBR according to the research project 19-07-01200.

References

1. Kravets, A.G., Salnikova, N.A., Mikhnev, I.P., Orudjev, N.Y., Poplavskaya, O.V.: Web portal for project management in electronics design software development. Conference: 2019 International Seminar on Electron Devices Design and Production (SED 2019), Proceedings, 8798472, pp. 1–6 (2019)
2. Vasiliev, S.S., Korobkin, D.M., Kravets, A.G., Fomenkov, S.A., Kolesnikov, S.G.: Extraction of cyber-physical systems inventions' structural elements of Russian-language patents. In: Cyber-Physical Systems: Advances in Design & Modelling, pp. 55–68. Springer, Cham (2020)
3. Korobkin, D., Fomenkov, S., Golovanchikov, A.: Method of identification of patent trendsbased on descriptions of technical functions. J. Phys: Conf. Ser. **1015**(7), 1–6 (2018)
4. Mysior, M., Hnat, W., Koziołek, S.: Method of identification of useful functions in the scope of technical system development. New Opportunities for Innovation Breakthroughs for Developing Countries and Emerging Economies, pp. 204–215 (2018)
5. Kizim, A.V., Kravets, A.G.: On systemological approach to intelligent decision-making support in industrial cyber-physical systems. In: Cyber-Physical Systems: Industry 4.0 Challenges. Studies in Systems, Decision and Control, vol. 260, pp. 167–183. Springer, Cham (2020)
6. Kamaev, V.A., Salnikova, N.A., Akhmedov, S.A., Likhter, A.M.: The formalized representation of the structures of complex technical devices using context-free plex grammars. Communications in Computer and Information Science, CIT&DS 2015, vol. 535, pp. 268–277. Russia Federation, Volgograd (2015)
7. Lee, C., Kan, B., Shin, J.: Novelty-focused patent mapping for technology opportunity analysis. Tech. Forec. and Soc. Chanc. **90**, 355–365 (2015)
8. Kravets, A., Shumeiko, N., Shcherbakova, N., Lempert, B., Salnikova, N.: "Smart Queue" approach for new technical solutions discovery in patent applications. In: Communications in Computer and Information Science, vol. 754, pp. 37–47, CIT&DS 2017. Volgograd, Russia (2017)
9. Kravets, A.G., Kolesnikov, S., Salnikova, N., Lempert, M., Poplavskaya, O.: The study of neural networks effective architectures for patents images processing. Commun. Comp. Inf. Sci. **1084**, 27–41 (2019)
10. Korobkin, D.M., Fomenkov, A.A., Kravets, A.G., Golovanchikov, A.B.: Patent data analysis system for information extraction tasks. In: 13th International Conference on Applied Computing (AC 2016), pp. 215–219 (2016)
11. Kravets, A.G., Belov, A.G., Sadovnikova, N.P.: Models and methods of professional competence level research. Recent Pat. Comput. Sci. **9**(2), 150–159 (2016)
12. Kravets, A., Salnikova, N., Dmitrenko, K., Lempert, M.: Industrial cyber-physical systems: Risks assessment and attacks modeling. Stud. Syst. Decis. Control **260**, 197–210 (2020)
13. Wang, F., Mei, X., Rodriguez, J., Kennel, R.: Model predictive control for electrical drive systems-an overview. CES Trans. Electr. Mach. Syst. **1**(3), 219 –230 (2017)

14. Korobkin, D.M, Fomenkov, S.A, Kravets, A.G, Kolesnikov, S.G.: Methods of statistical and semantic patent analysis. Communications in Computer and Information Science, CIT&DS 2017, pp. 48–61 (2017)
15. Shcherbakov, M., Groumpos, P.P., Kravets, A.: A method and IR4I index indicating the readiness of business processes for data science solutions. Commun. Comput. Inf. Sci. **754**, 21–34 (2017)
16. Kravets, A.G., Kravets, A.D., Korotkov, A.A.: Intelligent multi-agent systems generation. World Appl. Sci. J. **24**(24), 98–104 (2013)
17. Best, C.M., Gillespie, M.T., Hyatt, P., Rupert, L., Sherrod, V., Killpack, M.D.: A new soft robot control method: Using model predictive control for a pneumatically actuated humanoid. IEEE Robot. Autom. Mag. **23**(3), 75–84 (2016)
18. Kravets, A.G., Fomenkov, S.A., Kravets, A.D.: Component-based approach to multi-agent system generation. Commun. Comput, Inf. Sci. 466 CCIS, pp. 483–490 (2014)

The Software for Formation of Technical Function Assessments Based on the Patent Analysis

Dmitriy Korobkin, Sergey Fomenkov, Alexander Zlobin, Dmitriy Shabanov, and Alexander Golovanchikov

Abstract Based on the developed method of construction of a database of technical functions carried out by physical effects, realized the software with following functions: (a) extraction of technical functions; (b) search of the physical effect description; (c) construction of term-document matrices "Patent - Technical Function" and "Patent - Physical Effect"; (d) construction based on the reduced term-document matrices the matrix "Physical Effect - Technical Function". The system consists of two main and independent parts: the patents repository and the semantic core. The repository implements a standard CRUD interface for creating, reading, updating, and deleting documents. The semantic core is a library that implements all text processing functionality. The correctness of algorithms work was estimated on a test sample, the method of extraction of technical functions showed the following criteria: precision—0.87, recall—0.77, F—0.82, the method of search of physical effect description showed precision—0.92.

Keywords Technical functions · Physical effects · Patents

1 Introduction

The chapter shows the developed method for the automated construction of a database of technical functions performed by physical effects. For the synthesis of the physical principle of operation of new technical systems [1] in several scientific approaches [2, 3], physical effects (PE) are used. PE implements technical functions, which in turn constitute the constructive functional structure of the technical system [4]. The authors have developed a method for extracting descriptions of physical effects and technical functions from US patent documents (USPTO) and Rospatent. The method of automatic creation of a table of technical functions performed by physical effects is based on identifying latent dependencies in term-document matrices «Physical Effects-Patents» and «Technical Functions-Patents» [5].

D. Korobkin (✉) · S. Fomenkov · A. Zlobin · D. Shabanov · A. Golovanchikov
Volgograd State Technical University, 28 Lenin Av, Volgograd 400005, Russia

A. G. Kravets et al. (eds.), *Cyber-Physical Systems*, Studies in Systems, Decision and Control 350, https://doi.org/10.1007/978-3-030-67892-0_12

The purpose of this work is to programmatically implement a formation system of the matrix of technical functions performed by physical effects based on patent array analysis.

2 The Methodology

The automated system (AS) should provide the following functions:

- Extraction of technical functions in the «Subject - Action - Object» (SAO) [6–8] format from the texts of patent documents;
- Search for a description of the physical effect in the text of patent documents;
- Construction of the term-documentary matrix «Patent - Technical function», the elements of which are the values of the frequency response TF-IDF [9] for the corresponding technical function and patent document;
- Construction of the term-documentary matrix «Patent - Physical effect», the elements of which are the values of the frequency response TF-IDF for the corresponding physical effect and the patent document;
- Reduction of the space of technical functions for the term-document matrix “Patent - Technical function» and the space of physical and technical effects for the term-document matrix «Patent - Physical effect»;
- Construction from the reduced term-document matrices «Patent - Physical effect» and «Patent - Technical function» of the matrix «Physical effect - Technical function» based on the method of cosines as a characteristic of the representations of the physical effect and technical function in the space of patent.

AS is implemented in python version 3.7.2. For morphological tagging the program TreeTagger [10, 11] is used, for syntactic parsing—UDPipe [12]. The information structure of the input XML documents must conform to the document type declaration (DTD) «us-patent-application», the version of the patent document must conform to «v4.4 2014-04-03», which meets the general description of the «ST.36» standard.

The AS consists of two main and independent parts (Fig. 1): the patent array storage and the semantic core.

The patent array storage implements the functionality of storing and issuing to the user the texts of patent documents and their meta-data, such as number, class according to IPC classification [13], and so on. The storage implements the standard interface for CRUD operations for creating, reading (receiving), updating, and deleting documents, as well as the functionality of writing queries to retrieve data, which allows you to filter documents by the value of certain fields. Such an implementation allows, if necessary, to replace this module with any NoSQL storage in the future. The document storage implementation stores the patent data and all the necessary metadata locally in a specified directory. If cluster computing is required, the data folder can be placed on any network file system that supports FUSE technology. From the program interface side, this storage is an interface that provides

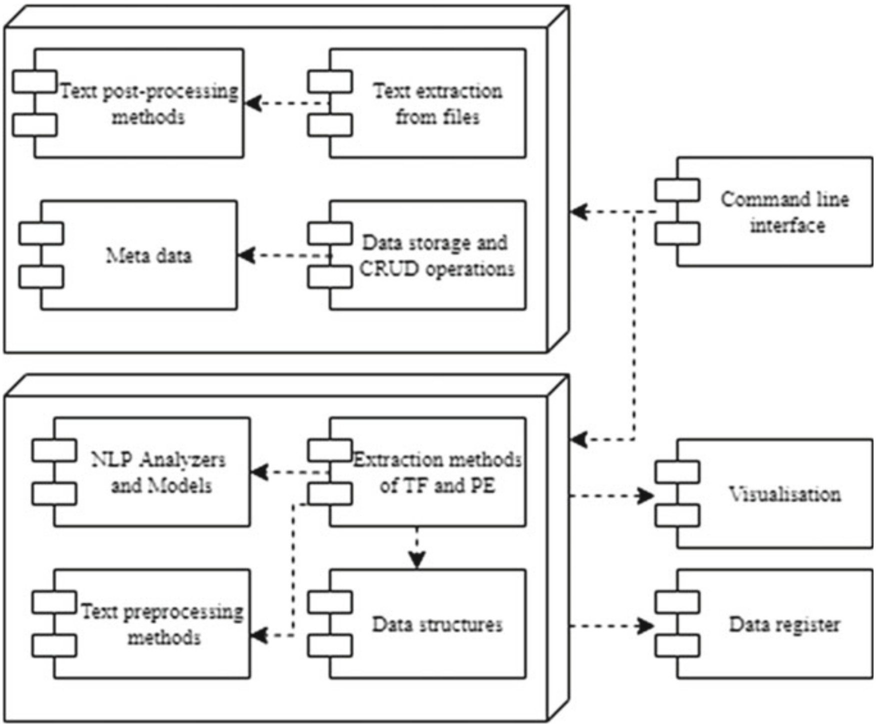

Fig. 1 Component diagram

a collection of documents in the form of a generator, which allows not to store the entire requested sample in memory, but to retrieve data only when accessing them.

All work on extracting data from files of patent documents is delegated to a separate library that implements the functionality of reading and extracting data for specific formats of patent documents. All communication between the store and the data extraction library is done through a set of data classes. The architecture of the block for working with the data warehouse is presented in the form of class diagrams (Fig. 2) and object diagrams (Fig. 3).

The functionality of the CRUD operation to the patent array is implemented in the «Bulk» class that works with objects that implement the «Document» interface—in this case, «Patent». The «DataFetcher» is responsible for extracting data and creating data document objects. For its operation, two objects of classes are needed that implement the «DocumentReader» and «DocumentParser» interfaces. «DocumentReader» extracts the text of patents from patent document files in their original formats (files from the USPTO database are contained in yourself several patents, archives, and other data at once). «DocumentParser» is responsible for the creation of document objects (class «Patent»). Since there are several dozen formats of input files and formats of the documents themselves, for simplicity, most of them are omitted in the diagram and replaced by the "…" sign, which symbolizes many

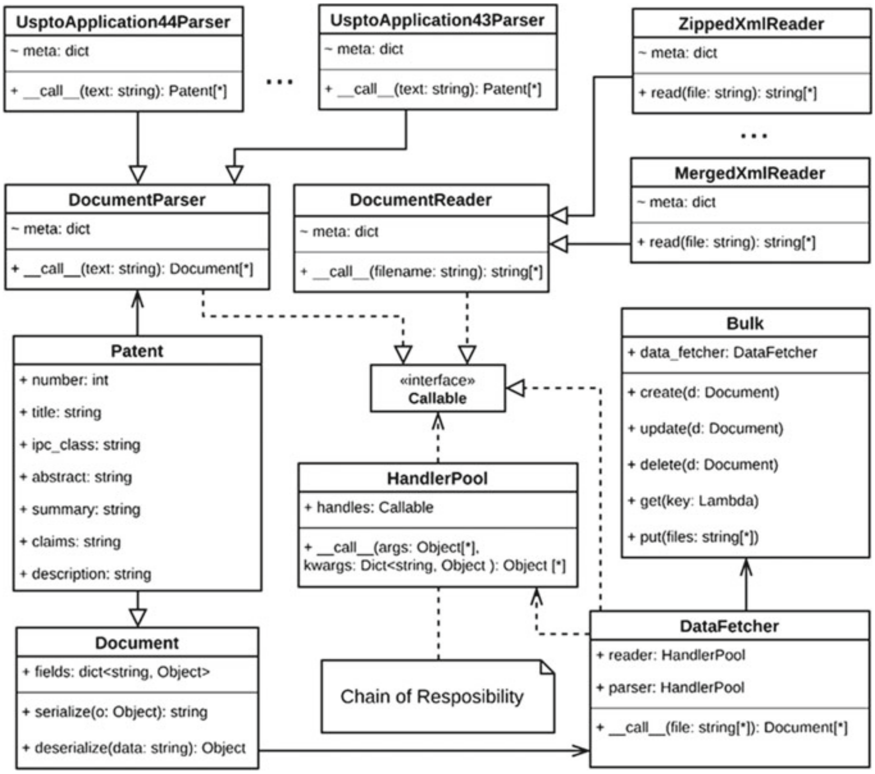

Fig. 2 Document storage class diagram

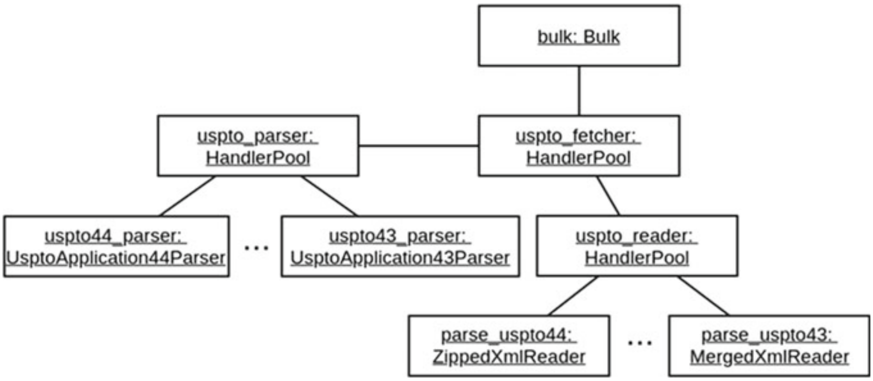

Fig. 3 Patent storage object diagram

different implementations for each format. For the same reasons, the «HandlerPool» class has been introduced, which is the standard «Chain-of-responsibility» design pattern. «HandlerPool» stores a list of all registered handlers and, when a request for processing arrives, delegates it to one of them, which makes it easy to add functionality for processing new input data formats with small code changes. The class object relationships are shown in Fig. 3.

The second part (semantic core) is a library that implements all the functionality for text processing:

- graphemic and lexical analysis, implemented in the form of text processors, as well as adapters to third-party word processing libraries such as NLTK [14];
- morphological and syntactic analysis, implemented in the form of adapters to third-party libraries TreeTagger, MaltParser [15, 16], UdPipe, and others;
- syntactic and semantic analysis—packages for working with PE and TF that programmatically implement the methods and data structures described in this work.

The architecture of the semantic core block is presented in the form of class diagrams (Figs. 4, 5) and object diagrams (Fig. 6).

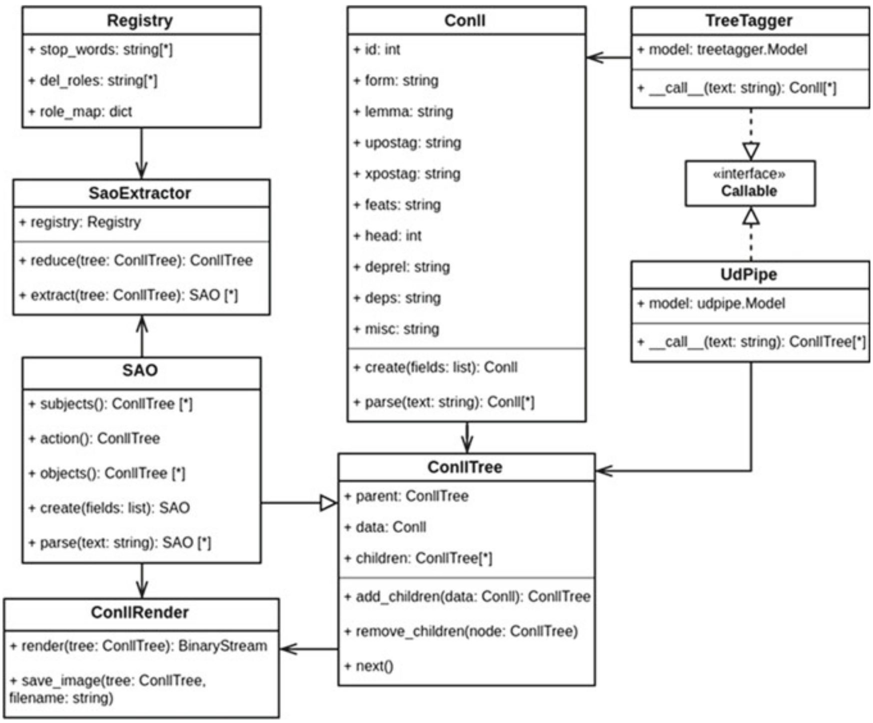

Fig. 4 Semantic core class diagram

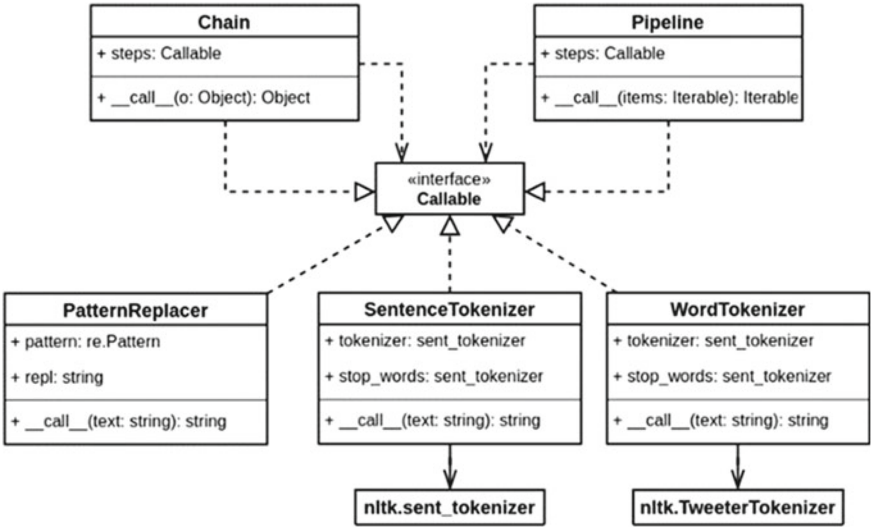

Fig. 5 Pipeline data processing class diagram

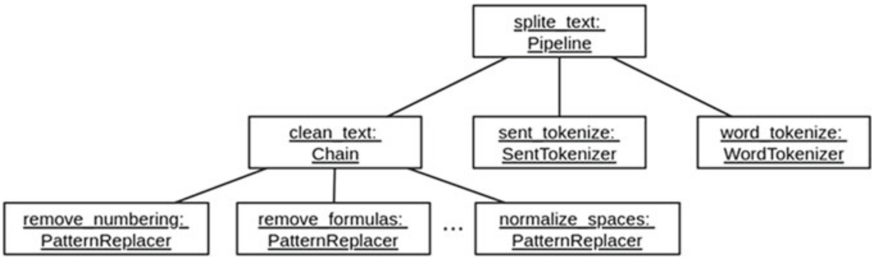

Fig. 6 Diagram of Pipeline data processing objects

In the approach when data is the root cause, the main emphasis is on: storage structures and work with different formats and notations (classes SAO, Conll, ConllTree, etc.) [17] and processors of this data, taking data in one format as input and producing morphological (class TreeTagger), syntactic (UdPipe class), semantic analysis, such as extracting technical functions (SaoExtractor class).

The main concept that is taken as a basis is the Data Pipeline. Most of the existing Batch Processing systems are based on this principle. In this work, we use several third-party libraries based on a data pipeline, which has its implementation specific to the data format they use (matrices, token sequences, etc.). It was decided not to use one of the existing pipelining systems due to their cumbersomeness and specificity, but to implement a simpler and more flexible implementation based on the «Iterator» design pattern and functional programming elements. The main idea is to build a chain of tasks, implemented based on the «Command» design pattern, which allows implementing delayed execution of a certain set of functions. Text processors are examples of this approach (Fig. 5). An illustrated principle has been applied to the entire system.

The diagram shows the text processors «PatternReplacer», «WordTokenizer» and «SentenceTokenizer» that process text at different levels: as a sequence of symbols, words, and sentences respectively. “PatternReplacer” is intended for replacing or deleting blocks of text by a pattern, instances of this class implement their specific functionality, for example, for deleting formulas and numbering paragraphs, as illustrated in Fig. 6. The classes «WordTokenizer» and «SentenceTokenizer» add functionality to similar classes of the NLTK library. «WordTokenizer» combines several words into one for named entities according to the input rules. «Sentence-Tokenizer» segments sentences. These classes are designed to eliminate from the text constructions that do not carry semantic significance in the framework of the problem being solved but negatively affect the correctness of the work of morphological and syntactic analyzers. The classes described above implement the standard «Command» design pattern, which allows you to create deferred objects and build task chains (the «Chain» class) or pipelines (the «Pipeline» class) for processing data. The «Chain» class represents a chain of execution, stores a list of handlers that implement the «Callable» interface, passes the input data (a single object) to the first, its result to the next, and so on along the chain. The Pipeline class implements similar functionality but works with a collection of objects.

3 Research Results

Command-line interfaces for working with the data storage (Fig. 7) and the semantic core (Fig. 8) were implemented.

By the physical effect model, each of its components is described by a regular expression, an example of a description is given in Table 1, for clarity, the pattern is

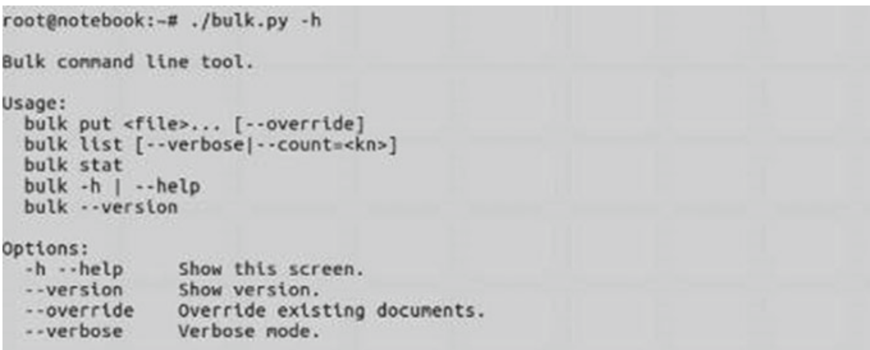

Fig. 7 Data storage command-line interface

```
root@notebook:~# ./semcore.py -h

SemCore command line tool.

Usage:
  semcore morph <file>...
  semcore synt <file>... [--output=(conll | picture)]
  semcore sao <file>... [--output=(conll | picture)]
  semcore effect <file>... [--output=(plain | table)]

  semcore -h | --help
  semcore --version

Options:
  -h --help     Show this screen.
  --version     Show version.
```

Fig. 8 Semantic core command-line interface

Table 1 Description of the physical effect "Ohm's Law"

Component		Description	Pattern
Input	Impact	Electrical field	[weak] electric[al] field
	Characteristic of impact	weak	
	Physical quantity	electric field strength (V/m)	(electric[al] field) density | pressure) | voltage
Output	Impact	electricity	
	Characteristic of impact	Direct, alternating, electronic, mixed, ionic	([alternating | direct | ionic | mixed] [electric[al]] current) | AC | DC
	Physical quantity	current density (A/m**2)	[electric[al]] current density
Object		conductor, semiconductor	[semi]conductor | resistance | resistor

presented in the following form: optional parts of the pattern are presented in square brackets, alternatives are listed, separated by the "|" symbol. Examples of found descriptions of the physical effects are shown in Table 2.

Examples of found descriptions of technical functions in SAO format are shown in Table 3.

The correctness of the algorithms was proved on a test sample prepared manually. Technical functions were extracted from the «Summary of Invention» [18, 19] field of the document, and physical effects were searched for in the «Description» field [20]. The test sample was composed of 60 patent documents and includes 480 technical functions and a description of 20 physical effects, with one document describing only one physical effect.

TF extraction method: accuracy—0.87, completeness—0.77, and F-measure—0.82.

Search for PE description: accuracy—0.92.

Table 2 Examples of searching for descriptions of technical functions in the text of a patent

№	Determined PE	Input data
1	PE № 303 «Thermo-photoelectric effect»	Patent US6380534B1 The amplitude of the Brillouin peaks and the frequency shift of the Brillioun peaks compared with the Rayleigh peak is a measure of the voltage and temperature of the optical fiber at the point from which the light was backscattered
2	PE № 37 « Ohm's law»	Patent US2965301A Conductors, as indicated, are connected to the resistors for application thereto of factor—representing voltages and/or currents and for deriving therefrom an output, all as more fully explained hereinafter

Table 3 Examples of searching for technical functions in the text of a patent

№	Determined SAO	Input data
1	S: method and apparatus A: measure O: temperature and strain within a structure	Patent US6380534B1 …A method and apparatus for measuring the temperature and strain within a structure consists of having optical fibres incorporated in the structure, passing pulses of light down the fibre and detecting the backscattered light…
	S: optical fibres A: pass O: pulses of light down the fibre	
	S: optical fibres A: detect O: backscattered light	
2	S: object of the invention A: provide O: simple and reliable multiplier-divider computer unit of increased capacity.	Patent US2965301A …object of the invention is the provision of a simple and reliable multiplier-divider computer unit of increased capacity. Another object of the invention is the provision of a simple and reliable D.C. multiplier-divider computer unit…
	S: object of the invention A: provide O: simple and reliable D.C. multiplier-divider computer unit	

To test the method of constructing a database of technical functions performed by physical effects, a combination of test and design samples was made, measuring 60 and 10 thousand patent documents, respectively.

We will assume that for a specific document of the test sample, a correspondence between the PE and the TFs implemented by it has been determined, if at least 80% of the technical functions marked by experts in the document and correctly found at the stage of testing the method for extracting TF technical functions were marked in the TF-PE matrix for this PE. This threshold value is introduced in connection with the possible exclusion of technical functions at the stage of reducing their space.

According to the results of testing, the accuracy of extracting technical functions performed by physical effects was 0.78.

4 Discussion

The theoretical value of this work lies in the developed methodology for analyzing graphical representations of mathematical formulas to expand the description of scientific and technical effects and create an automated system on its basis.

5 Conclusion

The reported study was funded by RFBR (research project 18-07-01086), RFBR and Administration of the Volgograd region (projects 19-47-340007, 19-41-340016).

References

1. Orloff, M.: Inventive Thinking Through TRIZ: A Practical Guide, p. 352. Springer, Heidelberg (2006). https://doi.org/10.1007/978-3-540-33223-7
2. Vayngolts, I., Korobkin, D., Fomenkov, S., Golovanchikov, A.: Synthesis of the physical operation principles of technical system. In: Kravets, A., Shcherbakov, M., Kultsova, M., Groumpos, P. (eds.) CIT&DS 2017. CCIS, vol. 754, pp. 575–588. Springer, Cham (2017). https://doi.org/10.1007/978-3-319-65551-2_42
3. Korobkin, D., Fomenkov, S., Kravets, A.: Methods for extracting the descriptions of sci-tech effects and morphological features of technical systems from patents. In: IISA 2018 (2018). https://ieeexplore.ieee.org/document/8633624
4. Davydova, S., Korobkin, D., Fomenkov, S., Kolesnikov, S.: Modeling of new technical systems using cause-effect relationships. In: IISA 2018 (2018). https://ieeexplore.ieee.org/document/8633683
5. Korobkin, D., Shabanov, D., Fomenkov, S., Golovanchikov, A.: Construction of a Matrix «Physical Effects – Technical Functions» on the Base of Patent Corpus Analysis. Creativity in Intelligent Technologies and Data Science (CIT&DS 2019), pp. 52–68. (Ser. Communications in Computer and Information Science (CCIS); Volume 1084) (2019)
6. Park, H., Yoon, J., Kim, K.: Identifying patent infringement using SAO based semantic technological similarities. Scientometrics **90**, 515 (2012)
7. Manning, C., Raghavan, P., Schütze, H.: Introduction to Information Retrieval. Cambridge University Press, Cambridge (2008)
8. Yufeng, D., Duo, J., Lixue, J.: Patent Similarity Measure Based on SAO Structure. Chin. Sentence Clause Text Inf. Process. **30**(1), 30–36 (2016)
9. Vasilyev, S., Korobkin, D., Kravets, A., Fomenkov, S., Kolesnikov, S.: Extraction of cyber-physical systems inventions' structural elements of Russian-language patents. Cyber-Physical Systems: Advances in Design & Modelling, pp. 55–68. https://link.springer.com/book/10.1007/978-3-030-32579-4#toc (Book ser. Studies in Systems, Decision and Control (SSDC); vol. 259) (2020)

10. Guo, J., Wang, X., Li, Q., Zhu, D.: Subject–action–object-based morphology analysis for determining the direction of technological change. Technol. Forecast. Soc. Change **105**, 27–40 (2016)
11. Lee, J., Kim, C., Shin, J.: Technology opportunity discovery to R&D planning: key technological performance analysis. Technol. Forecast. Soc. Change **119**, 53–63 (2017)
12. Moehrle, M.G., Walter, L., Geritz, A., Muller, S.: Patent-based inventor profiles as a basis for human resource decisions in research and development. R&D Manag. **35**(5), 513–524 (2005)
13. No, H.J., Lim, H.: Exploration of nanobiotechnologies using patent data. J. Intellect. Prop. **4**(3), 109–129 (2009)
14. Wang, X., Wang, Z., Huang, Y., Liu, Y., Zhang, J., Heng, X., et al.: Identifying R&D partners through subject–action–object semantic analysis in a problem & solution pattern. Technol. Anal. Strateg. Manag. **29**, 1–14 (2017)
15. Wich, Y., Warschat, J., Spath, D., Ardilio, A., König-Urban, K., Uhlmann, E.: Using a text mining tool for patent analyses: development of a new method for the repairing of gas turbines. In: 2013 Proceedings of PICMET 2013 Technology Management in the IT-Driven Services (PICMET), pp. 1010–1016. IEEE, 2013, July
16. Yoon, J., Kim, K.: Identifying rapidly evolving technological trends for R&D planning using SAO-based semantic patent networks. Scientometrics **88**(1), 213–228 (2011)
17. Yoon, J., Kim, K.: Detecting signals of new technological opportunities using semantic patent analysis and outlier detection. Scientometrics **90**(2), 445–461 (2012)
18. Yoon, B., Park, I., Coh, B.Y.: Exploring technological opportunities by linking technology and products: Application of morphology analysis and text mining. Technol. Forecast. Soc. Change **86**, 287–303 (2014)
19. Zhang, Y., Zhou, X., Porter, A.L., Gomila, J.M.V.: How to combine term clumping and technology roadmapping for newly emerging science & technology competitive intelligence: "problem & solution" pattern based semantic TRIZ tool and case study. Scientometrics **101**(2), 1375–1389 (2014)
20. Mel'čuk, I.: Dependency Syntax Theory and Practice. SUNY, New York (1988)

The Formation of Morphological Matrix Based on an Ontology "Patent Representation of Technical Systems" for the Search of Innovative Technical Solutions

Dmitriy Korobkin, Sergey Fomenkov, Grigoriy Vereschak, Sergey Kolesnikov, Dmitriy Tolokin, and Alla G. Kravets

Abstract Today, the active development of technology leads to a huge increase in the amount of information in patent databases. In this regard, it is necessary to process this information and extract the most relevant data from the array of patents. This article discusses component extraction methods, technical problems, and solutions. Structured information from patents is stored in a structured form in an ontology. Information about system components is retrieved by querying the ontology. The paper also describes the grammar for extracting technical functions in the form of a "solution-problem". The structure and components of the subsystem for allocating the functions of technical objects are described.

Keywords Technical systems · Patent · Ontology · Fact extraction

1 Introduction

With the development of the direction of the automated invention [1–5], CAI systems are being used more and more recently. Computer-Aided Invention is the search for innovative solutions using the computer. CAI systems are automated support systems and search for new technical solutions. The completeness of various knowledge bases and the completeness of ontologies of subject areas directly affect the success of support systems and the search for new technical solutions that find their application in the synthesis of new technical solutions. But one of the serious problems of CAI systems is the problem of updating the knowledge base since this process is rather difficult [6].

Scientific documents, patent documents, reference books can be the main sources of technical information to supplement existing knowledge bases. Patent documents

D. Korobkin (✉) · S. Fomenkov · G. Vereschak · S. Kolesnikov · D. Tolokin · A. G. Kravets
Volgograd State Technical University, Lenina Avenue, 28, Volgograd, Russia

A. G. Kravets
Dubna State University, Dubna, Moscow Region, Russia

A. G. Kravets et al. (eds.), *Cyber-Physical Systems*, Studies in Systems, Decision and Control 350, https://doi.org/10.1007/978-3-030-67892-0_13

can be considered one of the main sources of technical information since the number of patents in patent databases is quite large.

The existing more than 20 million worldwide patent database can act as a source of information for the initial stages of designing new technical solutions. Such volumes of data require automated processing.

One of the convenient ways of conceptualized knowledge representation about any subject area is the ontology model. Ontologies are a convenient organization of stored knowledge, thanks to which you can search and analyze data. Considering that the array of patent documents contains a lot of information useful for extraction and analysis, such as claims, classifications, country of origin, organization; ontologies provide the ability to structure and link information.

2 Analysis of the Patent Array

A patent document is a document issued by an authorized public authority confirming the exclusive right of the patent holder to an invention, utility model, or industrial design. One of the most useful for analysis is the patent claims, which are part of the specification of the patent document. The International Patent Classification (IPC) is a vehicle for internationally uniform classification of patent documents. This paper deals with patents belonging to the classes of electricity and mechanical engineering, that is, classes H and F, respectively.

In this study, as morphological features, which are concepts of ontologies of the subject areas "Technical functions" and "Implementation of technical objects", the technical implementation and the structure "problem-solution" are highlighted. The technical implementation determines the constructive composition of the invention, and the problem-solution structure expresses the problem solved by the technical implementation. The source of data for the first feature is the claims of the device, and for the second—the item of the technical result in the description section of the invention.

Using the SAO (Subject-Action-Object) [7–9] model, technical implementations of objects can be represented, and the problem-solution structure is an incomplete part of the model. Morphological features of technical objects from patent documents can be represented by certain syntactic constructions that can be used for the automated construction of ontologies.

The main methods for extracting concepts and relationships between concepts for building domain ontologies are dependency parsing and part-of-speech tagging [10–15]. The SAO model is used to represent the implementations of technical objects and technical functions. To extract concepts from the claims of a patent document, the latest version of the Stanford NLP called Stanza [16] is used. An example of concept extraction is shown in Fig. 1

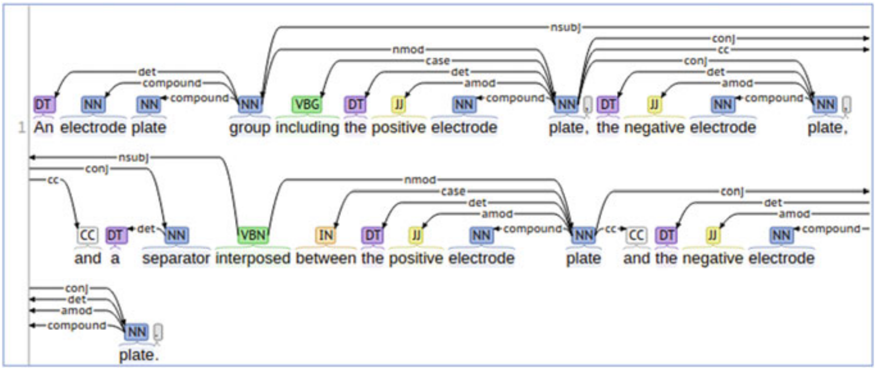

Fig. 1 Example of fact extraction

3 Developed Methods for Extracting Information from the Patent Array

Features of patent presentation of technical systems:

- Descriptions of realizations of technical objects are contained in the invention formula;
- The technical problem solved by the device (device from the name of the patent) is contained in the first paragraph of the summary of the patent.

Before proceeding to parse patent documents containing descriptions of implementations of technical devices, it is necessary to perform preliminary processing of the patent array, which is an XML file. The filtering of patents is carried out by classes H and F, which correspond to electricity, mechanical engineering, etc.

To search for and retrieve realizations of technical objects [17–20], the claims are analyzed. The first claim is the most generalized and contains the most complete description of the device, and it is he who is being analyzed.

3.1 Pre-segmentation Algorithm

The main idea of preparing the segments of the first paragraph of the formula is to "restore" sentences for correct analysis by the stanza parser. In Example 1, you can see a fragment of the first claim of the invention in its original form.

For the left side of the claims, the main device is searched. The claims begin with the main device, followed by the sequence of characters "comprising:". To restore the segments the left part is taken up to the ":" character and the right part containing the enumeration is split by the ";" character. At the beginning of each segment representing an enumerated element, a substring is added containing the main unit of the patent claims.

Each penultimate enumerated element has after the “;” the conjunction “and”, which can complicate the parsing of the sentence. Therefore, in the first claim, the combination of symbols “; and” is replaced with“; ”, after which the first occurrence of the word “ where ”is searched for. The claims are divided into two parts—before and after. If “where” is absent, then the whole formula is taken. Since there can be several “where”, then the part of the formula after the first mention of “where” is broken down by “where”, and for each resulting segment, whitespace characters are removed from the beginning and end of the segment.

Example 1. A fragment of the first claim of the invention

```
<claim-text> 1. A decoupled gas turbine engine
comprising:
  <claim-text> a low pressure compressor; </claim-text>
  <claim-text> a high pressure compressor;
</claim-text>
  …
  <claim-text> a second turning duct in fluid
communication between the combustor and the high
pressure turbine; </claim-text>
  <claim-text> where the low pressure compressor and
the low pressure turbine …
```

After preliminary segmentation, the first claim will have the form shown in Example 2.

Example 2. View of the first claim after preliminary segmentation

```
A decoupled gas turbine engine comprising a low
pressure compressor.
  A decoupled gas turbine engine comprising a high
pressure compressor.
```

3.2 SAO Extraction Algorithm

A global list of extracted SAOs is used to store and write retrieved device components in the form of an SAO model. For each pre-segmented segment, all SAOs are retrieved. The input segment is split into a sequence of tokens using a parser. Only those segments with tokens that contain key verbs typical for extracting the implementation of technical objects are subject to processing. Key verbs include the following: comprise, consist, connect, include, attach, have. The extraction of technical realizations should be continued until there are no unprocessed key verbs in the segment. Figure 2 shows an algorithm for extracting realizations of technical objects from the claims.

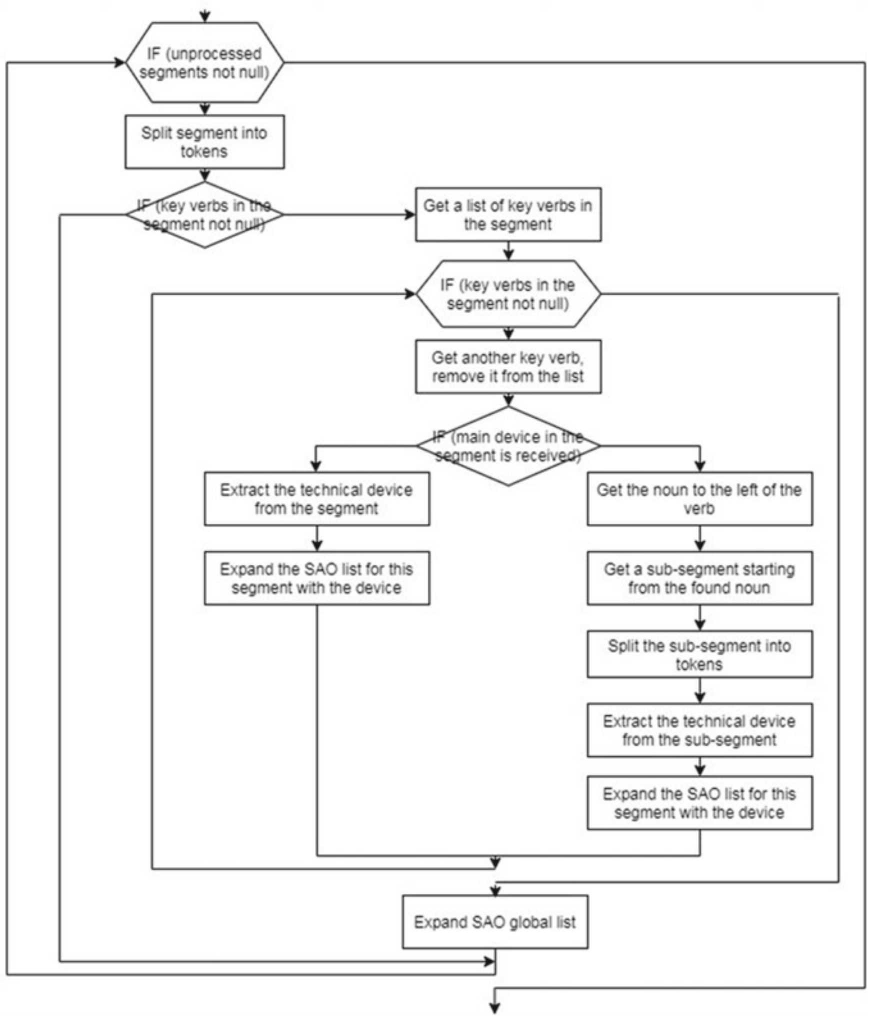

Fig. 2 Algorithm for extracting realizations of technical objects from the claims

Dependency parsing and parts of speech detection are used to directly extract the technical implementation. The algorithm for extracting technical implementation assumes the presence of a potential key vowel, for which it is necessary to find a subject and an object.

Figure 3 shows a detailed algorithm for extracting a specific implementation of a technical object.

An example of extracting the implementation of technical objects is shown in Fig. 4.

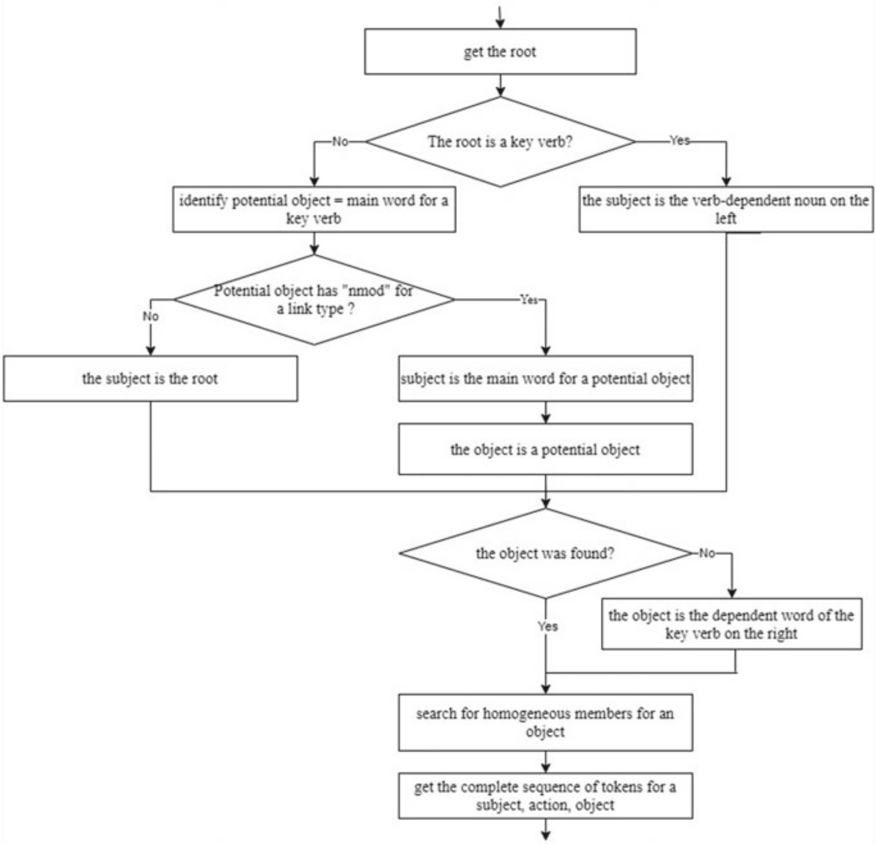

Fig. 3 Algorithm for extracting the implementation of a technical object

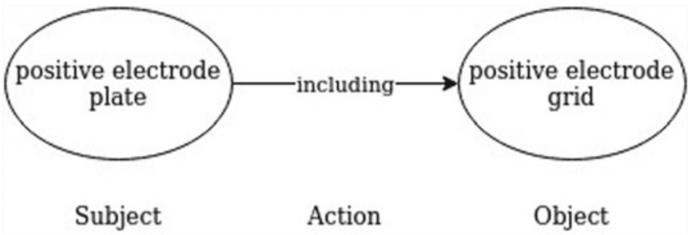

Fig. 4 Example of the method implementation

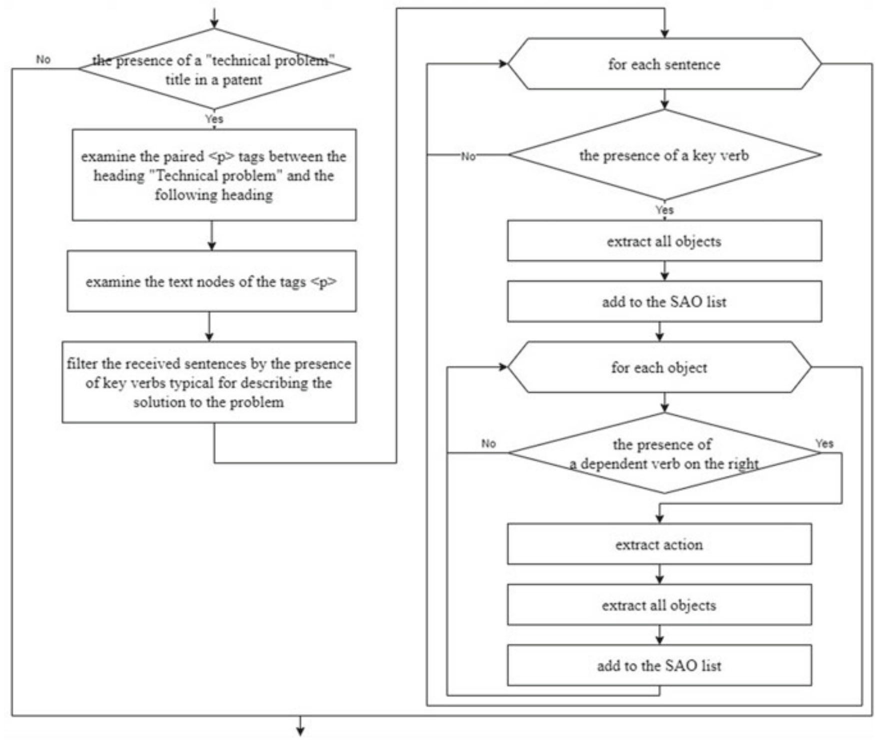

Fig. 5 Algorithm for extracting the problem of the device and technical functions to be solved

To extract technical functions and the problem to be solved, the device does not analyze the patent formula, but the section of the patent with the title "Technical Problem". Figure 5 shows an algorithm for extracting the device problem to be solved and technical functions.

4 The Ontology

Triplets are the main way of expressing information in ontologies. A triplet consists of three components—subject, predicate, and object. This model is ideal for storing retrieved realizations of technical objects as SAO. So, a triplet will consist of three components—subject, action, object.

In Fig. 6 you can see the class diagram of the ontology of the subject areas "Technical functions" and "implementations of technical objects".

The following properties of objects were selected:

- hasFunction—a property for linking a technical function and a component;

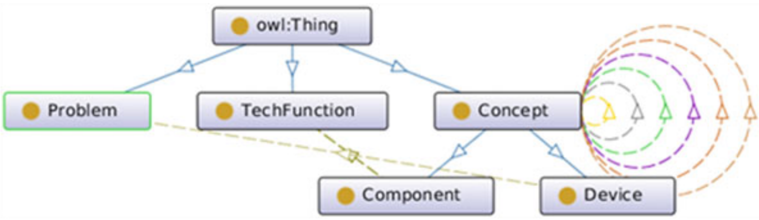

Fig. 6 Scheme of classes of the ontology of the subject areas "Technical functions" and "implementation of technical objects"

- comprises—a property for communication between the components of a device (the verb "comprise");
- connectedTo—property for communication between device components (verbs "connect", "attach");
- consists—a property for communication between device components (the verbs "consists", "include");
- parentFor—indication of the presence of a parent relationship between elements (the verb "have");
- partOf—indication of the belonging of the component to the device of the patent document;
- solutionFor—property for linking the problem and the device being solved by it;
- connected_to—connection between elements (verbs "install", "connect", "connect", etc.).

Figure 7 shows the ontology replenishment algorithm.

The resulting ontology is exported to an OWL file, which can then be opened for further work in Protege.

5 The Software

The automated system is implemented as a desktop application for Linux operating systems. Development was carried out on the Ubuntu 18.04.4 operating system. The system is implemented in the Python 3.6.9 programming language. The PyQt5 library was used to create the user interface. For the analysis of natural language texts, the latest version of Stanford NLP called Stanza was used. The MySQL DBMS was used to store the extracted SAOs, and the Python PyMySQL library was used for development. XML files were parsed using the lxml library. The Owlready2 library was used to work with ontologies.

The automated system allows you to download patent documents, extract technical functions and implementations of technical objects, display the extracted implementations of technical objects in a form, build ontologies for a user-selected patent, as well as for all uploaded patents for which technical functions and technical object

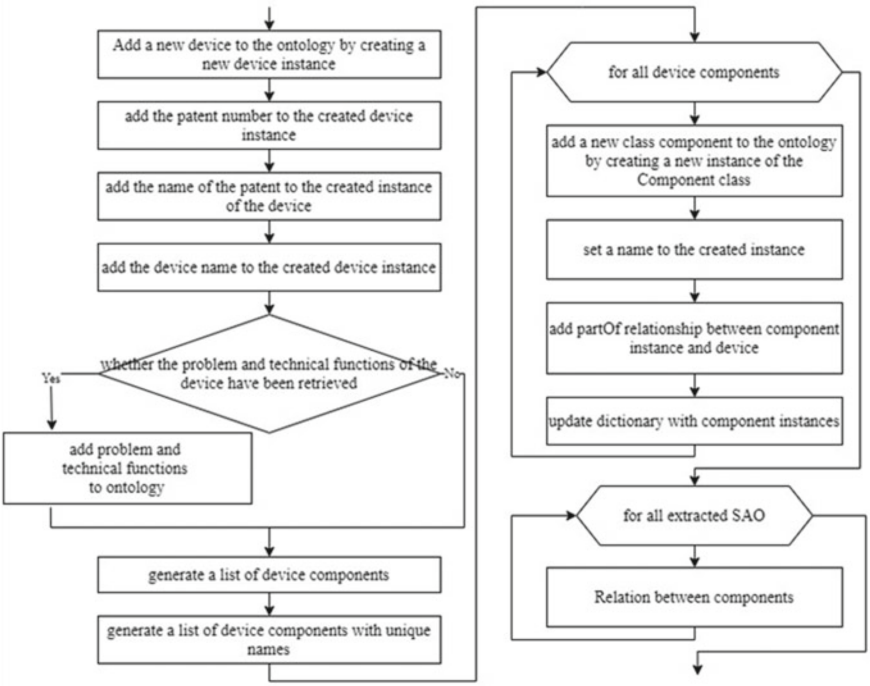

Fig. 7 Algorithm for replenishing the ontology of the subject areas "Technical functions" and "implementation of technical objects"

implementations have been extracted. Figure 8 shows the constructed ontology for one patent document.

As a computational experiment, patent documents were manually sorted out, the number of SAO retrieved for each patent and the time taken to parse each patent document were recorded. The extraction accuracy (P) was calculated using the formula (1)

$$P = \frac{\mathrm{E}}{\mathrm{N}}, \tag{1}$$

where E is the number of correctly extracted by the SAO system, N is the number of SAO in the patent document.

In Table 1 you can see the results of the experiment.

The average time for parsing one patent by the system was 1.72316 s, the average time for parsing one patent by an expert was 46.6 s. Accuracy rates are above 70%.

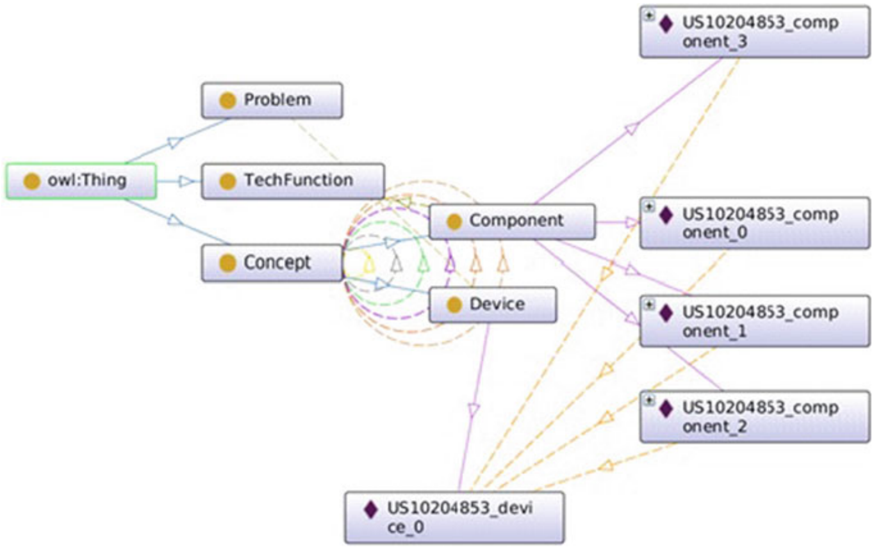

Fig. 8 The ontology for one patent document

Table 1 Results of the experiment

Experiment number	Time spent processing by the system, c	Time spent on processing by an expert, c	Extraction accuracy, %
1	1.324552	47.0	85.7
2	2.366441	54.0	100.0
3	2.608219	51.0	76.5
4	0.656219	38.0	100.0
5	1.660411	43.0	71.4

6 Discussion

This work solved the general problem of information support for the synthesis of new technical solutions based on the analysis of USPTO patents.

As concepts of the ontology of subject areas, the structural elements of a technical object (TO) and the relationship between them, as well as descriptions of the problems solved by the invention, were considered. The first claim of the patent document acted as the main source of information. The unit of extraction was the semantic structures SAO (Subject-Action-Object).

The main linguistic features of patent documents were identified. The method of preliminary processing of the patent mass has been formed. A separate auxiliary tool has been developed for the preliminary processing of the patent array. An algorithm for extracting SAO from the patent formula has been formed. A method has been developed for exporting extracted SAOs from English-language patents to a domain ontology.

The developed methods were tested on US patent documents

Acknowledgements The reported study was funded by RFBR (research projects 18-07-01086, 19-07-01200), RFBR and Administration of the Volgograd region (projects 19-47-340007, 19-41-340016).

References

1. Arel, E.: Goldfire Innovator. Volume II: Patents and Innovation Trend Analysis User Guide. Invention Machine Corporation, Boston, MA (2004)
2. Arel, E., Verbitsky, M., Devoino, I., Ikovenko, S.: TechOptimizer Fundamentals. Invention Machine Corporation, Boston, MA (2002)
3. Zlotin, B., Zusman, A.: Directed Evolution: Philosophy, Theory and Practice. Farmington Hills, Ideation International (2001)
4. Fey,V., Rivin, E.: Innovation on Demand: New Product Development Using TRIZ. Cambridge University Press, Cambridge (2005)
5. Souili, A., et al. Starting from patents to find inputs to the problem graph model of IDM-TRIZ. Procedia Eng. **131**, 150–161. https://doi.org/10.1016/j.proeng.2015.12.365 (2015)
6. Manning, C., Raghavan, P., Schütze, H.: Introduction to Information Retrieval. Cambridge University Press, Cambridge (2008)
7. Choi, S., et al. SAO network analysis of patents for technology trends identification: A case study of polymer electrolyte membrane technology in proton exchange membrane fuel cells. Scientometrics, 863–883. https://doi.org/10.1007/s11192-011-0420-z (2011)
8. Guo, J., et al.: Subject–action–object-based morphology analysis for determining the direction of technological change. Technol. Forecasting Soc. Change **105**, 27–40 (2016)
9. Yufeng, D., Duo, J., Lixue, J.: Patent similarity measure based on SAO structure. Chin. Sentence Clause Text Inf. Process. **30**(1), 30–36 (2016)
10. Asiryan, A.K.: Morphological tagging tools comparison. Intellectual potential of the XXI century 2017, November. https://www.sworld.com.ua/konferu7-317/27.pdf (2017)
11. Mel'čuk, I.: Dependency Syntax Theory and Practice. SUNY, New York (1988)
12. Link Grammar Parser. http://www.abisource.com/projects/linkgrammar (2020)
13. MaltParser. http://maltparser.org/ (2018). Accessed 26 Oct 2020
14. UFAL UDPipe. http://ufal.mff.cuni.cz/udpipe (2020). Accessed 26 Oct 2020
15. CoNLL-U Format. https://universaldependencies.org/format.html (2020). Accessed 26 Oct 2020
16. Stanza. https://stanfordnlp.github.io/stanza/ (2020). Accessed 26 Oct 2020
17. Korobkin, D., Shabanov, D., Fomenkov, S., Golovanchikov, A: Construction of a matrix «Physical Effects – Technical Functions» on the base of patent corpus analysis. In: Creativity in Intelligent Technologies and Data Science (CIT&DS 2019), pp. 52–68 (Ser. Communications in Computer and Information Science (CCIS); Volume 1084) (2019)
18. Vasilyev, S., Korobkin, D., Kravets, A., Fomenkov, S., Kolesnikov, S.: Extraction of cyber-physical systems inventions' structural elements of Russian-language patents. In: Cyber-Physical Systems: Advances in Design & Modelling, pp. 55–68. https://link.springer.com/book/10.1007/978-3-030-32579-4#toc (Book ser. Studies in Systems, Decision and Control (SSDC); vol. 259) (2020)

19. Fomenkova, M., Korobkin, D., Kravets, A., Fomenkov, S.: Extraction of knowledge and processing of the patent array. In: Creativity in Intelligent Technologies and Data Science (CIT&DS 2019), pp. 3–14 (Ser. Communications in Computer and Information Science (CCIS); Volume 1084) (2019)
20. Vayngolts, I., Korobkin, D., Fomenkov, S., Kolesnikov, S.: The Software and Information Complex Which Uses Structured Physical Knowledge for Technical Systems Design / Creativity in Intelligent Technologies and Data Science (CIT&DS 2019), pp. 42–51 (Ser. Communications in Computer and Information Science (CCIS); Volume 1084) (2019)

The Software for Computation the Criteria-Based Assessments of the Morphological Features of Technical Systems

Dmitriy Korobkin, Sergey Fomenkov, Marina Fomenkova, Ilya Vayngolts, and Alla G. Kravets

Abstract The software of computation criteria-based assessments of the morphological features of technical systems based on an analysis of trends identified from the patent array was considered in this article. This method is developed based on highlighting the most important technical functions, as well as based on an approach to comparing and identifying synonymous technical functions.

Keywords Patent analysis · DGH structures · Patent documents · Fact extraction · Technological trends

1 Introduction

Today, the massive development of technology leads to a huge increase in the amount of information in patent databases. In this regard, there is a need to process this information and extract the most relevant data from the patent array. There are several approaches to solving this problem. The most relevant approach seems to be the use of semantic units, such as the structures of the SAO [1–7] (subject, object, action), DGH (action, object, restriction), etc., which represent the basic semantic meaning of the sentence.

Researchers such as Yoon, Kim, and Wang are working in this direction [1–10]. Extracting from the patent documents the structures of the SAO [5–15] or extended structures of the SAO [15], they receive key information about the structure, materials of the invention, as well as information about its application. Which in the future can be used to analyze technological trends, compare patents, compile competitive maps, etc.

Due to the peculiarities of the Russian language, the most successful choice for research seems to be the structure of DGH, consisting of action, object, and restrictions.

D. Korobkin (✉) · S. Fomenkov · M. Fomenkova · I. Vayngolts · A. G. Kravets
Volgograd State Technical University, Lenina Avenue, 28, Volgograd, Russia

A. G. Kravets
Dubna State University, Dubna, Moscow Region, Russia

A. G. Kravets et al. (eds.), *Cyber-Physical Systems*, Studies in Systems, Decision and Control 350, https://doi.org/10.1007/978-3-030-67892-0_14

This chapter presents a method for the formation of criteria-based assessments of morphological features of technical systems based on an analysis of trends identified from the patent array. The method is based on the analysis and finding of the most relevant structures of DGH and the identification of patent trends based on them [11–15].

2 The Method of Extracting the Technical Functions from Natural Language Documents

Semantic analysis of a segment of a patent formula is carried out using Link Grammar Parser software that uses a grammar of relationships. The parser takes input segments of the sentence in a natural language and displays the connections found in the sentence with the markup of the morphological features of the words of the segment. As a result of the parser, we get not syntactic relations (subject to object), but relations between pairs of words.

The relationships found by the parser are interpreted to represent the technical function according to the DGH model.

By analyzing certain types of relationships, you can find words that are objects of the action, the action itself, and the condition for the action to be performed.

As a result, the description of the function of the technical object in the text is presented in the following form: F = <D, G, H>, where D is the set of actions (actions) per-formed and leading to the desired result; G is the set of objects to which these actions are directed; H—a lot of special conditions (conditions) of the performed actions.

A context-sensitive grammar was compiled to extract the components of the DGH model from Russian-language patent proposals through link analysis:

Gram = (T, N, <W>, R),
where T = {action, object, condition} is a set of terminals, N = {<MV>, <SI>, <E>, <J>, <I>, <A>, <M>} is a set of non-terminals, <W> is the initial non-terminal, R is the set of production rules:

<W> → action <MV> <E> | action <MV> | action <E> | action | ε
action <MV> → action <MV> | action <MV> <MV>
action → action | <I> action | action <I>
<I> action → action action | <I> action action | action <I> action
action <I> → action action | action action <I> | action <I> action
<MV> → object <MV> | <A> object | <A> object <M> | object <M> | an object
<A> → object → object object | <A> object object | object <A> object
object <M> → object object object | object <A> object | object object <M> | object <A> object <M>
condition <J> → condition | condition <E> | condition <J>

<A> condition → condition condition <M> | condition <A> condition <M>
condition <M> → condition condition | condition condition <M> | condition condition <J> | condition <A> con-dition
<MV> → <MV> | <SI>
<E> → <E> | <EI>
<A> → <A> | <AXP> | <PI>

To extract Russian-language descriptions of the functions of a technical object, it is necessary to carry out semantic analysis of a patent formula based on Link Gram-mar for Russian software using a grammar of relationships.

To parse Russian-language patent formulas, you need the following types of links Link Grammar for Russian:

- W—connects the border of the sentence and the main word, which is usually noun;
- MV—connects verbs with their objects;
- SI—connects verbs with their objects, answering the question what;
- E—connects an adverb with a verb;
- J—connects a preposition with a dependent noun or pronoun;
- I—connects the verb with another dependent verb;
- A—connects a pronoun or adjective with a noun;
- M—connects nouns with other dependent on them nouns;
- EI—connects a verb with an adverb;
- PI—connects verb adjectives or participles with
- nouns;
- AXP—connects pronouns or adjectives with adjectives.

3 The Method for the Computation of Criteria-Based Assessments of the Morphological Features of Technical Systems

Firstly, the term-document matrix is formed. The terms (functions of the technical object DGHi) are extracted from the totality of all documents {P} of the patent array and the frequency of their occurrence in patent documents is determined.

Metric TF of the i-th technical function DGHi in the j-th patent document Pj (section of the patent relating to the main purpose of the invention):

$$TF_{ij} = f_{ij} \tag{1}$$

where f_{ij} is the frequency of occurrence of DGHi in Pj.

At the initial stage, Table 1 in the cells will contain 0 if DGHi does not meet Pj, or some integer value.

Further, the contents of the term-document matrix are modernized based on the developed DGH comparison algorithm. If the technical function DGHi is found in

Table 1 Matrix of occurrence of technical functions in patents

	DGH_1	DGH_2	…	DGH_m
P_1	TF_{11}	TF_{21}	…	TF_{M1}
P_2	TF_{12}	TF_{22}	…	TF_{M2}
…	…	…	…	…
P_N	TF_{1N}	TF_{2N}	…	TF_{MN}

the j-th patent document Pj, then on the basis of DGHi, a subset of the technical functions {DGH} is searched for which the similarity coefficient DGHi is higher than the entered threshold value.

Consider an example comparison of two DGH structures that extracted from patents:

- SU245727A1 «Установка для очистки воздуха» (Air purifier)—«Установка предназначена для очистки воздуха в производственных помещениях…» (The unit is designed for air purification in industrial premises…)
- SU28860A1 «Фильтр для воздуха» (Air filter)—«Предлагаемый фильтр для воздуха, предназначенный для очищения пыльного теплого воздуха в жилых и промышленных помещениях…» (The proposed air filter designed to clean dusty warm air in residential and industrial premises).

The first step is a comparison of the “Action” (D). If the top of the first DGH (search query pattern, SQP) and the second DGH (search document pattern, SDP) do not match, then Word2Vec technology is used to identify the semantic proximity of the terms “Actions”. A set of word2vec algorithms for calculating vector representations of words implements two main architectures:

- Continuous Bag of Words: taking into account the four nearest neighbors of the term (two previous and two subsequent words) without taking into account the sequence.
- Skip-gram: a sequence of length n, where the elements are at a distance of no more than k from each other. The body of patent tests (claims of 200 thousand Russian-language patents) is fed to the input, and the output is a set of word vectors.

As a result of the operation of the algorithms, the following results are formed:

- Word2Vec in “CBoW” mode: the output is a list of words that characterize this.
- Word2Vec in “skipgrams” mode: the output is a list of words interchangeable with the data (contextual synonyms). For the word “Cleaning”, according to Word2Vec technology, we obtain the following list of contextual synonyms with part of speech and Cosine similarity coefficient:
  - Flushing—NOUN—0.61
  - Purification—NOUN—0.59

- Filtration—NOUN—0.58
- clean—VERB—0.56
- extraction—NOUN—0.54
- recycling—NOUN—0.54
- sorting—NOUN—0.54
- precipitation—NOUN—0.54
- drying—NOUN—0.53
- sewage—ADJ—0.53

Among the first 10 contextual synonyms, there is the term “purification”. We introduce the concept of the similarity coefficient DGH for the “Action” element:

$$K^D = \begin{cases} 1, \ \text{if } D \text{ matches for SQP and SDP} \\ \text{Cosine similarity, if contextual synonyms} \\ 0, \ \text{if not matches} \end{cases} \tag{2}$$

Consider the example in Fig. 1 in SQP, the D-vertex is “purification”, in SDP—“purification”, respectively, K^D (coefficient of similarity DGH for the element “Action”) is 0.59 (Cosine similarity).

At the second stage, the similarity of the “Object” is checked—a comparison of the vertices G and the associated child structures.

If the G vertices of the SQP and SDP do not match, then the similarity coefficient of DGH for the “Object” is 0. If the G-vertices of the SQP and SDP match, then their children associated with this G-vertex are compared.

At each level, when terms (words) do not match, a check is made for significance. The significance of the term is checked on the basis of a prepared table in which the IDF coefficients are determined (the inverse document frequency with which terms are found in all documents of the patent base). If the IDF term is less than the threshold value, then the word is not significant and is not taken into account in the calculation of the similarity coefficient.

We introduce the concept of the similarity coefficient DGH for the “Object” element:

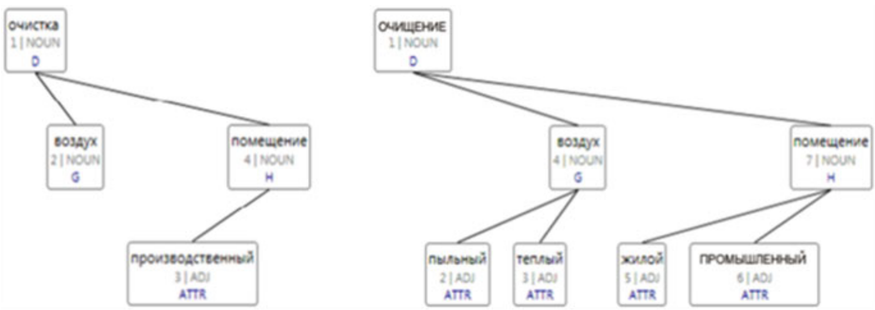

Fig. 1 Comparison of two extracted DGH (SQP, SDP)

$$K^G = \begin{cases} 1, \text{ if } G \text{ matches for SQP and SDP} \\ \text{Cosine similarity, if contextual synonyms} \\ 0, \text{ if not matches} \end{cases} \quad (3)$$

Let us introduce the concept of the similarity coefficient of children associated with a G-vertex ("Object"):

$$K_C^G = \begin{cases} \sum_{i=1}^{Nsqp} S(t1, t2) \\ 1, \text{ if } Nsqp = 0 \end{cases} \quad (4)$$

where Nsqp—the number of children of the G-vertex of the SQP taking into account IDF;

TG_{SQP}, TG_{SDP}—a set of child elements associated with the G-vertex for SQP and SDP, respectively (taking into account IDF)

S (t1, t2) is the operator that determines the coincidence of the $t1 \in TG_{SQP}$ and $t2 \in TG_{SDP}$

$$S(t1, t2) = \begin{cases} 1, \text{ if } t1 \text{ matches } t2 \\ \text{Cosine similarity, if contextual synonyms} \\ 0, \text{ if not matches} \end{cases} \quad (5)$$

Consider the example in Fig. 1 the coefficient K^G of the similarity of DGH in the "Object" is 1. There are no children in the SQP for G vertices, in the SDP—2 ("dusty", "warm"), respectively, Nsqp = 0. The coefficient K_C^G is 0.

In the third stage, the similarity "Constraints" is checked—a comparison of the vertices H and the associated child structures.

If the H-vertices of SQP and SDP do not coincide, then the similarity coefficient of DGH according to the "Constraint" is 0. If the H-vertices of SQP and SDP are the same, then their children associated with this H-vertex are compared.

We introduce the concept of the similarity coefficient DGH for the "Constraint" element:

$$K^H = \begin{cases} 1, \text{ if } H \text{ matches for SQP and SDP} \\ \text{Cosine similarity,if contextual synonyms} \\ 0, \text{ if not matches} \end{cases} \quad (6)$$

Let us introduce the concept of the similarity coefficient of children associated with an H-vertex ("Restriction"):

$$K_C^H = \begin{cases} \sum_{i=1}^{Nsqp} S(t1, t2) \\ 1, \text{ if } Nsqp = 0 \end{cases} \quad (7)$$

where $Nsqp$—the number of children of the H-vertex of the SQP, taking into account IDF;

TH_{SQP}, TH_{SDP}—a set of children associated with the H-vertex for SQP and SDP, respectively (taking into account IDF);

$S(t1, t2)$—the operator that determines the coincidence of the elements $t1 \in TH_{sqp}$ and $t2 \in TH_{SDP}$;

$$S(t1, t2) = \begin{cases} 1, \text{ if } t1 \text{ matches } t2 \\ \text{Cosine similarity, if contextual synonyms} \\ 0, \text{ if not matches} \end{cases} \tag{8}$$

Consider the example in Fig. 1 the coefficient K^H of the similarity of DGH in the "Constraint" is 1. In SQP 1, a child element for G peaks ("production"), in SDP—2 ("residential", "industrial"), respectively, Nsqp = 1. The term "production" passes the filter according to the IDF parameter.

For the word "production", according to Word2Vec technology, we obtain the following list of contextual synonyms with part of speech and Cosine coefficient similarity:

- production—NOUN—0.68
- company—NOUN—0.65
- technological—ADJ—0.65
- Technical—ADJ—0.63
- design—ADJ—0.60
- industrial—ADJ—0.60
- forestry—ADJ—0.59
- Equipment—NOUN—0.58
- operational—ADJ—0.57

Among the first 10 contextual synonyms, there is the term "industrial". The coefficient K_C^H is 0.6. We introduce the concept of the similarity coefficient of 2 structures:

$$K_{DGH} = \frac{K^D + \frac{K^G + K_C^G}{2} + \frac{K^H + K_C^H}{2}}{3} \tag{9}$$

For example in Fig. 1 $K_{DGH} = (0.59 + 2/2 + 1.6/2)/3 = 0.8$. Two DGHs can be called similar if their similarity coefficient is greater than a certain threshold value. The maximum value of the coefficient is 1.

Next, for each DGH, a search for similar structures is performed. If, on the basis of DGHi, a similar DGHj with a similarity coefficient K_{DGH} was found, then the TF characteristic for DGHj in the rows of the term-document matrix corresponding to patents in which TF (DGHi) is greater than 0 will take the value TF (DGHi) $*K_{DGH}$.

Table 2 An example of an initial matrix of occurrence of technical functions in patents

	DGH_1	DGH_2	…	DGH_m
P_1	*1*	*0*	…	*0*
P_2	*0*	*2*	…	*1*
…	…	…	…	…
P_N	*0*	*0*	…	*1*

Table 3 An example of a modernized matrix of occurrence of technical functions in patents

	DGH_1	DGH_2	…	DGH_m
P_1	1	1*0,8	…	0
P_2	2*0,58	2	…	0
…	…	…	…	…
P_N	0	0	…	1

For example, if, based on DGH1, a similar structure of DGH2 with a coefficient of $K_{DGH} = 0.8$ was found, and for DGH2, the similarity coefficient of DGH1 is 0.58. Tables 2 and 3 are examples of the conversion of the characteristic TF.

(2) The inverted document frequency is selected as the DGHi global weighting, which is 0 if the technical function appears in all patent documents of the array, and this weight increases as the number of documents in which the technical function occurs decreases:

$$IDF_i = log\left(\frac{N}{\sum_{j=0}^{N} \chi\left(f_{ij}\right)}\right) \tag{10}$$

where N is the number of documents in the patent array,

f_{ij} is the frequency of occurrence of DGHi in the patent Pj

$$\chi\left(f_{ij}\right) = \begin{cases} 1, \text{ if } f_{ij} > 0, \\ 0, \text{ if } f_{ij} = 0 \end{cases} \tag{11}$$

Thus, the inverted document frequency (IDF) will be one of the criteria for evaluating the morphological features of technical systems, which will identify “commonly used” technical functions and reduce their significance.

(3) The patent array is analyzed by time intervals (quarters), clusters with maximum increasing activity (patent trend) are identified, a set of key technical functions corresponding to modern technologies is formed.

Fuzzy clustering of the “Patent Technical Function” matrix is carried out to identify key modern technologies and inventions. In this case, patents registered over the past 10 years (2009–2019) are taken into account. Matrices “Patent Technical Function” are built for each time quarter (I quarter 2009, II quarter 2009, … III quarter 2019). Clustering is based on the LDA [16] model and the constructed model is used to obtain distribution vectors for clusters (unnamed topics). To do this, apply the Spark distributed computing framework and its MLlib [17] machine learning library.

A term document matrix is the mathematical matrix in which rows are patents and columns are terms. This matrix describes the statistical set of the document, describes the frequency of occurrence of each term in the document. In our case, terms are understood as technical functions in the DGH format, and documents are patents.

To construct the Dirichlet Latent Placement Model (LDA), a matrix based on TF [18] (term frequency) is used, which displays the frequency of DGH occurrence in patent texts.

A dictionary of all technical functions in the DGH format is used, extracted from the patent array, voc = $\{t_1, t_2, t_3, \ldots, t_n\}$, where t_i is another unique trending DGH of the patent array. Then each i-th row of the term-document matrix will be the resulting dictionary, and each column will be the number of occurrences of the DGH structure (including similar structures found according to the developed algorithm) in the i-th patent.

Based on the LDA model, it is possible to obtain simultaneous clustering of patents and technical functions on the same set of clusters called topics. As a result, "soft" clustering is built, that is, a patent (and a technical function) may belong to several topics to varying degrees. In the future, we will use the degree of membership of a fuzzy cluster equal to 0.7 as a pore value.

$$DGH_{Cl_i} = \{DGH_1\}, P_{Cl_i} = \{P_k\} \tag{12}$$

where i = 1,…, cl is the cluster index; cl—a given number of clusters (based on the experiments we set the number of clusters equal to 150); DGH_Cli—i cluster of technical functions in the DGH format; $DGH_l \in T_{DGH}$—the l-th technical function in the cluster DGH_Cli; P_cl—i cluster of patents; $P_k \in T_P$—k-th patent in the cluster P_Cli.

Next, we rank the resulting clusters by the number of patents and correlate their technical functions. We select the first 30 clusters with the maximum number of patents and the minimum distance from the centroid to the most remote patent (Euclidean distance) [19].

Thus, for each time quarter, we get a set of so-called "trending" technical functions in the DGH format, which make up the first 30 clusters from the ranked list. The set of trend DGH for a certain period of time is determined as follows:

$$T^t_{DGH} = \left\{DGH_i, DGH_j, \ldots DGH_{N^t_{DGH}}\right\} \tag{13}$$

A criterion assessment of the presence of a technical function in key modern technologies is formed as its frequency of occurrence in the sets of trend DGH for all 39 time quarters (I quarter 2009, II quarter 2009,… III quarter 2019):

$$TR_i = \sum_{j=0}^{29} \chi\left(f_{ij}\right) \tag{14}$$

where f_{ij} is the frequency of occurrence of DGHi in the list of trend technical functions T^t_{DGH},

$$\chi\left(f_{ij}\right) = \begin{cases} 1, & \text{if } f_{ij} > 0, \\ 0, & \text{if } f_{ij} = 0 \end{cases} \tag{15}$$

(4) The following criteria-based assessment of a technical function is formed on the basis of a forecast of its occurrence in a future period.

Time series are constructed on the basis of the vector of occurrence of the technical function in patent documents (the TF characteristic from the term-document matrix “Patent Technical Function” is used) [20]. In this case, patents registered during the last 30 years (1989–2018) are taken into account. Matrices “Patent Technical Function” are constructed for each temporary quarter (I quarter of 1989, II quarter of 1989,… IV quarter of 2018). Thus, for each technical function in the DGH format, we obtain a time series where the number of references to TF is recorded in patents issued in a certain time quarter.

This will be data set No. 1, which is used to implement the proposed method, and data set No. 2 (I quarter of 2019, II quarter of 2019, III quarter of 2019) will be used to verify the effectiveness of the proposed method.

The formula for the model for predicting the development of technology, expressed in terms of DGH, can be obtained using regression analysis.

3 indicators are used (2 quantitative and 1 qualitative):

- TI1 estimates the popularity (frequency of references) of DGH over an appropriate period based on the TF metric
- TI2 shows the potential for future references to DGH. We use the slope of the curve in the last retrospective period to show the trend of the curve in the future
- Qualitative criterion TI3 is formed by experts, used to minimize the expected deviation caused by two previous quantitative indicators. This criterion is used when choosing a technical solution based on a morphological table (paragraph 5 of the Report). Experts are invited to evaluate the importance of each implemented technical function (TF) by distributing points (on a 10-point scale) for each component of a technical object (TO), and then TF with a large contribution to solving specific problems that are supposed to be solved using a new technical solution, may get higher scores than others. The average value of all expert ratings is defined as TI3.

A criterion assessment of the significance of a technical function in a future period is formed by predicting time series based on the ARIMA method.

4 Conclusion

The method of forming criteria-based assessments of the morphological features of technical systems based on an analysis of trends identified from the patent array was considered in this chapter. The approach to extracting and ranking the main technical functions from the texts of the documents is shown, and a technique for extracting the most relevant information is given.

Acknowledgements The reported study was funded by RFBR (research projects 18-07-01086, 19-07-01200), RFBR and Administration of the Volgograd region (projects 19-47-340007, 19-41-340016).

References

1. Korobkin, D., Shabanov, D., Fomenkov, S., Golovanchikov, A.: Construction of a matrix «Physical Effects—Technical Functions» on the base of patent corpus analysis. In: Creativity in Intelligent Technologies and Data Science (CIT&DS 2019), pp. 52–68 (Ser. Communications in Computer and Information Science (CCIS), vol. 1084) (2019)
2. Vasilyev, S., Korobkin, D., Kravets, A., Fomenkov, S., Kolesnikov, S.: Extraction of cyber-physical systems inventions' structural elements of Russian-language patents. In: Cyber-Physical Systems: Advances in Design & Modelling, pp. 55–68 (Book ser. Studies in Systems, Decision and Control (SSDC), vol. 259). https://link.springer.com/book/10.1007/978-3-030-32579-4#toc (2020)
3. Guo, J., Wang, X., Li, Q., Zhu, D.: Subject–action–object-based morphology analysis for determining the direction of technological change. Technol. Forecast. Soc. Change **105**, 27–40 (2016)
4. Lee, J., Kim, C., Shin, J.: Technology opportunity discovery to R&D planning: key technological performance analysis. Technol. Forecast. Soc. Change **119**, 53–63 (2017)
5. Moehrle, M.G., Walter, L., Geritz, A., Muller, S.: Patent-based inventor profiles as a basis for human resource decisions in research and development. R&D Manag. **35**(5), 513–524 (2005). No, H.J., Lim, H.: Exploration of nanobiotechnologies using patent data. J. Intellect. Property **4**(3), 109–129 (2009)
6. Park, H., Yoon, J., Kim, K.: Identifying pa-tent infringement using SAO based semantic technological similarities. Scientometrics **90**(2), 515–529 (2011)
7. Wang, X., Wang, Z., Huang, Y., Liu, Y., Zhang, J., Heng, X., et al.: Identifying R&D partners through subject–action–object semantic analysis in a problem & solution pattern. Technol. Anal. Strateg. Manag. **29**, 1–14 (2017)
8. Wich, Y., Warschat, J., Spath, D., Ardilio, A., König-Urban, K., Uhlmann, E.: Using a text mining tool for patent analyses: development of a new method for the repairing of gas turbines. In: 2013 Proceedings of PICMET'13 Technology Management in the IT-Driven Services (PICMET), July, pp. 1010–1016 (2013)
9. Yoon, J., Kim, K.: Identifying rapidly evolving technological trends for R&D planning using SAO-based semantic patent networks. Scientometrics **88**(1), 213–228 (2011)
10. Yoon, J., Kim, K.: Detecting signals of new technological opportunities using semantic patent analysis and outlier detection. Scientometrics **90**(2), 445–461 (2012)
11. Yoon, B., Park, I., Coh, B.Y.: Exploring technological opportunities by linking technology and products: application of morphology analysis and text mining. Technol. Forecast. Soc. Change **86**, 287–303 (2014)

12. Zhang, Y., Zhou, X., Porter, A.L., Gomila, J.M.V.: How to combine term clumping and technology roadmapping for newly emerging science & technology competitive intelligence: "Problem & solution" pattern based semantic TRIZ tool and case study. Scientometrics **101**(2), 1375–1389 (2014)
13. Korobkin, D.M., Fomenkov, S.A., Kolesnikov, S.G., Voronin, Y.F.: System of physical effects extraction from natural language text in the Internet. World Appl. Sci. J. **24**(24), 91–97 (2013)
14. Korobkin, D.M., Fomenkov, S.A., Kolesnikov, S.G., Orlova, Y.A.: A multy-stage algorithm for text documents filtering based on physical knowledge. World Appl. Sci. J. **24**(24), 91–97 (2013)
15. Fomenkov, S., Korobkin, D., Kolesnikov, S.: Method of ontology-based extraction of physical effect description from Russian text. Communications in Computer and Information Science. T. 466 CCIS. C. 321–330 (2014)
16. Choi, S., Kim, H., Yoon, J., Kim, K., Lee, J.Y.: An SAO-based text-mining approach for technology roadmapping using patent information. R&D Manag. **43**(1), 52–74 (2013)
17. Chen, H., Zhang, G., Zhu, D., Jie, L.: A patent time series processing component for technology intelligence by trend identification function. Neural Comput. Appl. **26**(2), 345–353 (2014)
18. Mel'čuk, I.: Dependency Syntax Theory and Practice. SUNY, New York (1988)
19. Fomenkova, M., Korobkin, D., Kravets, A., Fomenkov, S.: Extraction of knowledge and processing of the patent array. In: Creativity in Intelligent Technologies and Data Science (CIT&DS 2019), pp. 3–14 (Ser. Communications in Computer and Information Science (CCIS), vol. 1084) (2019)
20. Vayngolts, I., Korobkin, D., Fomenkov, S., Kolesnikov, S.: The software and information complex which uses structured physical knowledge for technical systems design. In: Creativity in Intelligent Technologies and Data Science (CIT&DS 2019), pp. 42–51 (Ser. Communications in Computer and Information Science (CCIS), vol. 1084) (2019)

Models and Methods Flexible Documents Matching Based on the Recognized Words

Oleg Slavin, Vladimir V. Arlazarov, and Ivan Tarkhanov

Abstract The chapter discusses methods for business documents' recognition with a flexible structure. The subject of the research is algorithms for matching areas meant for the extraction of text data. This task is applicable, for instance, for scanned paper documents recognition and retrieval of attributes for further processing. A mock-up for hierarchical matching using recognized words is described. Classifying text objects methods (zones, lines, fields) for speculation of an object's boundaries are considered. A modification of the Levenshtein distance is proposed to compare a set of recognized words with a limited vocabulary. An algorithm for speculation of the fields' boundaries in recognized text line using text feature points is proposed. The proposed methods have been time-tested on our private data array. The proposed method showed high recognition quality for documents of Agreement and Consistent type.

Keywords Document image processing · Image segmentation · Feature point · Recognition of documents · Levenshtein distance

O. Slavin (✉) · V. V. Arlazarov · I. Tarkhanov
Federal Research Center "Computer Sciences and Control" Russian Academy of Sciences, 9 Prosp. 60-Letiya Oktyabrya, Moscow 117312, Russia
e-mail: oslavin@isa.ru

V. V. Arlazarov
e-mail: arl@isa.ru

I. Tarkhanov
e-mail: tarkhanov@isa.ru

O. Slavin
Moscow Institute of Physics and Technology (State University)—MIPT, Institutskiy Per 9, Dolgoprudny, Moscow Region 141701, Russia

V. V. Arlazarov
LLC "Smart Engines Service", 9 Prosp. 60-Letiya Oktyabrya, Moscow 117312, Russia

A. G. Kravets et al. (eds.), *Cyber-Physical Systems*, Studies in Systems, Decision and Control 350, https://doi.org/10.1007/978-3-030-67892-0_15

1 Introduction

The subject of this chapter is Document Image Processing and Document Understanding. The relevance of the study in this field is characterized by a significant amount of works on this topic to have been published recently, for instance [1–4].

We will call a business (administrative documents [5]) documents those that are involved in some kind of workflow. Business documents have attributes, they can be stored in electronic archives. The set of attributes of a business document is a document card that is not irrelevant in the context of searching for a document and analyzing its contents. Business documents' examples are: registration certificates, documents for personal identification (hereinafter referred to as identification documents), attorney letters, billing statements, application forms. We will distinguish business documents from discretionary documents that do not contain attributes necessary in some kind of workflow and are not irrelevant as an appendix to business documents. When it comes to entering documents into a computer, the most important function of modern systems is to recognize the structure and contents of digitized documents.

The document will be considered in the form of two layers: a document template and filling out of a document. Filling out contains unique document information in the form of single-line entry fields or wrapped fields. A document template consists of static elements: lines, sheets, static texts, images, note fields (checkboxes), markers, a complex background. There are fields in the template as well: areas for printed, handprinted or handwritten filling out. There are fixed and flexible patterns. A fixed template does not allow static texts' modification, for example, when using PDF format. Flexible templates can be used to allow static texts' modification, which are for example templates in Microsoft Office format. We will distinguish fixed and flexible documents respectively.

An example of a fixed document is an application form for the issuance of an international passport of the Russian Federation. Inflexible documents, static and filling out elements are not bound to a specific location and cannot possess similar geometrical characteristics. An example of a flexible document is an "invoice", in which the distances between specific fields can vary depending on the filling out with specific data and on the text layout. Another example is "attorney letter" documents, in which the fields are named entities (place of registration, address, ID number, Signature, Date, etc.) that can be located in any place of a large-sized zone. Business documents can be either fixed or flexible.

Fixed document recognition is described in [6]. Each document is described by a view model used to detect field borders. The stages of the proposed page recognition of a digitized document are: page image normalization, page type classification, page matchings (recognition field zone search), ANN-based recognition, post-processing. The most important stage in recognizing a video stream with documents in [6] is to integrate the separate pages' recognition results. Document page matching can be performed using feature points mechanism selected in such a way as to steadily detect a set of feature points for a single-valued forecast of area boundaries for recognition [7].

As for flexible documents, some systems are known for the extraction of fields' values from a document image without using a view model using text line recognition [8] or an additional graphic image analysis [9]. The disadvantage of such systems is the ability to solidly identify only a small quantity of relation types between documents' elements.

In this chapter, we will consider the model and algorithms for a flexible document matching for reliable speculation of the boundaries of area boundaries for recognition, which can be modified over a wide range.

2 Background

The group of authors [10–12] addressed flexible documents' geometrical structure analysis issues. In paper [12], a flexible document model was considered, which consists of structural elements (a static text or a field bounded by four-sided figures) and geometrical relations between them. It has been argued that simple geometrical relations like:

- element B is located below (above, to the left, to the right) element A;
- element B is located above (below, under, left, right) element A;
- element B is located in the upper left (upper right, lower left, lower right) corner regarding element A;
- the distance between elements A and B lies within a certain interspace.

The authors define an algorithm whose source data is a set of fuzzy logic statements over a formal description of the document structure. Fuzzy logic statements are formed in the process of analyzing training documents. The algorithm was used to parse the payment documents structure, in which the structural elements are defined by dividing lines.

In another paper [10], a segmentation algorithm is presented, consisting of identifying graphic images in different parts of a document indicated in a document template. The statement of the problem is considered, allowing non-rigid division of the document into pages and free flow of text blocks from page to page. A model of the segmentation "FrameStream" is proposed in the form of a graph, which changes during segmentation and recognition. The upper level of the model corresponds to the stream of scanned pages, the lower one—to the stream of characters in the text line. The model allows alternative options of partitioning and recognition, as well as the presence of different document types in one stream and various options for document formatting. In such a paradigm, the recognition problem is restricted to constructing and searching for the best path in the segmentation graph. The algorithm operation is illustrated by the example of "scientific investigation" document segmentation. The authors consider cases of alternative segmentation that are possible for the proposed model, leading to additional segmentation graph ramification.

The proposed model was developed in paper [12]. The model is described with formalized language based on simplified regular expressions using concatenation and alternative operations. The search for substrings was performed using the substring analysis procedure in recognition alternatives, allowing non-rigid matching of words in the form of substitution, omission, and addition of characters. A numerical estimate of substrings similarity was formed, resistant to typos and recognition errors. An oriented graph not supposed to contain cycles was used for geometrical structure recognition. The search for structural elements was based on predetermined elements' correspondence analysis regarding each relation set candidate. The relational graph was built manually, it was indicated that its construction was not single-valued, and the final document parsing reliability depended on the graph.

A system feature [12] was the ability to work with documents whose structural elements do not possess a fixed location on paper, as well as the ability to describe documents, well-defined examples of which are not presented.

In this chapter, a model developing the model [12] will be described below. The model consists of several structural elements types. Matching methods based on comparing recognized words using generalized Levenshtein distance will also be described.

3 Model

We will call *primitives* the simplest geometrical objects that are automatically pulled in from the document image. By the means of primitives, more complex objects are created for document analyzing and recognition. We will use the following primitives pulled in from color images:

- line segment;
- printed word frame;
- illustration, photo, or logo frame;
- handwritten notes frame (words, check-box, signature);
- print frame.

For images normalized by angle [13, 14], the primitives listed above can be considered rectangles. Of course, primitives are pulled in with a certain accuracy, and primitive detection errors are possible.

Searching rectangles primitives' algorithms can be either simple, based on binary representations and connected components, or based on machine learning, for instance, using image points belonging to a certain class of primitives [15].

Base elements are formed based on combining and refining primitives' features. Following on from the line segments, lines themselves are created that can be continuous or broken and can correspond to sheet division in the document template. By the means of line segments, barcode frames and checkboxes can also be formed.

Based on word frames recognized words or *textual feature points* are formed.

$$W = (T(W), (W))$$

where

- $T(W)$ is the *core* of a text feature point, that is, a sequence of word characters consisting of certain alphabet characters or a sequence of character location with conformity ratings of character location with alphabetical characters;
- $B(W)$ is the *frame* of the text feature point, consisting of the border coordinates to $B_{x1}(W)$, $B_{y1}(W)$, $B_{x2}(W)$, $B_{y2}(W)$; coordinates can be normalized in a certain range;
- *F(W)* is the *attributes* of a text feature point, such as family resemblance and font modification.

A text feature point is similar to "graphic" image feature points, which are understood as points that satisfy several conditions:

- difference from points in one's neighborhood,
- noise immunity,
- resistance to certain transformations (for example, to affine transformations or scaling) [16].

It is assumed that a text feature point is different from juxtaposed text feature points in its neighborhood. If by neighborhood we mean a text line, then most of the words in business documents differ from the neighbors in the line. Multiple identical words placed on the same line will not be considered text singular points. However, if by neighborhood we mean one or two neighboring words, then two identical words placed on the same line and distinguished by neighboring words will pass for text singular points.

The juxtaposition of feature points is performed using similarity *d*, which should receive next to none values in case of comparing two points corresponding to one image location, and large values when comparing points from different image locations. It is proposed to use the match threshold of two words *T(W)* and W^r in order to measure the similarity of text feature points. Comparisons of the two cores of text feature points in this chapter are based on the Levenshtein distance and its modifications. If $\rho_{\text{Lev}}(W, W^r) < d(W)$, then the word W^r and the text feature point *W* are *identical*, otherwise they are different. In the simplest case, *d(W)* is the maximum number of substitution operations when transforming one word into another.

A feature point's program control word is an identifier used when matching feature points. The program control word is expected to be invariant when matching feature points regarding image transformations. The text feature points comparison can be based on the core of *T(W)*, as well as on the use of additional features of *F(W)*.

The method of pulling in feature points from an image is called a detector. A text feature point *detector* is a recognition procedure using some OCR that pulls in feature point program control words from a document image. Word recognition is based on the search for word boundaries [17, 18] and their recognition, for example, using ANN [19, 20].

In the proposed model, the most important base element is a text line consisting of static words and, possibly, fields from printed or handwritten elements that need to be pulled in. For business documents, the assumption that most of the lines are different from juxtaposed lines is true.

The following structural elements were used in the proposed model:

- text *area*—a set of text lines arranged vertically;
- broken lines.

Relations between structural elements are defined according to the rules described above. A zone can be either a text column or part of it, for instance, a paragraph. The zone can also be placed in a table cell or be limited by several dividing lines.

4 Methods of Matching Flexible Documents

A document page model is a foregone set of lines consisting of text feature points that are a subset of the page static text. The document page image for analysis is converted by the primary OCR detector into a set of text lines corresponding to both static texts and filling in fields and other objects (stamp, signature). It is also known beforehand that static text lines are unequivocally divided into zones separated by lines or placed at a sizable distance from each other. There are geometrical relations between zones as structural elements. Indubitably, the number of zones is significantly less than the number of words of the page static text.

A multi-page document can also be represented as a set of lines grouped into zones. In the image of a multi-page document, some lines may move from page to page. Zones can be partially located on one or two pages.

Supposing that in some way the page was divided into zones consisting of text lines. If the number and location of the zones detected correspond to the zone graph known beforehand, then the zones analysis can be performed by the algorithm [12]. However, if for some reason the number and location of the zones detected do not correspond to the graph, it's necessary to take actions to adapt the zones detected to the ideal zones described in advance. For this, it is proposed to use text feature points comparison.

The word W is a text feature point on the assumption of distinction from other words W_1, W_2, … W_k in some neighborhoods of e(W). The coincidence of the two words W_i={w_{i1}, w_{i2}, …, w_{k1}} and Wj ={w_{j1}, w_{j2}, …, w_{k2}} is estimated by the Levenshtein distance $\rho_{\text{Lev}}\left(W_i, W_j\right)$. The Levenshtein distance takes the value 0 in the case when the word lengths Wi and Wj are the same (k_1= k_2) and the corresponding word characters coincide ($\forall p : w_{ip} = w_{jp}$), in other cases $\rho_{\text{Lev}}\left(W_i, W_j\right) > 0$. The correspondence of some document word Wi to the text feature point W is established using the threshold $d(W)$ subject to the conditions

$$\rho_{\text{Lev}}(\text{T}(W), W_i) < d(W).$$

Let us consider the recognized document area as a text line set. The correspondence of this region to a certain region where a text feature point, unique to the neighborhood representing a page of the document, is located, is established unambiguously. A part of this zone is classified the same way if some of the words are lost by the zone due to distortions or recognition errors. At the same time, at the training stage, text feature points that are unique for the page *TFP1, TFP2, …* and thresholds *d(TFP1), d(TFP2)* allowing to distinguish each of the text singular feature from the recognized words convincingly, must be preliminarily selected. Note that unique text feature points should be selected in static text captures, taking into account their appearance in the filling in fields.

In general, to determine a zone, several positive detectors (unique to the page of text feature points) and several negative detectors (words that should not be placed in this zone) are required. In other words, the zone Z is determined by the model M(Z) as a set of points

$$\mathrm{M(Z)} = \left\{W(\mathrm{Z})_1^+, W(\mathrm{Z})_2^+, \ldots, W(\mathrm{Z})_{k+}^+, W(\mathrm{Z})_1^-, W(\mathrm{Z})_2^-, \ldots, W(\mathrm{Z})_{k-}^-\right\} \quad (1)$$

for which thresholds are known. Based on weak classifiers (positive and negative detectors), a strong zone classifier is determined. We define the matching of a text point W to Z if there is a word w from Z that fulfills the condition $\rho_{\mathrm{Lev}}(W, w) < d(W)$. In the simplest case, the zone Z is attached to the model M(Z) if at least one of the points $W_1^+, W_2^+, \ldots, W_{k+(\mathrm{Z})}^+$ is attached, and at the same time, none of the points $W_1^-, W_2^-, \ldots, W_{k-(\mathrm{Z})}^-$ is attached. For greater accuracy, relations between bound text feature points of type W_1^+ above or below W_2^+ are checked. The zones recognized as pages are classified based on foregone models M(Z_1), M(Z_2), …, M(Z_q). For each of the allocated to the model of a zone (1), the correspondence estimates Δ(Z, M(Z_i)), are calculated equal to 0 or 1. There are three possible selected zone Z matching cases:

- single-valued matching: there is a unique model M(Zi) for which Δ(Z, M(Z_i)) = 1;
- no matching: for any model M(Z_i): Δ(Z, M(Z_i)) = 0;
- multivariate matching: there are several models to which zone Z is bound.

The last two cases are eliminated by selecting an appropriate zone via sorting out possible zones and checking limitations relation between the candidate zone and neighboring zones. More complex classifiers are possible, for example, in the form of disjunctive normal forms over positive and negative detectors, in which the distance control between words is additionally applied [16].

We mentioned zone boundaries allocation errors above. There may be cases of merging several zones into one and splitting one zone into several. The use of a classifier based on positive and negative detectors allows matching of two or more combined zones Z_1, Z_2, … to models M(Z_1)⊕M(Z_2) ⊕…, in which points $W_1^+(\mathrm{Z}_1), W_2^+(\mathrm{Z}_1), \ldots, W_{k+}^+(\mathrm{Z}_1), W_1^+(\mathrm{Z}_2), W_2^+(\mathrm{Z}_2), \ldots, W_{k+}^+(\mathrm{Z}_2), \ldots,$ $W_1^-(\mathrm{Z}_1), W_2^-(\mathrm{Z}_1), \ldots, W_{k-}^-(\mathrm{Z}_1), W_1^-(\mathrm{Z}_2), W_2^-(\mathrm{Z}_2), \ldots, W_{k-}^-(\mathrm{Z}_2)$ are used. The case of splitting one zone into several can be processed by combining the described method by sorting out the limitations of the structural elements [12].

Let us consider the features of comparing program control words of text feature points. Inherently, for the Levenshtein distance, the distance between different short words is small (not exceeding the word length), however, the distances between similar long words are drastic. Taking this circumstance into account, it is proposed to use unique thresholds for text feature points to compare them with recognized words. Thresholds d(W) are formed upon training.

There may be such pairs of words on one page for which most of the characters coincide, and the difference is observed in a small number of characters located in a certain location. These words can be identifiers and abbreviations. Such words can also be used as unique points, if we introduce the function Const(w, i), equal to 1, if, for the word character w placed in position i (i does not exceed the length of the word w), any editorial instructions are prohibited. When calculating the Levenshtein distance, it is necessary to calculate editorial instructions for each character and use the beforehand Const(w, i) set values. If an editorial instruction for a character with Const(w, i) = 1 is found, the process of calculating the Levenshtein distance is completed and the distance is determined as some a great number.

It is on record that characters with similar typefaces can be replaced with each other upon OCR recognition. Examples for the Latin alphabet include pairs of characters “B8”, “DO”, “1I”. When calculating the Levenshtein distance for compensation of such cases, the price of replacing a character with another character with a similar typeface can be reduced. The price of replacing a letter for characters with similar typefaces is chosen in the process of training.

Line classification (line matching) can be performed both for the entire page and for a separate zone. Classification within a separate zone increases both the validity and processing speed of the method. Valid lines models M_{s1}, M_{s2},…, M_{sq} are set beforehand, each M_S model consists of a text feature points set

$$M_S = \left\{W^+_{S1}, W^+_{S2}, \ldots, W^+_{S,k+}, W^-_{S1}, W^-_{S2}, \ldots, W^-_{S,k-}\right\} \quad (2)$$

and additional parameters, the most important of which is $d_{LINK}(M_S)$—the threshold value of bound points number for well-functioning matching. The line models M_l ranking method of matching the S_w lines found consists in calculating conformance evaluation for the models $\Delta(S_w, M_{si})$. The $\Delta(S_w, M_{si})$ evaluation is 0 if at least one point from $W^-_{S1}, W^-_{S2}, \ldots, W^-_{S,k-}$ is bound.

The $\Delta(S_w, M_{si})$ evaluation is 1 if no points $W^-_{S1}, W^-_{S2}, \ldots, W^-_{S,k-}$ were bound and at least $n_{LINK}3d_{LINK}(M_{Si})$ of points $W^+_{S1}, W^+_{S2}, \ldots, W^+_{S,k+}$. were bound. There are three possible cases of matching a S_w line detected:

– single-valued matching: there is only one M_{Si} model for which $\Delta(S_w, M_{Si}) = 1$;
– no matching: for any MSi model: M_{Si}: $\Delta(S_w, M_{Si}) = 0$;
– multivariate matching: there are several models to which S_w lines are bound.

The many-valued matching can be compensated via various heuristics, for instance, by choosing the line with the maximum $(n_{\text{LINK}\,-}\ d_{\text{LINK}}(\text{M}_{\text{S}i}))/d_{\text{LINK}}(\text{M}_{\text{S}i})$ value. The absence of line matching is eliminated by selecting the appropriate line by sorting out possible lines and checking the limitations relation between the candidate line and the upper or lower neighboring lines. Absence of matching is inevitable for lines in which there are no text feature points $W^{+}_{\text{S}1}, W^{+}_{\text{S}2}, \ldots, W^{+}_{\text{S},k+}$ applicable for matching, that is, for such lines that do not contain keywords.

After line matching, the main matching task becomes possible, which is finding field boundaries for attribute values pulling in. The described model (2) is supplemented by the boundaries of each field. For the boundaries of each field F, text feature points located to the right or left are known:

- …, W_{-2}(F), W_{-1}(F), F, W_1(F), W_2(F) …—for fields at central positions in the line;
- …, W_{-2}(F), W_{-1}(F), F—for fields at the last position in the line;
- F, W_1(F), W_2(F), …—for fields at the first position in the line.

Fields that have neither right nor left neighbors should have been matched before using the upper or lower neighboring lines. A correct frame prediction is possible if the neighbors of the field are bound:

- W_{-1}(F), F, W_1(F) …—for fields at central positions in the line, the field frame is determined via the left border of the word bound to W_{-1}(F) and the right border of the word bound to W_1(F);
- W_{-1}(F), F—for fields at last positions in the line, the field frame is determined using the left border of the word bound to W_{-1}(F) and the right border of the line;
- F, W_1(F)—for fields at the first position in the line, the field frame is determined using the left border of the line and the right border of the word bound to W_1(F).

If the nearest neighboring text feature points are not detected, then the precision of the prediction for the remote neighbors depends on the measure of discrepancy between the real and the model lines. By the same token, it is beneficial to bind all text feature points that are juxtaposed to the document fields. For this, the second matching step is used in the proposed method. In the second step, an attempt is made to find the boundaries of words recognized with a large count of errors, as well as words split into parts or combined with other words. In the second step, line segments between two bound keywords are considered, between which one or more words juxtaposed to the fields to be pulled in are not detected.

The following procedure is suitable for matching parts of the words recognized with simple errors. We consider the representation of a line segment without spaces. In this representation, we search for substrings that are not bound beforehand to text feature points, for example, using a modified algorithm "bitup" that uses Levenshtein distance [21]. In this case, the threshold value $d(\text{W}^{\sim})$ is increased in comparison with the matching threshold value used earlier in the line matching step.

5 Experimental Results

For an experiment, a private dataset containing images of the scanned documents "Consent" (333 samples) and "Attorney" (308 samples) was drawn up. These documents were created on the ground of flexible templates allowing changes in text layout and word placement. Documents were created by real users. Documents were printed and scanned on various devices, the quality of the documents was good and satisfactory (several significant superfluously highlighted areas were detected), the optical resolution ranged from 100 to 300 dpi. The text consisted of type size 8 symbols, some words were underlined.

For two types of documents, the $M_{consent}$ (32 text feature points) and $M_{attorney}$ (30 text feature points) were created, each document consisted of one zone. The zone classification method described above was used for document classification. In addition to the presence of positive detectors, unambiguous vertical relations between the text feature points frames were checked. OCR Smart ID Reader [6] was used for recognition. The quality of the algorithm was evaluated according to the following criteria:

- $Precision = tp / (tp + fp)$,
- $Recall = tp / (tp + fn)$,

in which the following values were used:

- the number of correctly classified documents of its class *tp*;
- the number of rejected classified documents of its class *fp*;
- the number of rejected classified documents of another class *tn*;
- the number of incorrectly classified documents of another class *fn*.

The results obtained are in Table 1. All errors ($fp \neq 0$) were caused by recognition errors in superfluously highlighted areas.

The validity of field matching was estimated (the proportion of correctly bound fields to the total number of fields of the entire dataset documents) using the proposed method. To bind 14 fields of the "Consent" document, the model contained 23 text feature points and 12 fields, 4 fields were multiple-line. For the matching of 14 fields of the "Attorney" document, the model contained 47 text feature points and 29 fields, 4 fields were multiple-line.

Matching accuracy was 96.4% for the Consent document and 97.9% for the Attorney document. 1.2% of Consent document fields and 0.3% of the Attorney document were not detected. The matching accuracy of the "Consent" document

Table 1 Experimental results of classifying the document type

$M_{consent}$		$M_{attorney}$	
tp = 331	fp = 2	tp = 307	fp = 1
tn = 308	fn = 0	tn = 333	fn = 0
Precision = 0.99	Recall = 1	Precision = 0.99	Recall = 1

fields is worse than the matching accuracy of the “Attorney” due to recognition errors in superfluously highlighted or glared areas.

6 Conclusion

The chapter proposed a model for the description of flexible documents structural elements based on text feature points. The elaborated text objects classification algorithms by the means of the proposed model are described.

The proposed algorithms make extraction of document field values that were printed via flexible templates allowing font modification and text layout possible. Disposal of lines’ parts, as well as transferring the lines from one page to another in a multi-page document, is available. Business document templates with a limited vocabulary in the static text were considered. Such documents are circulated in workflow systems in the banking and financial sectors.

The proposed models and methods have been field-proven on real datasets. High precision has been demonstrated, Precision and Recall, commeasurable to methods for recognizing fixed documents [6].

Acknowledgements The research is carried out with partial financial support of The Russian Foundation for Basic Research (projects: 19-29-09092, 18-29-03070).

References

1. Saha, R., Mondal, A., Jawahar, C.: Graphical Object Detection in Document Images, pp. 51–58. https://doi.org/10.1109/icdar.2019.00018 (2019)
2. Ray, A., Sharma, M., Upadhyay, A., Makwana, M., Chaudhury, S., Trivedi, A., Singh, A., Saini, A.: An End-to-End Trainable Framework for Joint Optimization of Document Enhancement and Recognition, pp. 59–64. https://doi.org/10.1109/icdar.2019.00019 (2019)
3. Jain, R., Wigington, C.: Multimodal Document Image Classification, pp. 71–77. https://doi.org/10.1109/icdar.2019.00021 (2019)
4. Qasim, S.R., Mahmood, H., Shafait, F.: Rethinking Table Recognition using Graph Neural Networks, pp. 142–147. https://doi.org/10.1109/icdar.2019.00031 (2019)
5. Rusiñol, M., Frinken, V., Karatzas, D., Bagdanov, A.D., Lladós, J.: Multimodal page classification inadministrative document image streams. IJDAR **17**(4), 331–341 (2014)
6. Smart IDReader: Document Recognition in Video Stream. In: Bulatov, K., Arlazarov, V., Chernov, T., Slavin, O., Nikolaev, D. 14th IAPR International Conference on Document Analysis and Recognition, vol. 6, pp. 39–44. IEEE (2017)
7. Skoryukina, N., Faradjev, I., Bulatov, K., Arlazarov, V.: Impact of geometrical restrictions in RANSAC sampling on the ID document classification, p. 78. https://doi.org/10.1117/12.2559306 (2020)
8. Breuel, T.M.: High performance document layout analysis. In: Proceedings of the Symposium on Document Image Understanding Technology, pp. 209–218 (2003)
9. Yang, X., Yumer, E., Asente, P., Kraley, M., Kifer, D., Giles, C.L.: Learning to extract semantic structure from documents using multimodal fully convolutional neural networks. IEEE Conference on Computer Vision and Pattern Recognition (CVPR 2017)

10. Postnikov, V.V.: Flexible Forms Identification. In: Proceedings of the 5th German-Russian Workshop on Pattern Recognition and Image Understanding (GRWS98). Infix, Hamburg (1999)
11. Postnikov, V.V.: Identification and recognition of documents with a predefined structure. Pattern Recogn. Image Anal. **13**(2), 332–334 (2003)
12. Marchenko, A.E., Ershov, E.I., Gladilin, S.A.: Sistema razbora dokumenta, zadannogo atributami strukturnykh elementov i otnosheniyami mezhdu strukturnymi elementami [The system for parsing a document specified by attributes of structural elements and the relations between structural elements]. Trudy ISA RAN **67**(4), 87–97 (2017) (in Russian)
13. Ballard, D.: Generalizing the Hough transform to detect arbitrary shapes. Pattern Recogn. **13**(2), 111–122 (1987)
14. Nikolaev, D.P., Karpenko, S.M., Nikolaev, I.P., Nikolayev, P.P.: Hough transform: underestimated tool in the computer vision field. In: Proceedings of 22nd European Conference on Modelling and Simulation (ECMS 2008), pp. 238–243. https://doi.org/10.7148/2008-0238 (2008)
15. Daniil, P., Matalov, S.A., Usilin, V.V.: ArlazarovSingle-sample augmentation framework for training Viola-Jones classifiers. In: Proceedings Volume 11433, Twelfth International Conference on Machine Vision (ICMV 2019), 114330I. https://doi.org/10.1117/12.2559435 (2020)
16. Slavin, O.A.: Using special text points in the recognition of documents. In: Studies in Systems, Decision and Control, vol. 259. pp. 43–53. Springer Nature Switzerland AG. https://doi.org/10.1007/978-3-030-32579-4_4 (2020)
17. Wu, J.C., Hsieh, J.W., Chen, Y.S.: Morphologybased text line extraction. In: Machine Vision and Applications, pp. 195–207 (2008)
18. dos Santos, R.P., Clemente, G.S., Ren, T.I., Calvalcanti, G.D.C.: Text line segmentation based on morphology and histogram projection. In: Proceedings of ICDAR '09, pp. 651–655 (2009)
19. Chernyshova, Y.S., Sheshkus, A.V., Arlazarov, V.V.: Two-step CNN framework for text line recognition in camera-captured images. IEEE Access **8**, 32587–32600 (2020). https://doi.org/10.1109/ACCESS.2020.2974051
20. Chirvonaya, A.N., Sheshkus, A.V., Arlazarov, V.L.: Monospaced font detection using character segmentation and Fourier transform. In: Osten, W., Nikolaev, D., Zhou, J. (ed.) ICMV 2019, 11433 ed., vol. 11433, pp. 1–7. SPIE, ISSN 0277-786X, ISBN 978-15-10636-43-9. https://doi.org/10.1117/12.2559373 (2020)
21. Baeza-Yates, R.A., Gonnet, G.H.: A new approach to text searching. In: Communications of the ACM. Band 35, Nr. 10, Oktober 1992, ISSN 0001-0782, S. 74–82. https://doi.org/10.1145/135239.135243

Search for Falsifications in Copies of Business Documents

Oleg Slavin, Elena Andreeva, and Vladimir V. Arlazarov

Abstract The present article is concerned with methods of comparison of scanned copies of business documents. Such a problem arises when comparing two copies of business documents signed by two parties to detect possible changes made by one of the parties. This problem is relevant, for example, in the banking sector when concluding contracts in paper form. It considers the partial matching method for the flexible form that allows modifying text attributes and inadvertent modifications of common words. It proposes the method of comparison of two scanned images based on recognition and analyses of N-grams words sequences. The proposed method has been tested on its private data set. The proposed method has demonstrated high quality and reliability of searching for differences in two copies of the same Agreement document.

Keywords Comparison of documents · Image segmentation · Feature point · Recognition of documents · Levenshtein distance

O. Slavin (✉)
Federal Research Center "Computer Sciences and Control" Russian Academy of Sciences, 9 Prosp. 60-Letiya Oktyabrya, Moscow 117312, Russia
e-mail: oslavin@isa.ru

Moscow Institute of Physics and Technology (State University)—MIPT, Institutskiy Per 9, Dolgoprudny, Moscow Region 141701, Russia

E. Andreeva · V. V. Arlazarov
LLC "Smart Engines Service", 9 Prosp. 60-Letiya Oktyabrya, Moscow 117312, Russia
e-mail: andreeva@phystech.edu

V. V. Arlazarov
e-mail: vva@smartengines.biz

V. V. Arlazarov
Federal Publicly Funded Institution of Science, Institute for Information Transmission Problems n.a. A.A. Kharkevich of Russian Academy of Science, 19 Bolshoy Karetny Per, Moscow 127051, Russia

A. G. Kravets et al. (eds.), *Cyber-Physical Systems*, Studies in Systems, Decision and Control 350, https://doi.org/10.1007/978-3-030-67892-0_16

1 Introduction

Often the process of signing contract documents by two parties takes place on different premises. For example, a template of the agreement with an organization is downloaded from the website, printed out and signed by the client outside the bank's office, and passed to the organization for signing. There are cases when bank clients made changes to the agreement and then took advantage of that.

Such a situation may occur when working with providers of various services. We have in mind the situation described below. Currently, many organizations attracting plenty of new customers offer them to prepare a contract on their own, by downloading the contract template from the organization's website. A contract thus printed, completed, and signed is then delivered to the other party for signing. The other party checks up contracts prepared by the potential customers, say, by checking up the delivered documents manually. There may be plenty of such documents; therefore, several attentive employees are to be involved in the check-up. However, when several dozens of documents with identical meaning are checked up during a day, even a diligent employee may miss errors. That's what accounts for the cases of fraud not detected during the manual check-up.

The procedure of comparing the copy of the business document (agreement, contract) with the standard is necessary for the reliability of the transaction. If there is a high flow of contract documents (hereinafter referred to as documents), their manual verification before signing takes a long time. Moreover, when the operator checks manually a large number of contract documents, omissions of possible modifications are unavoidable.

Agreement documents are of the category of business documents created for any record keeping and document management systems. The distinguishing feature of business documents is a limited glossary to be used and the method of execution thereof. That is due to the tendency of document templates unification to facilitate comprehension of business documents, primarily by humans.

The document template contains static text and margins for entering the information. Let's consider two widespread categories of templates: the fixed one and the flexible one. The fixed template does not allow modifying static texts when using, for example, the PDF format. Flexible templates can be used that allow modifying static texts, for example, Microsoft Office format templates. Thereafter, we will distinguish between fixed and flexible documents. The subject of this article is Document Image Processing and Document Understanding. The relevance of the study in this field is characterized by a significant amount of works on this topic to have been published recently, for instance [1–6].

There are known methods of automated comparison of the signed document image with its prototype [7–10]. They are checked for possible modifications to the content:

– replacing one or more characters in a word;
– replacing one word with another one;
– adding a character, word, or group of words;
– deleting a character, word, or group of words.

Modifications of the document design are also possible:

- changing the style of words (size, font, type);
- changing document margins of words;
- changing the number of paragraphs;
- changing margins.

Modification of a fixed template is an intended falsification. Modification of a flexible template maybe both falsification and an accidental misprint or a consequence of formatting improvement.

The paper will consider models and methods of search for falsifications in copies of business documents printed out using both fixed and flexible templates.

2 Background

A great problem with the development of forgery detection methods consists in the absence of public data set for algorithm assessment. It is explained by the fact that organizations do not want to share the information found about forgery of documents, among other things because there are their personal data in the documents. In this paper [7] a public data set is presented that has been composed of a package of 477 falsified (modified) pay sheets, wherein a total of about 6000 characters were modified. The authors [7] assumed that adding or deleting words occurred in static texts, the placement of which in the document image should be invariant. For the analysis, there were synthesized documents that were modified by volunteers.

The paper [8] describes the forgery automatic detection method focused both on detecting outliner of characters in a discriminant feature space and on detecting analogous (similar) character images. The feature set is calculated for all characters, and then, based on the distance between characters of the same category, the character is classified as genuine or fake. In the papers [9, 10] a simplified approach was used for comparing the documents coming from the same source. In the paper [11] the main distortion associated with the search for falsifications is called nonuniform vertical scaling. When a printed document is scanned, the content of the reprinted document differs from the original one by different vertical distances between text elements.

These methods show a high quality of document comparison. For example, the comparison methods proposed in the paper [11] allow us to find all forgeries for a test set containing invoices and medical statements (40 original documents and 12 fake ones), at that 30% of the original documents are classified as suspicious. However, these methods have not been tested for documents printed in Cyrillic, and they are not aimed at searching for modifications of individual words or characters, but at testing the hypothesis that the whole document is fake.

The present paper is dedicated to solving the problem of searching for modifications in a document with the known template that develops the authors' works [12, 13].

3 Statement of the Problem

The model of the one-page document is D the set of lines $\{L_i^d\}_{i=1}^{|D|}$, each line L^d is a set of words $\{W_j^l\}_{j=1}^{|L^d|}$.

Some lines can be clustered, for example, as paragraphs and sections. The word W is defined as a *textual key point*

$$W = (T(W), B(W), F(W)) \tag{1}$$

where

– $T(W)$ is *the core* of the textual key point, i.e. a sequence of characters of the word composed of characters of a specific alphabet or a sequence of character spaces with estimates of correspondence of the character space to the alphabet characters;
– $B(W)$ is *the frame* of the textual key point composed of the border coordinates $B_{x1}(W), B_{y1}(W), B_{x2}(W), B_{y2}(W)$; the coordinates can be normalized in a specific range
– $F(W)$ are *the features* of the textual key text, for example, the font style and modification.

The textual feature point is analogous to the "graphic" feature point of an image which is understood to be a point that fulfills some conditions:

– distinguishing from points in its neighborhood;
– noise resistance;
– resistance to some transformations (for example, to affine transformations or scaling) [14].

Properties of feature points are the following ([15]):

– Repeatability—the feature point must be located in the same place as the image object, regardless of changes in the viewing point and illumination;
– distinctiveness/informativeness—neighborhoods of feature points must differ significantly;
– locality—the feature point and its neighborhood must take up a small area of the image;
– quantity—the number of detected feature points must be big enough for detecting objects;
– accuracy—the detected feature points must be localized accurately both in the original image and in the image of another scale;
– efficiency—the time of detection of feature points on the image must be admissible for the time-critical applications.

Feature points mapping is carried out using the similarity measure d that shall take on values close to zero when comparing two points corresponding to the same place in the image, and big values when comparing the points from different places of the image.

It is supposed that the textual feature point differs from the proximate textual key points in their neighborhood. If a neighborhood is understood as a textual line, then most of the words in business documents differ from the proximate ones in the line. Several identical words placed in the same line are not textual feature points. However, if the neighborhood is understood as one or two proximate words, then two identical words placed in the same line and distinguished by the proximate words are textual feature points. Comparing the feature points is carried out using the similarity measure d that shall take on values close to zero when comparing two points corresponding to the same place in the image, and big values when comparing two points corresponding to the same place of the image.

Comparing the two cores of the textual feature points in this work is based on the Levenshtein distance ρ_{Lev} [8] and modifications thereof. The threshold $d(W)$ for comparing the word $T(W)$ with other words is calculated a priori. If $\rho_{\text{Lev}}(W, W^r) < d(W)$, then the word W^r and the textual feature point W are *identical*, otherwise they are distinguished.

The feature point descriptor is the identifier used when mapping feature points. The descriptor is expected to be invariant when mapping feature points relatively to image transformations. The mapping of textual feature points can be based on the core *T(W)*, as well as on the use of additional features *F(W)*.

The method for extracting key points from the image is called a detector. The detector of the textual feature point is a recognition procedure using some OCR that extracts feature point descriptors from the document image. The document image was generated based on the paper page, using a scanner or a digital camera.

The above-mentioned properties of feature points are valid for textual key points in case the modern OCR can compensate for different types of image distortions. The uniqueness of the textual feature point descriptors is determined by the structure of documents (unambiguous partitioning of the document into constellations—sections, paragraphs, and lines) and the properties of natural language (rare matching of two neighboring words in documents). A different relationship between the textual feature points (the relationship above—below, on the right—on the left or geometric distance between the frames) allows combining the points into constellations using the clustering algorithms.

Ideally, the OCR correctly extracts all textual key points from the images of the copy and the *ideal* of the document. This allows forming the lines. Comparison of the copy and the standard consists of the unambiguous matching of all or a part of the textual feature points of the standard and a set of the textual feature points of the copy. The process of matching of points or constellations of points is called coordination.

The coordination of fixed documents refers to the matching of all words and lines of the static text. The matching shall account for the additional features (typeface, size, etc.). The coordination of fixed documents includes:

– search for matching of any point of the standard in the copy points;

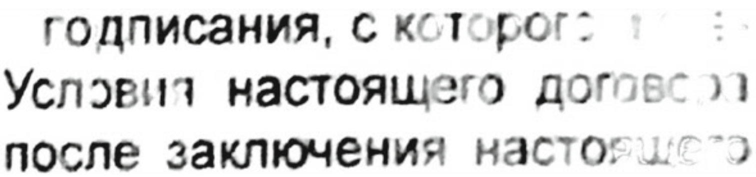

Fig. 1 Fragment of a textual image with distortions

– search for matching of any point of the copy in the standard points;
– search for matching of any static line of the standard in the copy points;
– search for matching of any static line of the copy in the standard points;
– check for the image identity of each pair of coordinated images.

Any detected mismatch is a potential modification. Certainly, the mismatch detected may have been caused by the detector errors (OCR) or distortions of the document image.

The coordination of flexible documents refers to matching between all words of the static text. However, unlike fixed documents, there is no matching between lines of the flexible document static text. In the flexible documents, there may be legitimate changes that do not change the meaning of the text, such as changing the font, changing the line borders, or line breaks. Such modifications may lead to line breaks to another page, so the comparison of multi-page flexible documents should be carried out for the entire page sequence.

In general, with no knowledge of the structure of the document, coordination of all words in the test and reference documents shall be necessary. The principal disadvantage of total coordination of words is a considerable number of mismatches detected. Mismatches occur due to recognition errors, specifics of photographic images (refer to the example—a fragment of a textual image with distortions in Fig. 1). Each mismatch shall be interpreted as a modification, and the person responsible for verification will have to spend extra time, checking the false modifications.

Notwithstanding the total coordination of words in the copy and the original, despite false recognition errors, there may be other insignificant mismatches. The fact is that, for the functional User of the program comparing the copy and the original, not all words are equally significant. The subset of words in a page of the document, determining the essential terms of the contract, is actually significant. It is assumed that a fraudster's goal is to make such modifications that, in court or pre-trial proceedings, may be deleterious to the organization that signed a contract with the fraudster. It is hardly possible to give a formal definition of such *essential* words, they are to be determined by specialists. Moreover, some words become significant in combination with neighboring words. For example, the particle "not" in combination with the adjacent word "accepted" is significant. Modification of the word "Agreement" into the word "Notagreement" is insignificant as the fraudster cannot benefit from it in the court proceeding.

Thus, another statement of the problem of the modifications search based on a subset of words in a document is possible. The statement of the problem uses knowledge of both the structure of the document and the placement of the words essential for a check-up. In such a statement, the document model consists of paragraphs and textual lines. Each textual line and each paragraph is represented by a set of textual feature points the sequence of which is unique for such a paragraph or line. Lines and paragraphs may also contain words that are not unique, i.e., which are repeated or even placed next to each other. Additionally, distances between the unique words, determined by the number of blank characters, or geometric distance between images of words, are used.

A special case of searching for falsifications is not the analysis of the full set of words $W_D = \{W_j^l\}_{j=1}^{|L^d|}$ of a document's page, but the analysis of a subset $W'_D \subset W_D$ of the set of words. The list of words W'_D for a partial check for falsifications may be determined based on the word value in terms of the responsibility of the person who has signed the document.

4 Description of the Method of Search for Falsifications in Scanned Documents

The proposed method of comparison of fixed documents is based on the coordination of pairs of textual feature points and further comparison of word images of one pair. The word coordination has been performed simultaneously with line coordination. An analogous problem is resolved when coordinating stereo images using feature points [16]. The paper [13] introduces the comparison of two digital images based on a combination of several methods of word image comparison:

- comparison of the cores $T(W_1)$ and $T(W_2)$ of two textual feature points W_1 and W_2;
- comparison of two sets of feature points RFD extracted from the borders of textual feature points $B(W)$;
- comparison of the expanded images extracted from the textual feature points $B(W)$.

The last two words comparison methods were used to compensate for OCR recognition errors. When comparing using the RFD descriptors, an algorithm based on the RANSAC method [17] was used to find the optimal transformation. The descriptors of points located in the reference image were calculated on the converted test image, and then two sets of binary point descriptors with geometrically close locations were compared. After comparing, outliner cleaning was performed and the similarity factor was calculated:

$$1 - |n_{\text{outliners}}| / (|n_{\text{outliners}}| + |n_{\text{inliners}}|),$$

where $n_{outliners}$ is the number of outliners, $n_{inliners}$ is the number of inliners. Two words were considered coordinated if the similarity factor for them is bigger than the predetermined threshold.

One more method of comparison of words images is based on the following symmetrics: for each image, I an expanded image $O^{(1)}(I)$ is created which includes the image I itself and its single neighborhood. The distance between images A and B is calculated using the following formula:

$$\mu_1(A, B) = \sum_{i=1}^{m} \sum_{j=1}^{n} (a_{ij} \cdot \bar{O}^{(1)}_{b,ij} + b_{ij} \cdot \bar{O}^{(1)}_{a,ij}),$$

where $O^{(1)}(A) = ||O^{(1)}_{a,ij}||$, $O^{(1)}(B) = ||O^{(1)}_{b,ij}||$ are the expanded images A and B. When comparing images A and B several shifts of image A were performed in different directions, and the minimum value from the reported values was chosen as the distance between the centered images A and B

$$d_1(A, B) = \min(m_1\left(A^{(h,v)}, B\right)),$$

where $h, v \in S_p(z) = \{-z, \ldots, 0, \ldots, z\}$, z is the natural number, $A^{(h,v)}$ is the shift of the image A to the vector (h,v).

The combination of several methods proposed in these papers [12, 13] allows resolving the problem of searching for mismatches between scanned copies of business documents. The experiments performed show that on the images scanned with a resolution of 300 dpi there has been obtained an accuracy of 90.9%; the completeness has been equal to 98.2%, for these images errors of the 2nd class.

Note that for fixed documents, in the same way as word comparison, the comparison of line images can be applied which should not be modified in the same way as word images.

For comparison of flexible documents, a partial modification search method based on the recognition and application of N-grams words is proposed. The recognition is preceded by image preprocessing which consists of normalizing the page image by size and inclination angle. The recognition result is represented as a set of textual feature points.

The developed method of searching for modifications includes two stages. At the first stage, one or more recognized document pages were analyzed as a set of textual feature points. (1) Clustering is performed using the nearest neighbor method; the criterion for entering the cluster is the closeness of a textual feature point to the textual feature points that have already entered the cluster. The recognized line Sr is represented as a cluster consisting of an ordered sequence of textual feature points WS = {W1(Sr), W2(Sr),…}.

The constructed lines are classified using the similarity estimation δ(Sr, Li) of the recognized line Sr and the model line Li. The model lines that convert δ(Sr, Li) to the minimum are selected.

At the second stage a search was performed for a predetermined sequence of mandatory keywords

$$w_1, w_2, \ldots w_n,$$

ordered using the ratio: if $B_{x2}(w_i) < B_{x1}(w_j)$ for the words from the same line ($w_j \in S_r$ и $w_j \in S_r$), or the words refer to different lines ($w_j \in S_r^1$ и $w_j \in S_r^2$), and with that the line S_r^1 is located higher than the line S_r^2.

For searching for keywords n-grams of words in the following forms are used:

- $n_1(w_i) = <w_i>$,
- $n_2(w_i) = <w_i, r_1(w_i)>$
- $n_3(w_i) = <w_i, r_1(w_i), r_2(w_i)>$
- $n_2(w_i) = <l_1(w_i), w_i>$
- $n_3(w_i) = <l_1(w_i), w_i, r_1(w_i)>$
- $n_4(w_i) = <l_1(w_i), w_i, r_1(w_i), r_2(w_i)>$ (2)
- $n_3(w_i) = <l_2(w_i), l_1(w_i), w_i>$
- $n_4(w_i) = <l_2(w_i), l_1(w_i), w_i, r_1(w_i)>$
- $n_5(w_i) = <l_2(w_i), l_1(w_i), w_i, r_1(w_i), r_2(w_i)>$,

where $r_k(w_i)$, $l_q(w_i)$ is the word located on the right or on the left from w_i; there are known also acceptable distances $\rho_{BT}(w_i, r_1(w_i))$, $\rho_{BT}(r_1(w_i), r_2(w_i))$, $\rho_{BT}(l_1(w_i), w_i)$, $\rho_{BT}(l_2(w_i), l_1(w_i))$ between adjacent words. Let us name index k in the designation of N-gram $n_k(w_i)$ length of N-gram.

The form $<w_i>$ is applied for the words that are present on the page in a single copy. For the words that occur in multiple instances on the page, the forms with adjacent words are used, for example $<l_2(w_i), l_1(w_i), w_i, r_1(w_i), r_2(w_i)>$. The comparison of the recognized word and the text key point was based on the Levenshtein distance, the threshold of comparison $d(w_i)$ was chosen differently for each keyword w_i. The forms allow identifying one or more recognized words as one of the N-grams (2). The evaluation of each form was determined based on the Levenshtein distance and the recognition evaluation of each word.

The model of paragraph consists of an ordered sequence of N-grams

$$n^1(w_1), n^2(w_2), \ldots, n^m(w_m),$$

with predetermined n-tuples of words $n^i(w_i)$, with distances between pairs $\{n^{j-1}\left(w_{j-1}\right), n^j\left(w_j\right)\}$ known beforehand. Note that some N-grams are unique to the paragraph, while some may be repeated. To ensure uniqueness, N-grams of various lengths may be used.

The construction of the document model was developed out in two stages of training. At the first stage, N-grams (2) were selected for an ideal document without errors, so that each word w_i surrounded by adjacent words could be unambiguously found. At the second stage, the thresholds $d(w_i)$ were selected for a validation set to minimize false identification errors due to character recognition errors; the words are considered identical when $\rho_{\text{Lev}}(W, W^r) \leq d(w_i)$.

When constructing the model of the paragraph, N-grams are formed to maximize the number of the unique N-grams. The use of N-grams by contrast to separate keywords ensures uniqueness for the majority of paragraphs of the Agreement documents, which is primarily due to the above-mentioned significant limitation of the set of words in the static text.

It makes sense to carry out training and parameter optimization on real datasets. Note that we will not be able to see possible modifications even on real datasets, which is primarily due to the classification of such data by the private dataset. So we have to make the modifications manually.

The trigram search algorithm resolves itself into selecting several consecutive words. The first thing we need is to generate a set of textual feature points. To do that, we have taken the following steps:

– halftone image processing,
– normalizing the image by angle, using the methods based on the fast Hough transformation [18].
– word boundary detection using the erase and dilate operations,
– recognition of characters within the boundaries of the words found.

A paragraph was presented in the form of a single long line. A comparison of the ideal words and recognized words in the paragraph was carried using a modified Levenshtein distance. The well-known Levenshtein distance calculation algorithms make it possible to detect not only the number of editorial instructions but also the instructions themselves.

The modified Levenshtein distance was used. First, the unique threshold was chosen to compare a particular word with other words. For refusal to identify pairs of words of the "ACCEPT" and "EXCEPT" with thresholds $d = 2$ type or for identifiers of the "IDENTIFIER196", "IDENTIFIER296", "IDENTIFIER199" type, another rule was used. For such words, segments that were to remain unmodified, were specified. That is, at the beginning of the words "IDENTIFIERddd" a greater number of errors were allowed, but identification was prohibited when the editorial instructions were found in the last 3 characters of a word.

Another modification was to compensate for the replacement of some characters with similar characters, done by OCR. Formally, replacement of the Latin alphabet characters B and 8, D and O, 1 and I are errors. However, reducing the significance of such replacements may improve word identification accuracy. Significance of replacement of a letter for similar style characters was chosen during training.

Based on several distances between the center and the N-gram neighborhoods to the analogs chosen, a heuristic evaluation of N-gram binding as a whole is formed. Parameters of the model (N-gram thresholds, length) were chosen during training to minimize the number of errors in N-gram binding, and to maximize the number of N-grams bound correctly.

After binding the N-grams to the words in the paragraph, the check-ups listed below may be carried out:

– availability of all the expected N-grams,

– availability of all the unique N-grams in a copy,
– N-grams sequence order,
– distances between the N-gram neighborhoods.

Failure to carry out any of the check-ups means the detection of modification of the essential keyword.

5 Experimental Results

The method was tested on the test samples consisting of document images of national (Cyrillic) scanned with resolution from 100 to 300 dpi. Was tested 161 documents of type "Agreement". The model consisting of 33 keywords was examined. A part of the keywords in the test samples images was deleted or modified intentionally. 740 deletions and 140 modifications of words were made. The OCR Smart ID Reader [19] and open-sourced OCR Tesseract [21] were used for recognition.

The algorithm quality was estimated using the following criteria:

– $Precision = tp / (tp + fp)$,
– $Recall = tp / (tp + fn)$,

in which the following values are used:

– count of found modified words *tp*;
– count of correct words classified as modifications *fp*;
– count of unfound modified words *fn*;
– count of correct words classified as correct *tn*.

The results are given in Tables 1 and 2. The tables contain the characteristics calculated for several thresholds of the word correctness $d(w_i)$. Note that when recognizing by ANN [20] in the OCR Smart ID Reader all modified words were found.

Table 1 Experimental results of detection for OCR Smart ID Reader

$d(w_i)$	*tp*	*fp*	*tn*	*fn*	*Precision*	*Recall*
1	216	414	738	0	0.34	1
2	216	90	1062	0	0.7	1
3 and more	216	54	1098	0	0.8	1

Table 2 Experimental results of detection for OCR Tesseract

$d(w_i)$	*tp*	*fp*	*tn*	*fn*	*Precision*	*Recall*
1	201	288	756	13	0.38	0.94
2	201	192	792	13	0.45	0.94
3 and more	201	80	972	13	0.66	0.94

The speed of comparison of a one recognized document without regard to the preliminary recognition was equal to 0.075s per document on the computer Intel® Core™ i7-4790 3.60 GHz. Whereby recognition time was equal to 1–1.5s per document.

6 Conclusion

The proposed new method is intended for analyzing incidents of possible distortion of the content of business documents. It is aimed at analyzing a part of the words that determine the legal significance of the document, for example, when dealing with a dispute in court or arbitration. The advantage of the method is a high accuracy, as well as a small number of cases for manual verification. The limitation of the method is word-level analysis; modifications of individual characters are either ignored or controlled manually.

The proposed method is applicable for searching for modifications of flexible documents printed using a well-known template that allows modification, for example, Microsoft Office document templates. The method has high detection accuracy. The method's errors are associated with recognition errors, mainly due to the scanning defects.

Acknowledgements The research is carried out with partial financial support of The Russian Foundation for Basic Research (projects: 17-29-03170, 18-07-01384).

References

1. Saha, R., Mondal, A., Jawahar, C.: Graphical Object Detection in Document Images, pp. 51–58. https://doi.org/10.1109/icdar.2019.00018 (2019)
2. Ray, A., Sharma, M., Upadhyay, A., Makwana, M., Chaudhury, S., Trivedi, A., Singh, A., Saini, A.: An End-to-End Trainable Framework for Joint Optimization of Document Enhancement and Recognition, pp. 59–64. https://doi.org/10.1109/icdar.2019.00019 (2019)
3. Jain, R., Wigington, C.: Multimodal Document Image Classification, pp. 71–77. https://doi.org/10.1109/icdar.2019.00021 (2019)
4. Qasim, S.R., Mahmood, H., Shafait, F.: Rethinking Table Recognition using Graph Neural Networks, pp. 142–147. https://doi.org/10.1109/icdar.2019.00031 (2019)
5. Moysset, B., Kermorvant, C., Wolf, C.: Learning to detect, localize and recognize many text objects in document images from few examples. IJDAR **21**, 161–175 (2018). https://doi.org/10.1007/s10032-018-0305-2
6. Nagy, G.: Document analysis systems that improve with use. IJDAR **23**, 13–29 (2020). https://doi.org/10.1007/s10032-019-00344-x
7. Sidère, N., Cruz, F., Coustaty M., Ogier, J.-M.: A dataset for forgery detection and spotting in document images. In: Proceeding of Seventh International Conference on Emerging Security Technologies (EST). https://doi.org/10.1109/est.2017.8090394, https://sci-hub.tw/10.1109/EST.2017.8090394 (2017)
8. Bertrand, R., Terrades, O., Gomez-Kramer, R., Franco, P., Ogier, J.: A conditional random field model for font forgery detection. In: 13th International Conference on Document Analysis and Recognition, Nancy, France. [Online] Available: https://doi.org/10.1109/icdar.2013.29 (2015)

9. Beusekom, J., Shafait, F., Breuel, T.M.: Automated OCR ground truth generation. In: Proceeding of the 8th IAPR Workshop on Document Analysis Systems, pp. 111–117. Nara, Japan, September. https://sci-hub.tw/10.1109/DAS.2008.59 (2008)
10. Beusekom, J., Shafait, F., Breuel, T.M.: Document signature using intrinsic features for counterfeit detection. In: Proceedings of the 2nd international workshop on Computational Forensics, ser. IWCF ’08, pp. 47–57. Springer-Verlag, Berlin, Heidelberg. https://link.springer.com/content/pdf/10.1007%2F978–3-540-85303-9_5.pdf (2008)
11. Ahmed, A.G.H., Shafait, F.: Forgery detection based on intrinsic document contents. 11th IAPR International Workshop on Document Analysis Systems. https://doi.org/10.1109/das.2014.26 (2014)
12. Andreeva, E., Arlazarov, V.V., Manzhikov, T., Slavin, O.: Comparison of the scanned pages of the contractual documents. In: The 10th International Conference on Machine Austria (ICMV 2017), November 13–15. Vienna, Austria. https://doi.org/10.1117/12.2309458 (2017)
13. Slavin, O.A.: Using special text points in the recognition of documents. In: Studies in Systems, Decision and Control, vol. 259, pp. 43–53. Springer Nature Switzerland AG. http://doi.org/10.1007/978-3-030-32579-4_4 (2020)
14. Rodehorst, V., Koschan, A.: Comparison and evaluation of feature point detectors (2006)
15. Lukoyanov, A., Nikolaev, D., Konovalenko, I.: Modification of YAPE keypoint detection algorithm for wide local contrast range images. In: Tenth International Conference on Machine Vision (ICMV 2017), vol. 10696. International Society for Optics and Photonics, vol. 10696. https://doi.org/10.1117/12.2310243 (2018)
16. Badino, H., Kanade, T.A.: Head-Wearable “Short-Baseline Stereo System for the Simultaneous Estimation of Structure and Motion”. In: Proceedings of MVA, pp. 185–189 (2011)
17. Skoryukina, N., Farajev, I., Bulatov, K., Arlazarov, V.V.: Impact of geometrical restrictions in RANSAC sampling on the ID document classification. In: Osten, W., Nikolaev, D., Zhou, J. (ed.) ICMV 2019, 11433 ed., vol. 11433, pp. 1–7. ISSN 0277-786X, ISBN 978-15-10636-43-9. https://doi.org/10.1117/12.2559306 (2020)
18. Bezmaternykh, P.V., Nikolaev, D.P.: A document skew detection method using fast Hough transform. In: Proceedings Volume 11433, Twelfth International Conference on Machine Vision (ICMV 2019); 114330 J. [Online] Available: https://doi.org/10.1117/12.2559069 (2020)
19. Smart IDReader: Document Recognition in Video Stream. In: Bulatov, K., Arlazarov, V., Chernov, T., Slavin, O., Nikolaev, D. 14th IAPR International Conference on Document Analysis and Recognition, vol. 6, pp. 39–44. IEEE. https://doi.org/10.1109/icdar.2017.347 (2017)
20. Chernyshova, Y.S., Sheshkus, A.V., Arlazarov, V.V.: Two-step CNN framework for text line recognition in camera-captured images. IEEE Access **8**, 32587–32600 (2020). https://doi.org/10.1109/ACCESS.2020.2974051
21. Tesseract OCR. Documentation. [Online] Available: https://tesseract-ocr.github.io. Accessed 26 Oct 2020

Text Classification in Emergency Calls Management Systems

Artur Sabitov, Rifkat Minnikhanov, Maria Dagaeva, Alexey Katasev, and Timur Asliamov

Abstract In this chapter text mining approach for emergency calls management systems is investigated. A data mining approach of emergency calls classification based on the machine learning decision tree method was proposed. As an input dataset for model building the data with 1.6 million textual emergency events descriptions was taken. Approbation results, finally, led to the conclusion that high effectiveness and a possibility of practical use in the emergency calls management information systems.

Keywords Natural language processing · Classification · Machine learning · Decision trees · Knowledge base · Decision support system

1 Introduction

In recent years a steady trend towards the digitalization of services and resources in many areas of human activity is observed. This process is aimed at the optimization of the various services work; it becomes actual due to the following factors: urbanization, modern cities' infrastructure is getting more complicated, increasing the significance of digital interaction between citizens, companies, and government structures. As a result, we can see an increasing necessity of data processing in different fields of life [1–5]. Usually, the data in information systems is heterogenic, partial incompleteness, and uncertainty. An emergency calls management system is an example of this kind of information systems.

Emergency calls management systems are systems that collect and process emergency event data [6]. Their main purpose is to centralize incoming calls, improve the

A. Sabitov (✉) · R. Minnikhanov · M. Dagaeva · A. Katasev · T. Asliamov
Kazan National Research Technical University named after A.N. Tupolev-KAI, Karl Marx str. 10, Kazan 420111, Russia

M. Dagaeva
e-mail: Dagaevam@rambler.ru

A. Katasev
e-mail: Kat_726@mail.ru

A. G. Kravets et al. (eds.), *Cyber-Physical Systems*, Studies in Systems, Decision and Control 350, https://doi.org/10.1007/978-3-030-67892-0_17

interaction between emergency services, and accelerate response time. The architecture of emergency calls management systems includes the collection of incoming messages about incidents, registration, and transmission to the competent emergency services. In the Republic of Tatarstan (Russian Federation) operates «The System for providing emergency services call operates under a single number "112" (Service-112)». The main purpose of the system:

- full-time monitoring, receiving, and registration of all incoming events reports;
- receiving a location of persons contacting with Service-112 from telecom operators;
- immediate initiation of work, operational processing of received messages, sending incident information to competent emergency services;
- collection, storage, classification, and archiving of the main characteristics of the registered incidents (location, retranslation time, results, etc.).

Service-112 has the ability to process phone calls (stationary or mobile) or text messages (Short Message Service). Operators of the Service-112 register and process received messages. Registration includes filling a specialized form in which the operator enters basic information about the incident. During message registration, the operator solves a problem of analyzing and classifying calls, makes a decision of sending the completed incident card to competent services. The operator makes the decision based on internal instructions and his personal experience, which, due to human factors, can lead to errors. In addition, the decision-making phase of redirecting information to competent services takes some time.

Modern technical solutions, big data analysis, and machine learning methods allow us to solve described problems by the implementation of automatic incidents classification approach. The main requirement for the approach is being highly effective and possible to be embedded into existing architecture, the openness of decision-making rules (possibility of interpreting classifier's work). Technology should be implemented as part of the decision support system. It should increase the efficiency of the Service-112 and leave for the operator only decision-making functions.

2 The Emergency Event Classification Technique

We proposed technology of text messages processing and classification for Systems for providing emergency services calls in the Republic of Tatarstan. The technology aims to automate a process of events data analysis and classification. Figure 1 shows a scheme of event messages processing by the operator.

As shown in Fig. 1 operator receives a message and fills a special form of basic information from a person (or information from automatic warning systems) and additional systems. The operator analyzes information and classifies calls. Our technology was developed for automatic events classification based on data received by the operator. Figure 2 shows some main stages of our technology running.

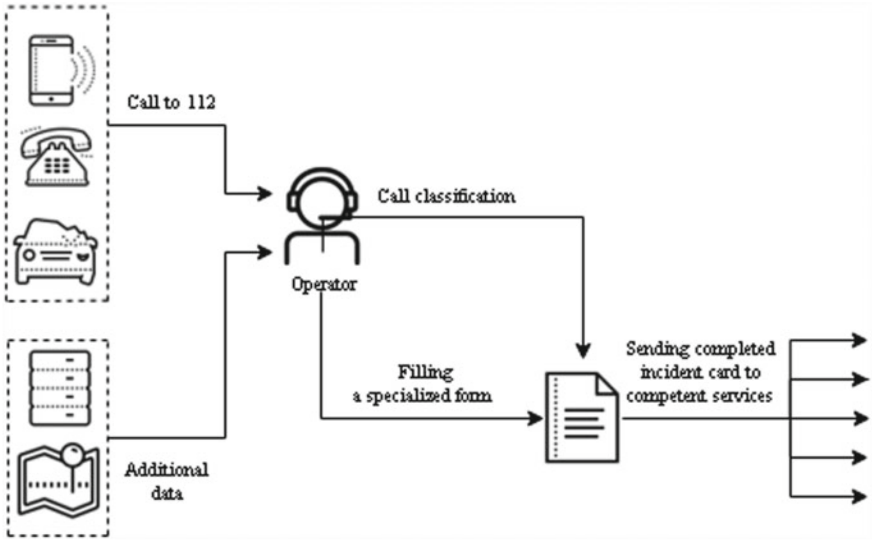

Fig. 1 Scheme of event messages processing by the operator

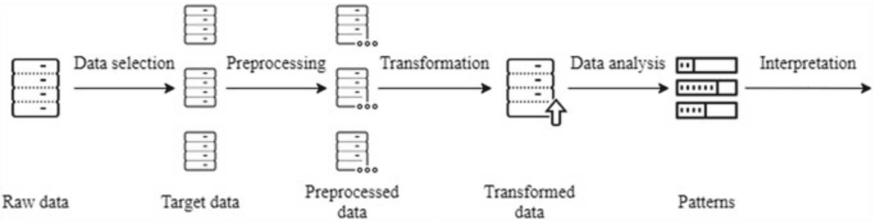

Fig. 2 Scheme of intelligent text processing technology

As shown in Fig. 2 technology of text messages processing and classification includes four serial steps [7–9]:

Step 1: initial data selection;
Step 2: data preprocessing;
Step 3: data transformation;
Step 4: data analysis.

Each of these steps is described in more detail below. On the step of initial data sampling, we selected data for subsequent analysis. The main requirements for data are sufficient completeness and representativeness to practical problems solving.

On the step of data preprocessing noises, outliers and anomalies are excluded from selected data. Using data without their preprocessing as an input for data mining approaches can lead to building inadequate models, characterized, for example, by low classification accuracy, and an increase of classifier working time, etc. [9–11].

In order to minimize the influence of negative factors, special methods of text data cleaning are used.

On the data transformation step, the input dataset is modified. Text transformation allows preparing text data for machine learning algorithms. Since converted data should be informative and representative of the original datasets, selection of the transformation method is based on a preliminary analysis of the subject area [9–11].

On the data analysis step, a machine learning-based classifier is implemented and applied. Selecting of algorithm main parameters was made on the basis of a preliminary analysis of the subject area, taking into account a number of additional requirements.

3 Raw Data Sampling and Preprocessing

As initial data, we use a set of historical textual descriptions of incidents recorded in the emergency call system of the Republic of Tatarstan from 2013 to 2018 and classes of events. The classification was made by Service-112 staff according to internal instructions, acts of the Ministry of Civil Defense and Emergencies of the Republic of Tatarstan, and the General Directorate of the Ministry of Emergencies of Russia for the Republic of Tatarstan. Information on the Service-112 is provided as part of the «Open Tatarstan» project.

According to the project documentation, 16 main categories of incidents were identified: anti-terror, salvation, medicine, fire, crimes, traffic accidents, gas services, natural phenomena, psychological assistance, national and religious conflicts, communal services, reference call, repeated call, service call, global emergency situation, other. Events of global emergency and national and religious conflict categories were excluded from consideration due to a low number of recorded events. The total volume of the initial dataset amounted to more than 1.6 million events descriptions recorded on the territory of the Republic of Tatarstan during the specified period. Some examples of dataset messages are presented in Table 1.

According to Table 1, each event of the initial dataset is characterized by a unique identification number, text description, timestamp, and corresponding class. Text data contain a certain amount of distortions, errors, and unnecessary, uninformative words. We made the following preliminary cleaning operations of text descriptions [9, 10]:

- identical messages, punctuation marks, and service symbols excluding;
- texts tokenizing;
- stop words excluding;
- words “stemming”.

Each of these operations is described in more detail below.

Identical messages exclusion was made due to the fact that inputting duplicates to algorithms data can lead to the building of inadequate models that could result in excessive classes’ significance. In addition, the exclusion was performed to clearly

Table 1 Examples of emergency text description

Id	Description	Timestamp	Category
1365	The house is on fire. The applicant sees fire from his home. There is no information about the victims	6 September 2016 02:06:18	Fire
527987	A suspicious yellow plastic bag measuring 50 * 40 cm was found in the underpass	13 November 2016 16:58:02	Anti-terror
548315	A bird fell into the chimney	26 November 2016 18:27:08	Other
563467	Repeated call on 02. A fight with two unknowns on the street	5 December 2016 23:02:33	Repeated call
662879	The taxi passenger broke the wiper, hit the applicant on the head, threatens … The applicant closed in the car	22 January 2017 22:56:08	Crime
684168	From the evening of February 3, 2017, hot water flows from the cold water and hot water pipelines	4 February 2017 09:39:43	Communal services
735270	High blood pressure 220/105 (fourth day), medications do not help. Anamnesys: stroke, hypertension	3 March 2017 20:26:30	Medicine
1288940	A traffic accident involving public transport, without injuries	24 December 2017 21:37:29	Traffic accidents
1618345	The smell of gas in the apartment	29 May 2018 17:01:43	Gas services

distinguish the initial dataset to training and test samples. Punctuation marks and other characters were excluded to make a correct representation of text data.

Text tokenization is a segmentation of a single text into separate words or word forms (tokens) by analogy with natural language [9, 12–14]. We divided texts by spaces, tabs, and line break characters.

Stop-words' exclusion is removing the most commonly used words. We deleted most common and uninformative Russian language words: introductory words, prepositions, conjunctions, etc.

Words stemming is a reduction of invariant word forms to lexical foundations by removing endings and suffixes [9, 10, 14, 15]. Stemming was made by Porter algorithm for the Russian language. Porter algorithm is based on reducing words by the set of rules [16–18].

4 Data Transformation

On the data transformation step, we analyzed text data presenting methods. Probability-weighted word methods are based on matching to each word a frequency of its occurrence in the text or corpus of texts. We concluded that the probability-weighted words approach is optimal for extracting text messages parameters in terms of efficiency and the possibility of interpreting decision rules [19–22]. Following methods of probability-weighted words described in more details below:

- Bag of Words (BOW);
- Time frequency-inverse domain frequency (Tf-IDF).

Bag of Words is a method that allows numerically to evaluate words' importance and represents texts as a vector. The Bag of Features vector represents an integer vector of N length, where N—number of all unique tokens in the set, vector values represent each token occurrences. An example of a message in the form of Bag of Words and Bag of Features is presented below.

Original message:

«A roommate stole two telephones (iPhone brand) worth 32000 (thirty-two thousand) rubles, 15000 (fifty thousand) rubles».

Message in BOW:

{'15000', '32000', 'iphon', 'two', 'brand', 'fift', 'rubl', 'roommat', 'worth', 'telephone', 'thirt', 'thousand', 'stol'}.

Message in Bag of Features (BoF):

{1, 1, 1, 1, 1, 1, 2, 1, 1, 1, 1, 2, 1}.

According to this example, each word of BOW corresponds to one number of a Bag of Features vector. Every Bag of Features vector value characterizes uses the word in a text.

Tf-Idf is a method that evaluates the numerical significance of the words in the text. Tf-Idf is based on calculating occurrence frequency or time-frequency (TF) of a word in the text (like in Bag of Feature's) and its domain frequency of occurrence (IDF) in the considered texts [20]:

$$f(t, d) = \frac{n_t}{\sum_k n_k}, \tag{1}$$

where n_t—the number of word occurrences in a document, $\sum_k n_k$—total number of words in a document;

$$idf(t, D) = \log \frac{N}{|d_i \in D : t \in d_i|}, \tag{2}$$

where N—number of documents in a corpus, $|d \in D : t \in d|$—number of documents, where the token t is found.

Coefficient Tf-IDF is calculated by TF and IDF values

$$TfIdf(t, d, D) = tf(t, d) * idf(t, D). \tag{3}$$

Calculation of Tf-IDF for each token of a text in corpus allows us to create a vector of parameters that characterize not the only number of each token occurrences, but also calculate some syntactic significance of words. This significance is expressed in the value of the parameter limited by [0; 1] values, where value tending to “0” expresses a low word significance, and to “1”—high. An example of a message in the form of Tf-Idf vectors is presented below.

Original messages:

«A roommate stole two telephones (iPhone brand) worth 32000 (thirty-two thousand) rubles, 15000 (fifty thousand) rubles».

«Applicant lost his documents on 08/26/08 at 8.50 on his name (passport, driver’s license. There is a video surveillance camera that recorded this fact».

Messages in BoW:

{‘08’, ‘15000’, ‘26’, ‘32000’, ‘50’, ‘iphon’, ‘vid’, ‘driv’, ‘this’, ‘two’, ‘documents’, ‘record’, ‘applicant’, ‘nam’, ‘camer’, ‘mark’, ‘surveillanc’, ‘passport’, ‘lost’, ‘licens’, ‘fift’, ‘rubl’, ‘his’, ‘roommat’, ‘worth’, ‘telephone’, ‘thirt’, ‘thousand’, ‘stol’, ‘fact’}.

Messages in Tf-Idf vectors:

{0.242, 0, 0.242, 0, 0.242, 0, 0.242, 0.242, 0.242, 0, 0.242, 0.242, 0.242, 0.242, 0.242, 0, 0.242, 0.242, 0.242, 0.242, 0, 0, 0.242, 0, 0, 0, 0, 0, 0, 0.242},

{0, 0.229, 0, 0.229, 0, 0.229, 0, 0, 0, 0.229, 0, 0, 0, 0, 0.229, 0, 0, 0, 0, 0.229, 0.458, 0, 0.229, 0.229, 0.229, 0.229, 0.458, 0.229, 0}.

According to the example, each Bag of Words corresponds to a number of Tf-IDF vector, which characterizes the occurrence number in the text and the corpus of texts.

Applying probability-weighted word models on high-volume text data causes computational difficulties [9, 22]. It is caused by an increase of each text vectors’ presentation dimension and increasing in a large number of useless and uninformative tokens. Therefore, the exclusion of such tokens before the data mining stage was performed. It was required due to the fact that such data does not affect classification accuracy, but their presence causes an exponential increase in a computational load on model training. Moreover, the Pearson coefficients of the statistical relationship between each token with each class of incidents were calculated. The Pearson correlation coefficients were calculated by the following formula [23]:

$$r_{XY} = \frac{\sum (X - \bar{X})(Y - \bar{Y})}{\sqrt{\sum (X - \bar{X})^2 (Y - \bar{Y})^2}}, \tag{4}$$

where $\bar{X} = \frac{1}{n}\sum_{t=1}^{n} X_t$ and $\bar{Y} = \frac{1}{n}\sum_{t=1}^{n} Y_t$—average values of dataset.

According to Pearson correlation coefficients, the most informative words of texts were selected. We heuristically established that an exception of tokens with correlation coefficients below |0.05| allows us to save classifiers’ accuracy and reduce the number of analyzed tokens. It allows us to reduce overall time (on training and evaluation steps) of algorithm performance, as well as to increase model interpretability.

The exclusion of non-informative tokens reduces the dimension of Tf-Idf vectors of each text message by more than 70 times (from 154 thousand to 2.2 thousand words).

5 Data Analysis

On the step of data analysis, a classification algorithm is selected. There are various machine learning algorithms that are used for classification issues. Therefore, machine learning algorithms were considered and it was revealed that the decision trees classification method has the most significant accuracy, high interpretability of obtained rules, and a possibility of large dimension input data processing. Decision trees algorithms are based on simple heuristic decision-making rules (CART—Classification and Regression Trees) [9, 10, 24–26].

A distinctive feature of these algorithms is the formation of explicit rules for solving problems and the possibility of their interpretation. Sets of decision rules have a hierarchical tree structure: each decision rule except the root belongs to other "parent" rule (Fig. 3). Therefore, each sequence of decisions from the root rule to the last can be interpreted by Boolean algebra operations [26].

Figure 3 shows an example of decision rules visualization for a model trained on a limited data sample (2.5 thousand examples and two categories of events).

We built classifier by "top-down induction" of decision trees creating: on each stage, the initial dataset is recursively divided into parts by a local criterion of the greedy algorithm [27]. Subsampling and rules formation stopped when data on some node was completely separated or when the algorithm was limited to the depth of rules, the threshold of separation criterion, and a minimum number of sample elements on the node.

The decision tree model is implemented on Python v3.7.3 (Jupyter Notebook) using special machine learning, natural language processing, support for multidimensional and sparse data arrays libraries (Scikit-learn, Scipy, NumPy, NLTK). Decision tree classifier was built with the following parameters:

- separation strategy: the best separator;

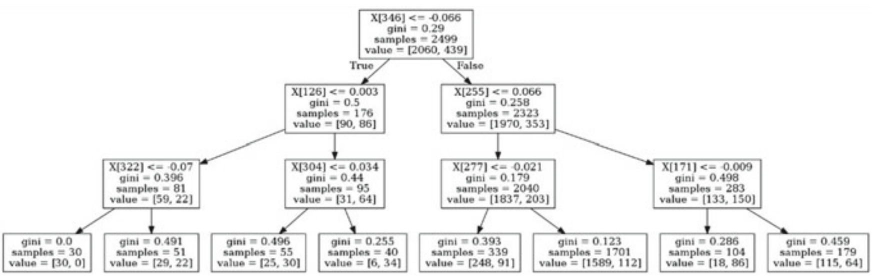

Fig. 3 Scheme of operator event processing

- criterion for the quality of separation assessing: Gini Impurity;
- threshold criteria for assessing the quality of division: 10-7;
- minimum number of samples for separation: 10;
- maximum depth of decision rules: 100.
- class weights: relative to the number of instances of each class.

Model building and evaluation were performed on a server with the following characteristics:

- CPU: AMD EPYC 7551P 2.00 GHz (32 cores 64 threads);
- GPU: 2 Nvidia Tesla V-100 (videomemory 16 Gb, Compute Capability 7.0);
- RAM: 512 Gb (clock frequency 2667 MHz).

6 Experimental Setup and Evaluation

The developed algorithm was tested on the analysis of a data sample in 896 thousand unique text messages. Training and verification data sets were formed to assess classifier accuracy, these data sets consist of 805 thousand and 89 thousand values of the initial sample, respectively. In both samples, the ratio of the number of objects of each class is preserved. Evaluation of classifier accuracy was carried out on test data that was not inputted into the algorithm during the learning process. The volume of data by each category of events presented in Table 2.

Table 2 The volume of data by each category of events

Category of event	Size of training data sample	Size of evaluation data sample
Medicine	340,159	37,796
Crimes	189,687	21,077
Communal services	42,644	4738
Traffic accidents	27,922	3102
Fire	24,972	2775
Salvation	13,936	1549
Gas services	12,252	1361
Natural phenomena	6536	726
Service call	4624	514
Psychological assistance	4171	464
Anti-terror	3789	421
Reference call	43,370	4818
Repeated call	30,896	3433
Other	60,650	6739

Table 3 Accuracy of classification

Category of event	Accuracy of data classification for training sample	Accuracy of data classification for evaluation sample
Medicine	0.981	0.978
Crimes	0.944	0.941
Communal services	0.880	0.875
Traffic accidents	0.966	0.966
Fire	0.943	0.942
Salvation	0.658	0.627
Gas services	0.949	0.932
Natural phenomena	0.782	0.763
Service call	0.558	0.550
Psychological assistance	0.850	0.831
Anti-terror	0.753	0.698
Reference call	0.973	0.968
Repeated call	0.917	0.909
Other	0.916	0.905
Full sample	0.945	0.941

As shown in Table 2, the algorithm was implemented on an unbalanced by categories data set. Therefore, in order to avoid inadequate learning of algorithms, each class was aligned with all others by introducing special weighting coefficients during model formation. The values of these coefficients are inversely proportional to a number of unique event descriptions of each class relative to the volume of the entire data set.

This operation was carried out to eliminate classes "outsiders", for which a sufficient number of decision rules will not be developed in a model. Results of training and accuracy evaluation presented in Table 3.

According to the results presented in Table 3, we can conclude that the developed algorithm shows the effective classification of most incidents. However, in four classes (service call, anti-terror, natural phenomena, and salvation), the algorithm showed insufficiently accurate results. It should be noted that implemented technology shows the same accuracy on the training and verification data sets. Moreover, in order to improve the accuracy of classification, we propose to use additional procedures for text data cleaning and transformation. In the future, the simultaneous use of several methods for selecting classification features will increase the information content of analyzed data and improve the accuracy of classification for classes that have shown insufficiently high results.

7 Conclusion

Evaluation results of proposed technology allow us to confirm a possibility of its effective practical use for automating the process of incidents classification in the existing architecture of emergency call management system of the Republic of Tatarstan and similar emergency systems as an element of decision support system and for messages classification knowledge base forming.

References

1. Kizim, A.V., Kravets, A.G.: On systemological approach to intelligent decision-making support in industrial cyber-physical systems. Stud. Syst. Decis. Control **260**, 167–183 (2020)
2. Kotenko, I., Parashchuk, I.: Determining the parameters of the mathematical model of the process of searching for harmful information. Stud. Syst. Decis. Control **260**, 225–236 (2020)
3. Korshikova, A.A., Trofimov, A.G.: Predictive model for calculating abnormal functioning power equipment. Stud. Syst. Decis. Control **260**, 249–259 (2020)
4. Golovanov, P., Livshits, M.Y., Tuponosova, E.: Analysis of impact made by the flagship university on the efficiency of petrochemical complex. Stud. Syst. Decis. Control **260**, 289–300 (2020)
5. Proletarsky, A., Berezkin, D., Popov, A., Terekhov, V., Skvortsova, M.: Decision support system to prevent crisis situations in the socio-political sphere. Stud. Syst. Decis. Control **260**, 301–314 (2020)
6. Dagaeva, M., Garaeva, A., Anikin, I., Makhmutova, A., Minnikhanov, R.: Big spatio-temporal data mining for emergency management information systems. IET Intell. Transp. Syst. **13**(11), 1649–1657 (2019)
7. Fayyad, U., Piatetsky-Shapiro, G., Smyth, P.: From data mining to knowledge discovery in databases. AI Magazine **17**(3), 1–34 (1996)
8. Suad, A.S., Bhaya, A.S., Bhaya, W.: Review of data preprocessing techniques in data mining. J. Eng. Appl. Sci. **12**, 4102–4107 (2017)
9. Kowsari, K., Meimandi, K.J., Heidarysafa, M., Mendu, S., Barnes, L., Brown, D.: Text classification algorithms: a survey. Information (Switzerland) **10**(4), 150 (2019)
10. Aggarwal, C.C., Zhai, C.: A survey of text classification algorithms. Mining Text Data, vol. 9781461432234. pp. 163–222 (2012)
11. Famili, A., Shen, W., Weber, R., Simoudis, E.: Data preprocessing and intelligent data analysis. Intell. Data Anal. **1**, 3–23 (1997)
12. Kaplan, R.: A method for tokenizing text. Inquiries into Words, Constraints and Contexts (5), 55–64 (2005)
13. Huang, C.H., Simon, P., Hsieh, S.K, Prevot, L.: Rethinking Chinese word segmentation: tokenization, character classification, or wordbreak identification. In: Proceedings of the ACL 2007 Demo and Poster Sessions, pp. 69–72 (2007)
14. Denny, M.J., Spirling, A.: Text Preprocessing for unsupervised learning: why it matters, when it misleads, and what to do about it. Polit. Anal. **2**(2), 1–22 (2017)
15. Singh, J., Gupta, V.: Text stemming: approaches, applications, and challenges. ACM Comput. Surv. **49**(3), 1–16 (2016)
16. Porter, M.F.: An algorithm for suffix stripping. Program: Electron. Librar. Inf. Syst. **14**(3), 130–137 (1980)
17. Willett, P.: The Porter stemming algorithm: then and now. Program: Electron. Librar. Inf. Syst. **40**(3), 219–223 (2006)
18. Paice, C.D.: An Evaluation Method for Stemming Algorithms, pp. 42–50. Springer, London (1994)

19. De Boom, C., Van Canneyt, S., Demeester, T., Dhoedt, B.: Representation learning for very short texts using weighted word embedding aggregation. Pattern Recogn. Lett. **80**, 150–156 (2016)
20. Tokunaga, T., Makoto, I.: Text categorization based on weighted inverse document frequency. Spec. Interest Groups Inf. Process Soc. Jpn. **94**, 33–40 (1994)
21. Aizawa, A.: An information-theoretic perspective of tf–idf measures. Inf. Process. Manage. **39**, 45–65 (2003)
22. Mikolov, T., Chen, K., S., Corrado, G., Dean, J.: Efficient estimation of word representations in vector space. International Conference on Learning Representations (2013)
23. Pearson, K.: Notes on regression and inheritance in the case of two parents. Proc. Roy. Soc. Lond. **58**, 240–242 (1895)
24. Quinlan, J.R.: Induction of decision trees. Mach. Learn. **1**, 81–106 (1986)
25. Breiman, L., Friedman, J. H., Olshen, R.A., Stone, C. J.: Classification and Regression TREES, p. 358. Wadsworth & Brooks and Cole Advanced Books & Software, Monterey, CA (1984)
26. Rokach, L., Maimon, O.: Decision Trees. Data Mining and Knowledge Discovery Handbook, pp. 165–192 (2010)
27. Azad, M., Chikalov, I., Moshkov, M., Zielosko, B.: Greedy algorithm for construction of decision trees for tables with many-valued decisions. Fundamenta Informaticae **928** (2013)

Computer Vision for Cyber-Physical Systems

Accented Visualization User Interfaces in Augmented Reality

Anton Ivaschenko, Sergey Orlov, and Arkadii Krivosheev

Abstract The features of using modern augmented reality devices (tablets, glasses, and helmets) in practice require the development of new principles for building user interfaces. Due to the three-dimensionality of the observed scene and the need to combine real objects with virtual ones in one scene, specific difficulties arise in ensuring effective human-computer interaction in industrial applications. To solve this problem, it is proposed to adapt the user interface in accordance with the concept of accented visualization and implement adaptive generation of virtual scene elements as necessary, as a result of analysis of the user's focus and current context. The chapter discusses the basic patterns and requirements for augmented reality interfaces for decision-making support systems that will improve the usability and effectiveness of augmented reality devices application. In order to personalize the interface and adapt it to the current operations and user interests, it is proposed to implement machine learning algorithms.

Keywords Augmented reality · User interface · Accented visualization · Artificial intelligence

1 Introduction

Nowadays, Augmented Reality (AR) develops from an innovative concept used primarily in computer games to a practically useful technology, which allows improving user interfaces in many applications. Modern AR devices, including specific ones like goggles and helmets as well as universal smartphones and tablets, provide the possibility to realize AR in addition to traditional user interfaces (UI). Despite this availability and ease in use, implementation of AR UI remains yet challenging due to the differences in perception of traditional and virtual objects.

At the same time, typical requirements for software applications deployed on smartphones and tablets include high usability and the possibility of personalization. The main trends come from Web services and social networks. From one side,

A. Ivaschenko (✉) · S. Orlov · A. Krivosheev
Samara State Technical University, Molodogvardeyskaya 244, Samara, Russia

A. G. Kravets et al. (eds.), *Cyber-Physical Systems*, Studies in Systems, Decision and Control 350, https://doi.org/10.1007/978-3-030-67892-0_18

any additional information or functionality can be provided to the user contextually considering his current interest. On the other side, software developers try to reduce redundant and annoying hints and notifications. Efficient usability is always a result of some compromise.

Based on some experience of AR UI implementation in practice [1] there was proposed an original concept of accented or focused visualization [2, 3], which provides additional facilities to capture and track the user's focus and adapt visualization and behavior of corresponding controls. Further developments have led to a new concept of the virtual mark-up approach, which describes the technology of docking and localization of virtual elements and controls to provide better usability. The details can be found below in this chapter.

2 Related Works

The fundamental trends in software development, including the requirement to provide high usability and personalization, are inspired by recent Internet developments [4]. Social media bring the user inside a virtual reality of continuous intercommunication with the network of users and devices. As a result, people perceive it naturally to keep some interactive controls always in the area of attention.

Modern technologies of Augmented Reality are widely used in the game industry, education, interactive manuals, and decision-making support [5–11]. We need to differentiate the use cases of AR application in computer games and entertainment from its continual use in professional activities. In the first case, the users are driven by their interest, and AR starts being the main instrument to involve the user in virtual reality and attract his attention.

Using AR devices in the professional sphere, e.g., in surgery assistance, interactive user guides or decision-making support runs into difficulties. The main problem is that these interfaces often play a secondary role. Due to high uncertainty and low-performance, AR devices do not become the basis of business processes and often duplicate the existing IT technologies. This feature makes it difficult to overcome implementation barriers.

Let us concentrate on this type of application. The main difference of AR interfaces is in their possibility to allocate virtual objects in the same space and time as the real ones. Hints and control panels can be presented for the user at any point in a 3D scene; they can overlap and even intersect with each other and real entities in view. Thus AR devices provide overlaid information additive or masking the real environment. AR technology allows developing interactive and context-dependent user interfaces that should provide the possibilities of computer vision and object recognition.

As a result, the user is put inside the "loop" of computer-human interaction [12, 13] and make user interfaces context and focus dependent. The system should interlink all related data sets (e.g., images, text, measured values, scans) and offer visual scenes [14]. It is proposed to involve the decision-maker in the process of data processing and visualization using continuously interacting with the system, which helps to optimize the learning behavior of both humans and algorithms.

AR interfaces behavior can be determined by the declarative logic in the form of rules. Considering the high complexity and uncertainty of virtual and real objects allocations and intersection in a 3D scene [15], necessary conditions can be determined using artificial intelligence [16–18]. Machine learning algorithms can be used to personalize the interface and adapt it to the current actions and interests of the user [19].

As a result of related works overview, there was formulated a new problem of AR UI development considering modern requirements of personalization. Its implementation in practice can be performed based on the concept of accented visualization as shown below.

3 Virtual Mark-Up Approach

The concept of accented visualization analysis for decision-making support is presented in Fig. 1. The idea is based on the formalization of <focus, context, and overlay context> for each user. Focus points on the object that is processed by the user or attracts his attention. The context describes the current situation and considers the history of previous actions and events that have led to it. Overlay context includes virtual entities (textual items, marks, or highlights) that attract user attention to the required scene objects when needed.

Such an approach allows changing the user focus to target values using the overlay context as a management tool. Therefore it refers to the soft manipulation techniques and provides higher user involvement and independence. These features increase the usability of AR-based systems and contribute to their implementation in practice.

Within the framework of the AR-based system is required to introduce an intelligent module of object recognition using, e.g., artificial neural network. In the provided solution, this module becomes a part of the Identifier that processes the images, includes identification of all critical objects in view, and handles this information to Navigator.

Navigator is responsible for user focus identification, processing, and control. For this purpose, it can incorporate an eye-tracking subsystem. Navigator detects the gaps in the viewer's perception if no required attention is given to particular scene objects at necessary times. As a result, it forms an overlay context for user focus coordination.

Let us consider the scene s_k, where $k = 1 \ldots N^s$ is the scene number that contains some real objects $w_{i,k}$, $i = 1 \ldots N_k^w$ and virtual entities $v_{j,k}$, $j = 1 \ldots N_k^v$:

$$s_k = \left\{ w_{i,k}, v_{j,k} \right\}. \quad (1)$$

In the mixed reality, each object at a time t_n can be described by geometrical parameters of size and shape $g_{i,k,n}$. Simplistically $g_{i,k,n}$ can be represented by a

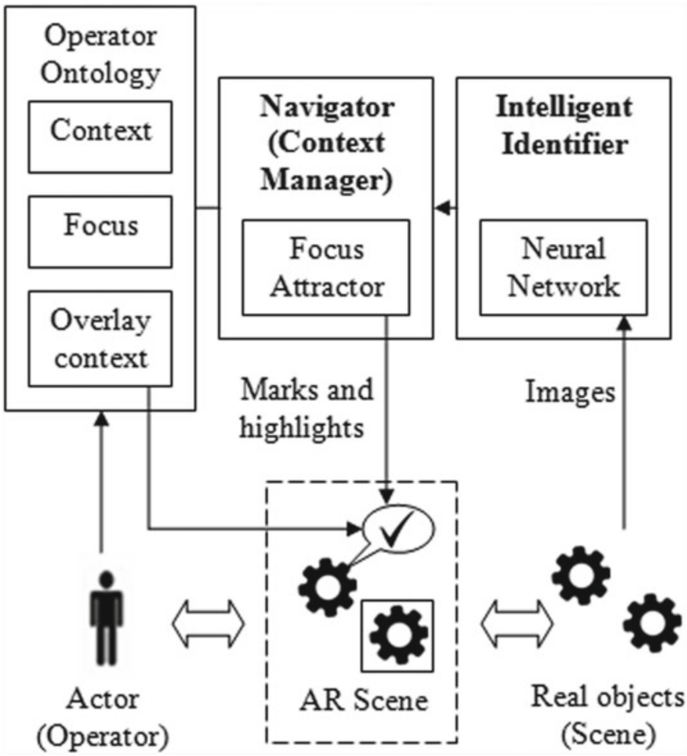

Fig. 1 Accented visualization solution for AR applications

polyhedron:

$$g_{i,k,n} = g_{i,k,n}\left(w_{i,k}, t_n, \left\{c_{i,k,n,m}\right\}\right), \tag{2}$$

described by a set of points in space projected to the view of an AR device $c_{i,k,n,m} = c_{i,k,n,m}\left(x_{i,k,n,m}, y_{i,k,n,m}, z_{i,k,n,m}\right)$.

Physical objects can have various locations in space and not interact, but in the view of AR user, their images can overlap, which can be described by a Boolean step function:

$$\delta\left(g_{j,k,n}, g_{i,k,n}\right) = \begin{cases} 1, & g_{j,k,n} \text{hides } g_{i,k,n}; \\ 0.5, & \text{partial overlap}; \\ 0, & \text{no overlap}. \end{cases} \tag{3}$$

There is no need for accurate calculation of overlapping percentages. In most cases, even extensive overlapping does not interfere with the recognition of the specific parts that are in view.

Overlapping of real objects in view does not depend on the application logic and cannot be reduced. However, the amount of intersection with virtual objects and critical physical objects in view must be reduced to minimum necessary cases:

$$\Omega(s_k, t_n) = \sum_i \sum_j \delta\left(g_{j,k,n}, g_{i,k,n}\right) \to \min. \tag{4}$$

To solve this problem, we need to analyze the couples of real and virtual objects considering their position and time of appearance. As a result, the following changes can be applied to virtual objects:

- the relative shift in space to minimize or reduce overlapping;
- prioritizing of hints and control elements at a specific moment;
- grouping and docking the hints and elements in certain space areas.

The last feature helps to solve an essential problem of user interface adequacy and stability. In case some elements disappear due to low demand, the user should remain confident that he will be able to find them in a particular place when needed. Especially active components like buttons and links should not migrate or move around.

Groups of hints and active elements can be placed on separate overlay contexts associated with specific events and requirements of a workflow. Overlay contexts can be switched on and off when needed. This helps in introducing adequate and understandable logic in AR user interfaces.

Solution architecture is shown in Fig. 2. Focus point data, the position of real objects in the image, and the initial location of the virtual entities are sent to the Matcher module. Matcher operates with logic and machine learning models. Its purpose is to choose the pre-processor that is best suited to improve the location of virtual entities to avoid overlapping with real objects.

Matcher also decides to leave the current position of virtual entities unchanged. The chosen pre-processor uses neural networks, machine learning models, or logic circuits to process the location of virtual objects. The results are then transferred to the postprocessor in the form of a new arrangement of virtual entities. Postprocessor evaluates the results from the pre-processors at a higher level.

After the evaluation, a decision is made to accept the result or sent it back to Matcher to continue processing. The result is chosen from all the options as one with the highest rating if a loop is detected as well as in the case of the expiration of the maximum allowable time.

4 Implementation

The proposed approach was implemented in a specialized intelligent system for industrial manual operation control, developed by Open Code LLC [3]. The system is illustrated by Fig. 3. The overall solution is used to identify gaps and failures

Fig. 2 Virtual mark-up solution architecture

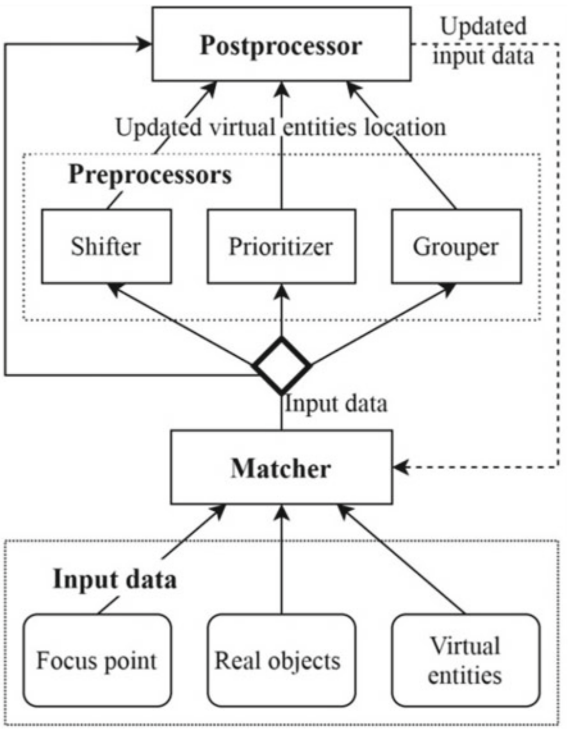

Fig. 3 AR-based intelligent manual operations' control

of the operator in real-time, predict possible operating mistakes, and suggest better procedures based on comparing the sequence of actions to the experience of highly qualified operators.

The objects are identified using the neural network and presented in an AR scene generated by the tablet or interactive dashboard. It is possible to use AR goggles, but the operators still refuse using it due to low comfort.

System functionality includes:

- scene object identification based on image analysis;
- complex devices analysis including components identification by the partial view and assemble tips generating;
- contextual description of the object in view;
- search and highlighting of the object required;
- user attention identification and contextual add-ons generating according to the principles of accented visualization;
- operating scenario processing, tracking, and control.

Virtual objects include two layers for all the identified objects (marked by blue) and hints for wrong or delayed operations (marked by red). For regular using the first layer is switched off. 3D models of the objects are not depicted as well. Overlapping of irregular operating notifications with the corresponding objects do not interfere with the workflow and help to attract attention in the required time and space.

Another example of an AR application is the specialized solution for electric meters surveying based on photo fixation [2]. The main challenge is concerned with a large variety of analog and digital meters available on the market. In addition to this, each meter has some additional digital notes on the front. Notes can be mixed up with an indication.

System functionality includes:

- automation of the process of recording the readings of electricity meters by employees of the company;
- identification of fraudulent and other illegal actions of consumers;
- collection of evidence of identified offenses for use in judicial and other proceedings.
- There was developed a specialized mobile application for photographing the readings of electricity meters (see Fig. 4), their transmission to the data processing center, recognition, and operational analysis by the staff of a regional energy distribution company.

To overcome this difficulty, there was proposed a solution of a pre-launch AI Matcher that distributes the identification procedure to separate layers, which corresponds to the idea of virtual mark-up. The first layer is used to identify the type of meter and an indication screen. Then the picture is processed to a separate neural network capable of digits recognition.

This approach allows using the solution in complex conditions with low light, screen pollution, and shading. The first layer has low sensitivity, and the second can identify digits using minimum information available.

Fig. 4 Examples of meters reading recognition

5 Discussion

User interface usability analysis can hardly be formalized. Some users prefer simple user interfaces that contain minimum necessary control elements; others find it comfortable to get access to all functionality available at a time. Nevertheless, the widespread use of smartphones and Internet browsers has formed the principles that are common for the majority.

In AR applications, the virtual objects are mixed to the projections of the real objects over the user screen. In this situation, it is impossible to split them off and isolate basic controls in a specific area. In computer user interfaces, this problem is usually solved by docking the controls to the borders of the screen. In AR interfaces, the screen borders disappear, which makes it impossible to find the best place for them.

It can be noticed that despite there remains such a critical point in space like the center of user view, determined by his focus. But any user expects to find there an important real object, not supplementary controls. So it is also not the best point for additional elements.

To analyze and compare various solutions of user interface comfort, there can be introduced the minimum time of finding the required element. With inefficient computer interfaces, the skilled user can find the necessary element for a fixed time easily. In case some controls are hidden or need multiple steps for access, this time can be increased, but the user should understand what chain of actions he has to perform to reach the point. In augmented reality, this challenge becomes more complicated, but the trained user should understand what controls are hidden and why as well as how to get them back.

Therefore the access time becomes not sufficient to estimate AR UI usability. In addition to it, we propose to study the track of the user focus. The latter can be captured by, e.g., eye tracker, a subsystem used in modern games. Eye tracker includes hardware capable of capturing the user's view and linking it to screen coordinates. In addition to application in computer games, it is successfully used in various experiments of user interfaces analysis [20]. Using this device, the system can understand how the user was looking for a hint or component.

Some research on performing various tasks by the users of different age and gender have proven that the trajectories of multiple users that look for the same elements in comparatively overloaded by objects screen can be significantly different. "Tobii eye tracker" was used for it. Some results are presented in Fig. 5. There was developed specialized software capable of tracking the users' focus for the AR user interface.

Fig. 5 Combined focus track of 10 users looking for an original element on the computer screen

The resulting trajectory characterizes the way between the points of expected and real locations. The experimental results prove that the implementation of the virtual mark-up approach allows decreasing the track of the user's view by grouping and adapting the positions of virtual objects to his expectations.

6 Conclusion

The proposed approach was implemented in a specialized intelligent control system developed based on the Open Code LLC platform for the assembly production of KAMAZ vehicles. Some cameras are used to track operations following the technological process and determine the objects that will be used in a real scene. Intelligent software provides recognition of images of objects and their comparison with the corresponding description in the knowledge base. Video panels or augmented reality glasses are used to deliver relevant contextual information to the operator.

Interactive visualization tools are implemented to generate prompts to users, control the execution of technological operations and transitions, and obtain feedback. As a result, the probability of identification increased to 0.95. The proposed solution allows ensuring the universality of the use of interactive electronic technical manuals in a given subject area, regardless of the number of types of products, parts, and designs.

Some studies on the performance of various tasks by users of different ages and sexes have proved that the trajectories of different users who are looking for the same elements on the screen can vary significantly. The experimental results confirm that the implementation of the virtual mark-up approach allows to reduce tracking of the user's gaze by grouping and to adapt the positions of virtual objects under his expectations.

Acknowledgements The chapter was supported by RFBR, according to the research project № 20-08-00797.

References

1. Ivaschenko, A., Kolsanov, A., Chaplygin, S., Nazaryan, A.: Multi-agent approximation of user behavior for AR surgery assistant. In: Information and Communication Technology for Intelligent Systems. Smart Innovation, Systems and Technologies, vol. 107, pp. 361–368. Springer, Singapore (2019)
2. Ivaschenko, A., Sitnikov, P., Katirkin, G.: Accented visualization in digital industry applications. In: Studies in Systems, Decision and Control, vol. 199, pp. 366–378. Springer, Cham (2019)
3. Ivaschenko, A., Kolsanov, A., Nazaryan, A.: Focused visualization in surgery training and navigation. In: Advances in Intelligent Systems and Computing, vol. 858, pp. 537–547. Springer, Cham (2019)

4. One Internet. Global commission on Internet Governance. https://www.cigionline.org/initiatives/global-commission-internet-governance (2016)
5. Krevelen, R.: Augmented Reality: Technologies, Applications, and Limitations. Vrije Universiteit Amsterdam, Department of Computer Science (2007)
6. Schmalstieg D., Reitmayr, G.: The World as a user interface: augmented reality for ubiquitous computing. In: Location Based Services and TeleCartography. Lecture Notes in Geoinformation and Cartography, pp. 369–391. Springer, Berlin, Heidelberg (2007)
7. Furmanski, C., Azuma, R., Daily, M.: Augmented-reality visualizations guided by cognition: perceptual heuristics for combining visible and obscured information. In: Proceedings of the International Symposium on Mixed and Augmented Reality, Darmstadt, Germany. IEEE Xplore, pp. 215–320 (2002)
8. Ke, C., Kang, B., Chen, D., Li, X.: An augmented reality based application for equipment maintenance. Lecture Notes in Computer Science, vol. 3784, pp. 836–841 (2005)
9. Navab, N.: Developing killer apps for industrial augmented reality. Technical University of Munich, IEEE Computer Graphics and Applications IEEE Computer Society (2004)
10. Osadchaya, I.A., Berestneva, O.G., Volovodenko V.A., Marukhina, O.V.: Multidimensional data visualization methods based on generalized graphic images. In: Communications in Computer and Information Science. Knowledge-Based Software Engineering, vol. 466, pp. 568–575. Springer, Cham (2014)
11. Singh, M., Singh, M.P.: Augmented reality interfaces. Natural web interfaces. IEEE Internet Comput. **17**, 66–70 (2013)
12. Holzinger, A.: Extravaganza tutorial on hot ideas for interactive knowledge discovery and data mining in biomedical informatics. Lecture Notes in Computer Science, vol. 8609, 502–515 (2014)
13. Holzinger, A.: Interactive machine learning for health informatics: when do we need the human-in-the-loop? Brain Inform. **3**(2), 119–131 (2016)
14. Julier, S., Livingston, M.A., Swan J.E., Bailot, Y., Brown, D.G.: Adaptive user interfaces in augmented reality. In: Proceedings of the Software Technology for Augmented Reality Systems, pp. 1–8 (2003)
15. Pechenkin, V., Korolev, M., Kuznetsova, K., Piminov, D.: Analysis of three-dimensional scene visual characteristics based on virtual modeling and parameters of surveillance sensors. In: Studies in Systems, Decision and Control, vol. 199, pp. 552–562. Springer Nature Switzerland (2019)
16. Baesens, B.: Analytics in a Big Data World: The Essential Guide to Data Science and Its Applications. Wiley, 232 p. (2014)
17. Egmont-Petersen, M., de Ridder, D., Handels, H.: Image processing with neural networks—a review. Pattern Recogn. **35**(10), 2279–2301 (2002)
18. Goodfellow, I., Bengio, Y., Courville, A., Bengio, Y.: Deep Learning, vols. 1, 925. MIT Press, Cambridge (2016)
19. Orlov, S.P., Girin, R.V.: Intelligent technologies in the diagnostics using object's visual images. In: Studies in Systems, Decision and Control. Cyber-Physical Systems: Advances in Design & Modelling, vol. 259, pp. 301–312. Springer Nature Switzerland (2020)
20. Lyamin, A.V., Cherepovskaya, E.N.: An approach to biometric identification by using low-frequency eye tracker. IEEE Trans. Inf. Forensics Secur. **12**(4), 881–891 (2017)

The Status Functions Application for Multispectral Data Images Processing in Virtual Reality Systems

I. V. Veshneva and R. A. Singatulin

Abstract The analysis of problems of feedback channel design in virtual reality training systems is presented. These problems are combined into groups of technical implementation, software processing of data, and mathematical models for assessing the state of a person studying in a virtual reality system. For the design of the technical implementation, possible technologies are considered. To create a non-invasive channel for assessing a person's condition, the possibility of using multispectral methods and image recognition technologies is highlighted. To develop mathematical support, a brief analysis of the mathematical representation of the signals in the communication channel was made. The methods based on the canonical expansions of random functions are singled out. To process the signal, a method of status functions is used, based on the canonical expansions of random functions. An experiment was conducted to develop a feedback channel based on multispectral imaging techniques and status functions. In the experiment, we used the study of the possibility of perceiving a 3D image of a volumetric display. The experiments demonstrated good prospects for the proposed technologies and mathematical methods. It was revealed that a short test demonstration of SIRDS-images or 3D-images before the beginning of the presentation of the main educational material promotes a holistic perception of pseudo-images. The proposed approach is advisable to use in modern educational platforms for the study and research of cyber-physical systems.

Keywords Status functions · Multispectral images · Data processing · Virtual reality systems · 3D images · Training · Feedback channel · Perception of three-dimensional images · Cyber-physical systems · Cognitive approach · Construing · Discourse · Elite · Engineering · Mind mapping · Model elite person · Social network · Semiolinguistics · Semiotics · Sign

I. V. Veshneva (✉) · R. A. Singatulin (✉)
Saratov State University, 83 Astrakhanskaya Street, Saratov 410012, Russian Federation

A. G. Kravets et al. (eds.), *Cyber-Physical Systems*, Studies in Systems, Decision and Control 350, https://doi.org/10.1007/978-3-030-67892-0_19

1 Systems of Virtual Reality in Training

Currently, the entire training system is being transformed [1, 2]. One of the aspects of this transformation is the introduction of virtual reality training systems (VRTS) in the process of education. The experience shows that the application of the VRTS provides high educational motivation and the success of the training. This is achieved through the activation of the brain, the realness of the objects and phenomena studied, the inclusion of all sensory organs. A new qualitative level can be realized by virtual reality methods in information processing, modeling, and design of experiments, the creation of complex machines and mechanisms, industrial objects, processes.

The main task of the development of VRTS is the development of technical and mathematical software. It is also necessary to create methods for assessing the cognitive and psycho-emotional state of a person [3, 4]. The set of problems arises when developing mathematical models of the state of the student, studying their psychological validity, and the means of technical and programmatic implementation of systems for assessing learning outcomes [5]. At the same time, it is required to preserve the continuity of the key concepts of interaction between the learner and the teacher.

To assess the levels of training, it is possible to use the following mathematical models: simple algebraic ones, taking into account the parameters of tasks, based on statistical methods, fuzzy sets theory, status functions [6].

The technical implementation of VRTS will most likely be based on applying a new concept of using the human-machine interface to create the effect of a three-dimensional environment in which the user interactively operates virtual objects, rather than images of these objects [7, 8].

The complex problem of the technical implementation of VRTS is the creation of a communication channel for the interaction of a person with the technical system affecting it. We considered ways to design a feedback channel in an ergatic VRTS using mathematical models based on status functions.

2 Technical Opportunities for Evaluating the Change in the Emotional State

For the application of modern methods of assessing learning outcomes, it is necessary to evaluate the result of mastering knowledge, as well as the change in the psychological state of a person. Human emotions are the physiological mechanisms of their interaction with the environment. Basic emotions have the simplest chemical and physical effects on the endocrine system of the body. If necessary, under certain circumstances they lead to a change in the type of behavior. Emotions act as key forces motivating behavior.

Objective assessment of systemic changes in emotions and brain work is possible based on methods for processing electro-encephalograms, Vibro images, or multispectral images.

Electro-encephalographic methods allow the analysis of subtle functional reconstructions of brain activity. This is their undeniable advantage. Data collection is carried out by a contact method. This imposes are significant.

Vibro image is a functional analog of the electroencephalographic method. The frequency of processed signals does not exceed 10 Hz, and 0–30 Hz, respectively. For registration of the Vibro image, it is enough to use webcams. This allows us to expect broad possibilities for applying this method for assessing the psychophysical state of a person and groups of people when several people are analyzed in the frame.

Non-invasive diagnosis with the use of multispectral technologies is based on photogrammetric methods of measuring the positioning of the human body in different spectral ranges. The novelty of the proposed approach is the use of webcams with multispectral diapason and a special software algorithm, mathematics model of the status function. The information-measuring system receives images from web cameras, then binds objects or fragments to the coordinate system and automatically identifies them with the corresponding fragments from the database, and then performs diagnostics. The scale and orientation of original fragments can be arbitrary.

To identify fragments, a stereo identification algorithm is used. It allows us to compare images of different geometries. The sequence of procedures based on photogrammetric and multispectral technologies allows solving the problem of recognition and selection of characteristic contour forms of the body. The implementation of the proposed procedure is designed to diagnose a typical motor pattern (smooth motion with constant motion), non-optimal dynamic stereotype, atypical motor pattern (the appearance of additional movements and distortion of the trajectory and speed of motion), and some other.

The measurement of motor deviations can occur anywhere in the eyeshot of the multispectral measuring system (at home, on the street, in the classroom). In the output of the measuring system, a three-dimensional description of the shape and dynamics of the object in a given format is shaped. Output data can be transmitted over the network. Information can also be visualized as a virtual three-dimensional object with its texture. The advantages of the method include low costs, the high accuracy of measurements, ease of use, high degree of automation, efficiency (diagnostics is performed in real-time).

3 Mathematical Methods for Describing the Feedback Channel of Ergatic Systems

The connection of input and output signals in the communication channel of the information measuring system can be realized by using a direct description, which is based on the use of differential or integral equations [7]. In this case, the description should use the consideration of the operator, which converts a multitude of input signals into output signals. Therefore models that use spaces in which coordinate functions are eigenfunctions of linear systems on infinite analyzed interval will be developed. This ensures the universality of the developed models.

It is advisable to use the mathematical model in the form of an operator for which bases of decompositions of input and output signals are given as harmonic functions [8]. It is assumed that the impact on the learner and assessment of his condition is presented in the form of a mixture of some signals. In this mixture, the learner state variables have a useful component $z(\boldsymbol{r}, t)$, and additive noise $n(\boldsymbol{r},t)$. The model of the communication channel is represented in the form of some operator H'. The operator displays the useful component of the output signal as the received mixture, which depends on the properties of the transmission medium, as well as on the characteristics of the input and output devices (performing the matching). Then the mathematical model of the communication channel can be represented in the following form:

$$H'(x(\boldsymbol{r}, t)) =< \Psi_r'\big(z'(\boldsymbol{r}, t), \boldsymbol{r}, t\big)| \frac{\partial z'(\boldsymbol{r}, t)}{\partial t} = \Psi_r\big(x(\boldsymbol{r}, t)z'(\boldsymbol{r}, t), \boldsymbol{r}, t\big) \quad (1)$$

where $z'(\boldsymbol{r}, t)$—learner state variables, Ψ_r, Ψ_r'—some nonlinear operators containing derivatives concerning spatial coordinates, $\boldsymbol{r}, t$—spatial and temporal variables. Various changes in the output signal can act as state variables.

The operator H′ is a system characteristic and reproduces the features of the signal observed in the output. The description of the feedback channel is reduced to the development of its system characteristics. Then the problem of numerical processing of a stationary random function can be based on canonical representations of random functions. They are based on the representation of a random function in the form of a deterministic function of random variables [9].

The development of methods for using canonical expansions for mathematical processing of signals in feedback channels in VRTS was carried out in [3]. These results should be used to solve the problem of assessing the state of a person trained in the VRTS for the formation of mathematical models of the state operator. Thus, when developing a mathematical model of a person's psychophysical state, which is affected by a technical system for training, status functions should be used [6].

As a result of the sequence of measurements of the interaction process between the trainee and VRTS and the representation of harmonic basic status functions from the form, mathematical models of human states can be determined. As a consequence, based on these models, we obtain an analog of the state vector of the system.

When the learner interacts with VRTS, the new concept of using the human-machine interface is realized for the creation of the effect of a three-dimensional environment in which the user copes interactively with virtual objects, not with images of these objects [7].

The problem of forming a mathematical model of the learner in the VRTS (1) can be solved by evaluating the perception of a three-dimensional image. There is a set of technical limitations in applying this approach.

4 Problems of the Feedback Channel Interface

Firstly, the user can work only with a complete prototype of a real object or phenomenon. The inclusion of focus groups at the stage of device modeling has not shown effectiveness due to different personal ability to abstract and indicators of spatial thinking of users. Secondly, final users have significant individual differences, which lead to a great mismatch of the usability ratings of the device. Also, the main methods of collecting estimates from users are questionnaire techniques and tests, the validity, and reliability of which also require additional evidence.

According to statistics, approximately 40% of people, when viewing the SIRDS-picture, almost immediately perceive a three-dimensional image. About 50–60% perceive a three-dimensional image only through special training, related to the selection of the optimal distance and focus of the view. Approximately 5–10% are not able to perceive an artificially formed volumetric image due to specific vision problems. Taking into account that modern multimedia educational technologies are oriented to the perspective of virtualization of educational material with the help of visualization of voluminous objects with new technical means [4], there is an urgent need to adapt (transform and switch) modern pedagogical methods and tools to a new qualitative level.

For each of the following indicators, we will use an estimate based on the status functions [6]:

1. Characteristics of two-dimensional images
   (a) Screen resolution.
   (b) Color of the image (color rendering quality).
   (c) Frame rate.
2. Characteristics of the three-dimensional image.
   (a) Viewing angle.
   (b) Image size.
3. Monocular properties of volume perception (I1)—these are taken into account when creating content for the display:
   (a) Parallax movement.
   (b) Perspective.
   (c) Shadows.
   (d) Mutual overlap of objects (occlusion).
   (e) Rotating object.
   (f) Gradient texture.
   (g) Heterogeneity of form.

For each of the indicators, and evaluation is based on status functions [5]. For each assessment objective (display characteristics, sensor readings, image analysis by software), and subjective indicators are used. Analysis of status functions allows us to conclude the perception of the image.

5 Experiment

When considering the volume pseudo-images (stereo images, 3D-images) without the use of special technical means (liquid crystal glasses, anaglyph glasses, etc.), it is required to perform two opposite actions:

- to direct a relaxed glance through the image,
- focus on the image, when each eye captures a clear and sharp image.

Studies were carried out at two independent levels:

I level—collective, classroom testing;
II level—"deep" individual testing.

In group testing, 87 people participated. The format of the messages of the textual-visual plan (lecture material) was selected depending on the target audience. The measurement of the physiological activity of students was made depending on their physiological activity (movement of the head, limbs, thermographic data of the open skin) when passing the test material in the audience. The technology of such an experiment is described in detail in [3, 4]. The difference was the way data is presented in 3D format. We used SIRDS-images, as well as 3D-images, formed based on the patent [9]. At the same time, publications in this subject area were taken into account [10–15].

List of used equipment:

- Stereo camera based on digital camera ELP USB8MP02G-MF80, 8.0 Megapixel, shooting mode 2K–4K;
- Digital camera GoPro 3+, shooting mode 2K–4K;
- Infrared laser flashlight with adjustable beam shape and backlight frequency;
- TV camera Flir® Tau®2 with uncooled VOx microbolometer;
- 3D-display designed based on the patent of the Russian Federation No. 2526901;
- Multimedia projector XGIMI H1;
- Laptop: Sony Vaio SVD1321M9RB, Intel® Core™ i5-4200U CPU @ 1.60 GHz 2.29 GHz, 4 Gb RAM, Windows 10 Pro (64-bit OS, x64 processor); Tablet: iPad Air, RAM 64 Gb, iOS 11.0.3.

The results of the 1st level audit are shown in Figs. 1 and 2. The first figure shows the placement of students in the classroom.

Classical university audiences are the best in overview for group testing. The second figure shows a graph of the total average amplitude of active movements (movements of hands, head, face mimic, eye movements, etc.) of students. The time interval is 45 min. During this period, the theoretical content of the discipline is presented. The presentation of the material is carried out in the feedback mode

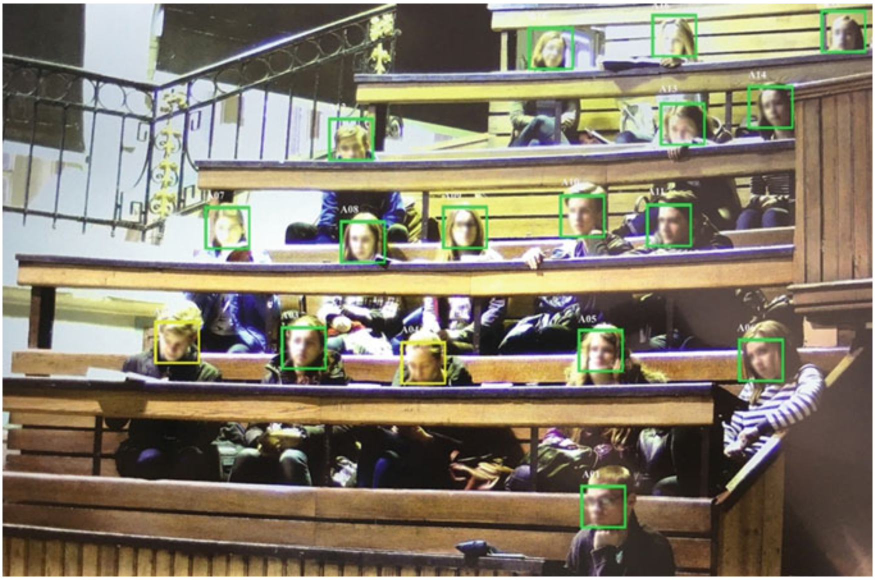

Fig. 1 Content placement trainees. The upper rows in the audience are scanned with a visible decrease in resolution accuracy. The *green* frame shows the faces of people in an active cognitive state, the *yellow* one indicates a decrease in attention, the *red* frame corresponds to a lack of attention

Fig. 2 The average amplitude of activity movements with clearly visible periods of decline and the increase in activity in the audience. The graph reflects the dynamics of the registered motility of movements in 25 min (in the so-called active phase of the perception of group information

(discussion and explanatory). On the chart, a fifteen-minute group climb of students' activity can be followed, followed by a "fatigue" decrease (8–10 min) and a new, more "effective" rise. In this case, the graph can be viewed as a conditional classroom "pro-file" of the learning group, which reflects the students' reactions to the instructional material presented by the teacher. Such visualization of the audit "profile", in real-time, significantly expands the possibilities of the educational and educational process, makes it possible to effectively evaluate and correct educational and methodological material.

In individual testing, the "deep immersion" method was used in a virtual environment, which was formed using the status function method, 17 people were tested. The experiment was conducted twice (one week after the first testing), with the same composition of participants. The study of eye tremors has been carried out

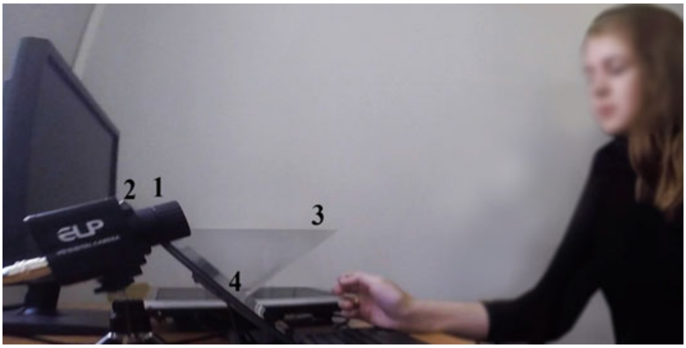

Fig. 3 General view of the information and measuring system of "deep" testing. Legend: 1—digital camera; 2—infrared searchlight; 3—3D-display; 4—laptop with a test program. The photo was taken at real field studies. Some parts of the image are veiled to maintain privacy. A feature of the installation is its hardware availability and high measurement efficiency. Setting the viewing angles (this is important) of web cameras and its adjustment can be done remotely (remotely) using the developed software

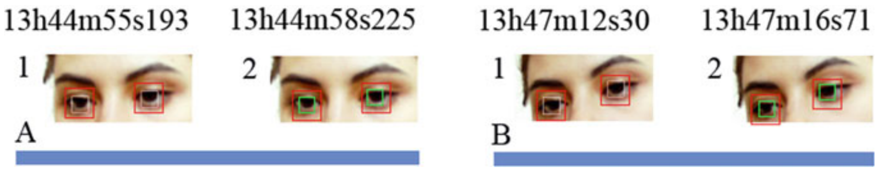

Fig. 4 An example of the work of an information-measuring system for "deep" testing: A1—eye-fixing (pupils) in the search mode; A2—eyes (pupils) in the perception mode; B1—fixation of the eyes (pupils) in the search mode (inclination of the head); B2—eyes (pupils) in the perception mode (inclination of the head)

in some works, for example [16]. Figure 3 are shown the system for conducting "deep" individual testing. Figure 4 are shown an example of the operation of the information-measuring system.

6 Conclusion

The effectiveness of the learning process directly depends on the applied methods and means, as well as the ability to most accurately assess the assimilation of educational material. In this case, the possibilities of using new educational technologies based on status functions are considered to form a feedback channel for training in specialized virtual reality systems.

The educational material using 3D technologies allows us to effectively achieve the planned learning goals. Unfortunately, three-dimensional images, due to the physiological features of the perception of 3D images by humans based on 3D technologies, are not always perceived by students.

In the proposed chapter, the development of actively studied methods was carried out [17–20]. Vibration imaging methods allow you to register minor vibrations of a living object using standard technical equipment, such as digital or analog video cameras [21, 22]. Processing data on the movement of body points in space reflects the psychophysiological state of a person and the level of his emotional arousal. All these allow to remotely scan people, revealing the level of their psychophysical state of activity, stress, and other characteristics of the psychophysical state of a person. In this chapter, these characteristics are used to collect data for constructing a mathematical model of a person's psychophysical state based on status functions. This method allows you to go to the quantum-mechanical operators describing the state of man. The prospects of these methods are considered in the early works of the authors. In the present work, the next step is taken to study the combination of the status function method for mathematical modeling based on the proposed and technically implemented laboratory setup.

The difference lies in the combination of cheap affordable devices and the demonstration of the use of medical research in education. The work is aimed at creating the foundations for the application of mathematical methods of quantum mechanics in creating mathematical models of the state of students in humanergatic machine systems. The basics of the application of status functions in models of the psychophysical state of a person have been developed and tested.

As shown by experiments, a short test demonstration of SIRDS-images or 3D-images of the target audience within 20–30 s. (the so-called "warm-up", "warm-up") before the beginning of the presentation of the main educational material, promotes the maximum inclusion of trainees in an active, holistic perception of volumetric images.

In the process of research and development of a system for remote diagnosis and monitoring of human conditions, the following were developed:

- a technique for diagnosing the psychophysical state of a person;
- algorithms for data analysis based on the method of status functions.

These results coincided with the experiments of other scientists who conducted similar studies, therefore, the identified relationships can be used for the correction of human conditions. If the results we obtained coincide with the results obtained in laboratory conditions and using additional measuring equipment, then it can be argued that they can also be used for the correction of the psychophysiological states of a person. The proposed approach is advisable to use in modern educational platforms for the study and research of cyber-physical systems.

Acknowledgements This chapter was prepared with the support of the RFBR grant 20-010-00465.

References

1. Gunal, M.M. et al.: Industry 4.0, Digitisation in manufacturing, and simulation: a review of the literature. In: Simulation for Industry 4.0, pp. 19-37. https://doi.org/10.1007/978-3-030-04137-3_2 (2019)
2. Jensen, L., Konradsen, F.: A review of the use of virtual reality head-mounted displays in education and training. Educ. Inf. Technol. **23**, 1515–1529 (2018). https://doi.org/10.1007/s10639-017-9676-0
3. Bolshakov, A.A., Veshneva, I.V., Chistyakova, T.B.: Model of formation of the feedback channel within ergatic systems for monitoring of quality of processes of formation of personnel competences. Int. J. Qual. Res. **9**(3), 495–512 (2015)
4. Meshchaninov, S., Ldovskaya, A.: Mathematical model of an adaptive system for remote monitoring of human's psychophysiological state. JCPEE **5**(1), 37–40. http://science.lpnu.ua/sites/default/files/journal-paper/2017/jul/5414/7.pdf (2015)
5. Stillman, G.A., Brown J. (eds.).: State of the art on modelling in mathematics education—lines of inquiry. In: Lines of Inquiry in Mathematical Modelling Research in Education. ICME-13 Monographs. Springer, Cham, pp 1–2. https://doi.org/10.1007/978-3-030-14931-4_1 (2019)
6. Veshneva, I.V., Chistyakova, T.B., Bolshakov, A.A.: The status functions method for processing and interpretation of the measurement data of interactions in the educational environment. SPIIRAS Proc. **6**(49), 144–166. https://doi.org/10.15622/sp.49.8. ISSN: 20789181 (2016)
7. Thakral, S., Manhas, P., Kumar, C.: Virtual reality and M-learning. Int. J. Electron. Eng. Res. **2**(5), 659–661 (2010)
8. Batenkov, K.A.: Modeling of continuous communication channels in the form of transformation operators for certain spaces. SPIIRAS Proc. **32**, 171–198 (2014)
9. Pugachev, V.S.: The Theory of Random Functions and Its Application to Problems of Automatic Control. Gos. Izd-vo fiz.-mat. lit-ry, Moscow (1963)
10. Tunable, L., Crystal, L., Yung-Yuan, K., Yan-Pean H., Kai-Xian, Y., Paul, C.-P., Chi-Chung, T., Chi-Neng, M.: An auto-stereoscopic 3D display using. https://doi.org/10.1889/1.3256482 (2012)
11. Robert, B., John, S.: Directional backlight lightguide considerations for full resolution autostereoscopic 3D displays. https://doi.org/10.1889/1.3500410 (2012)
12. Eurasia Patent No. 200601499 08.02.2005 Three-dimensional display using a variable focusing lens. Seo Cheong Soo, Gim Dong Woo, Cho Gioung Il [et al.] (2005)
13. Jones, A., McDowall, I., Yamada, H., Bolas, M., Debevec, P.: Rendering for an interactive 360° light field display. ACM Trans. Graph. **26**(3), 40 (2007)
14. Lens, S. H., Sung-min, J., Byung-joo, L., Hyung-ki, H., Hyun-ho, S.: 3D displays based on a LTPS 2.4" VGA LCD panel attached with lenticular. https://doi.org/10.1889/1.3069639 (2012)
15. Nagano, K., Jones, A., Unger, J. et al.: An Automultiscopic Projector Array for Interactive Digital Humans. SIGGRAPH ACM Press (2015)
16. Method for obtaining information about the psychophysiological state of a living being 2015-04-01. KR20140041382A. South Korea. https://patents.google.com/patent/KR20140041382A/en (2015)
17. Xueliang, X., Cheng, T., Xingyuan, F.: A health care system based on PLC and ZiGbee. In: International Conference on Wireless Communication, Networking and Mobile Computing, September 21–25, 2007, Shanghai, China, pp. 3063–3066 (2007)
18. Manohar, A., Bhatia, D.: Pressure detection and wireless interfaces for patient bed. In: IEEE Biomedical Circuits and Systems Conference, November 20–22, 2007, Baltimore, MD, pp. 389–392 (2007)
19. Stepanov, M., Musatov, V., Egorov, I., Pchelintzeva, P., Stepanov, A.: Cyber-physical control system of hardware-software complex of anthropomorphous robot: architecture and models. Cyber-Physical Systems: Industry 4.0 Challenges. Studies in Systems, Decision and Control, vol. 259. Springer Nature Switzerland AG 2020, pp. 13–24. https://doi.org/10.1007/978-3-030-32579-4 (2020)

20. Suyatinov, S.I.: Conceptual approach to building a digital twin of the production system. Cyber-Physical Systems: Industry 4.0 Challenges. Studies in Systems, Decision and Control, vol. 259. Springer Nature Switzerland AG 2020, pp. 279–290. https://doi.org/10.1007/978-3-030-32579-4 (2020)
21. Klovskij, D.D., Kontorovich, V., Shirokov, S.M.: Models of Continuous Communication Channels Based on Stochastic Differential. Radio i svyaz' Publ., Moscow (1984)
22. Bolshakov, A.A.: e.a. 3D display. Patent RF, no. 2718777 (2020)

Application of Faceted Neural Networks to Solving the Pattern Recognition Problem

Semen Podvalny, Varvara Mugatina, and Eugeny Vasiljev

Abstract The chapter considers the prospects and possibilities of using artificial neural networks based on the faceted principle of data storage when applied to solving the pattern recognition problem. Basic discrepancies of widely known neural networks with the direct signal flow and their biological prototypes are discussed. It is found out that the main reason for these discrepancies is the structural stability of neural network models in the course of training, i.e. their passivity. The analysis was made of the modern concept of a biological nervous system functioning as a process of selective transfer of excitement in the hierarchical structure consisting of the ensembles of the nervous cages with high selectivity. On the basis of this analysis, it is offered to give up the attempts of imitation of a biological nervous system functioning at the level of elementary neurons functioning processes and to pass to the reproduction of the information structure of data storage and processing. The concept of a multi alternative structure and functioning of complex systems based on the multileveled of structure, the division of functions, and modularity was chosen as the basic concept of this approach to the formation of neural networks. It is shown that this concept satisfies the transition to the faceted principle of data storage which allows creating alternative neural networks with a mutable structure. The example is given of the creation of a hierarchical faceted neural network for the recognition of geometrical objects.

Keywords Pattern recognition model · Principles of multialternativeness · Faceted neural networks

1 Introduction

The artificial neural networks used in the problems of pattern recognition in a classical case represent themselves as the functionality [1–4]:

S. Podvalny (✉) · V. Mugatina · E. Vasiljev
Voronezh State Technical University, Moskov av., 14, Voronezh 394026, Russia
e-mail: spodvalny@yandex.ru

A. G. Kravets et al. (eds.), *Cyber-Physical Systems*, Studies in Systems, Decision and Control 350, https://doi.org/10.1007/978-3-030-67892-0_20

$$y_{j_N}(x) = F\left(\sum_{i_N} b_{i_N j_N} \cdot \ldots \cdot F\left(\sum_{i_2, j_2} b_{i_2 j_2} \times F(\sum_{i_1, j_1} b_{i_1 j_1} x_{i_1 j_1} + c_{j_1}) + c_{j_2}\right) + \ldots + c_{j_N}\right),$$

where:

b, *c*—network settings configured in the process of training;

r—number of a layer;

j_r—number of neurons in the *r* layer;

i_r—input number;

N—number of layers;

x, *y*—input and output variables;

$x_{i_r j_r}$—an element *i* of vector *x*, as an input of neuron *j* in the *r* layer;

$F(b,c,x)$—activation function.

Formal justification of the use of such neural networks in the general theory of decision-making is the theorem of completeness, i.e., any continuous function can be approximated asymptotically by the $y(x)$ type functions if the first and the second derivative of the activation functions $F(b,c,x)$ are continuous too.

However, an experience of the application of the neural network in the problems of recognition has shown that the specified formal prerequisite is not sufficient for the machine realization of properties of a biological nervous system; hence the basic discrepancies to their biological prototype are inherent in the type $y(x)$ artificial neural networks [5–9].

These discrepancies are connected with the attempt to reproduce biological processes on the basis of $y(x)$ functionality with a constant invariable structure. Reorganization of this functionality is made on the lowest, i.e., the parametrical level only: the network in the course of training is not capable to change the structure, thus being passive.

The specified passivity of a neural network leads to the emergence in such networks of the shortcomings that are not inherent in general to their biological prototypes, as shown in Table 1.

The most essential shortcomings are [10–13]:

1. The retraining problem consisting of the distortion of previously saved data in an artificial network in case of presentation to it of some excess quantity of the

Table 1 Comparison of an artificial neural network to its biological prototype

Artificial neural network	Biological nervous system
Tendency to retraining	Selective, accumulative nature of training: «one event—one ensemble of neurons»
Low generalization ability	The developed hierarchy of the «private—general» relations
Rapid growth of a number of the configured settings (a so-called «dimensional damnation»)	An ability to training does not decrease with growth of the saved-up information volume
Structure immutability (constancy) in the process of training (passivity)	Developing structure (activity)

training samples that are unknown beforehand. In a biological nervous system, its memory is characterized by high selectivity, whereas the data storing itself possesses the accumulative character which allows saving previously-stored data without distortions and in the unlimited volume.
2. Low generalization ability, i.e. the limited ability to identification between the situationally recognizable relation «private—general» . For this purpose, the network has to possess a multilevel, hierarchical structure.
3. The lack of autonomy in the functioning of the artificial neural networks elements leading to the nonlinear growth of a number of the configured settings with the increasing dimension of the tasks i.e. the manifestation of a «dimension damnation» . In biological organisms, there are no restrictions on the dimension of vectors of the offered attributes.

Modern ideas of biological nervous systems [14–20] demonstrate that in these systems the characteristic principles are those of a multi alternative structure and functioning based on a multileveled of structure, division of functions, and modularity [21–25]:

1. Independent storage of the events of nervous activity in the form of an ensemble of connected neurons excited differentially only by certain sensor signals. Such independence excludes the retraining itself.
2. The organization of neuro ensembles into the hierarchical structure which connects them by various general attributes (properties) of sensor signals.
3. The activity of a neural network providing the reorganization of the communications structure between the ensembles after each fact of training (the formation of the new stable ensemble and its embedding in the general structure of a network).
4. To realize artificially the properties of biological neural networks listed above it is offered to refuse any attempts to imitate the biological nervous system functioning at the level of the elementary neurons functioning processes and to pass to the reproduction of the data storage and processing structure. To create such a structure, the faceted principle of objects' classification can be used (from the French word 'la facette' meaning the same).

2 Faceted Principle of Data Storage

The faceted principle of the objects' classification is that the ensemble (set) $\{f, s\}$ of attributes-facets f is formed for each event whose set of values s determines by itself the particular object a (f, s), as shown in Fig. 1:

$$a \in A,\ |A| = z,\ f = \{f_1, f_2, \ldots, f_p\},\ s = \{s^{f_1}, s^{f_2}, \ldots, s^{f_p}\},\ s^{f_i} = \{s_1^{f_i}, s_2^{f_i}, \ldots, s_t^{f_i}\},\ i = \overline{1, p}$$

The faceted principle of data storage allows to unite various objects into the network structure $A^i = a_1^i \cap a_2^i \cap \ldots \cap a_z^i$ separately by each attribute f_i, at the same time introduction of an additional attribute or object does not require reorganization of a previously created and available structure, it just supplements it with a new ensemble with the corresponding communications. It is essential that in the presence of several attributes-facets f_i, the hierarchical classification of objects is possible.

In Fig. 2 the possible structure of a faceted type neural network is shown with three hierarchical levels of ensembles $a(f,s)$ of neurons that can be excited or inhibited by certain receptors-facets f_i and/or from other ensembles.

In particular, the excitement of the receptors f_4, f_5, f_6 activates the ensemble $a_{1,2}$, and further, in the absence of inhibition from the ensemble $a_{1,1}$, the ensemble $a_{2,1}$ will be excited which is activated indirectly by primary receptors f and in the presence of the previous $a_{1,2}$ activation.

Thus, there will be a sequence of the operated events in the system corresponding to the ensembles $a_{1,2}$ and $a_{2,1}$. At the same time the excitement of ensemble $a_{2,1}$ in the absence of inhibition from other ensembles, for example, $a_{2,2}$, $a_{2,3}$, will lead to an activation of the event $a_{3,1}$.

As a result, under the influence of the external influence $\{f_4, f_5, f_6\}$ the sequence of events has been created corresponding to the specified excitement. This obtained sequence of the excited ensembles corresponds to the pattern or replica of the $\{f_4, f_5, f_6\}$ influence, i.e. the result is recognition of this pattern.

The training procedure of a faceted neural network includes:

1. addition of a new object in the form of an ensemble of the values of attributes $a(f,s)_{z+1}$;
2. inclusion of each attribute—the facet of an object in the structure of communications of a network.

Two situations are possible in the course of the solution of the pattern recognition problems in a faceted neural network:

1. Within the same facet, there is an internal hierarchical interrelation between the selected set of objects. In this situation, the family tree is built based on the degree of proximity of the objects by the considered attribute which determines

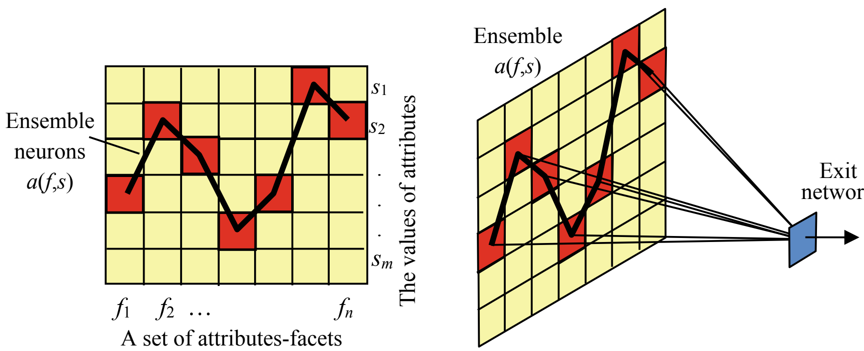

Fig. 1 The faceted memory organization in a neural network

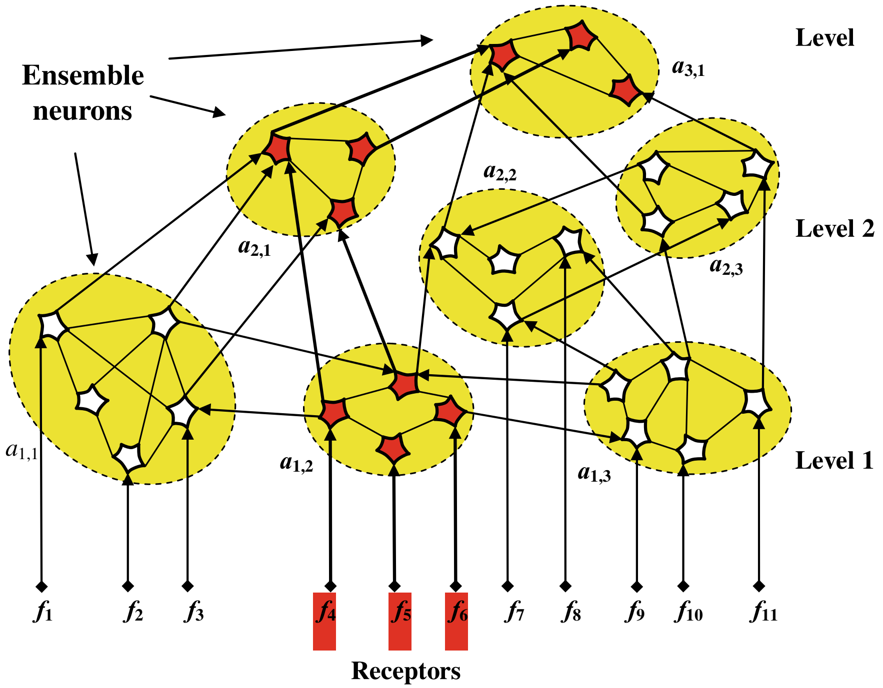

Fig. 2 Faceted type neural network structure

the interrelations between the events and defines the belonging of objects to either this or that branch of the family tree.

2. An object should be classified by some set of attributes, and the value of some attributes on which its classification should be made is unknown for this object. In this case, an artificial hierarchy (sequence) of attributes must be obeyed for the formation of a family tree to which the actual belonging of the recognizable object will be defined according to this hierarchy.

3 Example of the Creation of a Faceted Type Active Neural Network

Let's construct the active neural network model of pattern recognition for the problem of classification of objects with incompletely known attributes (here the set of features is applicable to all objects, but the values of some attributes may be unknown). The set of the classified objects is shown in Fig. 3.

The description of geometrical objects is provided by means of the attributes listed below:

1. equality of all sides;

2. an existence of right angles;
3. equality of all corners;
4. the number of all sides is equal to four;
5. the number of all sides is equal to three;
6. the color of the recognized object is white;
7. the area of the recognized object is greater than 1 sq.unit.

Each attribute can accept two values: 1—if the object possesses this attribute, 0—otherwise.

Such a description of the selected figures is shown in Table 2.

At the same time, it was accepted that the attribute value corresponding to the «existence of right angles» is unknown for Fig. 2. Here we set up the hierarchic sequence of classification so that the attribute which value for some object is unknown, is the last member in the classification hierarchy. It allows us to classify objects by all known values and to determine with maximum accuracy the belonging of the recognizable object, despite the absence of information on it by one of the applied classification attributes.

Let's apply the following sequence:

6. the color of the recognized object is white;

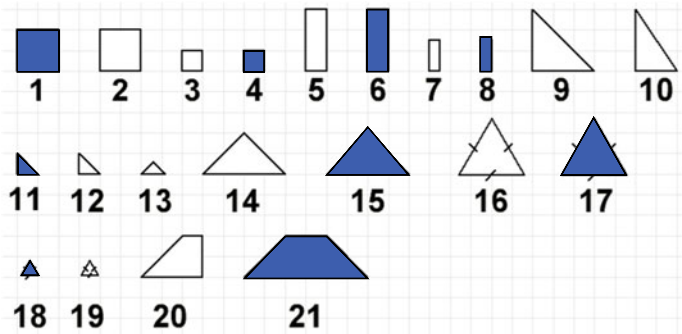

Fig. 3 A set of the classified objects

Table 2 A set of attributes-facets for the objects

Object Number	Attributes						
	1	2	3	4	5	6	7
1	1	1	1	1	0	0	1
2	1	–	1	1	0	1	1
3	1	1	1	1	0	1	0
…	…	…	…	…	…	…	…
20	1	0	1	0	1	1	0
21	0	0	0	1	0	0	1

4. the number of all sides is equal to four;
7. the area of the recognized object is greater than 1 sq.unit;
5. the number of all sides is equal to three;
1. equality of all sides;
3. equality of all corners;
2. an existence of right angles.

The constructed classification tree is shown in Fig. 4.

This drawing reflects the structure of a faceted neural network shown in Fig. 2. Each rectangle of the tree represents the ensemble of the values of attributes *a(f,s)* (see also Fig. 1 and Fig. 2). And the thing is that the ensembles of the first hierarchical level contain all attributes - facets, whereas the ensemble of the following level has one attribute less, etc. until the last known attribute. The sequence of the excited ensembles (these ensembles are highlighted with color in Fig. 4) creates the required pattern of the object. As soon as a new attribute is introduced to a problem, the existing network structure shall not collapse, it is supplemented instead with a new branch of a classification tree, i.e. the network attains an active character.

The result of classification shows that despite the absence of information on the presence of right angles in the second object, it can be judged from the constructed tree that this figure belongs to the class of quadrangles with equal corners, equal sides, and that the color of a figure is white and its area exceeds the value of 1 square unit. It should be noted that in the case considered above the existence of right angles in the recognized figure follows from the attribute of the equality of all corners in a quadrangle, i.e. an originally unknown attribute of an object can be restored as a result of the classification by the known attributes.

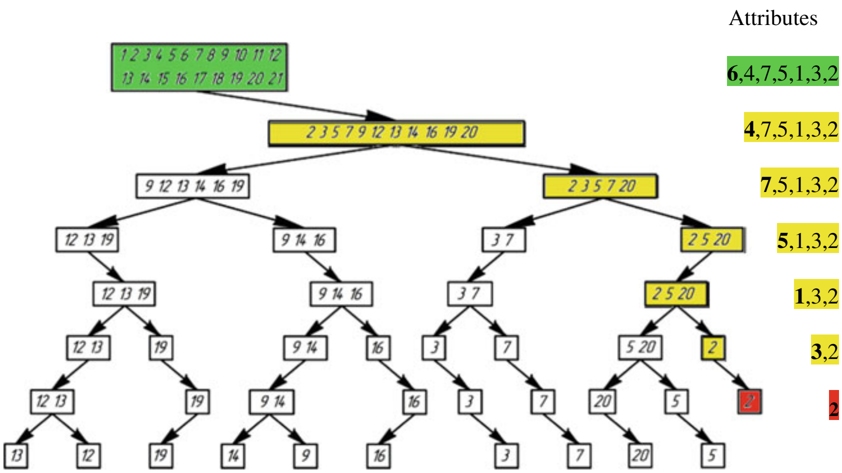

Fig. 4 Fragment of the classification tree

4 Discussion of the Results

Let's discuss two main properties of the considered faceted neural network that draw it closer to the properties of biological systems [26], i.e. the multileveled of structure and the property of activity, i.e. the restructuring ability.

Belonging to a concept «network» of the faceted memory structure is determined by the nature of interrelations between the subjects of recognition and attributes-facets which is described with a standard «many to many» notation, as shown in Fig. 5.

At the same time, the structure of interrelations between facets contains the relations «one to many» as well, that are characteristic for the hierarchical systems which operate in the problems of objects classification with the categories «particular-general» .

Such interrelation is given in Fig. 6 showing that the objects A and C belong to the same class basing on the f_1, attribute yet they belong to different classes basing on the f_2 attribute. According to f_1 the objects A, C, and B, D are united in different classes, and based on f_2 the objects A and D belong to the same class. Such hierarchy is shown

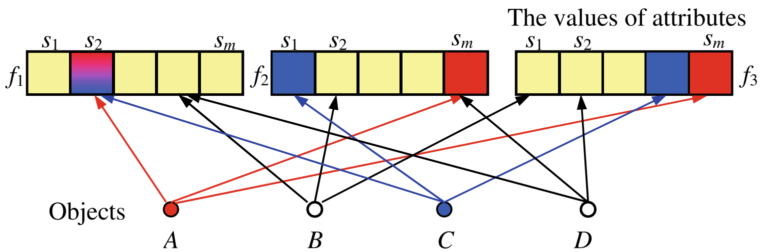

Fig. 5 Network interrelation between the objects and attributes-facets

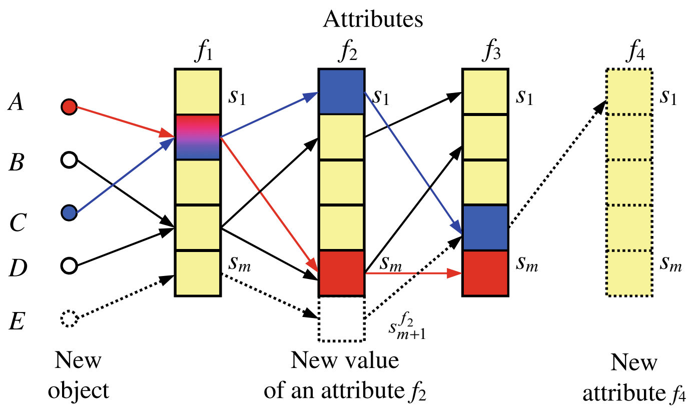

Fig. 6 Hierarchical interrelations between the attributes-facets

also in Fig. 4 which illustrates the more evident binary classification of objects by their geometric attributes.

It is important to note that the type of multilevel structure depends on the accepted sequence of the creation of a classification tree and it is defined by the priorities of the attributes in the problem of recognition. Nevertheless, for any chosen sequence the result of recognition will be defined by the obtained structure of interrelations, i.e. their unique sequence similar to the sequence of the excitement of the ensembles of neurons in biological nervous systems.

An activity of a faceted network is explained in Fig. 6 by an introduction of the new object E possessing an attribute f_4 which was absent in the known objects A, B, C, D. Moreover, the new object E can be characterized by the value $s_{m+1}^{f_2}$, of the attribute f_2 which was not found before, as well. As follows from Fig. 6, the new object E is built-in and inherent to the existing structure, expanding and supplementing it without the distortion of the existing system of communications.

5 Conclusions

An application of passive neural network models in the systems of pattern recognition meets the fundamental and based on principle difficulties connected with the discrepancy of properties of neural networks with their biological prototype.

To overcome these difficulties it is offered to refuse the attempts to imitate the biological nervous system at the level of the elementary neurons processes and to pass to the reproduction of the information structure of data storage and processing in these systems.

The faceted principle of classification of objects can be used to create such a structure. The faceted organization of memory allows to create of the active models of recognition with the reconfigured structure reproducing by their properties the evolutionary principles of a multi-alternative structure and functioning of biological systems, i.e.:

1. the creation of a memory structure based on the rule «one event-one ensemble» gives the chance to unlimited and selective building-up of any number of objects in the active system without the emergence of the retraining effect;
2. the modularity of a structure allows to build in the new ensembles of attributes-facets into an active neural network structure without meeting at the same time both the restrictions known as the «dimension damnation» and the retraining effect;
3. the multilevel structure of a faceted network is a replica of the hierarchy of the «particular—general» relations reproducing it directly and providing high generalizing properties of the recognition system.

References

1. Cichy, R.M., Kaiser, D.: Deep neural nnetworks as scientific models. Trends Cogn. Sci. **23**(4), 305–317 (2019)
2. Goyal A., Gupta V., Kumar M.: Recent named entity recognition and classification techniques: a systematic review. Comput. Sci. Rev. **29**, 21–43 (2018)
3. Nixon M.S., Aguado A.S.: Distance, classification and learning. In: Feature Extraction and Image Processing for Computer Vision, pp. 571–604. Academic Press, Elsevier Ltd, London (2020)
4. Davies, E.R.: Face detection and recognition: the impact of deep learning. In: Ferrari, V., Hebert, M., Sminchisescu, C., Weiss, Y. (eds.) Computer Vision-ECCV 2018, 15th European Conference, pp. 631–662. Munich, Germany (2018)
5. Barrett, D.G.T., Morcos, A.S., Macke, J.H.: Analyzing biological and artificial neural networks: challenges with opportunities for synergy? Curr. Opin. Neurobiol. **55**, 55–64 (2019)
6. Benitez V.H.: Pattern classification and its applications to control of biomechatronic systems. In: Artificial Neural Networks for Engineering Applications, pp. 139–154. Academic Press, Elsevier Ltd, London (2019)
7. Meshalkin, V., Puchkov, A., Dli, M., Lobaneva, Y.: Deep neural networks application in models with complex technological objects. In: Kravets, A., Bolshakov, A., Shcherbakov, M. (eds.) Cyber-Physical Systems: Advances in Design & Modelling. Studies in Systems, Decision and Control, vol. 259, pp. 291–300. Springer Nature Switzerland AG, Cham (2020)
8. Li, J., Makarychev, M., Popov, A.: Alternative approach to solving computer vision tasks using graph structures. In: Kravets, A., Bolshakov, A., Shcherbakov, M. (eds.) Cyber-Physical Systems: Industry 4.0 Challenges. Studies in Systems, Decision and Control, vol. 260, pp. 63–78 . Springer Nature Switzerland AG, Cham (2020)
9. Nashivochnikov, N.V., Bolshakov Alexander, A., Lukashin, A. A., Popov, M.: The system for operational monitoring and analytics of industry cyber-physical systems security in fuel and energy domains based on anomaly detection and prediction methods. In: Kravets, A., Bolshakov, A., Shcherbakov, M. (eds.) Cyber-Physical Systems: Industry 4.0 Challenges. Studies in Systems, Decision and Control, vol. 260. pp. 277–288. Springer Nature Switzerland AG, Cham (2020)
10. Abrosimov, M., Alexander Brovko, A.: High generalization capability artificial neural network architecture based on RBF-network. In: Dolinina, O., Brovko, A., Pechenkin, V., Lvov, A., Zhmud, V., Kreinovich,, V. (eds.) Recent Research in Control Engineering and Decision Making. ICIT 2019. Studies in Systems, Decision and Control, vol. 199, pp. 67–78. Springer Nature Switzerland AG, Cham (2019)
11. Barker, G.R.I., Warburton, E.C.: Multi-level analyses of associative recognition memory: the whole is greater than the sum of its parts. Curr. Opin. Behav. Sci. **32**, 80–87 (2020)
12. James, C.D., Aimone, J.B., Miner, N.E., Vineyard, C.M., Plimpton, S.J.: A historical survey of algorithms and hardware architectures for neural-inspired and neuromorphic computing applications. Biol. Inspired Cogn. Arch. **19**, 49–64 (2017)
13. Frazão, X., Alexandre, L.A.: Weighted convolutional neural network ensemble. In: Bayro-Corrochano, E., Hancock, E. (eds.) Progress in Pattern Recognition, Image Analysis, Computer Vision, and Applications. CIARP 2014. Lecture Notes in Computer Science, vol. 8827, pp. 674–681. Springer Nature Switzerland AG, Cham (2014)
14. Kandel, E.R., Dudai, Y., Mayford, M.R.: The molecular and systems biology of memory. Cell **157**(127), 163–186 (2014)
15. Sewards, T.V.: Neural structures and mechanisms involved in scene recognition: a review and interpretation. Neuropsychologia **49**(3), 277–298 (2011)
16. Di Carlo, J.J., Zoccolan, D., Rust, N.C.: How does the brain solve visual object recognition? Neuron **73**(39), 415–434 (2012)
17. Lacey, S., Sathian, K.: Visuo-haptic object perception. In: Multisensory Perception, pp. 157–178. Academic Press, Elsevier Ltd, London (2020)

18. Ennaceur, A.: Object novelty recognition memory. Handb. Behav. Neurosci. **27**, 1–22 (2018)
19. Sanes, J.R., Zipursky, S.L.: Synaptic specificity, recognition molecules, and assembly of neural circuits. Cell **181**(330), 536–556 (2020)
20. Miskovic, V., Lynn, S.J., Bagg, J.O., Pouliot, J.J., Wackermann, J.: Perceptual phenomena in destructured sensory fields: probing the brain's intrinsic functional architectures. Neurosci. & Biobehav. Rev. **98**, 265–286 (2019)
21. Podvalny, S.L., Vasiljev, E.M.: Evolutionary principles for construction of intellectual systems of multi-alternative control. Autom. Remote. Control. **76**(2), 311–317 (2015)
22. Podvalny, S.L., Vasiljev, E.M.: A multi-alternative approach to control in open systems: origins, current state, and future prospects. Autom. Remote. Control. **76**(8), 1471–1499 (2015)
23. Podvalny, S.L., Vasiljev, E.M., Barabanov, V.F.: Models of multi-alternative control and decision-making in complex system. Autom. Remote. Control. **75**(10), 1886–1891 (2014)
24. Podvalny, S.L., Vasiljev, E.M.: The Cybernetic Concept of Multialternativity in the Evolution of Biological Systems // J. Phys.: Conf. Ser., Applied Mathematics, Computational Science and Mechanics: Current Problems, 2019, Voronezh, Russian Federation. IOP Publishing, vol. 1479, 012109 (2020)
25. Podvalny,, S.L., Vasiljev, E.M.: Simulation of the multialternativity attribute in the processes of adaptive evolution. In: Kravets A., Bolshakov A., Shcherbakov M. (eds) Cyber-Physical Systems: Advances in Design & Modelling. Studies in Systems, Decision and Control, vol. 259, pp. 167–178. Springer Nature Switzerland AG, Cham (2020)
26. Jandel, M.: Biologically relevant neural network architectures for support vector machines. Neural Netw. **49**, 39–50 (2014)

Research of the ELA Algorithm for Identifying Editing Fact in Jpeg Images

Vladimir Polyakov, Dmitriy Buhanov, Maxim Panchenko, Margarita Redkina, and Sergey Chernikov

Abstract The process of detecting the fact of image modification using the method of analyzing the level of errors in jpeg images is considered. It is proposed to use artificial neural networks based on an adaptive resonance theory with a hierarchical memory structure as a classifier. A number of experiments were conducted to test the system for detecting the fact of modification of the original image. The results of the experiments show the speed and high accuracy to detect a modified image.

Keywords JPEG image modification · Video frame analysis · Error analysis method · Adaptive resonance theory artificial neural network · Clustering

1 Introduction

Modern society cannot be represented without a constant, intensive growth of information exchange. The fastest, most convenient, and affordable way to exchange information around the world is to use the Internet. Content produced, distributed, and consumed digitally is called digital content [1]. According to reports [1, 2], there is an increase in digital content on the Internet. The main types of digital content are audio and video files and streams.

The trend towards an increase in the volume of this kind of traffic in the global network has led to problems of quality control, reliability, and time of access to digital content. The most urgent and not fully resolved task is the verification of the authenticity and reliability of digital images, that is, revealing the fact of image falsification. In [3–5], a review of the main methods of checking digital images for falsification is carried out. These methods are based on ADJPEG and NADJPEG filters, primary quantization matrix detection, and JPEG ghost detection. However, according to [6], when checking these methods on the database of falsified images

V. Polyakov (✉) · D. Buhanov · M. Panchenko · M. Redkina · S. Chernikov
Belgorod State Technological University, Kostyukova Str. 46, Belgorod 308012, Russia
e-mail: p_v_m@mail.ru

S. Chernikov
e-mail: serg4315@mail.ru

A. G. Kravets et al. (eds.), *Cyber-Physical Systems*, Studies in Systems, Decision and Control 350, https://doi.org/10.1007/978-3-030-67892-0_21

[7], unsatisfactory results were obtained. Most approaches require an expert to find a fake area. This slows down and reduces the accuracy of the process of finding the image modification.

To solve this problem, it is proposed to use a method based on error level analysis (ELA), that automates the determination of the fake area. Error rate analysis examines lossy digital image compression artifacts such as JPEG. Using this method, it is possible to find modified areas of a JPEG image [8], based on the features of the JPEG encoding. In this chapter, noise is the difference between an image and its compressed version. The resulting noise is analyzed for the difference in the levels of compression artifacts. An image that has not been modified has a uniform level of compression artifacts. Thus, the part of the image that has been changed and the part that remains intact will have different levels of compression artifacts. The JPEG image encoding method [9] causes noise.

Consider JPEG encoding. An image in which each pixel is described by 3 bytes of the RGB model can be converted to the YCbCr model [10]. A group of 4 pixels, represented as a 2 × 2 block, can be described by a set of components: {Y, Y, Y, Y, Cb, Cr}, where Y—brightness, Cb—relative blue, Cr—relative redness of the image. The order of these components is specified in the image header. Totally, a group of 4 pixels is described not by 12 bytes, but by 6, which halves the file size.

Next comes the encoding stage, which includes lossy compression of the JPEG image. The image is split into 8 × 8-pixel blocks. A discrete cosine transform (DCT) is performed over each block [11, 12], at the stage of which the output matrix will contain the coefficients for the patterns, which are the basis for compiling any image of 8 × 8 pixels. This basis is shown in Fig. 1a.

The values of the output transformation matrix are arranged in ascending order of frequency according to the principle shown in Fig. 1b. The resulting coefficient matrix is divided by a rounding matrix, also called a quantization table [13], and the values in the cells are rounded to the nearest integer number. Quantization matrices

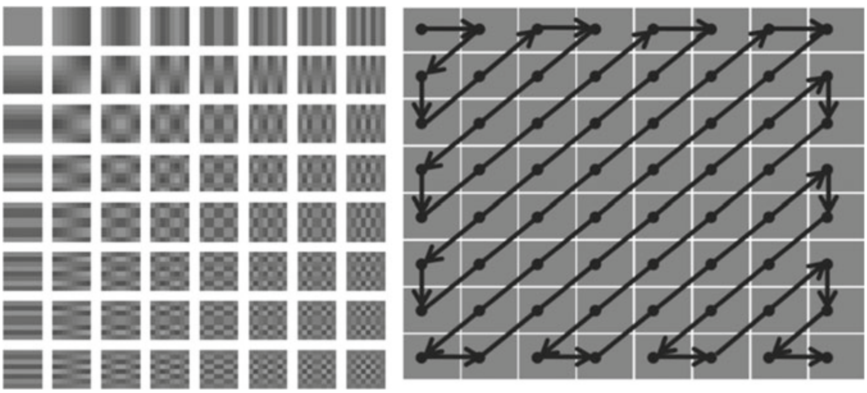

a b

Fig. 1 **a** basis matrix from [12], **b** principle of increasing frequencies in a matrix [13]

1	1	2	2	4	2	5	6
1	1	2	3	6	1	6	6
1	2	2	4	6	1	7	6
2	2	3	5	9	1	8	6
2	4	6	7	11	2	10	8
4	6	6	8	10	2	11	9
6	8	9	10	12	5	12	10
9	10	10	11	10	7	10	10

a

3	2	2	3	5	8	10	12
2	2	3	4	5	12	12	11
3	3	3	5	8	11	14	11
3	3	4	6	10	17	16	12
4	4	7	11	14	22	21	15
5	7	11	13	16	21	23	18
10	13	16	17	21	24	24	20
14	18	19	20	22	20	21	20

b

Fig. 2 Quantization matrices of modification of the original image **a** and its compressed version **b**

used for compressing the images on which the tests were carried out are formed depending on the set compression quality.

The quantization matrix for the modification of the original image in Fig. 2a is generated based on a quality score of 90%, and for its compressed version (Fig. 2b) based on a quality score of 95%.

The coefficients of the DCT matrix form a vector according to the pattern shown in Fig. 1b. The first coefficient of a vector is called the DC coefficient or sample mean. All subsequent vector coefficients are subdivided into 3 equal groups, each containing 21 elements: a group of low-frequency coefficients, a group of mid-frequency coefficients, and a group of high-frequency coefficients [13].

The quantization table values increase as you move along the scheme shown in Fig. 1b. When dividing and rounding the result of the DCT transform by the quantization table in Figs. 2a and b, the high-frequency elements of the resulting matrix have values close to or equal to zero.

Thus, the DCT output block goes through a sampling or quantization process - a process in which high frequencies are removed. This is where information loss occurs.

Further compression occurs without losses in three ways: length coding, delta, and Huffman's methods. An important stage for this work is the stage of lossy compression. Compression with a higher quality index removes more DCT coefficients and affects those that are more visible to the human eye. The difference between images with different compression levels is noise.

Table 1 Test data for the experiments

Exp. no	Number of images	Number of modifications	Size of modifications
1	5	20	100 × 100
2	5	50	100 × 100
3	3	20	100 × 100
4	3	10	200 × 200
5	3	30	200 × 200

2 Preparing Data for Experiments

The chapter proposes a system for detecting the facts of image modification by analyzing noise histograms of JPEG images based on the ELA method. An artificial neural network (ANN) ART-2 m is used as a classifier of data, frequencies represented by histograms.

Test data obtained by embedding in the original image into another image position obtained by the normal distribution, the size intersperse image remains unchanged with respect to all modifications obtained. Parameters of obtained test data are shown in Table 1.

The table shows the data for the experiments, the data for experiments 3–5 were obtained when analyzing the same video sequence, respectively.

3 Development of an Image Modification Detection System

The resulting test sample passes through the transform with the selected compression quality. The difference between the modified image and its compressed version is noise (Fig. 3).

Next, the resulting noise image is converted to a black-and-white version of the image and this version of the histogram of noise. The histogram of noise is described by a vector V, consisting of 256 elements. After repeating the algorithm overall modified images, we get vectors $V_i, i = 1..n$, where n- number of tests or modified images. Figure 3 illustrates an example of the modified video sequence frame (a), the noise (b), the histogram of the original frame noise (c), and the modified block noise histogram (d).

As seen from Figs. 3a and d, the histogram of the modified image noise has fewer black pixels (with a value of 0) and more colored pixels (with a value different from zero), this is due to a larger amount of high-frequency noise in the modified image.

Consider an algorithm for detecting image modification, the block diagram of which is shown in Fig. 4. Input data: *Images* and quality parameter *Quality*.

The algorithm is the following steps:

Step 1. Initializing an empty set of vectors V and its counter (iterator) i.

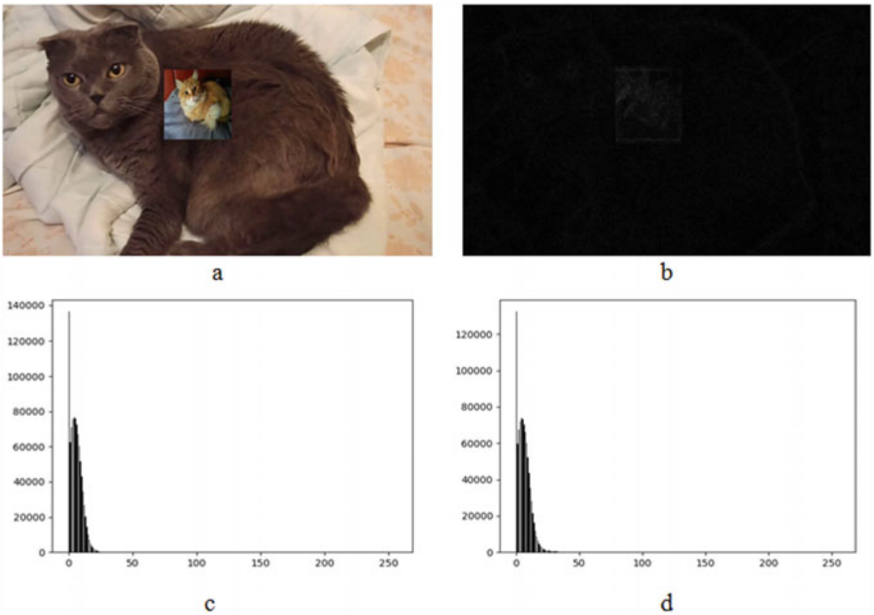

Fig. 3 **a** modified frame of the video sequence, **b** noise of the modified frame, **c** histogram of the noise of the original frame, **d** histogram of the noise of the modified frame

Step 2. Then carry out the following steps for all images in a given set:

Step 2.1. The *Image* is compressed according to the JPEG standard with the *Quality* parameter, the resulting image will be denoted as *Compressed_image*.

Step 2.2. Find the *Noise* as the *Difference* between the compressed and the given image.

Step 2.3. Convert *Noise* to *Monochrome_noise*.

Step 2.4. Building a histogram (*Hist*) based on the pixel values of a monochrome image of noise (*Monochrome_noise*).

Step 2.5. Create a vector *V* describing the histogram (*Hist*)

Step 3. Set of vectors *V*, resulting in the implementation of the algorithm is fed to the input of ART-2 m classifier.

The most popular methods for solving classification problems are methods based on ANN [14–16]. One of the most pressing problems inherent in different classes of ANN is instability during additional training. In [17], was presented the network that solves it. Subsequently, papers were published describing various modifications of the ART-2 network [18, 19].

As the classifier was selected ART-2 m network having a tree structure of memory. In [20] described the algorithm of such a network. It is an iterative process, represented by the following algorithm:

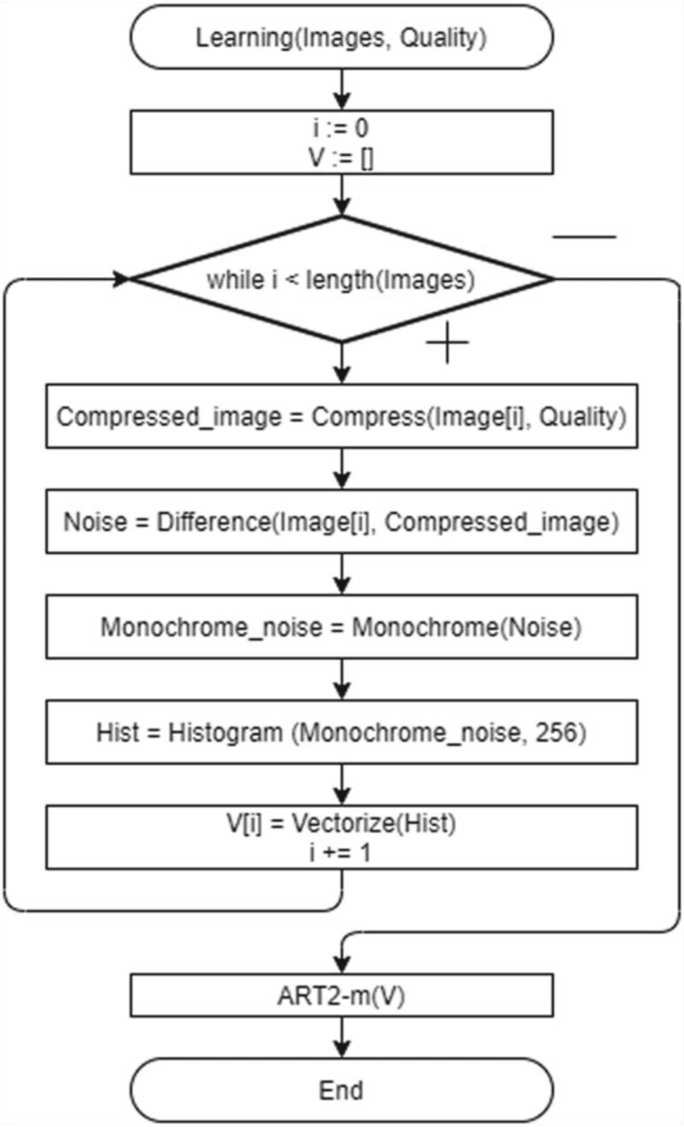

Fig. 4 Algorithm of image modification detecting

1. The image, which is a vector of numbers, is fed to the input of the comparison field of the ANN ART-2 m. The corresponding neuron is determined for it from the recognition field.
2. If the input image does not match with those already in memory, there is the ANN training mode, while it does not break the tree architecture. The generalized structure of the ART-2 m network is shown in Fig. 5.

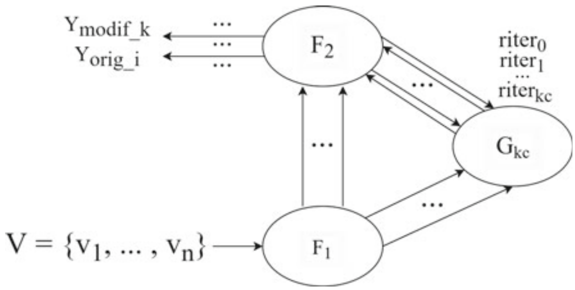

Fig. 5 Generalized structure of ART-2 m

The diagram shows: F_1 is a comparison field, F_2 is a recognition field and G_{kc} is a similarity field, represented by similarity parameters $riter_i$, where $i = 0..kc$ for each of kc ANN tree structure levels. The calculation of $riter_i$ is based on the following recurrent dependency:

$$riter_0 = 0.5; riter_{i+1} = riter_i + 0.75(1 - riter_i).$$

The input is a histogram V, ANN outputs are represented by images of originals noise Y_{orig} or modifications Y_{modif}

4 Results

A number of experiments were performed on the test data described in Table 1. The tree constructed on the basis of the results of experiment 1 using ART-2 m is shown in Fig. 6.

In Fig. 6 shows the result of the experiment with the test data of experiment 1. It can be seen from the results obtained that most of the noise of modifications ($modif\_i, i = 2\ldots5$) are less similar to the noises of the originals, for which these noises of modifications were obtained. The exception was the modification noise of the first original. ($orig\_1$). It is similar to the noises of the original with $riter_3 = 0.982$. It also shows that the original sounds and noises original versions are similar to each other. To analyze the image recognition rate at the network input filed different sets of fixed-size images with the number of inputs equal to 100. Figure 7 shows the performance of ART-2 m during the recognition of the input image. The average time for pattern recognition is 12.88 ms.

In experiments 1, 2, in which images not connected by a single video sequence were used as test data, all modifications of each original generate a new branch of the hierarchical memory of the classifier based on ART-2 m. This suggests that using this approach requires an original image. In the presence of the original image, the following binary classification results were obtained (Table 2). All original images were assigned to one group, all modifications to the other.

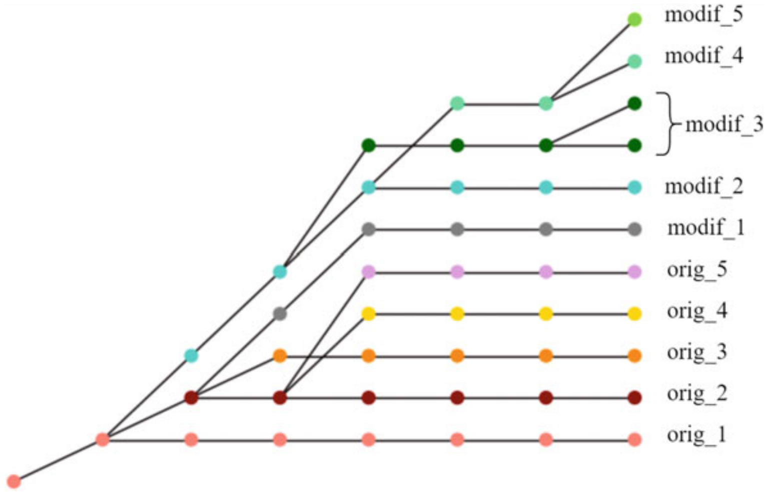

Fig. 6 ART-2 m memory tree

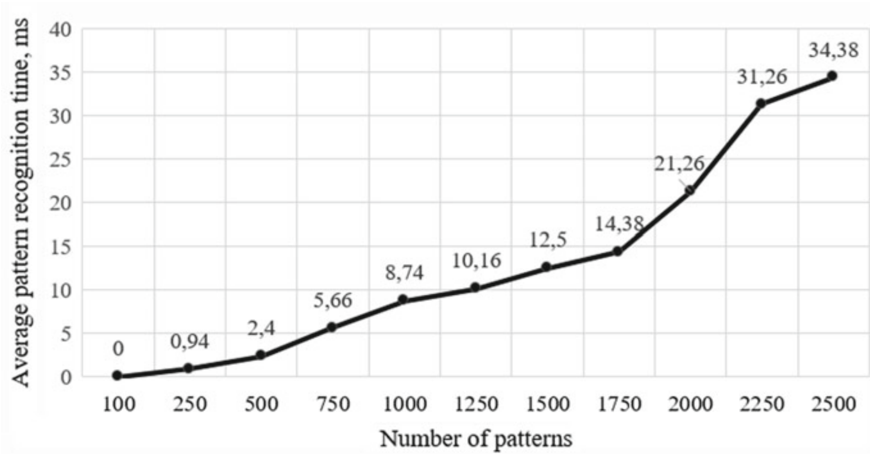

Fig. 7 Average speed of recognition of the input image ART-2 m

Table 2 Results of binary classification

Exp. 1	Orig.	Modif.	Exp. 2	Orig.	Modif.
Orig.	1.0	0	Orig.	1.0	0.004
Modif.	0	1.0	Modif.	0	0.996

Table 3 Results of a binary classification in the analysis of video sequences

Exp. 3–5	Orig.	Modif.
Orig.	1.0	0
Modif.	0	1.0

But this approach does not allow us to identify the original image without modification. If you use a video sequence as test data, as in experiments 3–5, then this allows you to identify a modification, having an incomplete set of original frames for training. Table 3 shows the general results of the binary classification for experiments 3–5.

The experiments show good classification results. Using a modification of ART-2 m to identify video editing due to the fact of high recognition rate. It should also be noted that the architecture of the ART-2 m ANN allows additional training of the network during operation.

5 Conclusion

The chapter presents the results of research to identify the fact of installation in JPEG images. For the study, algorithms for checking images for falsification were analyzed. From the considered algorithms was chosen algorithm ELA, because it allows you to automate the search for the modified region in the image. As an evaluation criterion has been selected image vector describing the brightness histogram of image noise. To obtain this vector, an algorithm presented in the work was developed, a feature of which is the use of ART-2 m for image classification. This feature allows you to increase the speed of image recognition, as well as perform additional training of the network in the process. After the experiments, conclusions were drawn, according to which the most effective application of the algorithm would be its use to identify the fact of editing in single-frame images. This is due to the fact that in order to identify the fact of editing, an original image is needed, which in the case of a single image may be absent, however, in the video stream, some frames may remain untouched, thereby providing original images for the algorithm. In the future, the algorithm requires modification to enable automated detection of the falsified image area.

Acknowledgements This research was supported by the Russian Foundation for Basic Research (project 19-29-09056 MK)

References

1. Digital content (2018). http://www.tadviser.ru/a/132656. Accessed 18 Sept 2020
2. The digital content market in Russia and the world. J'son & Partners Consulting. (2014) https://json.tv/ict_telecom_analytics_view/rynok-tsifrovogo-kontenta-v-rossii-i-mire-2010-2016-gg-2014092201340353. Accessed 22 Sept 2020
3. Mire, A.V., Dhok, S.B., Mistry, N.J., Porey, P.D.: Catalogue of digital image forgery detection techniques, an overview. Proceedings of the International Conference on Advances in Information Communication Technology & Computing. Amsterdam: Elsevier, pp. 502–508 (2013)
4. Mahdian, B., Saic, S.: A bibliography on blind methods for identifying image forgery. Signal Process.: Image Commun., **25**(6). Amsterdam: Elsevier, pp. 389–399 (2010)
5. Image Forgery Detection. A survey, IEEE Signal Processing Magazine, Volume 26, Issue 2. Austin, pp. 16–25 (2009)
6. Mire, A.V., Dhok, S.B., Porey, P.D., Mistry, N.J.: Digital Forensic of JPEG Images. 2014 Fifth International Conference on Signal and Image Processing. Washington: IEEE Computer Society, 8–10 Jan. 2014, pp. 131–136 (2014)
7. J. Dong, J., Wang,, W., Tan, T.: CASIA Image Tampering Detection Evaluation Database // 2013 IEEE China Summit and International Conference on Signal and Information Processing, pp. 6–10 (2013)
8. Wang, W., Dong, J., Tan T.: Tampered Region Localization of Digital Color Images Based on JPEG Compression Noise, 9th International Workshop, Seoul: IWDW 2010. October 2010, pp. 120–133. (2010)
9. Shehata O.: Unravelling the JPEG, Parametric press, Science + Society(2019). https://parametric.press/issue-01/unraveling-the-jpeg. Accessed 15 Sept 2020
10. Poynton A.: Frequently asked questions about color. http://poynton.ca/PDFs/ColorFAQ.pdf (2009). Accessed 5 Sept 2020
11. Cabeen K., Gent P.: Image compression and the DCT, Math 45. https://www.math.cuhk.edu.hk/~lmlui/dct.pdf. Accessed 21 Sept 2020
12. Sayood K.: Transform Coding, The Morgan Kaufmann Series in Multimedia Information and Systems.Introduction to Data Compression (Fourth Edition), pp. 409–446. Amsterdam: Elsevier (2012)
13. Dhanani, S., Parker, M.: Image Compression Fundamentals. Digital Video Processing for Engineers, pp. 103–109. Amsterdam: Elsevier, (2012)
14. Novikov, A.S., Ejov, A.A.: Rosenblatt multilayer neural network and its application for solving the problem of signature recognition. Izvestiya Tula State University. Technical science. No. 2. (2016)
15. Gorohovatskiy, V.A., Pupchenko, D.V.: Classification of images of visual objects by a set of descriptors of special points based on Kohonen's neural network. (2018)
16. Ershov, E.V. et al.: Software video detector for the detection, classification and counting of vehicles from CCTV cameras. Optoelectronic devices and devices in image recognition systems, image processing and symbolic information. Recognition. pp. 113–115 (2018)
17. Carpenter, G.A., Grossberg, S.: ART 2: self-organization of stable category recognition codes for analog input patterns. Appl. Opt. **26**(23), 4919–4930 (1987)
18. Dmitrienko, V.D., Zakovorotniy, A.U.: Neural network associative memory of adaptive resonance theory for determining the set of solutions, Mathematical and software systems in industrial and social spheres, vol. 7 No 1 (2019)
19. Dmitrienko, V.D., Zakovorotniy, A.U., Havina, I.P.: Nauchnie vedomosti BelSU. Ser. History. Political science. Economy. Informatics. No 7. pp. 110–119 (2010)
20. Buhanov, D.G., Polyakov, V.M.: Adaptive resonance theory network with multilevel memory. Nauchnie vedomosti BelSU. **45**(4), 709–717 (2018)

Analysis of Energy Characteristics for Issuing Areas of Significance When Compressing Images in Cyber-Physical Systems

Stella Lyasheva, Oleg Morozov, and Mikhail Shleymovich

Abstract The article discusses models and methods of image compression in cyber-physical systems. An approach is proposed to determine the significance of image areas in terms of their perception. An algorithm for identifying image significance regions based on an analysis of energy characteristics is described. The algorithm allows building a weight model, in which the image is considered at various scale levels. The multiple-scale wavelet transform is primarily applied, and then, based on the values of detailed wavelet coefficients, the pixel weights of the image copies at each level are calculated to build the weight model. Significant pixels are defined as pixels whose weight exceeds predetermined threshold values. The totality of these pixels forms a region of the significance of the image. The method of image compression using the algorithm for highlighting areas of significance is described. This method allows for reducing the image size by discarding the detailed wavelet coefficients associated with non-significant pixels. The method involves the use of additional quantization and entropy coding operations to improve image compression quality. Examples of image compression based on the described models, methods, and algorithms are given. It is shown that using the described approach it is possible to obtain compression and recovery characteristics that are comparable and, in most cases, exceed the quality of the corresponding characteristics of popular image presentation formats.

Keywords Cyber-physical systems · Image processing · Image analysis · Image compression · Image energy characteristics · Image significance areas · Image wavelet transform

S. Lyasheva (✉) · O. Morozov · M. Shleymovich
Kazan National Research Technical University Named After a. N. Tupolev-KAI, 10 K. Marx St, Kazan 420111, Russia
e-mail: salyasheva@kai.ru

O. Morozov
e-mail: ogmorozov@kai.ru

M. Shleymovich
e-mail: mpshleymovich@kai.ru

A. G. Kravets et al. (eds.), *Cyber-Physical Systems*, Studies in Systems, Decision and Control 350, https://doi.org/10.1007/978-3-030-67892-0_22

1 Introduction

Currently, there is the widespread use of models, methods, and tools for image processing and analysis for solving decision support tasks in various systems, including road safety systems, autonomous vehicles, and aircraft control systems, Earth remote sensing systems, access control systems to protected objects, etc. [1–5].

These systems should be considered within the framework of a relatively new actively developing scientific and technical direction—the theory of cyber-physical systems (CPS). CPS is understood as systems that provide reliable and secure control of remote physical objects in real-time using intelligent, info-communications, and computing technologies [6].

One of the intelligent technologies of cyber-physical systems is computer vision technologies based on models, methods, and tools for image processing and analysis [7].

According to the paradigm of D. Marr, image processing and analysis procedures can be divided into three levels [8]. At the first lowest level, images in the form of a set of attributes (brightness values or color intensity vectors) of pixels arrive at the input and output of the corresponding procedures. The second, middle, level procedures at the input also receive images in the form of a set of pixel attributes, and at the output, descriptors are formed that describe fragments of images. And finally, at the third, highest level, the corresponding procedures process image descriptors to determine their content.

As a rule, in the systems that process and analyze images, it is necessary to ensure their transmission and/or storage [9, 10]. At the same time, due to the fact that images represent large volumes of data, it is usually necessary to implement image compression procedures that reduce transmission time and/or increase the effective capacity of information storage devices and are related to the middle level of processing.

In the most general form, the main approaches to image compression are reduced to a scheme consisting of three steps, but not all of them are mandatory: reduction of inter-element correlation, quantization of data elements, and coding of data elements. The most complete general compression scheme is implemented in the JPEG standard [11–13]. In practice, not all of these steps are implemented in the compression procedure. This is due, for example, to the fact that it is necessary to provide compression of images without distortion, which is impossible when performing scalar or vector quantization or when interpolating the brightness of pixels based on reference values. However, distortion compression is most effective.

2 Compression Methods Based on Wavelet Transform

Many effective image compression methods are based on the use of the wavelet transforms. Distinguish between continuous and discrete wavelet transforms [14, 15]. Multiple-scale wavelet transforms also belong to discrete wavelet transforms. The image is presented in the form of a matrix of approximating coefficients and a set of matrices of detailed coefficients in the multiple-scale wavelet transform.

Based on multiple-scale wavelet transforms, it is possible to construct procedures for the analysis of detailed coefficients that allow localizing changes in brightness or color in images. For example, Fig. 1 shows the multi-scale orthogonal Haar wavelet transform of standard images of the boat, cameraman, and house, where the values of the detailed wavelet coefficients are represented by dots marked with gray gradations—darker brightnesses correspond to large absolute values of the coefficients. The standard images are 512 × 512 pixels in size and are taken from the USC-SIPI collection [16]. From the consideration of the figure, it is seen that a change in the brightness values in the source images (above) is observed at points corresponding to relatively large absolute values of the detailing wavelet coefficients (below). Figure 1 shows a two-level wavelet transform. Moreover, the approximating wavelet coefficients are shown as copies of the original image.

Based on the wavelet transform, many image compression methods have been developed [17, 18]. One of the most famous is JPEG2000 compression [19]. The scheme of this compression for color images contains operations of splitting images into tiles, shifting the database and converting color space (this operation is not required for grayscale images), discrete wavelet transform, quantization, and arithmetic coding.

In general, two methods are distinguished when encoding a wavelet-transformed image – intra-subband and inter-subband [20]. The intra-subband methods, for

Fig. 1 Examples of multi-scale Haar image transform

example, EBCOT, SPECK, SWEET, are based on eliminating the correlation between adjacent wavelet coefficients in each of the subbands individually. The inter-subband methods, for example, EZW, SPIHT, are based on eliminating the correlation between wavelet coefficients from different subbands.

One of the most popular methods is SPIHT, based on the following idea. The wavelet transform decomposes the image into subbands corresponding to low and high-frequency components. The bulk of the image energy is concentrated in the low-frequency ranges. Therefore, it can be expected that the coefficients of the parts decrease when moving from the high level to the lower one. In addition, there is a certain spatial similarity between the subbands.

3 Model of Energy Image Features Based on Wavelet Transform

The points in which there is a large difference in brightness can be determined energy characteristics model [21–24]. Within the framework of this model, estimates of the contribution of the pixels to the total energy of the image are considered based on the analysis of the values of the detailed wavelet coefficients at various levels of decomposition from the initial level j_0 to the final level $J-1$. The number J is determined by the formula:

$$J = \log_2 N, \tag{1}$$

where N—a number of rows and columns of the image.

When analyzing the level j of wavelet decomposition, the energy of the difference $\Delta E_j(m,n)$ at a point with coordinates (m, n) can be estimated using the expression:

$$\Delta E_j(m,n) = LH_j^2(m,n) + HL_j^2(m,n) + HH_j^2(m,n) \tag{2}$$

where $LH_j(m,n)$, $HL_j(m,n)$, $HH_j(m,n)$—detailing wavelet coefficients with coordinates (m, n) at the level j. In the case of applying the multiple-scale orthogonal Haar transform, these coefficients are calculated as follows:

$$\begin{aligned} LH_j(m,n) = (&LL_{j+1}(2m,2n) + LL_{j+1}(2m+1,2n)- \\ &-LL_{j+1}(2m,2n+1) - LL_{j+1}(2m+1,2n+1))/4, \end{aligned} \tag{3}$$

$$\begin{aligned} HL_j(m,n) = (&LL_{j+1}(2m,2n) - LL_{j+1}(2m+1,2n)+ \\ &+LL_{j+1}(2m,2n+1) - LL_{j+1}(2m+1,2n+1))/4, \end{aligned} \tag{4}$$

$$\begin{aligned} HH_j(m,n) = (&LL_{j+1}(2m,2n) - LL_{j+1}(2m+1,2n)- \\ &-LL_{j+1}(2m,2n+1) + LL_{j+1}(2m+1,2n+1))/4. \end{aligned} \tag{5}$$

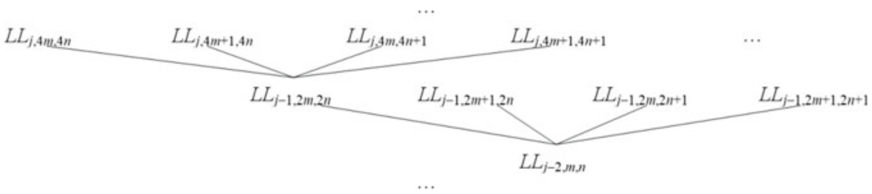

Fig. 2 The relationship between image copies at different levels of the multi-scale wavelet transform

In expressions (3)–(5) LL_{j+1} denotes a matrix of approximating wavelet coefficients at the level j+1. The values of the approximating coefficients are the brightness values of the copy of the original image at the corresponding level. Thus, in the multi-scale wavelet transform, each detail level coefficient j is associated with four pixels of a copy of the j+1 level image. This determines the relationship between pixels of different levels of image representation (Fig. 2). For the considered Haar transformation, this can be clearly observed from the expression for calculating approximating coefficients:

$$LL_j(m,n) = (LL_{j+1}(2m,2n) + LL_{j+1}(2m+1,2n)+ \\ +LL_{j+1}(2m,2n+1) + LL_{j+1}(2m+1,2n+1))/4 \quad (6)$$

and expressions for the inverse transformation:

$$LL_{j+1}(2m,2n) = (LL_j(m,n) + LH_j(m,n)+ \\ +HL_j(m,n) + HH_j(m,n))/4, \quad (7)$$

$$LL_{j+1}(2m+1,2n) = (LL_j(m,n) + LH_j(m,n)- \\ -HL_j(m,n) - HH_j(m,n))/4, \quad (8)$$

$$LL_{j+1}(2m,2n+1) = (LL_j(m,n) - LH_j(m,n)+ \\ +HL_j(m,n) - HH_j(m,n))/4, \quad (9)$$

$$LL_{j+1}(2m+1,2n+1) = (LL_j(m,n) - LH_j(m,n)- \\ -HL_j(m,n) + HH_j(m,n))/4. \quad (10)$$

Based on the above reasoning, all pixels and all points with coordinates (m, n) at the level j can be associated with the energy estimates of the brightness difference, both this level and all levels from j_0 to j-1. Therefore, in the framework of the image representation based on the model of energy features for its analysis, it is possible to determine the function of calculating weight values:

$$w_j(m,n) = T_j(\Delta E_{j_0}(m,n), \ldots, \Delta E_j(m,n)), \quad (11)$$

where $w_j(m, n)$—the weight of the point with the coordinates (m, n) of the image at the level j, which reflects its significance in terms of contribution to the total energy of the image; $T_j(\cdot)$—a function for calculating weights at the level j; $\Delta E_{j_0}(m, n)$, …, $\Delta E_j(m, n)$—the energy estimates at the point with coordinates (m, n), which are obtained at the levels $j_0, \ldots, j$.

Based on the weight values of all levels, it is possible to construct the weight model of the original image, as well as weight models of its representations at different levels. Examples of the weight models for standard images of the boat (left), cameraman (center), and house (right) are shown in Fig. 3, where darker brightnesses correspond to large values of weights.

The weighted models can be used to analyze the significance of changes in brightness at the image points, presented in the form of a wavelet decomposition. Since localization of the brightness changes in the image is associated with the values of the detailed wavelet coefficients, the weight models allow determining their significance for the inverse wavelet transform.

Figure 4 shows copies of the standard boat image, formed only from the approximating wavelet coefficients of levels 6 (left), 7 (center), and 8 (right). The presented copies of the original image can also be interpreted as "adding" to the approximating wave-let coefficients of level 6 detailed wavelet coefficients of higher levels.

Fig. 3 Examples of the weighted image models

Fig. 4 The copies of the boat image

At the same time, it is clear that when copies are formed from higher levels, their quality increases. It should also be noted that the original image in JPEG format has a volume of 101,7 Kb, and its copies at levels 6, 7, and 8—8,7 Kb; 54,8 Kb and 73,8 Kb, respectively. This shows how significantly reducing the number of detailing wavelet coefficients affects the quality of the compression and the quality of image recovery.

Thus, it is possible to determine the optimal set of detailing wavelet coefficients needed to represent the image. Representation of the image in the form of the approximating wavelet coefficients sets and the number of detailed wavelet coefficients ones significantly reduce its volume and can be used as the basis for its compression procedure.

4 Application of the Energy Features Model for Image Compression

The energy feature model (or weight model) of the image allows obtaining the weight values associated with the approximating and detailing coefficients for the various levels of the multi-scale wavelet transform. The weights obtained in the framework of this model can be used to analyze the significance of the detailed wavelet coefficients from the point of view of image reconstruction.

In general terms, the proposed image compression procedure using the energy feature model contains the following steps:

1. Determination of the final level of the wavelet decomposition $J - 1$.
2. Setting the initial level of the wavelet decomposition j_0.
3. Setting the function for calculating weights T_j for all levels of the wavelet decomposition $j_0, \ldots, J - 1$.
4. The calculation at each level j of the value of the weights $w_j(m, n)$ for all the detailed wavelet coefficients with coordinates (m, n).
5. Setting at each level j is a threshold value Δ_j.
6. Constructing a significance map of detailed wavelet coefficients by performing threshold processing of weight models of each level j:

$$w'_j(m, n) = \begin{cases} 1, \ w(m, n) \geq \Delta_j, \\ 0, \ w(m, n) < \Delta_j. \end{cases} \tag{12}$$

7. Transfer and /or storage of all approximating wavelet coefficients of the level j_0 and detailed wavelet coefficients of the level $j_0, \ldots, J - 1$, for which $w'_j(m, n) = 1$.

The final level of wavelet decomposition is determined by the size of the image $N \times N$ (the image is assumed to be square with $N = 2^K$, where K is a non-negative integer):

$$J - 1 = \log_2 N - 1 \tag{13}$$

The initial level j_0 is selected from the segment $[0, J - 1]$. The choice j_0 is determined by the requirements for the quality of the restored image and the quality of compression—the lower the initial level, the lower the quality of the restored image, and the higher the quality of compression. Based on the reasoning given above, the choice of the initial level determines the initial approximation of the original image. Moreover, the lower the initial level, the less approximating wavelet coefficients and the "rougher" the initial approximation to the original image. In addition, the smaller the initial level, the more detailing wavelet coefficients can be discarded. This can reduce the number of compressed images. However, discarding the detail coefficients leads to a deterioration in the quality of the reconstructed image. In this case, the quality of compression refers to the ratio between the volumes of the original and compressed images.

The functions for calculating weights T_j can be specified in various ways, based on heuristic considerations and implementation requirements. For example, the following method can be used:

$$w_{j_0}(m, n) = \Delta E_{j_0}(m, n), \tag{14}$$

$$w_j(m, n) = w_{j-1}(m/2, n/2)/4 + \Delta E_j(m, n),\ j = \overline{j_0, J - 1}. \tag{15}$$

Thresholds Δ_j should be calculated based on the requirements for the quality of the reconstructed image and the quality of compression. For example, these can be set as the values of a given ordinal statistics, calculated by the histogram of the weights. To simplify the construction of the histogram, the weight values can be reduced to a given range, for example, to a segment [0, 255].

To transmit and/or save the significant detailing wavelet coefficients for each level j, it is possible to build a significance map $\{w'_j(m, n)\}$ containing single-bit values. Also, the significant detailing wavelet coefficients can be quantized to bring to a given range, for example, to a range of single-byte values. In order to reduce the volume of the compressed image, the significance maps and the values of the quantized detailed wavelet coefficients can be further compressed using some encoding method, for example, the Huffman method or the arithmetic encoding method.

The compressed image will have a structure, a general view of which is shown in Fig. 5, where N—the image size; j_0—the initial level of decomposition; LL_{j_0}—a bulk of the approximating wavelet coefficients; $w'_{j_0}, \ldots, w'_{J-1}$—the significance maps

N	j_0	LL_{j_0}	w'_{j_0}	LH'_{j_0}	HL'_{j_0}	HH'_{j_0}	…	w'_{J-1}	LH'_{J-1}	HL'_{J-1}	HH'_{J-1}

Fig. 5 General view of the structure of a compressed image

Fig. 6 Examples of the recovered images with different quality

of the levels $j_0, \ldots, J-1$; $LH'_{j_0}, HL'_{j_0}, HH'_{j_0}, \ldots, LH'_{J-1}, HL'_{J-1}, HH'_{J-1}$—sets of the significant detailing wavelet coefficients.

Figure 6 shows examples of restoring standard images while maintaining a different number of detailed coefficients. The analysis of the image reconstruction quality was carried out using the criterion of the peak signal-to-noise ratio PSNR:

$$PSNR = 20\lg\left(\frac{I_{\max}}{RMSE}\right), \tag{16}$$

where $I_{\max}$—a maximum brightness in the original image I; $RMSE$—the mean square error between the original image I and restored image I' with dimensions $M \times N$ pixels:

$$RMSE = \frac{1}{MN}\sqrt{\sum_{m=0}^{M-1}\sum_{n=0}^{N-1}|I(m,n) - I'(m,n)|^2}. \tag{17}$$

The PSNR values for the reconstructed images in Fig. 6 are 38,4; 35,9 and 27,2 (from left to right).

For each level of the wavelet transform, the significance maps after threshold processing and the set of detailed wavelet coefficients after quantization are arrays of values that have good characteristics for additional compression using entropy coding methods. Moreover, each of these arrays can be compressed separately, which allows organizing progressive compression and recovery - this makes it possible to present the image first in the form of a rough copy, and then gradually improve it. The progressive compression interrupts the recovery process when an acceptable quality is achieved from the point of view of the end-user, which reduces the time it takes to transmit and analyze images.

In the framework of this chapter, the Huffman adaptive coding method was considered also [25]. The choice of this method is due to the high speed, the lack of the need to save additional information, and good compression characteristics.

Tables 1 and 2 show the characteristics of the proposed approach.

Table 1 The compression and recovery characteristics of the implementation for the proposed method

Images	Compression quality	Recovery quality	Compression time, sec	Recovery time, sec
boat	4,025	35,724	0,016	0,011
cameraman	4,461	40,819	0,013	0,008
house	4,968	42,169	0,012	0,009
jetplane	4,136	39,002	0,015	0,009
lake	3,893	34,792	0,016	0,011
livingroom	4,152	34,999	0,015	0,009
mandril	4,028	29,851	0,015	0,009
peppers	3,851	36,578	0,016	0,011
pirate	4,029	36,046	0,014	0,,009

Table 2 Volumes of test images in different raster formats

Images	WEIGHTS	JPEG	PNG	TIFF
Boat	65392	104143	324516	389120
Cameraman	59011	62222	254183	148938
House	52983	45023	202391	111390
Jetplane	63639	77034	277300	316366
Lake	67615	109389	329132	384722
Livingroom	63400	103133	322913	262750
Mandril	65347	107724	349977	262750
Peppers	68343	100589	210487	309918
Pirate	65330	99142	320518	262750

Table 1 shows the compression and recovery characteristics of the implementation of the proposed method for standard halftone images of 512 × 512 pixels. The following parameters were used: $J = 9$, $j_0 = 7$, $\Delta_7 = p_{50}$, $\Delta_8 = p_{80}$, where p_{50} and p_{80}—the 50th and 80th percentiles of ordered sets of weights of the corresponding levels. The characteristics were obtained relative to the original images in the BMP format. Table 2 for comparison shows the volume in bytes of test images in the proposed WEIGHTS format (Fig. 5) and the popular raster formats JPEG, PNG, TIFF, which are often used in practice. The volume of each test image in BMP format is 263,222 bytes. For experiments, a personal computer-based on 4 Intel (R) Core (TM) i5-8300H CPU@2.30 GHz processors and 8 GB RAM under the Microsoft Windows 10 operating system was used. The experiments were performed using a 64-bit software implementation performed in C ++ in the Microsoft Visual Studio 2017 programming environment using the OpenCV 3.4.9 computer vision library.

5 Conclusion

Based on the foregoing, the described method allows one to obtain the compression and recovery characteristics that are comparable and, in most cases, are superior in quality to the corresponding characteristics of popular image presentation formats.

Thus, the proposed approach can be effectively applied to compress images during their transmission and/or storage in cyber-physical systems based on computer vision technologies.

References

1. Kanellakis, C., Nikolakopoulos, G.: Survey on computer vision for UAVs: current developments and trends. J. Intell. Robot. Syst. **87**, 141–168 (2017)
2. Meshalkin, V., Puchkov, A., Dli, M., Lobaneva, Y.: Deep neural networks application in models with complex technological objects. In: Kravets, A., Bolshakov, A., Shcherbakov,, M. (eds.) Cyber-Physical Systems: Advances in Design & Modelling. Studies in Systems, Decision and Control, vol 259. Springer, Cham (2020)
3. Li, J., Makarychev, M., Popov, A.: Alternative approach to solving computer vision tasks using graph structures. In: Kravets, A., Bolshakov, A., Shcherbakov, M. (eds) Cyber-Physical Systems: Industry 4.0 Challenges. Studies in Systems, Decision and Control, vol 260. Springer, Cham (2020)
4. Alekseev, A.V., Orlova, Y.A., Rozaliev, V.L., Zaboleeva-Zotova, A.V.: Two-stage segmentation method for context-sensitive image analysis. In: Kravets, A., Shcherbakov, M., Kultsova, M., Iijima,, T. (eds) Knowledge-Based Software Engineering. JCKBSE 2014. Communications in Computer and Information Science, vol. 466. Springer, Cham (2014)
5. Eickeler, S., Valdenegro, M., Werner, T., Kieninger, M.: Future computer vision algorithms for traffic sign recognition systems. In: Schulze, T., Müller, B., Meyer, G. (eds.) Advanced Microsystems for Automotive Applications 2015. Lecture Notes in Mobility. Springer, Cham (2016)
6. Xiong, N.N., Shen, Y., Yang, K., Lee, C., Wu, C.: Color sensors and their applications based on real-time color image segmentation for cyber physical systems. J Image Video Proc. **2018**, 23 (2018)
7. Atat, R., Liu, L., Wu, J., Li, G., Ye, C., Yi, Y.: Big data meet cyber-physical systems: a panoramic survey. IEEE Access **6**, 73603–73636 (2018)
8. Stevens, K.A.: The vision of David Marr. Perception **41**(9), 1061–1072 (2012)
9. Coughlin, T.: Digital image storage and compression. In: Chen, J., Cranton, W., Fihn, M. (eds.) Handbook of Visual Display Technology. Springer, Cham (2016)
10. Ma, Z., Wang, X., Jiang, P., Jin, J., Guo, S.: Sequential record based compression for massive image storage in database. In: Gao, Y. et al. (eds.) Web-Age Information Management. WAIM 2013. Lecture Notes in Computer Science, vol. 7901. Springer, Berlin, Heidelberg (2013)
11. Raid, A.M., Khedr, W.M., El-dosuky, M.A., Ahmed, W.: JPEG Image Compression Using Discrete Cosine Transform—A SurveyInt. J. Comput. Sci. & Eng. Surv. (IJCSES) **5**(2) (2014)
12. Sayood, K.: Introduction to Data Compression, 5th edn. Morgan Kaufmann Publisher, Cambridge (2018)
13. Salomon, D., Motta, G.: Handbook of Data Compression, 5th edn. Springer-Verlag, London (2010)
14. Mallat, S.: A Wavelet Tour of Signal Processing, 3rd edn. Academic Press, New York (2009)
15. Tang, Y.Y.: Wavelet Theory and Its Application to Pattern Recognition. World Scientific Publishing Company, London (2009)

16. The USC-SIPI Image Database, http://sipi.usc.edu/database/database.php, last accessed 2020/04/30
17. Pearlman, W.A., Said, A.: Set partition coding: part I of set partition coding and image wavelet coding systems. Found. Trends Signal Process. **2**(2), 95–180 (2008)
18. Pearlman, W.A., Said, A.: Image wavelet coding systems: part II of set partition coding and image wavelet coding systems. Found. Trends Signal Process. **2**(3), 181–246 (2008)
19. Marcellin, M.W., Gormish, M.J., Bilgin, A., Boliek, M.P.: An Overview of JPEG-2000. Proc. of IEEE Data Compression Conference, 523–541 (2000)
20. Uthayakumar, J., Vengattaraman, T., Dhavachelvan, P.: A survey on data compression techniques: From the perspective of data quality, coding schemes, data type and applications. Journal of King Saud University—Computer and Information Sciences (2018). In press, https://www.sciencedirect.com/science/article/pii/S1319157818301101, last accessed 2020/04/30
21. Kostyukhina, G.V., Lyasheva, S.A., Shleymovich, M.P.: Edge detector based on wavelet transform energy attributes. Proc. SPIE **11146**, 111460L (2019)
22. Lyasheva, S.A., Medvedev, M.V., Shleymovich, M.P.: Contours detection in the images using energy characteristics of wavelet transform. Proc. SPIE **10774**, 1077417 (2018)
23. Shleymovich, M.P., Medvedev, M.V., Lyasheva, S.A.: Image analysis in unmanned aerial vehicle on-board system for objects detection and recognition with the help of energy characteristics based on wavelet transform. Proc. of SPIE **10342**, 1034210 (2017)
24. Lyasheva, S.A., Shleymovich, M.P.: Formation of energy features of the image based on wavelet transform. J. Phys: Conf. Ser. **1202**, 012006 (2019)
25. Patil, R.B., Kulat, K.D.: Image and text compression using dynamic huffman and RLE coding. In: Deep K., Nagar A., Pant M., Bansal J. (eds.) Proceedings of the International Conference on Soft Computing for Problem Solving (SocProS 2011) December 20–22, 2011. Advances in Intelligent and Soft Computing, vol 131. Springer, New Delhi (2012)

Improving the Method for Studying the Periodicity of Tissue Structure and Its Violations by Means of Wavelet Techniques

Olga Doubrovina

Abstract A method of the estimation of the parameters such as mean scatterer spacing (MSS) and scale index performed on the wavelet approximation of backscattered ultrasonic RF signals are used for the detection of the signals' periodicity and its violation. The results of the numerical experiment, registered data of the backscattered RF signal from phantom with pre-defined periodic structure, and the results of ultrasound examination of the human liver were considered as initial data. The proposed technique allows distinguishing the areas with tumor from healthy tissue.

Keywords Acoustic signal · Mean scatterer spacing · Scale index · Wavelet transform · Daubechies wavelets · Wavelet approximation · Cancer diagnostics

1 Introduction

Over the last thirty years, quantitative ultrasound techniques have been developed to improve tissue characterization for diagnostics made with the help of interpretation of images, obtained by medical ultrasound equipment [1]. The preferred imaging method for screening is ultrasonography (USG) which is well tolerated and widely available. However, the sensitivity of USG for the most popular primary cancer is low because small nodules can be missed in a cirrhotic liver. Any kind of additional parametric diagnostics-enhanced classical USG improves the diagnostic performance of USG for liver cancer [2].

It is known that the normal human liver lobule has periodic structure and its violation is caused by diseases such as, for example, tumors [3–5]. So it is important to have the possibility to detect the changes in periodic liver structure. As the emitted ultrasound beams interact with scatterers in the tissue [6], so backscattered signals from liver tissue in vivo should contain the information about weak diffuse sub-resolution scatterers in tissue cells, and also about stronger pseudo-periodic lobules formed from ordered cell groups.

O. Doubrovina (✉)
Belarusian State University, 5, Kurchatova, Minsk 220045, Belarus

A. G. Kravets et al. (eds.), *Cyber-Physical Systems*, Studies in Systems, Decision and Control 350, https://doi.org/10.1007/978-3-030-67892-0_23

The main idea of this chapter is to study the periodicity of the signals obtained by USG methods using the signals' wavelet approximation and special parameters such as mean scattering spacing and scale index. The research, there were used numerical models, a phantom with a pre-defined periodical structure, and the results of the ultrasound examination of the human liver.

2 Ultrasonic Backscattered Signals and Initial Data

When an ultrasonic impulse from the transmitter interacts with the tissue's scattering particles, each of them produces an echo signal [1, 5]. These echo signals are summarized on the surface of the transducer. As a result of many transmissions and receipts, an ultrasonic echo signal called the radiofrequency (RF) signal is formed. This signal contains information about ultrasound and tissue interaction, so the scattering properties of the tissue such as periodicity, for example, should be detected. The recorded data signal is amplitude dependence in time in the case of point transducer or a two-dimensional set of such signals for the linear transducer. The example of a one-dimensional signal is displayed in Fig. 1.

The example of the image obtained from the USG examination of the human liver is shown in Fig. 2.

The backscattered ultrasound signals recorded during the experiment, in vivo, and simulated numerically were used as initial data for study in this chapter. There were

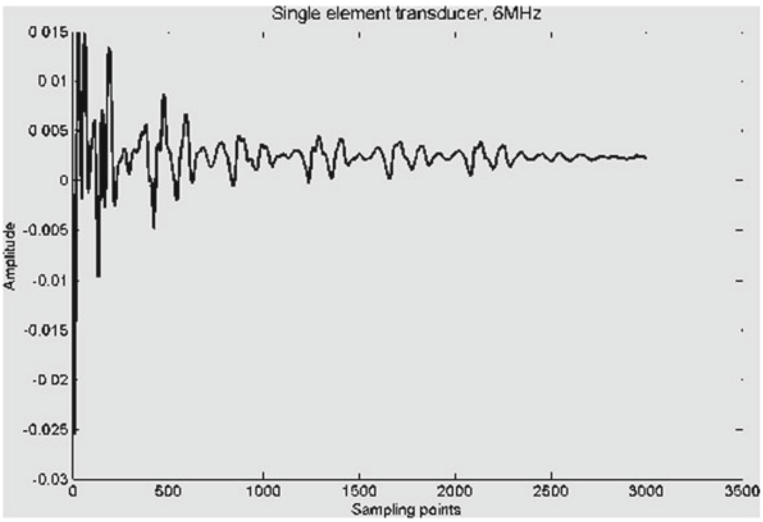

Fig. 1 An example of the RF signal, phantom experiment

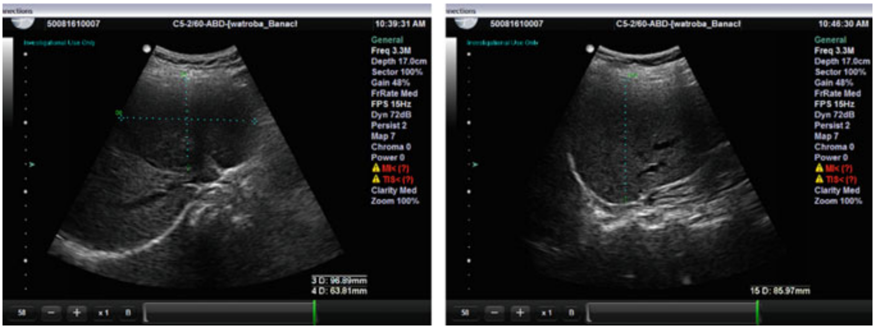

Fig. 2 Data obtained from the liver experiment, samples of the area with tumor and healthy

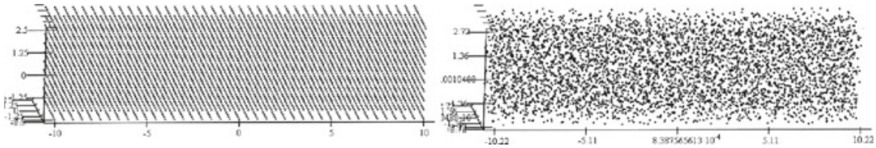

Fig. 3 The media with regular and quasi-periodic random structure

performed a numerical experiment, a series of experiments with phantom with predefined structure, and the recordings during ultrasound examination of the human liver.

Numerical experiment. The idea of the numerical experiment belongs to J. Wòcik [7], it is to construct the media with predefined periodical properties and to simulate the backscattered signal passing through it.

The generated medium is assumed to be composed of scatterers embedded in a homogeneous three-dimension matrix. The points are located in the centers of cubic cells forming a parallelogram in the Cartesian coordinate system of the size $41 \times 11 \times 11$. Each cube of dimension $0.5 \cdot 10^{-3}$ m contains one spherical scatterer, which is situated in the cell center and has a diameter of $0.5 \cdot 10^{-4}$ m. The local physical properties of the obtained two-phase medium such as the density and sound velocity of the host medium and scatterers are defined in [7]. The example of the medium is shown in Fig. 3 on the left.

Media of quasi-periodic structures are constructed by adding random fluctuations of the scatterers' position in the periodic cell, size, density, and sound velocity. There are defined four types of media:

I. Without randomness, the position, and properties of scatterers are periodic, physical properties are fixed.
II. With uniformly distributed summand for each scatterer's center coordinate. The numerical model of the medium is generated by moving the scatterer from the

center of the periodic cell by the random vector $\delta X_i = \begin{pmatrix} \delta z_i \\ \delta x_i \\ \delta y_i \end{pmatrix}$, where $\delta z_i, \delta x_i,$ δy_i are independent random variables, uniformly distributed in the intervals $[-0.45z_i, 0.45z_i]$, $[-0.45x_i, 0.45x_i]$, $[-0.45y_i, 0.45y_i]$ correspondingly and $i = 0, \ldots, 4960$ is an index of scatterers' numbering. The one realization of such a medium is presented in Fig. 3, on the right.

III. With normally distributed summands for physical parameters, such as density, speed of sound, and radius of the scattering particle. These summands are supposed to be normally distributed with zero mean value for each parameter and standard deviation $\sigma(c_i) = 0.05c_i$, $\sigma(q_i) = 0.05q_i$, $\sigma(r_i) = 0.025r_i$, where $c_i, q_i\ r_i$ are initial values of scatterers' radius, density, and speed of sound respectively, $i = 0, \ldots, 4960$.

IV. The media of this type is constructed as a combination of type II and III.

The equation for the plane wave is solved numerically for the scattered field, receiver and transmitter are simulated, and backscattered signals with plane wave transmitter, and point receiver for different media were obtained. The method is described in [7]. The dataset of initial signals is generated for each type of media to define the distinction of these RF signals.

Pre-defined periodic structure. To confirm the utility of the wavelet method for structural regularity recognition in backscattered ultrasound signals there was performed a series of experiments with phantom with pre-defined periodic properties to clarify the meaning of all applied procedures. There was used a phantom of a linear structure with nylon threads with the distance equal to 1.3 mm as a model to analyze the properties of ultrasound signal echoes registered with the use of different transducers, focusing and plane ones [8]. The phantom initially was immersed in water, but additionally, to study the influence of the background medium properties on the ultrasound backscattering signals there were also used oil and starch gel as quasi-noisy media.

From the whole dataset obtained from the scanners, there were chosen data corresponding to the area where threads had been located. The analyzed signal was treated as a mean for all signals from this area.

Liver tissue samples. The data were collected by the ultrasound scanner SonixTouch-Research with the linear head from cancerous tissue (Fig. 2, left image), and from healthy liver parenchyma (Fig. 2, right image) in both the left and right lobes of a patient. In Fig. 2 the initial data are displayed in a form of B-mode, or brightness mode [1, 9]. The area of the tumor was defined previously by medicians.

The common technique in such kind of study two dimensional USG data in acoustic imaging is to determine areas of the image called regions of interest (ROI) [10]. This method allows for avoiding the extra data and boundary effects because the measured region is usually much larger.

The chosen region of interest in there is the set of the rectangular areas 19.2×1.92 mm. To have the same features of the RF signal, these regions were taken from the same depth for each type of signal, equal to 48.1 mm. Figure 4 displays the

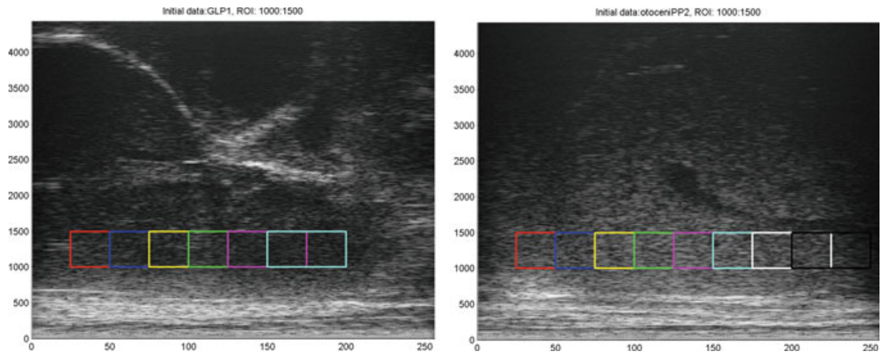

Fig. 4 Example of B-mode with chosen ROI, samples of the area with tumor and healthy

samples of initial data with tumor (left) and healthy (right), the colored rectangles border the area of ROI.

In [11] the lobule structure is described as roughly hexagonal and the liver can be considered as a composite of periodically distributed lobules, in which the plane normal to the central vein direction can be considered as the isotropic plane only at sufficiently long wavelengths (low frequencies) of acoustic excitation. But the ultra-sound excitation having a wavelength of less than a millimeter can detect the lobules as the periodic scatterers.

3 Mathematical Research Methodologies

Wavelet analysis. The idea of the application of wavelet transforms in signal processing is widely used as this method gives more information about the signal's behavior (see e.g. [12, 13]). Among others, this tool is also used to analyze the information registered from medical equipment. The usage of wavelet-based methods to study USG signals or other medical images for diagnosis is described in [14, 15]. The survey on the applications of wavelet methods for cancer diagnosis in soft tissues is given in [16, 17].

The main idea of this method is that any function $f(t) \in L_2(\mathbb{R})$ may be represented in the form

$$Wf(a,b) = \frac{1}{C_\psi} \int_{-\infty}^{\infty} f(t) \overline{\psi\left(\frac{t-b}{a}\right)} dt, \tag{1}$$

where $a \in (0, +\infty)$ is scale parameter (or scales), $b \in \mathbb{R}$ is the shift parameter, C_ψ is an admissible constant defined for each wavelet function ψ [10]. The signal function may be reconstructed in the space $L_2(\mathbb{R})$ by the formula

$$f(t) = \int_{-\infty}^{\infty} \int_{0}^{\infty} W_\psi(a, b)\psi\left(\frac{t-b}{a}\right)\frac{dadb}{a^2}.$$

For the scale parameter a, it is used the dyadic discretization scale $a_j = 2^{-j}$, where $j \in \mathbb{N}$. The coefficient b is linearly discretized $b_{ji} = i2^{-j}$, $i \in \mathbb{Z}$. The formula for discrete wavelets in general case may be written as $\psi_{ji}(t) = \frac{1}{\sqrt{a_j}}\psi\left(\frac{t-b_{ji}}{a_j}\right)$, and the discrete decomposition formula has form $w_{ji} = \int_{-\infty}^{\infty} f(t)\overline{\psi_{ji}(t)}dt$.

One of the reconstruction discrete formulae may be written as follows

$$f(t) = \sum_k g_{j_n,k}\varphi_{j_n,k} + \sum_{j \le j_n} h_{j,k}\psi_{j,k},$$

where ψ is a chosen wavelet function, φ is the corresponding to ψ scaling function. The set of functions $\{\psi_{j,k}\}$ is constructed as $\psi_{j,k} = 2^{\frac{j}{2}}\psi(2^j t - k)$, the set $\{\varphi_{j,k}\}$ may be obtained by using the additional relations for functions ψ and φ (see, e.g. [13, 18]). The value of j_n denotes the level of decomposition whose scale coefficients g and detail coefficients h are calculated for each chosen wavelet family.

One of the problems in the wavelet's application is to select the analyzing wavelet or family as there is no general algorithm to solve it because different bases would show different signal's features. P. Addison [13] proposed to use the special wavelet function if there is known about the signal's particularities or the form of the periodical patterns to find.

In the qualitative ultrasound Daubechies wavelet family [18] is used rather often as these functions match the reflection impulse [9]. The initial impulse is shown on the left image of Fig. 5. That is why the Daubechies 6 family had been chosen as analyzing wavelet, its wavelet function is represented in Fig. 5, right image.

Mean scatterer spacing. MSS (mean scatterer spacing) is a special parameter to characterize the periodicity in tissue. It shows the average periodicity in RF signal

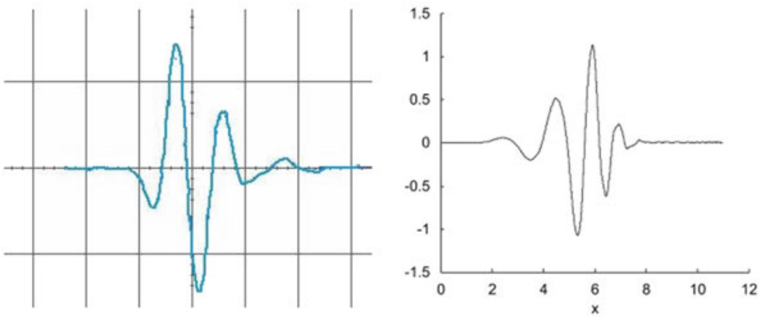

Fig. 5 The initial impulse (left) and Daubechies 6 wavelet function (right)

caused by the periodical structure of scattering media. The idea of measuring the distance of the peaks of the signal's transformation had been proposed in [17]. There are several approaches to computing the MSS.

The first approach is based on detecting the peaks in the Fourier transform spectrum and may be estimated by formulae $MSS = \frac{c}{2\Delta f}$ or $MSS = 2c\Delta t$, where c is the speed of sound, Δf is frequency interval, Δt is a time interval. This method had been used in [19] to investigate the mean scatterer spacing in bovine liver ex vivo samples.

The second approach suggests using the wavelet transform instead of the Fourier spectrum (see, e.g. [20, 21]) by studying modulus maxima at different decomposing scales corresponding to the location of coherent scatterers, so, the distance between modulus maxima may be treated as MSS. The best wavelet level J_n for MSS was proposed in [22], and the corresponding formula

$$\log_2\left(\frac{f_s}{f}\right) - 1 < J < \log_2\left(\frac{f_s}{f}\right), \tag{2}$$

where f_s is a sampling frequency, f is a fundamental frequency was used to estimate the MSS.

The percentage error of the MSS is obtained by the relation

$$e = \frac{|MSS_e - MSS_r|}{MSS_r} \cdot 100\%, \tag{3}$$

where MSS_e and MSS_r are measured and calculated approximate values of mean scatterers' spacing correspondingly.

Scale index. For detecting the periodicity in scattering media and corresponding RF signal there was used a scale index calculated for the levels of wavelet approximation (or scales) proposed in [23]. Here also the theorem connecting the wavelet decomposition level and the periodical structure of signal is proved and there is introduced a scale index ind_{sc} depending on the wavelet approximation level which allows identifying the periodical signals. It is underlined that usage of continuous wavelet transform is preferable.

The general idea of this method is based on the energy of the approximated signal calculated for each scale a

$$E(a) = \left(\int_{-\infty}^{\infty} |Wf(a,b)|^2 db\right)^{1/2},$$

where $Wf(a,b)$ is an integral wavelet transform defined in formula (1), a is supposed to change continuously on the set of real numbers.

To avoid the boundary effects, the set of possible values is narrowed down to the interval $[t_1(a), t_2(a)]$ which may be different for a different scale.

$$E^{in}(a) = \left(\int_{t_1(a)}^{t_2(a)} |Wf(a,b)|^2 db \right)^{1/2}.$$

Interval $[t_1(a), t_2(a)]$ should contain all the wavelets $\psi_{a,b}$ for all $a \in [t_1(a), t_2(a)]$. The scale index is calculated as

$$ind_{sc} = \frac{E(a_{\min})}{E(a_{\max})}, \tag{4}$$

where $E(a_{\max})$ is the smallest scale in for energy maximal value $[a_1, a_2]$ and $E(a_{\min})$ is the minimum of energy in the interval $[a_{\max}, a_2]$.

The scaled index takes its values in the interval $[0,\ 1]$. For periodic signals (i.e. periodic scattering structure) $ind_{sc} = 0$ and it for highly non-periodic signals $ind_{sc} = 1$ [23].

4 Results and Discussion

Mean scatterer spacing. The results of MSS and its errors are presented in Table 1 for initial data and the wavelet approximation at the chosen level.

Table 1 Mean scattering spacing and error estimation for initial data and wavelet approximation level

Thread Phantoms. Different transducers				
Transducer type	MSS for initial data, mm	Error for initial data, %	MSS for chosen level, mm	Error for chosen level, %
6F	1.99	7	1.81	1.85
3.5F	1.94	4.9	1.77	4.2
6P	2.1	12.7	1.98	7.2
Linear	1.88	0.14	1.848	0.11
Thread Phantoms. Different media				
Media Type	MSS for initial data, mm	Error for initial data, %	MSS for chosen level, mm	Error for chosen level, %
Water	1.88	0.14	1.848	0.11
Oil	2.1	13.4	1.89	1.9
Starch gel	1.89	2.4	1.85	0.11
Liver tissue				
ROI	MSS for initial data, mm	Error for initial data, %	MSS for chosen level, mm	Error for chosen level, %
Tumor	0.9919	1.5	1.01302	1.4
Environment	0.9912	1.8	1.009	1.14

For the thread phantom experiment, MSS was calculated for the experiment with different transducers and different media. According to formula (2) the approximation level $J = 5$. In the error relation (3) the value of $MSS_r = 1.3$ mm according to the experiment phantom's parameters.

In the liver tissue the main scatterers are the lobules, so and pathological changes in the structure of the liver can be reflected by the changes of the MSS. Therefore, the MSS may be used as the parameter to characterize the liver tissue having some kind of diseases that cause the infraction of its initial periodicity [2, 3, 22]. The inter scatter spacing of the liver is supposed to equal to 1 mm [18], that is why in formula (3) there was supposed $MSS_r = 1$. Due to formula (2), the optimal level for mean scatterer spacing $J = 2$. The MSS was computed as a mean value for MSS for each ROI from the dataset.

As it may be seen from Table 1 the wavelet approximation reduces the error value. It is important to point out that as the wavelet approximation provides also data filtering [13], each level of approximation reduces the number of sampling points twice, so the calculations will take less time.

For liver tissue samples it occurs that the greatest value of MSS belongs to the dataset corresponding to the tumor areas, i.e. to the tissue samples with the less periodic structure and the error for the second approximation level is less than for initial data.

Scale index. The scaled index was calculated by the formula (4) for the data from the numerical experiment, thread phantom, and liver tissue. The obtained values are shown in Table 2.

According to Table 2, the value of scale index for pure periodic numerically generated signal (type I, having no random components) is equal to $2.5121 \cdot 10^{-6}$ and may be treated as zero. The signal of type III having only a random physics component has a smaller value of the scale index than signals of type II and IV, so it may be concluded that these parameters are less influential to the periodicity. Signals of type II and IV have a larger value of scale index and besides, this index is ordering

Table 2 Scale index values

Numerical experiment				
Media Type	I	II	III	IV
Scale Index	$2.5121 \cdot 10^{-6}$	0.0035	$7.3322 \cdot 10^{-4}$	0.0045
Thread Phantoms				
Media	Water	Oil	Starch gel	Pure starch gel
Scale Index	0.0312	0.0635	0.0855	0.3153
Liver tissue				
ROI	Tumor		Environment	
Scale Index	0.1087		0.0451	

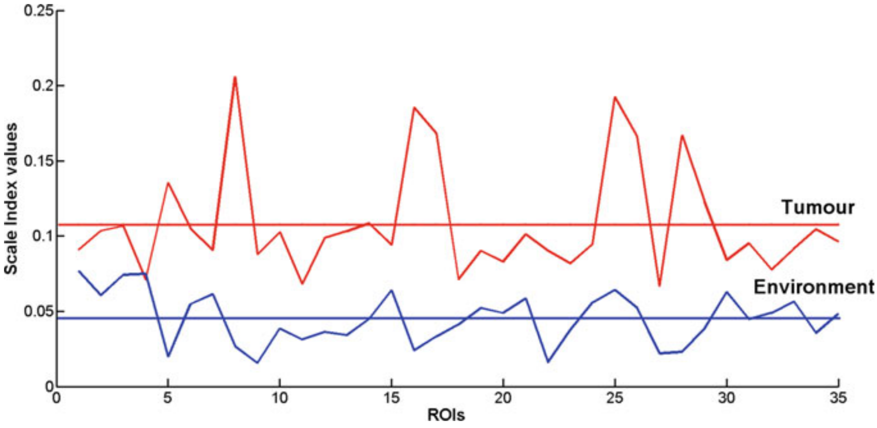

Fig. 6 Scale index for the samples of ROI with and without tumor

the degree of the randomness. Namely, the index value is greater for signal IV where randomness is a sum of both random physics and random geometry factors.

Table 2 also shows the scale index values for phantom experiments. Additionally, there was added a result of the USG measurements of the pure starch gel media with-out phantom as an example of a structure with a more random arrangement of scatterers.

It may be concluded that the obtained backscattered signals are close to periodic and the scale index increases with a noisier environment.

Figure 6 represents the distribution of index values, the red line here corresponds to the data from tumorous areas and the blue line displays the scale indexes for the environment area, horizontal lines indicate the mean value (also shown in Table 2).

It should be pointed out that for the areas with a more periodic structure of scatterers, i.e. for the healthy environment areas the value of scale index is less than for the areas where this periodicity is broken by cancerous changes. That is why this value may be used as a marker to recognize the cancerous tissue in vivo examination of the human liver.

5 Conclusion

The values of the mean scatterers spacing the quantitative parameter determined on the selected level of wavelet approximation of backscattered echo signals improve the parameter estimation accuracy.

A measure of structure chaoticity scale index defined on the base of signal wavelet transform properties may be applied in the processing of the ultrasonic RF signals. It allows arranging the scattering structures from a strictly periodic to completely chaotic structure, namely, to distinguish in vivo areas of healthy liver tissue from the tumor areas.

References

1. Nowicki, A.: Ultrasounds in Medicine (in Polish). 303 pp. Warszawa (2010)
2. Sudarshan, V.K., et al.: Application of wavelet techniques for cancer diagnosis using ultrasound images: a review. Comput. Biol. Med. **69**, 97–111 (2016)
3. Georgiou, G., Cohen, F.S.: Tissue characterization using the continuous wavelet transform. Part I: decomposition method. IEEE Trans. Ultrason. Ferroelect. Freq. Control **4**(2), 355–363 (2016)
4. Georgiou, G., Cohen, F.S.: Tissue characterization using the continuous wavelet transform. Part II: application on breast RF data, IEEE Trans. Ultrason. Ferroelectr. Freq. Control **48**(2), 364–372 (2001)
5. Abeyratne, U.R., Tang, X.: Ultrasound scatter-spacing based diagnosis of focal diseases of the liver. Biomed. Signal Process. Control **2**, 9–15 (2007)
6. Mamou, J., Oelze, M.L.: Quantitative Ultrasound in Soft Tissues, 444 pp. Springer, New York (2013)
7. Gambin, B., Wòjcik, J., Doubrovina, O.: Differentiation of random structure properties using wavelet analysis of backscattered ultrasound. Hydroacoustics **19**, 121–128 (2016)
8. Doubrovina, O., Tymkiewicz, R., Piotrzkowska-Wròblewska, H., Gambin, B.: Linking of structural parameters to properties of ultrasound backscattered signals by the threads phantoms study, Aktualności Inżynierii Akustycznej i Biomedycznej, Polskie Towarzystwo Akustyczne Kraków, pp. 67–79 (2018)
9. Najarian, K., Splinter, R.: Biomedical Signal and Image Processing, 411 pp. CRC Press, Boca Raton (2012)
10. Piotrzkowska, H., Litniewski, J., Szymańska, E., Nowicki, A.: Ultrasonic echosignal applied to human skin lesions characterization. Arch. Acoust. **37**, 103–108 (2012)
11. Gambin, B., Kruglenko, E., Gałka, A., Wojnar, R.: Macroscopic thermal properties of quasilinear cellular medium on example of the liver tissue. Comput. Assist. Methods Eng. Sci. **22**(4), 329–346 (2015)
12. Mallat, S.: A Wavelet Tour of Signal Processing, 805 pp. Elsevier, Burlington (1999)
13. Addison, P.: Illustrated Wavelet Transform Handbook, 368 pp. IoP, Bristol and Philadelphia (2002)
14. Rafiee, J., Rafiee, M.A., Prause, N., Schoen, M.P.: Wavelet basis functions in biomedical signal processing. Expert Syst. Appl. **38**(5), 6190–6201 (2011)
15. Shenga, L., Wangb, G., Lic, F., Luoc, J., Liu, J.: Ultrasound signal wavelet analysis to quantify the microstructures of normal and frozen tissues in vitro. Cryobiology **68**, 29–34 (2014)
16. Ramaraj, M., Raghavan, S.: A survey of wavelet techniques and multiresolution analysis for cancer diagnosis, International Conference on Computer, Communication & Electrical Technology, pp. 109–114 (2011)
17. Kucl, R., Haghkerdar, K., O'Donnel, M.: Presence of cepstral peak in random reflected ultrasound signals. Ultrason. Imaging **8**, 196–212 (1986)
18. Daubechies, I.: Ten Lectures on Wavelets, 350 pp. SIAM, Philadelphia (1993)
19. Rubert, N., Varghese, T.: Mean scatterer spacing estimation in normal and thermally coagulated ex vivo bovine liver. Ultrason. Imaging **36**(2), 79–97 (2014)
20. Tang, X., Abeyratne, U.R.: Wavelet transforms in estimating scatterer spacing from ultrasound echoes. Ultrason. **38**, 688–692 (2000)
21. Zhou, Z., Wu, W., Wu, S., Jia, K., Tsu, P.H.: A review of ultrasound tissue characterization with mean scatterer spacing. Ultrason. Imaging **39**(5), 263–282 (2017)

22. Machado, Ch.B., et al.: Continuous wavelet transform for tissue periodicity estimation: effect of noise and scatterers position variability. Proceedings of the 22nd International Congress on Acoustics, Buenos Aires, September 5–9, 10 p. (2016)
23. Benítez, R., Bolós, V.J., Ramírez, M.E.: A wavelet-based tool for studying non-periodicity. Comput. Math Appl. **60**, 634–641 (2010)

Implementation of the Observer on the Basis of the Digital Kalman Filter for the Lateral Deflection Control System of the Automatic Warehouse Platform

Evgenii Masliev, Alexander Bazhanov, Sergey Alekseevskiy, and Evgenij Karikov

Abstract The implementation of a digital filter for building the state observer that tracks changes in the operation of an automatic warehouse mobile platform, in particular, malfunctions, equipment wear is discussed in this article. The article presents a basic method for calculating state observers based on a digital filter. A mathematical model of an automatic warehouse platform in Matlab and the main blocks of the model are considered. Experiments were carried out with the appearance of system malfunctions and analyzed possible options for the system's behavior, thanks to which it is possible to quickly identify the area or source of system malfunction. This platform can be in the production and processing of black soldier fly in a warehouse where a large number of transport operations are required.

Keywords Modeling · Kalman filter · Matlab simulation · State-space representation

1 Introduction

When designing any automatic or automated cyber-physical system, they achieve obtaining the most independent process requiring minimal attention and human intervention. Such cyber-physical systems require achieving continuity of the process and ensuring prompt elimination of malfunction or damage during operation. To ensure this kind of system independence, it is possible to use an external observer of the system, which would track the indications of the system. In the event of a deviation, the observer warned in advance about the failed component of the system, which already needs a short-term repair, or introduced an additional compensating control action, allowing to extend the life of the component, which is on the verge of a malfunction. It is also possible to use backup elements of the cyber-physical system if such are incorporated in the design. The use of technologies based on modern digital filters allows us to evaluate the performance of the system. Examples

E. Masliev (✉) · A. Bazhanov · S. Alekseevskiy · E. Karikov
Belgorod State Technological University n.a. V.G. Shukhov, 46 Kostukova, Belgorod 308012, Russia

A. G. Kravets et al. (eds.), *Cyber-Physical Systems*, Studies in Systems, Decision and Control 350, https://doi.org/10.1007/978-3-030-67892-0_24

of such digital filters include the Kalman-Bucy filter or the Luenberger observer. However, the use of such filters requires certain computational powers and a sufficiently accurate representation of the behavior of the system in digital form, namely, as a mathematical model.

2 Initial Mathematical Formulation of System and Research Methodologies

A mathematical model in the state-space form obtained for the study of the object and the construction of the state observer based on the Kalman filter is used to solve the problems of assessing the state.

The Kalman filter algorithm allows the real-time construction of optimal estimation of the system X(t) state based on measurements of Y(t), which inevitably contain errors. The measurement vector Y(t) is considered as a multidimensional out-put signal of the system, which is noisy, and the vector of state variables X(t) is an unknown multidimensional signal to be determined. The optimality condition for the constructed estimation is the minimum of the standard deviation of the estimated value from the real one [1–6]. In the general case, the Kalman filtering problem is formulated for a linear stationary system (1) under the action of a correlated random process other than white noise.

$$\begin{cases} \frac{dX}{dt} = AX(t) + BU(t) \\ Y(t) = CX(t) + DU(t) \end{cases}, \tag{1}$$

where X(t) − n—is the n-dimensional state vector, Y(t) − p—is the p-dimensional vector of the output coordinates when p < n and rang C = p.

We make an assumption and consider the Kalman-Bucy estimation problem presented in the state-space representation for a linear stationary object with white noise acting (Fig. 1). One of the advantages of the Kalman filter is that the equations are recurrent in shape and can be easily implemented using digital computing devices [4–15].

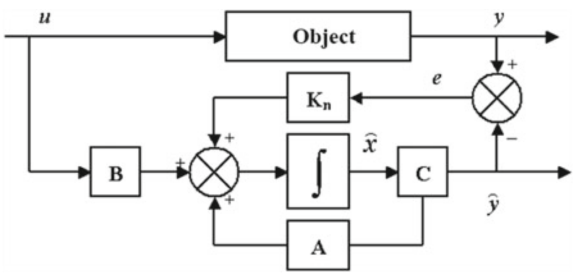

Fig. 1 Block diagram of the observer

We describe the algorithm for constructing a Kalman filter for a system represented in the state-space form:

1. we determine the n-dimensional space of functions and assume that temporary processes belong to this space;
2. we represent the control system in the state-space form by the equation of state:

$$\frac{dX}{dt} = AX(t) + BU(t) + \nu(t), \tag{2}$$

in which *X(t)* is a random Markov *n*-dimensional process defined by a priori information:

$$M\{X\} = X,$$
$$\operatorname{cov}\{X\} = P.$$

u(t)—vector input exposure, which may be a deterministic or random variable; ν(t) − k-dimensional random action vector corresponding to white noise processes:

$$M\{\nu\} = 0,$$
$$\operatorname{cov}\{\nu\} = M\{\nu(t)\nu(\tau)\} = V\delta(t - \tau),$$

where *δ(t)*—the delta function; *V*—symmetric non-negative definite white noise intensity matrix ν(t) with dimension $[k \times k]$;

3. the process X(t) is observed using a meter, and the vector of the measured coordinates is determined by the relation:

$$Y(t) = CX(t) + DU(t) + \eta(t), \tag{3}$$

where η(t)—p-dimensional vector of measurement noise assumed by a random process in the form of white noise:

$$M\{\eta\} = 0,$$
$$\operatorname{cov}\{\eta\} = M\{\eta(t)\eta(\tau)\} = R\delta(t - \tau).$$

Here R—is symmetric non-negative definite white noise intensity matrix η(t) of dimension [p × p];

4. the processes $\nu(t)$ and $\eta(t)$, as well as *X(t)* and $\eta(t)$, *X(t)* and $\nu(t)$ will be considered uncorrelated:

$$M\{\nu(t)\eta(\tau)\} = 0,$$
$$M\{X(t)\nu(\tau)\} = 0,$$
$$M\{X(t)\eta(\tau)\} = 0.$$

It is assumed that the forming filter satisfies the conditions of physical feasibility w(t) = 0, t < 0, and the dynamic system corresponding to (1) is completely controllable and observable.

5. the main task is to build a dynamic system that provides the estimation $\hat{X}(t)$ of the vector *X(t)*, with the error:

$$E(t) = X(t) - \hat{X}(t),$$

the optimality criterion is the condition of the minimum of its quadratic norm:

$$J = \int E(t)dt = \|E(t)^2\| \to \min.$$

Based on the above conditions, the solution of the Kalman filtering problem leads to the following structural scheme (Fig. 2).

The main idea of construction the Kalman filter is using a full-order n-dimensional observer, where a mathematical model of the system is taken as an identifier of the state.

The filter performs a recursive estimation based on the observation of the system input and output signals, and to reduce the variance of the estimate in the algorithm of the identifier is introduced the corrective feedback on the system output signal.

Given the requirements of an unbiased estimation $\hat{X}(t)$, the filter equation takes the form:

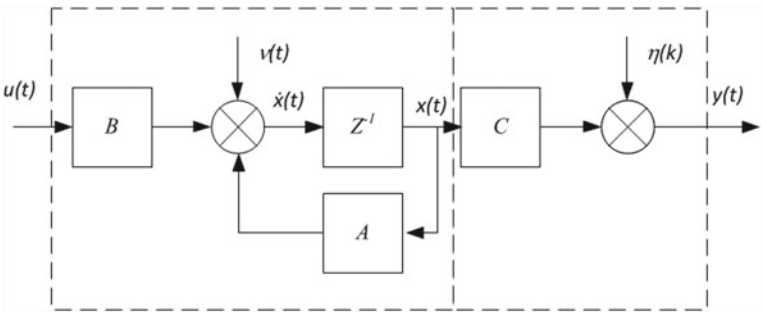

Fig. 2 The scheme of the forming filter (FF) and the meter in the presence of interference

$$\frac{d\hat{X}}{dt} = AX(t) + BU(t) + L\Big[Y(t) - C\hat{X}(t)\Big], \quad \hat{X}(t_0) = \hat{X}_{0,} \tag{4}$$

where *L*—is a matrix of gain of a filter of size *[n × 1]*, which provides an optimal state estimate in the sense of minimum dispersion, which is determined by the expression:

$$L = PC^T R^{-1},$$

where *P*—covariance matrix of estimation errors, which in the case of stationary processes is determined by solving the Riccati equation:

$$AP + PA^T - PC^T R^{-1} CP + GVG^T = 0. \tag{5}$$

Thus, the construction of the observer is a solution to the problem of optimal stochastic control, taking into account the conditions for the incompleteness of information about the vector of state variables. The implementation of the method of analytical regulators design is one of the ways to find the filter gain matrices.

To implement the filtering function of values on digital computing devices, we apply the discrete Kalman filter form [12, 16–20]. In this case, the filter gain matrix K($k + 1$) is independent of the observations and its calculation can be performed in advance using the following relations:

1. the apriori value of the covariance matrix of the signal is found based on k observations:

$$Q(k+1) = FP(k)F^T + V. \tag{6}$$

2. the posterior value of the covariance matrix of the signal is calculated based on $k + 1$ observations:

$$P(k+1) = Q(k+1) - Q(k+1)C^T\big[CQ(k+1)C^T + R\big]^{-1} CQ(k+1). \tag{7}$$

3. the matrix of gain $K\,(k+1)$ is determined, which sets the weight of the corrections to the initial conditions on the basis of covariance state estimation matrices:

$$K(k+1) = Q(k+1)C^T\big[CQ(k+1)C^T + R\big]^{-1} = P(k+1)C^T R^{-1}. \tag{8}$$

The calculations continue until the filter is stationary, the condition of which is the equality $P(k+1) = P(k) = P$ or, accordingly, $K(k+1) = K(k) = K$.

After determining the matrix *K(k)*, the Kalman filter algorithm reduces to sequential processing of incoming input and output data, in which the current signal estimation is obtained by adjusting the previously made estimation taking into account the information received at the filter input during the observation at each step:

$$K(k+1) = Q(k+1)C^T\left[CQ(k+1)C^T + R\right]^{-1} = P(k+1)C^T R^{-1}. \quad (9)$$

The general scheme of the system for the case of selective measurements of the time function, including the object and the observer, is shown in Fig. 3. The output of the object through the matrix of gain factors is supplied to the subsystem, which is an observer.

To confirm this theory, we construct an observer for the state of the lateral deviation control system of the mobile robot to estimate the unknown state vector X, while the optimality criterion will be the minimum standard deviation of the obtained estimate of the state of its true value [21, 22].

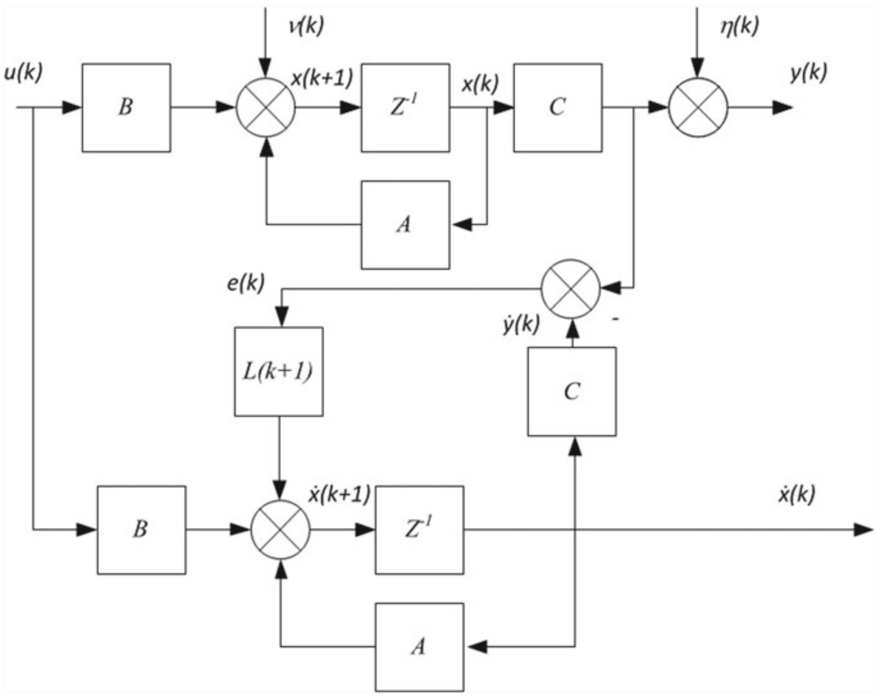

Fig. 3 Block diagram of an object and Kalman filter

3 Interpretation and Discussion of Research Results

During experiments on the full-scale model, there were obtained matrices that describe the dynamics of the study object in the state-space form (1):

$$A = \begin{pmatrix} -1.3947 & -160.0837 & -160.0837 \\ 0.0722 & 0 & 0 \\ 0 & 1 & 0 \end{pmatrix},\ B = \begin{pmatrix} 6.4033 \\ 0 \\ 0 \end{pmatrix},\ C = \begin{pmatrix} 0 & 0.5 & 0.5 \end{pmatrix},$$
$$D = (0).$$

Figure 4 shows a part of the model in the Simulink environment that reproduces the dynamics of the object of study in accordance with expressions (2) and (3). The used records *A*uvec*, *B*uvec*, *C*uvec*, and *R*uvec* in the blocks of the model denote the vector multiplication of the matrices *A*, *B*, *C*, *R* by the corresponding input signal.

The Kalman continuous filter calculation unit (Fig. 5) is implemented according to the model (4) and includes a gain matrix calculation unit (R_block) (Fig. 6) by solving the Riccati Eq. (5).

The discrete Kalman filter is calculated in accordance with the recursive expression (9), while the calculation of the matrix *K* is placed in a separate block (K_block, Fig. 7). The time sampling step was chosen as $dt = 100$ ms during constructing the discrete Kalman filter (Fig. 8). With such a relatively large value of the sampling step, the requirements for the computing power of embedded devices are significantly reduced, that allows real-time processing of the measured data by any widely used computing platforms, for example, microcontrollers, without significant losses in the estimation accuracy of the original system dynamics.

The general structure of the model in the Simulink environment is shown in Fig. 9.

Figure 10 presents the simulation results of the system under study and the discrete Kalman filter. The data obtained allow concluding that the assessment of the values of state variables corresponds to the dynamics of the original system taking into account

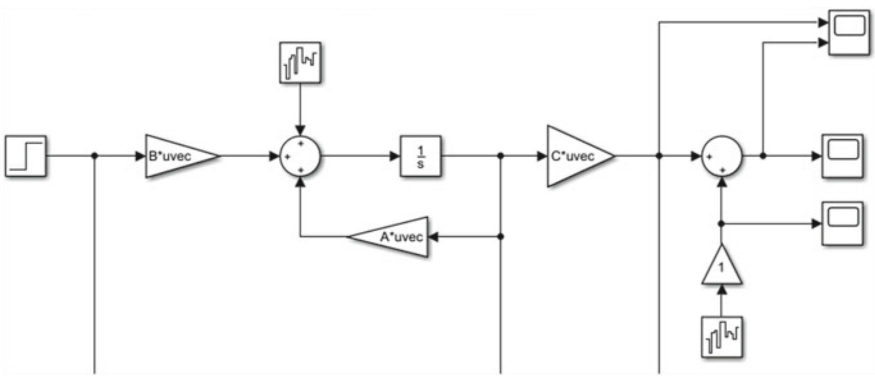

Fig. 4 Block modeling the dynamics of the study object

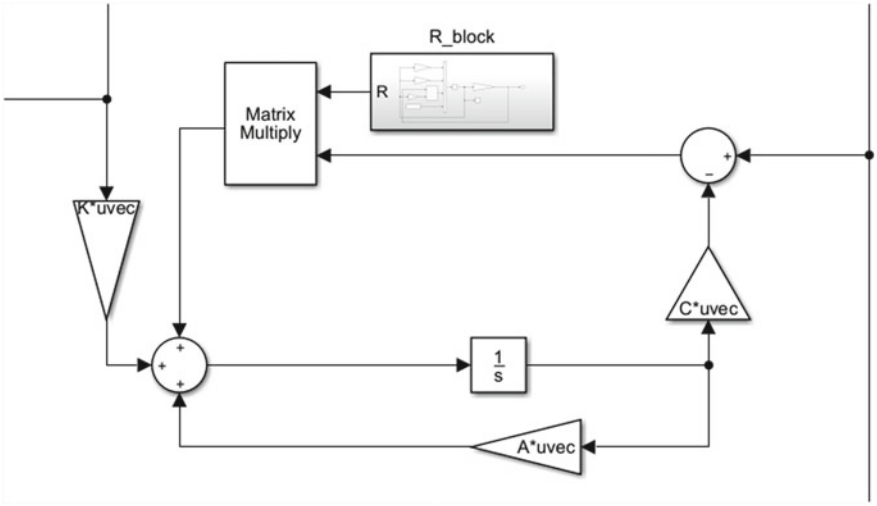

Fig. 5 Kalman continuous filter calculation unit

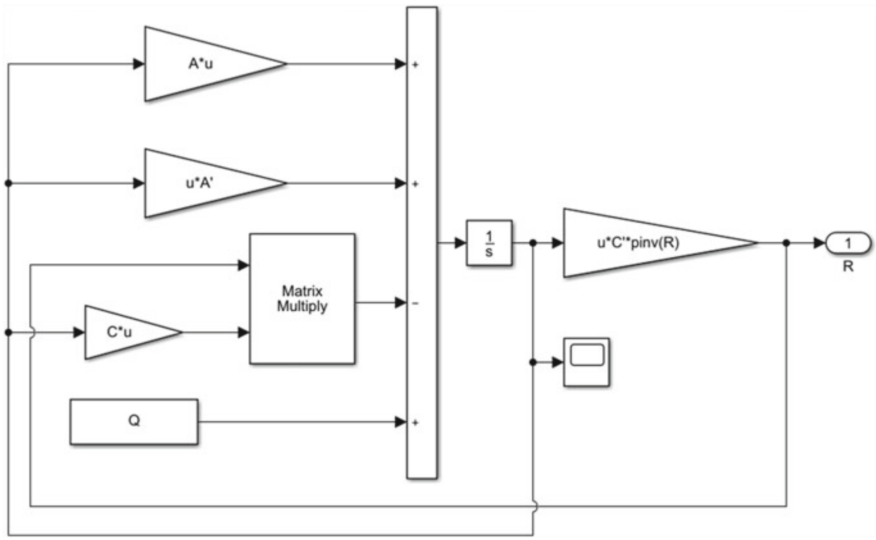

Fig. 6 Block calculation gain matrices of the continuous Kalman filter

errors at the input of the system, interference of the object itself, and measurement noise. So, for example, the maximum error of the obtained estimates was about 10 rpm for the value of the deviation rate of the mobile platform, and 0.2 degrees for the value of the deviation angle of the mobile platform.

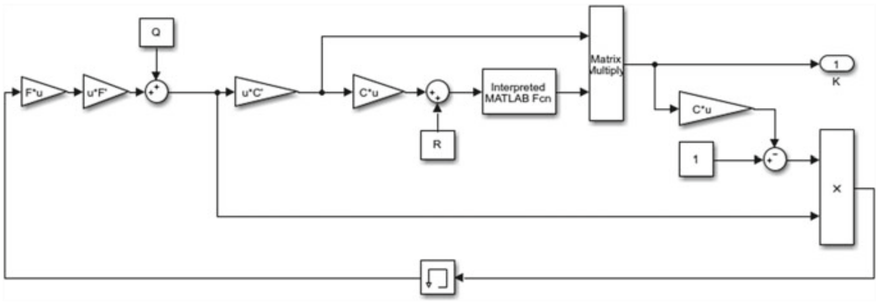

Fig. 7 Block calculation matrix gain of a discrete Kalman filter

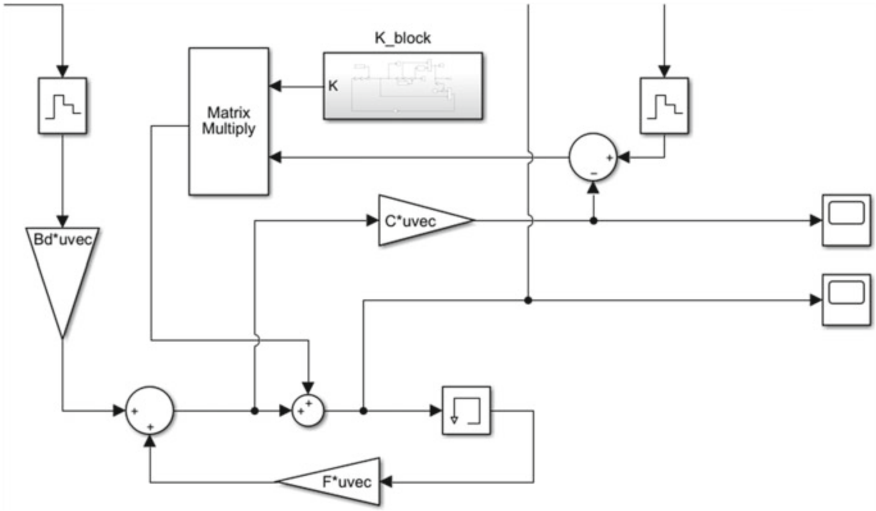

Fig. 8 Kalman discrete filter calculation unit

We will conduct a series of experiments to simulate changes in system performance for various malfunctions. As a first experiment, we check the operation of the system in the case of damage to the platform position sensor relative to a given path (Fig. 11, a, b).

Based on the experiment could be observed a shift in the characteristics not only in the signal amplitude but also in the time domain, which indicates the appearance of a delay in the system. There should be checked the effect of the considered engine defect on another state variable of the system (Fig. 12). Changing the parameter of the considered engine defect led to a sharp change in the speed of wheels rotation. Similar behavior of the system is observed when changing other parameters of the engines. Thus, for this system, two types of wear can be clearly distinguished:

1. damage of the sensors;

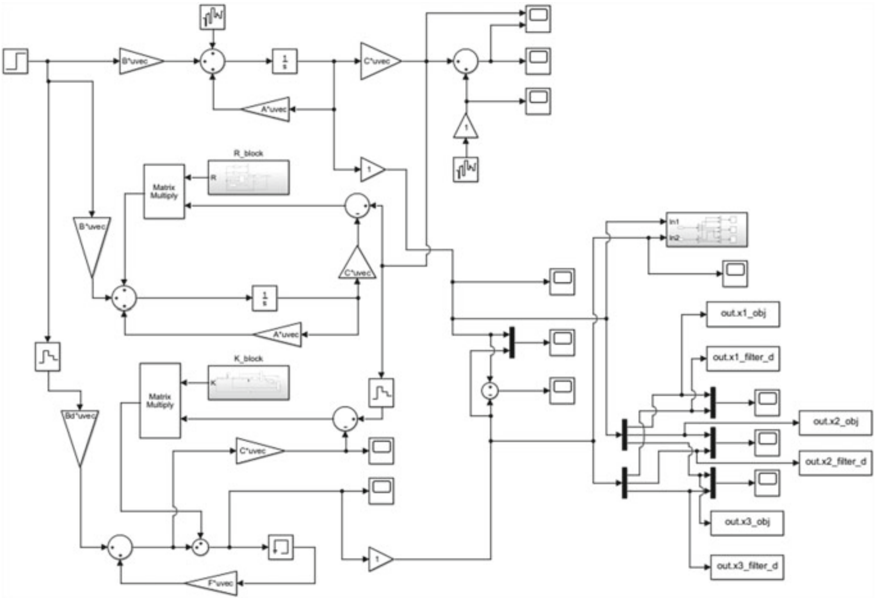

Fig. 9 The Kalman filter structure in Matlab Simulink environment

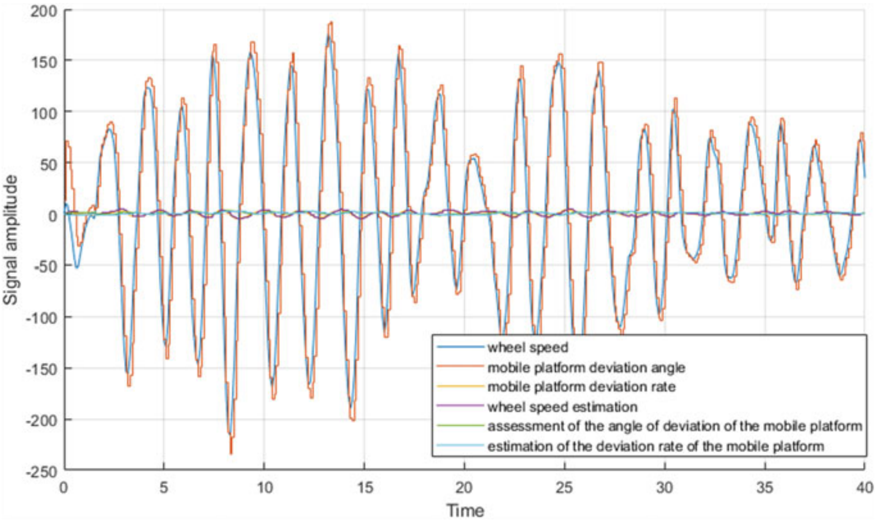

Fig. 10 Real and estimated deviations of control system values (X)

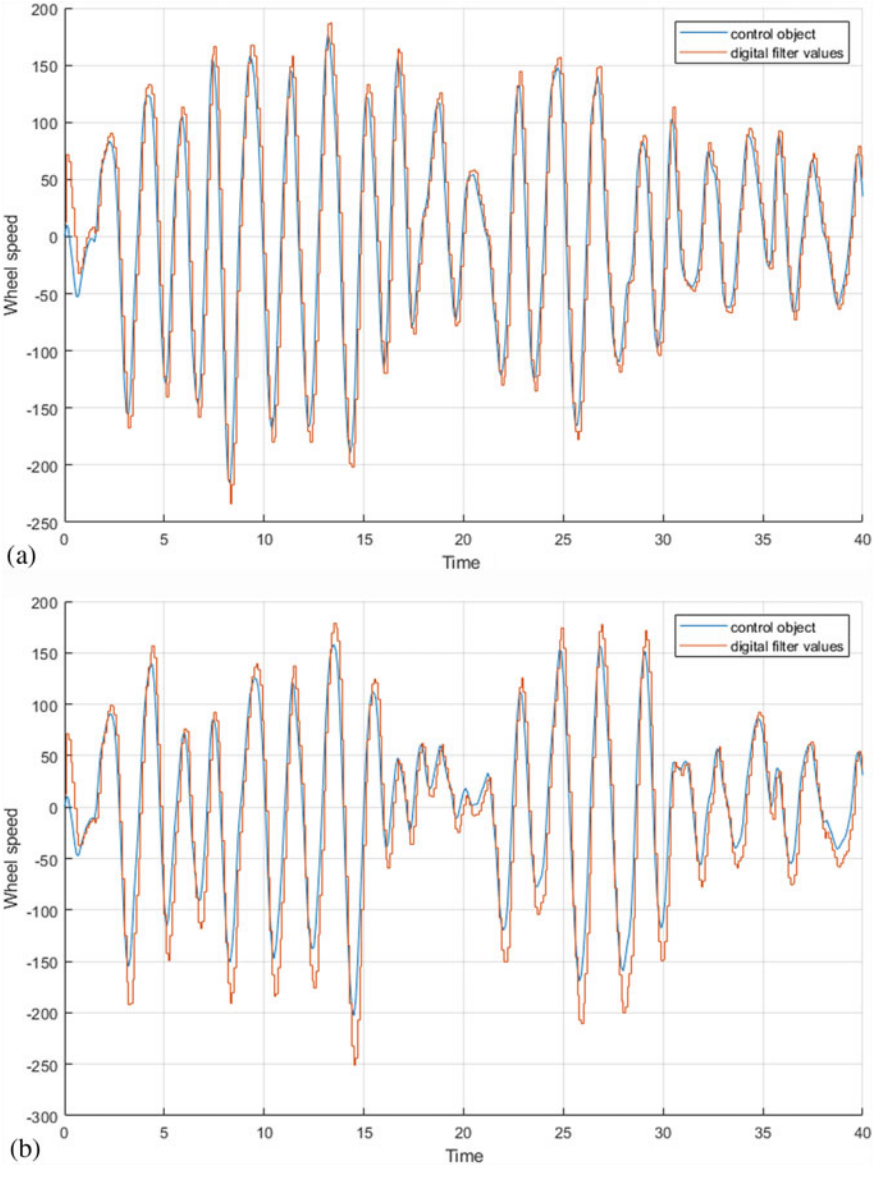

Fig. 11 Real and estimated values of the control system for deviation: (a)—without damage, (b)—with damage

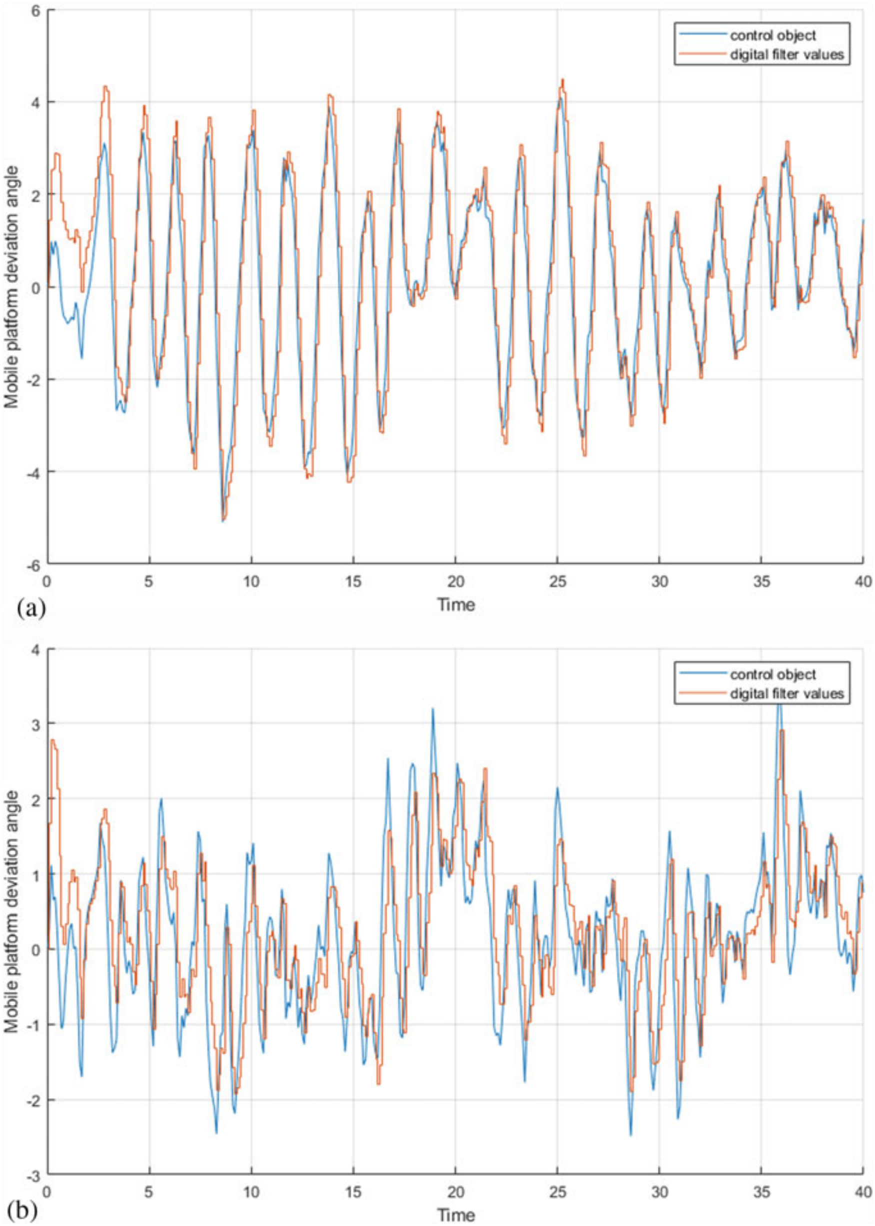

Fig. 12 Real and estimated values of the control system for deviation: (a)—without damage, (b)—with damage

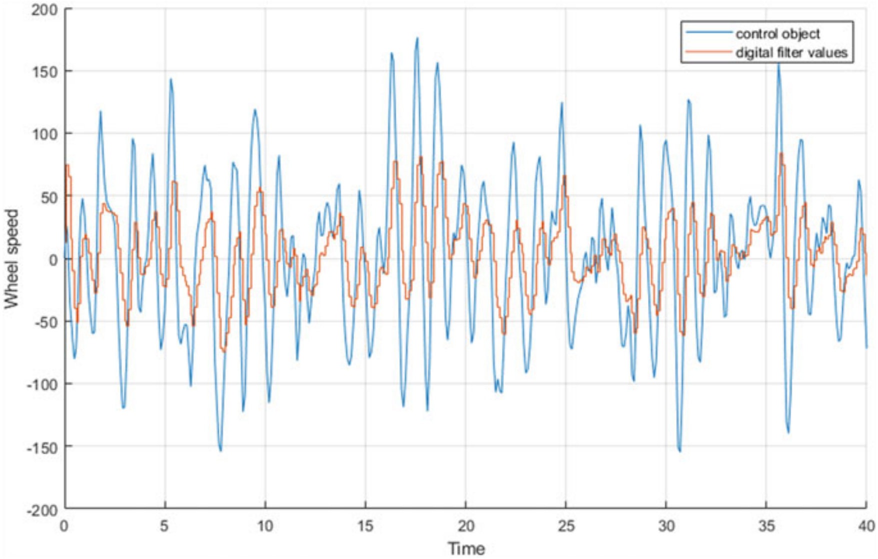

Fig. 13 Real and estimated values of the control system for the deviation in the case of a motor defect (state variable corresponding to the wheels rotation speed)

2. partial engine failure or wheelbase damage.

As can be seen based on the different behavior of the system with a certain type of defect, we can determine the nature and location of the system malfunction.

To verify this there should be conducted an additional experiment in the presence of a malfunction in the mobile platform chassis (Fig. 13, a, b):

As can be seen, the sensor defect introduces pronounced changes in the behavior of the system. This defect affects the amplitude of the signals characterizing the deviation of the mobile platform most of all for both the lower-order observer and the Kalman filter.

Another experiment related to the partial failure of the engines in the system (Fig. 14, a, b).

4 Conclusion

This experiment shows that the defect belongs to the second type of system malfunction since the delay of the system signals and the evaluation filter is clearly observed.

The results of the study show that the recurrent Kalman filters of continuous and discrete types obtained during synthesis allow reproducing the dynamics of the state variables of the study object.

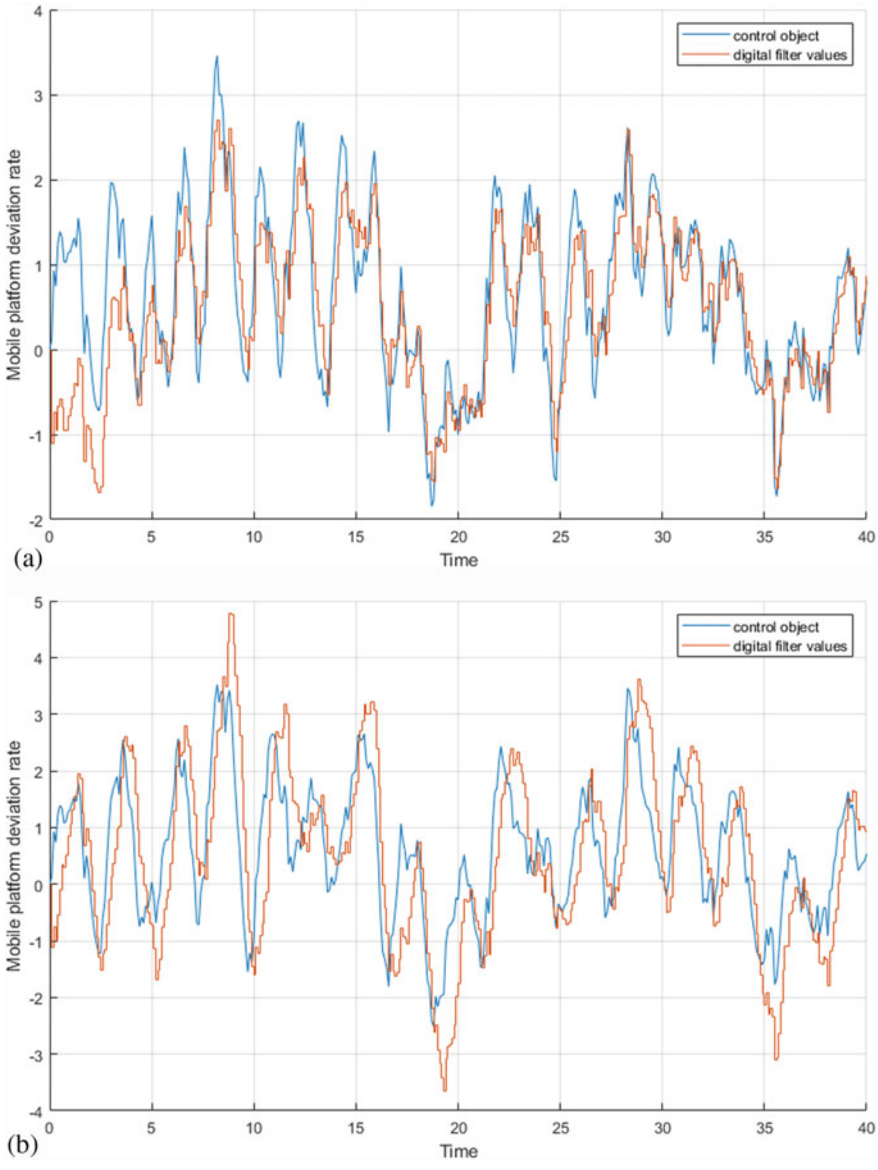

Fig. 14 Real and estimated values of the control system for the deviation during wear of the chassis: (a)—without damage, (b)—with damage

Thus, with the help of a state observer, it is possible to track the operation of the system and detect deviations of the system parameters, having discovered that it is possible to form a control action that compensates the negative effects caused by malfunctions or natural equipment wear.

However, state observer as a method could not give an accurate assessment of malfunction place occurrence, and it is extremely difficult to construct a system analyzer on their basis to accurately identify the source of the accident. However, for the control system by deviation, various behavior of the system was recorded in the case of sensor breakdown and motor apparatus elements.

Acknowledgements Research is done with financial support Ministry of Science and Higher Education of the Russian Federation under the contract 03/19 from 29.11.2019 in the framework of agreement №075-11-2019-070 of 29.11.2019 (unique number 07519SU2000000).

References

1. Rubanov, V.G., Rybin, I.A.: Modern Methods of Designing Control Systems: A Training Manual, 103 pp. Belgorod, BSTU (2017)
2. Rubanov, V.G., Kizhuk, A.S.: Mobile microprocessor automation systems for transport and storage operations. Mobile robotic systems: monograph, 288 pp. Belgorod, BSTU (2011)
3. Welch, G., Bishop, G.: An Introduction to the Kalman Filter. Los Angeles (2001)
4. Nikiforof, V.O.: Observers of external disturbances. 2. Objects with known parameters. Russian Academy of Sciences (Moscow). Automation and Telemechanics, No. 11, 40–48 (2004)
5. Dilegenskaya, A.N.: Identification of Management Objects, 136 pp. Samara, Samara State Technical University (2009)
6. Stenin, V.A.: The Space of States in the Problems of Automation of SEU, 94 pp. Severodvinsk, Sevmashvtuz (2008)
7. Rubanov, V.G., Luakurva, J.P., Porkhalo, V.A.: Modeling the dynamics of the lateral movement of a mobile robot in a Matlab environment. Ed. TulSU, Series. Comput. Eng. Inf. Tech. Control Syst. **1**, 126–134 (2006)
8. Grewal, M., Andrews, A.: Kalman Filtering: Theory and Practice Using MATLAB. New York (2001)
9. Aranovsky, S.V.: Synthesis of an observer under conditions of perturbation of the process of measuring the output variable. Proc. High. Educ. Inst. **E.52**(10), 28–32. Publishing House: RAS. (2009)
10. Eremenko, I.F., Krivonosov, V.A.: A control system with an observer of the coordinates of the state and indefinite disturbance. Devices Syst. Manage. Control Diagn. **7**, 10–13 (2005)
11. Baranov, A.M., Osipov, E.V.: Synthesis of the Kalman filter using matlab. Collection of master's articles. Issue V, 115–118. Tambov: TOGUP Tambov Polygraph (2006)
12. Kalman, R.E.: Contribution to the theory of optimal control. Bull. Soc. Mat. Mech **5**(1), 102–119 (1960)
13. Brown, R.G., Patrick Y.C. Hwang.: Introduction to Random Signal and Applied Kalman Filtering, 4th edn, 397 pp. John Wiley & Sons, Inc. (2012)
14. Kalman, R.E.: On the General Theory of Control Systems. Proceedings First International Conference on Automatic Control, 221 pp. Moscow, USSR (1960)
15. Garcia, E.A.: Deterministic nonlinear observer–based approaches to fault diagnosis: a survey. Control Eng. Pract **5**(5), 663–670 (1997)

16. Aranovskiy, S., Bobtsov, A., Pyrkin, A., Gritcenko, P.: Improved frequency identification via an adaptive filters cascade. 2014 IEEE Conference on Control Applications, pp. 140–145. Antibes, France: [s. n.] (2014)
17. Julier, S.J., Uhlmann, J.K.: Unscented filtering and nonlinear estimation. Proc. IEEE **92**(3), 401–422 (2004)
18. Arulampalam, S., Maskell, S., Gordon, N., Clapp, T.: A tutorial on particle filters for online nonlinear/non-Gaussian Bayesian tracking. IEEE Trans. Sig. Proc. **50**(2), 174–188 (2002)
19. Briers, M., Doucet, A., Maskell, S.: Smoothing algorithms for state-space models, Ann. Inst. Stat. Math. **62(**1), 61–89 (2008)
20. Carpenter, J., Clifford, P., Fearnhead, P.: An improved particle filter for non-linear problems. IEEE Proc. Radar Sonar Navig. **146**, 2–7 (1999)
21. Prokopev, A., Nabizhanov, Z., Ivanchura, V., Emelyanov, R.: Modeling cyber-physical system object in state space (on the Example of Paver). In: Kravets, A., Bolshakov, A., Shcherbakov, M. (eds.) Cyber-Physical Systems: Advances in Design & Modelling. Studies in Systems, Decision and Control, vol. 259. Springer, Cham (2020). https://doi.org/10.1007/978-3-030-32579-4_25
22. Bazhanov, A., Vashchenko, R., Rubanov, V., Bazhanova, O.: Development of an automated system for monitoring and diagnostics a guided robotic vehicle. In: Kravets, A., Bolshakov, A., Shcherbakov, M. (eds.) Cyber-Physical Systems: Advances in Design & Modelling. Studies in Systems, Decision and Control, vol. 259. Springer, Cham (2020). https://doi.org/10.1007/978-3-030-32579-4_8

Intelligent Cybersecurity

Security Providing for Cyber-Physical Systems Based on the Analysis of Service Dataflow

Roman Meshcheryakov, Sergey Iskhakov, and Andrey Iskhakov

Abstract In the chapter, we examine the possibility to use service dataflow extracted from logs of events of various elements for the analysis of the security of cyber-physical systems. The urgency of security providing for such complexes and their separate components is stipulated by a considerable number of security incidents as the violation of their faultless continuous functioning can lead to the damage of to people's life and health, to the disruption of the functioning of the subsistence means of the population and other technogenic catastrophes. A normalization procedure of service dataflow is offered, allowing to generate groups of objects and properties and to ensure the process is such a way that semantically similar data are allocated in the same taxonomic fields. Besides, we examined the possibility to use the correlation of events in the conditions of uncertainty of infrastructure to define the hierarchy of asset types and the most significant objects. The approach is based on the detection of connections between events of security and the estimation of the dependence of their relative force on the distribution of events in time, based on the calculation and use of correlation coefficients. Such an approach allows us to reveal the main types of objects of the infrastructure, their characteristics, and hierarchy by analyzing empirical data, as well as to compare the criticality of objects based on static and dynamic indexes. We present the results of the experiment according to which the application of the given procedure allows us to lower information loss during the transformation of models of identified objects. The implementation of the studied approach to the correlation of events has some limitations in the case with a heterogeneous infrastructure; however, it can be used to develop a short-term pattern of interaction object with a homogeneous infrastructure in cyber-physical systems. Also, it is shown that automation of the detection of elements and the hierarchy of connections between them as well as the estimation of their criticality allows us to more precisely and in more detail develop a model of risks for the security analysis.

R. Meshcheryakov (✉) · A. Iskhakov
V.A. Trapeznikov Institute of Control Sciences of Russian Academy of Sciences, Profsoyuznaya 65, 117997 Moscow, Russia

S. Iskhakov
Tomsk State University of Control Systems and Radioelectronics, Lenina 40, 634050 Tomsk, Russia

A. G. Kravets et al. (eds.), *Cyber-Physical Systems*, Studies in Systems, Decision and Control 350, https://doi.org/10.1007/978-3-030-67892-0_25

Keywords Cyber-physical systems · Normalization · Correlation · Taxonomy · Logging system · Event id

1 Introduction

The development and reduction in the price of the systems of extensive data gathering allow equipping technical objects with sensors and actuators to increase the efficiency of general processes. It has served as one of the reasons for the emergence of the class of cyber-physical systems (CPS). Currently, to ensure the competitiveness of production, the transition to such systems is carried out in various industries, and human life. CPS is a collection of components implementing computing and physical processes; and besides, physical processes are complex and continuous, and computing processes are discrete and determined.

The urgency of security provision for CPS and their separate components is caused by a considerable number of security incidents connected to critical fields of business and industrial production during the last years [1]. It proves to be true not only by the increasing number of cyber-attacks on technological objects of various levels but also by the intensification of research on the methods and technologies of the information protection for CPS from the scientific community, governors, standardization committees, as well as commercial manufacturers of information protection means.

One of the primary goals in the solution of this problem is the estimation of CPS security as a violation of their faultless continuous functioning can lead to the damage of people's lives and health; to the disruption of the functioning of the subsistence means of the population, transport infrastructure, communication networks; to requirement violations of the international contracts; to the damage of the environment; to the damage of defense of the country, security of the state and the law and order.

In its turn, when analyzing the security of CPS, as well as any information system, it's important to select and estimate the criticality of its elements. Practically all CPS elements are connected by various data channels and a number of semantic interrelations, and assets used in them can be considerably distributed. The assets, in this case, are understood as all informational-technological CPS objects (including sensors, controls, databases, applications, users, services, etc.). Thus, in an up-to-date CPS, the infrastructure can change with time—there can appear new nonregistered elements, new data channels, and semantic interrelations, which is interfaced with the occurrence of vulnerabilities and configuration errors. In such conditions, the estimation of assets and the degree of their criticality by experts requires considerable time and human resources. The automation of determining the elements and hierarchy of connections between them, as well as the estimation of their criticality, will allow us to more precisely and minutely build a risk model for the security analysis. Criticality, in this case, is understood as the importance of the object for the functioning of a CPS. The determination of criticality of all informational-technological objects is also important for the task of selection of protection measures as their implementation in distributed CPS with complex interconnections can lead to unforeseen incidental damage for critical assets at the expense of disconnecting or removal of auxiliary assets. In this connection, the problem of estimation of security of a cyber-physical system includes not only the estimation of security of the transmitted, processed, stored in it, and information systems interacting with it, but also the estimation of security of correctness and continuity of manufacturing processes.

Because at the heart of the interaction of components of modern CPS are often the local area networks technology, its specifics are reflected in the interaction of devices on the basis of network protocols that allow transforming the transmitted data into messages of a certain format. On the one hand, the application of network scanners allows one to define various objects of a network, such as the services, ports used by them, and the devices where they are deployed. On the other hand, such tools do allow selecting processes, sessions, users, and their privileges, thereby to select different types of both static and dynamic objects and their hierarchy. This condition does not allow one to receive an actual dynamic CPS model. Nevertheless, the determination and analysis of CPS elements are necessary for revealing its most critical elements.

The use of such data with the information on vulnerabilities and exploits, including hardware and software, templates of attacks will allow us to reveal malicious, illegitimate, and abnormal elements, to carry out monitoring of the state of CPS security for the development of preventive countermeasures. For today, various researchers offer procedures of automated determination of the propagation of damage from attacks and the criticality of information system objects. In particular, the approaches based on service dependence graphs performed well. For example, in [2] it is offered to use dependencies between system resources to determine the criticality of minority assets and subsequent selection of cyber-attack counteraction standards [3, 4]. At the same time, the authors do not consider the question of automation of determining the services and dependencies between them and they are oriented on the manual determination of the most important assets and their connection with the infrastructure objects.

Thus, within the limits of the CPS security estimation, the question of the automated determination of elements, hierarchical connections between them, and their criticalities are urgent. Paper [5] examines the idea of application of correlation methods for revealing the objects types of an indefinite infrastructure on the basis of the analysis of security events. Various types of analysis (statistical, structural, dynamic, etc.) of such events allow one to evaluate the criticality of assets from the point of view of the functioning of CPS and its separate elements.

The chapter proposes to examine the possibility of the use of service data extracted from the logs of events of various elements, for the analysis of CPS security. In this case, the determination of the hierarchy of asset types and their most significant objects is meant. The used approach of event correlation allows us to reveal the main types of infrastructure objects, their characteristics, and hierarchy by analyzing empirical data, and also to compare the object criticality on the basis of static and dynamic metrics.

2 Research Overview

The considerable quantity of the data sources in CPS affects not only the volume of processed data but also the variability of their representation. The prompt increase in the volumes and the heterogeneous nature of the processed data arrays negatively affect the velocity and complexity of their analysis, which, in turn, impedes the possibility of application of the given information for timely detection of incidents and generation of behavioral user profiles during adaptive authentication. Therefore, during the analysis of service data in CPS, it is necessary to solve the problem of processing large arrays of data in the various form of representation, including semi-structured data.

The thesis [6] proved the theorem of control sufficiency of a discrete message thread from devices for the analysis of their security. Therefore, it is possible to conclude that one of the sources for the analysis of the criteria of a user behavioral profile is the digital message thread in the various form of representation, generated by system components where a set of messages is generated by the device and contains both informational and status messages of various types [7, 8].

Thus, urgent is the development of the methods and algorithms of determination of the formats of the data generated by devices, the extraction of meaningful parameters, and their reduction to a uniform format for the further analysis of the state of security of protected objects. In papers [9–11] an approach to the formation of the expert knowledge for the development of control systems of security events is offered. The given approach is based on the prioritization of certain tags of system objects and heuristic search of known varieties of hidden incompatibilities between protection components of devices. The approach is based on the correlation of events on the basis of templates; thus, ensuring the adequate accuracy of anomaly detection and the possibility of the expandability of the template list. However, the interference of devices among themselves and a high number of factors influencing all devices is studied insufficiently. The main directions of scientific research in this area are the methods and mechanisms of normalization, aggregation, and correlation of events.

The search of event correlation is a process of detection of information security incidents by the analysis of a stream of normalized events. After in an event stream such sequence is detected, which is specified in the requirement of one of the rules of correlation defined in advance, a correlation event is registered. In [12, 13], a classification is presented which distinguishes rule-based and not-rule-based correlation methods. Rule-based methods refer to the manual development of certain rules of incident determination. Not-rule-based methods are based on the detection of anomalies by the principle of a black box. Among such methods, specification-based and data-mining based approaches are selected.

Let's consider the studies devoted to the correlation of events [14]. Initially, data correlation was applied within the limits of intrusion detection systems to find the connections between the network events for the purpose of their aggregation and subsequent attack detection [15–17]. However, the correlation of events occurring in an information system, besides finding incidents and security alerts, can be applied to the solution of various problems of security, including the determination of interconnections between the diverse security information, classification of low-level events into high-level meta-events, finding the types of objects of an information system and connections between them [18]. The most popular and simply implemented correlation method is the rule-based method [19]. The main disadvantage of this method consists of major time expenses needed by the administrator to assign the rules. The efficiency of the given method is directly connected to the administrator's qualification. Many methods, including those based on templates (scenarios) [20], graphs [21], finite state automatons, etc. use various models for mapping the events and the connections between them but can be implemented with the use of rules [22]. Now, more perspective is the approaches to correlation, based on self-training [23], such as Bayesian networks [24, 25], probability enumeration of events [26], immune networks, artificial neural networks [27], and others. The advantage of the given approaches is the possibility of an independent (unconditional) correlation of events with minimal manual adjustments. Nevertheless, a preliminary data analysis is necessary to build learning models, which is difficult to automate. Besides, there are requirements for the estimation of adequacy and quality of models, and initial learning sampling should be complete enough.

The main disadvantage of the majority of the above-mentioned research and development papers is the urgency of the problem of detail loss of the initial object during a simulation. For example, during the execution of a certain process, the operating system can transmit the data about its course into the local event logging system on the given device. In doing so, only that part of the information on the course of procedure execution, which is provided by developers, is transmitted. This leads to the loss of some details and to the simplification of the initial model. After this, the second stage follows, and the logging system either records the received information into the local storage or transmits it to its agent-collector for sending it into the SIEM-system. Here, the selected format of record storage or the protocol used for the information transfer, where the size of data fields is accurately defined, could be considered to be a restrictor. At this stage, there seems to be the next simplification of the model and a part of the data would also be lost.

As a result, received for processing is a simplified model of a real event in the form of a discrete record or structural unit of data. During the normalization of events, the obtained information is arranged in certain fields. At the same time, the number of fields in the diagram cannot reflect all possible semantics of all events from all sources, which leads to the further simplification of the model because of the elimination of some information.

For the development of diagrams of data normalization, many experts are often involved at different stages of the integration. For example, many products allow users to add new sources and to normalize the events by themselves. At the same time, each expert can differently define the semantic load of some data, which could lead to placing semantically similar data in various fields of normalization. In paper [28] an attempt is undertaken to formalize the normalization process; however, the development of accurate methodological instructions on the normalization of events from various sources is urgent.

The same disadvantage substantially restricts the development of such perspective direction as the development of methods of behavioral analysis of objects of heterogeneous IT infrastructures for which SIEM-systems are the most suitable data source. Nevertheless, the above-mentioned disadvantages show the impossibility to design such methods of the development of event correlation rules in isolation from the main problems in methodological and algorithmic support of the incident control process.

Thus, it is possible to select the following urgent problems in the researched domain:

1. Losses of data during the normalization, connected to the transformation of models.
2. Lack of the methodological apparatus of event normalization.
3. Lack of support for modifications of the protection object model.
4. Lack of methodology for developing the correlation rules.

Another important overlook of the above-mentioned studies is the insufficient development of the problem of the modification control of the states protected by CPS, including the retrospective analysis of the object state. In the course of functioning of systems, there inevitably occur modifications in their architecture and structure as a result of actions of administrators, users, and other staff interacting with the objects. The assets of the systems (objects) are constantly transforming into various states, which leads to the necessity to support regular upgrades of the model of the protected object.

The present chapter shows that the dynamic analysis of the events occurring in the system and the calculation of static-dynamic indexes, including frequency characteristics of event types, the variability of property values, paired usage, and variability of properties, helps to find the main sources of events (objects) and hierarchical interconnections between the types of objects.

3 Approach to the Analysis of Cyber-Physical System Security

When analyzing the CPS security, the criticality estimation is necessary to determine the damage from cyber-attacks, as well as to determine the incidental damage from the implementation of security measures. In various studies, criticality is defined both with qualitative and quantitative indicators.

To determine the damage inflicted on critical assets, dependence graphs of services are applied widely enough. They allow tracing the propagation of the damage from attacks on an information system. Their purpose is to determine how a certain vulnerability of informational infrastructure represented in the form of a service-oriented architecture would affect the organization's operation. The dependence graph of services represents a set of CPS services (assets) connected between themselves according to how the state of security of one service depends on the properties of the other. The records of damage propagation through dependencies of services allow one to adjust the expenses on security so that they would not exceed the possible damage, to justify them, as well as not to miss the important vulnerabilities which can lead to serious consequences.

In some cases, the index of damage from an attack is calculated on the basis of a dependence graph uniting priority resources, hierarchies of resources (classification of resources according to types with the selection of countermeasures for each type), and a cost model where the cost is assigned to the resources. At the same time, the given index is defined as the sum of costs of the nodes that were negatively affected by an attack action. In this case, resource criticality is defined by its cost. In some cases, to determine the incidental damage during the reaction, a tree of dependencies between the resources is used, and an index is offered that reflects the cost of service decrease as the result of the loss of its availability. Thereby, the service criticality is defined by its productivity. In [29], an approach to the determination of the extended damage level with the use of a dependence graph of services is offered. In this case, the criticality of assets is defined depending on its cost on a rank scale. In [30], a service dependence graph is used to determine the incidental damage during the reaction to attacks.

The mentioned studies allow us to define how the damage from cyber-attacks propagates in a system or to define the criticality of minority assets of an organization according to the damage that occurred as a result of the violation of their security. However, these studies are aimed at service-oriented architectures, and their purpose is not the automated determination of system services (or other objects of an information system) and connections between them.

The main means of autodetection of a network informational infrastructure are network scanners. The tools of network scanning are divided into activities such as Nmap and Nessus, and passive such as Wireshark. They allow us to define the topology of a network and partially reveal the network services by scanning ports, determination of services using them, and service hardware and software. However, these tools do not possess a sufficient degree of accuracy and completeness of information, and, besides, do not have the determination of dependencies between network resources as their task. Afterward, administrators can add gathered information manually. Besides, the information on the system services can be al-ready present in the information on the system configuration. Network scanners allow us to define objects with the structure defined in advance and are not designed to determine all types of dynamic objects, such as user's and system processes, sessions, their hierarchies, or their roles.

A detailed review of the automated detection procedures of dependencies between services is given in [31]. The author selects the inquiry of accessible knowledge of dependences, for example, in system files or in a specially created storage of configuration, program code used to determine dependencies, passive methods of identification on the basis of the analysis of object interaction, methods on the basis of neuro networks and methods of data mining. In [31], it is also noted that the problem is still not solved completely. The above-mentioned papers basically consider objects of one type (services).

In some cases, to select the objects, only frequency indexes of event types are used and the characteristics of the initial information are not used such as the use and variability of properties and their values, which could allow us to select objects types more precisely. The chains of events are researched; however, the determination of the hierarchy of elements and their types with the subsequent analysis of chains of events allows us to more precisely compare the chains of events in the future—to divide the events according to the belonging to the objects and to build connections between the objects. In other cases the correlation of the events and development of the rules (templates) of event correlation according to empirical data.

To analyze the CPS security, it is offered to automate the identification of its elements on the basis of the selection of various object types according to the information extracted from the service data logs of events. Although the examined methods were applied to detect intrusions, rather than to solve the problem of the asset type detection of an IT system and the connections between them, it is supposed that similar data analysis is also applicable for the solution of the problem discussed in the present research.

3.1 Domain Model

It is necessary to have a detailed idea about the CPS domain, including its components and the connections between them. The model of the domain constructed on the basis of ontologies represents the following advantages according to the sources [6, 32]:

1. the model is easily adapted and supplemented; the definition of new terms without the necessity to revise the existing definitions is possible;
2. the possibility to consider the intercomponent relations of the domain (internal and interlevel relations);
3. the possibility to consider the same objects of the domain from different points of view at the expense of their referring to different conceptual constructions;
4. the possibility to connect to an ontologic model other models designed to describe separate subsystems of the domain and using the concepts introduced in the ontologic model;
5. the fact that an ontologic model could be readable by a machine and could be translated into other universal languages;
6. the possibility to design a prototype of a protection system on the basis of a subject area model (Fig. 1).

The development of the domain model will allow us to examine the interaction of CPS elements implementing physical processes by means of messaging at different levels of abstraction, which then are transformed into events. Formally, an ontology represents a triplet $\{X, R, F\}$, where $X = \{x_i\}$—is a set of concepts, $R = \{r_i\}$—is a set of relations between concepts, $F = \{f_i\}$—is the function of concepts and relations [33]. The primary task is to describe the core (central) concepts of the ontology and relations between them. The interconnection of central concepts is presented in the

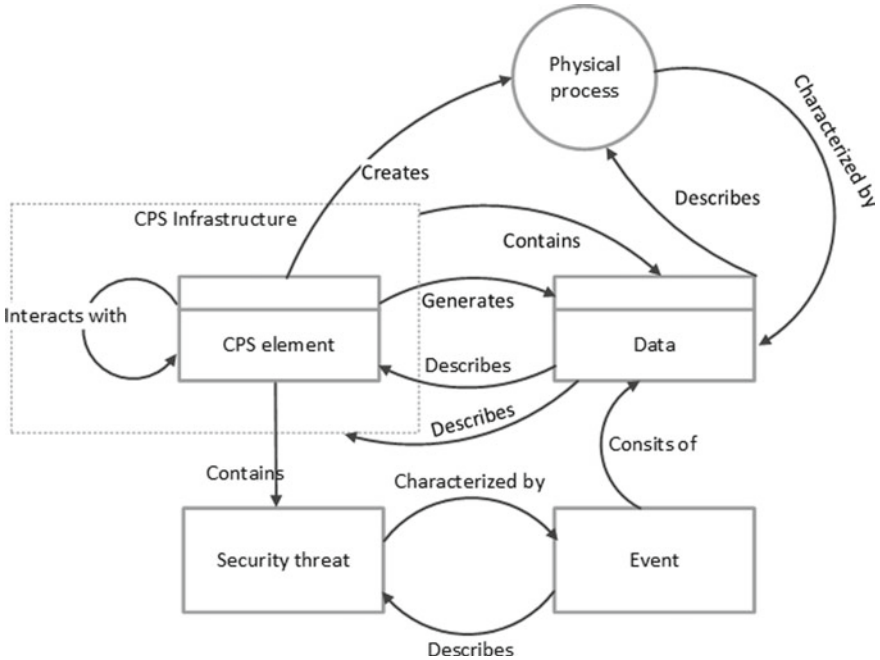

Fig. 1 Subject area model

figure, the arrows represent relations between concepts, and their meaning can vary. The description of levels of representation allows us to receive the requirements for the aspects of SIEM-system development. The following levels of representation are described:

– the level of CPS element representation characterizing the main sources of security threats connected to the finite device;
– the level of representation of message space and event space, characterizing the process of obtaining events processed by the SIEM-system;
– the level of security threat representation characterizing the process of detection of various anomalies in the data;
– the level of representation of security incidents characterizing the process of the development of the sequences of the interconnected events describing the process of the implementation of a security incident by a malefactor.

3.2 Identification of Assets of a Cyber-Physical System and Their Value

The thesis [6] proves the theorem of control sufficiency of a discrete message thread from devices for the analysis of their security. Therefore, it is possible to conclude that one of the sources for analyzing the criteria of a user's behavioral profile is a discrete message thread in a various form of the representation, generated by the system components where a set of messages is generated by the device, and contains both informational and status messages of various types.

The procedure is based on the assumption that in each event the following elements could be selected:

– the subject: the initiator of interaction the event narrates about;
– the object: the main entity described by the event;
– the source: an observer of the event, practically a subsystem of the certain element of the certain robotic system, the subsystem that generated and sent this message.

Proceeding from this, we could identify the following diagrams of events from the point of view of the interaction between the subject and the object.

1. The event does not contain the information on any interaction—the source transmits the object state information (Fig. 2a)
2. The event contains the information only about the object, but the subject is implied by the event context (Fig. 2b).
3. In the event, the object executes the operation on itself (Fig. 2c).
4. The event contains information on the subject and the object as well as their interaction (Fig. 2d).

An important factor at the CPS security estimation is the identification and estimation of the system asset value. The assets are all CPS elements (files, users, sensors, actuation devices, repositories, applications, servers, and others). The CPS structure

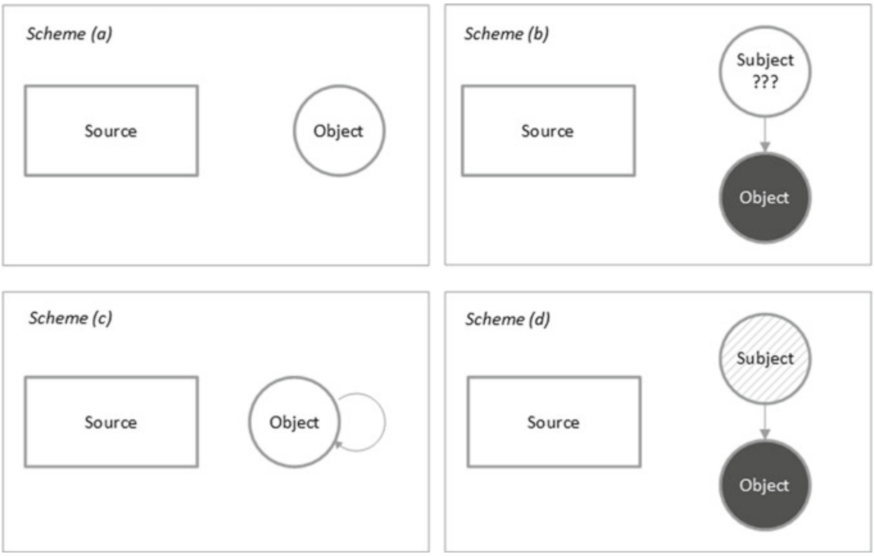

Fig. 2 Schemes of events in terms of subject-object interaction

can vary in the process of functioning, and also leads to the appearance of new vulnerabilities and configuration errors. With the increase in the CPS scale, the identification and estimation of asset value require considerable time expenditures. Therefore, this process is recommended to be automated. It is possible to organize that in a series of stages:

– Gathering and preprocessing of input data. At this stage, the data gathering about the events from CPS logs and bringing them to the normal mode for further analysis is implemented.
– Selection of element categories. The gathered data are exposed to the statistical analysis which allows defining the types of characteristics, categories of CPS elements, the connection between which is defined by static-dynamic indexes.
– Determination of asset value by means of the indexes of characteristics usage of assets and their quantitative values.

Gathering and preprocessing of input data. We consider infrastructure CPS indefinite. Input data is a set E of events of the security presented in register J of element CPS:

$$E^J = \{e_1, e_2, \ldots, e_n\} \tag{1}$$

The event, in this case, is the fact of operation execution of at its any stage: fulfillment attempt, beginning of the operation, the intermediate result of the operation (for events, duration in time), the total result of the completion of the operation (correct completion or completion with an error). Any event e includes a set of characteristics p and their values v, describing a certain operation:

$$e = \{p_i, v_i\}, \tag{2}$$

where p_i—is the event characteristics, $p_i \subset P$, P—is the set of all characteristics of events:

$$P = \{p_1, p_2, \ldots, p_m\}, \tag{3}$$

where m—is the total of characteristics; v_i—is the value of the event characteristics, $v_i \in V^{Pi}$, V^{Pi}—is the characteristics range p_i:

$$V^{P_i} = \{v_1, v_2, \ldots, v_k\}, \tag{4}$$

k—is the number of possible values of the characteristics p_i; $V^{Pi} \subset V$, and V—is the set of all values of all characteristics:

$$V = \left\{V^{P_1}, V^{P_2}, \ldots, V^{Pm}\right\} \tag{5}$$

At any moment these sets are finite and are not empty:

$$P \neq \emptyset,\ V^{P^i} \neq \emptyset,\ \forall i \in \{1, 2, \ldots, m\}$$

For further analysis, the event characteristics and their value are transformed into the normal mode by an expert. If it is not done, the quality of the results of the further stages can be essentially lowered. The gathered data can be divided according to their values on categorical and quantitative. The correlation approach at the following stage is selected depending on the type of values.

Selection of categories of elements. The infrastructure *I*, with indefinite composition and architecture, includes *l* information elements *O*:

$$O^I = \{o_1, o_2, \ldots, o_l\} \tag{6}$$

The state of the elements is defined by one or several characteristics c and their values:

$$o = (c_i, v_i), \tag{7}$$

where $o \in O^I$, $c_i \in C$, $C = \{c_1, c_2, \ldots, c_h\}$, $|C| \geq 1$, h—is the total number of possible characteristics of elements; $v_i \in V^{Ci}$, V^{Ci}—is the set of possible values of characteristic c_i:

$$V^{C_i} = \{v_1, v_2, \ldots, v_r\}, \tag{8}$$

r—is the number of possible values of characteristic c_i; $V^{Ci} \subset V$, V—is the set of all values of all characteristics:

$$\mathrm{V} = \left\{V^{C_1}, V^{C_2}, \ldots, V^{C_r}\right\} \tag{9}$$

The CPS elements are connected between themselves by membership relations: any element is either a part of a higher-level element of the system or contains lower-level elements. Also, the analysis of their immediate interaction helps to determine the direct relation of one element with another. It allows one to generate the hierarchy of elements. The complex of characteristics C^0, which describes the information element *o*, unambiguously defines the category of information element o_t. The examples of element categories: files, users, sensors, actuation devices, repositories, applications, servers, and others.

Model *R* of CPS infrastructure *I* consists of information element set *O*, and also sets of their categories *O*T and relations *OR*:

$$R^I = \langle O, OT, OR \rangle \tag{10}$$

Thus, the input data of the correlation process are transformed into the sets of elements and their categories of CPS infrastructure:

$$\{E, P, V\} \rightarrow (O, OT) \quad (11)$$

The stage of selecting categories of elements and their hierarchy consists of several steps:

– selection of event characteristics types on the basis of the analysis of their possible values;
– selection of element categories on the basis of characteristics types;
– determination of the hierarchy of the element categories on the basis of the common usage index.

4 Experiments and Discussions

For the experiments, platform Supermicro with two Intel Xeon E5 2.1 GHz processors and 64 Gb RAM was used. On the basis of the CentOS 7 operation system, a software complex was developed that was used to gather and process the data of several CPS logs, concerning various spheres of life. As input data, a stream of events from heterogeneous sources on various protocols was used, including Syslog for network equipment and objects with Unix-based system administration, Windows log events, as well as the data from various DBMS. The distribution of event stream intensity averaged on hours for days of the research and expressed in events in a second (EPS) is presented in Fig. 3.

During the analysis of input data, it was determined that all types of events can be divided into those occurring in the stream often enough, and those occurring seldom. The types of events occurring more than 1000 times during a day refer to the first group, the second kind includes the remaining events. It is thus determined that when using a heterogeneous infrastructure classification, the procedure becomes considerably complicated because even if the normalization stage is carried out properly enough and semantically similar fields are filled in correctly, in many cases their formats are various and the development of connections is not of practical use. Figure 4 can prove this; it shows the classification of the events received from assets provided by one vendor, but belonging to various product families where the properties defining the code of the event type are absolutely different.

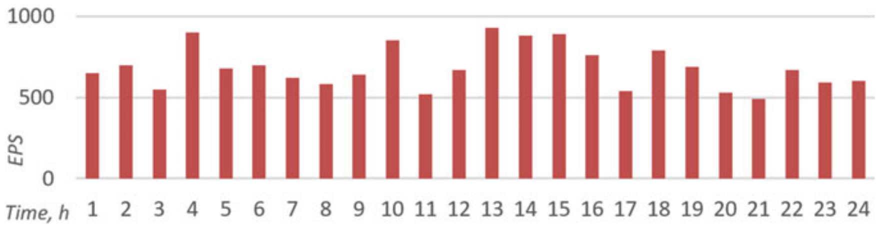

Fig. 3 Distribution of the intensity of the flow of events over a 24-hour period

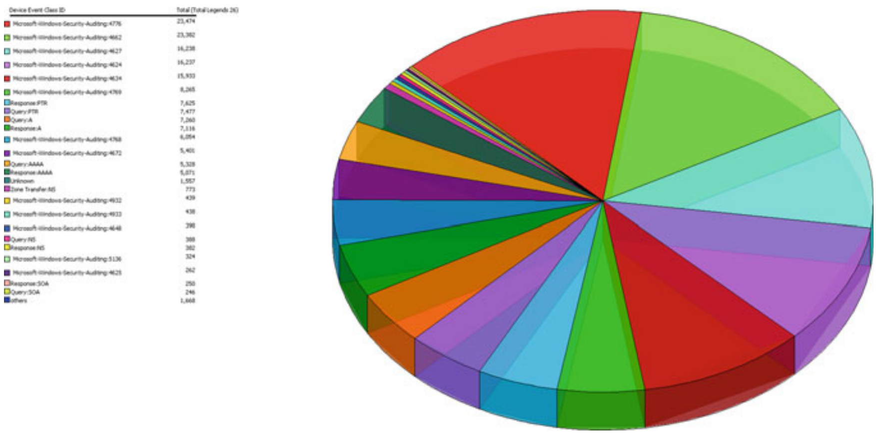

Fig. 4 Classification of the events received from assets provided by one vendor

As was mentioned earlier, for the full analysis of the characteristics of the received events, they should be transformed into a unified form and normalized. The fulfillment of the given procedure of the analysis of the initial event should be carried out according to the normalization formula defined in advance for the source and the type of event. A normalized event represents a collection of certain fields in which composition is defined within the limits of certain taxonomy, filled with the data from a raw event according to the rules specified in the normalization formula. At the same time, the normalization of the received events implies parsing (the analysis of the data of the initial event) and mapping (comparison of the extracted data to the taxonomy fields). Considering a great number of data sources generated by separate subsystems of various CPS elements, it is necessary to carry out filtering and integration of the samplings of the events which are subject to the analysis by applying aggregate methods. The data flow from the source can contain the events of the same type, differing by the value of one or several fields (for example, a long time). In such cases, it is expedient to organize the process of selection of such events which meet the requirement of the aggregate rule set in advance tuned, and their integration in one aggregated event. If the normalized and aggregated data about the state of information security of CPS infrastructure are present, it is possible to realize the actions directed on the analysis of the processes occurring in the system and on the detection of incidents. The main mechanism in the solution of the given task is the application of correlation methods.

We defined the normalization formulas for the most commonly encountered events in the studied object by implementing the procedure mentioned above. Each event was considered from the point of view of this procedure. In particular, Table 1 shows the ranking of event types from Windows logs according to the total number of events occurring during a day.

Table 1 Number of commonly encountered event types

Event ID	Event Name	Count
4776	The domain controller attempted to validate the credentials for an account	1,277 697
4662	An operation was performed on an object	1,224 824
4624	An account was successfully logged on	967 215
4634	An account was logged off	965 887
4627	Group membership information	961 710
4769	A Kerberos service ticket was requested	498 688
4768	A Kerberos authentication ticket (TGT) was requested	367 199
4672	Special privileges assigned to new logon	283 979
4648	A logon was attempted using explicit credentials	42 309

Some of the properties in the registered events can contain zero value from the point of view of semantics, but their elimination from the analysis can lead to considerable loss of quality of normalization and incorrect treatment of the structure and types of events. Besides, it is determined that the time distribution of practically all events is aperiodic. Figure 5 shows the diagram of the event distribution intensity

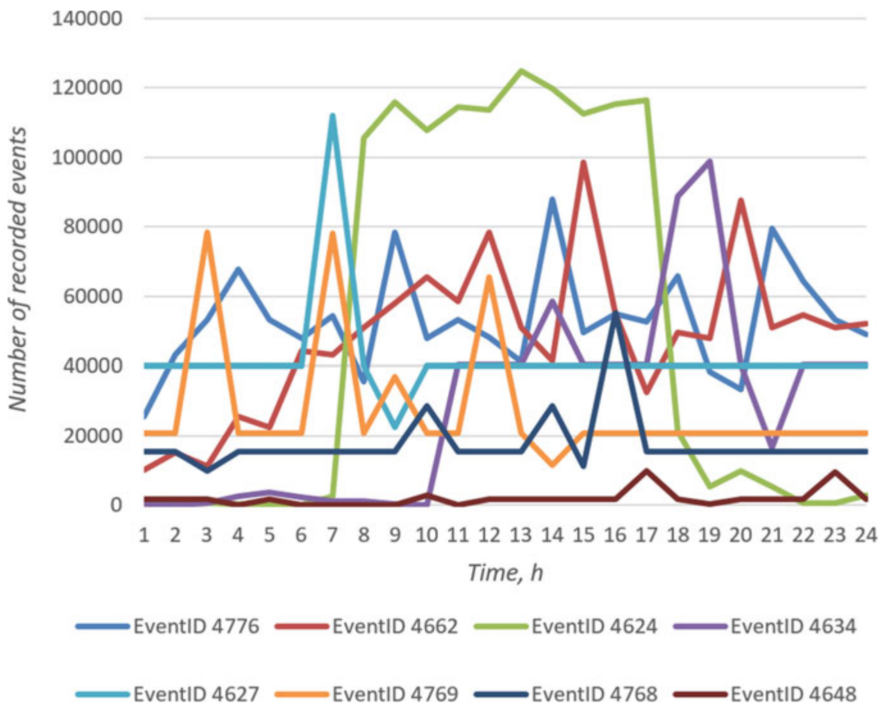

Fig. 5 Distribution of the intensity of event types by observation time range over a 24-hour period

from Table 1 on the time range of their observations (hours).

Figure 6 presents a screenshot of such dynamically varying graph built by means of Java visualization tools.

The experiments on the analysis of the events in the studied CPS infrastructure have shown that not in all cases the variability indexes can form a basis for decision-making on the automated identification of a CPS element. The reason for this can be either a high level of variability of property values or, on the contrary, extremely low variability of one of the properties. The given barriers can be overcome if we assume that if a certain value of a specific event is present, there is an object in the nearest point of time which can be described by means of this value and this object is active. If we define the lifetime of such objects, it is also possible to define the dynamics of the change in the values of properties. In this case, the comparison of properties in pairs and taking into account the time scale will allow us to minimize the

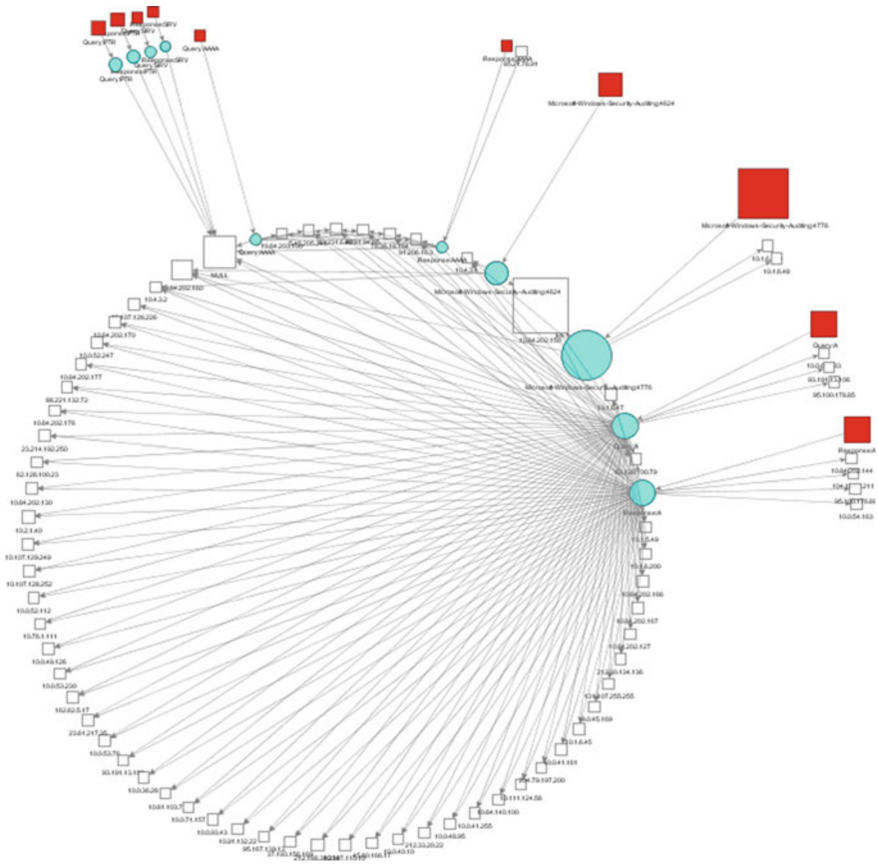

Fig. 6 Screenshot of a dynamically changing graph constructed using Java visualisation tools

above-mentioned errors and to define the life cycle of CPS element in the conditions of uncertainty.

For this reason, the application of pair correlation between properties of events from the sources of homogeneous environments can be used, including for the development of a short-term pattern of interaction between various elements. For example, using the data from events of Windows logs, it is possible to receive the current pattern of interaction in the domain, and in the case of visualization tool implementation, it can be used for monitoring of the CPS state and prompt investigation of incidents. Figure 6 presents a screenshot of such dynamically varying graph built by means of Java visualization tools.

The analysis of the received visualization allowed us to form the groups of objects and properties which are sufficiently expressed from the point of view of semantic value. The presented groups allow us to divide the studied objects into such types as the Subject and the Object, and also the Source and the Aim, which completely match the offered earlier procedure of considering each event during the process of normalization.

5 Conclusion

Currently, the urgency of the problem of security providing for the cyber-physical system so strongly entered into human life is beyond question. The constant growth of the number of cyber-attacks on technological objects is one of the main drivers of modern research and the development of new scientific and technical solutions. One of the primal tasks in the solution of this problem is the estimation of CPS security as the violation of their faultless continuous functioning can lead to the damage to the people's life and health; to the disruption of the functioning of the subsistence means of the population and other technogenic catastrophes.

When analyzing the CPS security, it is necessary to carry out an estimation of the criticality of its elements interconnected by various data channels and a set of semantic relations. In modern CPS, the infrastructure can vary with time—there can appear new nonregistered elements, new data channels, and semantic mutual relations, which is interfaced with the appearance of vulnerabilities and configuration errors. In such conditions, the determination of assets and the degree of their criticality by experts requires a considerable amount of time and human resources.

In the given chapter, the authors undertake an attempt to examine the possibility to use the service data extracted from logs of events of various elements for the analysis of the security of cyber-physical systems. Automation of detection of elements and connection hierarchy between them as well as the estimation of their criticality will allow us to more precisely and in greater detail develop the model of risks for the security analysis.

For this purpose, we offer a procedure of normalization of service message events for further identification of CPS assets and consider the possibility to use the correlation of events in the conditions of uncertainty of the infrastructure to define the hierarchy of asset types and their most significant objects. The used approach allows us to define the main types of infrastructure objects, their characteristics, and hierarchy by the analysis of empirical data as well as to compare the criticality of objects on the basis of static and dynamic indexes.

Earlier, statistical approaches to the execution of the process of security event correlation were also applied. The complexity of the application of probability estimation consists of the necessity to ensure that the input data meet certain requirements, for example, their homogeneity, normal distribution law, and others. The choice of a certain statistical index (correlation index, determination index, etc.) and the possibility to use it for correlation is possible to define in the course of the analysis of input data and results of the calculation of such index.

The carried out experiments have shown that the offered procedure of event normalization allows us to generate groups of objects and properties, ensuring the given process in such a way that semantically similar data were allocated in the same taxonomy fields. This, in turn, allows us to increase the quality of the received CPS model and the estimation of its security at the expense of decreasing the loss of the information during the transformation of the models of the identified objects. Also, the experiments have shown that in the case of a heterogeneous infrastructure, the examined approach to the correlation of events is applicable with some limitations because there are some problems with the determination of semantic similarity between the properties of objects. However, it has been determined that the implementation of the given approach to the correlation of events is the most applicable in the case of a homogeneous infrastructure and can be used for the development of a short-term pattern of interaction in order to monitor the CPS state and to promptly investigate the incidents.

Acknowledgements The reported study was partially funded by RFBR according to the research project №19-01-00767 and by ICS RAS according to the state project.

References

1. Cybersecurity Threatscape. https://www.ptsecurity.com/ww-en/analytics/cybersecurity-threatscape-2019 (2019). Accessed 28 Apr 2020
2. Kotenko, I., Doynikova, E., Chechulin, A.: Security Metrics Based on Attack Graphs for the Olympic Games Scenario, pp. 561–568 (2014). https://doi.org/10.1109/PDP.2014.113
3. Shcherbakov, M.V., Glotov A.V., Cheremisinov, S.V.: Proactive and Predictive Maintenance of Cyber-Physical Systems. In: Kravets, A., Bolshakov, A., Shcherbakov, M. (eds.) Cyber-Physical Systems: Advances in Design & Modelling. Studies in Systems, Decision and Control, vol. 259. Springer, Cham (2020)
4. Lee, E.A., Seshia, S.A.: Introduction to Embedded Systems—A Cyber-Physical Systems Approach, 2nd edn. Berkeley, CA (2015)
5. Teilans, A.A., Romanovs, A.V., Merkuryev, Y.A., Dorogovs, P.P., Kleins, A.Y., Po-tryasaev, S.A.: Assessment of cyber physical system risks with domain specific modelling and simulation. SPIIRAS Proc. **4**(59), 115–139 (2018)

6. Lavrova, D.: An approach to developing the SIEM system for the internet of things. Autom. Control Comput. Sci. **50**, 673–681 (2016). https://doi.org/10.3103/S0146411616080125
7. Jharko, E., Promyslov, V., Iskhakov, A.: Extending functionality of early fault diagnostic system for online security assessment of nuclear power plant. In: 2019 International Russian Automation Conference (RusAutoCon), pp. 1–6. Sochi (2019)
8. Shu, X., Smiy, J., Yao, D., Lin, H.: Massive Distributed and Parallel Log Analysis for Organizational Security // IEEE Globecom Workshops. December 2013, pp. 194–199 (2013)
9. Liang, W., Huang, W., Chen, W., Li, K.-C., Li, K.: Hausdorff distance model-based identity authentication for ip circuits in service-centric internet-of-things environment. Sensors. **19**, 487 (2019). https://doi.org/10.3390/s19030487
10. Iskhakova, A., Meshcheryakov, R., Iskhakov, A., Timchenko, S.: Analysis of the vulnerabilities of the embedded information systems of IoT-devices through the honeypot network implementation. In: IV International Research Conference Information Technologies in Science, Management, Social sphere and Medicine (ITSMSSM 2017), 363–367, Atlantis Press, Tomsk (2017)
11. Promyslov, V., Sakrutina, E., Meshcheryakov, R.: Coherence criterion for security architecture of digital control system. In: 2019 Inter/national Russian Automation Conference (RusAutoCon), pp. 1–5. Sochi (2019)
12. Iskhakov, A., Meshcheryakov, R., Iskhakov, S., Krainov, A.: Increase in security of authentication services through additional identification using optimal feature space. In: Proceedings of the IV International Research Conference "Information Technologies in Science, Management, Social Sphere and Medicine". pp. 443–446 (2017)
13. De Fuentes, J.M.: Applying information hiding in VANETs to covertly report misbehaving vehicles. In: de Fuentes, J.M., Blasco, J., González-Tablas, A.I., González-Manzano, L. (eds.) Int. J. Distrib. Sens. Netw. **10**(2), 1–15 (2014)
14. Doynikova, E., Fedorchenko, A., Kotenko, I.: Automated detection of assets and calculation of their criticality for the analysis of information system security. SPIIRAS Proc. **18**, 1182–1211 (2019). https://doi.org/10.15622/sp.2019.18.5.1182-1211
15. Artikis, A., Baber, C., Bizarro, P., Canudas-de-Wit, C., Etzion, O., Fournier, F., Goulart, P., Howes, A., Lygeros, J., Paliouras, G., Schuster, A., Sharfman, I., Scalable proactive event-driven decision making. Technology and Society Magazine, IEEE. **33**. 35–41 (2014). https://doi.org/10.1109/MTS.2014.2345131
16. Raju, B., Gopalan, G.: Event correlation in cloud: a forensic perspective. Comput. **98**(11) (2016). https://doi.org/10.1007/s00607-016-0500-2
17. Calyam, P., Dhanapalan, M., Sridharan, M., Krishnamurthy, A., Ramnath, R.: Topology-aware correlated network anomaly event detection and diagnosis. J. Netw. Syst. Manage. **22**, 208–234 (2014). https://doi.org/10.1007/s10922-013-9286-0
18. Alevizos, E., Artikis, A., Katzouris, N., Michelioudakis, E., Paliouras, G.: The complex event recognition group. ACM SIGMOD Record. **47** (2018). https://doi.org/10.1145/3299887.3299899
19. Limmer, T., Dressler, F.: Survey of Event Correlation Techniques for Attack Detection in Early Warning Systems (2008)
20. Michelioudakis, E., Artikis, A., Paliouras, G.: Semi-supervised online structure learning for composite event recognition. Mach. Learn. **108**(7), 1085–1110 (2018). https://doi.org/10.1007/s10994-019-05794-2
21. Han, Y., Zhu, M., Liu, C.: A service-oriented approach to modeling and reusing event correlations. 498–507 (2018). https://doi.org/10.1109/COMPSAC.2018.00077
22. Iskhakov, S.Yu., Shelupanov, A.A., Meshcheryakov, R.V.: Simulation modelling as a tool to diagnose the complex networks of security systems. J. Phys: Conf. Ser. **803**(1), 012057 (2017)
23. Selvamani, D., Selvi, V.A.: Association rule mining for intrusion detection system: a survey (2019)
24. Skarlatidis, A., Paliouras, G., Artikis, A., Vouros, G. Probabilistic event calculus for event recognition. ACM Trans. Comput. Logic **16**(2) (2014). https://doi.org/10.1145/2699916

25. Alevizos, E., Skarlatidis, A., Artikis, A., Paliouras, G.: Probabilistic complex event recognition: a survey. ACM Comput. Surv. **50**(5), 71 (2017). https://doi.org/10.1145/3117809
26. Harutyunyan, A., Poghosyan, A., Grigoryan, N., Marvasti, M.: Statistical normalcy determination based on data categorization. VMware Tech. J. **3**, 43–55 (2014)
27. Zhou, J., Guo, A., Celler, B.G., Su, S.: Fault detection and identification spanning multiple processes by integrating PCA with neural network. Appl. Soft Comput. **14**, 4–11 (2014). https://doi.org/10.1016/j.asoc.2013.09.024
28. Evsutin, O., Kokurina, A., Meshcheryakov, R., Shumskaya, O.: The adaptive algorithm of information unmistakable embedding into digital images based on the discrete Fou-rier transformation. Multimedia Tools Appl. **77**, 28567–28599 (2018)
29. Kheir, N., Debar, H., Cuppens-Boulahia, N., Cuppens, F., Viinikka, J.: Cost evaluation for intrusion response using dependency graphs. IFIP International Conference on Network and Service Security (N2S). 1—6 (2009)
30. Shameli-Sendi, A., Louafi, H., He, W., Cheriet, M.: Dynamic optimal countermeasure selection for intrusion response system. IEEE Trans. Dependable Secure Comput. **15**(5), 755–770 (2018)
31. Hanemann, A.: Automated IT Service Fault Diagnosis Based on Event Correlation Techniques (2007)
32. Munir, K., Anjum, M.: The use of ontologies for effective knowledge modelling and information retrieval. Appl. Comput. Inf. **14** (2017). https://doi.org/10.1016/j.aci.2017.07.003
33. Lavrova D.S.: Ontology-based big data approach to automated penetration testing of large-scale heterogeneous systems, T.V. Stepanova, A.I. Pechenkin, D.S. Lavrova, SIN '15 Proceedings of the 8th International Conference on Security of Information and Networks. ACM New York, NY, USA, P. 142–149 (2015)

A Variant of the Analytical Specification of Security Information and Event Management Systems

Igor Kotenko and Igor Parashchuk

Abstract The object of the study in the chapter is a variant of the analytical specification of the state change dynamics characterizing the quality indicators of the process fulfilled by a security information and event management (SIEM) system. A generalized model of such a system based on the state and observation equations taking into account advanced algorithms for converting excitation noise (spectral power density of excitation noise) is investigated. Moreover, the model is a formalized analytical description specified in terms of the Markov chain in the form of different stochastic equations. The dynamics of changes in the values of quality indicators characterizing the essential properties of the SIEM system functioning in the state space are analyzed. A mechanism for determining the values of the mathematical expectation increment of the simulated process is proposed. These values are obtained on the basis of a priori data on the Markov chain with respect to the mathematical expectation of white Gaussian noise exciting this process. The specified mechanism is used in conjunction with the calculation of the values of the coefficient that corrects the variance of random discrete realizations of the original white Gaussian noise. This approach allows one to make a decision about what values the elements of the vector of compensation additives will take in the state equation of this modified model of the SIEM system taking into account the excitation noise conversion.

Keywords Mathematical model · Security information and event management (SIEM) · SIEM system · Quality indicator · Functioning process · Matrix · Transition probabilities · State

---

I. Kotenko (✉) · I. Parashchuk
St. Petersburg Federal Research Center of the Russian Academy of Sciences (SPC RAS), 39, 14 Liniya, St. Petersburg 199178, Russia
e-mail: ivkote@comsec.spb.ru

I. Parashchuk
e-mail: parashchuk@comsec.spb.ru

A. G. Kravets et al. (eds.), *Cyber-Physical Systems*, Studies in Systems, Decision and Control 350, https://doi.org/10.1007/978-3-030-67892-0_26

1 Introduction

Information security systems for computer and telecommunication networks have a complex integrated structure. They include hardware and software systems (servers, databases, security tools, workstations), as well as personnel. All these components are organizationally and technically integrated and are designed to implement the information protection process. The purpose of this process is to minimize losses that may be caused by a violation of the availability, integrity, or confidentiality of information [1–4].

One of the possible and effective approaches to achieving this goal is the development and application of security information and event management systems (SIEM systems). They are designed for real-time analysis of security events (threats, alarms) emanating from network devices and applications, and allow one to respond to these threats before they occur and to prevent significant damage [5–9].

The traditional approach to the analytical description of the functioning processes of complex systems, for example, such as SIEM systems, consists of attempts to formally represent these processes through the dynamics of a linear or nonlinear change in the state (step-by-step values) of quality indicators (QIs) of these objects and processes in the state space. Markov process models, in this case, are an indispensable tool.

The necessary basic input data for the analytical description of the SIEM system functioning in this formulation is a vector of QIs for the SIEM system and the requirements for these QIs. Then the model of the SIEM system functioning can be represented through an analytical description of the process of changing the states (values) of its vector of QIs. Moreover, we denote the analytical description of the vector of QIs for the SIEM system functioning process by $x(k)$. The analytical relationship of individual QIs in the case of a dynamic, probabilistic, non-linear, and non-stationary process is associated with the need to specify multidimensional functions $F\left(x, \vec{\lambda}, t_0, \ldots, t_k, \ldots, t_K\right)$ or densities $W\left(x, \vec{\lambda}, t_0, \ldots, t_k, \ldots, t_K\right)$ of the probability distribution of the values of the functioning indicators for various elements of the SIEM system and the process of its operation as a whole on the interval of functioning of this system $(t_0 - t_K)$. Moreover, m is the number of process state variables $x(k)$, s is the number of distribution parameters λ and k is the number of time samples. The mathematical description, taking into account the dimension expansion in this case, is difficult.

2 Related Work

An analysis of such limitations leads to the need to search for a sufficiently rigorous analytical description of the SIEM system functioning process in dynamics. In our opinion, these restrictions can be most correctly taken into account in the framework of Markov models considered in a number of modern works.

The work [10] considers mathematical modeling based on the general theory of systems. A model has proposed here in abstract terms, which does not give the possibility to fully using it for modeling specific threats within the framework of the SIEM system.

In [11, 12], it is argued that the model of a complex controlled process can be implemented on the basis of stochastic differential equations. But these models require significant costs for collecting source data statistics to simulate the dynamics of changes in parameter values and quality indicators of SIEM systems. They do not provide the user's needs for unification and usability. These models are complex in terms of describing the process dynamics.

Thus, in [13–15], applications of the models based on stochastic differential equations were proposed, but the traditional methods, used to determine the parameters of the changes in the values of the quality indicators of the modeling object, are ineffective due to the need to consider many auxiliary parameters to fully describe all the properties of SIEM systems, but this is not always possible.

Works [16–21] are devoted to the possibilities of a mathematical description of processes in dynamics using Markov chains. Such approaches will be considered in our work as well, these will be dynamic models of the SIEM system functioning. They are the basis for modeling, however, these works do not address the problem of calculating the joint probability distribution density of various quality indicators of the SIEM system functioning.

The model considered in [22] is partially free from these drawbacks, however, this model, although it relies on Markov chains in the form of stochastic difference equations, is focused on modeling the processes of detecting malicious information.

The closest in essence to the idea proposed in this chapter is the work [23], where a Markov model of the decision-making process for managing information and security events is proposed.

Thus, the analysis of related works shows that Markov process models are highly versatile, and the combination of the theory of Markov processes with the theory of state variables opens up wide opportunities for the study of complex systems, such as SIEM systems.

In other words, we can assume the theoretical and practical possibility of constructing analytical, probabilistic-temporal models of state transition of the SIEM system functioning (as the mathematical models of the state change of QIs for these systems) based on Markov sequences. Besides, it is needed to achieve the required degree of adequacy for the probability-time properties of such system functioning while reducing the dimension of their mathematical description.

3 Theoretical Part

It is known that obsolescence of information about the state of the SIEM system functioning reduces the dependence of decisions made at the moment t_k on earlier observations, thereby providing the possibility of limiting the aftereffect ("memory") of the mathematical description of this system functioning.

Analysis of these restrictions leads to the need to search for a fairly rigorous description of the SIEM system functioning in dynamics. Most correctly, these restrictions can be taken into account in the framework of Markov models.

Markov process models are highly versatile, and the combination of the theory of Markov processes with the theory of state variables opens up wide possibilities for the analytical description of SIEM systems in dynamics.

The analysis of [10–23] shows that the application of Markov models to real processes occurring in complex information protection systems has a number of advantages based on the possibility to represent both discrete and continuous processes in the framework of Markov processes, which are characterized by both Gaussian, and non-Gaussian probability distributions, taking into account both the linear and non-linear nature of their change.

In addition, by expanding the connectedness ("memory") of the process and its dimension (for example, the transition to nested Markov chains) non-Markov processes can be mathematically correctly reduced to more complicated Markov processes [16].

As you know, most of the QIs of the SIEM system are continuously valued. The need and the possibility of approximating them mathematical

1. The generally accepted description of the dynamics of changes in continuously-valued QIs at discrete time instants is based on the apparatus of stochastic differential equations. But the use of this mathematical apparatus, although it provides high adequacy of the models to the processes that they describe, but leads to great computational complexity (known in mathematics as the "curse of dimensionality"). Ultimately, taking into account the variety of QIs of the SIEM system and their complex hierarchy, this makes the models and the entire apparatus for assessing the quality and effectiveness of the SIEM system cumbersome and re-quires large computational costs.
2. The possibility of approximating continuous processes by Markov sequences with discrete time allows, based on user-defined requirements for the QIs of the SIEM system and the accuracy of their estimation, one to simulate processes occurring in the system with a predetermined simulation error in time Δt_{perm} and state Δx_{perm}, whereas when modeling continuous processes using stochastic differential equations, the modeling error is unknown.
3. It is known that the space of process control resources implemented by the SIEM system is discrete and limited. This fact is an additional argument confirming the need to formalize the description of these processes and to control these processes within the framework of a single mathematical apparatus.
4. An important argument is a fact that currently there are methods for the reduction of the continuously-valued state and observation spaces based on the sensitivity theory methods.
5. In most cases, the user does not need to know all the continuous-valued states of the QIs of the SIEM system. To assess the state of the QIs of the SIEM system

at a certain point in time, it is quite enough to know its discrete value and the accuracy of maintaining this value.

Given all of the above, one can consider the possibility of constructing analytical, probabilistic-temporal models of state transitions of the SIEM system functioning process as mathematical models of state transitions QI of a system of this class based on Markov sequences, achieving the required degree of adequacy of the probabilistic-time properties of the SIEM process while reducing the dimension of their mathematical description.

The need to unify the mathematical specification of the SIEM system functioning, including the decision-making procedures, is caused by the desire for wider integration and integrated use of information protection methods and tools at all stages of investigating the interaction procedures of telecommunication, the local area, and global networks. It can be provided with sufficient description accuracy by using different classes of random processes with discrete-time.

Thus, to build an analytical probabilistic-temporal model of the state transition of the vector of QIs of the SIEM system that takes into account the dynamic and probabilistic nature, as well as the non-stationarity of the process of its functioning and control, we will use the apparatus of controlled Markov chains described in the form of difference stochastic equations.

An analysis of [10–23] allows one to say that all known classes of Markov random processes can be reduced to equivalent Markov chains (up to an admissible error of simulation in time Δt_{perm} and state Δx_{perm}). This type of models differs from that used previously since the possibility of using controlled Markov chains in the form of stochastic difference equations for vector analysis of the quality of the SIEM system functioning has not yet been investigated. Taking into account the results of the analysis, it can be argued that it is not difficult to pass from stochastic differential equations for discontinuous processes to difference stochastic equations, which for discrete models of state transition of QIs of the SIEM system functioning in the form of controlled Markov chains ($T = \text{const}$) will look like:

$$\vec{x}(k+1) = C^{\mathrm{T}}(k+1)\vec{\Theta}(k+1); \tag{1}$$

$$\vec{\Theta}(k+1) = \varphi^{\mathrm{T}}(k+1, k, k)\vec{\Theta}(k) + \vec{\vartheta}(k); \tag{2}$$

$$\vec{\vartheta}(k) = \left[\vartheta^{\mathrm{T}}(k)\vec{\Theta}(k)\right]\vec{\vartheta}'(k+1); \tag{3}$$

$$Z(k+1) = H(k, x(k))\vec{\Theta}(k+1) + \vec{\omega}(k+1), \tag{4}$$

where the expression (1) is the equation of the process x state at the $(k+1)$-th step (in our case, this is the state of some QIs of the SIEM system functioning), in which: $C^{\mathrm{T}}(k+1)$ is a matrix-row of possible values of the deviations of QIs of the SIEM system functioning; $\vec{\Theta}(k+1)$ is an auxiliary vector of QIs of the SIEM system functioning, taking values 0 or 1 and introduced for the convenience of recording the dynamics of transitions of this class system functioning from state to state ($m = \overline{1,\ M}$—the number of states).

Expression (2) is the equation of the state of the auxiliary vector of indicators, in which: $\varphi^{\mathrm{T}}(k+1, k, u)$ is the probability matrix of the transition of the process, which determines the change of states of the QIs of the SIEM system functioning; $\vec{\Theta}(k)$ is a vector of values of the status indicators in the previous step; $\vec{\vartheta}(k)$ is a vector of compensation additives, the elements of which are designed to compensate the non-integer part of the equation and are obtained by correcting the initial excitation noise—white Gaussian noise (WGN, wgn) $\vartheta^{\mathrm{wgn}}(k)$ with the mathematical expectation and dispersion corresponding to the initial state of the estimated QIs of the SIEM system functioning—Eq. (3)

The validity of the use of white Gaussian noise as excitation noise with parameters adequate to the real process is due to the nature of random values of the QIs of the SIEM system; $\vartheta^{\mathrm{T}}(k)$ is a diagonal block matrix of compensation additives, which is a stepped martingale, the elements of which are designed to compensate the non-integer part in Eq. (2); $\vec{\vartheta}'(k+1)$ is the vector of values of the modified exciting noise, which determines the values $\vec{\Theta}$ at the $(k + 1)$ step (values of auxiliary indicators of the process $x\ (k + 1)$).

Expression (4) is the equation for observing the state transition process of QIs for the SIEM system functioning $x(k)$, where $H(k, x(k))$ is the observation matrix containing known values for observing the state of the process $x(k)$:

$$H(k, x(k)) = \begin{vmatrix} x_1(k) & 0 & \cdots & 0 \\ 0 & x_1(k) & \cdots & 0 \\ \vdots & \vdots & \ddots & \vdots \\ 0 & 0 & \cdots & x_1(k) \end{vmatrix}; \tag{5}$$

$\vec{\omega}(k+1)$ is a vector of observation noise of the state transition process $x(k)$ of QIs of the SIEM system with zero mean and variance matrix $\vartheta_{\omega}(k)$.

4 Methodological Part and Discussion

The vector of values of the modified exciting noise $\vec{\vartheta}'(k+1)$, which determines the values $\vec{\Theta}$ at the $(k + 1)$ step (the values of the auxiliary process indicators $x\ (k + 1)$), is formed on the basis of comparison of the threshold values of the deviations of QIs of the SIEM system functioning process with the sample values of white Gaussian noise $\vartheta_m^{\mathrm{wgn}}(k)$, converted into exciting noise $\vartheta_m'(k+1)$ through a linear procedure:

$$\vartheta'_m(k+1) = |\Psi(k+1)|\vartheta^{\text{wgn}} + \Delta\varsigma_\vartheta(k) \underset{''0''}{\overset{''1''}{\gtrless}} x_{\text{thr}\,m}, \text{ at} \begin{cases} \text{M}[\vartheta'(k+1)] = \Delta\varsigma_\vartheta(k), \\ \text{D}[\vartheta'(k+1)] = \Psi^2(k), \end{cases} \tag{6}$$

which in matrix form has the form:

$$\begin{vmatrix} \vartheta'_1(k+1) \\ \vartheta'_2(k+1) \\ \vdots \\ \vartheta'_m(k+1) \end{vmatrix} = \begin{vmatrix} \Psi_1(k) & 0 & \cdots & 0 \\ 0 & \Psi_2(k) & \cdots & 0 \\ \vdots & \vdots & \ddots & \vdots \\ 0 & 0 & \cdots & \Psi_m(k) \end{vmatrix} \times \begin{vmatrix} \vartheta_1^{\text{wgn}}(k) \\ \vartheta_2^{\text{wgn}}(k) \\ \vdots \\ \vartheta_m^{\text{wgn}}(k) \end{vmatrix} + \begin{vmatrix} \Delta\varsigma_{\vartheta_1}(k) \\ \Delta\varsigma_{\vartheta_2}(k) \\ \vdots \\ \Delta\varsigma_{\vartheta_m}(k) \end{vmatrix}, \tag{7}$$

where $\Delta\varsigma_{\vartheta_m}(k)$ are the increments of the mathematical expectation of the process being formed, obtained on the basis of a priori data on the Markov chain, in relation to the mathematical expectation of white Gaussian noise exciting this process; $\Psi_m(k) = T\sqrt{2\sigma_\Theta^2 q_{mm}/N_{\vartheta_m}}$—coefficient correcting the dispersion of Gaussian noise based on a priori data on the Markov chain for this step; $|\Psi(k)| = G(t)T = diag\left\{T\sqrt{2\sigma_\Theta^2 q_{mm}/N_{\vartheta_m}}\right\}$—matrix of diffusion (excitation) of the process $\vec{\Theta}(k)$; σ_Θ^2—the dispersion of the process $\vec{\Theta}(k)$; q_{mm}—elements of the matrix of transition intensities of auxiliary indicators of the state of the SIEM system functioning.

Let us consider in detail the steps of the methodology for determining the elements of the vector of compensatory additives in the state equation of this modified model of the SIEM system taking into account the conversion of excitation noise.

The analysis results (based on a priori data on the Markov chain) to which state the process "tends" in the next step give us a decisive rule for choosing the vector of compensation additives and, ultimately, for determining the values of the elements of the vector of auxiliary state indicators $\vec{\Theta}_m(k+1)$ of the SIEM system functioning.

The values $\Delta\varsigma_{\vartheta_m}(k)$, that correct the probabilities of the state of the initial excitation noise $\vartheta^{\text{wgn}}(k)$, can be calculated for the case of a homogeneous circuit a priori, based on the expression:

$$\Delta\varsigma_{\vartheta_m}(k) = (1 - p_m(\varsigma_{\vartheta_m}(k)))^{-1} = \Phi^{-1}(-\varsigma_{\vartheta_m}(k)) \tag{8}$$

where (–1) is the symbol of the inverse function; $1 - \Phi^{-1}(-\varsigma_{\vartheta_m}(k))$—the probability integral; $p_m(\varsigma_{\vartheta_m}(k))$—the probability that the process takes the value $\vartheta'_m > 0$, numerically equal to the probability of the process Θ_m adopting a value $\Theta_m(k+1) = 1$,

$$p_m(\varsigma_{\vartheta_m}(k)) = p_m(k) = \sum_{i=1}^{M} p_i(k-1)\, p_{i\,m}(k-1\,|\,k), \quad m = \overline{1,\ M}, \tag{9}$$

where M—is the number of process states.

The calculation of the values of the coefficient $\Psi_m(k)$, correcting the variance of random discrete realizations of the initial white Gaussian noise $\vartheta^{\text{wgn}}(k)$, occurs as follows.

Given that the spectral density of the excitation noise power $\vartheta'(k)$ is related to its dispersion by the expression $N_\vartheta = \sigma_\vartheta^2 T$ and the intensity of the transition of the process $\Theta(k)$ from state to state is linked with the corresponding probabilities by the expression $q_{mm} = p_{mm} / T$, the equation for the coefficient $\Psi_m(k)$ can be written in the form

$$\Psi_m(k) = 2\ p_{mm}(k). \tag{10}$$

If the value of the modified excitation noise $\vartheta'_m(k+1)$, selected taking into account the entered coefficients, falls within the tolerance limits $-\Delta\varsigma_\vartheta \leq \vartheta'_m(k+1) \leq +\Delta\varsigma_\vartheta$ (which shows the "tendency" Θ_m at the $(k+1)$-th step to 1), in Eq. (3) it is decided that the element of the vector of compensation additives $\vartheta'_m(k)$ is positive and the remaining elements of this vector are negative, which, when solving the Eq. (2), gives us $\Theta_m(k+1) = 1$. The formation of the current values of the matrix of compensation additives $\vartheta(k)$ occurs in accordance with the rule:

If the process is described by two states Θ_0 and Θ_1, (i.e., $m = \overline{1,\ 2}$), then the vector of the excitation sequences for determining the value of the auxiliary indicator of the state Θ_1 of the SIEM system functioning is found from the matrix:

$$\vartheta_1(k) = \begin{vmatrix} \vartheta_1^{11}(k) & \vartheta_1^{12}(k) \\ \vartheta_1^{21}(k) & \vartheta_1^{22}(k) \end{vmatrix} = \begin{vmatrix} -p_{12}(k) & (1 - p_{12}(k)) \\ -p_{21}(k) & (1 - p_{21}(k)) \end{vmatrix}; \tag{11}$$

If we use three or more states Θ_m, (i.e. $m = 1, 2, \ldots, M$) to describe the process of changing the QIs states of the SIEM system functioning, then the matrix of compensation additives for the m-th state $\vartheta_m(k)$ is selected (at the first stage of solving the Eq. (3)) and the vector of compensation additives from this matrix $\vec{\vartheta}_m$ (at the second stage of solving Eq. (3)) comes from the block diagonal matrix of the form:

$$\|\vartheta(k)\| = \begin{vmatrix} |\vartheta_1(k)| & 0 & \cdots & 0 \\ 0 & |\vartheta_2(k)| & \cdots & 0 \\ \vdots & \vdots & \ddots & \vdots \\ 0 & 0 & \cdots & |\vartheta_m(k)| \end{vmatrix}. \tag{12}$$

The elements $\vartheta_m(k)$ of the matrix of the current compensation additives for various states of the QIs of the SIEM system functioning are in accordance with the rule

$$|\,\vartheta_m(k)\,| = \begin{vmatrix} \vartheta_{11}(k) & \vartheta_{21}(k) & \vartheta_{31}(k) & \cdots & \vartheta_{m1}(k) \\ \vartheta_{12}(k) & \vartheta_{22}(k) & \vartheta_{32}(k) & \cdots & \vartheta_{m2}(k) \\ \vartheta_{13}(k) & \vartheta_{23}(k) & \vartheta_{33}(k) & \cdots & \vartheta_{m3}(k) \\ \vdots & \vdots & \vdots & \ddots & \vdots \\ \vartheta_{1m}(k) & \vartheta_{2m}(k) & \vartheta_{3m}(k) & \cdots & \vartheta_{m}(k) \end{vmatrix} =$$

$$= \begin{vmatrix} (1-p_{m1}(k)) & -p_{m1}(k) & -p_{m1}(k) & \cdots & -p_{m1}(k) \\ -p_{m2}(k) & (1-p_{m2}(k)) & -p_{m2}(k) & \cdots & -p_{m2}(k) \\ -p_{m3}(k) & -p_{m3}(k) & (1-p_{m3}(k)) & \cdots & -p_{m3}(k) \\ \vdots & \vdots & \vdots & \ddots & \vdots \\ -p_{mm}(k) & -p_{mm}(k) & -p_{mm}(k) & \cdots & (1-p_{mm}(k)) \end{vmatrix}. \quad (13)$$

The number of states m is determined on the basis of the required accuracy of estimating the QIs of the SIEM system functioning.

Optimizing the dimension of the state and observation spaces of the SIEM system functioning, taking into account the requirements for an acceptable estimation error, is a separate theoretical and practical problem.

The final result of solving the Eq. (3) is the vector of compensating additives $\vec{\vartheta}_m(k)$ for the considered m-th state of the QIs of the SIEM system:

$$\vec{\vartheta}_m(k) = \begin{vmatrix} \vartheta_{m1}(k) \\ \vartheta_{m2}(k) \\ \vartheta_{m3}(k) \\ \vdots \\ \vartheta_{mm}(k) \end{vmatrix}. \quad (14)$$

Thus, it is shown that the proposed methodological approach allows one to determine the values of the increment of the mathematical expectation of the simulated process, obtained on the basis of a priori data on the Markov chain, in relation to the mathematical expectation of white Gaussian noise exciting this process.

This approach combines the calculation of the values of the mathematical expectation of the process being formed and the values of the coefficient that corrects the variance of random discrete realizations of the initial white Gaussian noise and allows one to decide what values the elements of the compensation additives vector will take in the equation of the state of this modified model of the SIEM system taking into account the noise excitation transformation.

5 Conclusions

Thus, on the basis of expressions (1–14), the chapter has suggested a variant of the analytical description of the dynamics of the change in the state of the quality indicators of the SIEM system functioning. In fact, the chapter has presented a generalized model of the functioning of this class system taking into account the conversion of excitation noise.

This model is a formalized analytical specification (in terms of a Markov chain in the form of difference stochastic equations) of the dynamics of changes in the values of the quality indicators of SIEM systems. The quality indicators characterize the essential properties of the SIEM system functioning in the state space.

The practical application of the improved model is possible both in the framework of research work and in integrated systems for automated control of information security. The direction of further research may be the development of models that take into account not only quantitative but also qualitative (for example, described using linguistic variables typical for fuzzy sets) nature of quality indicators of these class systems.

Acknowledgements This work was partially supported by the grant of RFBR (the projects No. 18-29-22034) and by the budget (the project No. 0073-2019-0002).

References

1. Kizza, J.M.: Guide to Computer Network Security, 3rd edn, 545 pp. Springer, New York (2015)
2. Sun, Y.: Research on security issues and protection strategy of computer network. The Open Autom. Control Syst. J. **7**, 2097–2101 (2015)
3. Dordal, P.L.: An Introduction to Computer Networks. Release 1.9.0. January 27, 745 pp (2017)
4. Pfleeger, C.P., Pfleeger, S.L.: Security in Computing, 944 pp. NJ, Prentice Hall (2015)
5. Miller, D.R., Harris, S., Vandyke, S.: Security Information and Event Management (SIEM) implementation, 430 pp. New York, McGrawHill (2011)
6. Kent, K., Souppaya, M.: Guide to Computer Security Log Management, 72 pp. NIST Special Publication 800–92. Gaithersburg, US, NIST (2006)
7. Maimbo, C.: Exploring the Applicability of SIEM Technology in IT Security: masters thesis, 116 pp. Auckland University of Technology (2014)
8. Kotenko, I., Parashchuk, I.: Synthesis of controlled parameters of cyber-physical-social systems for monitoring of security incidents in conditions of uncertainty. J. Phys.: Conference Series, IOP Publishing. **1069**(1), 012153, 1–6 (2018)
9. Kotenko, I., Doynikova, E.: Countermeasure selection in SIEM systems based on the integrated complex of security metrics. Proceedings of the 23th Euromicro International Conference on Parallel, Distributed and network-based Processing (PDP 2015). Turku, Finland. 4–6 March 2015. Los Alamitos, California. IEEE Computer Society. pp. 567–574 (2015)
10. La Padula, L.: Secure Computer Systems: A Mathematical Model. MTR-2547, Vol. I, The MITRE Corporation, 33 pp. Bedford, MA (1993)
11. Higham, D.: An algorithmic introduction to numerical simulation of stochastic differential equations. SIAM REVIEW **43**(3), 525–546 (2001)
12. Iacus, S.: Simulation and Inference for Stochastic Differential Equations. With R Examples, 214 pp. Springer Verlag (2008)

13. Yuksel, S.: Control of Stochastic Systems, 167 pp. Queen's University Mathematics and Engineering and Mathematics and Statistics (2017)
14. Van Handel, R.: Stochastic Calculus, Filtering and Stochastic Control, 261 pp. Springer, New York (2007)
15. Oksendal, B.: Stochastic Differential Equations. An introduction with Applications, 311 pp. Springer Verlag (2007)
16. Stewart, N., Thomas, G.: Markov processes. In: Proc. of Probability and Mathematical Statistics, pp. 214–234. John Wiley & Sons Inc., New York (1986)
17. Bini, D., Latouche, G., Meini, B.: Numerical Methods for Structured Markov Chains, 215 pp. Oxford University Press, New York (2005)
18. Dobre, T.G., Jose, G., Sanchez Marcano: Chemical Engineering: Modeling, Simulation and Similitude, 568 pp. Weinheim, Wiley-VCH (2007)
19. Oliver, D., Kelliher, T., Keegan, J.: Engineering Complex Systems with Models and Objects, 325 pp. McGraw-Hill Companies, New York (2007)
20. Quarteroni, A.: Mathematical Models in Science and Engineering. Proc. of Notices of the AMS **56**(1), 9–19 (2009)
21. Tweedie, R.: Drift conditions and invariant measures for Markov chains. Stoch. Process. Their Appl. **92**(2), 345–354 (2001)
22. Kotenko, I., Parashchuk, I.: Determining the parameters of the mathematical model of the process of searching for harmful information. In: Kravets, A.G. et al. (eds.) Cyber-Physical Systems: Industry 4.0 Challenges. Studies in Systems, Decision and Control 260, pp. 225–236. Springer Nature Switzerland AG 2020 (2019)
23. Kotenko, I., Parashchuk, I.: An approach to modeling the decision support process of the security event and incident management based on Markov chains. In: Proc. of 9th IFAC Conference on Manufacturing Modelling, Management and Control (MIM-2019). (Berlin, Germany, 28–30 August 2019) Ivanov, D. Dolgui, A., Yalaoui, F. IFAC-Papers OnLine **52**(13), 934–939 (2019)

Secure Data Transmission in Cyber-Physical Systems Based on the New Approach for Stream Cipher's Gamma Generation

Igor Anikin and Khaled Alnajjar

Abstract We suggested a new approach for secure gamma generation in stream ciphers with application to secure data transmission between components of cyber-physical systems (in terms of ensuring confidentiality). Secure gamma generation is based on using a new type of pseudo-random number generator (PRNG) with linear feedback shift registers (LFSR) and fuzzy logic. We used a nonlinear combination function based on fuzzy logic for selecting the best LSFR while generating the output. We adjusted some parameters of fuzzy PRNG (FPRNG) to get the best pseudo-random sequences (gamma), which are very close to white random noise. We also studied the structure of FPRNG to select the best design that better fits the requirements of good gamma generators with application to cyber-physical systems. We showed that the suggested approach allows generating gamma sequences with better quality than many others. It makes possible using this approach in new stream ciphers and applying them to ensure confidentiality of data transmission between different components of cyber-physical systems (CPS).

Keywords CPS · Stream cipher · Pseudo-random number generator · LFSR · Fuzzy logic

1 Introduction

Nowadays, cyber-physical systems (CPS) started to play an important role in Industry 4.0 and different smart applications [1, 2] including smart cities, smart grids, smart homes, smart manufacturing, intelligent transportation systems, and many others [3, 4]. Such systems involve a lot of different hardware and software components that are strongly interconnected and constantly interact with each other in different ways.

I. Anikin (✉)
Kazan National Research Technical University named after A.N. Tupolev-KAI, 10 K.Marx Str, Kazan 420111, Russia
e-mail: IVAnikin@kai.ru

K. Alnajjar
Higher Institute for Applied Science and Technology, Damascus, Syria
e-mail: Khaled.alnajjar@hiast.edu.sy

A. G. Kravets et al. (eds.), *Cyber-Physical Systems*, Studies in Systems, Decision and Control 350, https://doi.org/10.1007/978-3-030-67892-0_27

CPS is often considered as a complex distributed system, which is controlled by different algorithms (including AI), closely integrated with the Internet and people. It also involves different technologies such as simulation and modeling, big data, mechatronics, cloud computing, IoT, augmented reality, etc.

The progress of CPS is closely related to the efficiency of communication between its components. Modern CPS uses different communication mechanisms and protocols for such interconnection. They can use WIFI, 4G, Bluetooth, and other mechanisms for doing that. In this case, one the main problem which arises for CPS is ensuring the security of this communication, including data confidentiality, integrity, reliability, and availability. We have a lot of sensitive information that is transferring between CPS components. This information has to be protected.

Different protocols that could be used to provide the security of communication between CPS components. However, the problem of security enhancement for them is constantly relevant. In this case, it is needed to develop new methods and approaches for increasing the security of data transmission in CPS.

We suggested a new approach for increasing the data confidentiality in CPS communication channels. It is based on secure gamma generation for stream ciphers which are widely used for data encryption in different communication protocols.

2 Background

The security level of many ciphers strongly is based on the quality of embedded gamma generators that produce unpredictable long bitstreams (keystreams) with good statistical properties, close to random noise. Pseudo-random number generators (PRNGs) suggest an effective way to produce such sequences of random bits or numbers from a randomly chosen secret seed [5]. For example, we can see the diagram of a typical stream cipher in Fig. 1 where Key is the secret input (seed) of PRNG which produces a bitstream (keystream) as random white noise. The keystream is combined with the plain stream M using the bitwise exclusive-OR (XOR) operation.

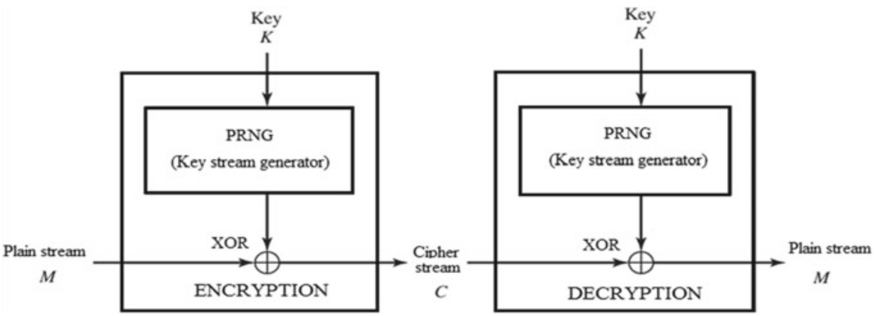

Fig. 1 General stream cipher diagram

The decryption stage requires the generation of the same pseudorandom sequence to get the plain stream. This approach is used widely in different stream ciphers and protocols of secure data transferring in cyber-physical systems: A5/1 (GSM cellular networks), RC4 (WIFI, Skype), SEAL, CryptMT, and others [6].

We have to ensure that generated keystreams have to be very close to the real true random sequences. They must be unpredictable, have long periods, and satisfy the cryptographic properties mentioned in [7]. They also have to pass successfully standard statistical tests from NIST STS and DIEHARD packets.

Linear feedback shift registers (LSFR) is one of the famous well-known elements of binary pseudorandom sequences generators [8] with very high performance which is important for gamma ciphers. The output sequence of LFSR can be described by the initial state $(s_0, s_1, \ldots, s_{n-1})$ and linear recurrence relation (1):

$$s_{k+n} = \sum\nolimits_{i=0}^{n-1} c_i s_{k+i}, \text{ where } k \geq 0 \tag{1}$$

Here the coefficients c_i are called feedback coefficients of the LFSR.

It has been shown that a binary stream generated by LFSR has good statistical properties if its characteristic polynomial is primitive. The period T of such sequence (M-sequence) is defined as $T = 2^n - 1$, where n is the degree of the characteristic polynomial. The quality of the M-sequences is also growing with the increasing degree of LFSR characteristic polynomial.

PRNG based on LFSRs is one of the fastest long-period generators currently available. They also require less hardware for implementation and produce pseudorandom sequences with good properties. It makes possible using such PRNG as embedded elements on CPS devices. However, the main drawback of such generators is their linearity which leads to insecurity. In this case, knowing only 2n consecutive bits enables the cryptanalyst to determine the feedback coefficients and thus the whole sequence. One way to overcome this problem is by using complex nonlinear functions to mix the outputs of several LFSR's. We consider the way for construction such a combination function by using fuzzy sets theory, linguistic variables, and fuzzy IF-THEN rules [9, 10].

3 Pseudo-Random Number Generator with Fuzzy Logic

We suggested the general structure of a pseudo-random number generator with fuzzy logic (FPRNG) in [11, 12]. This structure is presented in Fig. 2 and involves n LFSRs ($n \geq 2$), n buffers with a fixed size, which gather output bits from corresponding LSFRs, and a non-linear combination function based on fuzzy logic. This function includes two linguistic variables, fuzzy IF-THEN rules, and defuzzification block.

The goal of linguistic variables is to analyze the statistical properties of the buffers. The first linguistic variable assesses the number of ones (f_0) in the attached buffer. The second linguistic variable ($|f_1 - f_2|$) assesses the difference between the number of

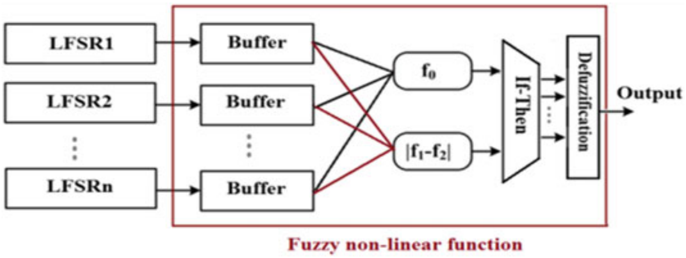

Fig. 2 The general structure of FPRNG

blocks (0110) consisting of two consecutive ones (f_1) and the number of gaps (1001) consisting of two consecutive zeros (f_2). The initial values of membership functions (MFs) for linguistic variables are presented in Fig. 3 (buffer size = 8).

The goal of IF-THEN rules is to compare the membership functions assessment results for the current buffer state and to select the best LSFR at the moment. Then least significant bit (LSB) of the associated buffer is passed to the output of FPRNG.

The gamma sequence generation flow chart is presented in Fig. 4.

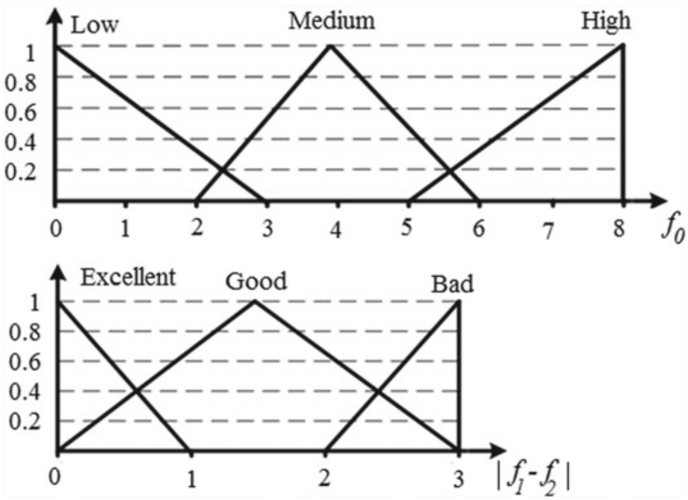

Fig. 3 Initial values of membership functions

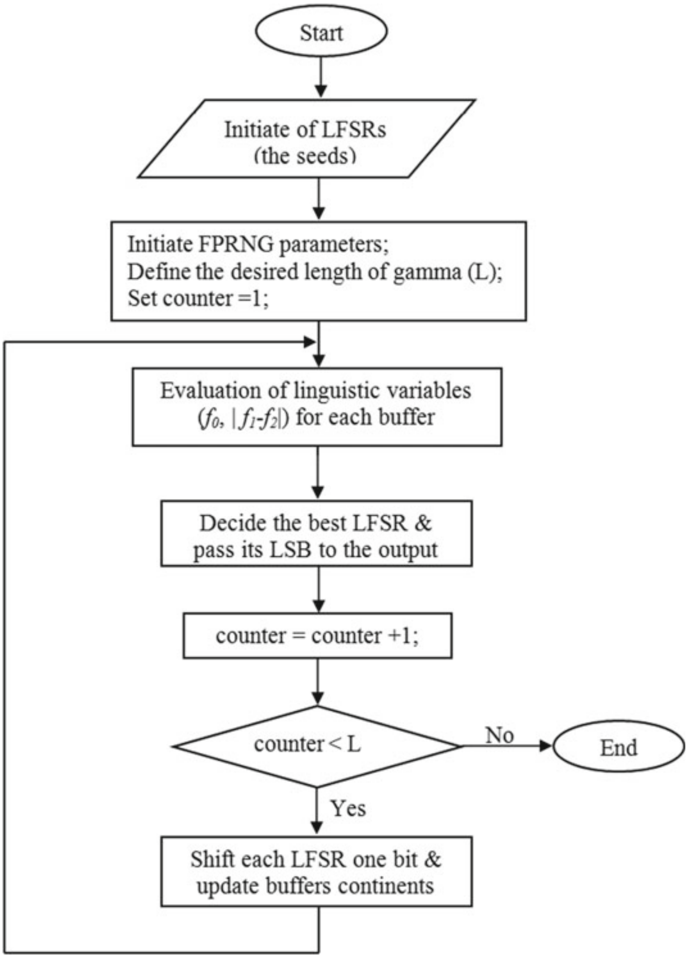

Fig. 4 Generation of gamma sequence based on FPRNG

4 Selection of the Rational Parameters' Values for FPRNG

We divide FPRNG's parameters into two groups. The first group contains one parameter related to LFSR. The second group contains several parameters related to the nonlinear function based on fuzzy logic.

4.1 FPRNG Parameter Related to LFSR

Selected LFSRs must guarantee the maximum period of the generated bitstream in addition to the randomness of the generated sequences. Thereby the characteristic polynomial of LFSR must be primitive, has a high degree and high Hamming weight (the number of the non-zero coefficients is not so different from half of its degree [13]). It should have low power consumption as well as low cost of hardware implementation. Finally, the selected polynomials should be co-prime with others to guarantee the maximum period of the generated sequence by FPRNG.

In [11, 13] authors recommended using a special type of primitive polynomial in FPRNG defined by expression (2). We proved that using such type of primitive polynomials allows satisfying all previously mentioned requirements. Low-power consumption and low cost of a hardware implementation for such polynomials make it possible to use corresponding FPRNGs as embedded elements on CPS devices.

$$P(x) = \left(1 + x^{b_1}\right)\left(1 + x^{b_2}\right)\ldots\left(1 + x^{b_m}\right) + x^n \tag{2}$$

Here $b_1, \ldots, b_{m,}n$ values satisfy the following conditions:

$$b_1 \geq 1, b_1 < b_2, (b_1 + b_2) < b_3, (b_1 + b_2 + \ldots + b_{m-1}) < b_m,$$
$$(b_1 + b_2 + \ldots + b_m) < n,$$

We selected characteristic polynomials defined by expression (3) for FPRNG with two LFSRs. They allow generating gamma with period $T = T^{1\cdot}T^2 = \left(2^{89} - 1\right)\left(2^{97} - 1\right) \approx 10^{56}$.

$$P_1(x) = (1 + x)\left(1 + x^5\right)\left(1 + x^{10}\right)\left(1 + x^{17}\right)\left(1 + x^{39}\right) + x^{89} \tag{3}$$

$$P_2(x) = (1 + x)\left(1 + x^4\right)\left(1 + x^7\right)\left(1 + x^{20}\right)\left(1 + x^{53}\right) + x^{97}$$

4.2 FPRNG Parameters Related to Non-Linear Function Based on Fuzzy Logic

We considered following FPRNG parameters related to non-linear function based on fuzzy logic: length of the buffers, number of fuzzy terms of linguistic variables $f_0, |f_1 - f_2|$, type of their membership functions, and used IF-THEN rules.

Initially, we defined these parameters as following: buffer size = 8 bit, three terms for each linguistic variable—“Low”, “Medium”, “High” for the linguistic variable f_0 and “Excellent”, “Good”, “Bad” for the linguistic variable $|f_1 - f_2|$ (see Fig. 3). IF-THEN rules were described in Table 1. Table 2 describes the rules for the

Table 1 Initial fuzzy IF-THEN rules

MF	Low	Medium	High
Excellent	Bad	Best	Bad
Good	Good	Good	Good
Bad	Bad	Good	Bad

Table 2 Defuzzification process

LSFR2\LSFR1	Best	Good	Bad
Best	Bit1	Bit2	Bit2
Good	Bit1	Bit1	Bit2
Bad	Bit1	Bit1	Bit1

defuzzification process, where Bit1 refers to the LSB of the buffer associated with LFSR1, Bit2 refers to the LSB of the buffer associated with LFSR2.

4.3 Evaluation of FPRNG Parameters

All parameters were investigated to find the best values for them. This evaluation was accomplished depending on the most important five randomness tests of the NIST packet that were defined by authors in [14]. The generated gamma bitstream was divided into subsequences. We applied five selected NIST tests for these subsequences and obtained the corresponding P-values. Then three statistical criteria were used to compare the sequences with each other and define the best one [14].

Criteria 1. Calculation of the mean and standard deviation of P-values and comparing them with the uniform distribution.
Criteria 2. Applying the chi-square criterion with 9 degrees of freedom on obtained P-values [15, 16].
Criteria 3. Computing the percent of the subsequences that failed the tests.

Table 3 presented the selected best values of FPRNG parameters after evaluation. Final FPRNG successfully passed all NIST and DIEHARD randomness tests.

4.4 Demonstration of Work and Nonlinearity of Fuzzy Combination Function

A function f defined over a field F is called as linear function if it satisfies the following two conditions: (1) $x,y \in F: f(x + y) = f(x) + f(y)$; (2) $\forall$ x $\in F, \lambda \in \{0,1\}$: $f(\lambda x) = \lambda f(x)$.

Table 3 Selected values for FPRNG parameters

Parameter	Value
Characteristic polynomials	Defined by Eq. 3
Size of buffers	32
Number of terms for $(f_0, \|f_1 - f_2\|)$	(3,3)
Type of the MFs	Trapezoidal
Configurations of MF f_0 for LFSR1	Low: {0,…,9}, Medium:{10,…,20}, High:{21, …, 32}
Configurations of MF $\|f_1 - f_2\|$ for LFSR1	Excellent:{0,…, 2}, Good:{3, 4}, Bad: {5,…10}
Configurations of MF f_0 for LFSR2	Low: {0,…, 11}, Medium: {12,…, 18}, High: {19,…, 32}
Configurations of MF $\|f_1 - f_2\|$ for LFSR2	Excellent: {0, 1}, Good: {2, 3}, Bad: {4,…, 10}

To prove that the function f is not linear, it's enough to find one opposite example showing that one of the mentioned above conditions is not fitted. In our case, the variables x, y are vectors of n values of the field $GF(2^m)$ and each value is related to the corresponding buffer, where m is the size of the buffer. To simplify the study without wasting the main goal, we will do it on the simplest structure of the FPRNG that contains only two LFSRs ($n = 2$) with buffer size ($m = 8$). After initialization of FPRNG and running it, we can find a lot of values of x, y that meet the desired purpose, for example:

$$x = \begin{cases} 10110110 \\ 11100101 \end{cases}, y = \begin{cases} 01101101 \\ 11001011 \end{cases}$$

Then we compute the sum modulo 2 of x, y bitwise:

$$x + y = \begin{cases} 10110110 \\ 11100101 \end{cases} + \begin{cases} 01101101 \\ 11001011 \end{cases} = \begin{cases} 11011011 \\ 00101110 \end{cases}$$

In the next step, we analyze the statistical properties of the buffers using the previously described linguistic variables $(f_0, |f_1 - f_2|)$ and the associated membership functions:

$$\mathrm{f_0(x)} = \begin{cases} 5 \\ 5 \end{cases} \overset{\text{fuzzification}}{\rightarrow} \begin{cases} \text{Medium} \\ \text{Medium} \end{cases}, |\mathrm{f_1(x)} - \mathrm{f_2(x)}| = \begin{cases} 2 \\ 1 \end{cases} \overset{\text{fuzzification}}{\rightarrow} \begin{cases} \text{Bad} \\ \text{Good} \end{cases}$$

$$\mathrm{f_0(y)} = \begin{cases} 5 \\ 5 \end{cases} \overset{\text{fuzzification}}{\rightarrow} \begin{cases} \text{Medium} \\ \text{Medium} \end{cases}, |\mathrm{f_1}(y) - \mathrm{f_2(y)}| = \begin{cases} 2 \\ 1 \end{cases} \overset{\text{fuzzification}}{\rightarrow} \begin{cases} \text{Bad} \\ \text{Good} \end{cases}$$

$$\mathrm{f}_0(\mathrm{x}+\mathrm{y}) = \begin{cases} 6 \\ 4 \end{cases} \overset{\text{fuzzification}}{\rightarrow} \begin{cases} \text{High} \\ \text{Medium} \end{cases}$$

$$|\mathrm{f}_1(\mathrm{x}+\mathrm{y}) - \mathrm{f}_2(\mathrm{x}+\mathrm{y})| = \begin{cases} |1-0| = 1 \\ |0-0| = 0 \end{cases} \overset{\text{fuzzification}}{\rightarrow} \begin{cases} \text{Good} \\ \text{Excellent} \end{cases}$$

In the next step, we apply the predefined set of fuzzy If-Then rules (Table 1) to determine the results for each buffer.

$$x : \begin{cases} Medium,\ Bad \\ Medium,\ Good \end{cases} \overset{If-Then}{\rightarrow} \begin{cases} Good \\ Good \end{cases}$$
$$y : \begin{cases} Medium,\ Bad \\ Medium,\ Good \end{cases} \overset{If-Then}{\rightarrow} \begin{cases} Good \\ Good \end{cases}$$
$$(x+y) : \begin{cases} High,\ Good \\ Medium,\ Excellent \end{cases} \overset{If-Then}{\rightarrow} \begin{cases} Good \\ Best \end{cases}$$

Finally we use rules from Table 2 for defuzzification: $f(x) = \mathrm{LSB(LFSR1)} = 0$, $f(y) = \mathrm{LSB(LFSR1)} = 1, f(x+y) = \mathrm{LSB(LFSR2)} = 0$. We can check the linearity of the function f by comparing values $f(x) + f(y) = 1, f(x+y) = 0$. So $f(x) + f(y) \neq f(x+y)$. We can conclude that the constructed combination function f based on fuzzy logic is nonlinear.

4.5 Linear Complexity Profile of Fuzzy Combination Function

LSFR combination function should also have a high degree of nonlinearity or linear complexity. This complexity for a binary sequence is defined by the length of the smallest LFSR that can generate the same sequence [16, 17]. The graph of linear complexity profile is one of the most important measurements of the randomness for a finite sequence. The linear complexity profile of an unpredictable sequence of length *n* over *GF(2)* should be close to the *n/2* line. Figure 5 illustrates the linear complexity profile of a sequence of a length of 70 bit generated by the proposed FPRNG. We can see that it satisfies the requirement.

The graph of the linear complexity profile of a random sequence should look like “an irregular staircase” with valid step lengths (≈4) and stair heights (≈2) [17]. So any regular characteristics should be excluded from a random sequence [5, 18]. Evaluation of the linear complexity profile for a long sequence (≈1 Mbits) generated by FPRNG showed that it has very good linear complexity.

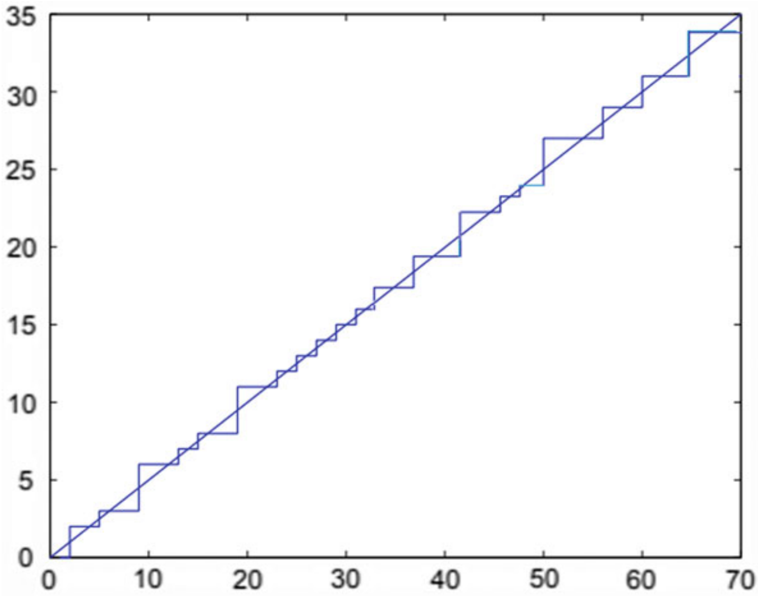

Fig. 5 Part of the linear complexity profile of the proposed FPRNG

5 Long LFSRs vs Many Short LFSRs

In this section, we answer the question "Is using a few long LFSRs better for generation good gamma than using a big number of relatively short LFSRs or not?".

To answer this question, we investigated two FPRNG variants: (1) FPRNG with 2 LFSRs which are defined by (3); (2) FPRNG with 4 LFSRs with the following characteristic primitive polynomials:

$$\begin{cases} P_1(x) = (1+x)(1+x^4)(1+x^{10})(1+x^{19}) + x^{37} \\ P_2(x) = (1+x)(1+x^6)(1+x^9)(1+x^{22}) + x^{41} \\ P_3(x) = (1+x)(1+x^2)(1+x^7)(1+x^{11}) + x^{47} \\ P_4(x) = (1+x^2)(1+x^8)(1+x^{14})(1+x^{27}) + x^{59} \end{cases}$$

We found the best parameter values for both FPRNG using the tuning technique presented in Chapter "The Methodology of Hybrid Modelling for Gas Turbine Subsystems Prescriptive Analytics" and checked that both generators passed all NIST and DIEHARD tests. However, we observed the difference between outputs of these FPRNGs related to their immunity against correlation attacks. We found that the probability of appearing the long runs (long blocks or gaps) is relatively high in the output stream of the LFSRs. In this case, the fuzzy nonlinear function selects the output of the other LFSR as the output of the generator (Fig. 6). Thus, considering the correlation attacks when performing the tuning process of the MFs, we can say that

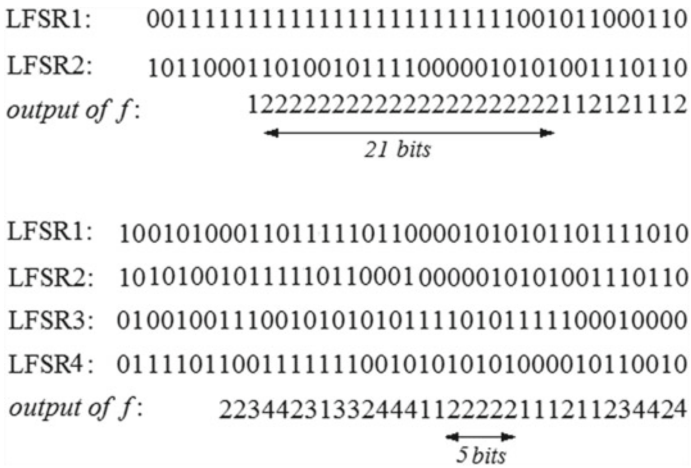

Fig. 6 Correlation magnitudes of two generators

using two long LFSRs leads to vulnerabilities in the generator's immunity against cor-relation attacks.

The second FPRNG which has a bigger number of shorter LFSRs showed higher immunity against correlation attacks. This happens due to the high frequency of switching between LFSRs and the lower probability of long runs on the output of the selected LFSRs. As a result, we can say, that the second FPRNG is better than the first one. So increasing the number of LFSRs increases the quality of the generated gamma sequences.

6 Comparison of FPRNG with Others

We compared FPRNG (2 LFSRs) with 21 well-known generators: 16 PRNG from the DIEHARD bundle [19] and 5 PRNG from different programming languages. 1Mbits length gamma sequences were generated by each of 21 PRNGs which compared with the 1Mbits gamma sequence generated by FPRNG. To compare the sequences we used the five most important tests from the NIST packet [20] and two statistical criteria (chi-square and number of failed subsequences). Table 4 summarizes the evaluation results.

The sign (+) in Table 4 means that the corresponding generator successfully passed all the five tests while the sign (−) means that the corresponding generator failed to pass one of the tests or more. We can see from Table 4 that the proposed FPRNG got the best results and increased the quality of the generated gamma sequence by 1.4 times compared with the best-obtained scores of the 21 famous PRNGs considering the number of failed subsequences criterion.

Table 4 FPRNG evaluation results

Generator	Chi-square ($\leq$ 21.67)	Number of fails
FPRNG	+	+ (36)
Multiply-with-carry	+	+ (47)
Multiply-with-carry on pairs of 16bits	+	−(51)
The mother of all random number generators	−	+ (55)
Kiss	−	+ (54)
Combo	+	+ (55)
The lagged Fibonacci-MWC combination ULTRA	−	+ (44)
A combination of multiply-with-carry & substract with borrow	−	+ (50)
Extended congruential	−	+ (43)
The super Duper generator	+	+ (63)
Substruct with borrow	−	+ (46)
Any specified congruential	−	+ (52)
The 31-bit ran2 from Numerical Recipes	−	+ (51)
Any specified shift register generator 31 or 32 bits	−	+ (53)
Microsoft Fortran	−	+ (58)
Any lagged-Fibonacci	+	− (94)
An inverse congruential	−	+ (35)
Java NB 8.1	−	+ (47)
Delphi	−	+ (45)
VB.Net Visual Studio	−	+ (51)
Wolfram Research Mathematica	−	+ (61)
MatLab R2014a	+	+ (50)

7 Conclusion

In this research, we proposed a new approach for secure gamma generation in stream ciphers. This approach could be easily used to increase the security of communication channels (in terms of ensuring confidentiality) between different components of cyber-physical systems. The suggested approach is based on the pseudo-random number generator with a fuzzy nonlinear combination function. The advantage of this approach is the possibility to make a tuning process for FPRNG to generate gamma sequences with good statistical properties.

We investigated the parameters of the proposed FPRNG and found the best values for them. Then we discussed the security of the produced sequences regarding correlation attacks and decided to use more LFSRs to avoid possible vulnerabilities. We compared FPRNG with 21 well-known PRNGs and proved that FPRNG has good statistical properties and improved the randomness quality of the generated sequences in 1.4 times comparing with the best PRNG. As a result, we can conclude the generated by FPRNG gamma sequences are very close to true random streams. They could be used safely in different ciphers. We used a special type of primitive polynomials in LSFRs with low-power consumption as well as low cost of hardware implementation. It makes possible using the suggested FPRNG as embedded elements on CPS devices.

Finally, we can conclude that the suggested approach can be effectively used to ensure the security of connections between different components of cyber-physical systems. Further research will be devoted to the possibility of the effective hardware implementation of suggested FPRNG which is very important for modern CPS. Suggested FPRNG could be also effectively used in different simulation models in cyber-physical systems. Further research could be devoted to this topic.

References

1. Suh, S.C., Tanik, U.J., Carbone, J.N., Egorlu, A.: Applied Cyber-Physical Systems, 253 pp. Springer-Verlag, New York (2014)
2. Ali, S., Al Balushi, T., Nadir, Z., Hussain, O.K.: Cyber Security for Cyber-Physical Systems, 768 pp. Springer International Publishing (2018)
3. Kravets, A.G., Bolshakov, A.A., Schervakov, M.V. (eds.): Cyber-Physical Systems: Advances in Design & Modelling, 340 pp. Springer Nature Switzerland, (2020)
4. Krushel, E.A., Stepanchenko, I.V., Panfilov, A.E., Berisheva, E.D.: An experience of optimization approach application to improve the urban passenger transport structure. In: Kravets, A., Shcherbakov, M., Kultsova, M., Lijima, T. (eds.) Knowledge-Based Software Engineering, 11th Joint Conference, JCKBSE, pp. 27–39, Springer, Cham, Heidelberg, New York, Dordrecht, London (2014)
5. Paar, C., Peizl, J.: Understanding Cryptography, 372 pp. Springer-Verlag, Berlin, Heidelberg (2010)
6. Huang, S.C.H., MacCallum, D., Du D.: Network Security. Springer US, 280 p (2010)
7. Rueppel R.A.: Analysis and Design of Stream Ciphers, 244 pp. Berlin, Heidelberg, Springer-Verlag (1986)
8. Henk, C.A.V.T.: Fundamentals of Cryptology: A Professional Reference and Tutorial. The Springer International Series in Engineering and Computer Science, 2000th edition, 492 pp (1999)
9. Zimmermann, H.J.: Fuzzy Set Theory—And Its Applications, 2nd edn. Springer Science + Business Media, LLC, 408 pp (1991)
10. Trillas, E., Eciolaza, L.: Fuzzy logic, 204 pp. Springer International Publishing (2015)
11. Anikin, I.V., Alnajjar, K.: Fuzzy Stream Cipher System, International Siberian Conference on Control and Communications (SIBCON), Omsk, Russia (2015). https://doi.org/10.1109/sibcon.2015.7146976
12. Anikin, I.V., Alnajjar, K.: Pseudo-random Number Generator Based on Fuzzy Logic, International Siberian Conference on Control and Communications (SIBCON), Moscow, Russia (2016). https://doi.org/10.1109/SIBCON.2016.7491667
13. Anikin, I.V., Alnajjar, K.: Primitive Polynomials Selection Method for Pseudo-Random Number Generator Based on Fuzzy Logic. IEEE Dynamics of Systems, Mechanisms, and Machines (Dynamics), Omsk, Russia (2017)
14. Anikin, I.V., Alnajjar, K.: Increasing the quality of pseudo-random number generator based on fuzzy logic generator. J. Phys.: Conf. Ser. **1096**(1), 012193 (2018)

15. Wasserstein, R.L., Lazar, N.A.: The ASA's statement on p-values: context, process, and purpose. Am. Stat. **70**(2), 129–133 (2016)
16. Knuth, D. E.: The Art of Computer Programming: Semi-numerical Algorithms, 624 pp. Addison-Wesley publishing company (1968)
17. Meidl, W., Niederreiter, H.: On the expected value of the linear complexity and the k-error linear complexity of periodic sequences. IEEE Trans. Inf. Theor. **48**, 2817–2825 (2002)
18. Rueppel, R.A.: Analysis and Design of Stream Ciphers, 244 pp. Springer-Verlag, Berlin (1986)
19. Marsaglia, G.: DIEHARD: Battery of Tests of Randomness. Available: http://stat.fsu.edu/pub/diehard (1996)
20. Rukhin, A., Soto, J., Nechvatal, J., Smid, M., Barker, E., Leigh, S., Levenson, M., Vangel, M., Banks, D., Heckert, A., Dray, J., Vo, S.: A Statistical Test Suite for Random and Pseudorandom Number Generators for Cryptographic Applications. NIST Special Publication 800–22. http://csrc.nist.gov/rng/SP800-22b.pdf (2001)

IoT for Cyber-Physical Systems

Neural Network Model for Evaluating Thermofluctuation Processes in Cable Systems Using a Multi-stage Forecasting Method

Nikolay Poluyanovich, Mikhail Medvedev, Marina Dubyago, Nikolay Azarov, and Alexander Ogrenichev

Abstract The chapter is a continuation of the consideration of the practical application of the elements of digital energy. The main focus of the work is on cyber-physical systems. A neural network (NN) was developed to assess the throughput, calculate and forecast the core temperature of a power cable line (PCL) in real-time based on data from a temperature monitoring system, and taking into account changes in the current load of the line. An analysis of obtained characteristics showed that the maximum deviation of the data received from the neural network from the data of the training sample was less than 3%, which is an acceptable result. A comparison of forecasted values with actual ones allows us to talk about the adequacy of the selected network model and its applicability in practice for reliable operation of the cable power supply system of consumers. An analysis of the results showed that the more aged PCL insulating material (IM) is the greater the temperature difference between the initial and aged sample.

Keywords Cyber-physical model · Artificial intelligence · Machine learning · Neural networks · Forecasting · Insulating materials · Thermal fluctuation processes · Reliability of energy supply systems

1 Introduction

Insulation materials of power cable lines (PCL) during operation are subject to various adverse external and internal factors (thermal, electrical, chemical, mechanical). Under their action, the state of electrical insulation during the operation of the cables is continuously reduced, which over time accelerates the occurrence of failures in the form of the insulation breakdown. This leads to the fact that in the places where defects (gas and solid inclusions) are located in the insulation, partial discharges (PD) are formed, the development of which leads to the insulation breakdown [1]. With an insulation temperature increase, chemical reactions in the insulation materials accelerated which are intensified by internal inhomogeneities, exposure to the

N. Poluyanovich (✉) · M. Medvedev · M. Dubyago · N. Azarov · A. Ogrenichev
Southern Federal University, Taganrog 347900, Russian Federation

A. G. Kravets et al. (eds.), *Cyber-Physical Systems*, Studies in Systems, Decision and Control 350, https://doi.org/10.1007/978-3-030-67892-0_28

environment, absorbed by moisture. With the core heating temperature increase, the specific thermal resistance of the insulating material (IM) decreases. This reduces the insulation electrical properties and leads to an insulation gap breakdown or insulation mechanical destruction. Many studies are devoted to research, diagnostics, and problem-solving in this area [2–4].

2 Literature Review

So the requirements for factory tests of PD and tests of medium voltage cables for PD in field conditions are described in [5]. The work [6] is devoted to the detection of PD in power cables at various AC voltages. Cost-effective online partial discharge measurements for cables are described in [7]. The problems of diagnosing a partial discharge of low voltage cables are shown in [8]. As well as a nonlinear analysis of the time series of PD in electric trees, crosslinked polyethylene cable insulation samples were considered in [9]. And the related new measurement of dielectric loss in the production cable is described in [10]. As shown in [11], the main factor having an adverse effect on the state of electrical insulation during operation of the power cable under load is heating:

- due to the loss of active power in his core, screen, and other elements, heat is generated—the temperature rises;
- when short-circuit currents flow through it (even during the protection operation time), a rapid increase in temperature.

If the core temperature approaches the maximum permissible, then the process of intense thermal insulation deterioration begins its thermal aging [12], which leads to the thermal breakdown of the insulation [13]. The distribution of degradation in insulating materials of cables during accelerated thermal and radiation aging is described in [14]. The study of the dielectric behavior of thermally aged cable made of cross-linked polyethylene in the high-frequency range is the subject of work [15]. Thus, one of the solutions to this problem is to monitor the cable temperature during operation [16]. This requires the creation of specialized cyber-physical models (CPS) systems, in which both are modeled as the operation of the automated control system (ACS) and info—telecommunication infrastructure and electrical parts electric power systems (EPS).

Thus, one of the solutions to this problem is to monitor the temperature of the cable during operation. The dependence of the time to breakdown can be explained on the basis of the thermal fluctuation theory of failure. In [17], a method for recognizing PD models based on an extended NN for high-voltage power devices [18] was proposed. The use of predictive modular NN for short-term forecasting was considered in [19].

The intellectualization of the cable monitoring system is based on the modern technology of Distributed Fiber-Optic Sensing, which allows temperature measurements along the entire length of the high-voltage cable in real-time [20]. The quality of the forecast largely depends on the chosen mathematical model [21]. CPS connect the physical processes of power transmission and distribution, which require the practical implementation of continuous control in real-time, with software and electronic systems [22].

The objectives of the study are:—the development of an intelligent system for the PCL core temperature forecasting for planning the operating modes of the power grid in order to increase the reliability and energy efficiency of their interaction with the integrated power system. One of the challenges of using CPS is to develop new mathematical methods.

3 Development of a PCL Thermal Equivalent Circuit

The long-term permissible current of a cable with SPE insulation in terms of throughput is determined by several factors.

$$I_{ADD} = f(n, \theta c, \theta en, \tau, S, R, P_n) \quad (1)$$

where n—number of cores in the cable, items; θc—permissible cable core heating temperature, °C; θE—environmental temperature, °C; S—total thermal resistance of the cable and the environment, deg cm W;—core electrical resistance, Ohm; Pn—power dissipated in cable insulation due to dielectric loss, W. Decrease of n, θE, S, R, and, as well as θc increase I_{ADD}.

The high-temperature coefficient of PE linear expansion, SPE cables, (0.00015–0.00018 $°C^{-1}$) leads to the appearance of high mechanical stresses in it when the temperature changes, which causes a decrease in the insulation service life [5], therefore, studies of the temperature field in the PCL section are necessary [6], Fig. 1.

The low thermal conductivity of the cable insulation, Fig. 1, causes a large temperature gradient. As a result, the temperature near the core as the most heated section in the cable section is very different from the temperature on the cable surface [23]. In this regard, the urgent task of creating an NN for calculating and forecasting the temperature of PCL conductors in real-time, taking into account changes in the current load of the line and the external conditions of heat removal.

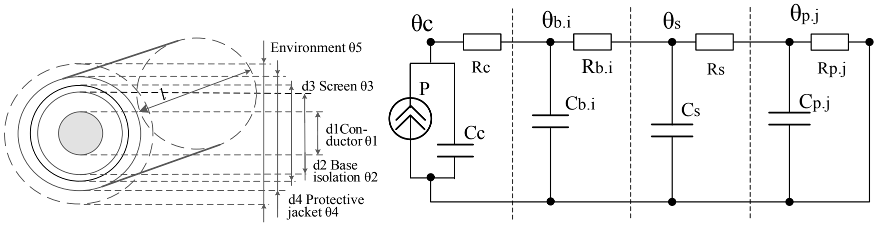

Fig. 1 Cable cross-section and its equivalent thermal equivalent circuit

4 Intellectualization of the Monitoring and Forecasting System

A promising direction is the creation of PCL fault diagnosis infrastructure based on the use of artificial neural networks (ANNs). NN in real-time allows us to calculate the temperature of the most heated points of its main parts and to detect abnormal heating due to the development of malfunctions in this object.

When solving the problem of PCL core temperature forecasting, a model is applicable, which in general terms is a nonlinear function:

$$Y_t = f(Y_{t-n}, T_{t-n}, N_t) + \varepsilon_t, \tag{2}$$

where X_t—core temperature; t—current time; $W_{t\text{-}n}$—previous observations of core temperature, $X_{t\text{-}n}$—previous environmental temperature observations; n—data retrospective index; I_t PCL core current ($I_{min} < I < I_{max}$); ε_t—random component (unobservable factors affecting core temperature).

When choosing the type of neural network (Table 1) and assessing the forecasting accuracy, we use the quality indicator in the form of a standard error, averaged over the number of output variables of the neural network and calculated on the basis of the predicted and real values of the test sample by the formula:

$$E = \frac{1}{N * K} \sum_{i=1}^{K} \sum_{j=1}^{N} \left(y_{ij}^{real} - y_{ij}^{predict} \right)^2 \tag{3}$$

where y_{ij}^{real}—the value of the i-th NN output variable for the j-th training or test example; $y_{ij}^{predict}$—the predicted value of the i-th output variable of the neural network for the j-th training or test example;—number of examples in a training or test sample;—the number of output variables of the neural network. To solve the problem of PCL resource forecasting when creating a model, based on the results of the mean square error calculation, the optimal configuration of the NN was made. A network with direct data distribution and feedback error Feed-forward backprop is selected, because Networks of this type, together with the activation function is

Table 1 Comparative analysis of various types of neural networks

No.	Neural network type	Average forecast error	
		ε, °C	ε, %
1	Multilayered perceptron (MLP)	0.9	2.3
2	Layer reccurent	1.2	2,5
3	Cascade forward backpropagation	1.63	4.2
4	Elman backpropagation	2.14	5.3
5	Backpropagation with delay	2.75	7.4

the hyperbolic tangent form $f(x) = (e^x - e^{-x}) \big/ (e^x + e^{-x})$ are to some extent a universal structure for approximation and forecasting. The analysis is carried out and the learning algorithm [24] is chosen by the Levenberg-Markard method and a cascade network with direct signal propagation and backpropagation of an error with 10 neurons, Table 1.

An analysis of the studies of NS various types allowed to determine the fact that the highest accuracy in solving the forecasting problem for a network of the type "Multi-layered perceptron" (Table 1).

5 Experimental Studies of the Neural Network Model

The forecasting of the limiting (maximum permissible) core temperature value at which the process of intense thermal insulation deterioration, it's thermal aging, and thermal breakdown of the insulation begins. To do this, we investigated thermal fluctuation processes in the power cable insulating material of APvPu $g^{-1} \times 240$ 25^{-10}. At the first stage of the experiment, samples were examined without damage. The study was conducted with a real diagram of the current value of the cable core current and the developed forecast model using NN on deep retrospective temperature data θp.c, θm.i (Fig. 1) of the studied cable for 2015–2019.

The average error in forecasting temperature of the cable core θc.c. for various values of the core current ($440 \leq$ Ic.c. ≤ 660, A) for any of the samples of the studied cable did not exceed 5 °C. Which indicates the possibility of using the artificial neural network method for forecasting the temperature of the cable core by temperature on the surface θp.c. Graphs of the actual temperature of the studied samples and graphs based on the data of the training sample of the neural network were constructed (Fig. 2).

Thus, the analysis of temperature conditions in the PCL electrically insulating materials showed that the maximum deviation of the values obtained by the developed NN from the values of the training sample is less than 2.5%, which is an acceptable result.

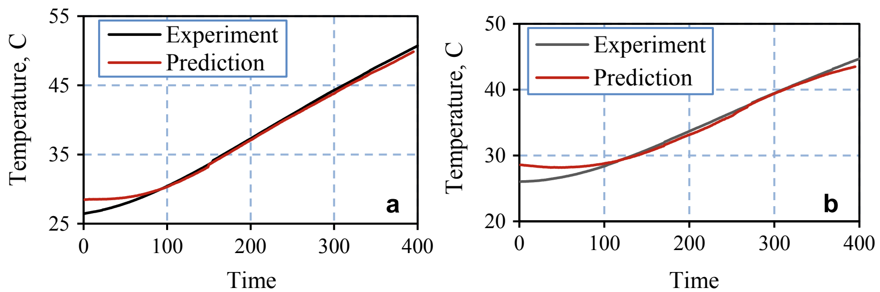

Fig. 2 Graph of the actual PCL core temperature samples No. 1–2, and forecast

Table 2 Results of an experimental study

Initial parameters			Temperature calculation, t °C			Predicted error	
Stages	№ sample	Time t_{ag}., hour	Experiment T_{av}.°C	Forecast T_{av}.°C	Δt_{exp} Δt_{for} °C	t °C	%
Training	1	–	33,97	34,18	–	– 0,35	1,02
	2	–	40,34	40,34	–	– 0,61	1,52
	3	–	38,28	39,60	–	– 1,32	3,33
Control	1	8	35,65	38,62	1,68 4,43	– 2,96	3,36
	2	16	42,59	42,37	2,2 2,02	1,54	4,51
	3	24	41,43	41,41	2,63 1,81	1,95	4,80

At the next stage, all cable samples were artificially aged in a heating cabinet at various temperatures, which corresponded to different aging times (second column of Table 2). The experimental study results of the control sample and aged samples are presented in Table 2.

Forecasting on two types of cable samples showed that the longer the aging time, the greater the temperature difference between the original (not damaged) and aged samples. We believe that this is due to the loss of material electrical insulating properties due to the accumulation of the destroyed structure fragments containing, in an increasing amount, inclusions of pure carbon and other conductive inclusions. The incomplete oxidation of polyethylene (insulating material) to produce carbon:

$$[-CH_2 - CH_2]n + nO_2 \rightarrow 2nC + 2nH_2O \tag{4}$$

6 Multi-stage Cable Temperature Forecasting

It is proposed to solve the problem of forecasting thermal fluctuation processes using models based on expert systems and artificial NN. It is known that the short-term forecasting of a parameter is performed by the step size of the sliding window in the training sample. If a long-term forecast is necessary, a sequential iterative forecast is applied for the step value that is a multiple of the step of the training sample. Moreover, the quality of long-term forecasting usually worsens with an increase in the number of iterations of the forecast (for example, with an increase in the time period of the forecast).

There is a task to improve the quality of the long-term forecast. To solve the problem, it was proposed to use, as an assessment of the training quality, not the deviation in the magnitude of the forecast for one step of the sliding window on the training sample, but the total deviation of the forecast for all values of the training sample. Moreover, based on the forecast, we obtain new values based on the forecast obtained on the previous one step.

To confirm the proposed method, a neural network algorithm for predicting the characteristics of electrical insulation was tested on a control sample of experimental data. Forecasting was carried out in two stages. At the first stage, the experimental data amounted to half the forecast. It should be noted that the training of the artificial neural network was carried out according to the first half of these data, Fig. 3a

To build a multi-stage forecast of a multidimensional series of input:

$$X_n = \theta_{p.c.}(n), I_c, N_k \tag{5}$$

and output:

$$Y_n = \theta_{p.c.}(n+1), \theta_{p.c.}(n+2) \tag{6}$$

variables are formed so that the width of the sliding window was equal to one step, and the forecast was two-stage, obtaining a transformed multidimensional time series. The algorithm iteratively makes a forecast based on the data of the training sample X(n) and is adjusted by updating the weight coefficients. Training stops after an acceptable level of efficiency is achieved (minimum forecast error ε).

To prove the method's work at the second stage, data were taken for all forecasted points of the forecasted temperatures. The graph of the experimental and forecasted temperatures of the aged cable sample is shown in Fig. 3b.

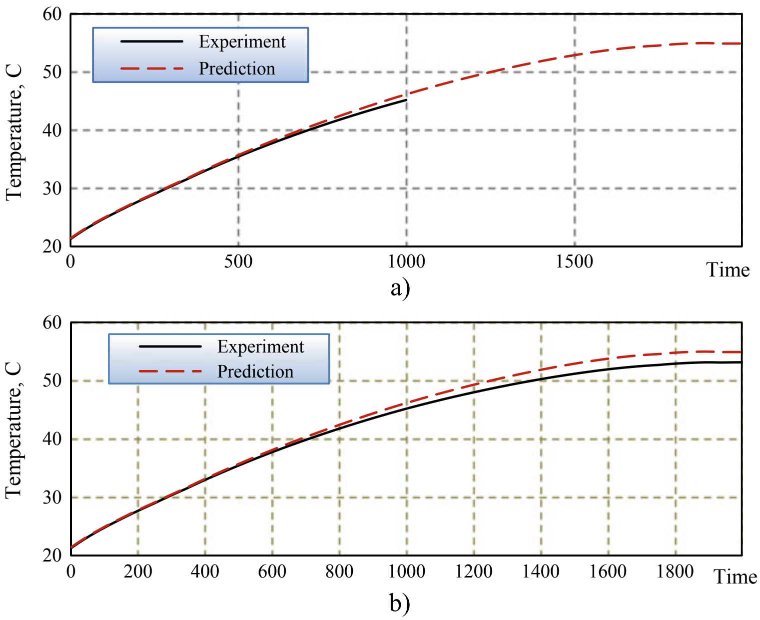

Fig. 3 Graphs of experimental and forecasted cable aging temperatures: **a** NN training for half of the sample; **b** experimental data were taken after the forecast

Table 3 Error multi-stage forecast of the core temperature

Type of test item	Average forecast error	
	ε, °C	ε, %
Sample cable № 7	2.3	5.1

The forecast results showed the effectiveness of the selected model. The error value of a multi-stage forecast of the core temperature of one of the cable samples is given in Table 3.

Thus, a multi-stage method for the resource forecast makes it possible to make a forecast with an error of 2.3 °C.

7 Dynamic Load Forecasting

In the mode of dynamically changing the load of the power cable, it is necessary to forecast its temperature regime not by one observation unit, but by several. For this purpose, the corresponding number of values, which is called the forecast horizon, is selected as the target.

At the first stage, it was necessary to solve the problems of selecting and analyzing the NN model, identifying its parameters, and finally checking the model for adequacy. The main task is to build sound computational forecasting algorithms and their neural network implementation.

Consider the task of building a forecast, not for one observation unit, but a few. For this purpose, the corresponding number of values, which is called the forecast horizon, is selected as the target. The number of observations in a series that are taken as input values is called the prediction depth.

A transformation algorithm that allows members of the time series (X(n)) of the PCL input parameters: θp.s. (1 … n)—temperature of the protective sheath, θe (1 … n)—environment temperature, Ic (1 … n)—current in the PCL core to form a "window", which is a training set for building a forecast. A window is a time interval containing a set of values (θp.s. (1 … n), Ic (1 … n), θe (1 … n), which are used to form a training example. During the operation of the algorithm, the window is shifted in time sequence by a unit of observation, and each position of the window forms one example. The transformation algorithm is shown in Fig. 4.

A sequential two-network NN architecture with a sequentially distributed structure was synthesized, Fig. 5. The first network forecasts PCL surface temperature, the second the core temperature.

Based on the method, a study was made of the PCL bandwidth for 10 kV cables with SPE insulation. To assess the long-term permissible values of heating the cable core with a voltage of 6^{-10} kV with XLPE insulation at various values of the cable core current and calculating the forecast in the mode of dynamically changing load of the power cable. A sequential two-network NN architecture with a sequentially distributed structure was synthesized. In Fig. 6 shows graphical dependencies of the

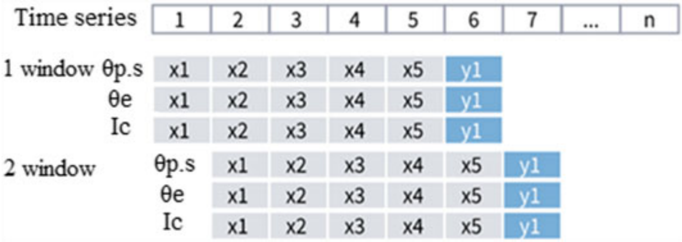

Fig. 4 Transformation algorithm

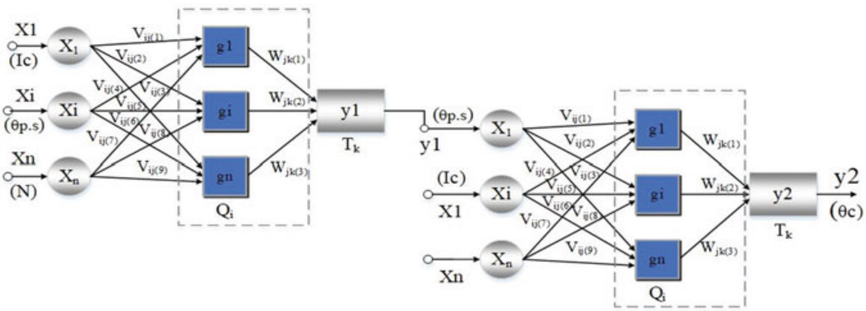

Fig. 5 The NN structure for multi-stage forecasting

temperature of the current-carrying core as a function of various values of the core current.

8 Conclusions

The mathematical model proposed in the chapter can be used as a base when calculating the thermal processes of power cables in real-time since its adequacy is confirmed by experimental studies. The error evaluation of the predicted and experimental temperatures of one of the studied cables samples showed that the average forecast error is 2.5 °C.

A sequential two-network NN architecture with a sequentially distributed structure was synthesized. The first network forecasts PCL surface temperature, the second—the core temperature. The obtained dependencies show that for cables with SPE insulation it is possible to predict the temperature of the current-carrying core with a dynamic change in the core current. Studies show that it is possible to pass significantly more current through the cable, while not exceeding the permissible temperature of the cable.

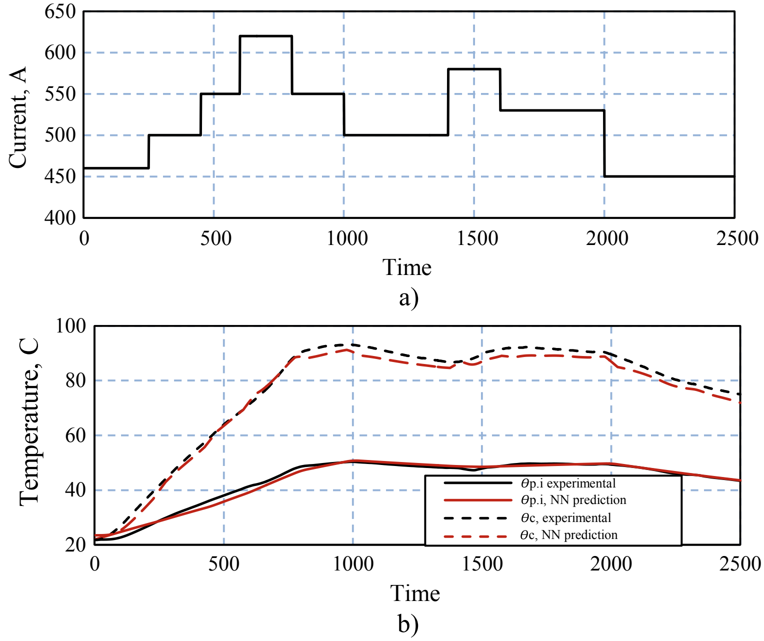

Fig. 6 Dynamic load forecasting: **a** cable test current diagram; **b** a graph of predicted and experimental temperatures

The model can be used in devices and systems for continuous diagnostics of power cables by thermal parameters. The results can be applied in an expert system for forecasting the technical condition of cable power supply systems.

The implementation of systems using temperature monitoring will allow virtually online monitoring of each CL state, including its real throughput. A comprehensive solution for temperature monitoring will help quickly monitor the current state of cable lines (PCL) and optimize the use of their real bandwidth.

Inertia when using neural network methods for PCL temperature forecasting is 5.2%, which is 2.5 times better than classical methods.

Acknowledgements This work was supported by the RFBR grant No. 18-08-00473 on the theme: “Development and research of methods for optimizing and controlling the processes of energy conversion in power plants of a complex type, including those converting a continuous flow of medium”.

References

1. Mashikian, M.S., Szatkowski, A.: Medium voltage cable defects revealed by off-line partial discharge testing at power frequency. Electr. Insul. Mag. **22**(4), 24–32 (2006)

2. Ushakov, V.Ya.: Electric power industry: Current state, problems, prospects, 234 p. Springer (2014)
3. Kories, R.: Schmidt-Walter H, Electrical Engineering, 626 p. Springer-Verlag, Berlin Heidelberg, ISBN 978-3-642-55629-6 (2003)
4. Pinto, T.: Electricity markets with growing levels of renewable generation: Structure, operation, agent-based modeling and new projects, 640 p. Springer (2018)
5. Walcott, E.E.: Partial discharge factory test requirements and in-field partial discharge testing of medium voltage cables. IEEE Electr. Insul. Mag. **21**(5), 29–30 (2005)
6. Wester, F.J., Gulski, E., Smit, J.J.: Detection of partial discharges at different AC voltage stresses in power cables. IEEE Electr. Insul. Mag. **23**(4), 28–42 (2007)
7. Zhou, Y., Qin, Y., Chappell, P.: Cost-effective on-line partial discharge measurements for cables. IEEE Electr. Insul. Mag. **22**(2), 31–37 (2006)
8. Cselkó, R., Berta, I.: Challenges of partial discharge diagnostics of low-voltage cables. J. Electrostat. **71**(3), 558–563 (2013)
9. Chen, X., Xu, Y., Cao, X.: Nonlinear time series analysis of partial discharges in electrical trees of XLPE cable insulation samples Dielectr. Electr. Insul. IEEE Trans. **21**(4), 1455–1461 (2014)
10. Yi, H., Zhou, C.: An novel in-service cable dielectric loss measurement 2017, pp. 119–122. IEEE Electrical Insulation Conference (EIC) (2017)
11. Luo, P.: Thermal and mechanical properties analysis for EHV XLPE cables with different operating years 2013 Annual Report Conference on Electrical Insulation and Dielectric Phenomena, vol. 3, pp. 47–51 (2013)
12. Crine, J.-P.: On the interpretation of some electrical aging and relaxation phenomena in solid dielectrics IEEE Trans. Dielectr. Electr. Insul. **12**(6), 1089–1107 (2005)
13. Li, H.J.: Estimation of soil thermal parameters from surface temperature of underground cables and prediction of cable rating. IEEE Proc. Gener. Transm. Distrib. **152**(6), 849–854 (2005)
14. Shimada, A.: Degradation distribution in insulation materials of cables by accelerated thermal and radiation ageing IEEE Trans. Dielectr. Electr. Insul. **20**(6), 2107–2116 (2013)
15. Kim, C.: Investigation of dielectric behavior of thermally aged XLPE cable in the high-frequency range. Polym. Test. **25**(4), 553–561 (2006)
16. Gulski, E., Cichecki, P., Wester, F.: On-site testing and PD diagnosis of high voltage power cables. IEEE Trans. Dielectr. Electr. Insul. **15**(6), 1691–1699 (2008)
17. Chen, H.-C., Gu, F.-C., Wang, M.-H.: A novel extension neural network based partial discharge pattern recognition method for high-voltage power apparatus. Expert Syst. Appl. **39**(3), 3423–3431 (2012)
18. Perpiñán, O.: Signal analysis and feature generation for pattern identification of partial discharges in high-voltage equipment. Electr. Power Syst. Res. **95**, 56–65 (2013)
19. Gross, G., Galiana, F. D.: Short-term load forecasting. Proc. IEEE **75**(12), 1558–1571 (1987)
20. Ukil, A., Braendle, H., Krippner, P.: Distributed temperature sensing: Review of technology and applications. Sens. J. IEEE **12**(5), 885–892 (2012)
21. Sarkar, R., Julai, S., Hossain, S., Chong, W.-T., Rahman, M.: A comparative study of activation functions of NAR and NARX neural network for long-term wind speed forecasting in Malaysia. Math. Probl. Eng. **2019**(6403081), 14. https://doi.org/10.115520196403081 (2019)
22. Wolf, W.: Cyber-physical systems. Computer **3**, 88–89 (2009)
23. Terracciano, M., Purushothaman, S.: Thermal analysis of cables in unfilled troughs: Investigation of the IEC standard and a methodical approach for cable rating. IEEE Trans. Power Delivery **27**(3), 1423–1431 (2012)
24. Belyavskiy, G., Puchkov, E.: Separate training of hybrid neural network. Int. J. Pure Appl. Math. **115**(4), 883–893 (2017)

Uncertain Big Data Stream Clustering

Alisa Makhmutova and Igor Anikin

Abstract Big data stream processing in real-time becomes very important for many IoT applications and modern cyber-physical systems. Sometimes such data streams are uncertain, which is caused by several reasons such as sensors inaccuracy and errors as well as, network faults. This fact leads to some problems during uncertain big data streams processing such as ensuring the results' veracity. Such tools as Storm, Samza, Spark Streaming, and Flink, which allow work with data streams in real-time, do not initially provide mechanisms for uncertain data stream mining. So implementation and evaluation of data mining mechanisms are very important for modern cyber-physical systems. In this chapter, we focused on implementation and study different algorithms for uncertain big data stream clustering for Apache Spark Stream. We studied CluStream and UMicro clustering algorithms, made evaluations of their robustness to noise, performance, and scalability. Finally, we selected the best one of them.

Keywords Data stream · Clustering · Uncertain data · Apache Spark Streaming

1 Introduction

The high growth of the IoT market has led to a significant data volume increase in cyber-physical systems. A big volume of information comes from different devices, including digital and analog sensors, interfaces, computer systems in form of the data stream. Nowadays, we have a lot of "smart" things: houses, cars, phones, media devices, and others, generating big data streams. Since 2003 the number of smart devices increased more than 50 times—from 500 million in 2003 to 26.66 billion in 2019 [1, 2]. Datastream processing is completely different from the processing

A. Makhmutova (✉) · I. Anikin
Kazan National Research Technical University Named After A.N.Tupolev-KAI,
10 K.Marx Str, Kazan 420111, Russia
e-mail: phd.makhmutova@griat.kai.ru

I. Anikin
e-mail: Anikin@kai.ru

A. G. Kravets et al. (eds.), *Cyber-Physical Systems*, Studies in Systems, Decision and Control 350, https://doi.org/10.1007/978-3-030-67892-0_29

of static data. We need to process data that arrives continuously in real-time. In this case, we have many additional requirements related to velocity, memory, veracity, and scalability [3].

Data mining techniques and machine learning methods are considering an effective tool for cyber-physical systems. Modern cyber-physical systems have to be focused on work with Big including data streams [4]. Data mining techniques allow identifying useful information or knowledge from the general mass of raw data. However, the processing of streaming data raises new challenges in comparing with usual mining techniques [5]:

- immediate processing of arriving data records in real-time to get relevant results;
- compact representation;
- identification and handling of outliers.

We can apply different data mining techniques adapted to data streams: association rule learning, clustering, classification, outliers' detection, etc. The clustering of big data streams is very important for different applications including sensors validation, identification of data source, data classification, etc. Clustering analysis implies searching patterns by dividing data into clusters (groups), which is similar in some way. Processing of huge data with meeting all the requirements of intensive data mining implies the usage of tools for distributed processing of Big Data, for example, Spark Streaming [6], Apache Flink [7], and Apache Storm [8]. These platforms have implementations of different stream data mining algorithms including clustering.

In some cases data in streams comes with some level of uncertainty: inaccuracy, imprecision, and sometimes even with lack of information. Although all distributed processing tools described above can solve many problems with data processing in streams, they do not initially provide mechanisms for data mining of uncertain data streams. In this chapter, we focused on implementation and study different algorithms for uncertain big data stream clustering for Apache Spark Stream platform. We also make an evaluation of uncertain data streams clustering approaches and epy effectiveness of existed solutions for performing data stream processing.

This chapter is organized as follows: in Sect. 2 we described different algorithms for clustering of uncertain data streams, in Sect. 3 we described the developed framework for online clustering of the uncertain data stream, in Sect. 4 we presented the evaluation part.

2 Clustering of the Uncertain Data Stream

2.1 Uncertainty in Data

Data that comes from sensors or other hardware can contain some part of the uncertainty, due to sensor fault or inaccuracy, transmission errors, or interruptions in the receiving process. There are two main approaches exist for dealing with such uncertainty [9]:

- preliminary processing of information and transformation of the uncertain dataset into deterministic;
- management of uncertainty, which means the implementation of data mining algorithms capable to work with uncertain data.

The first approach seems to be more preferable and reliable, but it cannot or difficult to be applied in the case of data streams. Therefore, many approaches to managing uncertainty in data streams exist.

In the database, uncertainty can be considered as tuple-level uncertainty, which means uncertainty of tuple relation, or as attribute-level uncertainty, which means a disputable value of the results is obtained. In the case of tuple-level uncertainty possible world semantics, a method exists, which expands the original database by all possible meanings and calculates a probability for each of them. In this chapter for cyber-physical systems, we will consider attribute-level as the most common form of uncertainty. Attribute-based uncertainty can be of two types: fuzzy value and ambiguity value [10]. Usually, continuous Probability Density Function (PDF) describes the most accurate assumption of attribute-based uncertainty.

We will consider attribute-level uncertain stream data as a group of records $\{D_t, f_t\}$, where t is a timestamp, D is the value and f is the corresponding PDF. Another case—records with discrete probability—$\{(x(t_1), 0.15); (x(t_2), 0.40); \ldots; (x(t_k), 0.05)\}$. The last model, a simple but common representation of arriving information from sensors is $(x_t \pm r)$, where r is a standard error.

2.2 Clustering of Uncertain Data

There many clustering algorithms which divide objects into clusters of different types:

- prototype (center)-based clusters (distance-based clustering);
- graph-based clusters (hierarchical clustering);
- density-based clusters (density-based clustering).

Modifications of existing clustering algorithms for work with uncertain data need to be done carefully. Cluster creation should take into account the degree of uncertainty in the dataset. As example we can give such modifications as DBSCAN [11] into FDBSCAN [12], OPTICS [13] into FOPTICS [14], K-means [15] into UK-means [16].

DBSCAN algorithm works with such concepts as *core points*, *density-reachable points,* and *outliers*. The main idea of DBSCAN is to find the density areas among the given set of points to build clusters from them. The cluster is built from core points and their reachable neighbors, identified by minimum threshold data density ε [31].

The FDBSCAN algorithm extends DBSCAN by introducing the concept of reachable probability between two data points because in the uncertain datasets we cannot find crisp accessibility from one point to another. Reachable probability is based on the properties of probabilistically specified objects and uncertain distances between them. This distance is represented in terms of the distribution function.

The basic idea of OPTICS is similar to DBSCAN. This method is to overcome the disadvantage of the DBSCAN algorithm and provide the clustering of spatial data, where data has a varying density. FOPTICS algorithm has probabilistically defined value for ordering and obtaining MinPts.

Traditional k-means algorithm [15] includes two basic steps: assignment, where point assign to the cluster with nearest mean, and update, where new clusters centers recalculate. In a crisp dataset, the distance obtaining process is easier because the existence of objects and their parameters are explicit. In an uncertain dataset, it causes difficulties. UK-means algorithm [16] aims to solve these problems. The uncertain data point is represented as a possible distribution region. The main idea of UK-means is to minimization the number of expected distance by computing the Minimum Bounding Rectangles (MBR) for the representative point of the cluster region.

There is also a fuzzy extension of the CobWeb algorithm (Fuzzy CobWeb), which can work with fuzzy values [32].

2.3 Clustering of Deterministic Data Stream

In many cases, the clustering of uncertain data streams is based on algorithms for deterministic data. In the case of data streams, clustering algorithms are often divided into two phases online and offline. Due to a big volume of records coming in a small time period, it is difficult to store them effectively in memory. So online phase processes in-formation about these records in real-time and single-pass [17] gathering some general information about these records. Then certain clusters are constructed on an offline phase based on information gathered online.

Different models of data windows could be used to cut the range of data for processing because some data may be outdated and doesn't represent interest for research (Fig. 1):

- Fixed sliding window model. It is one of the simple and fast, but inaccurate types, which takes a fixed number of records. Inaccuracy may be caused by the wrong window width if the researcher has poor knowledge about data properties [18].
- Adaptive window model. This model can be effective for streams with different values of coming information. This method assumes changing window width with adaptation for the current situation in the stream [19].

- Landmark window model. Looking at data in a stream from a fixed point in time landmark [20].
- Damped window model. Could be applied if the importance of new points is higher than the old ones [21]. Each arriving point gets its weight, which is damped over time.

In this chapter, we will focus on the online part of data stream processing, because there are years of research for clustering data in the offline phase. As it was mentioned previously, the online phase processes coming records and summarize it into so-called micro-clusters. This efficient representation of compressed data in streams was first proposed in [23] and then adapted in [24]. Micro-clusters are an extended concept of Cluster Feature Vector (CFV) [23], which contains a summary of statistical information about the cluster. Using micro-clusters significantly reduces the processing time for each record and allows saving involved memory. Micro-clusters are updated with coming to every record and offline clustering can be started at any time.

We have the stream of records $X_1, X_2, \ldots, X_n$, each of which contains d-dimensions, and the timestamps $T_{i_1}, T_{i_2}, \ldots, T_{i_n}$. Each record can be represented as $X_i = \left(x_i^1, \ldots, x_i^d\right)$. Micro-cluster can be defined as $(3 \times d + 2)$ tuple $(\overline{CF2^x}, \overline{CF1^x}, CF2^t, CF1^t, n)$, where $\overline{CF2^x}$ and $\overline{CF1^x}$ contain the sum of squares of values and the sum of data values respectively (both contain d values). $CF2^t$ and $CF1^t$ are sums of squares of timestamps and sum of timestamps respectively, n is the number of points, contained in the cluster. Micro-clusters have such properties as additivity and subtractive [22]. The first property means that two micro-clusters can be merged just by the sum of their values. Subtractive allows getting the summary information about data values, which arrived in some time interval.

2.4 Clustering of Uncertain Data Stream

There are two main principles in the online clustering of uncertain data streams: density and distance-based clustering. Density-based algorithms provide a more sophisticated function of determining the membership of record to the cluster. It allows handling of outliers, but can significantly decrease the processing time. DenStream [25] and DCUStream [26] algorithms relate to this approach. Distance-based methods are less accurate but fast. It can significantly increase the processing

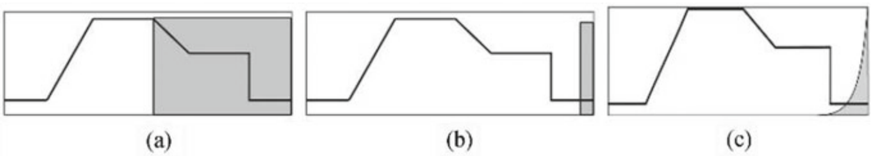

Fig. 1 Window models [22]. **a** landmark window model **b** fixed sliding window model **c** damped window model

throughput of the data stream. Umicro [27], LuMicro [28], and EMicro [29], algorithms relate to that. In our chapter, we focused on distance-based approaches.

Umicro algorithm is an adaptation of CluStream [24] for uncertain data streams. It has the same principle of work. Both of them use a two-phase concept (online/offline) and a micro-cluster model. They construct CFV in online mode and use the k-means clustering algorithm for the implementation of the offline mode. Uncertainty is represented as knowing the standard deviation or estimated error of each record. For dimension j in record X_i this error denotes as $(\psi_i X_i)$. Micro-cluster in Umicro algorithm is defined as $(3 \times d + 2)$ tuple $(\overline{CF2^x}, \overline{CF1^x}, \overline{EF2^x}, t(C), n)$, where additionally to $CF2^t, CF1^t)$ values, the sum of error squares $EF2^x$ as well as the last update of the micro-cluster $t(C)$ are keeping. On the online stage for each record, we have to calculate the expected distance, which includes, expected value v of the squared distance between record $X = (x_1, \ldots, x_d), (\psi_1(X), \ldots, \psi_d(X))$ and centroid Z of cluster C. It could be found as following (1):

$$v = E\left[\left\|X - Z^2\right\|\right] = \sum_{j=1}^{d} \frac{CF1(C)_j^2}{n(C)^2} + \sum_{j=1}^{d} \frac{EF2(C)_j}{n(C)^2} + \sum_{j=1}^{d} x_j^2 + \sum_{j=1}^{d} (\psi_j(X)^2 - 2\sum_{j=1}^{d} x_j \bullet \frac{CF1(C)_j}{n(C)} \tag{1}$$

For each coming record, it is necessary to identify, whether it is in a critical uncertainty boundary. If yes, the record has to be added to the micro-cluster. If no, then a new micro-cluster has to be created with this single point. The uncertainty boundary of the micro-cluster is determined as a standard deviation of data points' distances from the centroid of the micro-cluster. Let C be such centroid and the set of points will be denoted as $X_1, \ldots, X_r$. In this case, the uncertain radius is defined as

$$U = \sum_{i=1}^{r} \sum_{j=1}^{d} E\left[\left\|X_i - C_j^2\right\|\right] \tag{2}$$

UMicro algorithm is represented in Fig. 2, where n_{micro} is a maximum number of micro-clusters, which defined by the user and $S = \{\}$ represents the set of micro-cluster statistics with maximum n_{micro} elements.

In 2009 Zhang proposed LuMicro algorithm for tracking high-quality clusters over uncertain data streams [28]. The main difference is in considering the uncertainty: instead of working with standard deviation, they introduce instance uncertainty, which is based on probability. The algorithm also uses the concept of CFV, but it is named as Probability Cluster Feature (PCF), which is $(2 \times d + 3)$ vector $(CF2^x(C), CF1^x(C), U(C), t(C), n(C))$, where $CF2^x(C)$ and $CF1^x(C)$ are sums of squares and sum of tuple expectations for each dimension respectively, $U(C)$ keeps the average value of tuple uncertainty in micro-cluster, $t(C)$ contain the time of the

```
Data: Stream, each item of which contain pair of the vectors (X, ψ(X))
Result: set of micro-clusters S
S={};
while not the end of stream do
    Receive the next stream point X;
    if X not the first record then
        Compute the expected similarity of X to the closest micro-cluster M in S;
        Compute critical uncertainty boundary of micro-cluster M;
        if X lies inside uncertainty boundary then
            Add X to the statistics of M
        else
            Add a new micro-cluster in S with only one point X
        end
    else
        Create a new micro-cluster in S with only one point X
    end
    if S contain n_micro + 1 elements then
        Find the least recently updated cluster U;
        Remove U from S;
    else

    end
end
```

Fig. 2 The UMicro algorithm

recent record and $n(C)$ is the number of points. LuMicro method is based on work with tuple based uncertainty, while Umicro is a more standard error based approach. EMicro algorithm presented also by Zhang in 2010 [29], is based on LuMicro. It proposes a new model for outlier processing (buffer mechanism) and keeps two buffers in memory to store clusters and outliers.

In this chapter, we focused on the UMicro approach and its comparison with Clu-Stream when working with uncertain data.

3 Framework for Online Clustering of Uncertain Data Streams

We developed the framework for evaluation online clustering of uncertain data stream algorithms. CluStream and UMicro algorithms were selected for evaluation. In order to evaluate the robustness of these algorithms to noise, we add the Gaussian noise to stream data with zero mean and different standard deviations. After that, we compared the quality of clustering.

The huge amount of stream data that we have to process leads to the necessity of using distributed processing systems solutions like Apache Spark, Storm, etc. Different real-time intelligent data processing libraries were developed based on these solutions. In our work, we used StreamDM [30], which is an expansion of

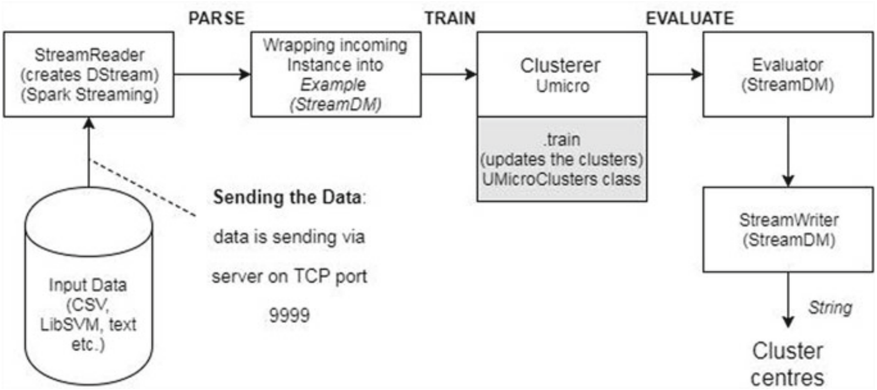

Fig. 3 General workflow of the framework

Apache SAMOA on Apache Spark Streaming. The main concept of Apache Spark is the Resilient Distributed Dataset (RDD) structure, which manages internal memory of distributed processing and allows providing fault-tolerant work of the system. Spark Streaming is an extension of the basic Spark API, which split the stream into small batches into time intervals. It uses DStream (discretized stream) abstraction, which can be perceived as a micro-package containing several RDDs.

The general workflow diagram of the developed framework is represented in Fig. 3. In the preprocessing step we prepare data into a form suitable for further processing. We also add some Gaussian noise into data for evaluation of the robustness of algorithms. On the clustering step, we apply UMicro and CluStream algorithms for pre-processed data. The evaluation step means the evaluation of some metrics of clustering algorithms including the performance, scalability, and robustness to noise.

4 Evaluation

4.1 *Accuracy and Robustness*

We used the following metrics for accuracy and noise robustness evaluation: standard deviation of cluster's center from original, cohesion, and separation.

The standard deviation of the cluster's center from the original ("clean") one, which caused by noise, is defined by Eq. (3)

$$S = \sqrt{\frac{1}{n}\sum_{i=1}^{n}(x_i - x)^2}, \tag{3}$$

where x is a "clean" value of the cluster center, x_i is a value of the cluster center under the noise. The lower value of the deviation is interpreted as more robustness to noise.

Cohesion is an internal parameter, which measures how items are close in the cluster, It is measured by the Sum of Square Error (SSE) between each point x in the cluster C and the cluster mean m_i Eq. (3):

$$SSE = \sum_i \sum_{x \in C_i} (x - m_i)^2 \tag{4}$$

Separation is an external measure, which defines how distant the clusters are from each other. This measure is calculated by Between-cluster Sum of Squares (BSS), taking into account the overall clustering mean m.

$$BSS = \sum_i |C_i|(m - m_i)^2 \tag{5}$$

We make an evaluation of these metrics on the dataset of 200 instances. The levels of noise were chosen from the range [0,1;3] because $\eta \geq 3$ creates a data set with a very high level of noise that completely changes the original meaning of the data. As a result, 7 different noise levels were applied. Equation (3) was applied to each dimension with n = 7. We can see the final evaluation results in Table 1. We can conclude that UMicro provides a more accurate result with data uncertainty than Clu-Stream algorithm. This algorithm is more robust to noise.

Evaluation of cohesion and separation metrics for CluStream and UMicro is presented in Table 2. SSE values of both algorithms are increasing, which means shuffle the values of points, included in the cluster. By analyzing SSE and BSS values, we can see that UMicro algorithm provides more stable cluster formation with an increasing level of noise in data.

Table 1 Cluster's center standard deviation for CluStream and UMicro

Number of clusters	CluStream			UMicro		
	Dimensions			Dimensions		
	1	2	3	1	2	3
1	28,77513	9,930413	61,45248	23,27297	9,182431	41,88777
2	23,34495	21,70004	32,18136	21,87622	6,963675	10,90682
3	39,47897	12,37348	36,23292	33,50327	12,06693	29,91255
4	29,59286	18,54312	28,4769	24,34	11,23197	27,12085
5	64,20629	19,2831	44,80376	28,93734	11,38293	22,11087

Table 2 Evaluation of cohesion and separation

Noise level (η)	CluStream		UMicro	
	SSE	BSS	SSE	BSS
0	3586	42404	3586	42404
0,1	3586	44297	3586	42404
0,3	4051	12239	3601	21779
0,5	6746	84097	3609	17421
0,7	8293	84146	4800	12062
1	8525	84146	5781	21864
1,5	8525	84146	4620	29127
2	8756	89141	4871	31456

4.2 Performance and Scalability

We evaluated the performance (in a sec) and scalability (distribution between several nodes) of CluStream and UMicro also with adding some level of noise. The original dataset included 500000 instances with an overall volume of 11,7 Mb. Noised data has a volume of 44,9 Mb. We used computation nodes with the following technical features: CPU—Intel Core (TM) i5—4590 CPU @3.30 GHz, RAM—8 GB. We can see the results in Fig. 4. We can see that the UMicro algorithm has a little bit better scalability than CluStream. It shows better performance when we increase the number of nodes.

5 Conclusion

In this chapter, we have presented a framework for the online clustering of the uncertain data streams. This framework was implemented in the Apache Spark Streaming environment with external library StreamDM. Using the developed framework we evaluated the robustness, performance, and scalability of UMicro and CluStream algorithms. We can say that the UMicro algorithm is better for all criteria for processing uncertain stream data. This algorithm provides accurate cluster formation despite existing noise in data.

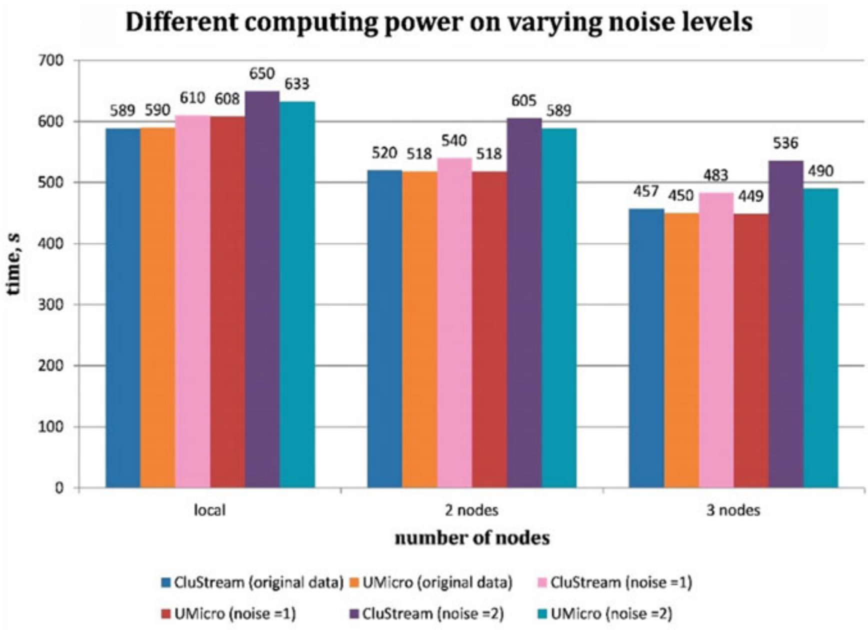

Fig. 4 Evaluation of performance and scalability

References

1. Evans, D.: The Internet of Things How the Next Evolution of the Internet Is Changing Everything, white paper, CISCO, Tech. Report (2010)
2. Maayan, G.D.: The IoT rundown for 2020: Stats, risks, and solutions. https://securitytoday.com/Articles/2020/01/13/The-IoT-Rundown-for-2020.aspx?Page=1. Accessed 8 Apr 2020
3. Stonebraker, M., Zdonik, S.: The 8 requirements of real-time stream processing. Sigmod Record **34**(4), 42–47 (2005)
4. Atat, R., Liu, L., Wu, J., Li, G., Ye, C.: Big data meet cyber-physical systems: A panoramic survey. IEEE Access **6**, 73603–73636 (2018)
5. Barbar, D.: Requirements for clustering data streams. ACM SIGKDD Explor. Newsl. **3**(2), 23–27 (2002)
6. Spark Streaming. https://spark.apache.org/streaming/. Accessed 8 Apr 2020
7. Apache Flink. https://flink.apache.org/. Accessed 8 Apr 2020
8. Apache Storm. https://storm.apache.org/. Accessed 9 Apr 2020
9. Lin, M.: Uncertainty in data stream processing. Master's thesis, Technical University Ilmenau (2015)
10. Goman, M.: Efficient query processing on probabilistic data streams. Master's thesis, Technical University Ilmenau (2017)
11. Simoudis, E., Han, J., Fayyadeds, U.M.: A density-based algorithm for discovering clusters in large spatial databases with noise. In: Second International Conference on Knowledge Discovery and Data Mining (KDD-96), pp. 1–13 (1996)
12. Kriegel, H.-P., Pfeifle, M.: Density-based clustering of uncertain data. In: ACM KDD Conference Proceedings (2005)

13. Ankerst, M., Breunig, M.M., Kriegel, H.-P., Sander, J.: Optics: Ordering points to identify the clustering structure. In: ACM SIGMOD international conference on Management of data, pp. 49–60 (1999)
14. Kriegel, H.-P., Pfeifle, M.: Hierarchical density based clustering of uncertain data. In: Proceedings of Fifth International Conference on Data Mining (ICDM'05) (2005)
15. Kanungo, T., Mount, D.M., Netanyahu, N.S., Piatko, C.D., Silverman, R., Wu, A.Y.: An efficient k-means clustering algorithm: Analysis and implementation. IEEE Trans. Pattern Anal. Mach. Intelli. **24**(7), 881–892 (2002)
16. Ngai, W., Kao, B., Chui, C., Cheng, R., Chau M., Yip, K.Y.: Efficient clustering of uncertain data. In: ICDM Conference Proceedings (2006)
17. Aggarwal, C.C., Reddy, C.K.: Data clustering: Algorithms and applications. Chapman and Hall/CRC, p. 617 (2013)
18. Lee, W., Stolfo, S., Mok, K.: Adaptive intrusion detection: A data mining approach. Artif. Intell. Rev. **14**(6), 533–567 (2000)
19. Bifet, A.: Adaptive stream mining: Pattern learning and mining from evolving data streams. Front. Artif. Intell. Appl. **11**(1), 55–56 (2010)
20. Zhu, Y., Shasha, D.: Statstream: Statistical monitoring of thousands of data streams in real time. Proceedings of the 28th International Conference on Very Large Data Bases (2002)
21. Chang, J.H., Lee, W.S.: Finding recent frequent item sets adaptively over online data streams. Proceedings of the ninth ACM SIGKDD international conference on Knowledge discovery and data mining (2003)
22. Matysiak, M.: Data stream mining. Basic methods and techniques. Technical report, Rheinisch-Westfalische Technische Hochschule Aachen (2012)
23. Zhang, T., Ramakrishnan, R., Livny, M.: Birch: An efficient data clustering method for very large databases. Proceedings of the 1996 ACM SIGMOD International Conference on Management of Data, pp. 103–114 (1996)
24. Aggarwal, C.C., Han, J., Wang, J., Yu, P.S.: A framework for clustering evolving data streams. Proceedings of the 29th International Conference on Very Large Data Bases, pp. 81–92 (2003)
25. Cao, F., Ester, M., Qian, W., Zhou, A.: Density-based clustering over an evolving data stream with noise. Proceedings the 2006 SIAM Conference on Data Mining, pp. 328–339 (2006)
26. Yang, Y., Liu, Z., Zhang, J., Yang, J.: Dynamic density-based clustering algorithm over uncertain data streams. Proceedings 9th International Conference on Fuzzy Systems and Knowledge Discovery, pp. 2664–2670 (2012)
27. Aggarwal, C., Yu, P.S.: A framework for clustering uncertain data streams. Proceedings of the 2008 IEEE 24th International Conference on Data Engineering, pp. 150–159 (2008)
28. Zhang, C., Gao, M., Zhou, A.: Tracking high quality clusters over uncertain data streams. Proceedings of the 2009 IEEE 25th International Conference on Data Engineering, pp. 1641–1648 (2009)
29. Zhang, C., Jin, C.-Q., Zhou, A.-Y.: Clustering algorithm over uncertain data streams. J. Softw. **21**(9), 2173–2182 (2010)
30. Bifet, A., Maniu, S., Qian, J., Tian, G., He, C., Fan, W.: Streamdm: Advanced data mining in spark streaming. Proceedings of IEEE International Conference on Data Mining Workshop (ICDMW), pp. 1608–1611 (2015)
31. Dagaeva, M., Garaeva, A., Anikin, I., Makhmutova, A., Minnikhanov, R.: Big spatio-temporal data mining for emergency management information systems. IET Intell. Transp. Syst. **13**(11), 1649–1657 (2019)
32. Nazarov, A.O., Anikin, I.V.: Clusterization of objects with fuzzy parameter's values. Proceedings of 2017 Dynamics of Systems, Mechanisms and Machines conference (Dynamics) (2017)

Frequency Characteristics of a Quantum Motherboard in Preprocessor and Distributed Sensor Mode

Nikolay Perminov and Diana Tarankova

Abstract In this work, we describe a quantum motherboard based on a system of five interacting resonators connected with two-level atoms via switched couplings. Based on algebraic methods, the frequency spectrum of the atomic-resonator platform was optimized and the dynamics in the preprocessor and distributed sensor mode were numerically studied. A comparative analysis of several optimization methods for the proposed scheme.

Keywords Quantum motherboard · High-Q resonators · Periodic frequency comb · Spectrum optimization · Preprocessor · Distributed sensor

1 Introduction

The development of a quantum motherboard (QMB) that plays the role of a multifunctional quantum interface, combined with long-lived atomic subsystems, is important for quantum computer science [1, 2]. The practical implementation of a multi-qubit QMB requires a reversible and controlled interaction of qubits with multi-particle long-lived quantum systems [3], in particular with NV centers in diamond [4], rare-earth ions in inorganic crystals [5], and quantum dots [6]. However, most approaches for implementing controlled qubit transfer between remote nodes provide quantum efficiency of up to 92% [7.8], whereas practical quantum computers require at least 99.9%.

N. Perminov (✉)
Kazan Quantum Center, Kazan National Research Technical University Named After A.N. Tupolev—KAI, 10 K. Marx, 420111 Kazan, Russia
e-mail: qm.kzn@ya.ru

FRC Kazan Scientific Center of RAS, Zavoisky Physical-Technical Institute, 10/7 Sibirsky Tract, Kazan 420029, Russia

D. Tarankova
Department of Radioelectronics and Information-Measuring Techniques, Kazan National Research Technical University Named After A.N. Tupolev—KAI, 10 K. Marx, 420111 Kazan, Russia
e-mail: tarankovadyu@ya.ru

A. G. Kravets et al. (eds.), *Cyber-Physical Systems*, Studies in Systems, Decision and Control 350, https://doi.org/10.1007/978-3-030-67892-0_30

One of the solutions is based on the use of rich properties of multiparticle dynamics [9]. The main problem here is the construction of multi-particle systems that provide convenient control of time-reversible dynamics. Significant progress in creating high-quality resonators [10, 11] with convenient spatial control opens up wide spectral properties for solving this problem in a system of coupled resonators [12, 13].

In particular, a system of resonators with periodic frequencies connected to a common resonator [13] can expand the dynamic capabilities of linear chains of resonators with the same frequencies [14]. Moreover, such multi-resonator schemes demonstrate a significant increase in the operating spectral range of the quantum interface [13]. In these systems, it is possible to significantly increase the interaction constant of light signals with resonant atoms, while the broadband system of resonators with high Q-factor allows reducing the effects of relaxation and decoherence by switching to faster storage processes. A multi resonator system with atoms and con-trolled coupling between resonators is useful as an effective tool for entanglement generators [15], quantum memory [13], multi-functional interface, and QMB [16, 17], and can also be used to construct photon-photon multi-qubit gates [19–22].

In this chapter, we show a QMB scheme based on a system of 5 interacting resonators connected to two-level atoms, with switchable couplings. This combination of a system of high-Q resonators with atoms (quantum dots, NV centers, or long-lived spin systems) located in these resonators can become a realistic approach for obtaining a full-fledged QMB for quantum calculations with different types of logical qubits [16, 18]. Analytically and numerically studied the criterion for optimizing the frequency characteristics of the QMB to obtain reversible and controlled atomic dynamics, as well as numerically investigate the dynamics of the QMB in the preprocessor and distributed sensor mode, which corresponds to different ratios of controlled connections in the platform.

2 Physical Model

Similarly, [16] here we consider the case of single-photon excitation in a system of 5 linearly coupled resonators (Fig. 1). Modes of resonator fields $b_n(t)$ with frequencies ν_n, each of which is connected to a single spin field $s_n(t)$ with frequency ν_n, which has relaxation yn, using the coupling constant fn. The coupling constants between the resonators n and m are $g_{nm}= g_{mn}$, and the non-zero initial excitation is as follows: $s_2(0) = exp(i\varphi)/sqrt(2) = s_4(0)^*$. In this work, we are interested primarily in sets of optimal parameters (parameters not specified in the solution are considered null by default, and the frequencies are counted from a certain reference central frequency) that correspond to different types of final solutions (preprocessor and sensor), and we also give a typical dependence of the spectrum on the connection between resonators.

Figure 1 schematically shows the typical structure of a single QMB block consisting of resonators with spins. The selected model is physically a chain of resonators with single spins inside them. From the point of view of geometry, a

Fig. 1 Principal scheme of a single QMB block in the form of a linear chain of resonators with spins

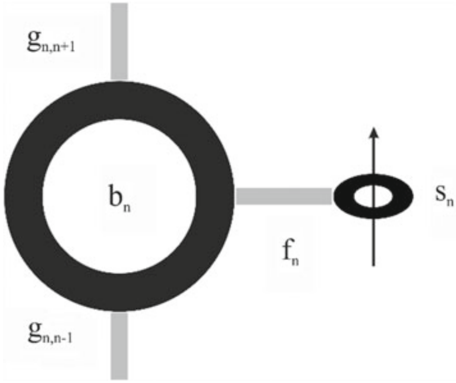

system of interacting resonators in the form of a chain has the maximum availability for control (for example, magnetic or electro-optical control of spin subsystems in resonators), which is very important for fine-tuning the operating mode and is critical for accurate control of all available parameters of the system, which in turn is necessary to obtain the highest possible quality characteristics of the system (efficiency, accuracy) in the preprocessor mode.

A qualitative feature of the model system under consideration is also the ability to load sufficiently pure single-photon States through spin subsystems by means of excitation by controlling fields. In this case, spin subsystems can actually act as state generators that respond to single excitations for performing any quantum calculations. In contrast to purely resonator systems that have a continuous excitation spectrum, single spins can have only two or three active transitions, which allows them to be used as qubits in a hybrid spin-resonator system of our type.

In a certain sense, for specialized quantum calculations/manipulations, the spins built directly into some of the resonators in a multi-resonator system can replace the complex, bulky remote state generator that is necessary for calculations using single-qubit writing. Thus, the proposed configuration can potentially have the qualities of a preprocessor and a generator at the same time, since the state generator is physically integrated into the computer system itself from the resonators. A more detailed discussion of these unique possibilities of combining multiple devices in a single scheme requires a separate discussion, and we will not go into this here. Note also that for all such devices, where manipulations with qubits and calculations are performed, a highly efficient state reading is required, which in our situation can be done, as well as loading information into spins, via spin sub-systems.

However, in reality, spin systems are effectively three-dimensional objects and practically cannot radiate stored energy equally effectively in the modes of planar resonators and in the perpendicular direction from which the loading is realized. Therefore, special fish-eye resonators are required to read information from the spins, which can only work in the unloading mode in the vertical direction.

An alternative solution for reading is to output energy from the system via integrated waveguides connected to resonators. At the same time, the connection between resonators and waveguides can be very efficient, with almost no energy loss. The planar waveguides themselves, in turn, can be effectively connected to highly efficient planar detectors of single quantum states. This configuration of energy output from a planar circuit from resonators to a planar quantum detector is the most promising in the context of fully integrated and very compact highly specialized quantum computers.

In the current work, we will consider the simplest and most analytically visible mode of operation of the system, which corresponds to the level of single-photon excitation. In this situation, the dynamics equations can be written in terms of the resonator spin modes as follows:

$$\begin{aligned}
&[\partial_t + i \cdot \nu_n] s_n + i \cdot f_n \cdot b_n = 0,\ [\partial_t + i \cdot \nu_1] b_1 + i \cdot f_1 \cdot s_1 + i \cdot g_{1,2} \cdot b_2 = 0,\\
&[\partial_t + i \cdot \nu_2] b_2 + i \cdot f_2 \cdot s_2 + i \cdot g_{2,1} \cdot b_1 + i \cdot g_{2,3} \cdot b_3 = 0,\\
&[\partial_t + i \cdot \nu_3] b_3 + i \cdot f_3 \cdot s_3 + i \cdot g_{3,2} \cdot b_2 + i \cdot g_{3,4} \cdot b_4 = 0,\\
&[\partial_t + i \cdot \nu_4] b_4 + i \cdot f_4 \cdot s_4 + i \cdot g_{4,3} \cdot b_3 + i \cdot g_{4,5} \cdot b_5 = 0,\\
&[\partial_t + i \cdot \nu_5] b_5 + i \cdot f_5 \cdot s_5 + i \cdot g_{5,4} \cdot b_4 = 0,
\end{aligned} \tag{1}$$

where the initial state corresponds to the single-photon excitation of the entire system, i.e. $\Sigma_n |s_n(0)|^2 + |b_n(0)|^2 = 1$, and is chosen as

$$\begin{aligned}
s_2(0) &= exp(i\varphi)/sqrt(2),\\
s_4(0) &= exp(-i\varphi)/sqrt(2),\\
s_1(0) &= s_3(0) = s_5(0) = 0.
\end{aligned} \tag{2}$$

With the selected initial loading of spins 2 and 4, we plan to investigate a potentially reversible state transfer from spins 2,4 to spins 1,3,5: the excitation from 2 nodes is transferred to 3 nodes with the possibility of additional manipulations. In general, the mapping of states in 2 nodes is possible in 1 node, which is similar to the schemes of balance/homodyne detection implemented in node systems, or in 2 nodes, which is used for implementing typical quantum operations such as controlled quantum negation (2 qubits in two nodes are displayed in 2 qubits in the other two nodes).

Mapping the state of 2 qubits in two nodes in 3 qubits in 3 nodes has additional features in terms of registering the final states that are the result of the system. Mapping the quantum state of a small number of qubits (quantum states of an arbitrary structure in a more general sense) to the states of a large number of qubits is used in tomographic schemes, where the largest number of components of the quantum state must be measured in a single measurement cycle.

The technique of splitting a state into several spatially distributed blocks together with the output of energy to a set of channels is a standard technique for quantum computing based on cluster entangled states and quantum memory. It is interesting that the scheme proposed here can be combined with the highly efficient multiresonator quantum memory proposed earlier [13, 17]. Thus, a system of resonators and spins can actually contain built-in state generators in the form of spins, dynamically switched resonators for processing, and a resonator block for quantum memory. In other words, such a system can potentially act as a full-fledged hybrid quantum computer aimed at solving highly specialized problems, such as solving nonlinear equations or simulating problems from quantum chemistry.

At the same time, problems from the theory of nonlinear equations in the system under study arise quite naturally, since the dependence of the eigenfrequencies of the composite system from interacting resonators depends in a nonlinear way on the initial frequencies of the resonators and spins.

To demonstrate this, we write the dynamic Eqs. (1) and (2) in the Laplace image after applying the Laplace transform of the form $h(t) = \int dt\ exp(-p\ t)\ h(p)$ to all modes of spins and resonators. Linear algebraic equations for Laplace images of modes have the following form:

$$
\begin{aligned}
&[p + i \cdot \nu_n] s_n + i \cdot f_n \cdot b_n = s_n(0),\\
&[p + i \cdot \nu_1] b_1 + i \cdot f_1 \cdot s_1 + i \cdot g_{1,2} \cdot b_2 = b_1(0),\\
&[p + i \cdot \nu_2] b_2 + i \cdot f_2 \cdot s_2 + i \cdot g_{2,1} \cdot b_1 + i \cdot g_{2,3} \cdot b_3 = b_2(0),\\
&[p + i \cdot \nu_3] b_3 + i \cdot f_3 \cdot s_3 + i \cdot g_{3,2} \cdot b_2 + i \cdot g_{3,4} \cdot b_4 = b_3(0),\\
&[p + i \cdot \nu_4] b_4 + i \cdot f_4 \cdot s_4 + i \cdot g_{4,3} \cdot b_3 + i \cdot g_{4,5} \cdot b_5 = b_4(0),\\
&[p + i \cdot \nu_5] b_5 + i \cdot f_5 \cdot s_5 + i \cdot g_{5,4} \cdot b_4 = b_5(0).
\end{aligned}
\tag{3}
$$

At the same time, despite the linearity of the equations themselves with respect to fields, the dependence of eigenfrequencies on parameters is determined by the determinant of systems, which is an essentially nonlinear function (a high-degree polynomial) both with respect to the Laplace frequency p and with respect to all controlled parameters.

Accordingly, all dynamic characteristics also depend in a non-linear way on natural frequencies and on the determinant. Despite its formally relatively simple algorithmic solvability, the presented system (3) does not allow us to directly formulate optimization problems that determine the modes of using the system that is in demand in physics.

Thus, even information about the presence of a given system with a large number of parameters (and dynamic capabilities) at least one mode of use in the form of a sensor or preprocessor, where the efficiency could be of any significance for physics and applications in quantum computing, remains unknown. In other words, we are dealing with a little-known system, the optimization of which is a complex mathematical problem.

Figure 2 shows the characteristic structure of the system's eigenfrequency spectrum depending on the coupling parameter g (specifically for Fig. 2, $g_{nm}= fn = g$, $\nu_n= 0$). It can be seen that the system has a rather complex structure, full control of which is implemented in a large multiparameter space of parameters g_{nm}, f_n, ν_n. Moreover, with the increase of the parameter g, the relative distances between frequencies change disproportionately, and therefore it is difficult to obtain such convenient cases for research when the eigenfrequencies are equidistant [16] and the

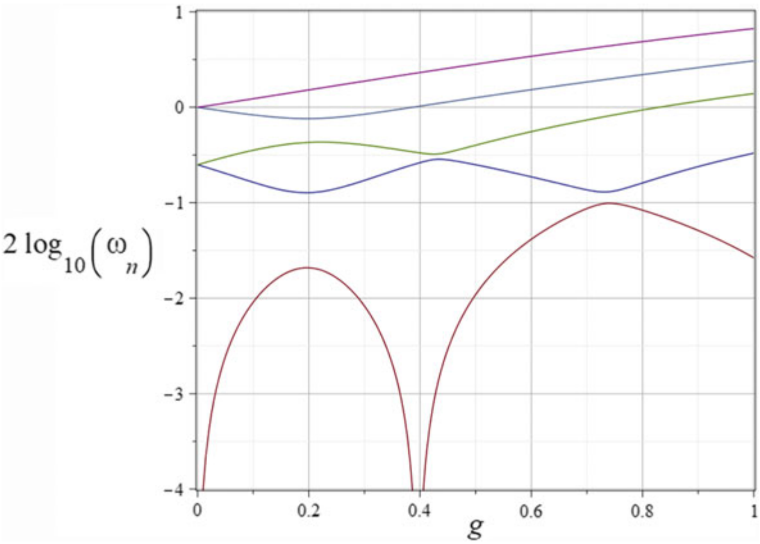

Fig. 2 Characteristic form of the system's own spectrum: the dependence of $log_{10}(\omega_n^2)$ on the parameter g for $n = \{\pm 1, \ldots, \pm 5\}$ ($\omega_n = -\omega_n$). As the coupling constant increases, the ratio of distances between frequencies increases quite rapidly and the spectrum cannot be equidistant at large g

dynamics become automatically reversible (which greatly simplifies the dynamic analysis of the system).

Despite the small number of elements in the complete system (10 elements: 5 spins and 5 resonators), the algebraic system presents significant complexity. At the same time, finding analytical algebraic relations can play a key role in quickly configuring the most effective modes.

3 Preprocessor Mode

The case of a 4-part subsystem. When the connections $g_{23} = g_{34} = 0$ are disabled, a reversible transfer of the field from spins 2 and 4 to spins 1 and 5 and back is possible (without using the central resonator number 3). When making initial assumptions about the ratios between the frequencies of the resonators

$$\nu_1 = \nu_2 = -\nu_4 = -\nu_5, \tag{4}$$

and about coupling constants

$$f_n = 1, \; g_{12} = g_{45} = g \tag{5}$$

the optimal transfer in forward and reverse direction is performed automatically due to the symmetry of the frequency spectrum of the system and the initial conditions (and hence in time representation, that is, there is reversibility), and the range of eigenfrequencies ωn (and conversion dynamics) controlled (according to (3), (4), (5)) by the constant g using the ratio

$$\omega_2 - \omega_1 = 2 \cdot g \cdot sqrt(1 + g^2) \quad (6)$$

At time $T = \pi/(\omega_2 - \omega_1)/2$, an equal division of energy between 4 channels 1,2,4,5 is possible, and at time $T = \pi/(\omega_2 - \omega_1)$, a complete transfer of energy from spins 2,4 to spins 1,5 is realized. Thus, due to the different distribution of energy between different subsystems, it becomes possible to manipulate quantum states due to external influence. Note also that such manipulations require some finite time and therefore require in fact some energy delay near the time zones chosen for manipulations. This condition is also achieved here but requires a more detailed study, which will be carried out in the continuation of the current study.

4 Distributed Sensor Mode

The simulation of a phase sensor on a resonator platform can be seen in the framework of a simple model – the decay of the field from spins 2 and 4 with frequencies $\nu_2 = -\nu_4 = 1$ to spin 3 with frequency $\nu_3 = 0$, which is the detecting element. We will choose the distribution of coupling constants as follows: $g_{12} = g_{45} = 0$, $g_{23} = g_{34} = g$. For the situation under study, the eigenfrequency spectrum is controlled by the ratio

$$\omega_2 - \omega_3 = sqrt(9 + 4 \cdot g^2) \quad (7)$$

At the moment of full energy transfer at $T = \pi/(\omega_2 - \omega_3)$, the phase difference $\varphi_2 - \varphi_4$ is actually detected, which is realized in the form of a rapid change of the parameter $\gamma_3 = 0$ to $\gamma_3 = \infty$. The detected energy fraction is $cos\ (\varphi_2 - \varphi_4 + Const)^2$, where the *Const* value follows from the equations, and the sensory sensitivity of such a system with respect to the phase change in the nodes 2,4 is determined in a standard way through the energy derivatives of the phase.

5 Reversible Dynamics and Spectra

Model examples of the system functioning in preprocessor and sensor mode show the fundamental capabilities of the system in terms of potential physical applications. However, an extensive study of the system's sensory capabilities involves the construction of reversible dynamics and other spectroscopic properties.

The presented system has 10 natural frequencies. For clarity, we can give a simulation of the spectrum dependence on the coupling parameter g for the case of a symmetrical arrangement of frequencies and couplings relative to the central frequency and the central resonator. When fixing the proper spectrum of growing positive frequencies $\omega_n = [0,1,1,\omega_4,\omega_5]$, using the ratios $\nu_n = [0,1,0,1,0]$, $f_n = 1$, the condition $\omega_3 = 2$ is fixed by the ratio $g_{23} = g_{34} = g\ sqrt((4-g^2)/(2\ g^2-4))$, where $g = g_{12} = g_{45}$. It can be seen that the optimal dependence of g_{23} on the parameter g is nonlinear but analytical. Thus, due to the analytical structure of this dependency, faster system configuration is possible, which simplifies the experimental implementation of the system (Fig. 3).

Figure 4 shows the dependence of the free frequency ω_5 on parameter g. When $g = sqrt(30\text{-}2\ sqrt(105))/2$ we get the minimum integer value $\omega_5 = 4$. In other words, we can't get an equidistant spectrum, but we can get a multiple frequency spectrum of the form *[0,1,1,2,4]*, which, like the equidistant spectrum, corresponds to reversible dynamics. The minimum requirement of ω5 is not mandatory, but for large values of ω_5, we get a high-frequency contribution to the dynamics, which will lead to a complication of the field dynamics in the vicinity of time zones, where external manipulations with states are assumed. Successful high-performance manipulation requires that the frequencies are in order equal to each other.

As a result, we saw 3 different ways to use the system: preprocessor mode, distributed sensor mode, and a mode that responds to reversible dynamics. In the case of a general situation, there is no general recipe for obtaining the necessary quantum dynamics, and it is often difficult to answer the question of what dynamic effects are fundamentally possible. If you know in advance what dynamics are possible and what you need to get, then formally the problem is solved by introducing the

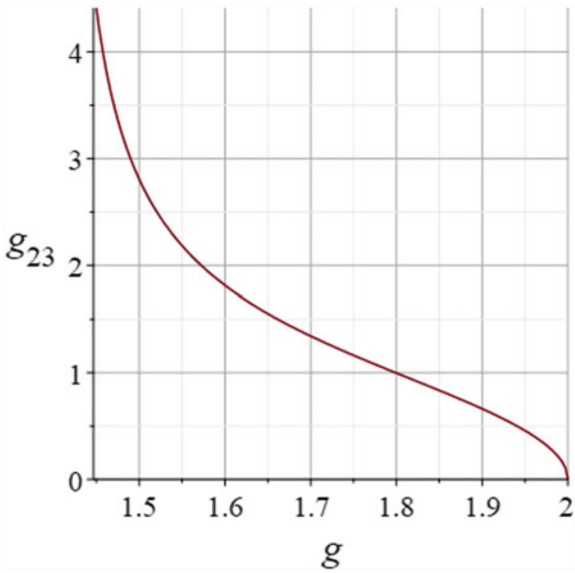

Fig. 3 The dependence of g_{23} on the parameter g, at which the condition $\omega_4 = 2$ is fixed

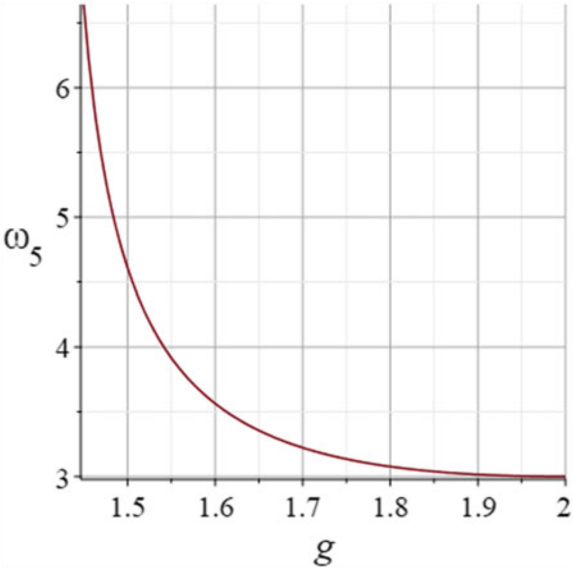

Fig. 4 Dependence of the free frequency ω_5 on the parameter g

necessary target optimization function for practice. If you need to use the system in several modes, then the first condition that is convenient to impose is the condition of reversibility (partial reversibility) of the dynamics. This allows us to consistently reduce the complexity of the optimization problem and most effectively use various dynamics capabilities to expand the computational functionality of the QMB.

The obtained algebraic dependencies that control modes with a frequency spectrum dominated by multiples of frequencies (corresponding to the reversible dynamics) are interesting for constructing QMB with pre-defined properties. Such modes for multiparticle systems with more than 10 subsystems are quite complex to describe and need to be systematically studied using methods of algebraic geometry [17].

6 Conclusion

Optimization of the multi-functional QMB showed the possibility of using the QMB simultaneously in the preprocessor mode, which plays the role of interface between logical qubits, as well as in the distributed sensor mode, which is potentially applicable for measuring the relative phase of cluster quantum states in different nodes of a multi-frequency quantum network of resonators.

Various optimization methods have shown that the proposed system has quite rich possibilities for spectral tuning, which is necessary to improve various modes of use. This makes it interesting to further study the proposed scheme in the form of a linear chain.

Acknowledgements The work was partially supported by the laboratory "Integrated Quantum Optics" of the Kazan Quantum Center of KNRTU-KAI (model construction and analysis of results—N.S.P.), partially supported by the budget theme of the laboratory of Quantum Optics and Informatics of the KPhTI—FRC KazSC RAS (algebraic methods for optimizing quantum systems—N.S.P., T.D.Y.), and partially supported by the RFBR grant 18-42-160007 (numerical modeling of dynamic properties of multifunctional quantum memory—N.S.P.).

References

1. Hammerer, K., Sørensen, A.S., Polzik E.S.: Quantum interface between light and atomic ensembles. Rev. Mod. Phys. **82**(2), 1041–1093 (2010). https://doi.org/10.1103/RevModPhys.82.1041
2. Kurizki, G., Bertet, P., Kubo, Y., Mølmer, K., Petrosyan, D., Rabl, P., Schmiedmayer, J.: Quantum technologies with hybrid systems. Proc. Natl. Acad. Sci. **112**(13), 3866–3873 (2015). https://doi.org/10.1073/pnas.1419326112
3. Roy, D., Wilson, C.M., Firstenberg, O.: Colloquium: Strongly interacting photons in one-dimensional continuum. Rev. Mod. Phys. **89**(2), 021001 (2017). https://doi.org/10.1103/RevModPhys.89.021001
4. Jiang, L., Hodges, J.S., Maze, J.R., Maurer, P., Taylor, J.M., Cory, D.G., Hemmer, P.R., Walsworth, R.L., Yacoby, A., Zibrov, A.S., Lukin, M.D.: Repetitive readout of a single electronic spin via quantum logic with nuclear spin ancillae. Science **326**(5950), 267–272 (2009). https://doi.org/10.1126/science.1176496
5. Zhong, M., Hedges, M.P., Ahlefeldt, R.L., Bartholomew, J.G., Beavan, S.E., Wittig, S.M., Longdell, J.J., Sellars, M.J.: Optically addressable nuclear spins in a solid with a six-hour coherence time. Nature **517**(7533), 177–180 (2015). https://doi.org/10.1038/nature14025
6. Zhang, X., Li, H. O., Cao, G., Xiao, M., Guo, G. C., & Guo, G. P.: Semiconductor quantum computation. Natl. Sci. Rev. **6**(1), 32–54 (2019). https://doi.org/10.1093/nsr/nwy153
7. Cho, Y.W., Campbell, G.T., Everett, J.L., Bernu, J., Higginbottom, D.B., Cao, M.T., Geng, J., Robins, N.P., Lam, P.K., Buchler, B.C.: Highly efficient optical quantum memory with long coherence time in cold atoms. Optica **3**(2), 100–107 (2016). https://doi.org/10.1364/OPTICA.3.000100
8. Hsiao, Y.F., Tsai, P.J., Chen, H.S., Lin, S.X., Hung, C.C., Lee, C.H., Chen, Y.H., Chen, Y.F., Yu, I.A., Chen, Y.C.: Highly efficient coherent optical memory based on electromagnetically induced transparency. Phys. Rev. Lett. **120**(18), 183602 (2018). https://doi.org/10.1103/PhysRevLett.120.183602
9. Hartmann, M.J., Brandao, F.G., Plenio, M.B.: Quantum many-body phenomena in coupled cavity arrays. Laser Photonics Rev. **2**(6), 527–556 (2008). https://doi.org/10.1002/lpor.200810046
10. Vahala, K. J.: Optical microcavities. Nature **424**(6950), 839–846 (2003). https://doi.org/10.1038/nature01939
11. Kobe, O.B., Chuma, J., Jamisola Jr., R., Chose, M.: A review on quality factor enhanced on-chip microwave planar resonators. Eng. Sci. Technol., Int. J. **20**(2), 460–466 (2017). https://doi.org/10.1016/j.jestch.2016.09.024
12. Pfaff, W., Axline, C.J., Burkhart, L.D., Vool, U., Reinhold, P., Frunzio, L., Jiang, L., Devoret, M.H., Schoelkopf, R.J.: Controlled release of multiphoton quantum states from a microwave cavity memory. Nat. Phys. **13**(9), 882–887 (2017). https://doi.org/10.1038/nphys4143
13. Moiseev, S.A., Gerasimov, K.I., Latypov, R.R., Perminov, N.S., Petrovnin, K.V., Sherstyukov, O.N.: Broadband multiresonator quantum memory-interface. Scientific Reports **8**(1), 1–8 (2018). https://doi.org/10.1038/s41598-018-21941-6

14. Smith, D.D., Chang, H.: Coherence phenomena in coupled optical resonators. J. Mod. Opt. **51**(16–18), 2503–2513 (2004). https://doi.org/10.1080/09500340408231809
15. Flurin, E., Roch, N., Pillet, J.D., Mallet, F., Huard, B.: Superconducting quantum node for entanglement and storage of microwave radiation. Phys. Rev. Lett. **114**(9), 090503 (2015). https://doi.org/10.1103/PhysRevLett.114.090503
16. Perminov, N.S., Tarankova, D.Y., Moiseev, S.A.: Programmable quantum motherboard for logical qubits. Laser Phys. **29**(12), 124016 (2019). https://doi.org/10.1088/1555-6611/ab4bd5
17. Perminov, N.S., Moiseev, S.A.: Spectral-topological superefficient quantum memory. Scientific reports **9**(1), 1–7 (2019). https://doi.org/10.1038/s41598-018-38244-5
18. Moiseev, S.A., Andrianov, S.N., Moiseev, E.S.: A quantum computer in the scheme of an atomic quantum transistor with logical encoding of qubits. Opt. Spectrosc. **115**(3), 356–362 (2013). https://doi.org/10.1134/S0030400X13090166
19. Andrianov, S.N., Arslanov, N.M., Gerasimov, K.I., Kalinkin, A.A., Moiseev, S.A.: CNOT gate on reverse photon modes in a ring cavity. Quantum Inf. Process. **18**(7), 235 (2019). https://doi.org/10.1007/s11128-019-2345-z
20. Tarasov, S.O., Andrianov, S.N., Arslanov, N.M., Moiseev, S.A.: A quantum transistor based on an atom-photon molecule. Bull. Russ. Acad. Sci.: Phys. **82**(8), 1042–1046 (2018). https://doi.org/10.3103/S1062873818080415
21. Moiseev, S.A., Ablayev, F.M., Andrianov, S.N., Vasiliev, A.V.: Quantum computer based on triangular atom-photon molecule. Int. Conf. Micro-And Nano-Electron. **11022**, 110222A (2019). https://doi.org/10.1117/12.2522445
22. Han, J.X., Wu, J.L., Wang, Y., Jiang, Y.Y., Xia, Y., Song, J.: Multi-qubit phase gate on multiple resonators mediated by a superconducting bus. Opt. Express **28**(2), 1954–1969 (2020). https://doi.org/10.1364/OE.384352

A Reinforcement Learning Approach for Task Assignment in IoT Distributed Platform

Oleg Eremin and Maria Stepanova

Abstract This chapter represents an adaptive method based on reinforcement learning for task assignment in IoT distributed platform. The described experiments and results present the ability to usage IoT nodes by themselves for task processing operations. Furthermore, previously designed program code for classical distributed and parallel systems could be executed on the IoT nodes with the described approach and method. The method was developed with the diversity and variability of IoT systems.

Keywords Internet of Things · Distributed systems · Computing nodes · Program code · Parallel systems · Machine learning · Reinforcement learning · Adaptive ε method

1 Introduction

Complex computing tasks require the use of specialized distributed or parallel computing systems such as multiprocessors, multi-core, multithreaded systems, and similar to them.

The Internet of Things platform consists of many heterogeneous computing nodes that could be arranged in a whole distributed computing system.

The main idea of IoT systems is embedding specialized modules in real-world objects. The modules implement data identification, gathering, processing, and transmitting.

Initial approaches to interacting elements of the Internet of Things were to transfer data from computing sensor modules embedded in real-world objects to a centralized computing node [1, 2]. The node provided data storing and processing,

O. Eremin · M. Stepanova (✉)
Bauman Moscow State Technical University, ul. Baumanskaya 2-ya, 5/1, Moscow 105005, Russia
e-mail: stepanova@bmstu.ru

O. Eremin
e-mail: ereminou@bmstu.ru

A. G. Kravets et al. (eds.), *Cyber-Physical Systems*, Studies in Systems, Decision and Control 350, https://doi.org/10.1007/978-3-030-67892-0_31

device coordination, and communication. Such architecture has a set of significant limitations:

- high latency,
- the complexity of supporting the diversity of the technology stack, and organizing their coherent interaction with the proliferation of different types of devices,
- the necessity of increasing capacity on the network bandwidth.

There were proposed architecture types to eliminate the disadvantages according to a principle: computing tasks that can be executed without its sending to a centralized node should be performed on a node by itself.

Such a principle is implemented in the edge computing concept that peripherals are organized in a distributed computing system for increasing data processing speed [2, 3]. Computing capabilities of embedded systems are constantly growing, especially of IoT devices. Thus, moving sensor and local node workloads from a central node to IoT nodes can provide the overall IoT platform with the same benefits which have been obtained in edge computing [4].

Existing node load distribution algorithms are applied to classical distributed systems and not suitable for the IoT platform [5]. That is caused by IoT specifics: heterogeneity of nodes, changeable number of nodes, variable level of network quality, etc.

Thus, there is an actual point for developing the distribution method that can be applied to the IoT platform with its mobility and changeability specifics. This chapter proposes such a method based on the reinforcement learning approach.

2 Distributed Computing System Based on IoT Platform

An IoT platform based distributed computing system consists of a great number of heterogeneous nodes that have various technical constraints. The nodes interact with each other with wired or wireless communication channels. It is necessary to provide an effective task distribution in distributed computing systems for the described issue:

- minimization of node downtime
- absence of node reboot
- quality assurance of task processing on each node

Furthermore, it is impossible to take into consideration the efficiency parameters of classical systems for the IoT platform as task assignment approaches are not applicable to the IoT platform [6].

The issue of node task assignment in the IoT platform is NP-hard. That means the issue can be solved by heuristic methods that allow receiving a solution close to the optimal one according to current constraints [7]. However, heuristic methods require the full model description of constraints variety and computing nodes states.

The procedure for assigning tasks to the nodes of a distributed system based on the Internet of Things platform, in general, can be with the following steps [8]:

– algorithm development for a distributed system specificity,
– implementation of the computational graph of the algorithm,
– dependencies detection among tasks,
– generating task sequences,
– tasks assignment and distribution to computing nodes,
– getting the results from each node.

The transformation of the computing issue algorithm into the graph [9] allows describing a solution with the help of a task set where each task can have a connection with other tasks. Moreover, it is necessary to determine the order of priority of the tasks: determine the tasks that need to be completed before the new one. Dependency and order control allows avoiding the deadlock state for the algorithm. Furthermore, each task can have individual requirements for a computing node to be able to be executed.

A task sequence generated according to node constraints then is assigned to the nodes of the distributed IoT platform. The proposed method based on reinforcement learning allows taking into consideration both the specialty of each task and each node as IoT nodes have a different computing capacity.

3 Methodology of Assigning Tasks to IoT Computing Nodes

It is proposed to implement a multi-armed bandit algorithm that is referred to the reinforcement learning to solve the issue of task assignment to the nodes of the distributed IoT platform.

The IoT platform is an environment in reinforcement learning [10] notation. The environment is defined by the number of nodes and their characteristics. The main node that is responsible for generating task sequences and tasks assignment is an agent. The agent is in the constant interaction process with the environment. The agent does not need the whole fully described model of the environment. It sends actions to the environment and gets back rewards instead (Fig. 1). The further agent actions depend on previously chosen actions and received rewards.

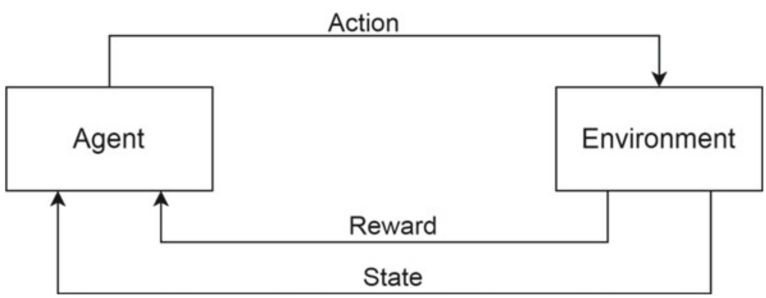

Fig. 1 The Agent-Environment interaction

Reinforcement learning belongs to the machine learning area and differs from supervised and unsupervised concepts. Unlike supervised machine learning type, it does not need predefined labeled data. To compare reinforcement learning with unsupervised machine learning type, it does not search for hidden structures.

The main characteristic of reinforcement learning is its self-creation of a set of decision-making actions according to the current environment state and constant adaptation to changing uncertain environment conditions.

The chapter proses a multi-armed bandit algorithm, the agent each time chose an action from a set of available actions A, R—a set of rewards from the environment [11]. Each reward r $\in$ R is matched to the action $a \in A$.

The expected reward for the selected a on time step t is:

$$q_*(a) \doteq \mathrm{E}[R_t \mid A_t = a]. \tag{1}$$

The uncertain distribution of reward probability with chosen a is:

$$R^a(t) = P(r|a). \tag{2}$$

The agent has two stages for implementation: exploration and exploitation. It is critical to balance the exploration-exploitation dilemma to ensure the optimal solution [12, 13]. Multi-armed bandit algorithms can follow various strategies for the dilemma. In this chapter, the ε-greedy strategy is described. The ε-greedy has an exploration probability $\varepsilon \in [0;\ 1]$, which defines the probability of each action to be chosen:

$$a_t = \begin{cases} a_t^*, \text{ with probability } 1 - \varepsilon \\ a \text{ random action, with probability } \varepsilon \end{cases} \tag{3}$$

Turning the ε parameter in the multi-armed algorithm makes the agent functioning in a completely greedy manner that provides the exploitation stage or in a variable way that is the exploration stage.

The strategy is greedy when ε = 0, and the agent never tries to explore new actions. The only action with the highest reward is chosen.

When ε = 1, the algorithm randomly chose an action on each time step.

The algorithm for task assignment into distributed IoT platform is given below:

Step 0. The step defines the initial states of a distributed computing system based on the IoT platform: environment, nodes number, nodes characteristics. The agent (main distributing node) generates task sequences with their interconnections.

Step 1. Exploration stage. The agent takes the R information from the nodes. If nodes are accessible, the rewards sequence R—integral characteristic is formed. Such characteristic is formed by computing nodes parameters: energy consumption, package processing time, etc.

Step 2. The integral characteristic of each node transforms into a probability value. It means that nodes' probability values show the ability of task processing from the main node.
Step 3. The exploitation stage. The agent saves the probabilities received at the previous step and sends tasks to nodes with the highest reward value.
Step 4. When the tasks are processed by the nodes, the nodes will send task processing results and the information of the current states of nodes to the main node, which will recalculate reward values R.
Step 5. If there are tasks in the task sequence in the main node, the algorithm will start back from Step 3 otherwise, it will move to Step 6.
Step 6. The end of the algorithm.

The multi-armed bandit algorithm can deal with a stationary or non-stationary environment [14].

In the stationary environment, its parameters do not change with time, opposite to the nonstationary environment.

For the IoT platform, both cases are possible as IoT nodes can be stationary located and the environment does not change. For the nonstationary case, IoT nodes can be unstable [15] and dynamically change their positioning, and network connection could be unstable or have a changeable bandwidth channel.

4 Method of Experiments: Stationary and Nonstationary Environment

The section presents two methods used in the experiments. The first method is for the stationary environment and the second is for the nonstationary environment.

In the stationary environment, the multi-armed bandit algorithm had constant:

- number of nodes,
- parameters of the integral characteristic of nodes,
- value of exploration probability ε.

The experimentally tested exploration probability values are:

$$\varepsilon \in [0, 0.001, 0.05, 0.25, 0.1, 0.2, 0.3, 0.4, 0.5, 1].$$

Figure 2 presents that output stabilizes with time and the system will produce the same level quality of task assignments. It is required more time for algorithm stabilization with the growing number of nodes. The experiment results are proved with the previously presented [16, 17]: increasing ε causes the algorithm to execute in the exploitation mode and reduces exploration rate.

Figure 3 shows the increase of cumulative reward that receives the main node time. Optimal algorithm execution is evaluated also with the help of the regret function (Fig. 4). The function has a logarithmic behavior [18, 19]. For 20 arms the optimal values ε are 0.1 and 0.2.

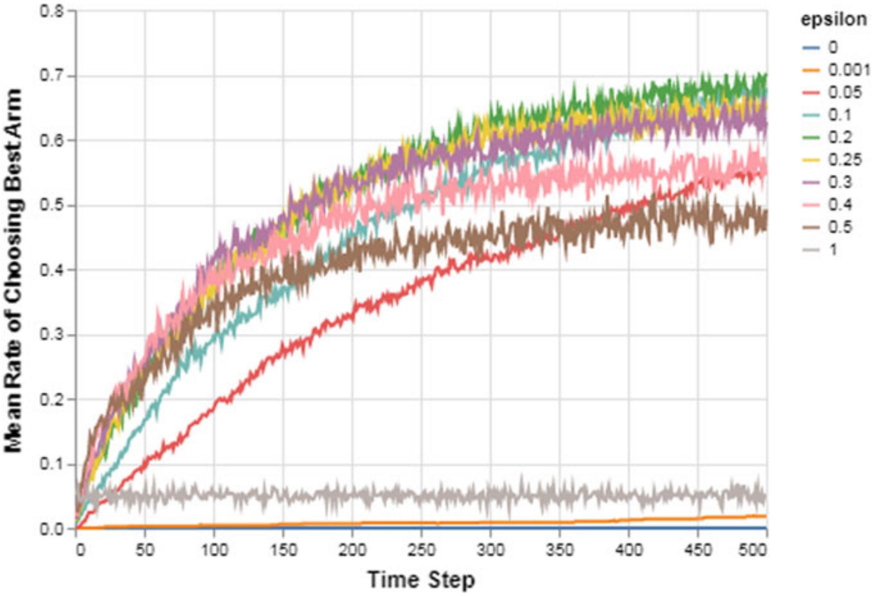

Fig. 2 Mean Rate of Choosing Best Arm (20 arms, 1000 simulations)

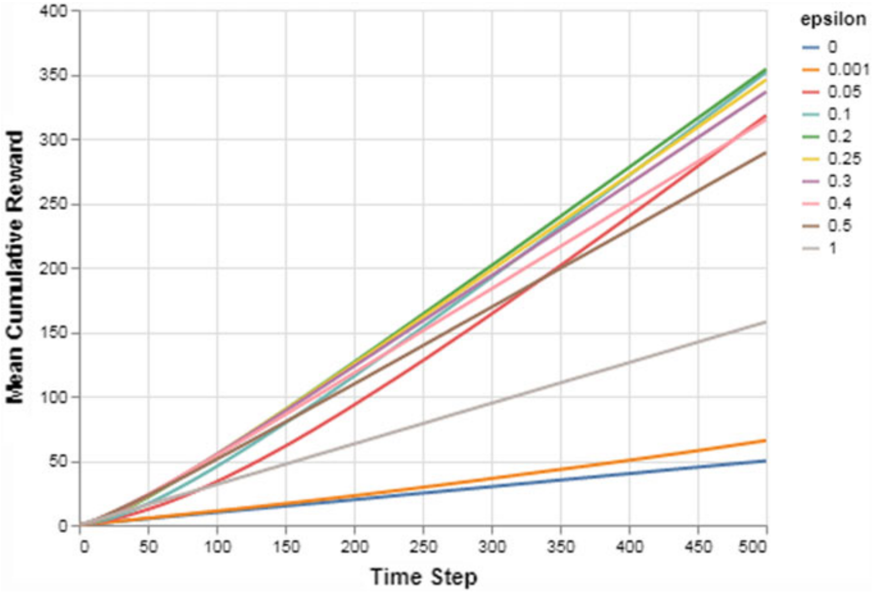

Fig. 3 Mean Cumulative Reward (20 arms, 1000 simulations)

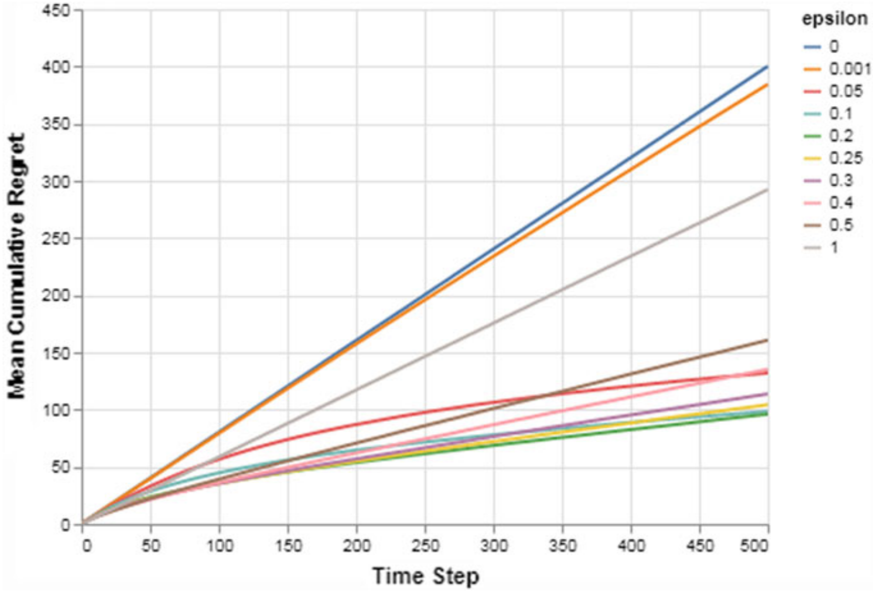

Fig. 4 Mean Cumulative Regret (20 arms, 1000 simulations)

For a nonstationary environment, there was an assumption that the environment was stationary for some time before a task was assigned to a node. The assumption was valid for every task waiting for an assignment to a node.

Previous approaches to an adaptive implementation were based on decreasing its value from a high rate at each time step or switching from exploration to exploitation after a specific amount of time [20, 21].

The chapter proposes to use adaptive ε that takes decisions to changes its value in [1;0] due to:

– number of correctly chosen arms for each task specifics from the task sequence,
– cumulative reward,
– reward statistics of each node for a specific task.

That means exploration probability can do self-regulation based on the described points. The adaptive ε self-tuning is more proper for a continuously changing environment, instead of the hand-tuning ε. Thus, the agent adaptably changes its behavior to the environment changes, and nodes are chosen optimally.

Figure 5 shows that the regret function is not stable in the changing environment and has a changing view. That tells that the agent in the algorithm constantly changes its node strategy choice depending on the environment—nodes states.

The value of the mean cumulative reward is reached quicker and greater with adaptive ε.

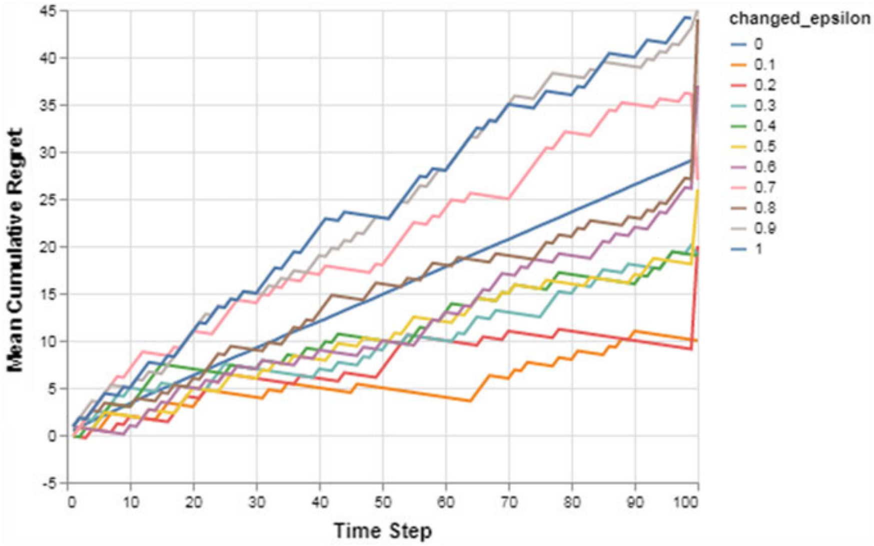

Fig. 5 Mean Cumulative Regret with an adaptive ε (20 arms, 1000 simulations)

Within the operation of the system, its quality gets higher and the optimal nodes are chosen for the task assignment process. The longer system operates with the adaptive approach the higher quality. Otherwise, without the adaptive approach, the system would operate but would choose non-optimal nodes for tasks' specifics.

Figure 6 presents a rough view of the mean cumulative reward due to the constantly changing parameters of the computational system.

The value of the reward function does not decrease in the dynamic system, which means that the proposed approach can be implemented in a computational system with constantly changing parameters on time.

5 Conclusion

The chapter describes the method of task assignment to computational nodes of a distributed system on the base of the IoT Platform.

The reinforcement learning approach implementing allows taking into account diversity and variability of the environment.

The proposed approach allows utilizing computational nodes by themselves for tasks' processing instead of sending the whole data stream to a central node for processing. Furthermore, the key feature of the proposed method is the usage of existing software, originally designed for classical distributed and parallel systems, for new distributed computations concepts with constantly changing parameters as it is in IoT.

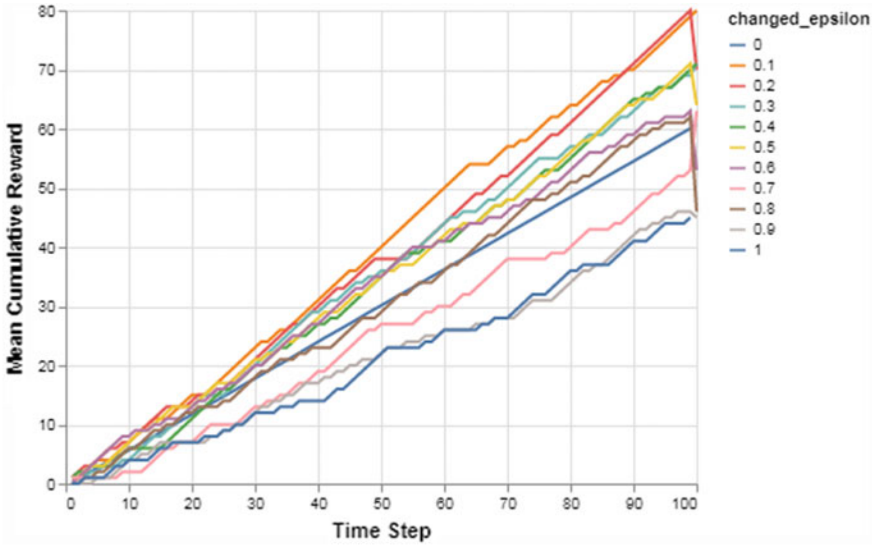

Fig. 6 Mean Cumulative Reward with an adaptive ε (20 arms, 1000 simulations)

References

1. Ai, Y., Peng, M., Zhang, K.: Edge computing technologies for Internet of Things: a primer. Digital Commun. Netw. **4**(2), 77–86 (2018)
2. Adi, E., Anwar, A., Baig, Z.: Machine learning and data analytics for the IoT. Neural Comput. Appl. (2020)
3. Verma, S., Kawamoto, Y., Fadlullah, Z.M., Nishiyama, H., Kato, N.: A survey on network methodologies for real-time analytics of massive IoT data and open research issues. IEEE Commun. Surv. Tutor. **19**(3), 1457–1477 (2017)
4. Chiang, M., Zhang, T.: Fog and IoT: an overview of research opportunities. IEEE Internet Things J. **3**, 854–864 (2016)
5. van Steen, M., Tanenbaum, A.S.: Distributed Systems, 3rd ed., distributed-systems.net (2017)
6. Chernen'kii, S.P.S.: Method for description of tasks in multiprogramming and multiprocessor systems. Vestnik MGTU, Seria "Priborostroenie" (1), 121–132 (2014)
7. Yeckle, J., Rivera, W.: Mapping and characterization of applications in heterogeneous distributed systems. In: Proceedings of the 7th World Multiconference on Systemics. Cybernetics and Informatics (SCI2003), pp. 1–6 (2003)
8. Eremin, O.Y., Stepanova, M.V.: Applying reinforcement learning in distribution computational system—Internet of Things. Dyn. Complex Syst. **14**(2), 84–92 (2020)
9. Voevodin, V.V., Voevodin, Vl.V.: Parallel'nye vychislenija, p. 608. SPb: BHV-Peterburg (2002)
10. Sutton, R.S., Barto, A.G.: Reinforcement learning: an introduction. The MIT Press (2008)
11. Robbins, H.: Some aspects of the sequential design of experiments. Bull. Am. Math. Soc. **58**, 527–535 (1952)
12. Rejeb, L., Guessoum, Z., M'Hallah, R.: An adaptive approach for the exploration-exploitation dilemma for learning agents. In: Pěchouček, M., Petta, P., Varga, L.Z. (eds.) Multi-Agent Systems and Applications IV. CEEMAS. Lecture Notes in Computer Science, vol. 3690. Springer, Berlin, Heidelberg (2005)
13. Yogeswaran, M., Ponnambalam, S.G.: Reinforcement learning: exploration–exploitation dilemma in multi-agent foraging task. OPSEARCH **49**, 223–236 (2012)

14. Manome, N., Shinohara, S., Suzuki, K., Tomonaga, K., Mitsuyoshi, S.: A multi-armed bandit algorithm available in stationary or non-stationary environments using self-organizing maps. In: Tetko, I., Kůrková, V., Karpov, P., Theis, F. (eds.) Artificial Neural Networks and Machine Learning—ICANN 2019: Theoretical Neural Computation. ICANN. Lecture Notes in Computer Science, vol. 11727. Springer, Cham (2019)
15. Hakim, A., Amirat, A., Oussalah, M.C.: Non-intrusive contextual dynamic reconfiguration of ambient intelligent IoT systems. J. Ambient. Intell. Human Comput. **11**, 1365–1376 (2020)
16. Akanmu, S., Garg, R., Gilal, A.: Towards an improved strategy for solving multi-armed bandit problem. Inter. J. Innovative Technol. Exploring Eng. (IJITEE) **8**(12) (2019)
17. Mignona, A., Rocha, R.: An adaptive implementation of ε-Greedy in reinforcement learning. Procedia Comput. Sci. **109C**, 1146–1151 (2017)
18. Peter, A., Fischer, N., Fischer, P.: Finite-time analysis of the multiarmed bandit problem. Mach. Learn. **47**, 235–256 (2002)
19. Agrawal, R.: Sample mean based index policies with O (log n) regret for the multi-armed bandit problem. Adv. Appl. Probab. **27**, 1054–1078 (1995)
20. Tokic M.: Adaptive ε-Greedy Exploration in Reinforcement Learning Based on Value Differences. In: Dillmann, R., Beyerer, J., Hanebeck, U.D., Schultz, T. (eds.) Advances in Artificial Intelligence. Lecture Notes in Computer Science, vol. 6359. Springer, Berlin, Heidelberg (2010)
21. Caelen, O., Bontempi, G.: Improving the exploration strategy in bandit algorithms. In: Learning and Intelligent Optimization. Number 5313 in LNCS, pp. 56–68. Springer (2008)